Filamentous Phage Display of Designed Ankyrin Repeat Proteins: from Conception to Applications

DISSERTATION

zur

Erlangung der naturwissenschaftlichen Doktorwürde

(Dr. sc. nat.)

vorgelegt der

Mathematisch-naturwissenschaftlichen Fakultät

der

UNIVERSITÄT ZÜRICH

von

Daniel Steiner

von

Neftenbach / ZH

Promotionskomitee

Prof. Dr. Andreas Plückthun (Vorsitz)

Prof. Dr. Raimund Dutzler

Zürich 2007

Die vorliegende Arbeit wurde von der Mathematisch-naturwissenschaftlichen Fakultät der Universität Zürich auf Antrag von Prof. Dr. Andreas Plückthun und Prof. Dr. Raimund Dutzler als Dissertation angenommen.

Publications

Steiner, D., Forrer, P., Stumpp, M. T. & Plückthun, A. (2006). Signal sequences directing cotranslational translocation expand the range of proteins amenable to phage display. *Nat. Biotechnol*. **24**, 823-31.

Steiner, D., Forrer, P. & Plückthun, A. (2006). Efficient Selection of DARPins with Subnanomolar Affinity using SRP Phage Display, *Manuscript*

Huber, T., Steiner, D., Rothlisberger, D. & Plückthun, A. (2007). In vitro selection and characterization of DARPins and Fab fragments for the co-crystallization of membrane proteins: The Na(+)-citrate symporter CitS as an example. *J. Struct. Biol*., Article in Press

Patent

Steiner, D., Forrer, P., Stumpp, M. T. & Plückthun, A. (2007). Phage display using cotranslational translocation of fusion polypeptides. WO2007006665

Additional publication

Zahnd, C., Wyler, E. , Schwenk, J.M., Steiner, D., Lawrence, M.C., McKern, N,M., Pecorari, P., Ward, C.W., Joos, T.O, Plückthun, A. (2007). A Designed Ankyrin Repeat Protein Evolved to Picomolar Affinity to Her2. *J. Mol. Biol.* **369**, 1015-1028.

Erklärung

Diese Dissertation im Fach Biochemie wurde von Prof. Dr. Andreas Plückthun betreut.

Die Dissertation wurde selbständig, ohne unerlaubte Hilfe angefertigt. Bei der Abfassung der Dissertation wurden im Sinne von § 3 lit. 1 der Promotionsverordnung vom 08. Juli 2002 keine anderen als die angegebenen Hilfsmittel verwendet.

Zürich, im September 2007

Daniel Steiner

For my parents

Acknowledgments

I owe most thanks to Prof. Dr. Andreas Plückthun for entrusting me with this project, for his constant support throughout my thesis, for many valuable discussions, and for the freedom to pursue my own ideas. I would also like to thank Prof. Dr. Raimund Dutzler for co-refereeing my thesis.

I am deeply grateful to Dr. Patrik Forrer and Dr. Michael Stumpp for their great supervision and support. Thank you both for the innumerous discussions, for sharing ideas, for correcting my manuscripts, for your trust in me, and for your friendship.

I would also like to thank Dr. Kaspar Binz, Dr. Patrick Amstutz and Dr. Christian Zahnd for many fruitful discussions, friendship and moral support. A big "thank you" goes also to Dr. Martin Kawe, Dr. Oliver Scholz, Chris Gehringer and Michael Hohl for creating an excellent atmosphere in M66. I wish to also thank Thomas Huber for an excellent collaboration on the selection and characterization of CitS binding DARPins as well as Christian Jost for the characterization of Her2 binding DARPins. Of course, special thanks go to Dr. Peter Lindner for everything necessary to keep our laboratory running and to all present and former colleagues in the Plückthun lab for creating such a nice working atmosphere.

Great thanks also to Petra Vogt and Ilse Plückthun for a great administration Job, Dr. Peter Hunziker, Dr. Serge Chesnov and Dr. Birgit Roth Z'Graggen for diverse analytic analysis, Dr. Stefan Klauser and Steve Rast for IT support, Jean-Claude Tomasina, Hermann Lüscher and Markus Imbach for technical support and Sibylle Strassmann and Mike Konia for material supply.

I wish to thank the „Swiss National Center of Competence in Research (NCCR) in Structural Biology" and the „KTI Discovery" for financial support.

Finally I would like to thank all good friends for their help and support and for creating a perfect balance to the laboratory working day. My biggest thank goes to Michèle, my parents and my sister Stefanie. Thank you for your understanding, support, tolerance and love.

Contents in Brief

Contents

Abstract

High affinity and specific binding molecules are important tools for many biotechnological and pharmaceutical applications. They can be obtained *in vitro* by using selection technologies that allow molecules with the desired binding properties to be extracted from large collections of variants. My thesis describes the development of a new selection technology and its subsequent application to select binders from a Designed Ankyrin Repeat Protein (DARPin) library.

In the first part of my thesis a new selection technology called ”SRP phage display“ was developed that allows the display of highly stable and fast folding proteins, such as DARPins, that are virtually refractory to conventional phage display. In SRP phage display, the proteins to be displayed are directed to the *Escherichia coli* cotranslational signal recognition particle (SRP) translocation pathway by using an appropriate signal sequence, whereas conventional phage display uses the posttranslational Sec translocation pathway. This simple change of the translocation route seems to prevent premature folding of stable and fast folding proteins in the cytoplasm and therefore allows their efficient translocation and subsequent display on filamentous phage particles. For example, the display levels of DARPins were improved up to 700-fold by simply exchanging Sec-dependent for SRP-dependent signal sequences. This allowed more than 1000-fold enrichment per phage display selection round in model experiments.

In the second part of my thesis, SRP phage display was used to generate a large phage DARPin library containing more than 10^{10} functional individual members. Using this library, well-behaved and highly specific DARPins were selected for a broad range of target proteins having affinities as low as 100 picomolar without affinity maturation.

In conclusion, SRP phage display makes filamentous phage display accessible for DARPins, which allows, for example, selections under hash conditions, such as high temperatures or in the presence of denaturants. I envision that the use of SRP phage display would be also beneficial to increase the functional diversity of other libraries, especially for those containing stable and fast folding proteins.

Zusammenfassung

Proteinbindende Moleküle mit hoher Affinität und Spezifität sind wichtige Werkzeuge für viele biotechnologische und biomedizinische Anwendungen. Solche Moleküle mit den gewünschten Binde-Eigenschaften können mit Hilfe von *in vitro* Selektionstechnologien aus grossen Bibliotheken isoliert werden. Diese Arbeit beschreibt die Entwicklung einer neuen Selektionstechnologie und deren erfolgreiche Anwendung zur Isolierung von proteinbindenden Molekülen aus einer Bibliothek von „Designed Ankyrin Repeat Proteinen (DARPin)".

Der erste Teil dieser Arbeit beschreibt die Entwicklung von „SRP Phage Display", einer neuen Selektionstechnologie die es ermöglicht, stabile und schnell faltende Proteine auf filamentösen Bakteriophagen zu präsentieren, was mit der konventionellen „Phage Display" Technologie nicht möglich ist. In „SRP Phage Display" wird das zu präsentierende Protein über den cotranslationalen Signalerkennungspartikel (SRP) Transportweg in das Periplasma von *E. coli* transportiert, wohingegen in der konventionellen „Phage Display" Technologie der posttranslationale Sec Transportweg benutzt wird. Dieser einfache Wechsel des Transportweges verhindert die vorzeitige Faltung von stabilen und schnell faltenden Proteinen im Zytoplasma und erlaubt deshalb einen effizienten Transport ins Periplasma, was den Einbau und die Präsentation auf den Phagen Partikeln ermöglicht. Durch den einfachen Austausch der Signal-sequenz wurde die Präsentation von verschiedenen DARPins auf den Phagen Partikeln bis zu 700-fach verbessert, was zu einer bis zu 1000-fachen Anreicherung pro Selektionsrunde in Modellexperimenten führte.

Im zweiten Teil dieser Arbeit wurde „SRP Phage Display“ angewendet, um eine DARPin Bibliothek präsentiert auf Phagen zu generieren, die mehr als 10^{10} funktionelle Mitglieder enthält. In Selektions-Experimenten wurden hochspezifische Binder gegen eine Vielzahl von Zielmolekülen isoliert und Affinitäten von bis zu 100 picomolar ohne Affinitätsmaturierung erreicht.

Zusammenfassend erweitert „SRP Phage Display“ die für DARPins zugänglichen Selektionstechnologien und erlaubt durch die Präsentation der DARPins auf filamentösen Bakteriophagen die Selektion von proteinbindenden Molekülen unter stringenten Bedingungen wie hoher Temperatur und Gegenwart von denaturierenden Reagenzien. Auch für andere Bibliotheken von stabilen und schnell faltenden Protein sollte „SRP Phage Display“ helfen, die funktionelle Diversität zu erhöhen.

Chapter 1

Introduction

Contents

1. General Introduction

In the era of intensive genomic discovery, the number of identified genes is strongly increasing. One of the major challenges is to understand the function of the proteins encoded by these genes. However, many of these proteins are difficult to handle and therefore difficult do investigate. One promising approach to study such proteins is to generate specific binding proteins against them allowing detection, purification and many further experiments. However, the large number of interesting proteins greatly exceeds the capacity of conventional methods for monoclonal antibody production and subsequently led to the development of alternative techniques.

My thesis addresses the development of a new selection technology for designed ankyrin repeat proteins (DARPins) and its applicability to enrich specific binding proteins from a DARPin library. The first part of this chapter will give a brief overview of the protein libraries and display scaffolds generally used for the generation of specific binding proteins. In the second part, different selection technologies with a focus on their limitations will be discussed.

2. Libraries and Display Scaffolds

Display scaffolds used to generate specific binding proteins can be very diverse in size, structure and composition of the interaction surface. Based on the parental proteins they are derived from, they can be grouped into immunoglobulin and non-immunoglobulin scaffolds[1]. To create molecules with novel binding specificities from such scaffolds, libraries which have randomized potential target interaction residues are generated. The proteins with the desired binding properties are then extracted from these large collections of variants by using different selection technologies (see below).

2.1 Immunoglobulin scaffolds

Antibodies are currently by far the most frequently used binding molecules. The reason for that is to some extent historic. The molecular diversity of the immune system was the first source available to generate target-specific binding proteins. The target protein is injected into a laboratory animal that reacts in most cases with an immune response and thus produces specific antibodies. For further applications, the polyclonal sera or monoclonal antibodies, obtained by hybridoma technology, are used. There are several problems encountered when producing antibodies by immunization. Some target proteins are not immunogenic, others too toxic or just not stable enough to elicit an antibody response in the laboratory animal. To avoid immunization and to gain better control over the selection process, a broad range of synthetic or natural libraries of antibody fragments[2] or even whole antibody molecules[3] have been generated which can be used in combination with an appropriate selection technology (see below) for the fast and convenient selection of specific binding molecules. For all of these immunoglobulin-based binding molecules, the variable surface loops on the antibody framework, called complementary determining regions (CDRs) are responsible for the interaction with the target protein and confer affinity and specificity. The major limitations of whole antibody molecules are based on their complex composition. The large, multidomain assembly with glycosylation and disulfide bonds makes them relatively difficult and expensive to manufacture. Smaller versions of antibodies, such as scFv or Fab fragments can be produced in microbial hosts albeit at relatively low yields. Furthermore, the stability of many of these antibody fragments still relies on stabilizing intradomain disulfide bonds which do not form in the reducing intracellular environment of the cell which might represent a bottleneck for some applications. Additionally, many antibodies or antibody fragments have unfavorable biophysical properties, resulting for example in aggregation or low stability, even though the most advanced antibodies are great clinical successes.

2.2 Non-immunoglobulin scaffolds

Due to the advances in protein engineering and the availability of selection technologies, binding proteins based on non-immunoglobulin scaffolds have become an appealing alternative to overcome the above-mentioned limitations of antibodies and antibody fragments. Preferentially such alternative scaffolds are small single-chain proteins, not containing disulfide bonds or free cysteines, while retaining the advantageous properties of antibodies, such as specific high affinity binding. Additionally, they should have favorable biophysical properties such as being monomeric in solution, highly soluble, thermodynamically stable and fast folding, altogether facilitating high expression levels. Numerous alternative scaffolds have been investigated and are discussed in detail in ref. 1.

DARPins comprise a recently established novel class of such non-immunoglobulin binding proteins, which rely on the modularity of repeat proteins[4,5]. Here, consensus design based on the sequence and structure analysis of natural ankyrin repeat proteins allows the discrimination of framework residues, which are important for stability of the scaffold and potential target interaction residues suitable to introduce the needed diversity. The resulting designed ankyrin repeat modules, composed of 33 amino acids (of which seven are randomized), were used to create combinatorial libraries of DARPins of different sizes. Most of the members of such DARPin libraries have very favorable biophysical properties[5] and specific binders with high affinities have been selected against a broad range of target proteins by using ribosome display[6-10]. My thesis describes the development of a new selection technology for designed ankyrin repeat proteins (DARPins) that allows selection conditions complementary to ribosome display.

3. Selection technologies

Natural evolution is based on consecutive rounds of diversification, selection of the fittest and amplification. A prerequisite for evolution is that the inheritable information is tightly linked to the functional principle and not mixed with competing individuals. This linkage allows the

genetic information (genotype) of each individual to be translated into its phenotype on which the selection pressure is applied, leading over several consecutive cycles to the enrichment of the fittest[11]. The linkage of phenotype and genotype is fundamental to all evolution processes and can be mimicked in the test tube for the directed evolution of proteins with desired properties. The key features of directed evolution are a genotypically diverse starting population (e.g. a combinatorial library, see above), a selection technology that allows the coupling of the genotype (i.e. the DNA encoding the displayed protein) and the phenotype (i.e. the displayed protein), a selection pressure and an amplification process. Different selection technologies use different strategies to achieve this linkage[1,12]. The success of every selection technology depends on the compatibility of the strategy used with the proteins to be displayed.

3.1 Phage display

Phage display[13] was the first display technology developed and is still the most widely used platform for the directed evolution of polypeptides. The protein (phenotype) is displayed on the surface of a phage particle while the respective DNA (genotype) is encapsulated inside[14,15]. Typically, filamentous bacteriophages that infect *Escherichia coli* (e.g. f1/M13/fd) are used for the display of foreign proteins. The power of phage display lies in the high stability of this linkage and the robustness of the phage particle itself, which allows selections to be performed under a wide range of conditions, including high temperature and in the presence of denaturants. The limiting factor of this selection technology is the involvement of an *in vivo* step. Bacterial transformation practically limits the library size to less than 10^{11} members and the *in vivo* assembly of the phage particle is not compatible with all proteins to be displayed (e.g. successful translocation of the protein to the periplasm and lack of aggregation in the periplasm is a prerequisite). Additionally, affinity maturation which involves cycles of randomization and library reconstruction is very unattractive due to the laborious transformation step. A scheme of the selection cycle is depicted in **Figure 1**. Other phages such as lambda or T7 that assemble intracellularly have been used for the display of proteins but most of them were not yet

investigated for library applications. In my thesis, the development of a new selection technology called “SRP phage display” is described. It expands the range of proteins amenable to phage display by allowing the display of fast folding and stable proteins such as DARPins that are refractory to conventional phage display.

3.2 Complete *in vitro* selection technologies

To overcome the limitations caused by the involvement of living cells, complete *in vitro* display technologies[16] have been developed of which most rely on the formation of a complex of the display scaffold and its encoding gene. Ribosome display, for example, is based on the formation of a non-covalent ternary complex of mRNA, ribosome and the displayed nascent polypeptide[17]. The formation of this ternary complex by *in vitro* translation allows the sampling of very large libraries, but due to its relatively low stability, the linkage of the genotype and the phenotype is only reliably maintained under non-denaturing buffer conditions at low temperature. The high sensitivity of the system to RNases additionally restricts the selection conditions applicable. A clear bonus of ribosome display is the built-in affinity maturation process, coming from the spontaneous mutations introduced during DNA amplification. The ease of increasing the mutations during the selection cycle by error-prone PCR makes this display technology a very powerful tool for affinity maturation of binding proteins. A scheme of the selection cycle is depicted in **Figure 2**. Ribosome display has been successfully used to select specific binders with high affinities from libraries of DARPins[6-10].

3.3 Cell surface display

Display on microbial cell surfaces exists for a variety of hosts and uses a variety of surface proteins for membrane anchoring[18]. For example, the affinity maturation of a fluorescein binding scFv antibody fragment by screening randomly mutagenized libraries of 10^5-10^7 yeast surface-displayed molecules enabled the isolation of clones with femtomolar antigen-binding affinity[19]. However, many of these systems have not yet been used in combination with highly diverse

naive libraries mainly due to the very low transformation efficiencies for most of the used host strains. One recent very promising approach is based on the anchoring of the display scaffold in the periplasmic membrane of *E. coli*, followed by disruption of the outer membrane, incubation with fluorescently labelled target protein and sorting of the spheroblasts[20]. This approach should allow libraries with sizes as large as for phage display to be generated. An extension of this system allows the functional display of full-length antibody libraries followed by the efficient selection of binders[3].

3.4 Other selection technologies

A broad range of complete *in vivo* selection technologies that are based on the reconstitution of a protein activity upon binder-target interaction (e.g. enzymatic or transcriptional) have been described. Examples, therefore, are the protein fragment complementation assay (PCA)[21] or yeast two-hybrid systems[22]. In all these systems, the interactions occur *in vivo* and the precise selection conditions are difficult to control. Display on microbeads by *in vitro* compartmentalization in the aqueous droplets of a water-in-oil emulsion[23] or protein-DNA linkage[24] are other methods that have been used as selection technologies.

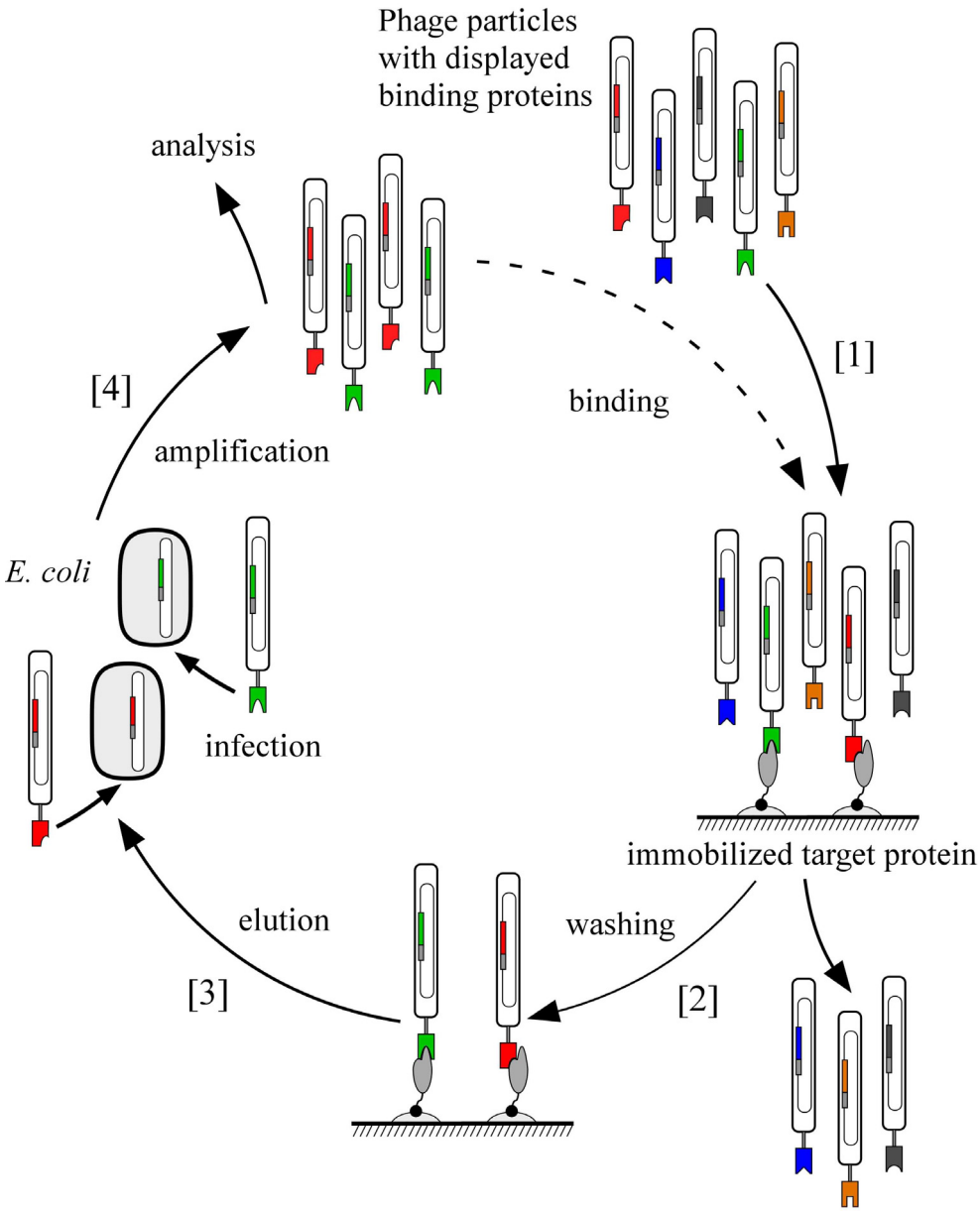

Figure 1: Schematic representation of a phage display selection cycle. A phage library displaying variants of the protein of interest on the surface while having the respective gene encapsulated inside the phage particle is used for the binding selection on the immobilized target [1]. After formation of the complexes between the binding protein and the target protein, unbound phage particles are washed away [2]. The bound phages are eluted from the immobilized target by a pH shift [3] and used for the infection of *E. coli*. Phage particles are amplified [4] and can then be analyzed or used as input for the next selection round.

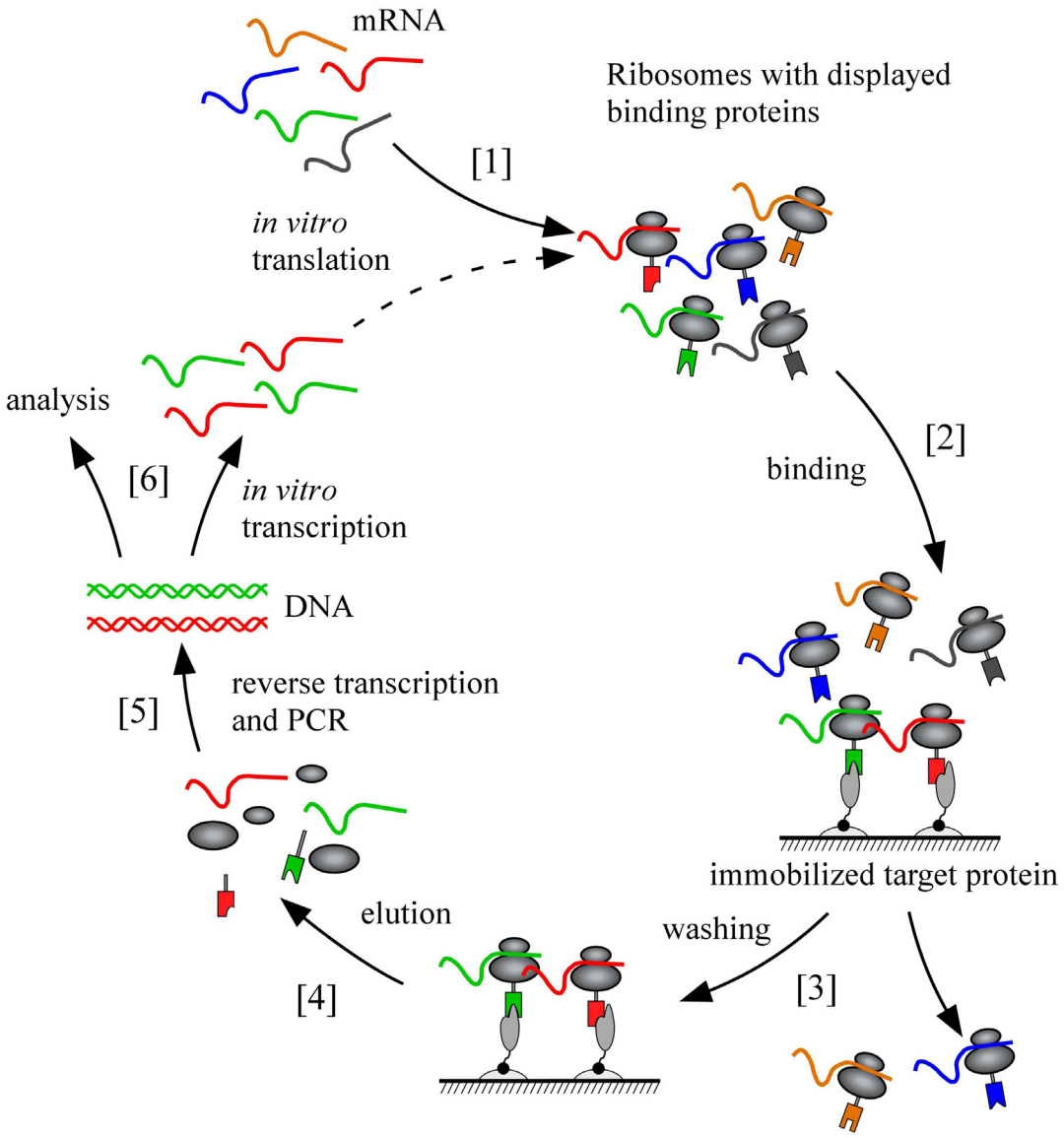

Figure 2: Schematic representation of a ribosome display selection cycle. An mRNA library encoding the proteins of interest without stop codon is translated *in vitro* [1]. After cooling, the translation yields stable ternary complexes of mRNA, ribosomes and nascent polypeptides. These complexes are used for the binding selection on the immobilized target [2]. After binding of the polypeptides to the target protein, unbound complexes are washed away [3]. The mRNA of the bound complex is eluted by dissociating the ribosomal complex with EDTA [4]. A reverse transcription reaction followed by PCR yields the genetic information of the selected clones [5]. The amplified genes can then be used as input for the next selection round starting with *in vitro* transcription [6] or cloned into plasmids for analysis.

4. The Project

As outlined above, the success of any directed evolution experiment (the "selection") depends on the compatibility of the selection technology used with the protein to be displayed (the "display scaffold"). This is crucial, since only functionally displayed library members will be accessible to the selection process and thereby contribute to the probability of finding individuals with the desired properties. In general, the larger the number of functionally displayed library members, the higher the probability to isolate diverse binders against a given target protein and the higher the affinities of the selected binders[25].

In my thesis, the development of a new selection technology called SRP phage display is described (**Chapter 2**, ref. 26). This technology expands the range of proteins amenable to display on filamentous phage particle by allowing the display of fast folding and stable proteins such as DARPins which are refractory to conventional phage display. In SRP phage display, the proteins to be displayed are directed to the *E. coli* cotranslational signal recognition particle (SRP) translocation pathway[27] by using an appropriate signal sequence, whereas conventional phage display uses the posttranslational Sec translocation pathway[28]. This simple change in the use of the translocation route seems to prevent premature folding of stable and fast folding proteins in the cytoplasm and therefore allows their efficient translocation and subsequent display on filamentous phage particles. The applicability of the system was shown for a broad set of proteins and different signal sequences.

Subsequently I investigated the potential of the developed display technology for library applications. We constructed a large phage DARPin library based on SRP phage display and performed selections on a panel of target proteins followed by the analysis of the thereby selected DARPins (**Chapter 3** and **Chapter 4**, ref. 29). The successful selection of high affinity binders against a broad range of target proteins supports the strength of SRP phage display and also underscores the excellent quality of the current phage DARPin library.

5. References

1. Binz, H.K., Amstutz, P. & Plückthun, A. Engineering novel binding proteins from nonimmunoglobulin domains. *Nat. Biotechnol.* **23**, 1257-1268 (2005).
2. Bradbury, A.R. & Marks, J.D. Antibodies from phage antibody libraries. *J. Immunol. Methods* **290**, 29-49 (2004).
3. Mazor, Y., Blarcom, T.V., Mabry, R., Iverson, B.L. & Georgiou, G. Isolation of engineered, full-length antibodies from libraries expressed in Escherichia coli. **25**, 563-565 (2007).
4. Forrer, P., Stumpp, M.T., Binz, H.K. & Plückthun, A. A novel strategy to design binding molecules harnessing the modular nature of repeat proteins. *FEBS Lett.* **539**, 2-6 (2003).
5. Binz, H.K., Stumpp, M.T., Forrer, P., Amstutz, P. & Plückthun, A. Designing repeat proteins: Well-expressed, soluble and stable proteins from combinatorial libraries of consensus ankyrin repeat proteins. *J. Mol. Biol.* **332**, 489-503 (2003).
6. Binz, H.K., Amstutz, P., Kohl, A., Stumpp, M.T., Briand, C., Forrer, P., Grütter, M.G. & Plückthun, A. High-affinity binders selected from designed ankyrin repeat protein libraries. *Nat. Biotechnol.* **22**, 575-582 (2004).
7. Amstutz, P., Binz, H.K., Parizek, P., Stumpp, M.T., Kohl, A., Grütter, M.G., Forrer, P. & Plückthun, A. Intracellular kinase inhibitors selected from combinatorial libraries of designed ankyrin repeat proteins. *J. Biol. Chem.* **280**, 24715-24722 (2005).
8. Amstutz, P., Koch, H., Binz, H.K., Deuber, S.A. & Plückthun, A. Rapid selection of specific MAP kinase-binders from designed ankyrin repeat protein libraries. *Protein Eng. Des. Sel.* **19**, 219-229 (2006).
9. Kawe, M., Forrer, P., Amstutz, P. & Plückthun, A. Isolation of Intracellular Proteinase Inhibitors Derived from Designed Ankyrin Repeat Proteins by Genetic Screening. *J. Biol. Chem.* **281**, 40252-40263 (2006).
10. Zahnd, C., Pecorari, F., Straumann, N., Wyler, E. & Plückthun, A. Selection and Characterization of Her2 Binding-Designed Ankyrin Repeat Proteins. *J. Biol. Chem.* **281**, 35167-35175 (2006).
11. Matsuura, T. & Yomo, T. In vitro evolution of proteins. *Journal of Bioscience and Bioengineering* **101**, 449-456 (2006).
12. Hoogenboom, H.R. Selecting and screening recombinant antibody libraries. *Nat. Biotechnol.* **23**, 1105-1116 (2005).
13. Smith, G.P. Filamentous fusion phage: novel expression vectors that display cloned antigens on the virion surface. *Science* **228**, 1315-1317 (1985).
14. Hoogenboom, H.R. Overview of antibody phage-display technology and its applications. *Methods Mol. Biol.* **178**, 1-37 (2002).
15. Smith, G.P. & Petrenko, V.A. Phage Display. *Chem. Rev.* **97**, 391-410 (1997).
16. Amstutz, P., Forrer, P., Zahnd, C. & Plückthun, A. In vitro display technologies: novel developments and applications. *Curr. Opin. Biotechnol.* **12**, 400-405 (2001).
17. Zahnd, C., Amstutz, P. & Plückthun, A. Ribosome display: selecting and evolving proteins in vitro that specifically bind to a target. **4**, 269-279 (2007).
18. Lee, S.Y., Choi, J.H. & Xu, Z. Microbial cell-surface display. *Trends Biotechnol.* **21**, 45-52 (2003).
19. Boder, E.T., Midelfort, K.S. & Wittrup, K.D. Directed evolution of antibody fragments with monovalent femtomolar antigen-binding affinity. *Proc. Natl. Acad. Sci. U. S. A.* **97**, 10701-10705 (2000).
20. Harvey, B.R., Georgiou, G., Hayhurst, A., Jeong, K.J., Iverson, B.L. & Rogers, G.K. Anchored periplasmic expression, a versatile technology for the isolation of high-affinity antibodies from Escherichia coli-expressed libraries. *Proc. Natl. Acad. Sci. U. S. A.* **101**, 9193-9198 (2004).

21. Mössner, E., Koch, H. & Plückthun, A. Fast selection of antibodies without antigen purification: adaptation of the protein fragment complementation assay to select antigen-antibody pairs. *J. Mol. Biol.* **308**, 115-122. (2001).
22. Visintin, M., Settanni, G., Maritan, A., Graziosi, S., Marks, J.D. & Cattaneo, A. The intracellular antibody capture technology (IACT): towards a consensus sequence for intracellular antibodies. *J. Mol. Biol.* **317**, 73-83. (2002).
23. Sepp, A., Tawfik, D.S. & Griffiths, A.D. Microbead display by in vitro compartmentalisation: selection for binding using flow cytometry. *FEBS Lett.* **532**, 455-458 (2002).
24. Odegrip, R., Coomber, D., Eldridge, B., Hederer, R., Kuhlman, P.A., Ullman, C., FitzGerald, K. & McGregor, D. CIS display: In vitro selection of peptides from libraries of protein-DNA complexes. *Proc. Natl. Acad. Sci. U. S. A.* **101**, 2806-2810 (2004).
25. Ling, M.M. Large antibody display libraries for isolation of high-affinity antibodies. *Comb Chem High Throughput Screen* **6**, 421-432 (2003).
26. Steiner, D., Forrer, P., Stumpp, M.T. & Plückthun, A. Signal sequences directing cotranslational translocation expand the range of proteins amenable to phage display. *Nat. Biotechnol.* **24**, 823-831 (2006).
27. Luirink, J. & Sinning, I. SRP-mediated protein targeting: structure and function revisited. *Biochim. Biophys. Acta* **1694**, 17-35 (2004).
28. Fekkes, P. & Driessen, A.J. Protein targeting to the bacterial cytoplasmic membrane. *Microbiol. Mol. Biol. Rev.* **63**, 161-173 (1999).
29. Huber, T., Steiner, D., Röthlisberger, D. & Plückthun, A. In vitro selection and characterization of DARPins and Fab fragments for the co-crystallization of membrane proteins: The Na^+-citrate symporter CitS as an example. *J. Struct. Biol.* **159**, 206-221 (2007).

Chapter 2

Expanding the range of proteins amenable to phage display with signal sequences directing cotranslational translocation

Steiner, D., Forrer, P., Stumpp, M.T. & Plückthun, A. (2006)

Nat. Biotechnol. **24**, 823-831.

Contents

ARTICLES

nature biotechnology

Signal sequences directing cotranslational translocation expand the range of proteins amenable to phage display

Daniel Steiner[1], Patrik Forrer[1,2], Michael T Stumpp[1,2] & Andreas Plückthun[1]

Even proteins that fold well in bacteria are frequently displayed poorly on filamentous phages. Low protein presentation on phage might be caused by premature cytoplasmic folding, leading to inefficient translocation into the periplasm. As translocation is an intermediate step in phage assembly, we tested the display levels of a range of proteins using different translocation pathways by employing different signal sequences. Directing proteins to the cotranslational signal recognition particle (SRP) translocation pathway resulted in much higher display levels than directing them to the conventional post-translational Sec translocation pathway. For example, the display levels of designed ankyrin-repeat proteins (DARPins) were improved up to 700-fold by simply exchanging Sec- for SRP-dependent signal sequences. In model experiments this exchange of signal sequences improved phage display from tenfold enrichment to >1,000-fold enrichment per phage display selection round. We named this method 'SRP phage display' and envision broad applicability, especially when displaying cDNA libraries or very stable and fast-folding proteins from libraries of alternative scaffolds.

Phage display is an *in vitro* selection method that allows polypeptides with desired properties to be extracted from large collections of variants[1,2]. Most commonly, filamentous phages, such as f1, M13 and fd, that infect *Escherichia coli* are used for phage display. Filamentous phages have been intensively investigated for the selection of peptides or antibodies with desired properties from combinatorial libraries[3,4]. Although the major coat protein (protein-8, p8) of the filamentous phage M13, present at ~2,700 copies, and all four minor M13 coat proteins (p3, p6, p7, p9), present at ~5 copies each, have been used for display[2], fusions with p3 have been used most frequently. The peptide or protein of interest (POI) to be displayed is placed between an N-terminal signal sequence and either the whole mature p3 or its C-terminal domain. The POI fused to p3 is translocated into the periplasm by the *E. coli* translocation system while remaining anchored to the cytoplasmic membrane by the C-terminal hydrophobic extension of p3. Upon completion of the extrusion of the phage particle, the p3 fusion protein is incorporated into the tip of the phage coat in a complex with p6 (ref. 5).

Many intra- or extracellular proteins with different sizes and structures have been functionally displayed on filamentous phage[2]. Nevertheless, numerous proteins are only poorly selected from phage display libraries, because they are displayed with very low efficiency or are refractory to display[6]. There are many reasons why a POI might fail to be displayed[6]; for example, (i) the POI can aggregate in the periplasm[7,8] or cytoplasm, sometimes resulting in *E. coli* lysis[9]; (ii) certain disulfide-containing proteins are displayed at lower levels than their nondisulfide-containing counterparts, presumably because of inefficient folding as a result of nonnative disulfide bond formation[10]; (iii) the POI can be refractory to translocation into the periplasm because of incompatibility of local sequence stretches with translocation[11] and (iv) the POI or the linking peptide to p3 can be degraded by periplasmic or cytoplasmic proteases.

Various attempts have been made to circumvent poor display. The host-cell toxicity of the p3 fusion protein can be limited when its expression is reduced[12]. Periplasmic folding of the POI has been improved when phage display vectors coexpressing the periplasmic chaperones Skp[13] or FkpA[14] have been employed. In phagemid/helper phage systems[2], wild-type p3 and the fusion protein compete for incorporation into the phage particles. Therefore, to improve display levels in these phagemid systems, different helper phages have been engineered that encode either no wild-type p3, or defective or proteolysis-sensitive p3 variants[15–18]. Interestingly, the display level of the Stoffel fragment of *Taq* DNA polymerase (*Taq*) was improved by partial randomization of the signal sequence of *Erwinia carotovora* pectate lyase PelB (PelBss) and subsequent selection for increased display, but the mechanism of the improvement was not investigated[18].

Despite these numerous improvements in phage display, many proteins still display poorly[2,6]. DARPins[19,20], which have been successfully selected by ribosome display for specific binding to different target proteins from corresponding combinatorial libraries[21,22], were virtually refractory to display on filamentous phage using a standard phagemid. DARPins have no cysteines, can be expressed in soluble form with high yields in the cytoplasm of *E. coli*, show high thermodynamic stability[20] and fast cooperative folding (S. Wetzel & A.P., unpublished data), and are very resistant to proteolysis (H.K. Binz & A.P., unpublished data). We therefore reasoned that premature cytoplasmic folding of DARPins, and proteins with similar properties,

[1]Department of Biochemistry, University of Zürich, Winterthurerstrasse 190, 8057 Zürich, Switzerland. [2]Molecular Partners AG, c/o Department of Biochemistry, University of Zürich, Winterthurerstrasse 190, 8057 Zürich, Switzerland. Correspondence should be addressed to A.P. (plueckthun@bioc.unizh.ch).

Received 30 November 2005; accepted 12 May 2006; published online 2 July 2006; doi:10.1038/nbt1218

ARTICLES

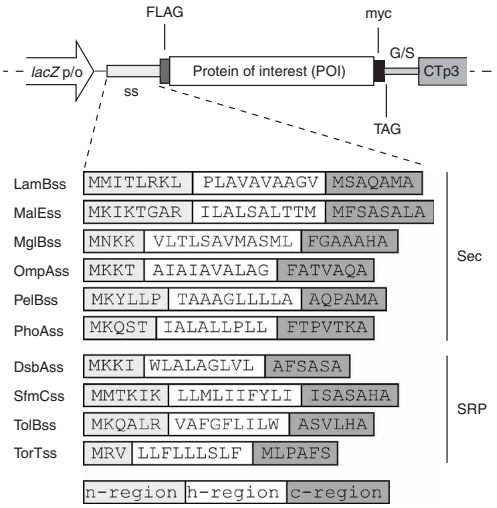

Figure 1 Scheme of the expression cassette of the pDST phagemid vector series. The expression cassette is composed of a promoter/operator element of the *lacZ* gene of *E. coli* (*lacZ* p/o), the coding sequences for the signal sequence (ss) and a protein of interest (POI) to be displayed, a suppressable stop codon (TAG), the coding sequences for a flexible glycine/serine linker (G/S) and for the C-terminal domain (amino acids 250–406) of protein 3 of filamentous phage M13 (CTp3), mediating incorporation of the fusion protein into the phage particle, two stop codons (TGATAA, not depicted) and a transcription terminator element (not depicted). The coding sequence of the POI is flanked by DNA sequences encoding a FLAG-tag (FLAG) and a myc-tag (myc). Shown are the single letter amino acid sequences for the LamB signal sequence (LamBss), the MalE signal sequence (MalEss), the MglB signal sequence (MglBss), the OmpA signal sequence (OmpAss), the PelB signal sequence (PelBss) and the PhoA signal sequence (PhoAss) as representatives of signal sequences targeting the Sec pathway (Sec), and for the DsbA signal sequence (DsbAss), the TorT signal sequence (TorTss), the SfmC signal sequence (SfmCss) and the TolB signal sequence (TolBss) as representatives of signal sequences targeting the SRP pathway (SRP). The positively charged N-terminal region (n-region), the apolar hydrophobic core and the more polar C-terminal region (c-region) of the signal sequences are highlighted. They were assigned by the method described[49], as implemented on the website http://www.cbs.dtu.dk/services/SignalP/. It should be noted that the Sec dependence of PelBss is only putative.

might result in their inefficient translocation into the periplasm and, as a consequence their poor display levels.

Three major pathways[23] are known for the translocation of polypeptides across the cytoplasmic membrane into the periplasm of Gram-negative bacteria: the Sec pathway[23], the signal recognition particle (SRP) pathway[24–26] and the Tat pathway[27,28]. The respective signal sequences strongly favor the targeting of proteins to one of these pathways. The Sec pathway translocates polypeptides post-translationally, whereas the SRP pathway translocates polypeptides cotranslationally. These two pathways converge at the Sec translocon, which transports the polypeptides in an unfolded state across the cytoplasmic membrane. In contrast to these two pathways, the Tat pathway translocates only folded proteins post-translationally through the Tat translocon.

The majority of secreted *E. coli* proteins and phage p3 (ref. 29) use the Sec-dependent translocation pathway. In early phage display experiments using well-secreted proteins, such as antibody fragments, the translocation or display levels showed no major systematic dependence on the signal sequence used, but the only signal sequences tested were Sec dependent[30]. Consequently, bacterial Sec-dependent translocation signal sequences, such as those from PhoA or OmpA, have been used predominantly in phage display.

The Sec pathway can transport only polypeptides that are kept in an unfolded conformation, either by intrinsic features of the protein or by the specialized cytoplasmic chaperone SecB, and perhaps other cytoplasmic chaperones[27]. Therefore, this pathway is inherently incapable of translocating proteins that do not remain in an unfolded state in the cytoplasm. We reasoned that such inefficient translocation could also lead to inefficient display, thus rendering phage display selections very inefficient or even impossible for proteins that fold prematurely in the cytoplasm.

Indeed, the rapidly folding cytoplasmic protein thioredoxin can be translocated into the periplasm only at very low yields using the Sec-dependent PhoA signal sequence (PhoAss)[31]. However, the signal sequence of DsbA (DsbAss) efficiently allowed the translocation of this rapidly folding protein into the periplasm[32]. It has been shown[33] that the reason for this effect is that DsbAss directs the fused protein to the cotranslational SRP pathway, thereby obviating inhibitory effects of cytoplasmic protein-folding on translocation.

We found that DsbAss and other signal sequences that engage the SRP pathway allow the efficient display of DARPins on filamentous phage, and strongly improve the display levels of a range of other proteins. No negative effects of the SRP-directing signal sequences were observed, suggesting that this method, termed SRP phage display, is generally applicable to expand the range of proteins that can be efficiently displayed on filamentous bacteriophage.

RESULTS

Phagemids with Sec- or SRP-type signal sequences

To test whether cotranslational translocation mediated by the SRP pathway would improve display of proteins on filamentous phage particles, compared to the post-translational translocation using the Sec pathway, we constructed two phagemid series, which are identical except for the signal sequence. They contained either the signal sequence of *E. coli* PhoA (PhoAss), directing the p3 fusion proteins to be displayed to the post-translational Sec pathway, or the signal sequence of *E. coli* DsbA (DsbAss)[33], directing the p3 fusion proteins to be displayed to the cotranslational SRP pathway. All further elements of the phagemids and their expression cassettes are described in detail in **Figure 1** and **Supplementary Figure 1** online. To test the applicability of the SRP translocation pathway for phage display, we cloned genes encoding a range of proteins into both phagemids (**Table 1**).

Increased display yields using DsbAss

The display yields of p3 fusion proteins on phage particles were compared between phage particles produced from phagemids differing only in the signal sequence (PhoAss versus DsbAss). Phage particles were purified by CsCl-gradient centrifugation, and the display yields were analyzed by western blot analysis (**Fig. 2a**,**b**). A single-chain Fv antibody (scFv) showed about the same display yield, independent of the signal sequence used. In stark contrast, all four DARPins tested could be efficiently displayed only when using the DsbAss-containing phagemids; when using the PhoAss-containing phagemids, we could not detect displayed protein for the nonbinding DARPin E3_5 (unselected DARPin, without target specificity)[20] or only very low amounts for the other DARPins tested.

To test the scope of this increased display, we compared several other proteins with the DsbAss and PhoAss. The use of

Table 1 Description of proteins tested for display on the surface of filamentous bacteriophage

Protein	Abbr.	Phagemid PhoAss	Phagemid DsbAss	Description[a]	Acc. no.[b], references
scFv_gpD	scFv	pDST24	pDST31	E1 - T245 of single-chain Fv binding to gpD	unpublished
DARPin 3a	3a	pDST22	pDST23	D13 - Q166 of DARPin 3a binding to APH	ref. 22
DARPin JNK2_2_3	2_3	pDST34	pDST37	D13 - Q133 of DARPin JNK2_2_3 binding to JNK2	ref. 21
DARPin E3_5	E3_5	pDST30	pDST32	D13 - Q166 of nonbinding DARPin E3_5	GB: AAO25689, ref. 20
DARPin E3_19	E3_19	pDST65	pDST66	D13 - Q166 of nonbinding DARPin E3_19	GB: AAO25690, ref. 20
GCN4	GCN4	pDST39	pDST40	GCN4 derivative (RMKQLEDKVELLPKNYHLENEVARLKKLVGER)	SP: P03069
pDΔN2	gpD	pDST41	pDST42	T21 - V110 of the capsid stabilizing protein of bacteriophage λ	SP: P03712
JNK2α2	JNK2	pDST45	pDST46	S2 - R424 of c-jun N-terminal kinase 2 (JNK2α2)	SP: P45984
TrxA	TrxA	pDST47	pDST48	S1 - A108 of thioredoxin (*trxA* gene of *E. coli*)	SP: P00274
Taq polymerase	*Taq*	pDST51	pDST52	S290 - E832 Stoffel fragment of *Taq* DNA polymerase	SP: P19821
λ-phosphatase	λPP	pDST53	pDST54	M1 - A221 of bacteriophage λ Ser/Thr protein-phosphatase	SP: P03772
APH	APH	pDST55	pDST56	A2 - F264 of aminoglycoside phosphotransferase (C19S, C156S, S194C)	SP: P0A3Y5

[a]The first and last amino acid used are indicated in single letter amino acid code. [b]Accession numbers: GB, GenBank; SP, Swiss-Prot. DARPin, designed ankyrin-repeat protein; DsbAss, DsbA signal sequence; PhoAss, PhoA signal sequence; scFv, single-chain Fv antibody fragment.

DsbAss-containing phagemids resulted in considerably higher display yields for p3 fusions with the phage λ coat protein D (gpD)[34], thioredoxin (TrxA) and aminoglycoside phosphotransferase IIIa (APH). Slightly higher display yields were observed with the DsbAss for the leucine zipper region of GCN4, *Taq* and the bacteriophage λ protein-phosphatase (λPP). In every case tested to date the display level was either maintained or increased by switching from PhoAss to DsbAss. Displayed c-jun N-terminal kinase 2α2 (JNK2) could not be detected with either signal sequence, suggesting that for this protein, lack of display is not due to premature folding (see below). These results demonstrate that the SRP-dependent DsbAss strongly increased display levels of p3 fusion proteins on phage particles for most polypeptides tested.

To quantify the protein display yields (**Fig. 3**), we analyzed phage particles displaying the target-specific APH-binding DARPin 3a or the JNK2-binding DARPin 2_3 (refs. 21,22) by enzyme-linked immunosorbent assay of phage (phage ELISA) (**Fig. 3a**). Phage particles displaying DARPins specifically binding to the target proteins APH and JNK2 were compared after production under identical conditions from either DsbAss-containing phagemids or PhoAss-containing phagemids. Based on the detection of bound phage particles with an anti-M13 antibody, an increased display yield of up to 600-fold was observed when the SRP-dependent DsbAss was used (**Fig. 3a,d**).

To exclude any dependence on the *E. coli* strain, we confirmed these results of DsbAss causing improved display yields (obtained in *E. coli* XL1-Blue) with another strain. Thus we tested the genotypically different *E. coli* strain TG1, frequently used in phage display (data not shown; for genotypes and strain references, see **Supplementary Table 1** online).

Faster enrichment when using DsbAss

To demonstrate that the higher display yields obtained by using DsbAss also dramatically improved selection experiments, we mixed two test mixtures containing four different types of phage particles produced from phagemids encoding either DsbAss or PhoAss in various ratios. For both test mixtures, phage particles displaying the target-specific DARPins 3a and 2_3 (binding the proteins APH and JNK2, respectively)[21,22] were spiked at a ratio of 1:10^7 into phage

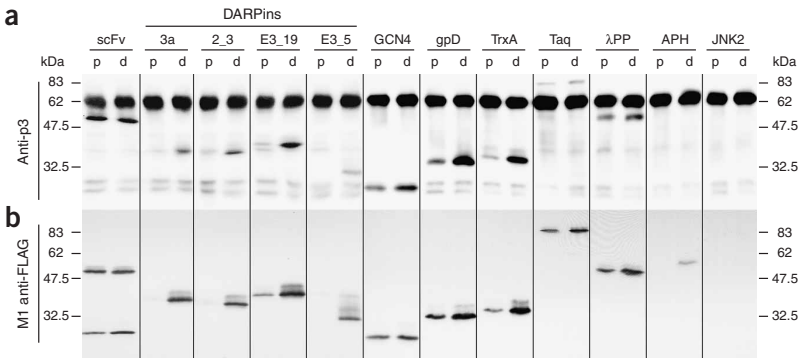

Figure 2 Display yields of the various POIs on phage particles. (**a**,**b**) CsCl-purified phage particles produced by the use of the respective phagemid indicated and normalized by UV absorbance to the same number of phage particles were separated by SDS-PAGE, blotted onto PVDF membranes and detected with antibodies specific for the C-terminal domain of protein 3 (anti-p3) (**a**) or the FLAG-tag (M1 anti-FLAG) located at the N terminus of the POI (**b**). The abbreviated names of the polypeptides are indicated on top of the lanes and refer to the polypeptides listed in **Table 1**. The display yields are compared for each polypeptide using either the PhoA signal sequences (lanes labeled 'p') or the DsbA signal sequence (lanes labeled 'd') translocating the corresponding fusion protein by the Sec pathway or the SRP pathway, respectively. The molecular weights of marker proteins are indicated in kDa at both sides of the blot. The band at 62 kDa in the anti-p3 blot corresponds to wild-type p3 and provides an additional normalization of the amount of phage particles loaded. Wild-type p3 is well known[50] to run at a seemingly higher MW. Note that DARPin E3_5-p3 fusion runs at an apparently lower MW than other DARPin-fusions. This is also observed for this very stable protein in nonfused form, for which mass spectrometry indicated the expected mass, and may indicate incomplete denaturation on the SDS gel, compared to the less stable E3_19 which runs at the expected MW.

ARTICLES

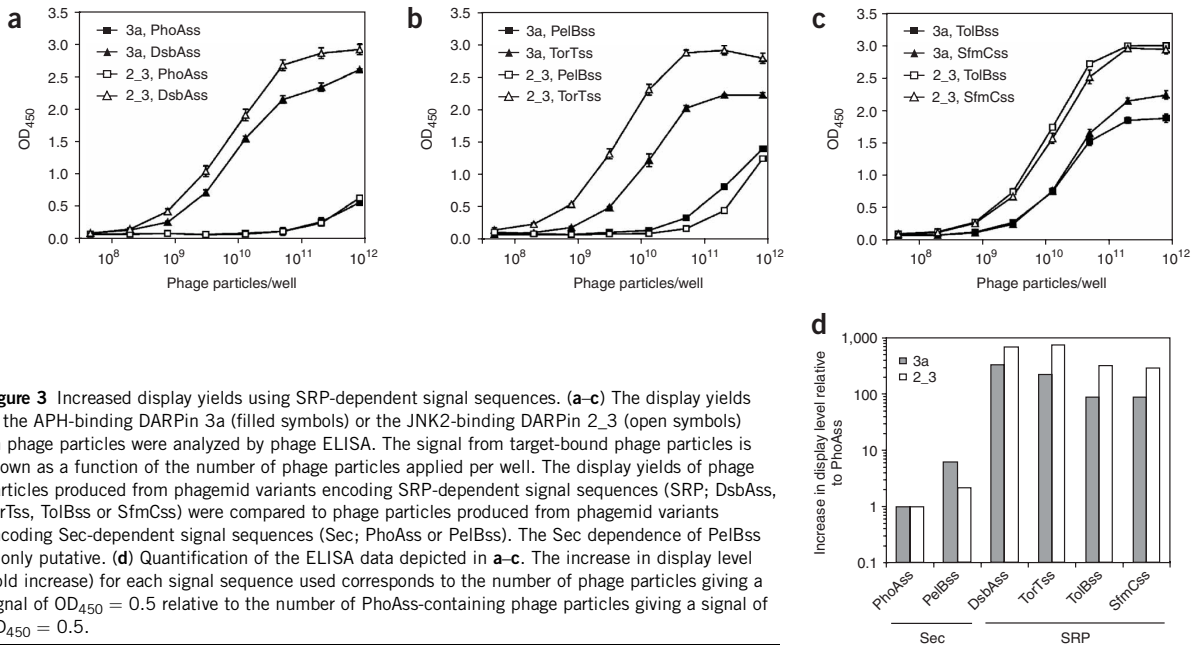

Figure 3 Increased display yields using SRP-dependent signal sequences. (**a**–**c**) The display yields of the APH-binding DARPin 3a (filled symbols) or the JNK2-binding DARPin 2_3 (open symbols) on phage particles were analyzed by phage ELISA. The signal from target-bound phage particles is shown as a function of the number of phage particles applied per well. The display yields of phage particles produced from phagemid variants encoding SRP-dependent signal sequences (SRP; DsbAss, TorTss, TolBss or SfmCss) were compared to phage particles produced from phagemid variants encoding Sec-dependent signal sequences (Sec; PhoAss or PelBss). The Sec dependence of PelBss is only putative. (**d**) Quantification of the ELISA data depicted in **a**–**c**. The increase in display level (fold increase) for each signal sequence used corresponds to the number of phage particles giving a signal of $OD_{450} = 0.5$ relative to the number of PhoAss-containing phage particles giving a signal of $OD_{450} = 0.5$.

particles displaying the nonbinding DARPins E3_5 and E3_19 (unselected DARPins, without target specificity)[20] (**Table 2**). Whereas the APH- and JNK2-specific phage particles could be enriched from the test mixture produced from DsbAss-encoding phagemids by a factor of more than 1,000 per selection cycle (>10% of the tested clones were specific for their target after only two cycles of selection, as determined by PCR with clone-specific primers), the corresponding PhoAss-containing APH- and JNK-specific phagemids were not enriched from the test mixture even after five selection cycles (no specific clones were observed). To quantify the enrichment of phage particles produced from phagemids encoding PhoAss, we spiked the phage particles displaying target-specific DARPins at much lower dilution (1:100 and 1:10) into phage particles displaying the nonbinding DARPins E3_5 and E3_19. One cycle of standard phage display selections on the target proteins APH and JNK2 was performed (**Table 2**). The enrichment of APH- and JNK2-specific phage particles from these test mixtures was less than a factor of 10 per cycle for PhoAss, as calculated from the number of specific clones. This observed improvement in enrichment of >100-fold in DsbAss-containing compared to PhoAss-containing phage particles corresponds well to the several hundredfold increased display level observed by western blot analysis (**Fig. 2**) and quantitative ELISA measurements (**Fig. 3a,d**).

Other SRP-type signal sequences increase display

To analyze if the SRP-dependence of the signal sequence is really the key determinant for the observed increased display levels using DsbAss, we tested additional signal sequences known to direct proteins either to the SRP pathway or the Sec pathway. The phagemids encoding the target-specific DARPins 3a and 2_3 (binding APH and JNK2, respectively) were adapted by exchanging the signal sequences. We additionally used the SRP-dependent signal sequences of the *E. coli* proteins TolB (TolBss), SfmC (SfmCss) and TorT (TorTss)[35] (**Fig. 1**). The *E. carotovora* PelB signal sequence (PelBss), which is frequently used in phage display, was also tested and is probably Sec dependent because it lacks a strongly hydrophobic region, a typical feature of SRP-dependent signal sequences[35]. To quantify the difference in display levels, the corresponding phage particles were analyzed by phage ELISA (**Fig. 3b–d**) as described above. An increased display yield of up to 700-fold was observed for the SRP-dependent TorTss, compared to the Sec-dependent PhoAss. The SRP-dependent SfmCss and TolBss gave an increased display yield up to 300-fold. The putative Sec-dependent PelBss showed only a two- to sixfold increased display yield, compared to PhoAss. For all SRP-dependent signal sequences the ELISA readings obtained for phages displaying

Table 2 Enrichment of phages displaying target-specific DARPins[a]

			Round of phage selection (positive colonies/number of colonies tested)[b]				
Signal seq. of phagemid	Dilution	Antigen	1st	2nd	3rd	4th	5th
DsbAss	$1:10^7$	APH	0/14	4/16	14/14	–	–
		JNK2	0/14	2/16	14/14	–	–
PhoAss	$1:10^7$	APH	0/11	0/15	0/14	–	0/9
		JNK2	0/14	0/16	0/14	–	0/11
	$1:10^2$	APH	2/16	–	–	–	–
		JNK2	1/16	–	–	–	–
	$1:10^1$	APH	4/16	–	–	–	–
		JNK2	7/16	–	–	–	–

[a]Input mixtures produced from phagemids encoding either PhoAss or DsbAss were produced as described in Methods. To a 1:1 mixture of phage particles displaying the nonbinding DARPins E3_5 and E3_19, phage particles displaying the target-specific DARPins 3a (recognizing APH) or 2_3 (recognizing JNK2) were added in a $1:10^7$ dilution for both mixtures and, additionally, in 1:100 and 1:10 dilutions for the mixtures generated from phagemids encoding the PhoAss. [b]Colonies were screened by PCR using primers specific for the DARPins 3a or 2_3.

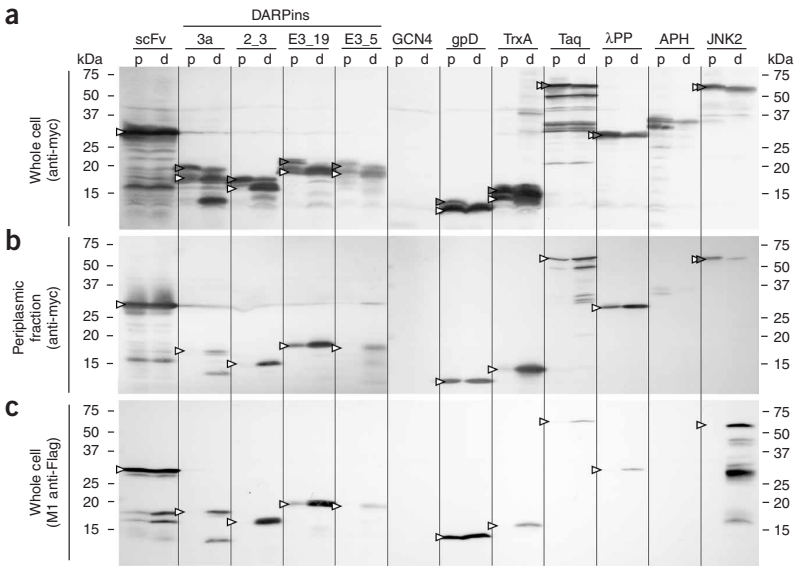

Figure 4 Protein translation and translocation of the various unfused POIs to the periplasm. (**a**–**c**) Whole cell and periplasmic extracts from nonsuppressor *E. coli* JM83 cells, harboring the respective phagemid and normalized to the same amount of cells, were separated by SDS-PAGE, blotted onto PVDF membranes and detected with antibodies specific for the C-terminal myc-tag (anti-myc) (**a**,**b**) and the N-terminal FLAG-tag (M1 anti-FLAG) (**c**). The anti-FLAG antibody M1 selectively recognizes the N-terminal FLAG-tag of the processed, mature POI (**Fig. 1**) having a freely accessible α-amino group. The protein translation and translocation yields are compared for each polypeptide using either the PhoA signal sequence (lanes labeled 'p') or the DsbA signal sequence (lanes labeled 'd') to translocate the corresponding protein by the Sec pathway or the SRP pathway, respectively. The abbreviated names of the polypeptides are indicated on top of the lanes and refer to the polypeptides listed in **Table 1**; for all other abbreviations see **Figure 2**. Mature protein (open triangles) and precursor protein (closed triangles) are indicated where possible. The degradation products of JNK2 detected with the anti-FLAG antibody M1 in whole cell extracts (**c**) could not be detected in the periplasmic fraction with the same antibody (data not shown), suggesting that the degradation products are insoluble and pelleted during centrifugation.

the DARPin 3a were always somewhat lower than for the phages displaying the DARPin 2_3.

Periplasmic levels of POIs correlate with display

We further wanted to investigate whether the increased display of these proteins on phage particles correlates with elevated translocation of these proteins to the periplasm and is not just caused by higher cytoplasmic protein translation yields. We therefore expressed the proteins from identical phagemids as used above (**Table 2**) in the nonsuppressor *E. coli* strain JM83. In contrast to the suppressor strain XL1-Blue, which is used for phage production, this nonsuppressor strain prevents read-through of the amber stop codon after the C terminus of the POI (**Fig. 1**). Whole cell extracts or periplasmic fractions were analyzed by western blotting (**Fig. 4**). To determine the total amount of POI, we used the C-terminal myc-tag of the precursor and mature protein for detection. The amount of periplasmically located, mature POI was additionally determined with the anti-FLAG antibody M1 that selectively recognizes the N-terminal FLAG-tag of the mature POI (**Fig. 1**)—precise cleavage of the signal sequence after translocation is required before this antibody can recognize the freely accessible α-amino group as part of the FLAG tag of the mature POI[36].

Detection of mature and precursor protein with the anti-myc antibody showed that the total protein expression of the different POIs is only influenced to a small extent by the signal sequence (**Fig. 4a**). However, the translocation into the periplasm depends directly on the signal sequence (**Fig. 4b**,**c**). As expected, the signals of the periplasmic fractions detected with the anti-myc antibody (**Fig. 4b**) on western blots correlated well with the signals from whole-cell western blots developed with the anti-FLAG antibody M1 (**Fig. 4c**), which detects only mature protein. The mature protein is thus located in the periplasm. Importantly, precursors of several fusion proteins are accumulating in the cytoplasm when using PhoAss, but not when using DsbAss, as seen in the whole cell blots with detection of the C-terminal myc-tag (**Fig. 4a**).

Independent of the signal sequence used, the scFv antibody fragment is well translocated across the cytoplasmic membrane. In stark contrast, all four tested DARPins could be efficiently translocated only when using the DsbAss-containing phagemids, and almost no protein translocation could be detected when using the PhoAss-containing phagemids. In agreement with previous observations[32,33], the expression of TrxA from DsbAss-containing phagemids resulted in considerably higher translocation yields. Only moderately higher translocation yields were observed for *Taq*, phage λ protein-phosphatase (λPP) and phage λ coat protein D (gpD). The unfused zipper region of GCN4 could not be detected in any of the western blots because of its small size. Very low translocation levels were detected for APH. For JNK2α2, only small amounts of protein were detected in the periplasmic fraction with the anti-myc antibody (JNK2, **Fig. 4b**), whereas a number of insoluble degradation products were detected with the anti-FLAG antibody M1 (JNK2, **Fig. 4c**), suggesting that this degradation may lead to low display (**Fig. 2**).

When these results are compared to those in **Figure 2**, a strong correlation between the translocation yields and the display levels of the different POIs is observed.

Other Sec-type signal sequences cause low display

We analyzed additional signal sequences known to direct proteins to the post-translational Sec-dependent translocation pathway. We chose as the proteins to be displayed DARPin E3_5, a protein with very high thermodynamic stability, and TrxA, a protein previously shown to be efficiently translocated only by SRP-dependent signal sequences[35]. The corresponding phagemids were adapted by exchanging the signal sequences to the SRP-dependent signal sequences (TolBss, SfmCss or TorTss), the Sec-dependent signal sequences (LamBss, MalEss, MglBss or OmpAss)[23] or the putative Sec-dependent PelBss (**Fig. 1**). To compare the difference in display levels, we analyzed the corresponding phage particles by western blotting (**Fig. 5a**). For DARPin E3_5 essentially no displayed protein could be detected with any of the

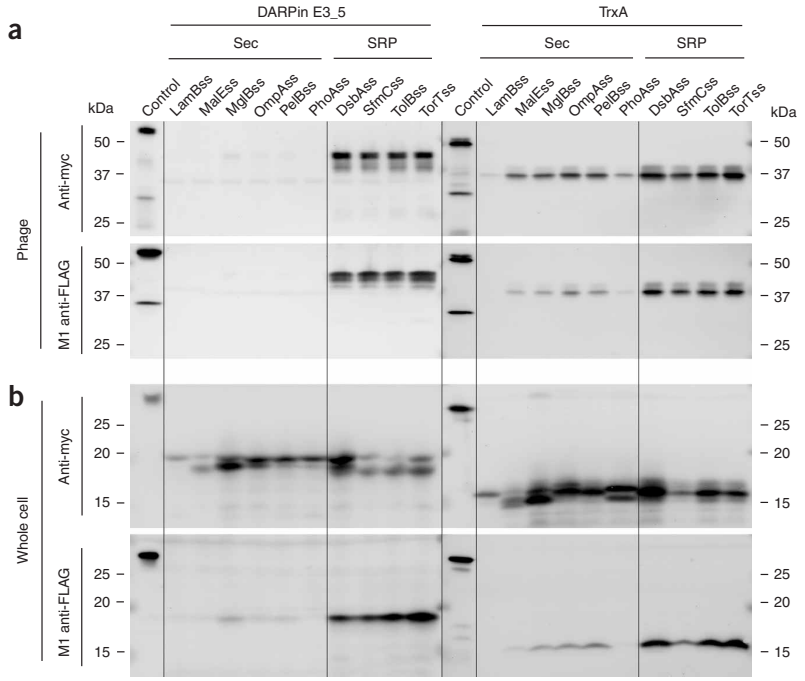

Figure 5 Display yields and periplasmic translocation of DARPin E3_5 and TrxA using various Sec- and SRP-dependent signal sequences. (**a**) Phage particles, produced by the use of the respective phagemid indicated and normalized by UV absorbance to the same number of phage particles, were separated by SDS-PAGE, blotted onto PVDF membranes and detected with antibodies specific for the myc-tag (anti-myc), located at the C terminus of the POI, or the FLAG-tag (M1 anti-FLAG), located at the N terminus of the POI. (**b**) Whole cell extracts from JM83 cells harboring the respective phagemid indicated were analyzed as described for **Fig. 3a**,**c**. The display, protein translation and translocation yields for DARPin E3_5 and TrxA are compared between phagemids encoding Sec-dependent signal sequences (Sec; LamBss, MalEss, MglBss, OmpAss, PelBss or PhoAss) and SRP-dependent signal sequences (SRP; DsbAss, TorTss, TolBss or SfmCss). The Sec dependence of PelBss is only putative. SDS-PAGE of the phage particles produced from phagemids encoding the DARPin E3_5 and whole cell extracts from JM83 cells harboring the phagemids encoding the DARPin E3_5 were run at 60 °C to reduce the partial refolding and therefore smearing of this very stable protein during separation. Control lane: the phagemid encoding the scFv with PhoAss was used as control for western blotting of phage particles or of whole cell extracts.

Sec-dependent signal sequences used, whereas all SRP-dependent signal sequences gave display levels in the same range as found for DsbAss (**Figs. 2** and **5a**). For TrxA the display yields were also considerably higher for all SRP-dependent signal sequences tested than for Sec-dependent signal sequences. However, in contrast to the DARPin E3_5, where almost no displayed protein could be detected for the Sec-dependent signal sequences, TrxA was displayed at moderate levels when using the Sec-dependent MalEss, MglBss and OmpAss and the putative Sec-dependent PelBss, yet substantially lower than with the SRP-dependent signal sequences.

The periplasmic expression yields of the DARPin E3_5 and TrxA correlate well with the display levels observed (**Fig. 5a**,**b**) and are also higher for all SRP-dependent signal sequences than for the Sec-dependent ones. This effect is not caused by increased protein translation (**Fig. 5b**).

DISCUSSION

Some polypeptides are refractory to conventional filamentous phage display because of their individual molecular properties. The reasons have generally not been elucidated[2]. This makes the success of the display of a particular polypeptide unpredictable.

A unique aspect of filamentous phage assembly, in contrast to the assembly of many other bacteriophages, is that it is a secretory process. Incorporation of the coat proteins into the growing phage particle occurs in the cytoplasmic membrane, and nascent phages are extruded from the cell as they assemble[2]. This phage assembly mechanism requires that the POI is translocated across the cytoplasmic membrane into the periplasm to be displayed on the phage particle.

In conventional filamentous phage display, signal sequences directing the POI to the Sec pathway[23] are used for translocation. In this pathway, the polypeptide is first synthesized by the ribosome and then post-translationally translocated, in its unfolded state, by the Sec translocon. This post-translational translocation poses a challenge for keeping the protein in a transport-competent, unfolded state. Transport capability may be achieved by intrinsic features of the polypeptide or by its interaction with the specialized cytoplasmic chaperone SecB and perhaps other cytoplasmic chaperones[27]. However, such mechanisms may not be effective for fast-folding and stable proteins; they may fold prematurely in the cytoplasm making them translocation incompetent.

By merely exchanging the signal sequence targeting the Sec pathway (e.g., LamBss, MalEss, MglBss, OmpAss or PhoAss) by one targeting the SRP pathway (e.g., DsbAss, SfmCss, TolBss and TorTss) in a standard phage display system, we were able to increase the functional display levels for numerous proteins up to 700-fold (**Fig. 3**), resulting in enrichment factors per selection round of more than 1,000 (**Table 2**). This increase of the display levels correlates well with an increase of translocation across the cytoplasmic membrane into the periplasm and is not caused by an overall increase in protein translation (**Fig. 4**).

Similar improvements of periplasmic expression levels when using the SRP pathway instead of the Sec pathway for protein translocation to the periplasm were described with the model protein TrxA[33,35]. Using a total of ten signal sequences, targeting either the Sec or the SRP pathway, we were able to demonstrate in the present study that the improvements in display were indeed a result of the targeted translocation pathway and not caused by individual properties of a particular signal sequence (**Fig. 3**).

For all proteins tested, the display levels on phage particles using SRP-dependent signal sequences were greater than or at least equal to those obtained using the Sec-dependent signal sequences (**Figs. 2** and **5**). This is also true for proteins, such as an scFv-fragment, that are already very well displayed using the conventional Sec-dependent signal sequences. These findings strongly suggest that the use of the cotranslational SRP pathway substantially expands the range of

proteins that can be efficiently displayed on phage particles without having negative effects on already well-displayed proteins.

It is reasonable to assume that cotranslational SRP-dependent translocation obviates the inhibitory effect of premature cytoplasmic protein folding on translocation and thereby allows the display of fast-folding and stable proteins that could not be displayed using the post-translational Sec pathway (**Figs. 2** and **5a**). These latter proteins are efficiently displayed only when SRP-dependent signal sequences are used. Oxidized TrxA, for example, has a high ΔG_o value of 8.1 kcal/mol and a very fast burst phase in folding with a first-order rate constant of 400 s^{-1} (ref. 37).

DARPins possess even higher thermodynamic stabilities than TrxA and have folding rates within the same order of magnitude. Thermal and denaturant-induced unfolding studies revealed T_m values above 66 °C, and ΔG values between 9.5 and 21.1 kcal/mol. In addition, DARPins show fast folding with first-order rate constants around 800 s^{-1} (S.Wetzel & A.P., unpublished data). Interestingly, the less stable DARPin E3_19 (ΔG value of 9.6 kcal/mol) is still displayed at some low level when using Sec-dependent signal sequences, whereas the more stable DARPin E3_5 (ΔG value of 14.8 kcal/mol) is essentially not displayed (**Figs. 2** and **5a**). Interestingly, TrxA variants having slower folding rates and lower thermodynamic stabilities than the wild-type protein also show improved translocation by the Sec pathway[38]. In line with our hypothesis, much higher display levels are seen for TrxA wt when the SRP-dependent signal sequences are used (**Fig. 2**). Whereas the Sec-dependent signal sequences do not enable translocation of DARPin E3_5 and translocate TrxA only at a low level, SRP-dependent signal sequences translocate both proteins, only at a much higher level (**Fig. 5b**).

The SRP-dependent signal sequence only moderately improved the display level for gpD, a protein with a ΔG_o value of 5.1 kcal/mol[39] and a moderate folding rate with the fastest phase estimated at 5 s^{-1} (P.F. & A.P., unpublished data). In contrast, antibody fragments can be translocated and displayed equally well with the Sec- or SRP-dependent signal sequences (**Figs. 2** and **4**). For antibody fragments, no evidence of a decrease in translocation with increasing thermodynamic stability is apparent[40], presumably because the fastest phases of folding of these proteins do not exceed 10 s^{-1} (ref. 41), and folding rates of many such molecules are much smaller.

Proteins that need cytoplasmic cofactors for folding or function may be refractory to display using the SRP translocation pathway. A recently described phage display system based on the post-translational Tat translocation pathway[42] might be better suited for the display of such proteins. Because it has been proposed that p3 itself cannot be displayed with the Tat system[42], the POI may have to be secreted separately and then assembled in the periplasm. A general limitation of this Tat-based approach is that only folded proteins can be translocated through the Tat translocon[43]. For example, disulfide-containing proteins such as antibody fragments can be secreted with the Tat system, and presumably displayed, only from a strain that allows disulfide formation in the cytoplasm[43].

As with any selection technology, the success of phage display selections strongly depends on the diversity of functionally displayed library members. A large combinatorial DNA library alone does not guarantee great functional diversity. We propose that SRP phage display could increase the functional diversity of many libraries, especially those expected to contain members with widely different folding rates and stabilities, such as for example, cDNA libraries. With SRP phage display, selections from such libraries can probably be performed with similar enrichment factors and numbers of selection rounds as typical for 'Sec-compatible' proteins and peptides. The enrichment factor for displaying DARPins was increased from about 10 to over 1,000 by switching to SRP phage display (**Table 2**).

We envision that SRP phage display will be applicable to all variants of phagemid or phage-based systems[12,15–18,44,45], including monovalent or polyvalent display, and will be compatible with all filamentous-phage coat proteins used for display. SRP phage display requires only the POI to be rerouted to the SRP pathway by simply exchanging the signal sequence. CysDisplay[45] and pJuFo phage display[44], two methods in which the POI is disulfide linked but not directly fused to p3, may also benefit from the SRP pathway. In these systems, the POI would be translocated by the SRP pathway, whereas the corresponding phage coat protein could still be translocated by the conventional Sec pathway, in analogy to the strategy described for the Tat pathway[42].

We identified post-translational protein translocation across the cytoplasmic membrane as a major bottleneck of conventional filamentous phage display. By redirecting the fusion proteins to the cotranslational SRP pathway using an appropriate signal sequence, we achieved efficient display of a wide range of POIs, presumably by avoiding premature folding in the cytoplasm. In particular, highly stable and fast-folding POIs were refractory to display using a Sec-dependent signal sequence, but can be efficiently displayed using a SRP-dependent signal sequence. In all cases tested the protein display levels were either maintained or improved by using a SRP-directing signal sequence. Therefore, this method seems to be a simple and broadly applicable way to expand the range of proteins that can be efficiently displayed and selected on filamentous phage.

METHODS

Materials. All chemicals were of the highest quality and purchased from Fluka unless stated otherwise. Oligonucleotides were from Microsynth. Vent DNA polymerase, restriction enzymes and buffers were from New England Biolabs or Fermentas. Helper phage VCS M13 was from Stratagene. All cloning and phage amplification was performed in *E. coli* XL1-Blue from Stratagene. Additionally, *E. coli* TG1 was used for phage production. Periplasmic protein expression was examined in the nonsuppressor *E. coli* strain JM83 obtained from the American Type Culture Collection. Genotypes and references for the *E. coli* strains used are described in the **Supplementary Table 1** online.

Molecular biology. Unless stated otherwise, all molecular biology methods were performed according to standard protocols[46].

Cloning. The phagemid vectors (plasmids with phage origin) that were prepared for the present study are described in detail in the **Supplementary Methods** online. The DNA encoding the proteins to be displayed was inserted into phagemids encoding either PhoAss or DsbAss, resulting in the phagemids listed in **Table 1**. The first and the last amino acids of the cloned proteins of interest are given in **Table 1** as well as the reference or accession number for either GenBank or Swiss-Prot databases.

For the DARPins 3a and 2_3, phagemids encoding the PelBss (pDST80 and pDST81, respectively), SfmCss (pDST86 and pDST87, respectively), TolBss (pDST84 and pDST85, respectively) and TorTss (pDST88 and pDST89, respectively) were generated.

For the DARPin E3_5 and thioredoxin (TrxA), phagemids encoding the LamBss (pDST110 and pDST117, respectively), MalEss (pDST109 and pDST116, respectively), MglBss (pDST111 and pDST118, respectively), OmpAss (pDST103 and pDST104, respectively), PelBss (pDST105 and pDST112, respectively), SfmCss (pDST108 and pDST115, respectively), TolBss (pDST106 and pDST113, respectively) and TorTss (pDST107 and pDST114, respectively) were generated. All signal sequences used are described in detail in **Supplementary Table 2** online.

Phage production and purification. The protocols were adapted from refs. 47 and 48. Five ml 2× YT medium containing 1% glucose, 34 μg/ml

chloramphenicol (cam) and 15 μg/ml tetracycline (tet) was inoculated with a single colony of *E. coli* XL-1 Blue harboring the phagemid of interest, and the cells were grown overnight at 30 °C with shaking. Five ml fresh 2× YT medium containing 1% glucose, 34 μg/ml cam and 15 μg/ml tet was inoculated with the overnight cultures at a ratio of 1:100 (OD_{600} ≈ 0.04) and grown at 37 °C to an OD_{600} of 0.5 with shaking. The cultures were infected with VCS M13 helper phage at 10^{10} (at plaque forming units per ml (multiplicity of infection ~ 20) and the cells were incubated for 30 min at 37 °C without agitation and then for 30 min at 37 °C with shaking. The medium was changed by harvesting the cells by centrifugation (3,500*g*, 24 °C, 10 min) and resuspending the pellet in 50 ml of 2× YT medium containing 34 μg/ml cam, 50 μg/ml kanamycin (kan) and 0.1 mM isopropyl-β-D-thiogalactoside (IPTG). After growth for 14 to 16 h at 30 °C with shaking, the cells were removed by centrifugation (5,600*g*, 4 °C, 10 min).

The culture supernatant was incubated on ice for 1 h with one-fourth volume of ice-cold PEG/NaCl solution (20% polyethyleneglycol (PEG) 6000, 2.5 M NaCl). The precipitated phage particles were then collected by centrifugation (5,600*g*, 4 °C, 15 min) and redissolved in 1 ml of TBS_{150} (25 mM Tris/HCl, 150 mM NaCl, pH 7.5). The phage particles were further purified by CsCl-gradient centrifugation as described[13]. The total concentration of phage particles was quantified spectrophotometrically[48]. The infective titer of the phage samples was determined by titration on *E. coli* XL-1 Blue cells using 2× YT agar plates containing 1% glucose, 34 μg/ml cam and 15 μg/ml tet. The colonies were counted after overnight incubation at 37 °C.

Phage blots. We applied 5 × 10^{11} phage particles, purified by CsCl gradient, to 15% SDS-PAGE under reducing conditions and transferred them to polyvinylidene fluoride (PVDF) Immobilon-P Transfer Membranes (Millipore) by electroblotting. The membranes were blocked with $MTTBS_{150}$ (TBS_{150}, 0.1% Tween-20, 5% skimmed milk) for 1 h at about 22 °C and incubated with a mouse anti-p3 antibody (MoBiTec) (1:1,000 in $MTTBS_{150}$, 20 min at about 22 °C) as primary antibody, which recognizes the C-terminal domain of p3. A $F(ab')_2$ fragment goat anti-mouse IgG horseradish peroxidase conjugate (Pierce) (1:10,000 in $MTTBS_{150}$, 1 h at about 22 °C) was used as the secondary antibody. The proteins were detected with ChemiGlow West substrate (Alpha Innotech).

In a second experiment, the blocked membranes were incubated with mouse anti-FLAG antibody M1 (Sigma) (1:5,000 in $MTTBS_{150}$, 1 h at about 22 °C) as primary antibody. A goat anti-mouse IgG alkaline phosphatase conjugate (Sigma) (1:10,000 in $MTTBS_{150}$, 1 h at about 22 °C) was used as secondary antibody. The proteins were detected with the substrates 5-bromo-4-chloro-3-indolyl phosphate (BCIP) and nitroblue tetrazolium (NBT).

Phage ELISAs. Phage ELISAs were carried out to assay the amount of functionally displayed DARPins on M13 phage particles. The targets, biotinylated APH and JNK2 proteins[21], were immobilized as follows: Neutravidin (66 nM, 100 μl/well; Pierce) in TBS_{150} was immobilized on MaxiSorp plates (Nunc) by overnight incubation at 4 °C. The wells were blocked with 300 μl $BTTBS_{150}$ (TBS_{150}, 0.1% Tween-20, 1% BSA) for 1 h at about 22 °C. Binding of the biotinylated APH and JNK2 proteins (100 μl, ≈ 1 μM) in $BTTBS_{150}$ was done for 1 h at 4 °C.

Dilution series of phage particles in $BTTBS_{150}$ were pipetted to the wells and incubated at about 22 °C for 2 h. After washing the wells five times with 300 μl $TTBS_{150}$ (TBS_{150}, 0.1% Tween-20) for 5 min, bound phage particles were detected with mouse anti-M13 antibody horseradish peroxidase conjugate (Amersham Pharmacia Biotech) and soluble BM Blue POD substrate (Roche Diagnostics).

Phage panning. Phage particles displaying DARPins E3_5, E3_19, 3a and 2_3 were produced from either phagemids encoding the PhoAss (pDST30, pDST65, pDST22 and pDST34, respectively) or from phagemids encoding the DsbAss (pDST32, pDST66, pDST23 and pDST37, respectively). These phage particles were subsequently mixed according to the experiment. To a 1:1 mixture of phage particles displaying the nonbinding DARPins E3_5 and E3_19, phage particles displaying the target-specific DARPins 3a or 2_3 were added in $1:10^7$ dilutions (for phage particles produced from phagemids encoding the PhoAss, additionally in 1:100 and 1:10 dilutions).

Biotinylated APH and JNK2 proteins were coated as described for the phage ELISAs. To each well, 0.1 ml of phage particle mixtures (10^{13} colony-forming units/ml) and 0.1 ml $BTTBS_{150}$ were added and incubated for 2 h. After washing with $TTBS_{150}$ (3× for the first selection cycle, 4× for the second cycle and 5× for additional cycles) for 5 min and with TBS_{150} (3× for the first selection cycle, 4× for the second cycle and 5× for additional cycles) for 5 min, the phage particles were eluted by incubating for 15 min with 0.2 ml elution buffer (0.2 M glycine/HCl, pH 2.2) at about 22 °C, followed by an elution for 30 min with 0.2 ml trypsin (10 mg/ml in TBS_{150}) at 37 °C. The combined eluates (neutralized with 10 μl of 2 M Tris-base) were used for the infection of 4 ml of exponentially growing *E. coli* XL1-Blue cells. After 30 min at 37 °C without agitation and 30 min at 37 °C with shaking, the cells were spread on 2× YT agar plates containing 1% glucose and 34 μg/ml cam and 15 μg/ml tet and grown overnight at 37 °C. The cells were washed from the plates with 2× YT containing 1% glucose, 15% glycerol, 34 μg/ml cam and 15 μg/ml tet and used for the phage production for the next cycle of panning. After each panning cycle, the identity of 9 to 16 eluted phage particles was determined. This was done by infection of *E. coli* with these phage particles and screening of the colonies by PCR with clone-specific primers.

Western blot analysis of cellular extracts. Five ml 2× YT medium containing 1% glucose, 34 μg/ml cam and 15 μg/ml tet were inoculated with a single colony of *E. coli* JM83 harboring the phagemid of interest and grown overnight at 30 °C with shaking. Fresh 5 ml 2× YT medium containing 1% glucose, 34 μg/ml cam and 15 μg/ml tet were inoculated with the overnight cultures at a ratio of 1:100 (OD_{600} ≈ 0.04) and grown at 37 °C to an OD_{600} of 0.5. The medium was changed by harvesting the cells by centrifugation (3,500*g*, 24 °C, 10 min) and resuspending the pellet in 50 ml of 2× YT medium containing 34 μg/ml cam and 0.1 mM isopropyl-β-D-thiogalactoside (IPTG). After growth for 14 to 16 h at 30 °C with shaking, the cells were harvested by centrifugation (5,600*g*, 4 °C, 10 min) for the whole cell extracts or treated as described[35] for subcellular fractionation.

Western blot analysis of the whole cell extracts and periplasmic fractions was carried out as described above. The blocked membrane was either incubated with mouse anti-FLAG antibody M1 (Sigma) (1:5,000 in $MTTBS_{150}$, 1 h at about 22 °C) or mouse anti-myc antibody (Cell Signaling Technology) (1:1,000 in $MTTBS_{150}$, 1 h at about 22 °C) as primary antibodies, then goat anti-mouse IgG alkaline phosphatase conjugate as secondary antibody. The proteins were detected with the substrates BCIP and NBT.

Note: Supplementary information is available on the Nature Biotechnology website.

ACKNOWLEDGMENTS

We thank Patrick Amstutz and H. Kaspar Binz for valuable discussions and J. Beckwith and D. Huber for advice on experimental procedures. This work was supported by the Swiss National Center of Competence in Research (NCCR) in Structural Biology and by KTI Discovery.

AUTHOR CONTRIBUTIONS

A.P. conceived the project; D.S., P.F., M.T.S. and A.P. designed experiments; D.S. performed the experiments; D.S., P.F., M.T.S. and A.P. analyzed the data; D.S., P.F., M.T.S. and A.P. wrote the manuscript.

COMPETING INTERESTS STATEMENT

The authors declare competing financial interests (see the *Nature Biotechnology* website for details).

Published online at http://www.nature.com/naturebiotechnology/
Reprints and permissions information is available online at http://npg.nature.com/reprintsandpermissions/

1. Smith, G.P. & Petrenko, V.A. Phage Display. *Chem. Rev.* **97**, 391–410 (1997).
2. Russel, M., Lowman, H.B. & Clackson, T. Introduction to phage biology and phage display. in *Phage Display: A Practical Approach* (eds. Lowman, H.B. & Clackson, T.) 1–26, (Oxford University Press, New York, USA, 2004).
3. Sidhu, S.S., Lowman, H.B., Cunningham, B.C. & Wells, J.A. Phage display for selection of novel binding peptides. *Methods Enzymol.* **328**, 333–363 (2000).
4. Bradbury, A.R. & Marks, J.D. Antibodies from phage antibody libraries. *J. Immunol. Methods* **290**, 29–49 (2004).
5. Rakonjac, J., Feng, J. & Model, P. Filamentous phage are released from the bacterial membrane by a two-step mechanism involving a short C-terminal fragment of pIII. *J. Mol. Biol.* **289**, 1253–1265 (1999).

6. Wilson, D.R. & Finlay, B.B. Phage display: applications, innovations, and issues in phage and host biology. *Can. J. Microbiol.* **44**, 313–329 (1998).
7. Deng, S.J. *et al.* Selection of antibody single-chain variable fragments with improved carbohydrate binding by phage display. *J. Biol. Chem.* **269**, 9533–9538 (1994).
8. Jung, S. & Plückthun, A. Improving *in vivo* folding and stability of a single-chain Fv antibody fragment by loop grafting. *Protein Eng.* **10**, 959–966 (1997).
9. Krebber, A., Burmester, J. & Plückthun, A. Inclusion of an upstream transcriptional terminator in phage display vectors abolishes background expression of toxic fusions with coat protein g3p. *Gene* **178**, 71–74 (1996).
10. Brinkmann, U., Chowdhury, P.S., Roscoe, D.M. & Pastan, I. Phage display of disulfide-stabilized Fv fragments. *J. Immunol. Methods* **182**, 41–50 (1995).
11. Rodi, D.J., Soares, A.S. & Makowski, L. Quantitative assessment of peptide sequence diversity in M13 combinatorial peptide phage display libraries. *J. Mol. Biol.* **322**, 1039–1052 (2002).
12. Krebber, A. *et al.* Reliable cloning of functional antibody variable domains from hybridomas and spleen cell repertoires employing a reengineered phage display system. *J. Immunol. Methods* **201**, 35–55 (1997).
13. Bothmann, H. & Plückthun, A. Selection for a periplasmic factor improving phage display and functional periplasmic expression. *Nat. Biotechnol.* **16**, 376–380 (1998).
14. Bothmann, H. & Plückthun, A. The periplasmic *Escherichia coli* peptidylprolyl cis,-trans-isomerase FkpA. I. Increased functional expression of antibody fragments with and without cis-prolines. *J. Biol. Chem.* **275**, 17100–17105 (2000).
15. Kramer, R.A. *et al.* A novel helper phage that improves phage display selection efficiency by preventing the amplification of phages without recombinant protein. *Nucleic Acids Res.* **31**, e59 (2003).
16. Baek, H., Suk, K.H., Kim, Y.H. & Cha, S. An improved helper phage system for efficient isolation of specific antibody molecules in phage display. *Nucleic Acids Res.* **30**, e18 (2002).
17. Rondot, S., Koch, J., Breitling, F. & Dübel, S. A helper phage to improve single-chain antibody presentation in phage display. *Nat. Biotechnol.* **19**, 75–78 (2001).
18. Jestin, J.L., Volioti, G. & Winter, G. Improving the display of proteins on filamentous phage. *Res. Microbiol.* **152**, 187–191 (2001).
19. Forrer, P., Stumpp, M.T., Binz, H.K. & Plückthun, A. A novel strategy to design binding molecules harnessing the modular nature of repeat proteins. *FEBS Lett.* **539**, 2–6 (2003).
20. Binz, H.K., Stumpp, M.T., Forrer, P., Amstutz, P. & Plückthun, A. Designing repeat proteins: well-expressed, soluble and stable proteins from combinatorial libraries of consensus ankyrin repeat proteins. *J. Mol. Biol.* **332**, 489–503 (2003).
21. Binz, H.K. *et al.* High-affinity binders selected from designed ankyrin repeat protein libraries. *Nat. Biotechnol.* **22**, 575–582 (2004).
22. Amstutz, P. *et al.* Intracellular kinase inhibitors selected from combinatorial libraries of designed ankyrin repeat proteins. *J. Biol. Chem.* **280**, 24715–24722 (2005).
23. Fekkes, P. & Driessen, A.J. Protein targeting to the bacterial cytoplasmic membrane. *Microbiol. Mol. Biol. Rev.* **63**, 161–173 (1999).
24. Koch, H.G., Moser, M. & Müller, M. Signal recognition particle-dependent protein targeting, universal to all kingdoms of life. *Rev. Physiol. Biochem. Pharmacol.* **146**, 55–94 (2003).
25. Valent, Q.A. Signal recognition particle mediated protein targeting in *Escherichia coli*. *Antonie Van Leeuwenhoek* **79**, 17–31 (2001).
26. Luirink, J. & Sinning, I. SRP-mediated protein targeting: structure and function revisited. *Biochim. Biophys. Acta* **1694**, 17–35 (2004).
27. Fisher, A.C. & DeLisa, M.P. A little help from my friends: quality control of presecretory proteins in bacteria. *J. Bacteriol.* **186**, 7467–7473 (2004).
28. Robinson, C. & Bolhuis, A. Tat-dependent protein targeting in prokaryotes and chloroplasts. *Biochim. Biophys. Acta* **1694**, 135–147 (2004).
29. Rapoza, M.P. & Webster, R.E. The filamentous bacteriophage assembly proteins require the bacterial SecA protein for correct localization to the membrane. *J. Bacteriol.* **175**, 1856–1859 (1993).
30. Plückthun, A. *et al.* in *Antibody Engineering,* edn. 1 (eds. McCafferty, J., Hoogenboom, H.R. & Chiswell, D.J.) 203–252, (IRL Press, Oxford, 1996).
31. Debarbieux, L. & Beckwith, J. The reductive enzyme thioredoxin 1 acts as an oxidant when it is exported to the *Escherichia coli* periplasm. *Proc. Natl. Acad. Sci. USA* **95**, 10751–10756 (1998).
32. Jonda, S., Huber-Wunderlich, M., Glockshuber, R. & Mössner, E. Complementation of DsbA deficiency with secreted thioredoxin variants reveals the crucial role of an efficient dithiol oxidant for catalyzed protein folding in the bacterial periplasm. *EMBO J.* **18**, 3271–3281 (1999).
33. Schierle, C.F. *et al.* The DsbA signal sequence directs efficient, cotranslational export of passenger proteins to the *Escherichia coli* periplasm via the signal recognition particle pathway. *J. Bacteriol.* **185**, 5706–5713 (2003).
34. Yang, F. *et al.* Novel fold and capsid-binding properties of the lambda-phage display platform protein gpD. *Nat. Struct. Biol.* **7**, 230–237 (2000).
35. Huber, D. *et al.* Use of thioredoxin as a reporter to identify a subset of *Escherichia coli* signal sequences that promote signal recognition particle-dependent translocation. *J. Bacteriol.* **187**, 2983–2991 (2005).
36. Slootstra, J.W., Kuperus, D., Plückthun, A. & Meloen, R.H. Identification of new tag sequences with differential and selective recognition properties for the anti-FLAG monoclonal antibodies M1, M2 and M5. *Mol. Divers.* **2**, 156–164 (1997).
37. Georgescu, R.E., Li, J.H., Goldberg, M.E., Tasayco, M.L. & Chaffotte, A.F. Proline isomerization-independent accumulation of an early intermediate and heterogeneity of the folding pathways of a mixed alpha/beta protein, *Escherichia coli* thioredoxin. *Biochemistry* **37**, 10286–10297 (1998).
38. Huber, D. *et al.* A selection for mutants that interfere with folding of *Escherichia coli* thioredoxin-1 in vivo. *Proc. Natl. Acad. Sci. USA* **102**, 18872–18877 (2005).
39. Forrer, P., Chang, C., Ott, D., Wlodawer, A. & Plückthun, A. Kinetic stability and crystal structure of the viral capsid protein SHP. *J. Mol. Biol.* **344**, 179–193 (2004).
40. Ewert, S., Huber, T., Honegger, A. & Plückthun, A. Biophysical properties of human antibody variable domains. *J. Mol. Biol.* **325**, 531–553 (2003).
41. Jäger, M., Gehrig, P. & Plückthun, A. The scFv fragment of the antibody hu4D5–8: evidence for early premature domain interaction in refolding. *J. Mol. Biol.* **305**, 1111–1129 (2001).
42. Paschke, M. & Höhne, W. A twin-arginine translocation (Tat)-mediated phage display system. *Gene* **350**, 79–88 (2005).
43. DeLisa, M.P., Tullman, D. & Georgiou, G. Folding quality control in the export of proteins by the bacterial twin-arginine translocation pathway. *Proc. Natl. Acad. Sci. USA* **100**, 6115–6120 (2003).
44. Crameri, R., Hemmann, S. & Blaser, K. PJuFo: a phagemid for display of cDNA libraries on phage surface suitable for selective isolation of clones expressing allergens. *Adv. Exp. Med. Biol.* **409**, 103–110 (1996).
45. Löhning, C., Urban, M. & Knappik, A. Novel methods for displaying (poly) peptides/proteins on bacteriophage particles via disulfide bonds Patent WO0105950 (2001).
46. Sambrook, J. & Russell David, W. (eds.). *Molecular Cloning: A Laboratory Manual,* edn. 3. (Cold Spring Harbor Laboratory Press, Cold Spring Harbor, NY, 2001).
47. Clackson, T. & Lowman, H.B.. *Phage Display: A Practical Approach* (Oxford University Press, New York, 2004).
48. Barbas, C.F., III, Burton, D.R., Scott, J.K. & Silvermann, G.J.. *Phage Display: A Laboratory Manual.* (Cold Spring Harbor Laboratory Press, Cold Spring Harbor, NY 2001).
49. Nielsen, H., Engelbrecht, J., Brunak, S. & von Heijne, G. Identification of prokaryotic and eukaryotic signal peptides and prediction of their cleavage sites. *Protein Eng.* **10**, 1–6 (1997).
50. Gailus, V. & Rasched, I. The adsorption protein of bacteriophage fd and its neighbour minor coat protein build a structural entity. *Eur. J. Biochem.* **222**, 927–931 (1994).

Supplementary Material

Supplementary Methods

Phagemid cloning. The phagemid pDST22, a derivative of the vector pMorph7 (ref. 1) which is functionally equivalent to the vector pAK100 (ref. 2) was the starting point for the cloning (**Supplementary Fig. 1**). It encodes the DARPin 3a and the signal sequence of the E. coli PhoA (PhoAss). The E. coli alkaline phosphatase (Swiss-Prot database accession number P00634) has the signal sequence MKQSTIALALLPLLFTPVTKA, given in single letter amino acid code.

To allow direct experimental comparison to phagemids encoding the signal sequence of DsbA (DsbAss), a second phagemid called pDST23 was generated. The *E. coli* thiol-disulfide interchange protein DsbA (Swiss-Prot database accession number P0AEG4) has the signal sequence MKKIWLALAGLVLAFSASA, given in single letter amino acid code. To replace the PhoAss of pDST22, the oligonucleotides oDST4 (AGAGCATGCGTAGGAGAAAATAAAAT GAAAAAGATTTggctggcgctggctgg), oDST5 (TCTTTGTAGTCCGCCGATGCGCTAAACGC TAAAACTAAAccagccagcgccagcc), oDST6 (GCTCTagagcatgcgtaggag (*Xba*I)), and oDST8 (GCGGATCCAtctttgtagtccgccg (*Bam*HI)) that encode the *E. coli* DsbAss were designed (Lower case letters indicate the regions designed for annealing, restriction sites are underlined and restriction enzymes given in brackets).

The oligonucleotides oDST4 and oDST5 were annealed and amplified with oligonucleotides oDST6 and oDST8 by PCR. The resulting DNA fragment encodes the DsbAss and is flanked by the restriction endonuclease sites *Xba*I and *BamH*I. This DNA fragment was digested with *Xba*I and *BamH*I and ligated into the similarly treated and dephosphorylated pDST22. The resulting phagemid pDST23 (**Supplementary Fig. 1**) was isolated and the sequence was verified by DNA sequencing.

The other phagemids used in this study are listed in **Table 1** of the publication and were obtained as follows: The coding sequences of the proteins of interest were PCR amplified using appropriately designed PCR primers and template DNA. Thereby, either a *BamH*I or a *Bgl*II restriction site was introduced 5' to each of the coding sequences and two restriction sites (*EcoR*I and *Pst*I) were introduced 3' to each of the coding sequences. These PCR fragments were digested either with *BamH*I or *Bgl*II and either *EcoR*I or *Pst*I, and then ligated into the similarly treated and dephosphorylated phagemids pDST23 and pDST22. The open reading frame of the expression cassette for the fusion polypeptide comprising the cloned PCR product was maintained for all constructs, especially the correct reading frame for the C-terminal fusion to the C-terminal domain of phage protein 3 (CTp3) was maintained. The first and the last amino acids of the cloned proteins of interest (POI) are given in **Table 1** of the publication as well as the reference or accession number for either the GenBank or the Swiss-Prot databases. The sequence of all phagemids was verified by DNA sequencing.

For the designed ankyrin proteins (DARPins) 3a and 2_3, additional phagemids encoding the PelBss (pDST80 and pDST81, respectively), SfmCss (pDST86 and pDST87, respectively), TolBss (pDST84 and pDST85, respectively) and TorTss (pDST88 and pDST89, respectively) were generated, using the same cloning strategy with 4 oligonucleotides as described above for DsbAss, using appropriate oligonucleotides**.**

For the DARPin E3_5 and thioredoxin (TrxA), additional phagemids encoding the LamBss (pDST110 and pDST117, respectively), MalEss (pDST109 and pDST116, respectively), MglBss (pDST111 and pDST118, respectively), OmpAss (pDST103 and pDST104, respectively), PelBss (pDST105 and pDST112, respectively), SfmCss (pDST108 and pDST115, respectively), TolBss (pDST106 and pDST113, respectively) and TorTss (pDST107 and pDST114, respectively) were generated. Again, the same strategy as for DsbAss was used.

Signal sequences used are described in detail in **Supplementary Table 2** and *E. coli* strains used are described in detail in **Supplementary Table 1**.

References

1. Knappik, A. et al. Fully synthetic human combinatorial antibody libraries (HuCAL) based on modular consensus frameworks and CDRs randomized with trinucleotides. *J. Mol. Biol.* **296**, 57-86 (2000).

2. Krebber, A. et al. Reliable cloning of functional antibody variable domains from hybridomas and spleen cell repertoires employing a reengineered phage display system. *J. Immunol. Methods* **201**, 35-55 (1997).

Supplementary Table 1: *E. coli* strains

Name	Genotype	Ref
JM83	F$^-$ *ara* Δ(*lac-proAB*) *rpsL* (Str^r)[Φ*80, lacZ*Δ*M15*] *thi*	a
TGl	F' [*lacI^q lacZ*Δ*M15 proAB$^+$ traD36*] *hsd*Δ*5* Δ(*lac-proAB*) *supE thi*	b
XL1-Blue	F' [*lacI^q lacZ*Δ*M15 proAB$^+$* Tn*10*(Tet^r)] *endA1 supE44 gyr*A96 *hsdR17 lac recA1 relA1 thi*	c

[a] Yanisch-Perron, C., Vieira, J. & Messing, J. Improved M13 phage cloning vectors and host strains: nucleotide sequences of the M13mp18 and pUC19 vectors. *Gene* **33**, 103-119 (1985).
[b] Gibson, T.J. (1984) Studies on the Epstein-Barr virus genome. PhD Thesis. Cambridge University, Cambridge, UK
[c] Bullock, W.O., Fernandex, J.M. & Short, J.M. Xl1-Blue: A High Efficiency Plasmid Transforming recA Escherichia coli Strain With Beta-Galactosidase Selection. *BioTechniques* **5**, 376-379 (1987).

Supplementary Table 2: Signal sequences

Abbr.	Source[a]	Amino acid sequence[b]	Accession number[c]
DsbAss	*E. coli* thiol-d. interchange protein DsbA	MKKIWLALAGLVLAFSASA	P0AEG4
LamBss	*E. coli* lambda receptor protein LamB	MMITLRKLPLAVAVAAGVMSAQAMA	P02943
MalEss	*E. coli* maltose-binding protein MBP	MKIKTGARILALSALTTMMFSASALA	P0AEX9
MglBss	*E. coli* galactose-binding protein GBP	MNKKVLTLSAVMASMLFGAAAHA	P0AEE5
OmpAss	*E. coli* outer membrane protein A OmpA	MKKTAIAIAVALAGFATVAQA	P0A910
PelBss	*Erwinia carotovora* pectate lyase PelB	MKYLLPTAAAGLLLLAAQPAMA	P11431
PhoAss	*E. coli* alkaline phosphatase PhoA	MKQSTIALALLPLLFTPVTKA	P00634
SfmCss	*E. coli* chaperone protein SfmC	MMTKIKLLMLIIFYLIISASAHA	P77249
TolBss	*E. coli* protein TolB	MKQALRVAFGFLILWASVLHA	P0A855
TorTss	*E. coli* periplasmic protein TorT	MRVLLFLLLSLFMLPAFS	P38683

[a] Organism and protein from which signal sequence is derived
[b] Signal sequence given in single letter amino acid code
[c] Swiss-Prot

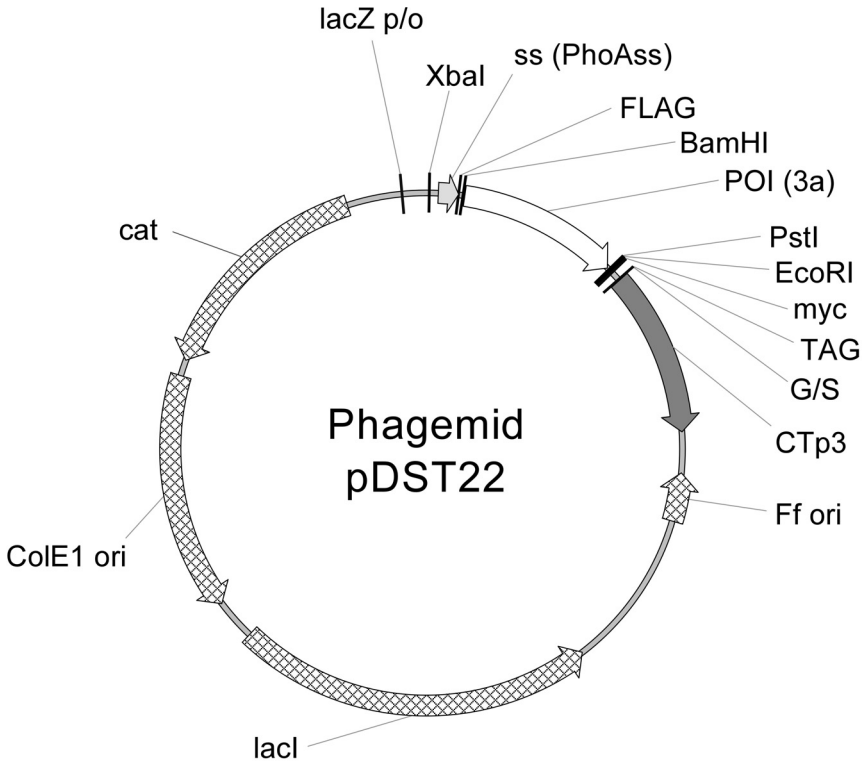

Supplementary Figure 1: Schematic representation of the phagemid pDST22. In addition to the elements shown in **Figure 1**, the filamentous phage replication origin (Ff *ori*), the *lac* repressor gene from *E. coli* (*lacI*) producing *lac* repressor needed for the control of the *lacZ* p/o, the ColE1 origin of replication (ColE1 *ori*) for bacterial replication of the vector, the antibiotic resistance gene (*cat*) encoding a chloramphenicol acetyltransferase conferring chloramphenicol resistance, and the restriction sites *Xba*I, *Bam*HI, *Pst*I, and *Eco*RI are depicted.

Chapter 3

Efficient Selection of DARPins with Sub-nanomolar Affinities by using SRP Phage Display

Daniel Steiner[1], Patrik Forrer[1,2] and Andreas Plückthun[1,3]

[1] Department of Biochemistry, University of Zürich, Winterthurerstrasse 190, 8057 Zürich, Switzerland

[2] Molecular Partners AG, Grabenstrasse 11a, 8952 Zürich-Schlieren, Switzerland

[3] To whom correspondence should be addressed:

Email: plueckthun@bioc.uzh.ch

Tel: +41-44-635 55 70

Fax: +41-44-635 57 12

Keywords:

Phage display, library generation, SRP phage display, DARPin, novel scaffold

Contents

1. Abstract

There is an ever increasing demand to select specific, high-affinity binding molecules against target proteins of biomedical interest. The success of such selections strongly depends on the design and functional diversity of the library of binding molecules employed, as well as on the performance of the selection strategy. We have recently developed SRP phage display that allows filamentous phage display of highly stable and fast folding proteins, such as Designed Ankyrin Repeat Proteins (DARPins) that are virtually refractory to conventional phage display. DARPins comprise a novel class of binding molecules suitable to replace or complement antibodies in many biotechnological or biomedical applications; and so far all DARPins had been selected by using ribosome display. Here, we harnessed SRP phage display and generated a phage DARPin library containing more than 10^{10} individual members. We were able to select well behaved and highly specific DARPins against a broad range of target proteins having affinities as low as 100 picomolar directly from this library, without affinity maturation. Thus, SRP phage display makes filamentous phage display accessible for DARPins, allowing, for example, selections under hash conditions or on whole cells. We envision that the use of SRP phage display would be also beneficial for other libraries of stable and fast folding proteins.

2. Introduction

The demand for good quality binding molecules for biotechnological and biomedical applications is ever increasing. Antibodies are currently by far the most frequently used binding molecules, but proteins based on non-immunoglobin scaffolds have become an appealing alternative.[1] From both antibody and non-antibody scaffolds, binding molecules with high affinity and high specificity against almost any chosen target protein can be generated *in vitro* using appropriately designed combinatorial libraries in combination with selection technologies such as phage display or ribosome display.[1,2,3] The success of such selections is mainly based on the design and size of the combinatorial library and the selection technology employed.

Together, these factors will determine the functional size of the library that is accessible for the selection of binding molecules. Further important factors are the selection strategy chosen and the biophysical properties of the target protein; even with the best library and an optimized selection protocol it might be very difficult or even impossible to obtain reasonable binding molecules against a "sticky" and unstable target protein.

The underlying principle of all selection technologies is the physical linkage of the phenotype (i.e. the displayed protein) and the genotype (i.e. the DNA encoding the displayed protein). Different selection technologies use different strategies to achieve this linkage. The success of any selection experiment depends on the compatibility of the strategy used with the proteins to be displayed. Ribosome display, for example, is a complete *in vitro* display technology that relies on the formation of a non-covalent ternary complex of mRNA, ribosome and the displayed nascent polypeptide.[4] The formation of this ternary complex by *in vitro* translation allows the sampling of very large libraries, and the ease of introducing mutations by error-prone PCR allows efficient affinity maturation. However, the linkage of the genotype and the phenotype is only reliably maintained under non-denaturing buffer conditions, in the absence of RNases and at low temperature. In contrast, in filamentous phage display[5] this linkage is very robust, allowing a broader range of selection conditions. Filamentous phage display achieves this robustness by physically linking the displayed protein to the surface of a very stable phage particle,[6] which encapsulates the corresponding genotype. Nevertheless, the limiting factor in this selection technology is the involvement of an *in vivo* step to produce the protein displaying phage particles. The bacterial transformation needed limits the library size that can reasonably be achieved to usually much less than 10^{11} members. Furthermore, the *in vivo* assembly process of the phage particle is not necessarily compatible with a protein to be displayed (e.g. successful translocation of a protein to the periplasm is a prerequisite). Ideally, high affinity binders should be obtained directly in a single selection experiment, without further time consuming affinity maturations.

Fist of all the success of a phage selection experiment strongly depends on the transformed library size. In general, the larger the library size the higher the probability to isolate diverse binders against a given target protein and the higher the affinities of the selected binders.[7] For example, to isolate antibody fragments with sub-nanomolar affinities libraries with more than 5×10^9 members were employed.[8,9,10] Nevertheless, even more important than the transformed library size (number of independent clones), is the functional library size, i.e. the number of different correct molecules available for selections, as often only a fraction of all library members can be functionally displayed. Factors influencing the functional diversity are therefore, the above-mentioned compatibility of the selection system with the protein to be displayed, the actual library design and the size and quality of the assembled library using synthetic genes.

In the case of libraries of designed binding molecules, the use of a very stable scaffold as starting point to introduce diversity helps to ensure that almost all library members are stable and well expressed proteins, as diversification of a scaffold will almost inevitably result in reduced stability. Another important aspect is the design of diversity, meaning the careful design of randomized parts into the scaffold; the challenge is here to introduce a diversity high enough to allow successful selections of binders against any target protein, yet low enough to not destabilize library members too much.

In the case of designed ankyrin repeat proteins (DARPins),[11,12] which comprise a novel class of binding proteins, we used consensus design[13] to generate a very stable scaffold amenable to the introduction of the needed diversity. This consensus design is based on the sequence and structure analysis of natural ankyrin repeat proteins and allows the delineation of framework residues, which are important for stability of the scaffold, and the definition of potential target interaction residues (inspired by the study of natural ankyrin complexes) suitable to introduce the needed diversity. Most members of such DARPin libraries have very favorable biophysical

properties.[12] They are very well expressed, monomeric in solution, highly soluble, thermodynamically stable and do show fast cooperative folding behavior.

From such DARPin libraries, specific binders with high affinities have been selected for a broad range of target proteins[14,15,16,17,18] by using ribosome display. Nevertheless, and much to our initial surprise, the display of DARPins on filamentous phage was highly inefficient using conventional systems, despite the good biophysical properties of the proteins. We identified this problem as one of inefficient translocation of the DARPins into the periplasm due to their premature folding in the cytoplasm, and one that can be solved by using the signal recognition particle (SRP) translocation pathway for phage display.[19]

In SRP phage display,[19] the proteins to be displayed are directed to the *Escherichia coli* cotranslational signal recognition particle (SRP) translocation pathway by using an appropriate signal sequence, whereas conventional phage display uses the posttranslational Sec translocation pathway. This simple change in the use of the translocation route seems to prevent premature folding of stable and fast folding proteins in the cytoplasm and therefore allows their efficient translocation and subsequent display on filamentous phage particles. These results indicated that the use of SRP phage display may help to obtain a high functional diversity of phage DARPin libraries leading to efficient selections.

In the present study we describe the generation of a large phage DARPin library by using SRP phage display, selections on a panel of target proteins using this library and analysis of the thereby selected DARPins. In addition, we discuss the potential of SRP phage display to generate novel binding molecules with excellent properties for biotechnological or biomedical applications.

3. Results

3.1 Construction of the phage DARPin library

The phage DARPin library described here is based on the phagemid vector pPDV1 that allows the display of a protein of interest (POI) fused to the minor phage coat protein 3 (p3) on filamentous phage (**Supplementary Figure 1**). In contrast to most other phage display vectors, it fuses the POI to a signal sequence using the cotranslational signal recognition particle (SRP) pathway for the translocation of the POI-p3 fusion across the cytoplasmic membrane of *E. coli*. The use of the SRP pathway ensures the efficient display of stable and fast folding DARPins on phage particles.[19]

We used the N3C DARPin library[12] (N3C denoting an N-terminal capping repeat, three randomized internal repeats and a C-capping repeat) and brought it to the phage display format by PCR amplification and subcloning it into pPDV1. XL1-blue cells were transformed with the library yielding 2.6×10^{10} independent colonies (transformed library size; see **Material and Methods** for details). The transformed XL1-blue cells were infected with helper phage VCS M13, and subsequently IPTG was added to the culture to induce the expression and thus the display of the DARPins on the phage particles. For all initial rounds of selection, as described below, the input library phage particles were directly used from a frozen phage library stock. There was no need to reamplify the library to obtain functional display, as the DARPins displayed on phage particles seem to tolerate at least one freeze-thaw cycle very well.

3.2 High functional diversity of the phage DARPin library

The functional diversity of the transformed 2.6×10^{10} independent clones of the DARPin library was assessed by sequencing, determining the display level and subsequent cytoplasmic expression analysis. DNA sequencing of 55 randomly picked clones showed that 26 (47%) encode functional DARPin sequences, composed of 18 (33%) N3C, 7 (13%) N2C and 1 (2%)

N1C DARPin library members, all with different amino acids at randomized positions. The presence of library members having less than three internal repeats (N1C and N2C) can be attributed to *in vitro* recombination during library construction, requiring the PCR amplification of the DARPins, and do result from their repetitive nature. The remaining 29 (53%) clones had frameshifts, deletions or insertions in the DARPin sequence or contained no insert at all (non-functional part of the library). Phage particles produced form the same 55 clones of the library as sequenced above were analyzed for DARPin display by western blotting. All 26 (47%) clones correct on sequence level showed bands at the size expected for a DARPin-p3 fusion protein and signal intensities similar to the signal obtained for a scFv using a standard phagemid for monovalent display. Thus, it can be assumed that single DARPins are displayed on about one to ten percent of phage particles.[20] Of the non-functional part of the library only one clone encoding the N-terminal part of a DARPin, in frame with the phage coat p3, a prerequisite for display on phage particles showed a band on the western blot. To analyze cytoplasmic expression of the DARPins, a pool of DARPin inserts from the library was subcloned into pDST67 (see **Materials and Methods**), a vector for high-level, soluble cytoplasmic expression derived from pQE30 (QIAgen), followed by small scale expression in 96-deep well plates and SDS-PAGE analysis of 57 randomly picked clones which were not sequenced. Thirty-two (56%) of the clones showed expression levels of soluble DARPins above 0.1 mg/ml *E. coli* culture. Together, these results show that all clones that are correct on the amino acid level are well displayed on the phage particles and can be expected to be well expressed in the cytoplasm. Thus, we can estimate that the Phage DARPin library contains about 1.2×10^{10} correct clones which encode well-behaved displayable molecules (functional library size; 47% of the transformed library size), taking also into account that the library which was used as template contained at least 10^{10} individual members.[14]

The non-functional part of the library may sometimes lead to the enrichment of background binding clones encoding defective DARPins that have parts of the scaffold replaced

by unstructured and sticky polypeptides. This background enrichment could be successfully circumvented in all cases by applying the optimized selection protocol described in detail in the **Supplementary Material**.

3.3 Target protein preparation, immobilization and optimized selection protocol

For the validation of the phage DARPin library we performed selections against a broad range of purified target proteins (**Table 1**). To avoid partial protein denaturation of the target due to direct immobilization on solid plastic (i.e. polystyrene) surfaces, samples of all target proteins were chemically or enzymatically (using an Avi-tag[21]) biotinylated. This allows selections to be performed either on biotinylated target protein bound to neutravidin or streptavidin, which are directly immobilized on a solid plastic surface (referred to as: "immobilized target protein") or on biotinylated target protein in solution, which was subsequently captured with streptavidin-coated beads (referred to as: "target protein in solution"). From the analysis of a number of selection experiments, we found that the most efficient enrichment of specific binders from our phage DARPin library is obtained with an optimized selection protocol which is composed of a first round of selection on immobilized target protein, followed by one to two further rounds of selection on target protein in solution. The development of this optimized selection protocol is described in the **Supplementary Material**. Unless stated otherwise, selections were performed at room temperature, enzyme-linked immunosorbent assay (ELISA) experiments were performed on biotinylated target protein bound to neutravidin, which had been directly immobilized on a solid plastic surface, and by using non-biotinylated target protein for competition experiments. The different selection approaches needed for the different target proteins and characterizations of the binders obtained are described below. This partial listing illustrates the versatility of the library, but also the great influence of the target protein on peculiarities of the selection.

3.4 Efficient selection of DARPins specific for huIgG1_Fc

Binders against the Fc domain of antibodies are of interest not only as an in vitro detection reagent, but also for biomedical applications to, for example, extend the *in vivo* half-life of molecules fused to such a binder by attaching to antibodies present in the blood stream. To enrich binders against the Fc domain of human IgG1 (huIgG1_Fc, **Table 1**) we performed three rounds of selection using our optimized selection protocol as described above. From each selection round we analyzed the recovered and amplified polyclonal pool of phage particles for target binding by phage ELISA. Enrichment of phage particles displaying target specific DARPins was already observed after the second selection round with a strong increase after the third round, and no background enrichment of phage particles binding to the corresponding non-target-coated matrix was observed (**Figure 1(a)**).

To screen individual DARPins for binding to their target protein, and at the same time eliminate any conceivable dependence on the p3-fusion format, we did not carry out single clone analysis with phages but directly subcloned the selected pool of binders from round three into the cytoplasmic expression vector pDST67. From 94 individual DARPins analyzed for full length huIgG1 binding by a crude extract ELISA (see **Materials and Methods**), 82 gave a specific binding signal (signal/background > 10) (**Figure 1(b); Table 2**). Crude cell extracts of ELISA-positive clones were further analyzed by SDS-PAGE (**Figure 1(c)**), confirming that, in general, the excellent expression properties are maintained throughout. It should be noted that some DARPins having more than two internal repeats run at lower apparent molecular mass or show additional bands with faster running behavior. The same behavior was also observed for the respective purified proteins, even though they were subsequently shown by sequencing and MS to be precise in sequence and not degraded. As shown previously,[12,19] this is due to an incomplete denaturation of these stable molecules by SDS. N2C DARPins do not have this extreme SDS resistance and do run where expected. Based on the ELISA signals, 21 clones were submitted for sequencing, resulting in eight different sequences of DARPins confirmed by

repeated ELISA experiments to bind the target protein (data not shown). The six most promising candidates (**Table 2**) named I_02, I_07, I_13 (N2C library members) and I_01, I_11, I_19 (N3C library members) were further analyzed. Expression and immobilized metal ion chromatography (IMAC) purification was performed in 96-well format in parallel with binders selected against other target proteins (see **Material and Methods**), yielding on average more than 1 mg of > 95% pure protein for each clone from 8 x 1.3 ml *E. coli* culture. These purified DARPins were used for all further experiments.

To investigate the specificity of the selected DARPins, ELISA experiments with the four high-affinity clones I_01, I_02, I_07 and I_19 (**Figure 1(c)**) and the two lower affinity clones I_11 and I_13 (**Figure 1(d)**) were performed. All of the binders do show specific binding to full length human IgG1 (huIgG1) but do not bind to neutravidin, mouse IgG1 (muIgG1) or mouse IgG2b (muIgG2b). In the competition ELISA setup the binding to immobilized huIgG1 could be well inhibited by preincubation of the DARPins with free huIgG1 (**Figure 1(c), (d)**). From the concentrations of free huIgG1 needed for an inhibition of > 50% the affinities of these binders can be estimated to be in the nM range, as could be confirmed by surface plasmon resonance (SPR, see below).

The binders were further characterized by size exclusion chromatography (SEC) and compared to the well characterized, non-binding DARPin E3_5 (ref. 12). At a concentration of 10 μM four of the six clones tested eluted at the size expected for the monomer (**Figure 2**). Clone I_19 showed a second elution peak at lower elution volume, indicating some dimer formation at this concentration. I_01 elutes as a single peak but at lower elution volume (higher apparent molecular weight) than expected, indicating an increase hydrodynamic radius due to multimerisation or partial unfolding. Further analysis of this binder by SEC combined with multi-angle light scattering (SEC-MALS) revealed a clearly dimeric mass of the DARPin I_01.

Four of the clones were further analyzed by SPR (**Table 3** and **Supplementary Figure 2**) and the data obtained were evaluated with a global kinetic fit. I_19 had the highest affinity for

huIgG1_Fc (K_D = 2.1 nM) and I_11 the lowest affinity (K_D = 137 nM), in good agreement with the competition ELISA experiments performed. To calculate the affinity of I_19 we assumed that the DARPin would be completely monomeric at all concentrations used for the SPR measurements (the maximal DARPin concentration was 75 nM), and the global fit agrees very well with a 1:1 interaction (see **Supplementary Material**).

In summary, we were able to enrich a diverse set of highly specific binders with affinities in the low nanomolar range in just three rounds of selection, from our phage DARPin library.

3.5 Selection of DARPins binding to TNFα

Antibodies to TNFα have been developed for a number of therapeutic applications,[22] as has the soluble recombinant receptor of TNFα, Etanercept (Enbrel™, see below),[23] and binding molecules based on novel scaffolds are currently being developed to do the same. To enrich binders specific for the soluble trimeric form of TNFα (**Table 1**) we performed selections and screenings as described above for huIgG1_Fc using biotinylated TNFα (see **Materials and Methods**). Fast enrichment of phage particles displaying DARPins specific for TNFα was already observed after the second selection round. From round two and three, 94 individual DARPins each were screened by crude extract ELISA for TNFα binding, giving 15 and 87 specific binding signals, respectively (**Table 2**). Based on the ELISA signals, 52 clones were submitted for sequencing, resulting in a highly diverse set of 29 different sequences of DARPins; interestingly, all selected DARPins were of the N3C type. Binders were expressed in the cytoplasm, purified by IMAC and further analyzed by SEC; they show high-level expression and most of them monomeric elution behavior, similar to the results obtained for the huIgG1_Fc binders described above.

To investigate the specificity of the selected DARPins, ELISA experiments were performed (**Figure 3**). All of the binders do show specific binding to TNFα, do not interact with neutravidin, and in the competition ELISA setup the binding to immobilized TNFα could be well inhibited by preincubation of the DARPins with free TNFα. From the competition ELISA signals

obtained with 10 nM of free TNFα, the affinities of the binders were estimated to be in the low nM range. Interestingly, the binding of all selected DARPins can be almost completely inhibited by preincubation of the immobilized TNFα with Etanercept (Enbrel^{TM}, recombinant human soluble tumor necrosis factor alpha receptor fused to Fc domain of human IgG1, Amgen, USA) (**Figure 3**). In the complementary experiment, where immobilized TNFα was preincubated with different DARPins, the inhibition of Enbrel binding could not be detected. It was clearly detected, however, in SPR measurements (see **Supplementary Figure 4),** where soluble TNFα, preincubated with DARPins could be prevented from binding to immobilized Enbrel. From SEC-MALS experiments (see **Supplementary Figure 5**), the DARPin TNFα complex has only a molar mass of about 53.5 kDa (theoretical molecular weight for the TNFα trimer plus one DARPin is 70.2 kDa and for the TNFα trimer plus three DARPins is 106.2 kDa). It thus appears that the DARPins selected in this particular experiment do possibly not bind to the TNFα trimer but to another form of TNFα, while the dimeric Enbrel chelates the TNFα trimer. This information thus helps to steer further selections to other epitopes and stoichiometries.

Up to this stage all binding and washing steps in the selection and ELISA experiments had been carried out using our standard buffers containing 0.1 % Tween-20. During further analysis, very much to our surprise we discovered that all the selected DARPins show specific TNFα binding that is dependent on the presence of the detergent Tween-20 in the binding buffer. In ELISA experiments, excellent and specific binding to the immobilized target protein was observed in buffers HBST, TBST and PBST all containing 0.1% (v/v) Tween-20, but not in the buffers alone. Also, in SEC experiments complex formation of the DARPins with TNFα could only be observed in PBST, but not in PBS alone. One speculation is that Tween-20 induces conformational changes in TNFα needed for the accessibility of the DARPin epitopes. To prevent the enrichment of such binders, Tween-20 could be omitted or replaced by other detergents in new selection approaches on TNFα. We did not further analyze these DARPins, since we do not expect them to bind their target protein *in vivo*.

3.6 Selection of DARPins to members of the ErbB receptor family

Antibodies to ErbB1 (EGFR) and the other members of the ErbB receptor family, notably ErbB2 (HER2), are being developed as anti-tumor therapeutics.[24] We describe in the present study the selection of DARPin binders against ErbB1, ErbB2 and ErbB4. The extracellular part of all members of this family is composed of four domains (domain I-IV).[25] For both ErbB1 and ErbB4 the extracellular domains I-III of the respective receptor fused to huIgG1_Fc were used in selections (see **Table 1**). The different selection approaches performed on these two target proteins are described in detail in the **Supplementary Material**.

Individual DARPins were screened for specific target protein binding by crude extract ELISA as described for huIGg1_Fc. For ErbB1, 97 out of 369 and for ErbB4, 55 out of 143 screened clones gave a specific binding signal (**Table 2**). Based on ELISA signals 64 clones for ErbB1 and 48 clones for ErbB4 were submitted for sequencing. Surprisingly, this resulted in only one dominant ErbB1 binder (E_01) and five ErbB4 binders (B4_01, B4_02, B4_07, B4_33 and B4_45), of which B4_02 was strongly overrepresented among the sequenced clones (about 66 %).

To increase the diversity of the selected binders and to avoid dominant enrichment of these binders we used a selection procedure termed “epitope-masking”.[26] For this purpose we expressed and purified the two dominant binders (E_01 and B4_02) by IMAC and performed one round of selection on the two target proteins in solution in the presence of an only two-fold excess of the respective purified binder. By this partial masking of the epitope of the dominant binder we expected to select DARPins which recognize a different epitope, but at the same time still allow new high-affinity DARPins competing for the same epitope to be enriched. Using higher concentrations for competition resulted in a lower diversity of the selected binders (see below). For both target proteins equivalent amounts of amplified, partially enriched pools of phage particles after selection round one on immobilized target proteins (**Supplementary Figure 3(a)** and **3(b)**) and after selection round two on target proteins in solution (**Supplementary**

Figure 3(c) and **3(d)**) were used as input. After one round of selection, input and output pools of phage particles were analyzed by phage ELISA for binding to their target protein in the absence and the presence of a large excess (2 μM) of the respective dominant binders (**Figure 4(a)** and **4(b)**). For ErbB1, the binding signal obtained on target protein alone was much higher than the signal obtained on ErbB1 in the presence of the DARPin E_01, indicating that most of the DARPins selected indeed recognize the same or an epitope overlapping with that of DARPin E_01 (**Figure 4(a)**). For ErbB4, the binding signal obtained on target protein alone or in the presence of B4_02 was identical, indicating that in this case, most of the selected DARPins recognize an epitope different from that of DARPin B4_02 (**Figure 4(e)**).

To analyze the success of the epitope-masking, individual selected DARPins were first screened for binding to their target protein by crude extract ELISA as described for huIGg1_Fc. For ErbB1, 81 of 105, and for ErbB4, 84 of 94 screened clones gave a specific binding signal (**Table 2**). Based on the ELISA signals, 20 clones of each selection were submitted for sequencing, resulting in four new binders for ErbB1 and six new binders for ErbB4. Binders were expressed in the cytoplasm of *E. coli*, purified and further analyzed by SEC; they show high-level expression and most of them monomeric elution behavior, similar to the results obtained for the huIgG1_Fc binders described above. All of the clones did bind specifically to the respective target protein, as shown by competition ELISA, but only the ErbB1 binders (E_67, E_68, E_69) and ErbB4 binders (B4_50, B4_58) were analyzed in detail, as in these cases inhibition of ELISA signals to less than 50% was already observed with 10 nM (50 nM for E_69) competitor, suggesting a high affinity (cf **Figure 1(d)**). This was confirmed by SPR analysis (see below).

3.7 Clones selected by epitope masking show diverse specificities

Binding and epitope localization of the clones selected by epitope masking were tested by ELISA. All high-affinity ErbB1 and ErbB4 binders were tested for interaction with the respective biotinylated target protein bound to immobilized neutravidin, or the non-biotinylated

target protein bound to the immobilized DARPins (E_01 or B4_02, respectively) used for epitope-masking (**Figure 5(a)** and **5(b)**). In the selection on ErbB1 using an only two-fold excess of E_01, three new high affinity clones were selected. E_69 recognized an epitope not competing with E_01, whereas the other two binders, E_67 and E_68, could not bind to their target immobilized over E_01. In contrast, the clone E_69 was very dominant when performing the same epitope-masking selection in the presence of a much higher excess (20-fold) of the masking DARPin E_01. This finding shows that somewhat higher diversities can be obtained by only partially masking the dominant epitope than by completely blocking it. In contrast, for ErbB4, one of the clones (B4_01) selected on ErbB4 in solution and both of the clones selected by epitope-masking recognized another epitope than B4_02. None of the binders did show cross-reactivity when analyzed in ELISA experiments for binding to other receptors of the ErbB-family (ErbB1, ErbB2 and ErbB4), which share about 50% sequence identity and have highly conserved structures (**Figure 5(b)** and **(c)**). Competition experiments were performed as described for huIgG1_Fc, and ELISA binding signals were inhibited to less than 50% already with 10 nM competitor (50 nM for E_69), suggesting low nanomolar affinities (data not shown). This was confirmed by SPR analysis (see below).

Four well behaved clones for each of the target proteins were further analyzed by SPR (**Table 3** and **Supplementary Figure 2**) and the data were evaluated with a global kinetic fit. Five of the measured binders showed affinities in the picomolar range, and the other binders were all below 15 nM.

In conclusion, dominant epitopes on a target protein may hinder the direct selection of diverse binders. This hidden diversity present in the library can be made accessible, however, by masking the dominant epitope during the selection cycle.

3.8 Epitope removal allows to select more diverse DARPins

To enrich binders against ErbB2 containing all four domains (I – IV) of the extracellular part of the receptor and thus comprising the first 631 amino acid residues of the mature protein

(termed ErbB2-631, see **Table 1**), we performed three initial rounds of selection on target protein in solution. Good enrichment of phage particles displaying DARPins binding to ErbB2-631 but not to ErbB2-509 (see **Table 1**), which only comprises the first 509 amino acid residues of the mature protein and therefore lacks domain IV, was observed after the third selection round as shown by phage ELISA (**Figure 6(a)**). This is in good agreement with previously performed ribosome display selections, where all selected high-affinity binders recognized domain IV, which seems to contain one ore more dominant epitopes of that protein.[18]

We followed two strategies to obtain binders that recognize domain I – III of the target protein. First, we directly performed selections on ErbB2-509. Surprisingly, all of the selection approaches on ErbB2-509, independent of whether the selection had been performed on immobilized target protein or on target protein in solution, failed to yield an enrichment of target specific DARPins. We reasoned that this might be due to a lower stability or higher flexibility of the truncated version of the receptor at room temperature and therefore performed further selections at 4 °C. Indeed, after three rounds of selection on ErbB2-509 by using the optimized selection protocol at 4 °C, target-specific binding of the enriched pools was observed in phage ELISA (**Figure 6(b)**). For the pool of round three, specific binding to both target proteins ErbB2-631 and ErbB2-509 was observed and suggested that target stability is indeed a very important parameter for optimal selections.

After round three, 94 individual DARPins were screened by crude extract ELISA for binding to ErbB2-509, resulting in 83 specific binding signals (**Table 2**). Based on the ELISA signals, 29 binders were sequenced, resulting in a diverse set of 13 different sequences of DARPins. Binders were expressed in the cytoplasm, purified and further analyzed by SEC; they show high-level expression and most of them monomeric elution behavior in SEC, similar to the results obtained for the huIgG1_Fc binders described above.

ELISA experiments showed high specificity (no cross-reactivity with ErbB1 and ErbB4), and inhibition of ELISA signals to less than 50% was observed for more than half of the clones

using 10 nM competitor, suggesting nanomolar affinity (cf **Figure 1(d)**). Three of the binders (9_16, 9_26 and 9_29) were further analyzed by SPR measurements showing affinities in the low nM range (**Table 3**).

The results obtained indicate that, similar to the epitope masking strategy described above, this strategy of removing an epitope by deleting a domain makes the hidden diversity of the library accessible for selection. It also shows that attention must be paid to the conformational integrity of the target protein, in this case by lowering the temperature during selection.

Additionally, as described for ErbB1 and ErbB4, we again partially masked one of the epitopes (see above) on domain IV by adding a two-fold excess of the high affinity DARPin H10-2-G3 (ref. 27) in one round of selection on ErbB2-631. The amplified, partially enriched pool of phage particles after two rounds of selection on the target protein in solution (**Figure 6(a)**) was used as input. Screening of 94 clones by crude extract ELISA resulted in 24 specific binding signals. Based on the ELISA signals 16 binders were sequenced, resulting in eight different sequences of which four had been already found in the selection on ErbB2_509. Of the three new binders two recognized ErbB2-509 as well as ErbB2_631 (domain I-III binders) and one (H_14) recognizes only ErbB2_631 (domain IV binder). Due to its exceptionally high binding signal binder H_14 was further analyzed by SPR measurements and the data were evaluated with a global kinetic fit showing an affinity in the picomolar range (**Table 3**) (C. Jost & A.P., unpublished data).

4. Discussion

4.1 Large functional DARPin library obtained by SRP phage display

The quality of a combinatorial library of binding proteins can be functionally described by the ability to isolate high affinity binders against a broad set of target proteins. Three major factors contribute to successful selections from such a library. First, the library design, which encompasses the scaffold used as well as its diversification strategy employed. Second, the theoretic diversity of the combinatorial DNA library and the percentage of clones that actually have sequences as specified. Finally, the display technology must be able to present all members of the library in a functional form allowing efficient selection. Together, these factors determine the functional diversity of the library which is accessible for the selection of binding molecules.

We have developed SRP phage display that allows the efficient display of fast folding and stable proteins such as DARPins that are partially refractory to conventional phage display that uses Sec dependent translocation of the POI into the periplasm.[19] We generated our phage DARPin library using the previously described combinatorial N3C DARPin library[12,14] as template and a phagemid containing an SRP-dependent signal sequence.[19] Analysis of single unselected members of this new library revealed that all clones that are correct on sequence level are also displayed on the phage particles at levels, comparable to the display yield obtained for a single chain Fv (scFv) antibody fragment using a conventional phagemid. This results in a functional library diversity of at least 1×10^{10} which is within the size reported for the largest phage libraries displaying non-immunoglobulin domains[28] and within the size of large phage libraries displaying antibody fragments.[7]

The functional part of the phage DARPin library is composed of N1C (4%), N2C (27%) and N3C (69%) DARPins as determined from the sequencing and display analysis of unselected clones. The constructs shorter than the N3C are probably side products of the PCR of the initial combinatorial N3C library necessary during construction; this is also regularly observed when

doing ribosome display selections and results from the repetitive nature of DARPins. Interestingly, we even selected N4C and N5C DARPins (**Table 3**). Since no repeat duplication or deletion that would indicate *in vivo* recombination of the DARPin scaffold was ever observed, we expect these longer constructs, just as the shorter ones to be already present to a low extent in the initial library. Since the selection for binding works well, as demonstrated by the successful selection against diverse targets, the occurrence of DARPins with a different number of repeats, (presumably) already in the initial library, can be seen as a source of additional diversity. A larger contiguous patch of randomized residues in the DARPins with more than three randomized repeats may allow binding to additional epitopes, where contacts by residues in the capping repeats might not have been favorable or where a larger binding surface is needed. An accumulation of these longer constructs during selections with epitope masking supports this theory.

In just two to three phage display selection rounds we were able to select high affinity binders against a broad range of target proteins without a single failure (**Table 2**). This validates the high functional library diversity and the optimized diversity design of the DARPin scaffold, and that SRP phage display is robust to select specific binders from this library. Good performance of SRP phage display was recently also reported for the display of a library based on the fibronectin type III domain.[29] We suppose that SPR phage display could increase the functional diversity of many other libraries, especially those expected to be composed of similarly stable and fast folding scaffolds or those containing members with widely different folding rates and stabilities, such as expected e.g., in cDNA libraries.

It should be noted that also for SRP phage display, as reported for conventional phage display,[30] it might be necessary to optimize the phagemid in combination with the scaffold used, in order to tune the expression level to achieve efficient but still monovalent display of the POI.

4.2 Selected DARPins have favorable biophysical properties

The selected DARPins retain the favorable biophysical properties of the initial library members.[12] They can be expressed in large amounts in soluble form in the cytoplasm of *E. coli* (**Figure 1(b)**), and routinely more than 100 mg protein is purified per one liter of shake-flask culture. Of the 84 clones analyzed by SEC, 46 (55 %) show a single peak at the elution volume expected for the monomer (**Figure 2**) and another 10 (12%) show a single peak at a too high elution volume, indicating interaction with the column material but were confirmed to be monomeric by SEC-MALS measurements. The other DARPins are presumably a mixture of monomer and dimer or elute at higher apparent molecular weight, indicating oligomerization or partial unfolding. Because of the broad diversity of clones isolated for each target, purely monomeric tight binding DARPins have always been found.

The selected clones specifically recognize the target protein which they were selected on and do not cross-react with other proteins tested as shown by ELISA (**Figure 5(c)** and **5(d)**), and these ELISAs were always carried out with recloned non-fused protein, and thus independent of being fused to the phage coat protein 3 or being displayed on phage particles.

4.3 DARPins with picomolar affinities were selected on a regular basis

The highest affinities of the selected binders are in the sub-nanomolar range (**Table 3**) and thus as good as the affinities obtained when performing ribosome display selections with the identical initial DARPin library.[14,15,16] There are several factors which may contribute to this, at first, surprising observation. First, the functional size of the present phage library is very large, and is expected to cover the diversity of 10^{10} members present in the initial ribosome display library[14] which was used as template. Therefore, the same input library will be sampled in ribosome display and phage display. Second, by the construction of the phage library, which involved PCR steps, also some additional variation has been introduced — and some may have existed already at the level of the synthetic individual modules — , as can be seen by the framework mutations regularly obtained in the selected clones. We have no evidence that these

would have been introduced during the selection and propagation steps in *E. coli*. Third, a growing experience in designing selection experiments, as summarized in the optimized selection protocol, may improve the quality of the selected clones. Ribosome display does allow, however, a seamless integration of additional randomization and affinity maturation steps, should they be needed.[4,27]

From the comparison of affinities obtained form various antibody libraries, it is widely accepted that the affinities of the selected antibodies correlate with the size of the library.[7] From phage antibody fragment libraries containing 10^7 to 10^9 members, affinities of up to 10 nM, and for libraries with over 5 x 10^9 members, sub-nanomolar affinities have been selected.[7] From our phage DARPin library containing about 10^{10} functional members we obtained against all target proteins multiple DARPins with affinities in the low nanomolar or, in most cases, even the sub-nanomolar range (**Table 3**). These affinities compare very favorably with those obtained for synthetic antibody repertoires of similar or even larger size.[8,9,10,31] Our very promising results can be attributed to the optimized diversity design of the DARPin library as well as the high functional display rate of the SRP phage display system. This will make affinity maturation for most applications unnecessary.

4.4 Broadening diversity of selected DARPins by epitope masking or removal

One frequently observed phenomenon in phage display when performing selection experiments on certain target proteins is low diversity and narrow specificity of the selected binders, even when using large libraries (e.g. ref. 8, 32, 33, 34). Different to ribosome display, where due to the generation of mutations during the selections, low affinity binders may stochastically acquire mutations that make them survive selection rounds with high stringency, and thus, different binder families can be obtained in parallel experiments.[35] In phage display, where the library is "static", there are many reasons why a certain binder might be selected with preference and dominate the selected pool: for example, (i) the binder has much higher affinity than the other binders; (ii) the binder is more efficiently displayed than the other binders, (iii) the

target protein contains a preferred binding site on its surface[33] or (iv) there are only limited epitopes on the target protein accessible to potential binders. When performing selections on the receptors of the ErbB family we obtained binders with low diversity and/or narrow specificity, suggesting that some epitopes in this family appear to be very well suited for the DARPin binding interface such that they dominated the selection. The dominant DARPin E_01 was also shown to be displayed at slightly higher levels than other library members (data not shown) and both E_01 and B4_02 have very high affinities, indicating that also point (i) and (ii) can influence the selection of DARPins by phage display. Note that a much broader diversity was obtained for other targets (TNFα, huIgG1_Fc, CitS[36] and others, data not shown). We followed several strategies to increase the diversity of the selected DARPins and to broaden the range of selected specificities.

For ErbB1, where essentially only one binder was found in the primary selections, and for ErbB4, where one binder was very dominant (**Table 2**), we performed one round of selection on the target protein in the presence of a two-fold excess of the purified dominant binder using pools of phage particles partially enriched on the target protein as input. This strategy of epitope-masking was recently described for antibodies.[37,38] In both cases this approach resulted in increased diversity and specificity of the binders (**Figure 6**). For ErbB1, two of the three further analyzed clones still bound to the same or an overlapping epitope than the binder used for epitope-masking. This is presumably due to the low, two-fold excess of competitor used, leading only to a partial masking of the epitope, and thus making it possible to find binders to the same domain.

For the full-length ectodomain of ErbB2 (ErbB2-631), the selection yielded a pool of binders that only recognize this full length ectodomain but not a truncated construct lacking domain IV (**Figure 6(a)**). Therefore, we performed selections on the truncated version. Probably due to the lower stability of ErbB2-509, selections on this target protein were only successful at low temperature. They yielded a pool of binders recognizing ErbB2-631 as well as ErbB2-509

(**Figure 6(b)**). Therefore, both strategies, epitope-masking and epitope removal, were successfully applied, and combining such binders recognizing different epitopes would give the possibility of constructing multivalent binders for a given target protein.

4.5 Conclusions

We have validated our phage DARPin library by successfully selecting well-behaved and high affinity binders against a broad range of target proteins. The SRP phage display used within this work has thus proven to be a powerful method to display libraries of fast folding and stable DARPins that would be refractory to conventional phage display using the Sec secretion pathway. Therefore we envision that this novel phage display method may also be beneficial for other libraries containing stable and fast folding proteins. The addition of phage display to the selection repertoire for the generation of specific DARPins further expands the application range of this novel class of binding molecules.

5. Materials and Methods

5.1 Materials

All chemicals were of highest quality and purchased from Fluka (Switzerland) unless stated otherwise. Oligonucleotides were from Microsynth (Switzerland). Vent DNA polymerase, restriction enzymes and buffers were from New England Biolabs (USA) or Fermentas (Lithuania). Helper phage VCS M13 was from Stratagene (USA). All cloning and phage amplification was performed in *E. coli* XL1-Blue from Stratagene (USA).

5.2 Molecular biology

Unless stated otherwise, all molecular biology methods were performed according to standard protocols.[39]

5.3 Phagemid and expression vectors

The phagemid pPDV1 (**Supplementary Figure 1**) is related to pDST23 (ref. 19) and comprises following features: (i) the signal sequence of *E. coli* DsbA (DsbAss) ensures efficient SRP phage display; (ii) sequences for display are inserted in the multiple cloning site (MCS) between the DsbAss and the coding sequence of the C-terminal domain (amino acids 250-406) of protein 3 (p3) of filamentous phage M13; (iii) the fusion protein (p3 fusion) is under the control of a *lac* promoter/operator element and the *lacI*^{q} gene provides high levels of the lac repressor in *cis*; (iv) an amber stop codon (TAG) is interposed between the displayed sequence and the C-terminal domain of p3; (v) the fusion protein contains a Flag-tag; (vi) the vector carries a f1 origin of replication to permit production of virions using an appropriate helper phage, such as VCS M13; and (vii) the vector has a plasmid origin (ColE1 *ori*) and an antibiotic resistance marker (the gene for chloramphenicol acetyl transferase (*cat*) providing resistance to chloramphenicol (cam)) to allow propagation as a plasmid in *E. coli.*

The vector pDST67 was used for high-level, soluble cytoplasmic expression of the selected DARPins containing an N-terminal MRGS$(H)_6$ tag. pDST67 is a derivative of pQE30 (QIAgen) in which the single amber stop codon (TAG) after the *Hind*III restriction site has been replaced by a double stop codon (TAA TGA), avoiding the formation of a read-through product when using suppressor *E. coli* strains such as XL1-Blue. pDST67 was generated via PCR cloning using the oligonucleotides oDST29 (5'-GGCCAAGCTTAATTAATGACTGAGCTTGGACTCCTG-3') and oDST30 (5'-AAAGCCAAGCTAGCTTGGATTCTC-3') and pQE30 as template. The resulting PCR product was *Hid*III/*Nhe*I digested and ligated into the identically treated and dephosphorylated pQE30 vector. Coding sequences of the selected DARPins were cloned into pDST67 via *BamH*I/*Hind*III yielding pDST67_(DARPin Name). Protein expression and purification was done as described below.

The vector pAT223 (GenBank accession number AY327138) was used for the expression of fusion proteins with an N-terminal avi-tag for in vivo biotinylation, followed by phage lambda protein D (pD) as fusion protein, followed by a His_6-tag for IMAC purification and then the protein of interest, e.g. a DARPin to be biotinylated and immobilized. Coding sequences of the selected DARPins E_01 and B4_02 were cloned into pAT223 via *BamH*I/*Hind*III, yielding pDST126 and pDST127, respectively. Protein production, purification and confirmation of biotinylation was done as described.[15]

5.4 Library construction

The N3C DARPin library in the ribosome display format[12] was PCR amplified using primers introducing a *BamH*I and *Hind*III site (EWT3 and WTC4, ref. 14), enabling subsequent subcloning into phagemid pPDV1. Two hundred PCR reactions of 50 µl yielded about 600 µg of purified PCR product that was ligated after restriction digest of the components using *BamH*I and *Hind*III into pPDV1. About 300 µg of ligated and purified DNA were first transformed by electroporation into MP1 cells (*E. coli* strain MC1061 (ref. 40) containing the F episome

transferred from XL1-blue cells) as these cells can be very efficiently transformed,[41] yielding 3.6×10^{10} independent colonies. From these cells the plasmid DNA was isolated and re-transformed into XL1-blue cells, for subsequent phage production, yielding 2.6×10^{10} independent colonies. The transformed XL1-blue cells were infected with helper phage VCS M13 and IPTG was subsequently added to the culture to induce the expression and thus the display of the DARPins, thereby producing the phage particles of the phage DARPin library. The DARPin displaying phage particles were PEG-precipitated from the culture supernatant, resuspended in PBS (137 mM NaCl, 3 mM KCl, 8 mM Na_2HPO_4, 1.5 mM KH_2PO_4, pH 7.4) containing 10% glycerol, aliquoted and stored at -80 °C. They were found to be stable for at least one year.

5.5 Library characterization

To determine the percentage of transformed clones encoding functional DARPins, 55 randomly picked clones were sequenced using standard techniques. To analyze the fraction of DARPin-p3 fusion proteins displayed, phage particles produced form the 55 sequenced clones were analyzed by western blotting as described,[19] using the anti-FLAG antibody M1 (Sigma, USA) for detection. Phage particles displaying a scFv, known to be well displayed using a conventional phagemid were used as a reference (phage particles produced form phagemid pDST24, ref. 19). To quantify the percentage of DARPins showing high level, soluble cytoplasmic expression, a pool of DARPin inserts from the phage library was subcloned into pDST67 via *Bam*HI/*Hind*III. Small scale expression and 15% SDS-PAGE analysis of 57 randomly picked clones which were not sequenced was performed.

5.6 Target proteins

Purified target proteins were used for all experiments and are described in detail in **Table 1**. ErbB receptors were kindly provided by Dr. Tim Adams and coworkers (CSIRO, Melbourne, Australia). The Fc domain of human IgG1 was purchased from R&D Systems, UK. For

immobilization, aliquots of these target proteins (200 µg to 600 µg) were chemically biotinylated using EZ-Link Sulfo-NHS-SS-Biotin (Pierce, USA). Due to the size difference of the target proteins a variable molar excess of the biotinylating reagent relative to the target protein was used (4-fold for huIgG1_Fc, 9-fold for ErbB1, 6-fold for ErbB2-509, 6-fold for ErbB2-631 and 9-fold for ErbB4). Reaction conditions were used according to the supplier's manual (Pierce, USA). Successful biotinylation was confirmed by ELISA and Western blotting experiments, the extent of biotinylation was not quantified.

Non-biotinylated and biotinylated TNFα, shown to be biologically active was expressed and purified from *E. coli* (C. Zahnd and A.P., unpublished data). In brief, human TNFα was amplified using the primers rTNFstopHind (5'-GATGAGAAGCTTTCATTACAGGGCAATGATCCCAAAG-3') and fTNFa (5'-CACCACCATGGCTGTCAGATCATCTTCTCGAAC-3'). The resulting PCR product was *Nco*I and *Hind*III digested and ligated into the identically treated and dephosphorylated vector pAT222 (GenBank accession number AY327137), yielding the construct with an N-terminal Avi-tag[21] used for the expression of biotinylated TNFα and into pQE60 (QIAgen) vector yielding the construct with no tag used for the expression of non-biotinylated TNFα. For biotinylation, the biotin-ligase BirA of *E. coli* was cotransformed and co-expressed with the Avi-tagged construct in *E. coli* XL1-Blue to yield *in vivo* biotinylated TNFα as described[21]. The biotinylated TNFα was purified, *via* a monomeric avidin column. To allow intermolecular disulfide bond formation, the soluble protein was dialyzed against TBS (20 mM Tris, 150 mM NaCl, pH 7.6) containing 1 mM reduced glutathione (GSH) and 0.2 mM oxidized glutathione (GSSG). The trimeric species was obtained by preparative gel filtration in using TBS as running buffer. The TNFα construct with no tag was expressed in *E. coli* XL1-Blue, purified via a cationic exchange column using washing buffer (100 mM MES, pH 5.8) with a NaCl gradient from 150 mM to 1 M, followed by a dialysis step against the same GSH/GSSG buffer mentioned above and subsequent preparative gel filtration. The biological activity of both constructs was

shown by their cytolytic activity on L929 mouse fibroblast cells (ATTC, USA) and compared to commercial TNFα.

5.7 Immobilization of target proteins

Target proteins had to be immobilized for selection and ELISA experiments. To avoid partial protein denaturation of the target proteins that may result from direct immobilization on solid plastic (i.e. polystyrene) surfaces, biotinylated target proteins were bound to neutravidin or streptavidin, which had been directly immobilized on a solid plastic surface, as follows: neutravidin (66 nM, 100 µl/well, Pierce, USA) or streptavidin (66 nM, 100 µl/well Sigma, Switzerland) in PBS was immobilized on MaxiSorp plates (Nunc, Denmark) by overnight incubation at 4 °C. The wells were blocked with 300 µl PBSTB (PBS containing 0.1% Tween-20, 0.2% BSA) for 1 h at RT. Binding of the biotinylated target proteins (100 µl, ~ 100 nM for selection and ~ 20 nM for ELISA) in PBSTB was allowed to occur for 1 h at 4 °C.

For the first selection round on immobilized target protein, requiring larger volumes, neutravidin (66 nM, 4 ml/tube) in PBS was immobilized on MaxiSorp Immunotubes (Nunc, Denmark) by overnight incubation at 4 °C. The tubes were blocked with 4 ml PBSTB for 1 h at RT. Binding of the biotinylated target proteins (4 ml, ~ 100 nM) in PBSTB was allowed to occur for 1 h at 4 °C.

For selections on immobilized target protein, neutravidin and streptavidin were used alternately in selection rounds to avoid selection of binders against these proteins.

5.8 Selection of phage DARPins

Unless stated otherwise, all steps of the phage display selection were carried out at room temperature. Selection rounds were performed either on biotinylated target protein in solution with subsequent capturing on streptavidin-coated magnetic beads (referred to as: “target protein in solution”) or on biotinylated target protein bound to neutravidin or streptavidin, which had been directly immobilized on a solid plastic surface (referred to as: “immobilized target

protein"), as described below. Very good results were obtained when performing the first selection round of selection on immobilized target protein, presumably because of the greater efficiency of capturing binders —especially important in the first round —, followed by further rounds on target protein in solution, presumably because of the lower enrichment of background binders (for the optimized selection protocol, see **Supplementary Material**). Protocols were adapted from ref. 42.

5.9 Selection on target proteins in solution

When the first selection cycle was done in solution, about 2.5 x 10^{13} phage particles of the phage DARPin library were incubated for 1 hour with 100 nM biotinylated target protein in 2 ml PBSTB for the first round of selection. In subsequent selection rounds, about 10^{12} phage particles were used (see below). The phage-antigen complexes were then captured on 100 µl streptavidin-coated paramagnetic beads (10 mg/ml, Dynabeads MyOne Streptavidin T1, Dynal) for 20 min. After washing the beads eight times with PBST (PBS, 0.1% Tween-20) the phage particles were eluted with 200 µl of 100 mM triethylamine (Et_3N, pH not adjusted) for 6 min, followed by 200 µl of 100 mM glycine-HCl, pH 2, for 10 min. Eluates were neutralized with 100 µl of 1 M Tris-HCl, pH 7, or 18 µl of 2 M Tris-base, respectively, combined and used to infect 5 ml of exponentially growing *E. coli* XL1-Blue cells. After shaking for 1 hour at 37 °C, cells were expanded into 50 ml of fresh 2YT medium (5 g NaCl, 10 g yeast extract, 16 g tryptone per liter) containing 10 µg/ml cam and incubated at 37 °C with shaking. After a maximum of 5 h (shorter times if OD_{600} = 0.5 was reached earlier), isopropyl-β-D-thiogalactoside (IPTG) was added to a final concentration of 0.2 mM and 15 minutes later the phage library was rescued by infection with VCS M13 helper phage at 10^{10} pfu (plaque forming units) per ml (multiplicity of infection ~ 20). Cells were grown overnight at 37 °C without the addition of kanamycin. Cells were removed by centrifugation (5600 g, 4 °C, 10 min) and 40 ml of the culture supernatant was incubated on ice for 1 hour with one-fourth volume of ice-cold PEG/NaCl solution (20 %

polyethyleneglycol (PEG) 6000, 2.5 M NaCl). The precipitated phage particles were then collected by centrifugation (5600 g, 4 °C, 15 min) and redissolved in 2 ml of PBS and used for the second round of selection.

For the subsequent selection rounds, about 10^{12} of the amplified phage particles were used as input and incubated with 100 µl of streptavidin-coated paramagnetic beads for 1 h to remove unspecific and streptavidin binding phage particles. After removing the beads, phage particles were incubated for 1 hour with 100 nM biotinylated target protein, complexes were captured on fresh beads, beads were washed 12 times with PBST, phages eluted with 400 µl of 100 mM glycine-HCl, pH 2, for 10 min, the eluate neutralized with 36 µl of 2 M Tris-base and phage particles amplified and purified as described above.

After three rounds, enrichment of phage particles displaying DARPins binding specifically to the target protein was monitored by phage ELISA. About 5 x 10^{10} phage particles (estimated spectrophotometically[43]) of the initial library and the amplified pools of each selection round were pipetted to wells with and without immobilized target protein and incubated at RT for 2 h. After washing the wells four times with 300 µl of PBST, bound phage particles were detected with mouse anti-M13 antibody horseradish peroxidase conjugate (Amersham Pharmacia Biotech, UK) and soluble BM Blue peroxidase (POD) substrate (Roche Diagnostics, Germany).

5.10 Selection on immobilized target proteins

For the first selection cycle about 3.5 x 10^{13} phage particles of the phage DARPin library were added to an immunotube containing the immobilized target protein (biotinylated target protein bound to neutravidin, which had been directly immobilized on the solid plastic surface) and incubated with rotation for 2 h. After rinsing the tube ten times with PBST, the phage particles were eluted with 500 µl of 100 mM Et_3N (pH not adjusted) for 6 min, followed by 500 µl of 100 mM glycine-HCl, pH 2, for 10 min. Eluates were neutralized with 250 µl of 1 M Tris-

HCl, pH 7, or 45 µl of 2 M Tris-base, respectively, combined and used to infect 13 ml of exponentially growing *E. coli* XL1-Blue cells. After shaking for 1 hour at 37 °C cells were expanded into 130 ml of fresh 2YT medium containing 10 µg/ml chloramphenicol (cam) and incubated at 37 °C with shaking. Phage amplification and precipitation was done as described above.

In the subsequent selection rounds about 10^{12} of the amplified phage particles were first incubated in a blocked immunotube (coated either with neutravidin or streptavidin used for immobilization of the target protein in the previous round of selection and BSA) one hour to remove neutravidin, streptavidin or unspecific binding phage particles. For the binding selection the phage particles were incubated for one hour in four wells containing the immobilized biotinylated target protein (directly coated neutravidin or streptavidin were alternately used in subsequent selection rounds). The wells were washed 12 times with PBST, phages eluted from each well with 100 µl of 100 mM glycine-HCl, pH 2, for 10 min, the combined eluates neutralized with 36 µl of 2 M Tris-base and phage particles amplified and purified as described above. After three rounds, enrichment was determined by phage ELISA as described above.

5.11 Selection with epitope-masking

The respective DARPins used for the epitope masking were expressed in 50 ml shake flask cultures and purified by IMAC as previously described.[12] Pools of phage particles already partially enriched for binders against the respective target protein (1-2 rounds of selection on the target protein alone as described above) were used as input. Biotinylated target protein (100 nM) was pre-incubated for 1 hour with the respective DARPin (200 nM or 2 µM) prior to performing a standard selection round on soluble target protein as described above. After one round of selection with epitope-masking, amplified phage particles were analyzed by phage ELISA. Binding to immobilized target protein alone and in the presence of an excess of the respective DARPin (2 µM) used for epitope-masking was done as described above.

5.12 Screening of single clones

From the selected phage pools showing specific binding to the respective target protein the DNA fragments encoding the DARPin inserts were subcloned into the expression vector pDST67 via *Bam*HI/*Hind*III.

Single selected DARPins were expressed in 96-deep-well plates. In brief, 1.2 ml of 2YT medium containing 1 % glucose and 50 µg/ml ampicillin was inoculated with a single, randomly picked colony of *E. coli* XL1-Blue harboring pDST67 encoding one of the respective selected DARPins and incubated overnight at 37 °C with shaking. Fresh 2YT medium (1.1 ml) containing 50 µg/ml ampicillin was inoculated with 100 µl of the overnight culture. After incubation at 37 °C for 1-2 h with shaking, 100 µl of 6.5 mM IPTG in 2YT were added to each well and protein expression was continued for 4 hours. Cells were harvested by centrifugation, resuspended in 50 µl B-PER II (Pierce, USA) by vigorous shaking for 20 min at room temperature. Then, 950 µl PBSTB was added and cell debris removed from the crude extract by centrifugation.

For the ELISA, 10 µl to 100 µl of the above crude extracts were applied to wells with or without immobilized target protein and incubated at RT for 1 h. After washing the wells three times with 300 µl PBSTB, wells were incubated with an anti RGS-His antibody (QIAgen, Germany) (1:5,000 in PBSTB, 1 h at RT), as primary antibody. A goat anti–mouse IgG alkaline phosphatase conjugate (Sigma, USA) (1:10,000 in PBSTB, 1 h at RT) was used as secondary antibody. The bound DARPins were detected with the substrate di-sodium 4-nitrophenyl phosphate (pNPP, 3 mM) (Fluka, Switzerland) in buffer containing 50 mM $NaHCO_3$ and 50 mM $MgCl_2$ (**Figure 1(b)**).

5.13 96 well purification of DARPins

Selected DARPins identified as binders were expressed 96-deep well plates as described above. Eight plates containing fresh 2YT medium were inoculated in parallel with the overnight

culture, resulting in a total expression culture volume of about 10 ml for each clone. Cells were lysed as described above, the 400 µl B-Per II lysates for each clone were pooled and 400 µl of TBS_{500} (50 mM Tris/HCl, pH 8, 500 mM NaCl), containing 20% glycerol and 40 mM imidazol, were added. After centrifugation the cleared lysates were used for the 96-well IMAC purification (SwellGel Nickel Chelated Discs, 96-well filter plate, Pierce, USA) according to the supplier's manual, yielding on average more than 1 mg of > 95% pure protein for each clone. Purified proteins were used for all further expereiments.

5.14 Analytical size-exclusion chromatography (SEC)

All IMAC-purified DARPins were analyzed at 10 µM concentration on a Superdex 75 gel-filtration column (Amersham Pharmacia Biotech, USA) using a Pharmacia SMART system at a flow-rate of 60 µl/min and with PBS as running buffer (**Figure 2**). Phage protein D (gpD) with an apparent mass of 17.6 kDa and phage protein SHP, a trimer with and apparent mass of 50.2 kDa were used as molecular mass standards.

A subset of DARPins showing too high or too low elution volume in SEC were further analyzed by SEC multi-angle light scattering (SEC-MALS) measurements as recently described.[36]

5.15 Competition ELISA measurements

Biotinylated target proteins were bound to neutravidin, which had been directly immobilized on a MaxiSorp plate as described above. For competition, purified DARPins were incubated with varying amounts of non-biotinylated target protein present before (1 h at RT) and during the binding reaction (12 min at RT). After washing the wells three times with 300 µl PBSTB, wells were incubated with an anti RGS-His antibody horseradish peroxidase conjugate (QIAgen, Germany) (1:5,000 in PBSTB, 1 h at RT) and the bound DARPins were detected with soluble BM Blue POD substrate (Roche Diagnostics, Germany).

5.16 Epitope mapping by ELISA

Biotinylated target proteins as well as biotinylated DARPin-pD fusions (see above) were bound to neutravidin, which had been directly immobilized on a MaxiSorp plate as described above. To the wells with immobilized DARPin-pD fusions the respective non-biotinylated target protein (100 µl, ~ 20 nM) in PBSTB was added for binding for 1 h at 4 °C. Purified non-biotinylated DARPins (100 µl, ~ 50 nM) were used for the binding reaction (1 h at RT) and detection of bound DARPins was performed as described for the ELISA using crude cell extracts (see above).

5.17 Surface plasmon resonance (SPR)

SPR was measured by using a BIAcore 3000 instrument (BIAcore, Sweden). All measurements were performed in HBST buffer (20 mM HEPES, 150 mM NaCl, 3 mM EDTA pH 7.4, 0.005% Tween-20) at a flow rate of 50 µl/min throughout. The following amounts of biotinylated target protein described in **Table 1** were immobilized on SA chips (BIAcore): ErbB1 (1000 RU), ErbB2-509 (400 RU), ErbB4 (600 RU), huIgG1_Fc (500 RU). For the determination of kinetic data, the interactions were measured as follows: five minutes initial buffer flow, followed by a 2 to 15 min injection of DARPin at different concentrations (1 nM to 250 nM) and a final off-rate measurement of 10 to 75 minutes with buffer flow. The signal of an uncoated reference cell and buffer response was always subtracted from the sensograms (double referencing). The kinetic data of the interaction were evaluated with a global fit using Scrubber 2 (BioLogic Software Ltd, USA). All sensograms are shown in the **Supplementary Figure 2**.

6. Acknowledgment

We thank Dr. Michael T. Stumpp for valuable discussions and sequence analysis of selected DARPins, Dr. H. Kaspar Binz for the PCR amplification of the DARPin library, Christian Jost for providing affinity data of ErbB2-631 binder H_14 and for help with ErbB2 binder characterization, Thomas Huber for SEC-MALS measurements and Dr. Christian Zahnd and Dr. Tim Adams for providing target proteins. This work was supported by the Swiss National Center of Competence in Research (NCCR) in Structural Biology and in part by KTI Discovery.

7. References

1. Binz, H.K., Amstutz, P. & Plückthun, A. Engineering novel binding proteins from nonimmunoglobulin domains. *Nat. Biotechnol.* **23**, 1257-1268 (2005).
2. Hoogenboom, H.R. Selecting and screening recombinant antibody libraries. *Nat. Biotechnol.* **23**, 1105-1116 (2005).
3. Sergeeva, A., Kolonin, M.G., Molldrem, J.J., Pasqualini, R. & Arap, W. Display technologies: Application for the discovery of drug and gene delivery agents. *Advanced Drug Delivery Reviews, 2006 Supplementary Non-Thematic Collection* **58**, 1622-1654 (2006).
4. Zahnd, C., Amstutz, P. & Plückthun, A. Ribosome display: selecting and evolving proteins in vitro that specifically bind to a target. **4**, 269-279 (2007).
5. Smith, G.P. & Petrenko, V.A. Phage Display. *Chem. Rev.* **97**, 391-410 (1997).
6. Smith, G.P. & Scott, J.K. Libraries of peptides and proteins displayed on filamentous phage. *Methods Enzymol.* **217**, 228-257 (1993).
7. Ling, M.M. Large antibody display libraries for isolation of high-affinity antibodies. *Comb Chem High Throughput Screen* **6**, 421-432 (2003).
8. Vaughan, T.J., Williams, A.J., Pritchard, K., Osbourn, J.K., Pope, A.R., Earnshaw, J.C., McCafferty, J., Hodits, R.A., Wilton, J. & Johnson, K.S. Human Antibodies with Sub-nanomolar Affinities Isolated from a Large Non-immunized Phage Display Library. **14**, 309-314 (1996).
9. Hoet, R.M., Cohen, E.H., Kent, R.B., Rookey, K., Schoonbroodt, S., Hogan, S., Rem, L., Frans, N., Daukandt, M., Pieters, H., van Hegelsom, R., Neer, N.C.-v., Nastri, H.G., Rondon, I.J., Leeds, J.A., Hufton, S.E., Huang, L., Kashin, I., Devlin, M., Kuang, G., Steukers, M., Viswanathan, M., Nixon, A.E., Sexton, D.J., Hoogenboom, H.R. & Ladner, R.C. Generation of high-affinity human antibodies by combining donor-derived and synthetic complementarity-determining-region diversity. **23**, 344-348 (2005).
10. Sheets, M.D., Amersdorfer, P., Finnern, R., Sargent, P., Lindquist, E., Schier, R., Hemingsen, G., Wong, C., Gerhart, J.C. & Marks, J.D. Efficient construction of a large nonimmune phage antibody library: the production of high-affinity human single-chain antibodies to protein antigens. *Proc. Natl. Acad. Sci. U. S. A.* **95**, 6157-6162 (1998).
11. Forrer, P., Stumpp, M.T., Binz, H.K. & Plückthun, A. A novel strategy to design binding molecules harnessing the modular nature of repeat proteins. *FEBS Lett.* **539**, 2-6 (2003).
12. Binz, H.K., Stumpp, M.T., Forrer, P., Amstutz, P. & Plückthun, A. Designing repeat proteins: Well-expressed, soluble and stable proteins from combinatorial libraries of consensus ankyrin repeat proteins. *J. Mol. Biol.* **332**, 489-503 (2003).
13. Forrer, P., Binz, H.K., Stumpp, M.T. & Plückthun, A. Consensus design of repeat proteins. *Chembiochem* **5**, 183-189. (2004).
14. Binz, H.K., Amstutz, P., Kohl, A., Stumpp, M.T., Briand, C., Forrer, P., Grütter, M.G. & Plückthun, A. High-affinity binders selected from designed ankyrin repeat protein libraries. *Nat. Biotechnol.* **22**, 575-582 (2004).
15. Amstutz, P., Binz, H.K., Parizek, P., Stumpp, M.T., Kohl, A., Grütter, M.G., Forrer, P. & Plückthun, A. Intracellular kinase inhibitors selected from combinatorial libraries of designed ankyrin repeat proteins. *J. Biol. Chem.* **280**, 24715-24722 (2005).
16. Amstutz, P., Koch, H., Binz, H.K., Deuber, S.A. & Plückthun, A. Rapid selection of specific MAP kinase-binders from designed ankyrin repeat protein libraries. *Protein Eng. Des. Sel.* **19**, 219-229 (2006).
17. Kawe, M., Forrer, P., Amstutz, P. & Plückthun, A. Isolation of Intracellular Proteinase Inhibitors Derived from Designed Ankyrin Repeat Proteins by Genetic Screening. *J. Biol. Chem.* **281**, 40252-40263 (2006).

18. Zahnd, C., Pecorari, F., Straumann, N., Wyler, E. & Plückthun, A. Selection and Characterization of Her2 Binding-Designed Ankyrin Repeat Proteins. *J. Biol. Chem.* **281**, 35167-35175 (2006).
19. Steiner, D., Forrer, P., Stumpp, M.T. & Plückthun, A. Signal sequences directing cotranslational translocation expand the range of proteins amenable to phage display. *Nat. Biotechnol.* **24**, 823-831 (2006).
20. Russel, M., Lowman, H.B. & Clackson, T. in Phage Display: A Practical Approach. (eds. H.B. Lowman & T. Clackson) 1-26 (Oxford University Press, New York, USA; 2004).
21. Cull, M.G. & Schatz, P.J. Biotinylation of proteins in vivo and in vitro using small peptide tags. *Methods Enzymol.* **326**, 430-440 (2000).
22. Rigby, W.F. Drug insight: different mechanisms of action of tumor necrosis factor antagonists-passive-aggressive behavior? *Nat Clin Pract Rheumatol* **3**, 227-233 (2007).
23. Goffe, B. & Cather, J.C. Etanercept: An overview. *J. Am. Acad. Dermatol.* **49**, 105-111 (2003).
24. Hynes, N.E. & Lane, H.A. ERBB receptors and cancer: the complexity of targeted inhibitors. *Nat Rev Cancer* **5**, 341-354 (2005).
25. Burgess, A.W., Cho, H.S., Eigenbrot, C., Ferguson, K.M., Garrett, T.P., Leahy, D.J., Lemmon, M.A., Sliwkowski, M.X., Ward, C.W. & Yokoyama, S. An open-and-shut case? Recent insights into the activation of EGF/ErbB receptors. *Mol. Cell* **12**, 541-552 (2003).
26. Ditzel, H.J. Rescue of a broader range of antibody specificities using an epitope-masking strategy. *Methods Mol. Biol.* **178**, 179-186 (2002).
27. Zahnd, C., Wyler, E., Schwenk, J.M., Steiner, D., Lawrence, M.C., McKern, N.M., Pecorari, F., Ward, C.W., Joos, T.O. & Plückthun, A. A Designed Ankyrin Repeat Protein Evolved to Picomolar Affinity to Her2. *J. Mol. Biol.* **369**, 1015-1028 (2007).
28. Silverman, J., Lu, Q., Bakker, A., To, W., Duguay, A., Alba, B.M., Smith, R., Rivas, A., Li, P., Le, H., Whitehorn, E., Moore, K.W., Swimmer, C., Perlroth, V., Vogt, M., Kolkman, J. & Stemmer, W.P. Multivalent avimer proteins evolved by exon shuffling of a family of human receptor domains. *Nat. Biotechnol.* **23**, 1556-1561 (2005).
29. Koide, A., Gilbreth, R.N., Esaki, K., Tereshko, V. & Koide, S. High-affinity single-domain binding proteins with a binary-code interface. *PNAS* **104**, 6632-6637 (2007).
30. Krebber, A., Burmester, J. & Plückthun, A. Inclusion of an upstream transcriptional terminator in phage display vectors abolishes background expression of toxic fusions with coat protein g3p. *Gene* **178**, 71-74 (1996).
31. Knappik, A., Ge, L., Honegger, A., Pack, P., Fischer, M., Wellnhofer, G., Hoess, A., Wölle, J., Plückthun, A. & Virnekäs, B. Fully synthetic human combinatorial antibody libraries (HuCAL) based on modular consensus frameworks and CDRs randomized with trinucleotides. *J. Mol. Biol.* **296**, 57-86 (2000).
32. Krebs, B., Rauchenberger, R., Reiffert, S., Rothe, C., Tesar, M., Thomassen, E., Cao, M., Dreier, T., Fischer, D., Hoss, A., Inge, L., Knappik, A., Marget, M., Pack, P., Meng, X.Q., Schier, R., Sohlemann, P., Winter, J., Wölle, J. & Kretzschmar, T. High-throughput generation and engineering of recombinant human antibodies. *J. Immunol. Methods* **254**, 67-84. (2001).
33. DeLano, W.L., Ultsch, M.H., de Vos, A.M. & Wells, J.A. Convergent Solutions to Binding at a Protein-Protein Interface. *Science* **287**, 1279-1283 (2000).
34. Dennis, M.S., Zhang, M., Meng, Y.G., Kadkhodayan, M., Kirchhofer, D., Combs, D. & Damico, L.A. Albumin binding as a general strategy for improving the pharmacokinetics of proteins. *J. Biol. Chem.* **277**, 35035-35043 (2002).
35. Hanes, J., Jermutus, L., Weber-Bornhauser, S., Bosshard, H.R. & Plückthun, A. Ribosome display efficiently selects and evolves high-affinity antibodies in vitro from immune libraries. *PNAS* **95**, 14130-14135 (1998).

36. Huber, T., Steiner, D., Röthlisberger, D. & Plückthun, A. In vitro selection and characterization of DARPins and Fab fragments for the co-crystallization of membrane proteins: The Na^+-citrate symporter CitS as an example. *J. Struct. Biol.* **159**, 206-221 (2007).
37. Ditzel, H., Binley, J., Moore, J., Sodroski, J., Sullivan, N., Sawyer, L., Hendry, R., Yang, W., Barbas, C., 3rd & Burton, D. Neutralizing recombinant human antibodies to a conformational V2- and CD4-binding site-sensitive epitope of HIV-1 gp120 isolated by using an epitope-masking procedure. *J. Immunol.* **154**, 893-906 (1995).
38. Tsui, P., Tornetta, M.A., Ames, R.S., Silverman, C., Porter, T., Weston, C., Griego, S. & Sweet, R.W. Progressive epitope-blocked panning of a phage library for isolation of human RSV antibodies. *J. Immunol. Methods* **263**, 123-132 (2002).
39. Sambrook, J. & Russell David, W. (eds.) Molecular cloning: a laboratory manual, Edn. 3. (Cold Spring Harbor Laboratory Press, Cold Spring Harbor; 2001).
40. Casadaban, M.J. & Cohen, S.N. Analysis of gene control signals by DNA fusion and cloning in Escherichia coli. *J. Mol. Biol.* **138**, 179-207 (1980).
41. Sidhu, S.S., Lowman, H.B., Cunningham, B.C. & Wells, J.A. Phage display for selection of novel binding peptides. *Methods Enzymol.* **328**, 333-363 (2000).
42. Clackson, T. & Lowman, H.B. Phage Display: A Practical Approach. (Oxford University Press, New York, USA; 2004).
43. Barbas, C.F., 3rd, Burton, D.R., Scott, J.K. & Silvermann, G.J. Phage display: A laboratory manual. (Cold Spring Harbor Laboratory Press, Cold Spring Harbor, NY; 2001).
44. Garrett, T.P., McKern, N.M., Lou, M., Elleman, T.C., Adams, T.E., Lovrecz, G.O., Kofler, M., Jorissen, R.N., Nice, E.C., Burgess, A.W. & Ward, C.W. The crystal structure of a truncated ErbB2 ectodomain reveals an active conformation, poised to interact with other ErbB receptors. *Mol. Cell* **11**, 495-505 (2003).

Table 1: Description of target proteins used for the selections[a]

Target Protein	Abbr.	Selected Binders[b]	Description[c]	Acc. no.[d]
Fc of huIgG1	huIgG1_Fc	I_xx	P100 – K330 of human IgG1 (Fc domain)	SP: P01857
TNFα	TNFα	T_xx	A76 - L233 of human tumor necrosis factor precursor (TNFα)	SP: P01375
ErbB1 (1-501)[e]	ErbB1	E_xx	L25 – S525 of human receptor tyrosine-protein kinase ErbB1 fused to huIgG1_Fc	SP: P00533
ErbB2 (1-631)[e]	ErbB2-631	H_xx	S22 – T652 of human receptor tyrosine-protein kinase ErbB2	SP: P04626
ErbB2 (1-509)[e]	ErbB2-509	9_xx	S22 – N530 of human receptor tyrosine-protein kinase ErbB2	SP: P04626
ErbB4 (1-500)[e]	ErbB4	B4_xx	Q26 – R525 of human receptor tyrosine-protein kinase ErbB4 fused to huIgG1_Fc	SP: Q15303

[a]Abbreviations used: Fc, fragment crystallizable; IgG1, immunoglobulin G1. [b]Nomenclature of selected binders, xx corresponds to the number of a specific binder. [c]The first and last amino acid used as denoted in the respective Swiss-Prot reference are indicated in single letter amino acid code. [d]Accession number: SP, Swiss-Prot. [e]ErbB receptors and in parentheses the amino acids of the mature extracellular domain as described in ref. 44.

Table 2: Summary of the phage selection of DARPins against different target proteins

Target Protein	Round of selection	No. positive clones[a]	No. different sequences[b]	Abbr. of binders further analyzed in this study
huIgG1_Fc	R3	82/94	8/21	I_01/02/07/11/13/19
TNFα	R2/3[c]	102/188	29/52	T_01/02/07/08/09/16/25/27/37/40
ErbB1	R2/3[d]	97/369	1/64	E_01
ErbB1	R1 (epitope-masking)[e]	81/105	4/20	E_67/68/69
ErbB2-509	R3	83/94	13/29	9_16/26/29
ErbB2-631	R1 (epitope-masking)[e]	24/94	8/16	H_14
ErbB4	R3	55/143	5/48	B4_01/02/07/33/45
ErbB4	R1 (epitope-masking)[e]	84/94	6/20	B4_50/58
CitS (ref. 36)	R3/4	110/124	11/21	cp34_15/16 (ref. 36)

[a]Ratio of the number of positive clones to the total number of clones screened in ELISA experiments. [b]Number of clones with different sequences confirmed by ELISA experiments using purified DARPins to bind the target protein., identified in the total number of clones sequenced. [c]Sum of the analysis of the 2nd and 3rd round of selection. [d]Sum of the analysis of the 2nd and 3rd round of different selection approaches. [e]One round of selections with epitope-masking using preselected pools as input as described in the results section.

Table 3: Affinities and binding kinetics of DARPins

Target Protein	Clone (NxC)[a]	K_D [nM]	k_{on} [10^5 $M^{-1}s^{-1}$]	k_{off} [$10^{-3}s^{-1}$]
ErbB1[b]	E_01 (N3C)	0.5	4.4	0.2
	E_67 (N3C)	7.3	0.3	0.2
	E_68 (N3C)	0.7	26	1.9
	E_69 (N4C)	15	0.7	1.1
ErbB2-509[b]	9_16 (N3C)	6.9	1.2	0.9
	9_26 (N3C)	1.4	0.7	0.1
	9_29 (N3C)	3.8	2.0	0.8
ErbB2-631[c]	H_14 (N3C)	0.2	4.1	0.1
ErbB4[b]	B4_01 (N4C)	0.1	7.3	0.1
	B4_02 (N3C)	0.4	1.2	0.1
	B4_50 (N4C)	0.3	35	1.0
	B4_58 (N5C)	9.0	16	14
IgG1_Fc[b]	I_02 (N2C)	41	2.8	12
	I_07 (N2C)	25	0.7	1.7
	I_11 (N3C)	140	4.9	67
	I_19 (N3C)	2.1	3.4	0.7
CitS[d]	cp34_15 (N3C)	10	-	-
	cp34_16 (N3C)	1.9	-	-

[a]Name of the respective clone and in parentheses number of internal repeat modules (x) stacked between N-Cap (N) and C-Cap (C). [b]Association (k_{on}) and dissociation (k_{off}) rate constants were measured by using surface plasmon resonance, and the respective dissociation constants K_D was calculated as (k_{off}/k_{on}). Kinetic data, evaluation with a global kinetic fit and statistical error in the parameters is given in the **Supplementary Figure 2.** [c]C. Jost & A.P., unpublished data. [d]Dissociation constants K_D were measured by using equilibrium titration (BioVeris) and are described in detail in ref. 36.

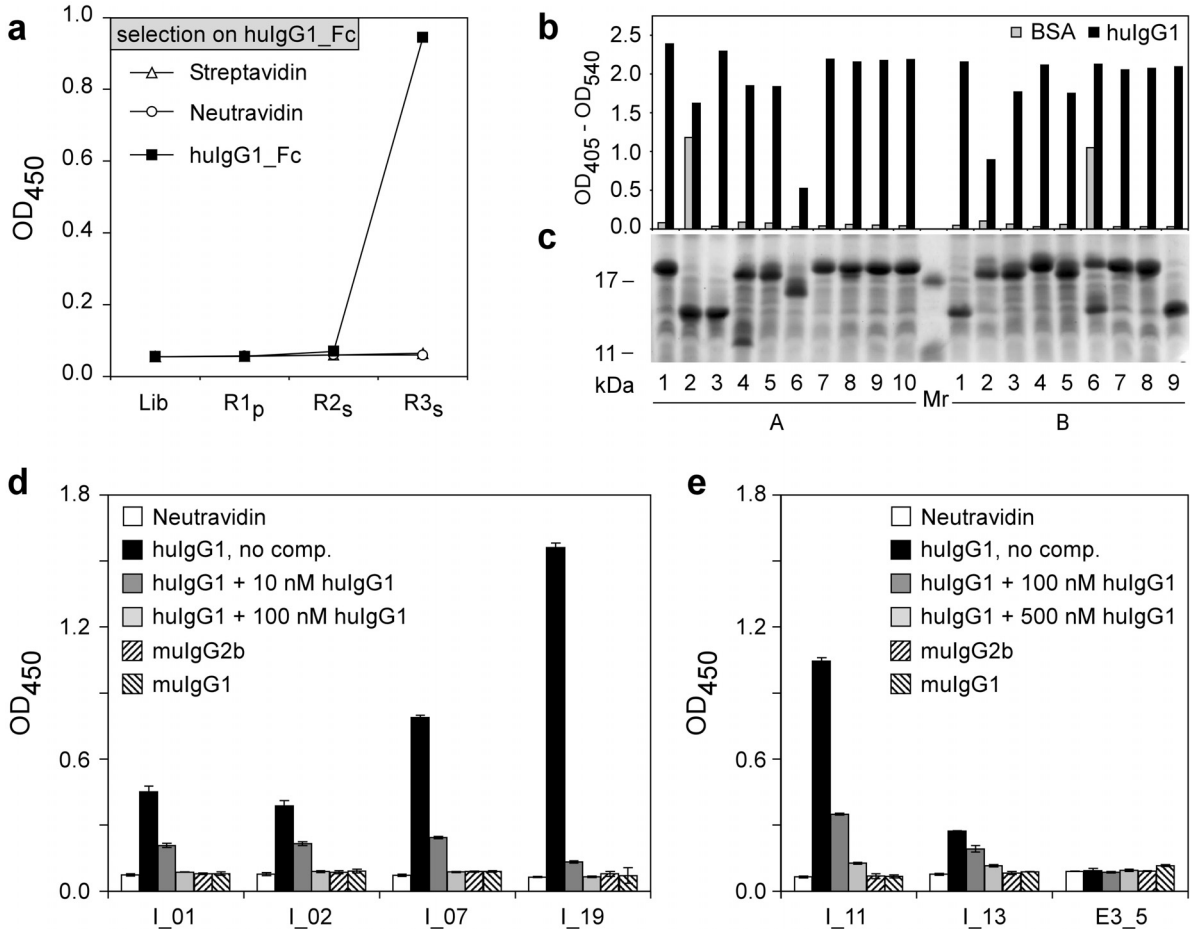

Figure 1: Selection, screening and characterization of binders against huIgG1_Fc. (a) The enrichment for the selection performed on huIgG1_Fc was analyzed by phage ELISA. Equivalent amounts of the initial library (Lib) and pools of amplified phage particles from each selection round ($R1_i$, $R2_s$ and $R3_s$, subscript i denotes selection on immobilized target protein, subscript s denotes selection on soluble target protein) were tested for binding to immobilized streptavidin, neutravidin and immobilized huIgG1_Fc. For each sample applied the signal of bound phage particles, detected with an anti-M13 antibody is shown. (b) ELISA screening to identify DARPins with affinity for huIgG1_Fc. *E. coli* extracts of randomly picked clones expressing soluble DARPins of selection round three were analyzed for binding to immobilized full length huIgG1 and BSA (control). Positions A1 - A10 and B1 - B9 of a 96-well plate are shown. (c) SDS-PAGE analysis of the *E. coli* extracts used for ELISA screening (**Figure 1b)**. Size of the SDS-PAGE protein marker (Mr) is indicated in kDa. (d) ELISA with high affinity huIgG1_Fc binders. To analyze specificity 1 nM solutions of the binders I_01, I_02, I_07 and I_19 were tested for binding on neutravidin, huIgG1, mouse IgG1 (muIgG1) and mouse IgG2b (muIgG2b), and in parallel, competition was tested by preincubation of 1 nM solutions of the DARPins with 10 nM or 100 nM free huIgG1 before binding on immobilized huIgG1. (e) ELISA with low affinity huIgG1_Fc binders and control DARPin E3_5. To analyze specificity, 5 nM solutions of the binders I_11, I_13 and control DARPin E3_5 were tested for binding on neutravidin, huIgG1, muIgG1 and muIgG2b, and in parallel, competition was tested by preincubation of 5 nM

solutions of the DARPins with 100 nM or 500 nM of free huIgG1 before binding on immobilized huIgG1. All full length IgGs were directly immobilized on solid supports. The first word in the legend denotes the protein immobilized, *no comp.* denotes the absence of a competitor and + *huIgG1* denotes the presence of competitor in 10 nM, 100 nM or 500 nM concentrations.

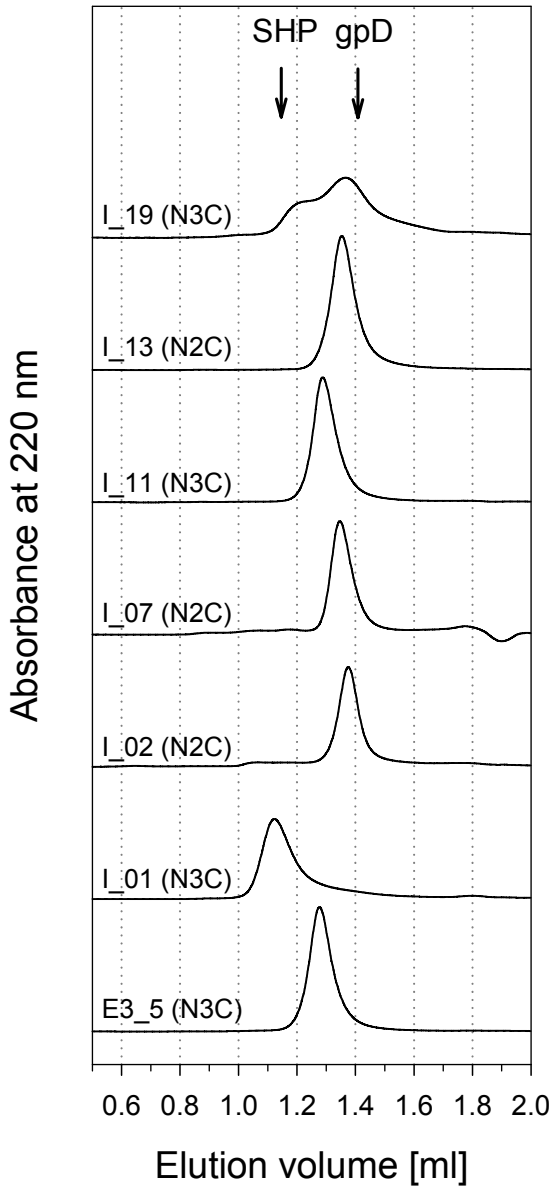

Figure 2: Size exclusion chromatography (SEC) of selected DARPins. The chromatograms of the six huIgG1_Fc binders and the unselected DARPin E3_5 are shown as examples. For each DARPin the number of repeats stacked between N-Cap (N) and C-Cap (C) is given in brackets. The molecular mass standards, phage protein D (gpD) with an apparent mass of 17.6 kDa and phage protein SHP, a trimer with an apparent mass of 50.2 kDa are indicated by arrows.

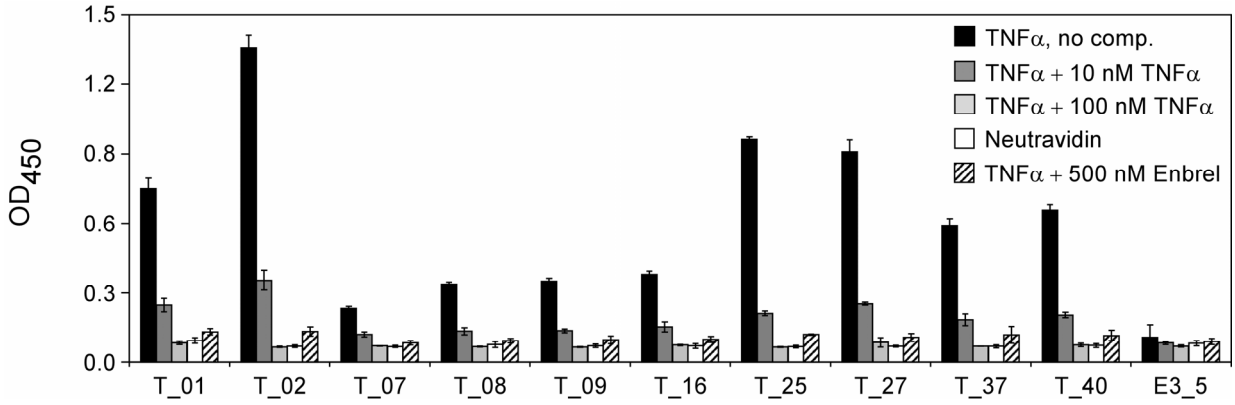

Figure 3: ELISA of selected TNFα binding DARPins. To analyze specificity 5 nM solutions of the selected DARPins were tested for binding on neutravidin, immobilized TNFα and immobilized TNFα preincubated with an excess (500 nM) of Etanercept (Enbrel™, recombinant human soluble tumor necrosis factor alpha receptor fused to the Fc domain of human IgG1). In parallel, competition was tested by preincubation of 5 nM solutions of the DARPins with 10 nM or 100 nM free TNFα before binding on immobilized TNFα. Only a subset of the selected TNFα binders is shown and unselected DARPin E3_5 was used as control. The first word in the legend denotes the protein immobilized, *no comp.* denotes the absence of a competitor and + *TNFα* or + *Enbrel* denotes the presence of competitor (respective concentrations given in nM).

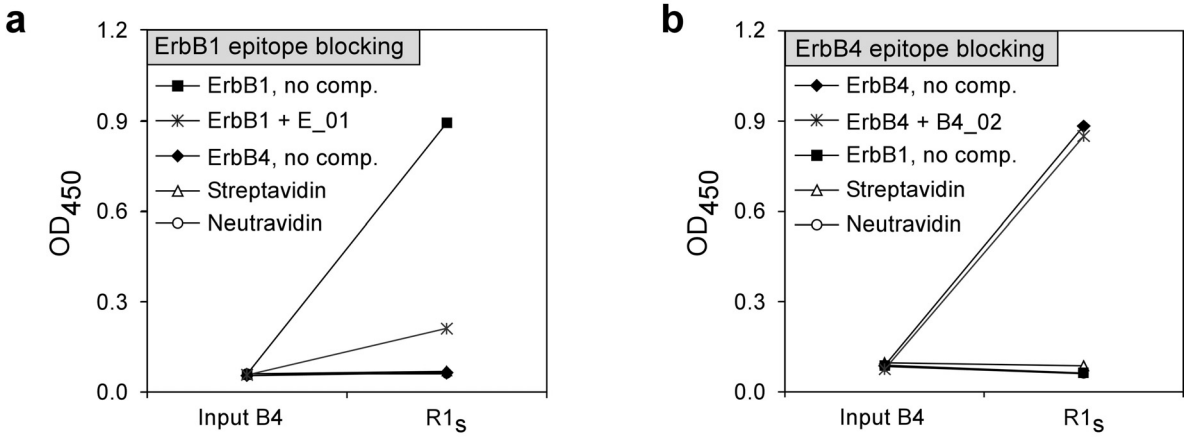

Figure 4: Equivalent amounts of the input and output phage particles form one round of epitope-masking performed on ErbB1 (by adding soluble DARPin E_01) and on ErbB4 (by adding soluble DARPin B4_04) were analyzed by phage ELSIA as described in **Figure 1**. Additionally, binding was tested on the respective target protein preincubated with an excess of the respective DARPin (ErbB1 + E_01 or ErbB4 + B4_02). Subscript s denotes selection on target protein in solution. The first word in the legend denotes the protein coated, *no comp.* denotes the absence of a competitor and + *E_01* or + *B4_02* denotes the presence of 2 µM competitor.

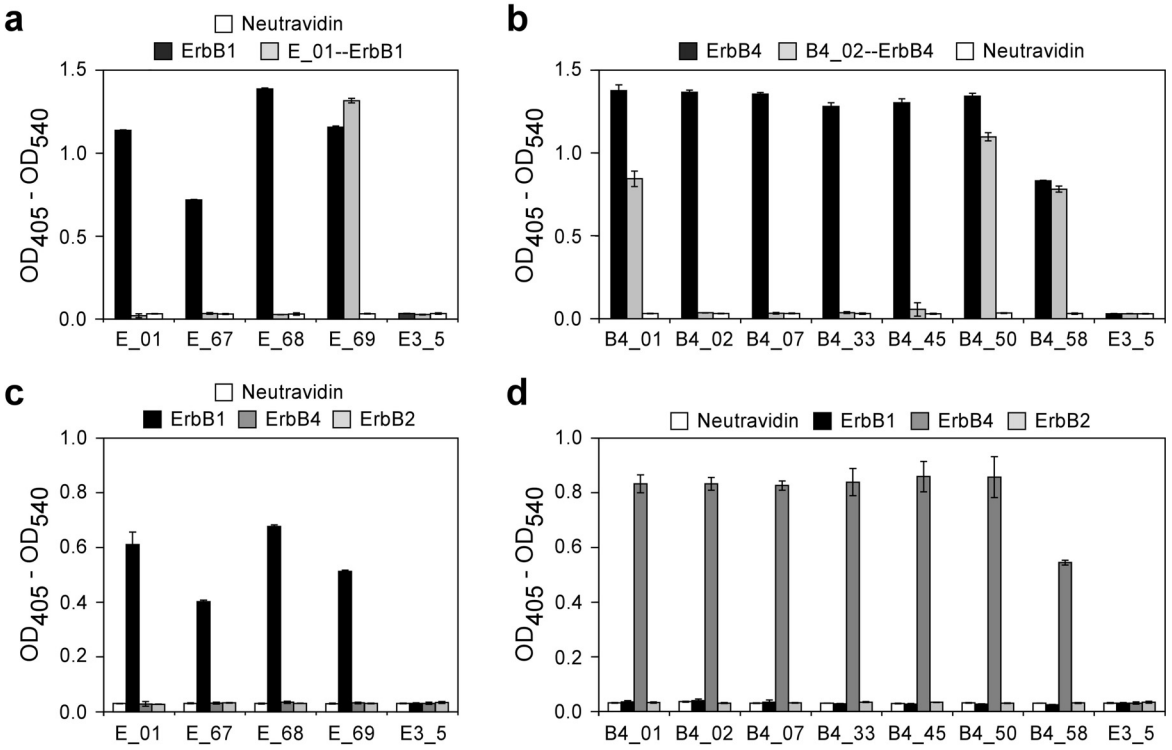

Figure 5: ELISA of selected ErbB1 and ErbB4 binding DARPins. 50 nM solution of the selected (a) ErbB1 and (b) ErbB4 binders was tested for interaction with immobilized target protein (ErbB1 or ErbB4, respectively), target protein bound to immobilized DARPin used for epitope-masking during the selection round (E_01—ErbB1 or B4_02—ErbB4, respectively) and neutravidin. (c, d) Specificity was tested by applying a 50 nM solution of the selected ErbB1 (c) and ErbB4 (d) binders on immobilized ErbB-receptors (ErbB1, ErbB2-631 and ErbB4) and neutravidin. DARPin E3_5 was used as control in all experiments. ErbB1 binders E_67, E_68 and E_69 and ErbB4 binders B4_50 and B4_58 were selected by epitope masking.

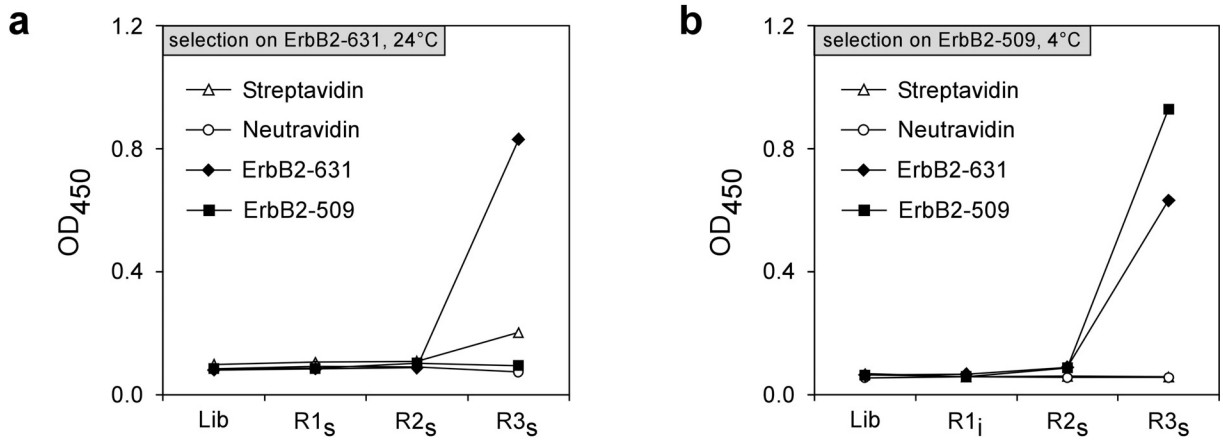

Figure 6: The enrichment for the selections performed on ErbB2-631 in solution at RT and on ErbB2-509 at 4 °C were analyzed by phage ELISA. Equivalent amounts of the initial library (Lib) and pools of amplified phage particles from each selection round (R1, R2 and R3) were tested for binding to immobilized streptavidin, neutravidin and immobilized ErbB2-631 and ErbB2-631. For each sample applied the signal of bound phage particles, detected with an anti-M13 antibody, is shown. For each round the subscript denotes if the selection was performed on immobilized target protein (i) or on target protein in solution (s).

8. Supplementary Material:

Efficient Selection of DARPins with Subnanomolar Affinity using SRP Phage Dipslay (Daniel Steiner, Patrik Forrer and Andreas Plückthun)

8.1 Supplementary Results: Development of the „optimized selection protocol“

This section describes the development of an optimized selection protocol for our DARPin phage library, based on experiences from the different selection approaches using members of the ErbB receptor family as target proteins. For both, ErbB1 and ErbB4, the extracellular domains I-III of the respective receptor fused to huIgG1_Fc were used as targets (see **Table 1** of the publication). For the first panning we had performed three rounds of selection on immobilized target protein as described in the **Material and Methods** section of the publication. During the second and third selection rounds we added an excess of soluble huIgG_Fc (1 μM) to the selection reaction to counter-select binders against the Fc domain. From each selection round we analyzed the amplified pool of phage particles by phage ELISA (**Supplementary Figure 3(a)** and **3(b)**). For ErbB1 good enrichment of phage particles displaying target specific DARPins was observed for the second and third round, with a slight enrichment of phage particles showing unspecific background binding (binding of non-target-coated matrix) (**Supplementary Figure 3(a)**). For ErbB4 the enrichment of such background binding phage particles was much stronger, and almost equal signals were obtained on neutravidin, streptavidin and immobilized target protein (**Supplementary Figure 3(b)**). This background binding could be reduced by applying extensive prepanning steps on non-target-coated matrix before performing the selection round on the target protein, but not to the level required for efficient screening of single clones (data not shown). Sequence analysis of some of

these background binders revealed defective DARPins of which part of the DARPin framework is not consensus due to multiple deletions or insertions (members of the non-functional part of the initial library). The C-terminal part of all of the clones analyzed was in frame with the phage coat protein, a prerequisite for display on phage particles.

Selection on target protein in solution was previously reported to results in less background enrichment when compared to selections on immobilized target proteins.[1] Thus, to avoid enrichment of phage particles with such background binding properties we performed another three rounds (starting with a fresh library aliquot) of selection on ErbB1 and ErbB4 in solution as described in the **Material and Methods** section of the publication. During the second and third selection rounds soluble huIgG1_Fc was added for competitions as described above. Analysis of the amplified pools of phage particles by phage ELISA showed for both selections highly specific binding signal on the respective target protein in round three (**Supplementary Figure 3(c)** and **3(d)**) without enrichment of background binding phage particles. When comparing the results obtained for selection on immobilized ErbB1 (**Supplementary Figure 3(a)**) and ErbB1 in solution (**Supplementary Figure 3(c)**) a faster enrichment of binders is revealed when performing the selection on immobilized target protein, however, with the disadvantage of a higher tendency for the enrichment of background binding phage particles. As a consequence, we combined both methods performing the first round of selection on immobilized target protein (high recovery of phage particles needed in order not to irreversibly lose binders), followed by two rounds on target protein in solution, turned out to be the most effective selection strategy and was used as optimized selection protocol for our phage DARPin library. Results obtained by using this protocol for selection of binders against ErbB1 (**Supplementary Figure 3(e))** do show fast enrichment of target specific binders without any enrichment of background binding phage particles (see also selections on huIgG1_Fc, TNFα and Her2-509 described in the results section of the publication).

8.2 Supplementary Discussion: Target protein dependent selection approaches

Many methods of target protein presentation have been used for phage selections[2] including panning on whole cells, on tissues or even using living organisms, but if available, purified target protein is preferentially used. The biophysical properties of a purified target protein do strongly influence the selection procedure, and, therefore, the chance of successful selection of binders from a given library. For "well behaved" target proteins such as the huIgG1_Fc domain the selection is simple and straightforward (**Figure 1(a)** of the publication). For more complicated target proteins (e.g. membrane proteins or proteins with low stability) the careful design of the selection procedure is essential to guide the selection into the desired direction in order to obtain specific binders. Background enrichment, meaning the accumulation of binders that do unspecifically bind to the non-target coated matrix, was highly target-protein dependent in our hands. When comparing selections on immobilized ErbB1 and ErbB4, much lower background enrichment was observed for ErbB1 (**Supplementary Figure 3(a)**), than for ErbB4 where background binding signals were almost equal to the specific binding signals on the target protein (**Supplementary Figure 3(b)**). Prepanning on non-target coated matrix only slightly improved the result. Performing the selections on the same target protein in solution completely abolished unspecific background binding signals (**Supplementary Figure 3(c)** and **3(d)**). This might be attributed to the short capturing step and the possibility to change the reaction vial during the selection process.

Target protein presentation not only has an influence on background enrichment but also on enrichment factors. Even if accompanied by background enrichment we observed a faster enrichment when performing selections on immobilized target protein, compared to selections on soluble target protein (**Supplementary Figure 3(a)** and **3(c)**). One possible explanation is that the immobilization of the target protein on solid plastic support leads to a locally very high concentration of the target protein, favorable for the capturing of all potential binders, which is especially important for the first selection round.

From the observations described above we used for most other selections our optimized selection protocol composed of a first selection round on immobilized target protein, followed by two rounds of selection on soluble target protein. In the case of ErbB1 this lead to the very fast enrichment of specific binders (**Supplementary Figure 3(e)**) without any detectable background enrichment and was further successfully used for the selection on huIgG1_Fc, TNFα and ErbB2-509.

8.3 References

1. Dennis, M.S. in Phage display in biotechnology and drug discovery. (ed. S.S. Sidhu) 143 - 164 (CRC, Boca Raton; 2005).
2. Bradbury, A.R. & Marks, J.D. Antibodies from phage antibody libraries. *J. Immunol. Methods* **290**, 29-49 (2004).

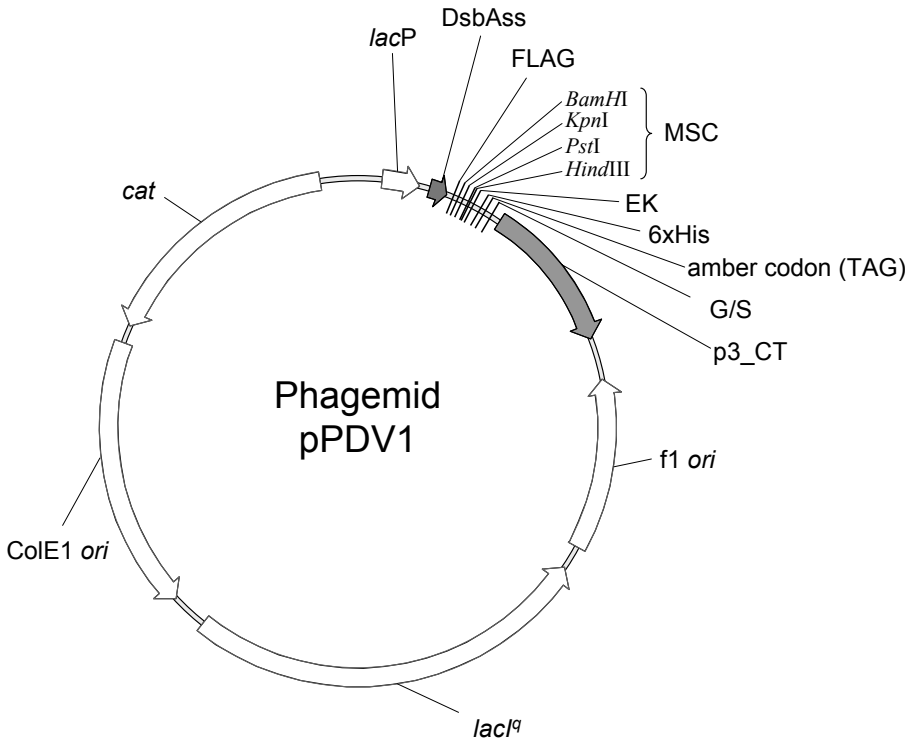

Supplementary Figure 1. Schematic representation of the phagemid pPDV1. The expression cassette is composed of a *lac* promoter/operator element (*lac*P), the coding sequences for the signal sequence of *E. coli* DsbA (DsbAss) leading to SRP dependent translocation, the multiple cloning site (MCS) to introduce the gene encoding the protein of interest (POI) with the restriction sites *Bam*HI, *Kpn*I, *Pst*I, and *Hind*III depicted, a suppressable stop codon (amber codon (TAG)), the coding sequences for a flexible glycine/serine linker (G/S) and for the C-terminal domain (amino acids 250-406) of protein 3 of filamentous phage M13 (p3_CT), mediating incorporation of the fusion protein into the phage particle. The coding sequence of the POI is flanked by DNA sequences encoding a FLAG-tag (FLAG), an enterokinase site (EK) and a His_6 tag (6xHis). In addition, the vector carries a f1 origin of replication (f1 *ori*) to permit production of virions using an appropriate helper phage, such as VCS M13; a plasmid origin (ColE1 *ori*), the *lacI*^{q} gene providing high levels of the *lac* repressor for the control of the lacP *in cis* and an antibiotic resistance marker (the gene for chloramphenicol acetyl transferase (*cat*), providing resistance to chloramphenicol) to allow propagation as a plasmid in *E. coli*

Supplementary Figure 2: Affinity determination of selected DARPins. Surface plasmon resonance (SPR) was measured using a BIAcore 3000 instrument (BIAcore, Uppsala Sweden). All measurements were performed in HBS-T buffer (20 mM HEPES, 150 mM NaCl, 3 mM EDTA pH 7.4, 0.005% Tween-20) at a flow rate of 50 µl/min. The following amounts of biotinylated target protein described in Tabel 1 of the man publication were immobilized on SA chips (BIAcore): ErbB1 (1000 RU), ErbB2 (509) (400 RU), ErbB4 (600 RU), huIgG1_Fc (500 RU). For the determination of kinetic data, the interactions were measured as follows: five minutes initial buffer blow, followed by a 2 to 15 min injection of DARPin at different concentrations (1 nM to 250 nM) and a final off-rate measurement of 10 to 75 minutes with buffer flow. The signal of an uncoated reference cell and buffer response was always subtracted from the sensograms (double referencing). The kinetic data of the interaction were evaluated with a global fit using Scrubber 2 (BioLogic Software Ltd). For each DARPin analyzed a representative set of curves with the corresponding fits are shown below. The statistical errors in the parameters given are those obtained from the best fit error and underline data quality and the good description of the data by the model. However, the true error of the parameter, estimated from measurements of independent protein preparations will be at least ±20%. Results are shown for DARPins binding ErbB1: (a) E_01, (b) E_67, (c) E_68 and (d) E_69, ErbB2: (e) 9_16, (f) 9_26 and (g) 9_27, ErbB4: (h) B4_01, (i) B4_02, (j) B4_50 and (k) B4_58 and huIgG1_Fc: (l) I_02, (m) I_07, (n) I_11 and (o) I_19.

a) E_01

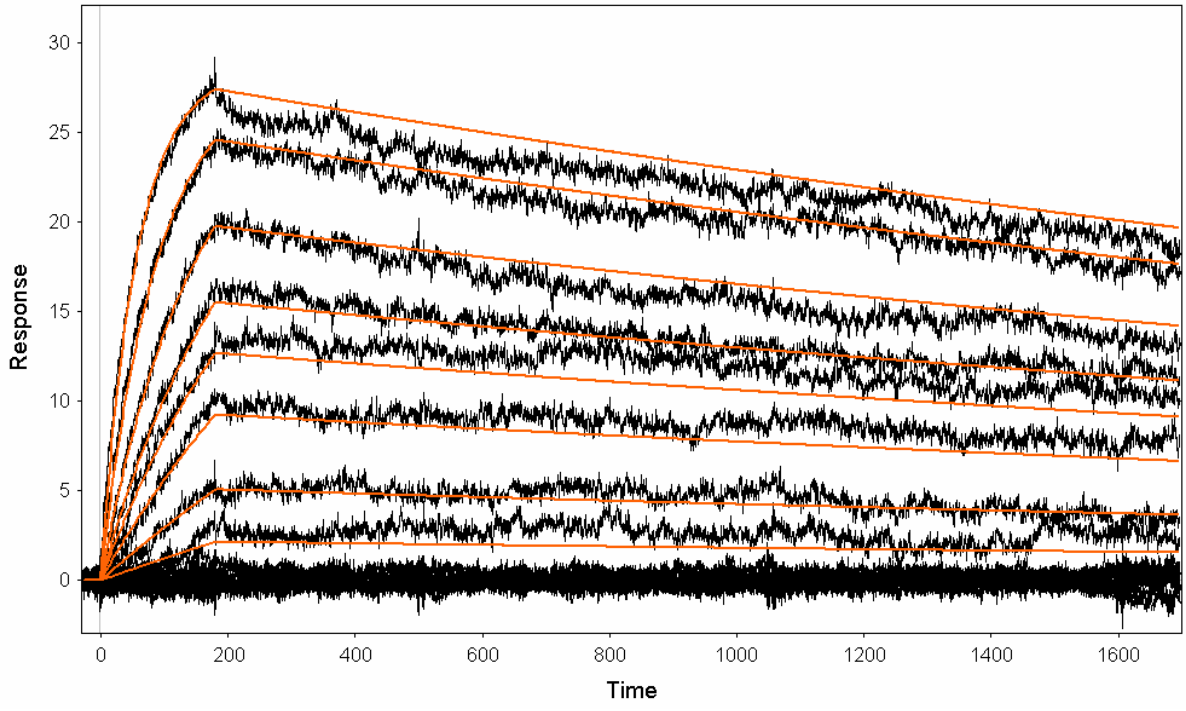

K_D = 496 ± 2 pM k_{on} = (44.2 ± 0.2) x 10^4 $M^{-1}s^{-1}$ k_{off} = (0.2194 ± 0.0007) x $10^{-3}s^{-1}$

DARPin concentrations [nM]: 1, 2.5, 5, 7.5, 10, 15, 25, 40

b) E_67

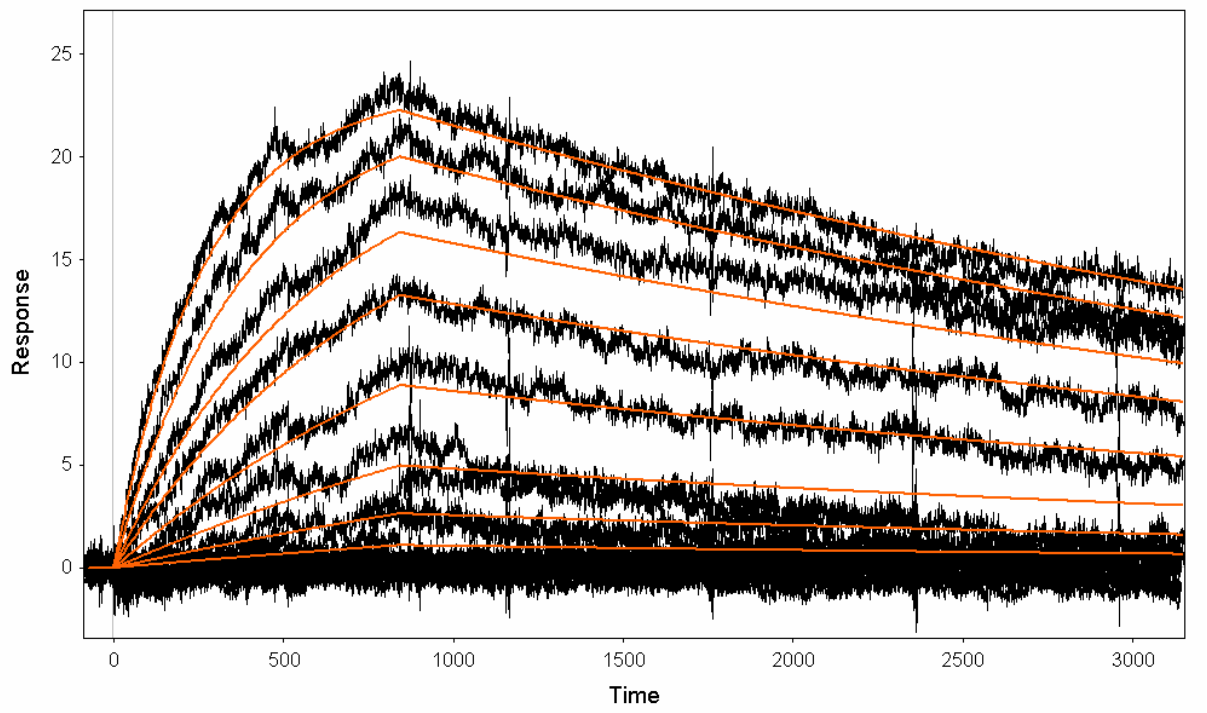

K_D = 7.3 ± 0.1 nM k_{on} = (2.95 ± 0.04) x 10^4 $M^{-1}s^{-1}$ k_{off} = (0.215 ± 0.002) x $10^{-3}s^{-1}$

DARPin concentrations [nM]: 2, 5, 10, 20, 35, 50, 80, 120

c) E_68

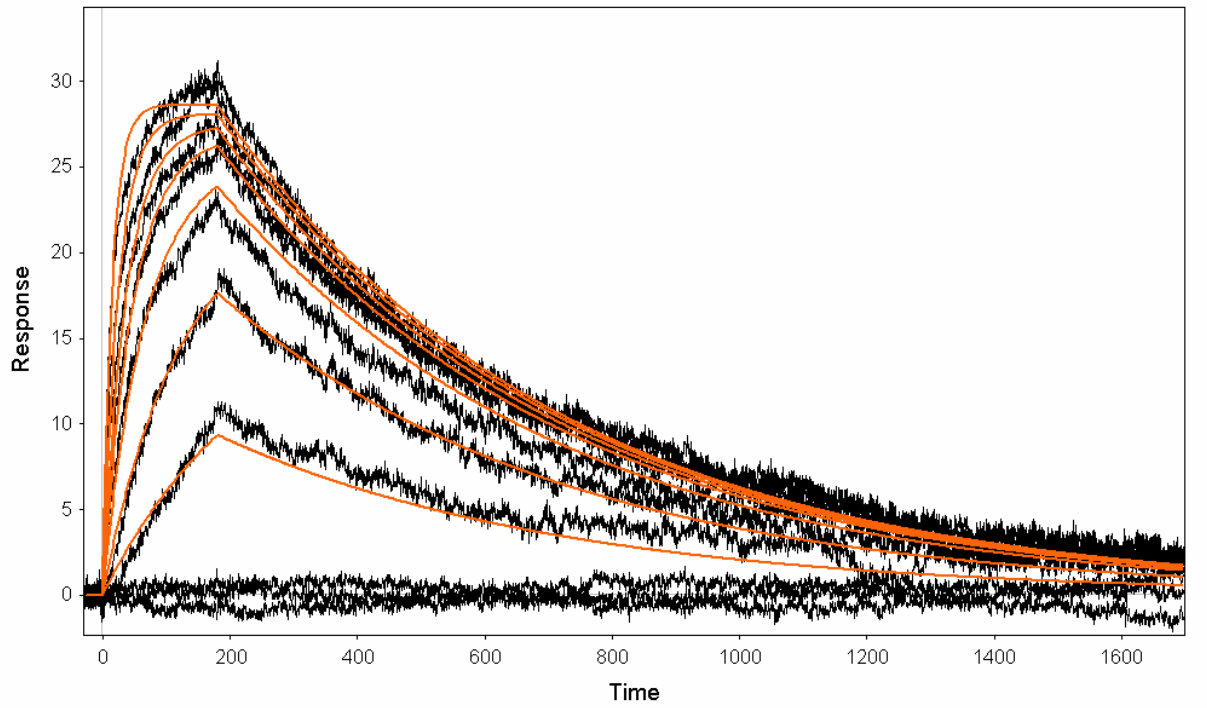

K_D = 724 ± 3 pM k_{on} = (258.6 ± 0.8) x 10^4 $M^{-1}s^{-1}$ k_{off} = (1.873 ± 0.006) x $10^{-3}s^{-1}$

DARPin concentrations [nM]: 1, 2.5, 5, 7.5, 10, 15, 25

d) E_69

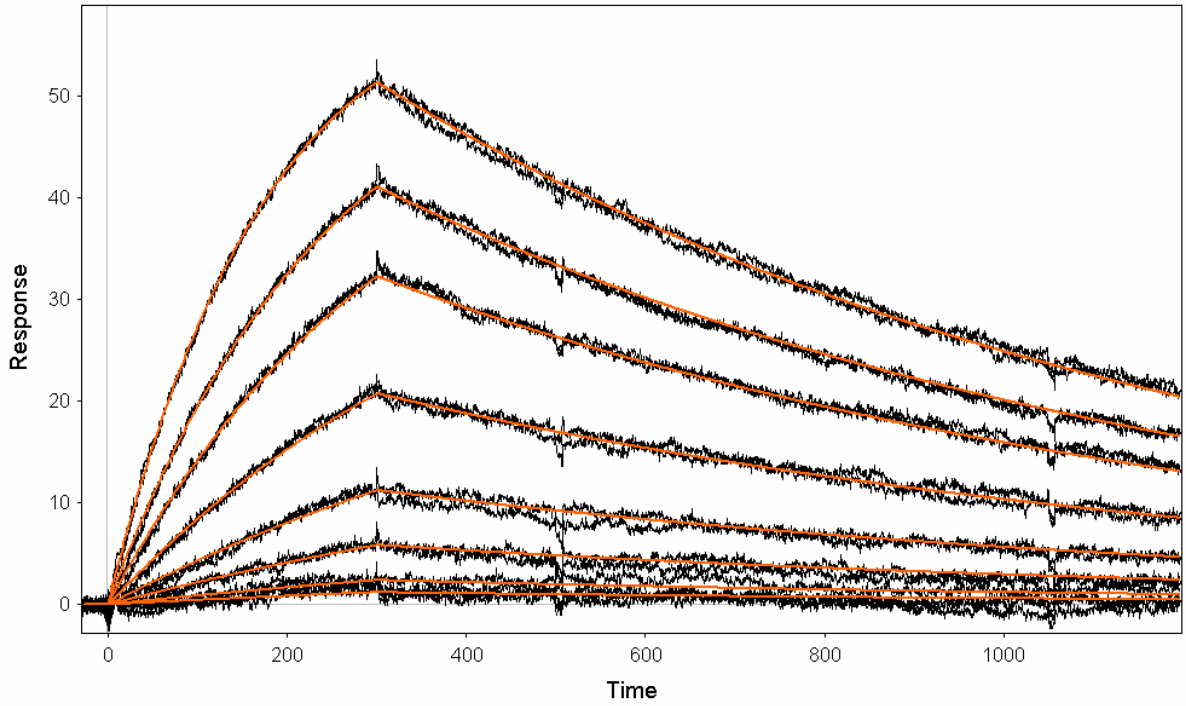

K_D = 15.20 ± 0.08 nM k_{on} = (7.32 ± 0.03) x 10^4 $M^{-1}s^{-1}$ k_{off} = (1.113 ± 0.003) x $10^{-3}s^{-1}$

DARPin concentrations [nM]: 1, 2, 5, 10, 20, 35, 50, 75

e) 9_16

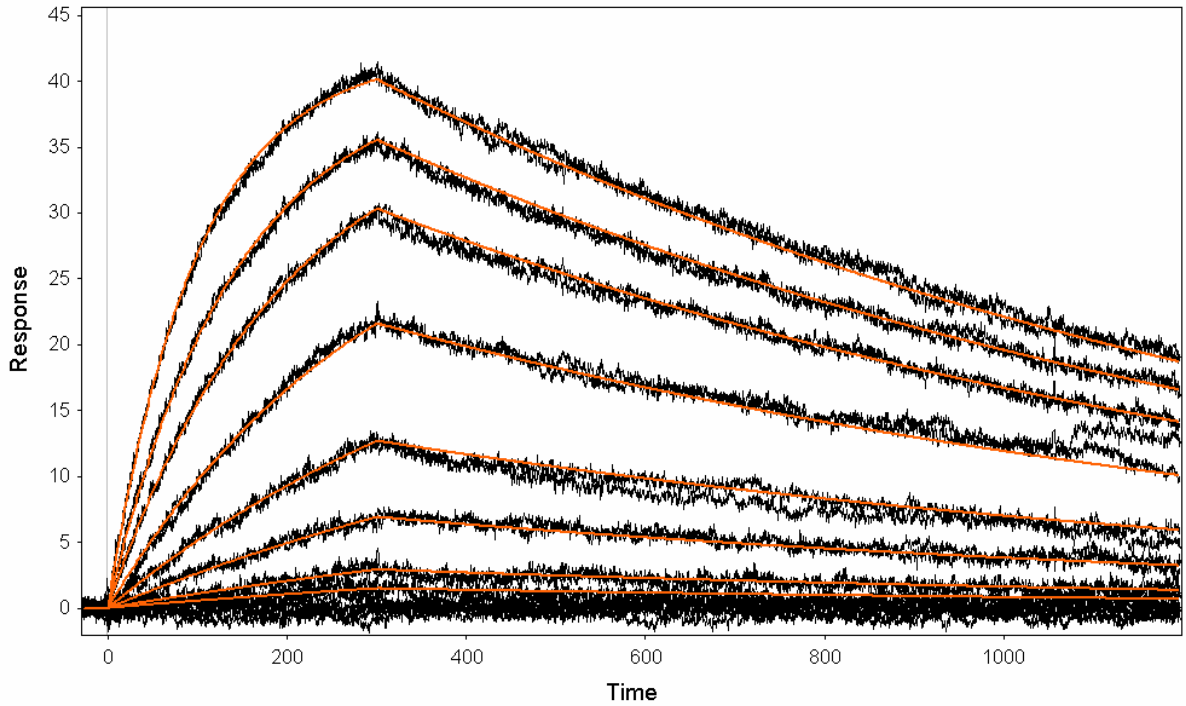

K_D = 6.90 ± 0.02 nM k_{on} = (12.36 ± 0.01) x 10^4 $M^{-1}s^{-1}$ k_{off} = (0.853 ± 0.003) x $10^{-3}s^{-1}$

DARPin concentrations [nM]: 1, 2, 5, 10, 20, 35, 50, 75

f) 9_26

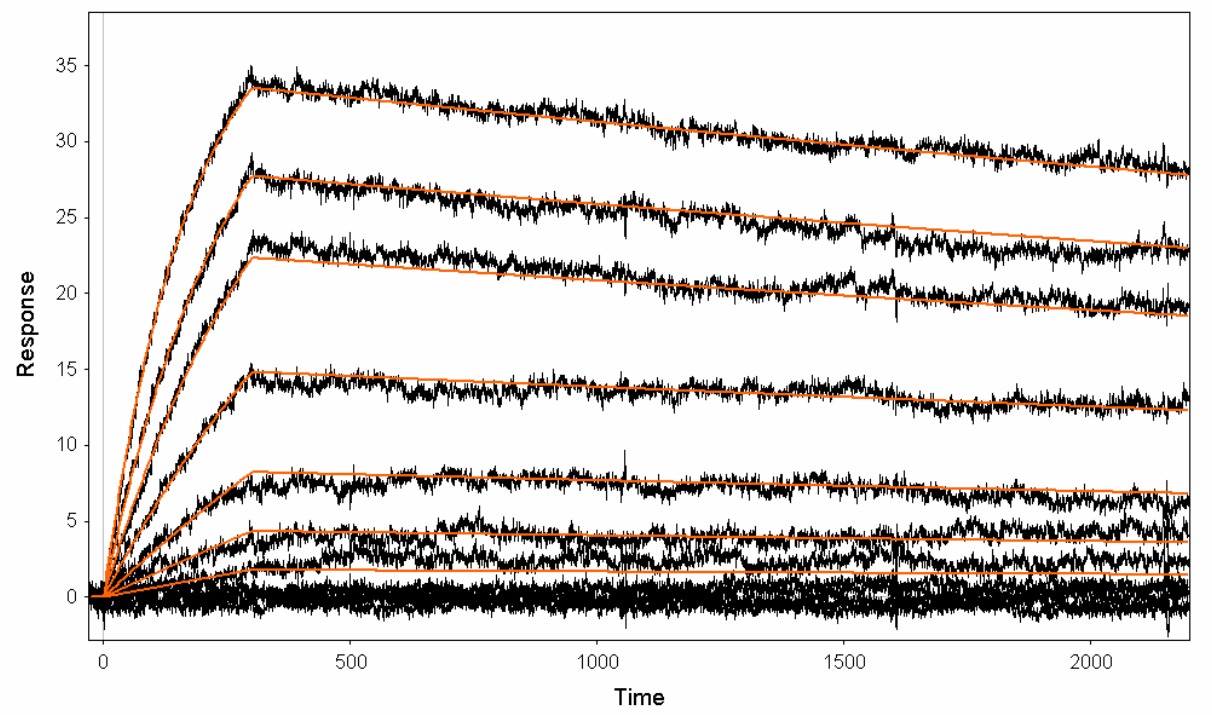

K_D = 1.36 ± 0.03 nM k_{on} = (7.38 ± 0.01) x 10^4 $M^{-1}s^{-1}$ k_{off} = (0.101 ± 0.002) x $10^{-3}s^{-1}$

DARPin concentrations [nM]: 2, 5, 10, 20, 35, 50, 75

g) 9_29

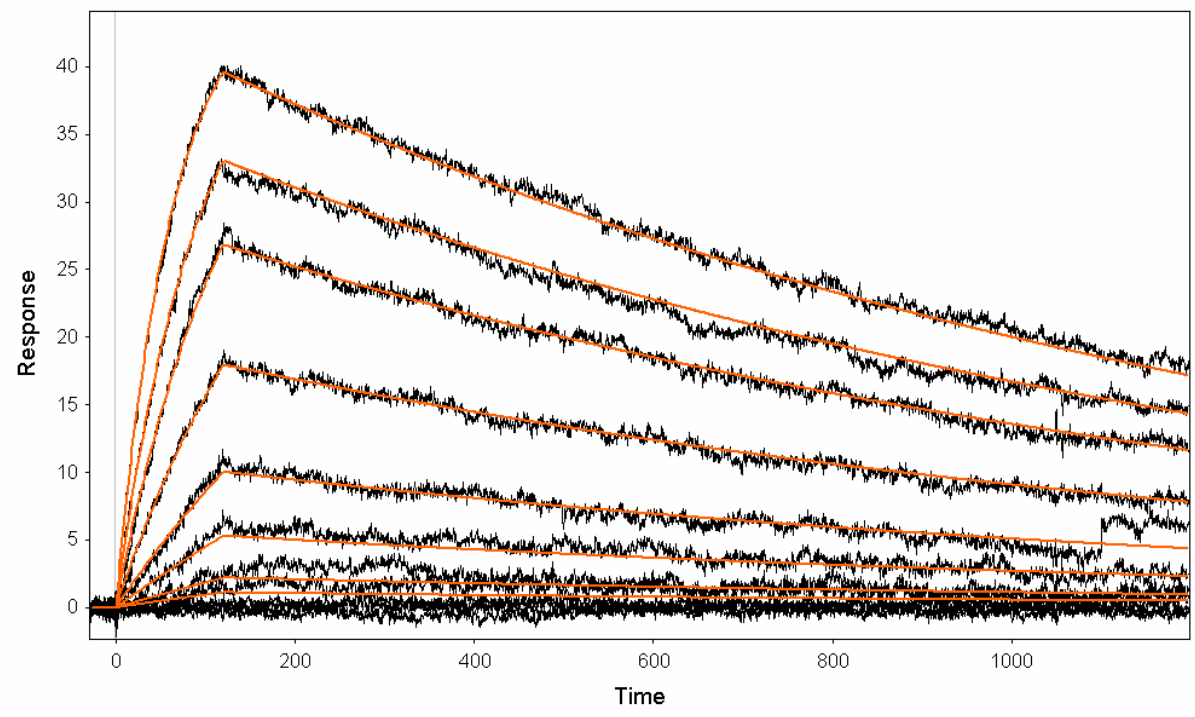

K_D = 3.83 ± 0.03 nM k_{on} = (20.25 ± 0.04) x 10^4 $M^{-1}s^{-1}$ k_{off} = (0.776 ± 0.007) x $10^{-3}s^{-1}$

DARPin concentrations [nM]: 1, 2, 5, 10, 20, 35, 50, 75

h) B4_01

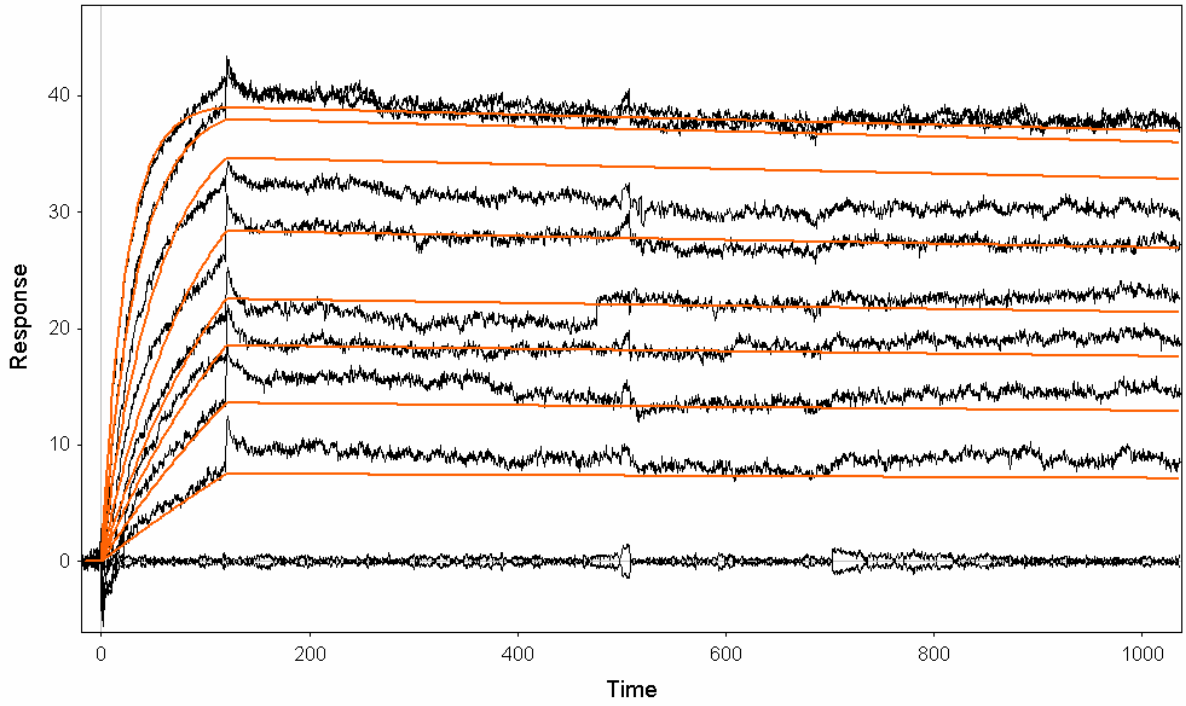

$K_D = 80 \pm 2$ pM $k_{on} = (72.8 \pm 0.5) \times 10^4\ M^{-1}s^{-1}$ $k_{off} = (0.058 \pm 0.001) \times 10^{-3}s^{-1}$

DARPin concentrations [nM]: 2.5, 5, 7.5, 10, 15, 25, 40, 60

i) B4_02

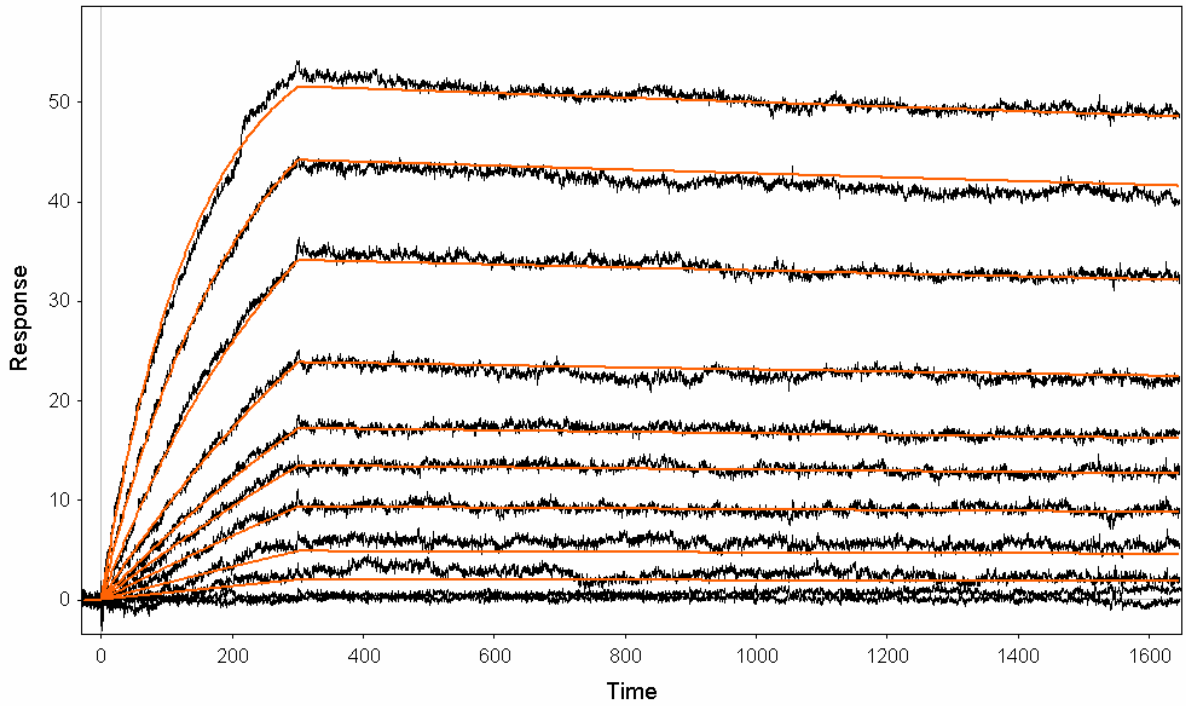

$K_D = 387 \pm 3$ pM $k_{on} = (11.63 \pm 0.06) \times 10^4\ M^{-1}s^{-1}$ $k_{off} = (0.045 \pm 0.004) \times 10^{-3}s^{-1}$

DARPin concentrations [nM]: 1, 2.5, 5, 7.5, 10, 15, 25, 40, 60

j) B4_50

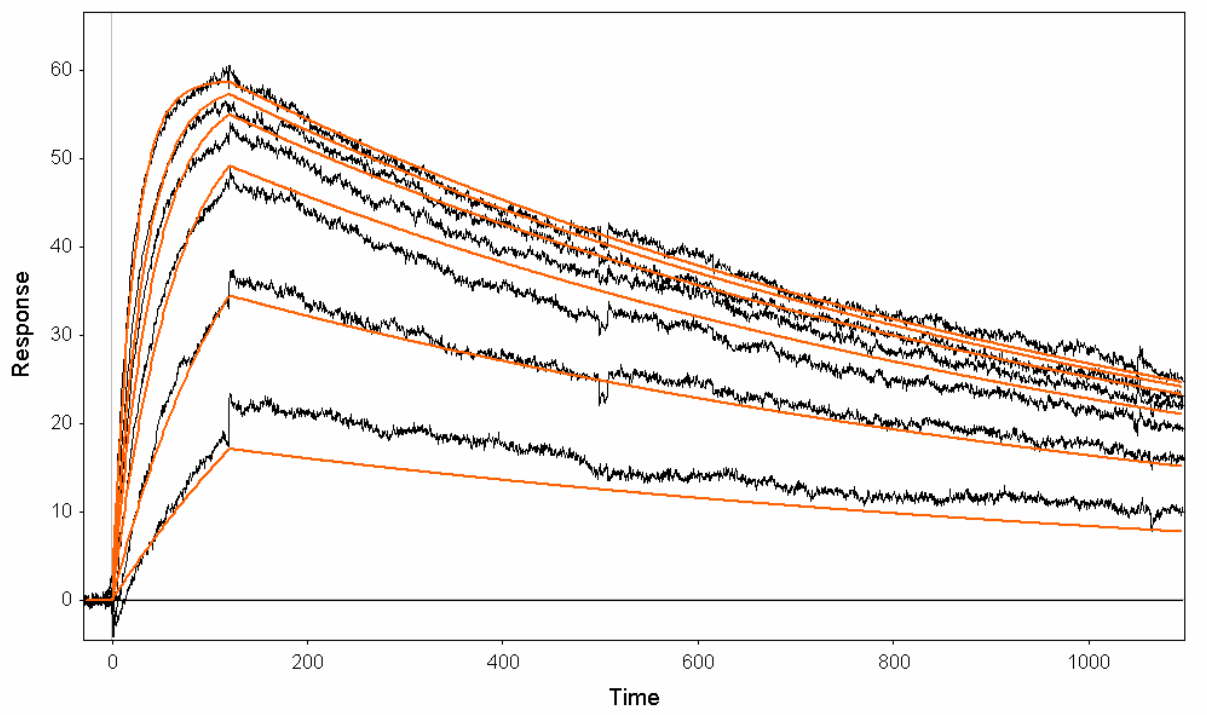

K_D = 273.7 ± 0.7 pM k_{on} = (348 ± 2) x 10^4 $M^{-1}s^{-1}$ k_{off} = (0.952 ± 0.003) x $10^{-3}s^{-1}$

DARPin concentrations [nM]: 1, 2.5, 5, 7.5, 10, 15

k) B4_58

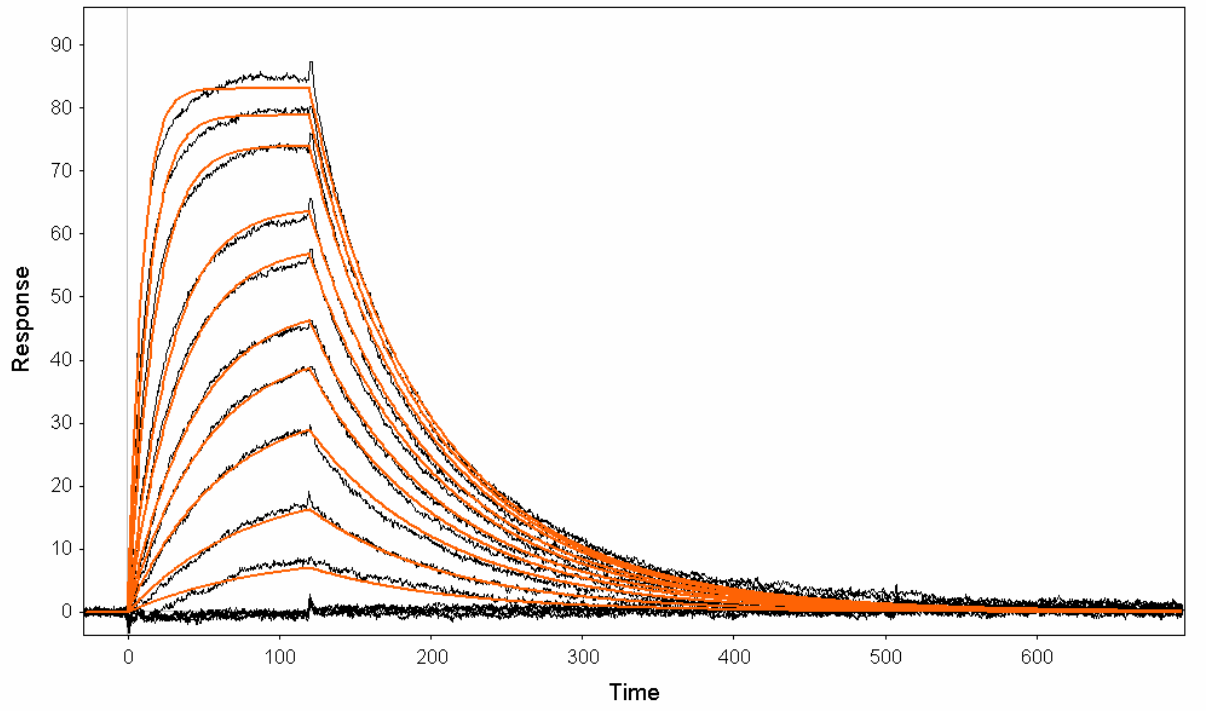

K_D = 9.00 ± 0.01 nM k_{on} = (159.3 ± 0.05) x 10^4 $M^{-1}s^{-1}$ k_{off} = (14.34 ± 0.05) x $10^{-3}s^{-1}$

DARPin concentrations [nM]: 1, 2.5, 5, 7.5, 10. 15, 20, 35, 50, 75

l) I_02

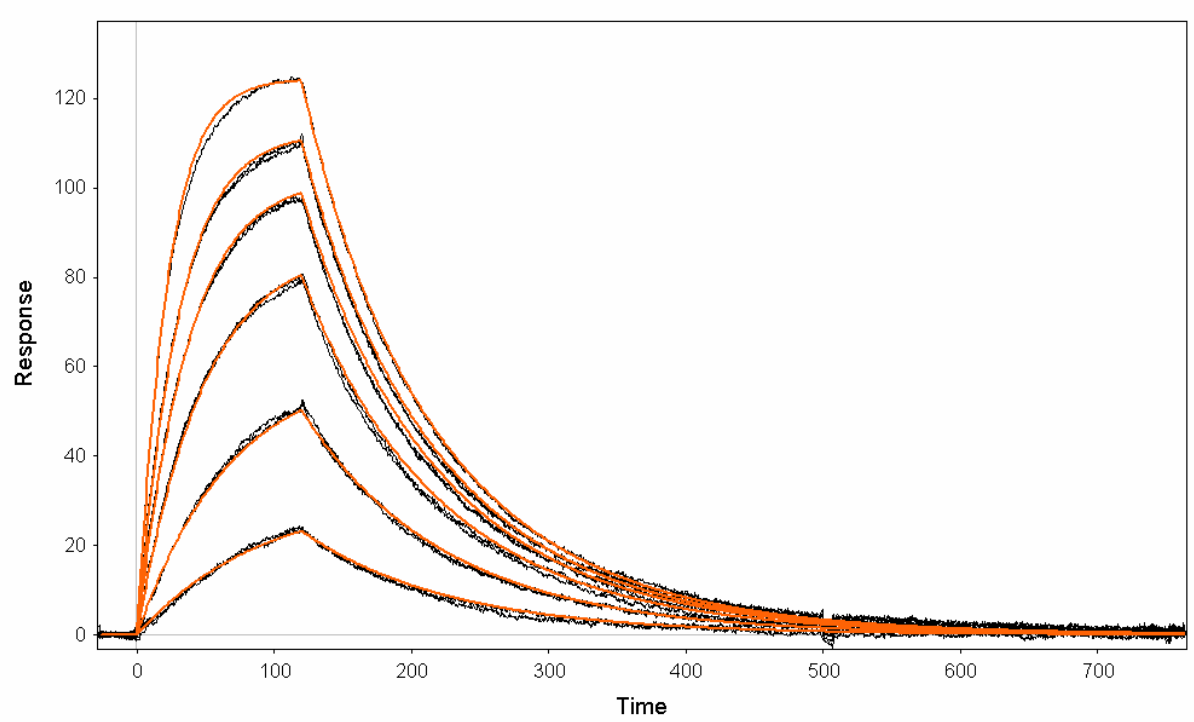

K_D = 41.1 ± 0.1 nM k_{on} = (28.29 ± 0.06) x 10^4 $M^{-1}s^{-1}$ k_{off} = (11.62 ± 0.02) x $10^{-3}s^{-1}$

DARPin concentrations [nM]: 10, 25, 50, 75, 100, 150

m) I_07

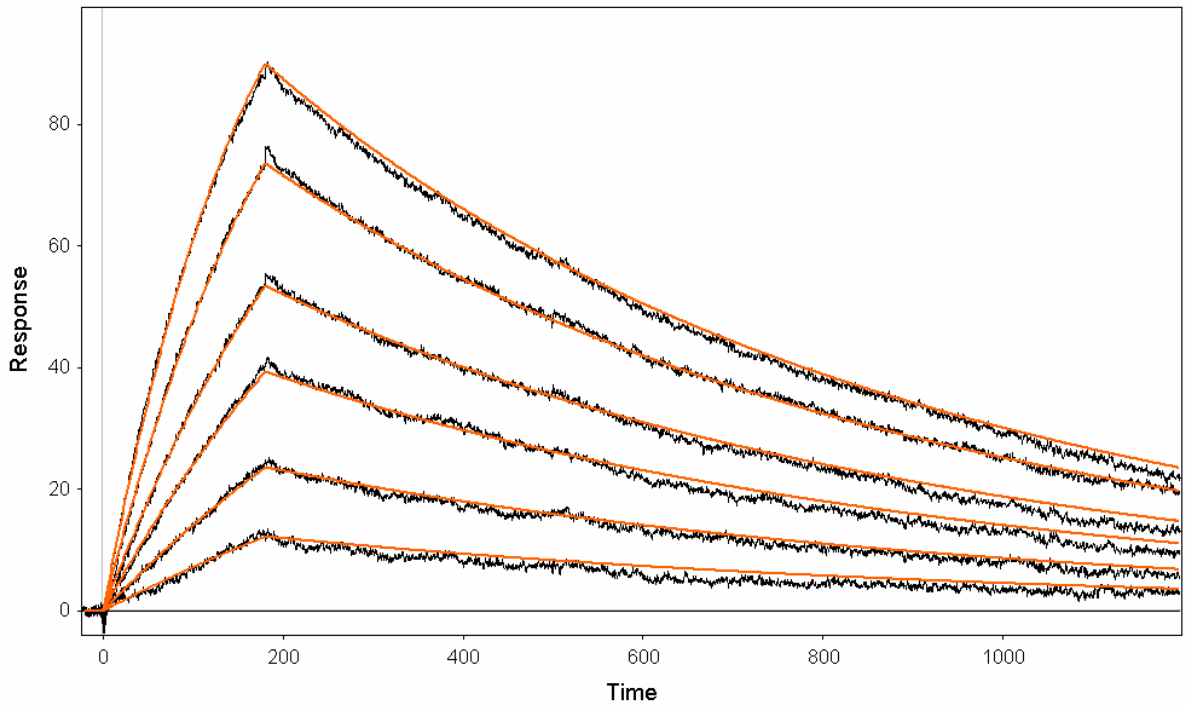

K_D = 24.5 ± 0.1 nM k_{on} = (7.03 ± 0.03) x 10^4 $M^{-1}s^{-1}$ k_{off} = (1.723 ± 0.007) x $10^{-3}s^{-1}$

DARPin concentrations [nM]: 10, 20, 35, 50, 75, 100

n) I_11

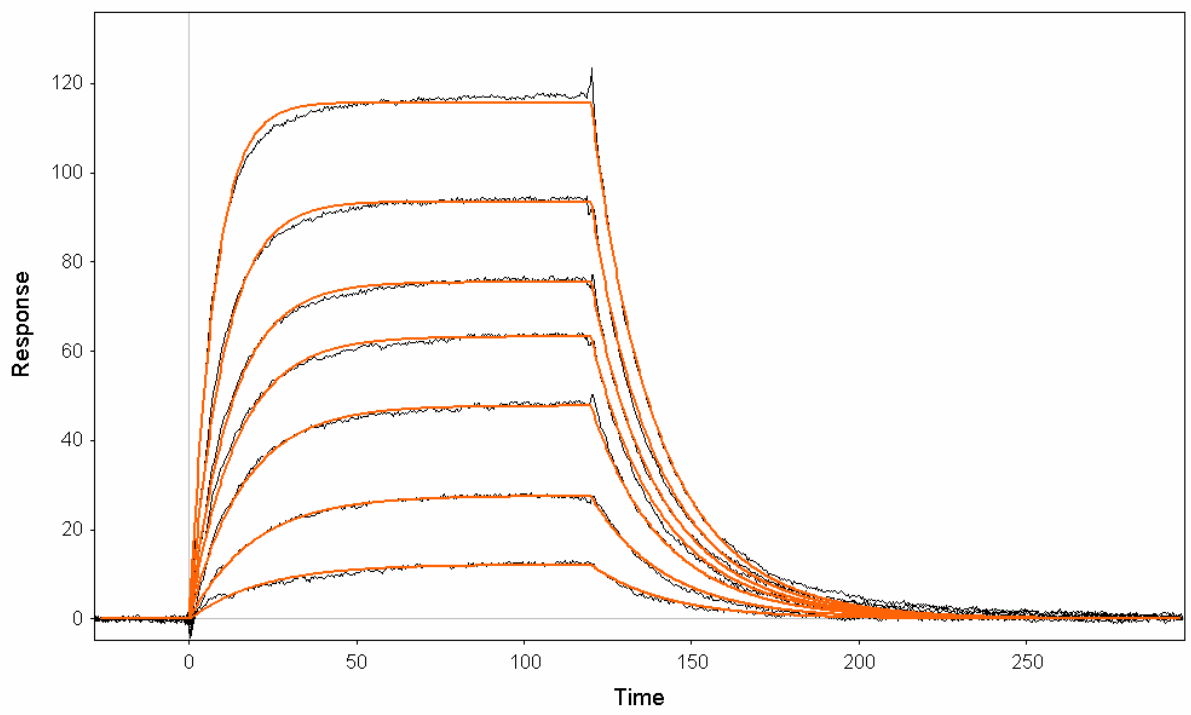

K_D = 137 ± 1 nM k_{on} = (48.6 ± 0.3) x 10^4 $M^{-1}s^{-1}$ k_{off} = (66.5 ± 0.5) x $10^{-3}s^{-1}$

DARPin concentrations [nM]: 10, 25, 50, 75, 100, 150, 250

o) I_19

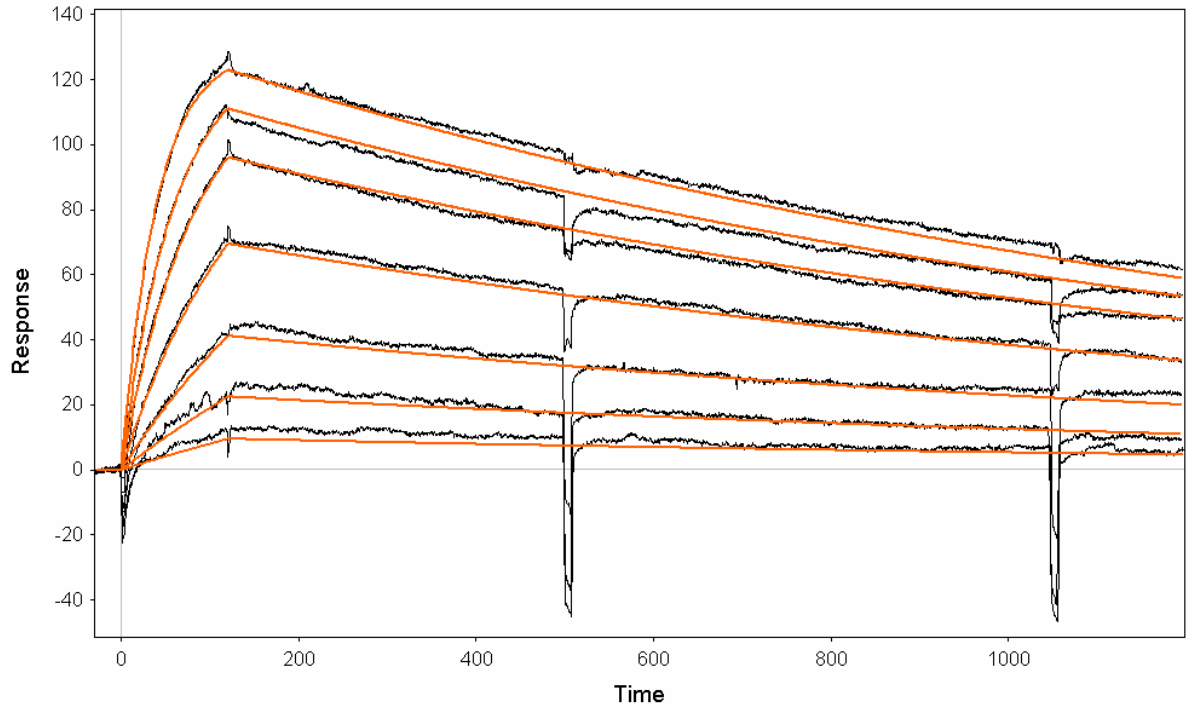

K_D = 2.07 ± 0.01 nM k_{on} = (33.7 ± 0.3) x 10^4 $M^{-1}s^{-1}$ k_{off} = (0.695 ± 0.004) x $10^{-3}s^{-1}$

DARPin concentrations [nM]: 2, 5, 10, 20, 35, 50, 75

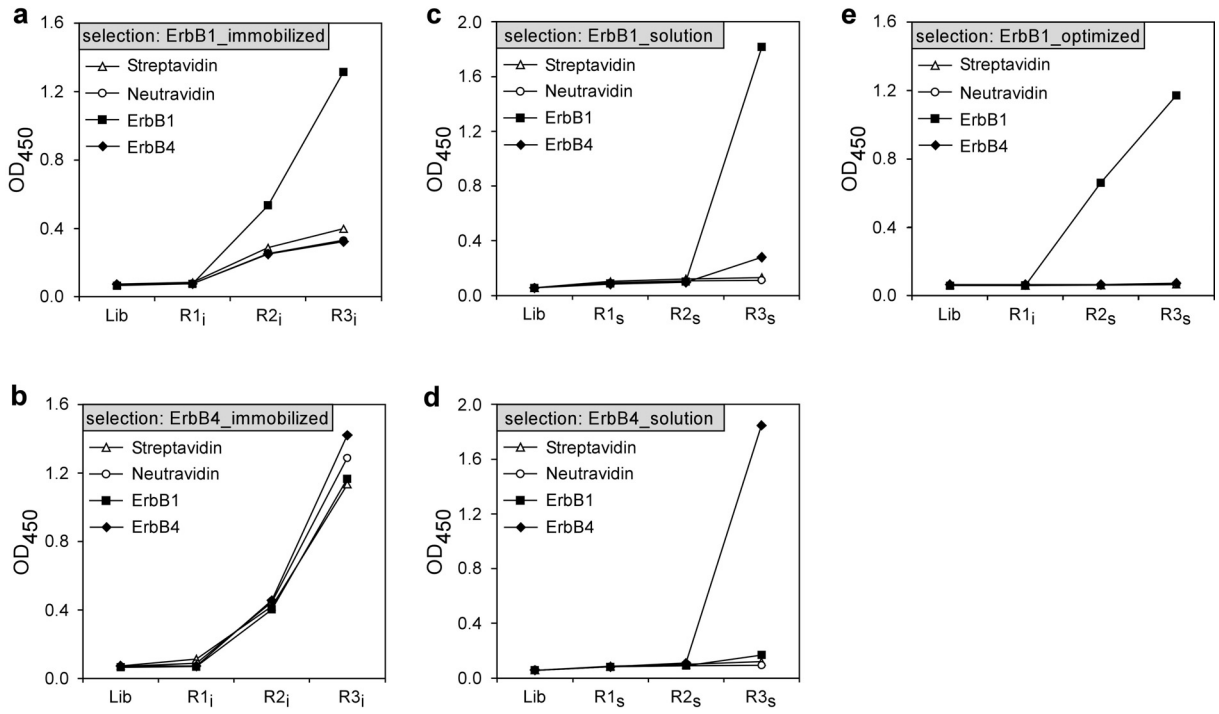

Supplementary Figure 3. Selection approaches on ErbB1 and ErbB4. The enrichments for the selections performed on (a) immobilized ErbB1, (b) immobilized ErbB4, (c) ErbB1 in solution, (d) ErbB4 in solution and (e) ErbB1 by using the optimized selection protocol were analyzed by phage ELISA. Equivalent amounts of the initial library (Lib) and pools of amplified phage particles from each selection round (R1, R2 and R3) were tested for binding to immobilized streptavidin, neutravidin, immobilized ErbB1 and ErbB4. For each sample applied the signal of bound phage particles, detected with an anti-M13 antibody, is shown. For each round the subscript denotes if the selection was performed on immobilized target protein (i) or on target protein in solution (s).

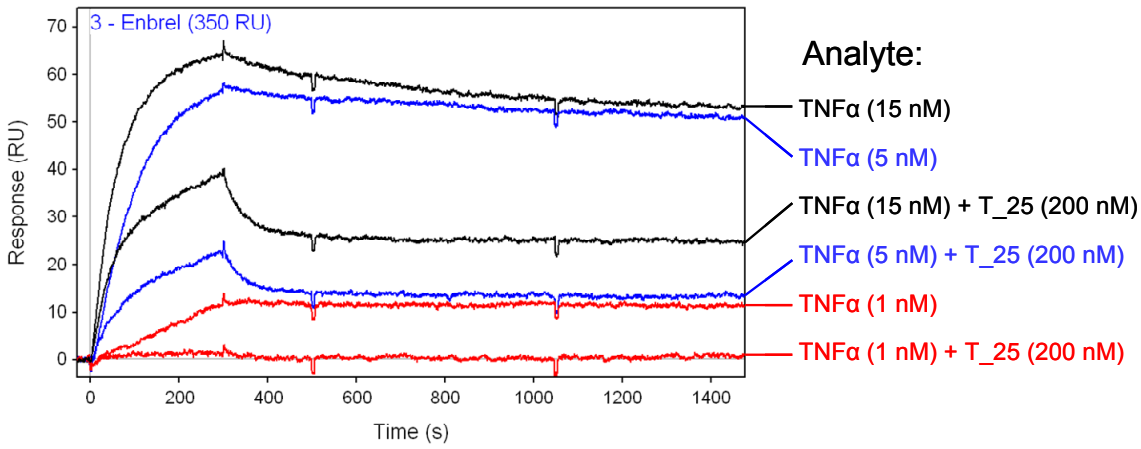

Supplementary Figure 4. Surface plasmon resonance (SPR) was measured using a BIAcore 3000 instrument (BIAcore, Uppsala Sweden). Measurements were performed in HBST buffer (20 mM HEPES, 150 mM NaCl, pH 7.4, 0.1% Tween-20) at a flow rate of 50 µl/min. Enbrel was directly coupled to a dextran-chip according to the manufacturer's protocol (CM5, Biacore, 350 RU) and soluble TNFα (1 nM, 5 nM and 15 nM) alone and preincubated with DARPin T_25 (200 nM) injected for 4 minutes and the dissociation recorded for 20 minutes with buffer flow. The signal of an uncoated reference cell was subtracted from the sensograms.

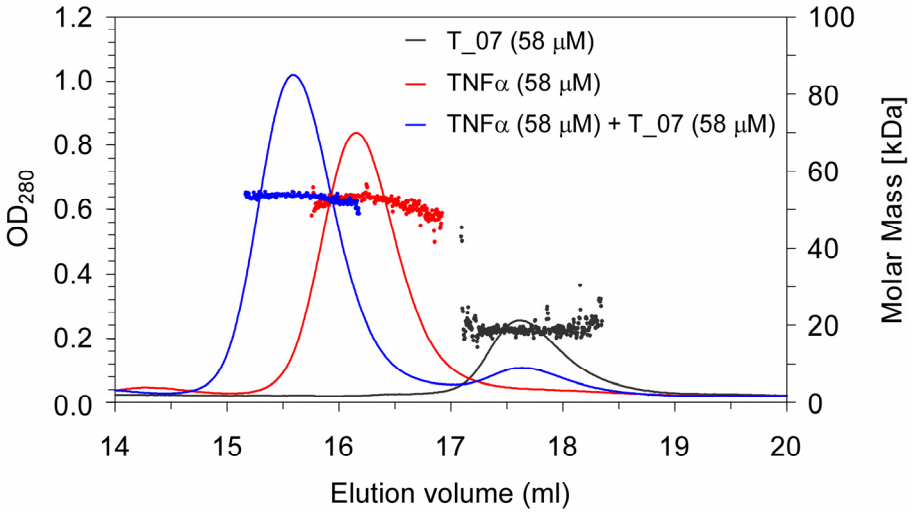

Supplementary Figure 5. Characterization of the DARPin T_07 – TNFα complex formation by size-exclusion chromatography combined with multi-angle light scattering (SEC-MALS). The OD_{280} signals are depicted as solid lines (left y-axis) and the molar mass of the respective elution peak indicated with filled circles (right y-axis). TNFα alone (red line), T_02 alone (grey line) and TNFα preincubated with an equimolar amount of DARPin (blue line) were analyzed at the concentrations described in the figure. The weight-average molar mass over the respective elution peaks are: TNFα alone (52.8 kDa, red circles), T_02 alone (18.8 kDa, grey circles) and TNFα preincubated with an equimolar amount of DARPin (53.5 kDa, blue circles). Protein samples were incubated in PBS containing 0.1% Tween-20 for at least 1 h at room temperature before injection and concentrations for TNFα are given for the monomer.

Chapter 4

In vitro selection and characterization of DARPins and Fab fragments for the co-crystallization of membrane proteins: The Na^+-citrate symporter CitS as an example.

Huber, T., Steiner, D., Rothlisberger, D. & Plückthun, A. (2007)

J. Struct. Biol. **159**, 206-221.

(**My contribution**: Selection and Screening of DARPins form phage display)

Contents

Available online at www.sciencedirect.com
ScienceDirect
Journal of Structural Biology 159 (2007) 206–221
Journal of Structural Biology
www.elsevier.com/locate/yjsbi

In vitro selection and characterization of DARPins and Fab fragments for the co-crystallization of membrane proteins: The Na^+-citrate symporter CitS as an example

Thomas Huber, Daniel Steiner, Daniela Röthlisberger [1], Andreas Plückthun *

Department of Biochemistry, University of Zürich, Winterthurerstrasse 190, CH-8057 Zürich, Switzerland

Received 1 December 2006; accepted 26 January 2007
Available online 3 February 2007

Abstract

The determination of 3D structures of membrane proteins is still extremely difficult. The co-crystallization with specific binding proteins may be an important aid in this process, as these proteins provide rigid, hydrophilic surfaces for stable protein–protein contacts. Also, the conformational homogeneity of the membrane protein may be increased to obtain crystals suitable for high resolution structures. Here, we describe the efficient generation and characterization of Designed Ankyrin Repeat Proteins (DARPins) as specific binding molecules for membrane proteins. We used both phage display and ribosome display to select DARPins *in vitro* that are specific for the detergent-solubilized Na^+-citrate symporter CitS of *Klebsiella pneumoniae*. Compared to classical hybridoma technology, the *in vitro* selection systems allow a much better control of the structural integrity of the target protein and allow the use of other protein classes in addition to recombinant antibodies. We also compared the selected DARPins to a Fab fragment previously selected by phage display and demonstrate that different epitopes are recognized, unique to each class of binding molecules. Therefore, the use of several classes of binding molecules will make suitable crystal formation and the determination of their 3D structure more likely.

Keywords: Co-crystallization; Designed ankyrin repeat proteins (DARPins); *In vitro* selection; Membrane protein; Multi-angle (static) light scattering (MALS); Na^+-citrate symporter CitS; Phage display; Recombinant antibody Fab fragment; Ribosome display; Protein engineering

1. Introduction

Multitopic membrane proteins, such as channels, transporters or receptors, are involved in many fundamental biological processes and today, the majority of drug targets are integral membrane proteins. Therefore, there is an immediate and growing need for high-resolution structure information to gain detailed insight into the function of membrane proteins at the atomic level.

In the different genomes analyzed to date, 20–30% of all open reading frames encode integral membrane proteins (Wallin and von Heijne, 1998). As of September 2006, only about 100 membrane protein structures[2,3] have been deposited in the Protein Data Bank (Berman et al., 2000), and this even includes all homologs from different species and a number of relatively robust bacterial outer membrane proteins with β-barrel topology. The even smaller number of non-redundant α-helical membrane proteins remains in stark contrast to the about 12,000[4] solved structures of non-redundant[5] soluble proteins. This contrast points out the difficulties in membrane protein structure determination.

* Corresponding author. Fax: +41 44 635 57 12.
E-mail address: plueckthun@bioc.unizh.ch (A. Plückthun).
[1] Present address: Department of Biochemistry, University of Washington, Seattle, WA 98195, USA.

1047-8477/$ - see front matter © 2007 Elsevier Inc. All rights reserved.
doi:10.1016/j.jsb.2007.01.013

[2] www.mpibp-frankfurt.mpg.de/michel/public/memprotstruct.html
[3] http://blanco.biomol.uci.edu/Membrane_Proteins_xtal.html
[4] http://www.pdb.org/pdb/holdings.do
[5] Proteins with less than 70% identity.

1.1. Crystallization of membrane proteins

A major bottleneck in structure determination of membrane proteins is the production of high quality crystals. The difficulties are mainly attributed to the inherent protein flexibility and conformational inhomogeneity of the detergent-solubilized membrane protein–detergent complex. Additionally, the polar surface of those membrane proteins having only very short solvent-exposed loops cannot reach beyond the detergent layer wrapped around the hydrophobic surface, and therefore stable protein–protein contacts essential for crystal packing are not formed.

1.2. Co-crystallization

A relatively new approach to overcome these problems is the co-crystallization of membrane proteins with antibody fragments (reviewed in Hunte and Michel, 2002). For successful co-crystallization a stable complex of an antibody fragment bound to a structural epitope present in the native conformation of the membrane protein is needed. Thereby, the bound antibody fragment reduces the protein flexibility and increases the conformational homogeneity of the membrane protein–detergent complex since it recognizes—ideally—only the native and functional conformation of the membrane protein. This specificity can also be exploited during membrane protein purification to increase the homogeneity of the protein sample (Kleymann et al., 1995). Equally important, the bound antibody fragment provides additional polar surfaces to mediate stable protein–protein contacts for well-ordered crystal packing. However, this specificity comes at a cost: a new binding molecule fulfilling all the above requirements has to be generated for each membrane protein structure to be solved.

Published co-crystals of membrane proteins and antibody fragments include cytochrome *c* oxidase from *Paracoccus denitrificans* (PDB entries 1QLE/1AR1), cytochrome bc1 complex from *Saccharomyces cerevisiae* alone (PDB entries 1EZV/1KB9) and in complex with cytochrome *c* (PDB entry 1KYO), potassium channel KcsA from *Streptomyces lividans* (PDB entries 1K4C/1K4D/1R3I/1R3J/1R3K/1R3L/2BOB/2BOC), and the ClC chloride channel from *Escherichia coli* (PDB entries 1OTS/1OTT/1OTU). Interestingly, in all crystal structures the antibody fragment fills the gap between adjacent membrane proteins in the crystal lattice and mediates important protein–protein interactions for well-ordered packing.

1.3. Monoclonal antibodies

In all published examples the antibody fragments used for co-crystallization were ultimately derived from monoclonal antibodies, and Fab fragments were either produced by proteolysis of the IgG or the antibody fragment genes from hybridomas were cloned and expressed in *E. coli*.

Several fundamental problems are encountered, however, in the generation of monoclonal antibodies with the desired properties from animals. When the solubilized membrane protein is injected into the animals, the detergent is diluted and the further fate of the protein and its conformational integrity cannot be controlled. The use of adjuvants such as mineral oil casts an additional shadow of doubt on maintaining the native structure for a long time. The membrane protein is processed by antigen-presenting cells and at the same time, some molecules need to be bound to IgM on the surface of B-cells, which triggers the antibody response in the animal. It is at least doubtful whether the conformational epitopes would still be intact at this stage, unless the protein is very stable. Subsequent screening of hybridomas for reactivity with the native state of the protein will detect those antibodies that bind to epitopes present in the folded structure—if such antibodies have been elicited at all. However, when producing antibodies against less rigid molecules, e.g. GPCRs, it is highly likely that most binders that do crossreact with the native protein will be directed against exposed N- or C-terminal tails (Niebauer et al., 2006) or extracellular compact domains, rather than that binders recognize the loops connecting the helices in their native conformation. If the protein denatures during the immunization process, many "real" conformational epitopes will be lost and conformation-specific antibodies are not found.

1.4. Our approach

Here, we demonstrate the use of *in vitro* selection methods to overcome the above limitations and we report a fast downstream screening process to efficiently identify suitable binding partners of membrane proteins for co-crystallization. After we showed in a previous study that conformation-specific, high-affinity antibody Fab fragments that bind to the detergent-solubilized Na^+-citrate symporter CitS can be generated by phage display (Röthlisberger et al., 2004), we now expand this approach to another selection system as well as to another class of binding proteins. With the use of a different class of binding proteins the shape of the binding module can be varied and we intended by using different binding molecules to obtain binders to different epitopes. Both factors can lead to different crystal packing, which should clearly increase the chance of crystal formation suitable for high resolution structure determination.

1.5. Recombinant Fab fragments and Designed Ankyrin Repeat Proteins

The two classes of binding proteins investigated and compared here are antibody Fab fragments and Designed Ankyrin Repeat Proteins (DARPins). The heterodimeric Fab fragment (Fig. 1a) consists of the entire light chain (V_L and C_L domains) and the Fd fragment (V_H and C_H domains) of the heavy chain, which—in the format used in this study—are not disulfide-linked to each other (Röthlisberger et al., 2004). The antigen binding site is formed by

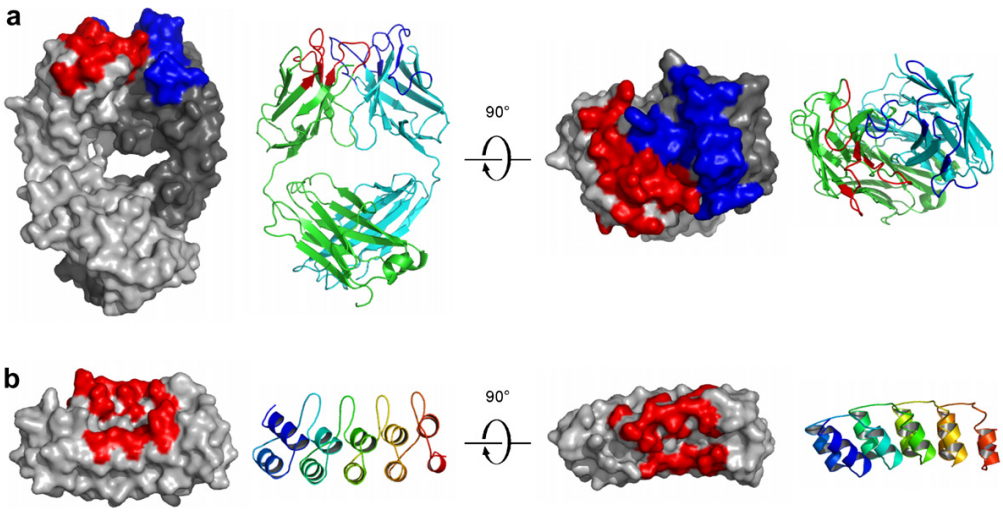

Fig. 1. (a) Surface and corresponding cartoon representation of a Fab fragment. Left, side view where the binding site is on top. The surface of the light chain ($V_L + C_L$) is depicted in light grey and its binding site (CDRs) in red. The corresponding elements of the heavy chain ($V_H + C_H$) are dark grey and the CDRs are depicted in blue. In the cartoon representation, the two chains are colored green (light chain) and cyan (heavy chain). Right, top view on the binding site of the Fab fragment. (b) Surface and corresponding cartoon representation of an N3C consensus DARPin (PDB entry: 1MJ0). The variable positions are colored red in the surface representation. The individual repeats are colored differently in the cartoon picture. Side view (left) and top view (right) on the binding site. Figures were generated with PyMol (DeLano, 2002).

the V_L and V_H domains and is constituted of three loops (complementarity determining regions, CDRs) from each domain, which are highly diverse in sequence and length. We have used a fully synthetic antibody library, based on the original HuCAL consensus design (Knappik et al., 2000), but limiting the library to the most stable and best expressing V_H and V_L frameworks (Ewert et al., 2003), which are randomized in all 6 CDRs and were used in the format of Fab fragments (Röthlisberger et al., 2004). Even though the *in vitro* selection by phage display and the subsequent preparation of milligram quantities of Fab fragments is possible, there are still good reasons to explore alternative frameworks. First, the Fab fragment contains four intramolecular disulfide bonds and can thus not be exposed to reducing conditions that some membrane proteins may require, and second, the preparation of Fab fragments for crystallization trials typically requires five to ten liters of *E. coli* culture. Finally, despite the variety of shapes of antibody binding sites, caused by the length and sequence variation of the CDRs, we have no information on how many different epitopes we actually targeted on a given detergent-solubilized integral membrane protein.

Ankyrin repeat proteins occur in all phyla and mediate important protein–protein interactions in all cell compartments (Bork, 1993). Their modular structure is built from stacked, 33-amino acid repeats, each forming a β-turn followed by two antiparallel α-helices and a loop connecting to the β-turn of the next repeat. Using a combination of sequence and structural alignments, potential interaction residues were identified in the β-turn and first α-helix and were randomized in the library design, while conserved intra- and inter-repeat interactions characteristic for the ankyrin fold were preserved (Fig. 1b) (Binz et al., 2003). Varying numbers of designed ankyrin repeats (typically 2 or 3) were cloned in between specialized N- and C-terminal capping-repeats which seal the hydrophobic core of a stack of the ankyrin repeats that are carrying the potential binding interface. These DARPins are termed N2C and N3C, respectively, denoting their internal repeat numbers. This procedure yielded libraries of DARPins with varying size of randomized interaction surface. Their members have very favorable biophysical properties, very high expression yields (Binz et al., 2003) and have been selected for specific binding to soluble targets before (Binz et al., 2004).

1.6. In vitro selection

The interest in rapid isolation of specific, high-affinity polypeptide binders against a broad range of target molecules lead to the development of different display technologies (Hoogenboom, 2005; Binz et al., 2005). The underlying principle of all these display technologies is the linkage of phenotype and genotype. Thereby, specific binders with desired properties can be enriched from large collections of variants over several consecutive selection cycles. In the present study, phage display and ribosome display were used.

1.7. Phage display

The most widely used display technology is phage display, where the protein (phenotype) is displayed on the sur-

face of a filamentous phage particle while the respective DNA (genotype) is encapsulated inside (Smith and Petrenko, 1997; Hoogenboom, 2002). The power of phage display lies in the robustness of the phage particle, which allows selections to be performed under a wide range of conditions, including the presence of many detergents. A limiting step in phage display, however, is the involvement of *E. coli* transformation, which restricts the diversity of the initial library to 10^9–10^{10} members. In the case of affinity maturation, this *in vivo* step makes the iteration between random mutagenesis, repeated library construction and selection unattractive, as it is very laborious. Furthermore, the *in vivo* amplification of the phage particles can lead to a bias in selection due to growth advantage of certain clones. However, the assembly pathway of filamentous phages allows heterodimers (e.g. Fab fragments) to be displayed on the phage surface. A scheme of the selection cycle is depicted in Fig. 2a.

1.8. Ribosome display

To overcome the limitations caused by the involvement of living cells, ribosome display was developed as a completely *in vitro* display technology (Hanes and Plückthun, 1997). This method relies on the formation of a non-covalent ternary complex of mRNA (genotype), ribosome and nascent polypeptide (phenotype). These complexes are formed during *in vitro* translation, and therefore very large libraries of up to 10^{14} members can be sampled (limited by the amount of cell-free translation extract used and the amount of diverse input DNA). The ease of introducing mutations during the selection cycle by methods such as error-prone PCR or DNA shuffling makes this display technology a very powerful tool for affinity maturation of binding proteins. The relatively low stability of the ternary complex narrows the range of selection conditions, but we show here that selection in detergent for binding to a solu-

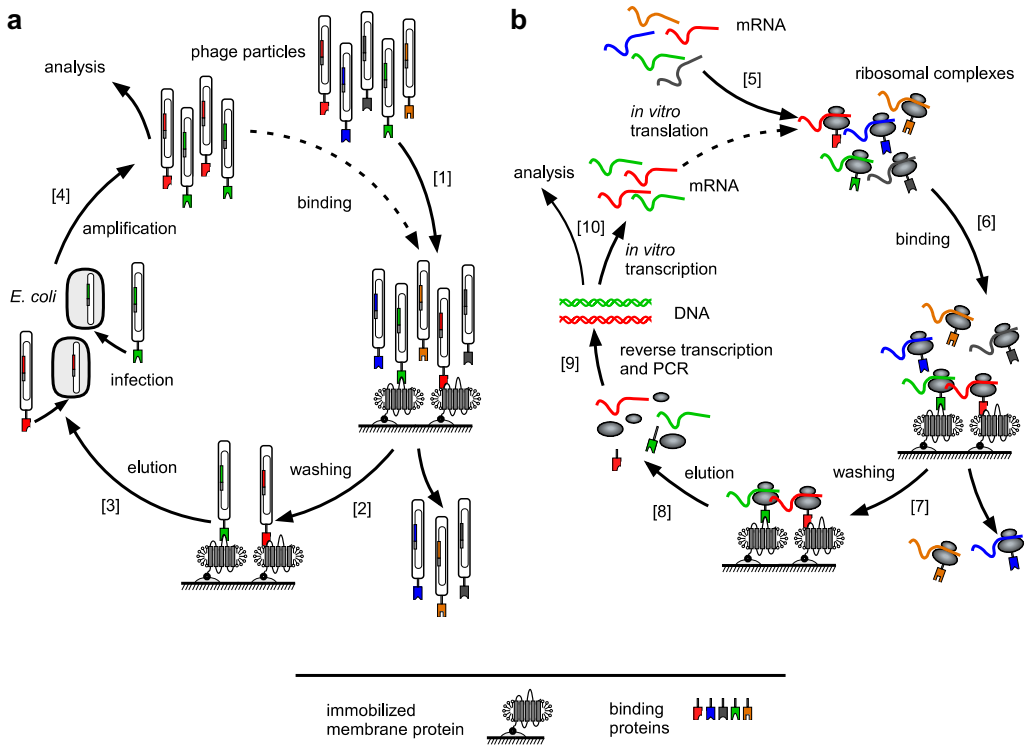

Fig. 2. (a) Schematic representation of a phage display selection cycle. A phage library displaying variants of the protein of interest on the surface while having the respective gene encapsulated inside the phage particle is used for the binding selection on the immobilized target [1]. After formation of the complexes between the binding protein and the membrane protein, unbound phage particles are washed off [2]. The bound phages are eluted from the immobilized target by a pH shift [3] and used for the infection of *E. coli*. Phage particles are amplified [4] and can then be analyzed or used as input for the next selection round. (b) Schematic representation of a ribosome display selection cycle. An mRNA library encoding the proteins of interest without stop codon is translated *in vitro* [5]. After cooling, the translation yields stable ternary complexes of mRNA, ribosomes and nascent polypeptides. These complexes are used for the binding selection on the immobilized target [6]. After binding of the polypeptides to the membrane protein, unbound complexes are washed off [7]. The mRNA of the bound complex is eluted by dissociating the ribosomal complex with EDTA [8]. A reverse transcription reaction followed by PCR yields the genetic information of the selected clones [9]. The amplified genes can then be used as input for the next selection round starting with *in vitro* transcription [10] or cloned into plasmids for analysis.

bilized membrane protein is possible. A scheme of the selection cycle is depicted in Fig. 2b.

1.9. Na^+-citrate symporter CitS as model target

The model system used for this study is the Na^+-citrate symporter CitS from *Klebsiella pneumoniae*, a typical integral membrane protein of the helix-bundle type. CitS has a predicted molecular mass of about 50 kDa and belongs to the family of 2-hydroxy-carboxylate transporters (2HCT)[6] found exclusively in bacteria. Currently, almost 40 members of the 2HCT family are known (Sobczak and Lolkema, 2005). The determined hydropathy profile is highly conserved throughout the family, and it is assumed that all members of the 2HCT family share a common fold. However, no 3D structure is available so far for any member of the 2HCT family. CitS is responsible for citrate uptake during the anaerobic breakdown of citrate in *K. pneumoniae* which ultimately leads to ATP formation. CitS transports the citrate dianion ($Hcit^{2-}$) in symport with two Na^+ ions and one H^+ ion across the membrane. A topology model of CitS was determined using PhoA fusions, site-directed Cys labeling, insertion of reporter proteins, and expression in an *in vitro* translation/insertion system (van Geest and Lolkema, 2000). According to this model, CitS consists of 11 transmembrane segments (TMS) with the N-terminus in the cytoplasm and the C-terminus in the periplasm and relatively short loops connecting the TMS (Fig. 3a). CitS is so far the only member of the 2HCT family that has been purified to homogeneity and functionally reconstituted into proteoliposomes (Pos and Dimroth, 1996). Therefore, it is assumed that CitS is in a functional state when detergent-solubilized. This is not only important for crystallographic studies of the membrane protein but is also crucial for successful *in vitro* selections.

There are certain advantages of using detergent-solubilized membrane proteins as targets for selection over the use of whole cells or reconstituted proteoliposomes. The advantages are the accessibility of both extracellular and intracellular epitopes, the higher monodispersity of the target, and the simplification of the selection procedure. Nevertheless, it must be kept in mind that the detergent may also shield regions (epitopes) of the membrane protein and that the membrane protein might, at least in principle, adopt a non-functional conformation.

[6] *Abbreviations used:* 2HCT, 2-hydroxy-carboxylate transporters; 4NPP, 4-nitrophenyl phosphate; AP, alkaline phosphatase; BAD, biotin acceptor domain; BSA, bovine serum albumin; CDR, complementary determining region; DARPin, Designed Ankyrin Repeat Protein; DDM, *n*-dodecyl-α-D-maltopyranoside; ECL, electrochemiluminescence; HuCAL, human combinatorial antibody library; IMAC, immobilized metal ion affinity chromatography; IPTG, isopropyl-β-D-thiogalactopyranoside; K_D, equilibrium dissociation constant; MALS, multi-angle (static) light scattering; MBP, maltose binding protein; pfu, plaque forming units; SEC, size-exclusion chromatography; TMS, transmembrane segment.

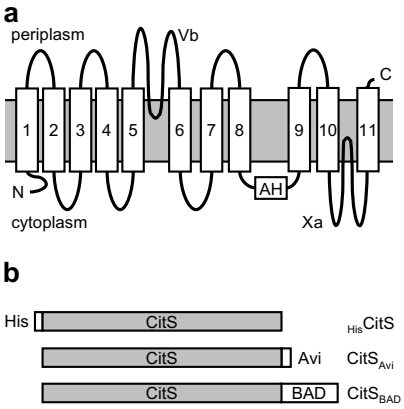

Fig. 3. (a) Simplified topology model of CitS. It contains 11 transmembrane segments, with the N-terminus (N) in the cytoplasm and the C-terminus (C) in the periplasm. The segments Vb and Xa are thought to extend into the membrane. The segment AH is an amphipathic surface helix. This figure is adapted from Sobczak and Lolkema (2005). (b) Schematic representation of the three CitS constructs with corresponding annotation used in this study. The length of the boxes is proportional to the actual length of the protein chain.

2. Materials and methods

2.1. Protein expression and purification

2.1.1. Na^+-citrate symporter CitS from K. pneumoniae

CitS containing an N-terminal His tag. The amino acid sequence M-G-$(H)_{10}$ was fused to the N-terminus of the full length CitS (M83146, aa M1-I446) in the vector pET16b (the expressed protein is termed $_{His}$CitS, Fig. 3b) and expressed in *E. coli* C43(DE3) (Miroux and Walker, 1996) as described by Kästner et al. (2000). *E. coli* C43(DE3) cells were lysed using a French press and CitS was directly solubilized with 2% DDM in 20 mM Tris–HCl, pH 7.5 and 300 mM NaCl. The cleared lysate containing the solubilized CitS was purified by IMAC (Ni^{2+}–NTA, Qiagen). The eluate was further passed over a size-exclusion chromatography column (Superose 6 10/300 GL, GE Healthcare).

Biotinylated CitS. The vector pMalccitSabirA (Kästner et al., 2000) was used to express biotinylated CitS. Biotin ligase BirA was co-expressed from the same plasmid allowing *in vivo* biotinylation. Two constructs were cloned in the vector pMalccitSabirA. One had the biotin acceptor domain (BAD) of oxaloacetate decarboxylase from *K. pneumoniae* (J03885, aa V492-A596) fused to the C-terminus of CitS (the expressed protein is termed $CitS_{BAD}$, Fig. 3b) (Kästner et al., 2000), the other carried an Avi tag (G-L-N-D-I-F-E-A-Q-K-I-E-W-H-E) fused to the C-terminus (the expressed protein is termed $CitS_{Avi}$, Fig. 3b). Both constructs were expressed in *E. coli* DH5α as described by Kästner et al. (2000). Cells were lysed using a French Press and biotinylated CitS was directly solubilized with 2% DDM in 100 mM sodium phosphate, pH 7,

300 mM NaCl and 10% glycerol. Solubilized CitS was purified from the cleared lysate by a monomeric avidin column (Pierce). To remove the free biotin the eluate was passed over a desalting column (NAP-5, GE Healthcare) and subsequently dialyzed twice against 250 buffer volumes each.

2.1.2. Designed Ankyrin Repeat Proteins (DARPins)

Selected DARPins were cloned into pQE30-based (Qiagen) vectors containing an N-terminal M-R-G-S-$(H)_6$ tag. Behind the DARPin coding region, the vector contained either the double stop codon TAA-TGA ($pQE30_{ss}$; the expressed protein is termed $_{His}$DARPin) or a five times repeated myc-tag (M-E-Q-K-L-I-S-E-E-D-L-N-E)$_5$, ($pQE30_{myc5}$; the expressed protein is termed $DARPin_{myc5}$) in front of the double stop codon. Expression of DARPins was performed in *E. coli* XL1-Blue (Stratagene) in dYT medium (5 g NaCl, 10 g yeast extract, 16 g tryptone for 1 liter of media). Expression was induced with 1 mM IPTG (final concentration) at an OD_{600} of 0.6 and continued for 3–4 h at 37 °C.

Cells were resuspended in lysis buffer (40 mM Tris–HCl, pH 7.5, 300 mM NaCl, 20 mM imidazole, 10% glycerol, and 1 mg/ml lysozyme), and passed through a French press, and the cleared lysate was applied to an IMAC column (Ni^{2+}–NTA, Qiagen). Elution fractions were passed over a desalting column (NAP-5, GE Healthcare).

2.2. Ribosome display

The PCR-amplified N3C DARPin DNA-library, described previously (Binz et al., 2004), was transcribed *in vitro* and selection was performed by ribosome display as described by Hanes and Plückthun (1997). MaxiSorp plates (Nunc) were coated with NeutrAvidin (100 µl, 66 nM, overnight at 4 °C), blocked with BSA (200 µl, 0.5%, 1 h at room temperature) and $CitS_{BAD}$ was immobilized via its biotin residue on NeutrAvidin (100 µl, 200 nM $CitS_{BAD}$, 1 h at 4 °C, 10 mM Tris–HCl, pH 7.5, 150 mM NaCl, and 0.05% DDM). Binding and washing buffers (50 mM Tris–HOAc, pH 7.5, 150 mM NaCl, 50 mM $Mg(OAc)_2$, 0.5% BSA, and 0.05% DDM) contained DDM as detergent to keep the membrane protein in its functional conformation. The translation mix, containing the ternary mRNA–ribosome–DARPin complexes, was first pre-panned in two wells (30 and 60 min) against biotinylated MBP, immobilized the same way as $CitS_{BAD}$ to remove DARPins that would bind to the plate for other reasons than recognizing CitS. Subsequently, the translation mix was transferred to the well containing immobilized $CitS_{BAD}$. The library was incubated for 45 min, and the washing time was increased from round to round (15 min total washing time in the first round to 90 min total washing time in the fourth round). After washing, the mRNA was eluted with 100 µl elution buffer (50 mM Tris–HOAc, pH 7.5, 150 mM NaCl, and 25 mM EDTA). A total number of four rounds of ribosome display were performed. The number of PCR cycles after reverse transcription was reduced from round to round from 45 to 35 to 30 to 25, adjusting to the yield due to progressive enrichment of binders in each round.

2.3. Phage display

The generation and characterization of the DARPin-phage library based on SRP-Phage display (Steiner et al., 2006) will be described elsewhere (Steiner et al., manuscript in preparation). All steps of the phage display selection were performed at room temperature. For the first selection cycle 1.6×10^{13} phage particles displaying the DARPin library were incubated for 1 h with 100 nM biotinylated $CitS_{BAD}$ in 2 ml of CitS-buffer (20 mM potassium phosphate, pH 7.0, 500 mM NaCl, 20% glycerol, and 0.1% DDM) containing 0.4% BSA. The phage–antigen complexes were captured on 100 µl streptavidin-coated paramagnetic beads (10 mg/ml, Dynabeads MyOne Streptavidin T1, Dynal) for 20 min. After washing the beads eight times with CitS-buffer the phage particles were eluted with 200 µl of 100 mM Et_3N for 6 min, followed by 200 µl of 100 mM glycine, pH 2, for 10 min. Eluates were neutralized with 100 µl of 1 M Tris–HCl, pH 7, or 18 µl of 2 M Tris–base, respectively, combined and used to infect 5 ml of exponentially growing *E. coli* XL1-Blue cells (Stratagene). After shaking for 1 h at 37 °C cells were plated on dYT agar plates containing 10 µg/ml chloramphenicol and 1% glucose and grown overnight at 37 °C. The cells were scraped off the plates and used to inoculate 15 ml of dYT containing 10 µg/ml chloramphenicol to an initial OD_{600} of 0.1. The culture was incubated at 37 °C with shaking and at an OD_{600} of 0.5 the phage library was rescued by infection with VCSM13 helper phage (Stratagene) at 10^{10} pfu (plaque forming units) per ml (multiplicity of infection ~20). After 1 h at 37 °C, 45 ml of fresh dYT containing 10 µg/ml chloramphenicol, 16.7 µg/ml kanamycin, and 0.27 mM IPTG were added and the culture grown overnight at 30 °C. Cells were removed by centrifugation (5600*g*, 4 °C, 10 min) and the culture supernatant was incubated on ice for 1 h with one-fourth volume of ice-cold PEG/NaCl solution (20% polyethyleneglycol (PEG) 6000, 2.5 M NaCl). The precipitated phage particles were then collected by centrifugation (5600*g*, 4 °C, 15 min) and resuspended in 3 ml of CitS-buffer and used for the second round of selection.

For the subsequent selection rounds, 10^{12} of the amplified phage particles were used as input, beads were washed 12 times with CitS-buffer, phages eluted with 400 µl of 100 mM glycine, pH 2 for 10 min, the eluate neutralized with 36 µl of 2 M Tris–base and used to infect 5 ml of exponentially growing *E. coli* XL1-Blue cells.

Infection was allowed to occur for 1 h at 37 ° C and cells were directly expanded into 50 ml of fresh dYT containing 10 µg/ml chloramphenicol. After 3–4 h at 37 °C, IPTG was added to a final concentration of 0.2 mM and 15 min later VCSM13 helper phage was added to a final concentration of 10^{10} pfu per ml. Cells were grown overnight at 37 °C

without the addition of kanamycin and phage particles harvested as described above.

To determine enrichment of binders, amplified polyclonal phage pools from each selection round were analyzed by phage ELISA as described by Röthlisberger et al. (2004). Further, single clones of round three and four were randomly picked and analyzed by phage ELISA. Positive clones were sequenced and recloned into $pQE30_{ss}$ and $pQE30_{myc5}$ for further analysis.

2.4. Analytical size-exclusion chromatography (SEC)

Size-exclusion chromatography was performed on an Agilent 1100 HPLC system. A molar excess of selected DARPins (30–60 μM) was mixed with $_{His}$CitS (15–30 μM) and incubated in 10 mM Tris–HCl, pH 7.5, 150 mM NaCl, 0.05% DDM for at least 30 min at 10 °C for complex formation. For analysis of the ternary CitS–DARPin–Fab fragment complex, $_{His}$CitS (15 μM) was incubated with both DARPin (30 μM) and Fab fragment (30 μM) for 60 min at 10 °C for complex formation. With a well plate autosampler (Agilent 1100) sample volumes of 75 μl were loaded on a Superdex 200 10/300 GL column (GE Healthcare) with a flow rate of 0.5 ml/min. Fractions of 250 μl were collected with an analytical fraction collector (Agilent 1100).

2.5. Multi-angle light scattering (MALS)

SEC-MALS measurements were performed on an Agilent 1100 HPLC system connected to a tri-angle light scattering detector and a differential refractometer (miniDAWN Tristar and Optilab, respectively; Wyatt Technology, Santa Barbara, CA, USA). Specific refractive index increment (dn/dc) values of 0.186 ml/g (Wen et al., 1996) and 0.133 ml/g (Strop and Brünger, 2005) were used for the protein and the detergent fraction (DDM), respectively. Sample volumes of 200 μl with a CitS protein concentration of 20 μM were injected on a Superose 6 10/300 GL column (GE Healthcare). The data were recorded and processed using the ASTRA V software (Wyatt Technology). To determine the detector delay volumes and normalization coefficients for the MALS detector, a BSA sample (Sigma, A8531) was used as reference. Neither despiking nor a band broadening correction was applied.

2.6. ELISA

Buffers for binding and washing in all ELISA experiments were 10 mM Tris–HCl, pH 7.5, 150 mM NaCl (TBS) supplemented with 0.05% DDM (TBS-D), 0.2% BSA (TBS-B) or both (TBS-DB), if not stated otherwise.

2.6.1. Crude extract ELISA

2.6.1.1. Coating. A MaxiSorp Plate (Nunc) was coated with protein A (Sigma, 100 μl, 10 μg/ml in 100 mM phosphate, pH 7.0, and 150 mM NaCl) for 2 h at 4 °C and blocked for 2 h with 0.2% BSA (Fluka, 200 μl TBS-B) at room temperature. The wells were incubated with 100 μl of a 1:500 dilution of anti-myc antibody (Cell signaling, 9B11) in TBS-B for 1 h at 4 °C.

2.6.1.2. Crude extract from single clones. One milliliter medium (dYT containing 1% glucose and 100 μg/ml ampicillin) was inoculated with single colonies of *E. coli* XL1-Blue, harboring $pQE30_{myc5}$ encoding a selected DARPin, in a 96-deep-well plate and was grown overnight at 37 °C. One milliliter of fresh dYT with 100 μg/ml ampicillin was inoculated with 100 μl of the overnight culture. After incubation for 2 h at 37 °C, expression was induced with IPTG (1 mM final concentration) and continued for 3 h. Cells were harvested, resuspended in 100 μl B-PERII (Pierce) and incubated for 15 min at room temperature with vortexing from time to time. Then, 900 μl TBS-D was added and cell debris was removed by centrifugation.

2.6.1.3. ELISA of lysate. Of each lysate, 100 μl were applied to a well of a MaxiSorp plate containing immobilized anti-myc antibody and incubated for 45 min. After extensive washing with TBS the plate was incubated with 40 nM biotinylated $CitS_{BAD}$ in TBS-DB for 45 min. For competition experiments, 400 nM of the competitor was pre-incubated with biotinylated CitS. After washing with TBS-D, binding was detected with streptavidin-AP conjugate (Roche, 1:1000 dilution in TBS-DB, 30 min at 4 °C) by using di-sodium 4-nitrophenyl phosphate (4NPP, Fluka) as a substrate for AP. The color development was stopped by addition of 3 M NaOH (100 μl) and measured at 405 nm (540 nm reference wavelength) with a plate reader (HTS 7000 Plus, Perkin-Elmer). As negative control the crude extract of an expression culture containing the expression vector without an insert was used.

2.6.2. Competition ELISA with purified proteins

2.6.2.1. Fab directly coated/detection of biotinylated CitS. MaxiSorp plates were coated directly with 250 nM Fab fragment (in TBS, purified as described by Röthlisberger et al. (2004)), incubated for 2 h at 4 °C and blocked with 200 μl TBS-B for 1 h. The plate was then incubated with 40 nM biotinylated $CitS_{BAD}$ in TBS-DB for 45 min. For competition experiments, 400 nM of the competitor was pre-incubated with biotinylated $CitS_{BAD}$. Detection of the bound protein was done as above. In the negative control no Fab fragment was coated.

2.6.2.2. Sandwich ELISA/detection of DARPin via myc tag. Coating of MaxiSorp plates with 250 nM Fab fragment was carried out as described above. Then the plate was incubated with 40 nM $_{His}$CitS in TBS-DB for 45 min. After washing, purified $DARPin_{myc5}$ (50 nM in TBS-DB) was added to the well for 30 min. Detection was performed by incubation with anti-myc antibody (1:1000 dilution in TBS-DB; 45 min at 4 °C) followed by, after washing, goat anti-mouse antibody fused to AP (Sigma, 1:2000 in

TBS-DB; 30 min at 4 °C). Color development and measurements were carried out as above. In negative controls there was either no Fab fragment coated or the Fab fragment was incubated with buffer only instead of $_{His}$CitS.

2.7. Determination of dissociation constants by equilibrium titration

To determine the dissociation constants of the DARPins electrochemiluminescence (ECL)-based equilibrium titration was performed using the ECL-detection system of BioVeris (Witney, Oxfordshire). Streptavidin-coupled paramagnetic beads were coated with $CitS_{Avi}$, and bound $DARPin_{myc5}$ was detected by an anti myc-tag antibody (Cell signaling, 9B11), which in turn was detected with an anti-mouse IgG labeled with the BV-tag (BioVeris). The BV-tag consists of a tris(2,2′-bipyridine)ruthenium(II) complex, covalently linked to the protein, that emits light when electrooxidized in the presence of aliphatic amines, such as tri-*n*-propylamine (Miao et al., 2002). The amount of DARPin bound to immobilized $CitS_{Avi}$ was measured as a function of competing $_{His}$CitS in solution. The assay buffer used for all dilution, wash and assay steps was 10 mM Tris–HCl, pH 7.5, 150 mM NaCl containing 0.05% DDM and 0.2% BSA (TBS-DB). Coating of the beads with $CitS_{Avi}$ was performed at 4 °C, all other steps at room temperature.

2.7.1. Detection mix

A suspension of 40 μg/ml streptavidin-coupled paramagnetic beads (Dynabeads MyOne Streptavidin T1, Dynal biotech) was washed and then incubated with 2.5 nM $CitS_{Avi}$ for 45 min under vigorous shaking. The beads were washed to remove free $CitS_{Avi}$. Subsequently, anti-myc antibody (Cell signaling, 9B11) as well as anti-mouse IgG antibody carrying the BV-tag (BioVeris) were added, each at 1:200 dilutions.

2.7.2. Assay

Dilutions of $_{His}$CitS in the range from 50 pM to 2 μM were mixed with 5 nM of $DARPin_{myc5}$ and 15 μl of detection mix to yield a total assay volume of 150 μl. Under vigorous shaking, the samples were incubated at room temperature for at least 4 h. Subsequently, ECL signals were detected in 96-well format with a M1M analyzer (BioVeris Corporation). The plate was incubated for 10 min in the M1M analyzer under shaking.

2.7.3. Data analysis

The DARPin can either bind to immobilized $CitS_{Avi}$ on the beads or to free $_{His}$CitS in solution. This can be described by two equilibria, assuming a 1:1 interaction Eq. (1).

$$C + A \rightleftharpoons CA \text{ and } C_b + A \rightleftharpoons C_bA \quad (1)$$

where C is the His-tagged CitS ($_{His}$CitS), A is the myc-tagged DARPin ($DARPin_{myc5}$) and C_b is the bound Avi-tagged CitS ($CitS_{Avi}$) present on the beads.

Assuming the same dissociation constant K_D for both equilibria and that each CitS monomer interacts with one DARPin independently, we derived Eq. (2) from the basic equations that describe the two equilibria Eq. (1) (see Online Supplement for derivation)

$$ECL = \frac{Const.}{2\left(\frac{[C]_t}{[C_b]_t}+1\right)}\left\{([A]_t+[C]_t+[C_b]_t+K_D) - \sqrt{([A]_t+[C]_t+[C_b]_t+K_D)^2-4\left(\frac{[C]_t}{[C_b]_t}+1\right)[C_b]_t[A]_t}\right\} + BG \quad (2)$$

where $[C]_t$ is the total concentration of added $_{His}$CitS, $[C_b]_t$ is the total amount of $CitS_{Avi}$ present on the beads (given as a molar concentration in the assay), $[A]_t$ is the total concentration of added $DARPin_{myc5}$, *Const.* is a proportionality constant that correlates the concentration of C_bA to the measured signal, *ECL* is the measured signal and *BG* is the background signal.

The parameters K_D, $[A]_t$, *Const.* and *BG* were fitted to the data using Eq. (2) with Prism 4 (GraphPad software Inc.). Measurements where carried out in duplicates. In order to be able to compare the different DARPins in one plot the ECL signals were normalized between 0 and 1 according to the fitted curves.

3. Results

We describe here the selection of Designed Ankyrin Repeat Proteins (DARPins) by ribosome display and phage display for binding to detergent-solubilized Na^+-citrate symporter CitS. We adapted several methods to be able to quickly and efficiently screen and characterize the binding proteins. Furthermore, we compare the obtained DARPins to a previously selected HuCAL Fab fragment binding to CitS.

We used CitS immobilized via a biotinylation tag as the target for selection. Both constructs (see Fig. 3b), CitS carrying a C-terminal BAD domain ($CitS_{BAD}$) or an Avi tag ($CitS_{Avi}$), were functional in *E. coli*, as determined with an *in vivo* assay based on growth of transformed *E. coli* on Simmons citrate agar (Kästner et al., 2000). We previously found the biotin–NeutrAvidin/streptavidin interaction to be the most robust linkage for immobilizing detergent-solubilized membrane proteins. By contrast, the binding of many other tags to their cognate antibodies is weakened by detergent. The immobilization via the His tag to immobilized Ni^{2+}–NTA is much too weak (Lata and Piehler, 2005) and further destabilized by the detergent-containing buffer (Ott and Plückthun, unpublished experiments). Even though we cannot prove directly that CitS is active in detergent, it can be reconstituted into lipid vesicles from the detergent mixture (Pos and Dimroth,

1996). Therefore, it is a reasonable assumption that it is in a state very close or identical to that in the native bilayer.

3.1. Ribosome display selection against CitS

For ribosome display, biotinylated CitS ($CitS_{BAD}$) was immobilized to microtiter plates coated with NeutrAvidin. The selected DARPin pools of all four rounds of ribosome display were subcloned into the expression vector pQE_{myc5}. After transformation, randomly picked single clones were sequenced to estimate the diversity of the pools. None of the 12 sequenced clones of each round carried the same DARPin. This result indicates that the pools are still diverse and that a wide variety of different binding molecules can be obtained. A strong enrichment of binding signal was observed after the fourth selection round by ELISA of the pool (data not shown).

Single clones (70) of the fourth round were further analyzed by crude extract ELISA. To quickly and reliably screen for positive clones, the selected DARPins were immobilized on the plate via the myc-tag, and the binding of solubilized membrane protein was detected. In this setup, the membrane protein was exposed to a minimum of washing and incubation steps (see Section 2). About 35% of the clones (25 out of 70 initially screened clones) showed a binding signal to $CitS_{BAD}$. To test whether binding was really specific for the membrane protein, free $_{His}$CitS, carrying no biotinylation tag, was used as competitor. For around 40% of the positive clones (10 out of 70 initially screened clones) the binding signal was decreased or even reduced to the background level upon addition of excess competitor $_{His}$CitS, consistent with specific binding. None of the sequenced CitS-specific DARPins showed the same sequence, indicating that even more DARPins may be found with further screening.

About half of the clones showing binding signal (15 of 25 clones) were false-positive. For biotinylation, BAD (biotin acceptor domain from oxaloacetate decarboxylase (Schwarz et al., 1988), about 100 amino acids long) was fused to CitS, and the presence of an additional folded domain in the selection procedure has apparently also resulted in—unwanted—selection of some DARPins specific for the BAD domain. Nevertheless, as determined by ELISA of the selection pools (data not shown), a greater percentage of non-CitS binders that became enriched is due to truly unspecific binding and only a smaller percentage shows binding to BAD.

3.2. Phage display selection against CitS

The phage display library used for the selection has a functional diversity of 1.1×10^{10} (Steiner et al, in preparation). Since DARPins are normally cytoplasmic proteins that fold very fast and are very stable, they are not compatible with standard phage display systems, and they have to be directed to the *E. coli* signal recognition particle (SRP) translocation pathway by the use of an appropriate signal sequence (Steiner et al., 2006). With the appropriate phagemid, phage display is then at least as efficient as with libraries of other proteins and peptides.

Since unspecific binding was observed in ribosome display, where CitS had been immobilized to a microtiter plate, the selection procedure in phage display was carried out by first letting solubilized $CitS_{BAD}$ bind to DARPin-carrying phages in solution and then capturing the complexes with streptavidin-coated beads. This "solution panning" requires larger amounts of $CitS_{BAD}$, but has the advantage of reducing unspecific interaction with the plate surface.

Four rounds of selection on solubilized $CitS_{BAD}$ in solution, followed by capturing of the antigen with streptavidin-coated paramagnetic beads, were performed. An enrichment of the binding signal was observed already after the second selection round. After the third and fourth round of selection, 62 clones each were screened in phage ELISA format for binding to immobilized $CitS_{BAD}$ in the absence or presence of an excess of soluble $_{His}$CitS as competitor. Eighty-nine percent of the clones (110 out of 124 initially screened clones) showed a binding signal on immobilized $CitS_{BAD}$, of which 17% (19 clones) could be inhibited by the addition of competitor ($_{His}$CitS). Sequencing revealed 11 different sequences (around 9% of initially screened clones).

Compared to panning on microtiter plates, solution panning lead to a reduction of unspecific binders, but the percentage of—undesired—BAD-specific binders was increased (data not shown). While in the ribosome display experiment described above the membrane protein was immobilized via its biotin tag prior to adding the ribosomal complex (thereby making the BAD domain less accessible), in phage display the selection was carried out in solution and the BAD domain was fully accessible. To increase the fraction of binders specific for CitS itself, a prepanning step on the BAD domain alone can be included, or a CitS version without BAD domain (e.g. carrying an Avi tag) can be used in the future. It should be emphasized that either immobilization strategy, solution panning or plate panning, can of course be used with either display technology, phage display or ribosome display.

3.3. Size-exclusion chromatography (SEC) of complexes

By using SEC, the formation of stable complexes in solution can be monitored directly. Additionally, the potential aggregation tendency of any selected binder can be assessed, usually an undesired property for co-crystallization. Furthermore, the use of purified $_{His}$DARPins for the subsequent analysis eliminates possible influences of the phage or crude lysate on the binding and solubility behavior.

The subset of different DARPins chosen based on efficient inhibition of ELISA signals by soluble $_{His}$CitS and on sequencing (10 from ribosome display and 11 from phage display, as described above) was further analyzed

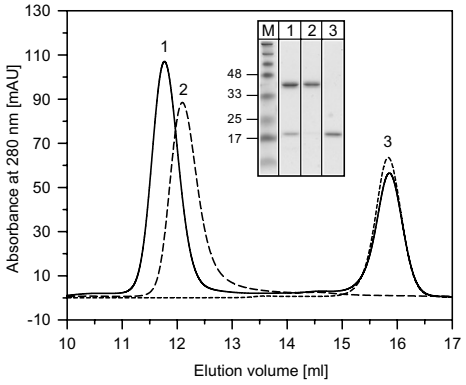

Fig. 4. Superposition of size-exclusion chromatography (SEC) elution profiles. Free CitS (dashed line, peak 2), free DARPin cp34h_15 (short dashed line, peak 3) and CitS mixed with excess DARPin cp34h_15 (solid line, peak 1) were loaded on a Superdex 200 column. The elution peak of the CitS–DARPin (peak 1) complex is shifted to smaller elution volume (i.e. bigger molecular size) compared to free CitS (peak 2). The Coomassie brilliant blue-stained SDS–polyacrylamide gel of the corresponding peak fractions is shown in the inset. The DARPin has a molar mass of 18 kDa, $_{His}$CitS of 50 kDa, but runs on SDS–PAGE at about 40 kDa.

by SEC. A molar excess of purified DARPin was mixed with $_{His}$CitS and loaded on a SEC column. Since the binding stoichiometry of CitS–DARPin complexes was not known, the DARPin was used in excess (relative to the subunit concentration of the presumed dimeric CitS) and at micromolar concentrations to allow complex formation of all CitS molecules. Complex formation is indicated by a shift of the CitS elution peak to smaller elution volume (i.e. bigger molecular size) relative to the uncomplexed $_{His}$CitS. SDS–PAGE analysis of the corresponding peak fraction of the presumed complex showed that the fraction contained both CitS and DARPin (Fig. 4).

Only a few of the initially screened binders (1 out of the 70 from ribosome display and 2 out of 124 from phage display) fulfilled the stringent criteria of forming complexes that showed a clear shift in elution volume and having only one distinct elution peak (i.e. no aggregation or residual uncomplexed CitS). We further characterized this one DARPin selected by ribosome display (cr34_8C4) and the two selected by phage display (cp34h_15 and cp34h_16) in more detail and compared them to each other and to the Fab fragment (f3p4) that had been previously selected as binder to solubilized CitS by phage display (Röthlisberger et al., 2004). An overview of the properties of the characterized binders is given in Table 1.

3.4. SEC-MALS of CitS and complexes

The SEC system was further connected to a multi-angle (static) light scattering (MALS) detector and a differential refractive index detector (dRI). These two detectors together with the UV-detector allow the direct comparison

Table 1
Properties of selected DARPin in comparison to a selected Fab fragment

	cr34_8C4	cp34_15	cp34_16	f3p4[a]
Protein class	DARPin	DARPin	DARPin	Fab fragment
Selection method	Ribosome display	Phage display	Phage display	Phage display
Molar mass (kDa)	18.2	18.2	18.4	47.9
p*I*	5.1	5.3	4.9	4.8
Affinity (nM)	2.5 ± 0.6[b]	5.4 ± 1.9[b]	1.3 ± 0.3[b]	4 ± 2[c]
Yield[d] (mg/liter)	>30[e]	>75[e]	>20[e]	3

[a] Previously described by Röthlisberger et al. (2004).
[b] Equilibrium titration (BioVeris).
[c] Competition BIAcore.
[d] Yield of purified protein from a 1 liter *E. coli* shake flask culture.
[e] IMAC column was strongly overloaded, therefore the yield is greatly underestimated.

of the corresponding molar masses of CitS alone and the complexes. The scattered light (the Rayleigh ratio $R_{(\theta)}$) measured by the MALS-detector is directly proportional to the product of the weight-average molar mass and the solute concentration (Wyatt, 1993; Wen et al., 1996; Folta-Stogniew and Williams, 1999). Either a UV-detector or a dRI-detector alone can be used to calculate online the concentration of a soluble, non-conjugated protein. In contrast, as membrane proteins consist of a protein core surrounded by a detergent fraction, both UV-detector and dRI-detector are required to calculate molar masses. If the UV-extinction coefficient and the differential refractive index increment (dn/dc) of the protein and the detergent are known, the molar masses of the protein fraction and the detergent fraction can be determined. In case of CitS, we calculated the UV-extinction coefficient based on the amino acid sequence and assumed a dn/dc of 0.186 g/ml (Wen et al., 1996) for the protein fraction and a dn/dc of 0.133 (Strop and Brünger, 2005) for the detergent fraction (DDM). In our buffer, we detect for CitS a monodisperse peak with a molar mass of the protein fraction (protein without detergent) of 105–115 kDa (Fig. 5a). This molar mass corresponds to the CitS dimer (theoretical molar mass of 100 kDa including His tag). The dimeric state of CitS is in agreement with single molecule fluorescence spectroscopy experiments (Kästner et al., 2003).

In the case of the CitS complexes, we first have to assume an extinction coefficient, as we do not know the binding stoichiometry initially. In the case of the CitS–Fab fragment complex (molar masses of both are about 50 kDa) only a 2:1 (CitS:Fab fragment) stoichiometry gives a meaningful result. The molar mass of the protein fraction is then determined to be 155–165 kDa (Fig. 5b). For the smaller CitS–DARPin complexes, however, the assumption of different binding stoichiometries (2:2 CitS:DARPin or 2:1 CitS:DARPin) and therefore different extinction coefficients does not lead to an unequivocal distinction and therefore both stoichiometries remain possible.

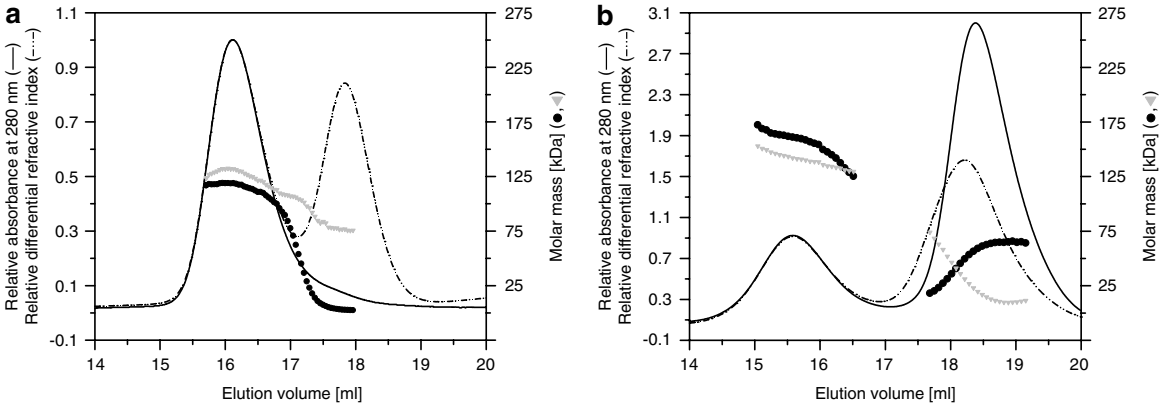

Fig. 5. (a) Characterization of CitS with size-exclusion chromatography combined with multi-angle light scattering (SEC-MALS). CitS (200 μl, 20 μM) was loaded on a Superose 6 column. Only the protein fraction of CitS contributes to the UV-A_{280} signal (solid line), whereas both the protein and the detergent fraction contribute to the differential refractive index signal (dashed-dotted line). The membrane protein–detergent complex elutes at 16.1 ml. The molar mass of the protein fraction is calculated to be 105–115 kDa (filled circles), which corresponds to a CitS dimer (theoretical molar mass of 100 kDa). With 125–140 kDa, the detergent fraction (grey triangles) has a slightly larger molar mass. The empty detergent (DDM) micelles, originating from concentration of the sample prior to injection, elute at 17.9 ml and have a calculated molar mass of 74–76 kDa and are characterized by a peak in refractive index, but not in UV-A_{280}. (b) Characterization of CitS–Fab fragment complex with size-exclusion chromatography combined with multi-angle light scattering (SEC-MALS). CitS (20 μM) was incubated with excess of Fab fragment (f3p4, 60 μM) complex for 1 h at 4 °C and loaded (200 μl) on a Superose 6 column. The UV-A_{280} signal is depicted as solid line, the differential refractive index increment as dashed-dotted line. The molar mass of the protein fraction of the CitS–Fab fragment–detergent complex is 155–165 kDa (filled circles). This corresponds to the molar mass of one Fab fragment bound to a CitS dimer (theoretical molar mass 150 kDa). The molar mass of the detergent fraction is indicated with grey triangles. The elution peak of the excess of Fab fragment (UV-A_{280} at 18.5 ml, and filled circles for the molar mass) superimposes with the empty detergent micelle (peak in differential refractive index at 17.9 ml and grey triangles for the molar mass).

Nevertheless, we can clearly demonstrate a larger molar mass of the complexes by the increased Rayleigh ratio $R_{(\theta)}$, compared to CitS alone.

3.5. Competition ELISA

$DARPins_{myc5}$ were immobilized via the myc-tag on a MaxiSorp plate coated with anti-myc antibody and the binding of biotinylated $CitS_{BAD}$ was competed with a 10-fold excess of either non-biotinylated $_{His}$CitS to confirm specificity, or a 10-fold excess of another $_{His}$DARPin or Fab fragment (f3p4) to test whether they recognize identical or overlapping binding epitopes.

The binding signal of all DARPins can be reduced to background levels with an excess of free $_{His}$CitS (Fig. 6a). This finding demonstrates that the characterized DARPins bind specifically to solubilized CitS, confirming the results from the first ELISA screens. All analyzed DARPins do recognize the same or overlapping epitopes, as the binding of one DARPin to CitS can be inhibited with an excess of another free DARPin. However, the Fab fragment (f3p4) seems to recognize a different epitope, as it does not significantly reduce the binding signal of the DARPins.

To further confirm this finding, the setup of the ELISA was inverted. The Fab fragment (f3p4) was directly coated on the plate and its binding to $CitS_{BAD}$ alone or to $CitS_{BAD}$ pre-incubated with either non-biotinylated $_{His}$CitS, free Fab fragment (f3p4) or free $_{His}$DARPin was compared. The binding signal could be fully competed with excess of $_{His}$CitS or Fab fragment (f3p4) but not with any of the selected DARPin. These results strongly indicate that the two scaffolds do indeed recognize different, non-overlapping epitopes (Fig. 6b).

3.6. Sandwich complex with Fab, CitS and DARPin

To determine if the selected DARPins and the Fab fragment (f3p4) can bind simultaneously to CitS and can therefore form a ternary complex, we performed a sandwich ELISA. In this setup, the Fab fragment (f3p4) was immobilized directly on the plate and subsequently incubated with $_{His}$CitS and $DARPin_{myc5}$. The binding of the $DARPin_{myc5}$ to the $_{His}$CitS–Fab complex was detected. In the negative controls, the Fab fragment was either incubated with BSA instead of $_{His}$CitS or BSA was coated on the well instead of the Fab fragment. The binding signal of the DARPin to $_{His}$CitS-Fab complex is significantly higher than that of the negative controls (Fig. 6c), and therefore the ternary complex seems to be formed for all DARPins.

If the DARPin, the Fab fragment and CitS are able to form a ternary complex, an additional shift in size-exclusion chromatography should be observed. The DARPin (cp34h_15), the Fab fragment (f3p4) and $_{His}$CitS were incubated for 1 h at 10 °C and the mixture was injected on a SEC column. The elution profile of the putative ternary complex is indeed shifted, compared to the binary complex of CitS and DARPin (Fig. 7) and the SDS–PAGE analysis

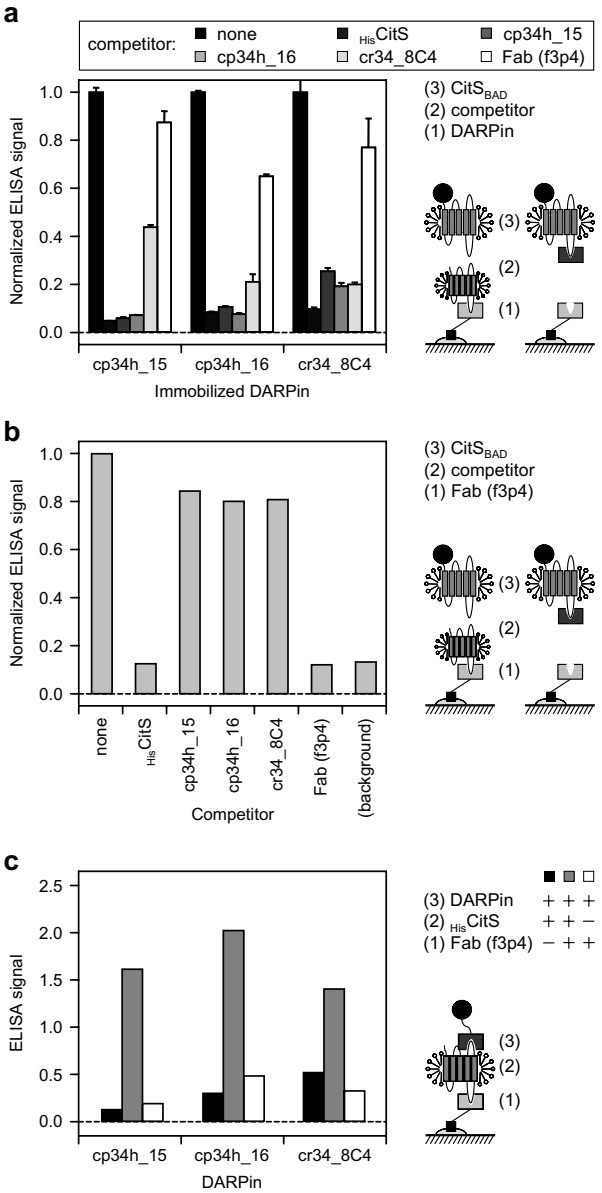

Fig. 6. (a) Competition ELISA assay of DARPins and Fab fragment reveals whether the binding molecules recognize the same or different epitopes. $DARPins_{myc5}$ (40 nM) were immobilized and binding to $CitS_{BAD}$ (40 nM) was detected. The binding signal without competition was normalized to 1. Competition with excess of $_{His}$DARPin and Fab fragment (all 400 nM) was examined. DARPins compete with each other for the same epitope, as the binding signal is clearly reduced. In contrast, there is no significant decrease when competed with the Fab fragment (f3p4). Competition with $_{His}$CitS (400 nM) is included as a control for specific binding. (b) Competition ELISA assay. The binding of $CitS_{BAD}$ to the immobilized Fab fragment (f3p4, 250 nM) was competed with an excess of either non-biotinylated $_{His}$CitS, Fab fragment or $_{His}$DARPins (all 400 nM). Both $_{His}$CitS and Fab fragment reduce the binding signal to background levels, which demonstrates the specificity of the binding. All DARPins do not significantly influence the binding, indicating that they bind to another epitope than the Fab fragment. (c) Sandwich ELISA assay. The Fab fragment f3p4 was immobilized on the plate (250 nM) and incubated with $_{His}$CitS (40 nM). The amount of $DARPin_{myc5}$ that binds was detected via the myc-tag. Binding signal of $DARPin_{myc5}$ to the CitS–Fab complex (grey), binding to $_{His}$CitS on a BSA-coated plate (black) and to Fab fragment without $_{His}$CitS (white).

of the elution peak reveal the presence of CitS, DARPin and Fab fragment in this peak fraction. Beside the main peak of the ternary complex, an additional peak appears, indicating higher aggregates. This peak shows the same SDS–PAGE band pattern as the main peak (data not shown).

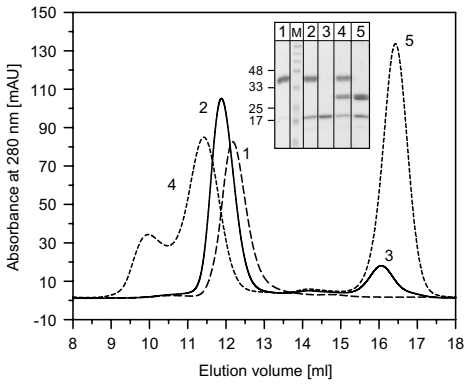

Fig. 7. Characterization of CitS–DARPin–Fab complex with size-exclusion chromatography. Elution profile of $_{His}$CitS (dashed line, peak 1), $_{His}$CitS mixed with an excess of DARPin cp34h_15 (solid line, peaks 2 and 3) and $_{His}$CitS mixed with an excess of both DARPin cp34h_15 and Fab fragment f3p4 (short dashed line, peaks 4 and 5). The Coomassie brilliant blue-stained SDS–polyacrylamide gel of the corresponding peak fractions is shown in the insert. The DARPin has a molar mass of 18 kDa, the two chains of the Fab fragment of 23 and 25 kDa, $_{His}$CitS of 50 kDa (but runs on SDS–PAGE at about 40 kDa). The Fab fragment elutes with some retardation from this size-exclusion column (Röthlisberger et al., 2004).

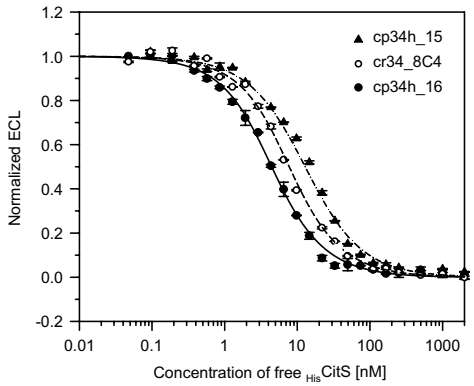

Fig. 8. Determination of dissociation constants by equilibrium titration in solution. Titration curves of three DARPins incubated with varying concentrations of $_{His}$CitS (0.05 nM to 2 μM). The amount of DARPin$_{myc5}$ that still binds to CitS$_{Avi}$ immobilized on beads is measured by ECL. Cp34h_16 (filled circles), cr34_8C4 (open circles) and cp34h_15 (filled triangles) show a K_D of about 1.3, 2.5, and 5.4 nM, respectively. The fits are according to Eq. (2).

3.7. Affinity determination by equilibrium titration

After demonstrating the specificity of the selected binder in ELISA experiments and the formation of well defined stable complexes in SEC experiments, the binding affinity of the selected DARPins was assessed by equilibrium titration in solution. This method is suitable for determination of dissociation constants (K_D) in a high-throughput format needed for the fast characterization of larger number of binding proteins (Haenel et al., 2005). Constant amounts of DARPin were incubated with varying amounts of $_{His}$CitS as competitor and the detection mix containing CitS$_{Avi}$ coated on magnetic streptavidin beads and two detection antibodies. The binding signal was detected with a BioVeris workstation. The binding curves reveal dissociation constants (K_D) in the low nanomolar range (1–6 nM) for all DARPins (Fig. 8) tested. Even though CitS is a dimer, the data could be fitted well to a simple model (Eq. (2), see Section 2), where each CitS monomer interacts with one DARPin independently. We cannot exclude a more complicated model, where the two binding sites may influence each other, but we can get a reasonable fit to the binding data already for the simple model.

4. Discussion

Future efforts in the structure determination of membrane proteins will have to be focused on the development of new tools and technologies to expedite the process and increase the likelihood of success. Co-crystallization with binding molecules is a promising approach to achieve crystals suitable for high resolution structure determination. However, the generation of new monoclonal antibody fragments by the classical hybridoma approach for each membrane protein is not only a costly and time-consuming procedure but may not even be particularly promising for helical, multi-spanning flexible membrane proteins. The fundamental obstacle is that the conformational integrity of the detergent-solubilized proteins cannot be controlled once injected into an animal. In contrast, the use of synthetic libraries and *in vitro* selection technologies, such as phage display and ribosome display, provide a powerful tool to generate such binding molecules in a fast and reliable way. Furthermore, selection conditions can be adapted to the need of the target protein as the binding step is performed *in vitro*.

Since the Na^+-citrate symporter CitS is a multi-spanning integral membrane protein with relatively short loops, it serves us as a model system for selecting such binding proteins for stabilization and mediating additional crystal contacts. By carrying out the comparative analysis of different selections systems and classes of binding molecules, we could demonstrate that both selection technologies (ribosome display and phage display) can be applied. To generate binding molecules against as many epitopes as possible several scaffolds (e.g. DARPin and Fab fragment) need to be considered simultaneously.

4.1. DARPins vs. Fab fragments

Although both scaffolds (DARPin and Fab fragment) compared in this study are used in nature for specific and high affinity binding interactions, they have quite different properties, each with its advantages and disadvantages. DARPins can be obtained in extremely high yields (up to 200 mg soluble protein per liter *E. coli* shake flask culture), and they tolerate the presence of reducing agents, as

DARPins do not contain any disulfide bonds or free cysteines. The Fab fragments are about 2.5 times the size of DARPins (50 vs. 18 kDa, Fig. 1) and may present a larger hydrophilic surface for stable protein–protein contacts in the crystal. As the binding site resides at the tip of the Fab fragment, compared to a more shallow binding groove along the DARPin, the Fab fragment can protrude further out and potentially leave more space in the crystal for the membrane bound detergent molecules. However, Fab fragments are built from several domains and therefore display more conformational flexibility than the very rigid and stable ankyrin fold. Most importantly, the binding surface is realized completely differently in the two scaffolds. In DARPins, the binding residues reside in stable secondary structure elements and short β-turns, displaying an ideal shape complementary to folded proteins (Fig. 1), whilst being less suitable to bind unstructured peptides. Therefore, both the molecular design and the *in vitro* selection strategy significantly increase the likelihood of obtaining binders against structural epitopes, rather than unstructured tails. In antibodies, flexible loops with varying size form the binding site to ensure the recognition of a wide range of antigens (such as small molecules, peptides or entire proteins). Therefore, completely independent epitopes can be bound by the two scaffolds (as shown in this study), which can and should be exploited for the *in vitro* generation of binding molecules for co-crystallization.

4.2. Ribosome display vs. phage display

This study demonstrates that both phage display and ribosome display are well suited for *in vitro* selection of binding proteins, even in detergent-containing buffers needed for membrane proteins. Phage display, when carried out in solution, showed higher enrichment of binding molecules after four cycles than ribosome display, which was carried out on immobilized membrane protein in the example described here. However, fast enrichment obtained by very stringent selection conditions can lead to lower diversity within the selected binding molecule population, with the caveat that none of the selected binders may have the desired properties needed for co-crystallization. It is therefore important to find the right balance between the number of selection cycles, the stringency of washing steps and the selection system applied. We would like to reemphasize that both ribosome display and phage display can be carried out in solution or on surfaces (see next section).

4.3. Solution panning vs. surface panning

The—unwanted—selection of BAD-specific DARPins shows how the applied immobilization method can influence the outcome of a selection. First, the use of a fusion protein for selection always bears a risk to generate unwanted binders against the fusion partner. However, if a fusion partner is needed because of solubility or stability issues, fusion proteins should be changed between subsequent selection rounds or a prepanning step on the fusion partner should be included. Second, the immobilization of the antigen prior to the panning step can mask potential binding epitopes. The use of a longer linker between protein and immobilization tag or a mixture of antigens which carry the immobilization tag either at the N- or the C-terminus can circumvent such an event.

4.4. Workflow

We established an efficient workflow for the characterization of potential binding proteins that allows rapid identification of binding molecules suitable for co-crystallization (Table 2). First, we had to evaluate and adapt the

Table 2
Overview of the workflow for the screening and characterization of DARPins after the selection

Step	Ribosome display	Phage display	Comments
Pool ELISA	Fourth round (then 70 clones were picked for screening)	Third and fourth round (then 62 clones of each round were picked for screening)	Defines of which round the analysis of single clones is worthwhile
Crude extract ELISA	35% (25)[a]	n.d.[b]	Clones that show binding
Phage ELISA	n.a.[c]	89% (110)[a]	Clones that show binding
Competition ELISA	14% (10)	17% (19)	Competition with free CitS indicates specificity
Sequencing	14% (10)	9% (11)	Identification of non-identical DARPin sequences
SEC	1.4% (1)	1.6% (2)	Formation of a well defined, stable complex in solution, no aggregation even at high concentration
Affinity	2.5 nM	1.3 nM, 5.4 nM	Equilibrium titration for affinity determination; ranking of binders according to the K_D
Competition ELISA	All recognize overlapping epitopes as all are competable		Competition with free DARPins distinguishes overlapping or different epitopes

Binding proteins that pass each screening step are given as percentage of the number of initially screened binders.
[a] For this study, initially 70 single clones of ribosome selection and 124 of phage display selection were screened (then 62 from round 3 and 62 from round 4). In parentheses the absolute number of clones is given.
[b] n.d., not done.
[c] n.a., not applicable.

methods, with respect to reliability to work under conditions required for membrane proteins. Then, we chose a format to screen and fully characterize the binding molecules with the least effort and time consumption. As first screen, single clone crude extract ELISA is used. This assay must distinguish specific binding to the membrane protein from binding to fusion partners, tags, streptavidin or BSA used for blocking. The most straightforward test for all of the requirements above in a single experiment is the competition of the binding signal with the membrane protein itself. This assay also tests whether binding occurs only to a surface-bound form of the membrane protein, which would indicate that binding is most probable to a non-native state of the membrane protein. As second screen, SEC is performed using purified DARPins to check for complex formation in solution. Binding proteins which show complete complex formation and form no soluble aggregates are then retested at high concentration (data not shown), in order to predict whether they might be aggregation-prone under crystallization conditions. As last screen, a K_D determination of the binder will help to further rank the selected binders to ensure the isolation of intact complexes. A competition ELISA with several purified DARPins finally reveals whether the binding proteins recognize the same or different, non-overlapping epitopes.

Even without robotic systems, several hundreds of clones can by analyzed by ELISA a day. A SEC-system with an autosampler runs 20–30 samples a day, and with the BioVeris workstation we can determine the binding affinities of around 20 binding proteins a day, both with a minimum of hands-on time. We have developed a workflow that allows us to obtain a characterized binder for co-crystallization within the time period of less than a month.

5. Conclusions

We have selected specific and high-affinity binding molecules to the Na^+-citrate symporter CitS and established an efficient way of characterizing them. All steps of the characterization (ELISA, automated SEC-MALS, affinity determination with BioVeris) are compatible with higher throughput to obtain binding molecules against one or preferentially several membrane proteins. Additionally, the use of two classes of binding molecules is very useful to obtain binders against different epitopes. Therefore, the combination of *in vitro* selection and screening presented here opens up a robust approach for the generation of specific, high-affinity binding molecules suitable for co-crystallization experiments with membrane proteins. Indeed, preliminary results of co-crystallization with selected DARPins seem to corroborate this approach, as well-diffracting crystals of CitS complexes have been obtained.

Acknowledgments

This work was supported by the NCCR Structural Biology. The authors thank Prof. Markus Grütter, Dr. K. Martin Pos, Daniel Frey, Dr. Patrick Amstutz, and Dr. Michael T. Stumpp for helpful discussions.

Appendix A. Supplementary data

Supplementary data associated with this article can be found, in the online version, at doi:10.1016/j.jsb.2007.01.013.

References

Berman, H.M., Westbrook, J., Feng, Z., Gilliland, G., Bhat, T.N., Weissig, H., Shindyalov, I.N., Bourne, P.E., 2000. The Protein Data Bank. Nucleic Acids Res. 28, 235–242.

Binz, H.K., Amstutz, P., Plückthun, A., 2005. Engineering novel binding proteins from nonimmunoglobulin domains. Nat. Biotechnol. 23, 1257–1268.

Binz, H.K., Stumpp, M.T., Forrer, P., Amstutz, P., Plückthun, A., 2003. Designing repeat proteins: well-expressed, soluble and stable proteins from combinatorial libraries of consensus ankyrin repeat proteins. J. Mol. Biol. 332, 489–503.

Binz, H.K., Amstutz, P., Kohl, A., Stumpp, M.T., Briand, C., Forrer, P., Grütter, M.G., Plückthun, A., 2004. High-affinity binders selected from designed ankyrin repeat protein libraries. Nat. Biotechnol. 22, 575–582.

Bork, P., 1993. Hundreds of ankyrin-like repeats in functionally diverse proteins: mobile modules that cross phyla horizontally? Proteins 17, 363–374.

DeLano, W.L., 2002. The PyMOL Molecular Graphics System. DeLano Scientific, Palo Alto, CA, USA. Available from: <<http://www.pymol.org>>.

Ewert, S., Huber, T., Honegger, A., Plückthun, A., 2003. Biophysical properties of human antibody variable domains. J. Mol. Biol. 325, 531–553.

Folta-Stogniew, E., Williams, K., 1999. Determination of molecular masses of proteins in solution: Implementation of an HPLC size exclusion chromatography and laser light scattering service in a core laboratory. J. Biomol. Tech. 10, 51–63.

Haenel, C., Satzger, M., Ducata, D.D., Ostendorp, R., Brocks, B., 2005. Characterization of high-affinity antibodies by electrochemiluminescence-based equilibrium titration. Anal. Biochem. 339, 182–184.

Hanes, J., Plückthun, A., 1997. In vitro selection and evolution of functional proteins by using ribosome display. Proc. Natl. Acad. Sci. USA 94, 4937–4942.

Hoogenboom, H.R., 2002. Overview of antibody phage-display technology and its applications. Methods Mol. Biol. 178, 1–37.

Hoogenboom, H.R., 2005. Selecting and screening recombinant antibody libraries. Nat. Biotechnol. 23, 1105–1116.

Hunte, C., Michel, H., 2002. Crystallisation of membrane proteins mediated by antibody fragments. Curr. Opin. Struct. Biol. 12, 503–508.

Kästner, C.N., Dimroth, P., Pos, K.M., 2000. The Na^+-dependent citrate carrier of *Klebsiella pneumoniae*: high-level expression and site-directed mutagenesis of asparagine-185 and glutamate-194. Arch. Microbiol. 174, 67–73.

Kästner, C.N., Prummer, M., Sick, B., Renn, A., Wild, U.P., Dimroth, P., 2003. The citrate carrier CitS probed by single-molecule fluorescence spectroscopy. Biophys. J. 84, 1651–1659.

Kleymann, G., Ostermeier, C., Ludwig, B., Skerra, A., Michel, H., 1995. Engineered Fv fragments as a tool for the one-step purification of integral multisubunit membrane protein complexes. Biotechnology (NY) 13, 155–160.

Knappik, A., Ge, L., Honegger, A., Pack, P., Fischer, M., Wellnhofer, G., Hoess, A., Wölle, J., Plückthun, A., Virnekäs, B., 2000. Fully synthetic human combinatorial antibody libraries (HuCAL) based on modular consensus frameworks and CDRs randomized with trinucleotides. J. Mol. Biol. 296, 57–86.

Lata, S., Piehler, J., 2005. Stable and functional immobilization of histidine-tagged proteins via multivalent chelator headgroups on a molecular poly(ethylene glycol) brush. Anal. Chem. 77, 1096–1105.

Miao, W., Choi, J.P., Bard, A.J., 2002. Electrogenerated chemiluminescence 69: the tris(2,2′-bipyridine)ruthenium(II), $(Ru(bpy)_3^{2+})$/tri-*n*-propylamine (TPrA) system revisited—a new route involving $TPrA^{*+}$ cation radicals. J. Am. Chem. Soc. 124, 14478–14485.

Miroux, B., Walker, J.E., 1996. Over-production of proteins in Escherichia coli: mutant hosts that allow synthesis of some membrane proteins and globular proteins at high levels. J. Mol. Biol. 260, 289–298.

Niebauer, R.T., White, J.F., Fei, Z., Grisshammer, R., 2006. Characterization of monoclonal antibodies directed against the rat neurotensin receptor NTS1. J. Recept. Signal Transduct. Res. 26, 395–415.

Pos, K.M., Dimroth, P., 1996. Functional properties of the purified Na(+)-dependent citrate carrier of *Klebsiella pneumoniae*: evidence for asymmetric orientation of the carrier protein in proteoliposomes. Biochemistry 35, 1018–1026.

Röthlisberger, D., Pos, K.M., Plückthun, A., 2004. An antibody library for stabilizing and crystallizing membrane proteins-selecting binders to the citrate carrier CitS. FEBS Lett. 564, 340–348.

Schwarz, E., Oesterhelt, D., Reinke, H., Beyreuther, K., Dimroth, P., 1988. The sodium ion translocating oxalacetate decarboxylase of *Klebsiella pneumoniae*. Sequence of the biotin-containing alpha-subunit and relationship to other biotin-containing enzymes. J. Biol. Chem. 263, 9640–9645.

Smith, G.P., Petrenko, V.A., 1997. Phage display. Chem. Rev. 97, 391–410.

Sobczak, I., Lolkema, J.S., 2005. The 2-hydroxycarboxylate transporter family: physiology, structure, and mechanism. Microbiol. Mol. Biol. Rev. 69, 665–695.

Steiner, D., Forrer, P., Stumpp, M.T., Plückthun, A., 2006. Signal sequences directing cotranslational translocation expand the range of proteins amenable to phage display. Nat. Biotechnol. 24, 823–831.

Strop, P., Brünger, A.T., 2005. Refractive index-based determination of detergent concentration and its application to the study of membrane proteins. Protein Sci. 14, 2207–2211.

van Geest, M., Lolkema, J.S., 2000. Membrane topology of the Na(+)/citrate transporter CitS of *Klebsiella pneumoniae* by insertion mutagenesis. Biochim. Biophys. Acta 1466, 328–338.

Wallin, E., von Heijne, G., 1998. Genome-wide analysis of integral membrane proteins from eubacterial, archaean, and eukaryotic organisms. Protein Sci. 7, 1029–1038.

Wen, J., Arakawa, T., Philo, J.S., 1996. Size-exclusion chromatography with on-line light-scattering, absorbance, and refractive index detectors for studying proteins and their interactions. Anal. Biochem. 240, 155–166.

Wyatt, P.J., 1993. Light-scattering and the absolute characterization of macromolecules. Anal. Chim. Acta 272, 1–40.

Online Supplement

***In vitro* selection and characterization of DARPins and Fab fragments for the co-crystallization of membrane proteins: The Na^+-citrate symporter CitS as an example**

Thomas Huber[1], Daniel Steiner[1], Daniela Röthlisberger[1,2] and Andreas Plückthun[1,3]

[1] Department of Biochemistry, University of Zürich, Winterthurerstrasse 190, CH-8057 Zürich, Switzerland

[2] present address: Department of Biochemistry, University of Washington, Seattle, WA 98195, USA

[3] to whom correspondence should be addressed:

Email: plueckthun@bioc.unizh.ch

Tel: +41-44-635 55 70

Fax: +41-44-635 57 12

Derivation of equations for the affinity determination

The two equilibria of CitS and DARPin in the assay solution can be described by Eq. 1, when assuming a 1:1 interaction.

$$C + A \overset{K_{D1}}{\rightleftharpoons} CA \quad \text{and} \quad C_b + A \overset{K_{D2}}{\rightleftharpoons} C_bA \quad \text{(Eq. 1)}$$

Here C is the his-tagged CitS ($_{His}$CitS) in solution, A is the myc-tagged DARPin (DARPin$_{myc5}$) and C_b is the bound AVI-tagged CitS (CitS$_{AVI}$) present on the beads.

The equilibria are characterized by the following basic relationships (Eq. 2 to 6):

$$K_{D1} = \frac{[C][A]}{[CA]} \text{ (Eq. 2)} \qquad K_{D2} = \frac{[C_b][A]}{[C_bA]} \text{ (Eq. 3)}$$

$$[C]_t = [C] + [CA] \text{ (Eq. 4)} \qquad [A]_t = [A] + [CA] + [C_bA] \text{ (Eq. 5)}$$

$$[C_b]_t = [C_b] + [C_bA] \text{ (Eq. 6)}$$

where $[C]$ is the concentration of free $_{His}$CitS, $[C]_t$ is the total concentration of added $_{His}$CitS, $[C_b]$ is the uncomplexed amount of CitS$_{AVI}$, present on beads, $[C_b]_t$ is the total amount of CitS$_{AVI}$ present on the beads, $[A]$ is the concentration of free DARPin$_{myc}$, $[A]_t$ is the total concentration of added DARPin$_{myc}$, and $[CA]$ and $[C_bA]$ are the concentrations of the corresponding complexes. All bead-bound species are treated like molecules in solution and therefore molar concentrations were used. K_{D1} and K_{D2} are the dissociation constants of the two equilibria. We assume here that the dissociation constants K_{D1} and K_{D2} are the same (therefore, named K_D). Using the mass balances in Eq. 2 and Eq. 3, we obtain:

$$K_D = \frac{([C]_t - [CA])([A]_t - [CA] - [C_bA])}{[CA]} \quad \text{(Eq. 7)}$$

$$K_D = \frac{([C_b]_t - [C_bA])([A]_t - [CA] - [C_bA])}{[C_bA]} \quad \text{(Eq. 8)}$$

From these two equations, it follows that

$$[CA] = \frac{[C_bA][C]_t}{[C_b]_t} \quad \text{(Eq. 9)}$$

Combining Eq. 8 and Eq. 9 will give Eq. 10:

$$K_D = \frac{([C_b]_t - [C_bA])\left([A]_t - \frac{[C_bA][C]_t}{[C_b]_t} - [C_bA]\right)}{[C_bA]} \quad \text{(Eq. 10)}$$

Solving Eq. 10 for [C_bA] will yield Eq. 11 (solution of the quadratic equation).

$$[C_bA] = \frac{([A]_t + [C]_t + [C_b]_t + K_D) - \sqrt{([A]_t + [C]_t + [C_b]_t + K_D)^2 - 4\left(\frac{[C]_t}{[C_b]_t} + 1\right)[C_b]_t [A]_t}}{2\left(\frac{[C]_t}{[C_b]_t} + 1\right)}$$

(Eq. 11)

The measured ECL signal is proportional to the concentration of bound complex [C_bA]. Taking also a term of background binding (*BG*) into account we obtain Eq. 12.

$$ECL = Const. \cdot [C_bA] + BG \quad \text{(Eq. 12)}$$

where *Const.* is simply a proportionality constant which is obtained from the fit and relates the measured ECL signal to bound complexes. We can then express the measured ECL signal by Eq. 13.

$$ECL = \frac{Const.}{2\left(\frac{[C]_t}{[C_b]_t} + 1\right)}\left(([A]_t + [C]_t + [C_b]_t + K_D) - \sqrt{([A]_t + [C]_t + [C_b]_t + K_D)^2 - 4\left(\frac{[C]_t}{[C_b]_t} + 1\right)[C_b]_t [A]_t}\right) + BG$$

(Eq. 13)

We thus fit the parameters K_D, $[A]_t$, *Const.* and *BG*. Even though $[A]_t$ should be known, possible errors in the concentration of active molecules make it advisable to fit this term as well.

Chapter 5

Discussion, Conclusions and Outlook

Contents

1. Discussion and Conclusions

The quality of a combinatorial library of binding proteins can be functionally described by the ability to isolate high affinity binders against a broad set of target proteins[1]. Three major factors contribute to successful selections from such a library. First, the library design, which encompasses the scaffold used as well as its diversification strategy employed. Second, the theoretic diversity of the combinatorial DNA library and the percentage of clones that actually have sequences as specified. Finally, the display technology must be able to present all members of the library in a functional form allowing efficient selection. Together, these factors determine the functional diversity of the library which is accessible for the selection of binding molecules.

The observation that the display of highly stable and fast folding proteins, such as DARPins, on filamentous phage is very inefficient using a conventional phage display system was the starting point of my thesis. I identified posttranslational protein translocation across the cytoplasmic membrane as a major bottleneck of this display technology. By simply directing the proteins to be displayed to the *E. coli* cotranslational signal recognition particle (SRP) translocation pathway by using an appropriate signal sequence I was able to solve this problem. This simple change in the use of the translocation route seems to prevent premature folding of stable and fast folding proteins in the cytoplasm and therefore allows their efficient translocation and subsequent display on filamentous phage particles. For all stable and fast folding proteins tested, the display levels on phage particles using SRP-dependent signal sequences were strongly increased and for all other proteins the display levels were at least equal to those obtained using the Sec-dependent signal sequences. This is also true for proteins, such as a scFv-fragment tested, that are already very well displayed using the conventional Sec-dependent signal sequences. Thus, SRP phage display seems to be a simple and broadly applicable way to expand the range of proteins that can be efficiently displayed on phage particles without having negative effects on already well displayed proteins. Therefore, I expected SRP phage display to increase

the functional diversity of many libraries, especially those containing stable and fast folding proteins, such as DARPins.

The logical subsequent step was to use SRP phage display to generate a large phage DARPin library using the previously described combinatorial N3C DARPin library[2,3] as template. As expected, all clones correct at sequence level were shown to be efficiently displayed, resulting in a functional library diversity of at least 1 x 10^{10}. Using this library I was able to select in just two to three phage display selection rounds well behaved and highly specific DARPins against a broad range of target proteins without a single failure until now, which is technically true, but the outcome of selections on TNFα is somehow unusual (see **Chapter 3**). The selected DARPins do show high specificity, have affinities as low as about 100 picomolar without affinity maturation, and retain the favorable biophysical properties of the initial library members such as high expression level, being monomeric in solution and high solubility. The fast enrichment, the high affinities, the very good biophysical properties of the selected binders compare very favorable with results described for antibody or other non-immunoglobulin phage libraries. This can be attributed to the optimized diversity design of the DARPin library as well as the high functional display rate of the SRP phage display.

The results described in my thesis show that the newly developed selection technology SRP phage display ensures a high functional diversity of a phage DARPin library leading to efficient selections. Thus, SRP phage display has proven to be a powerful method to display libraries of fast folding and stable proteins that would be refractory to conventional phage display using the Sec secretion pathway. Good results using SRP phage display were recently also reported for the display of a fibronectin type III domain library and subsequent selections[4]. This scaffold has previously been displayed by using conventional phage display[5] but the change

to SRP phage display seems to give superior results, supporting the broad applicability of our technology.

I expect SRP phage display to be also beneficial for other libraries containing members with widely different folding rates and stabilities, such as e.g. cDNA libraries. Here, a conventional phage display system using the Sec translocation pathway is expected to select against members with fast folding rates. In contrast, a recently described phage display system using the Tat translocation pathway[6] which only translocates natively folded proteins and is therefore expected to select against members that need disulfide bonds for proper folding or even against proteins with slow folding rates. Selection of a mutant with an increased folding rate by using a selection system based the Tat translocation pathway was reported recently, supporting this hypothesis[7].

2. Outlook

Thus, SRP phage display makes filamentous phage display accessible for DARPins, allowing additional selection approaches for DARPins not applicable to ribosome display and will therefore help to broaden the scope of DARPin application. For example, selections under hash conditions, such as high temperatures or in the presence of denaturants which may be valuable ways to select for highly stable interactions with their target proteins. Selections on target proteins in their natural environment such as for example whole cells, tissue sections or even *in vivo* may be even more important[8]. The spectrum of possible applications of such selections is broad and includes for example selections for functions such as internalization[9], thus opening the door to completely new drugs.

3. References

1. Ling, M.M. Large antibody display libraries for isolation of high-affinity antibodies. *Comb Chem High Throughput Screen* **6**, 421-432 (2003).
2. Binz, H.K., Stumpp, M.T., Forrer, P., Amstutz, P. & Plückthun, A. Designing repeat proteins: Well-expressed, soluble and stable proteins from combinatorial libraries of consensus ankyrin repeat proteins. *J. Mol. Biol.* **332**, 489-503 (2003).
3. Binz, H.K., Amstutz, P., Kohl, A., Stumpp, M.T., Briand, C., Forrer, P., Grütter, M.G. & Plückthun, A. High-affinity binders selected from designed ankyrin repeat protein libraries. *Nat. Biotechnol.* **22**, 575-582 (2004).
4. Koide, A., Gilbreth, R.N., Esaki, K., Tereshko, V. & Koide, S. High-affinity single-domain binding proteins with a binary-code interface. *PNAS* **104**, 6632-6637 (2007).
5. Koide, A., Bailey, C.W., Huang, X. & Koide, S. The fibronectin type III domain as a scaffold for novel binding proteins. *J. Mol. Biol.* **284**, 1141-1151 (1998).
6. Paschke, M. & Höhne, W. A twin-arginine translocation (Tat)-mediated phage display system. *Gene* **350**, 79-88 (2005).
7. Ribnicky, B., Van Blarcom, T. & Georgiou, G. A scFv Antibody Mutant Isolated in a Genetic Screen for Improved Export via the Twin Arginine Transporter Pathway Exhibits Faster Folding. *J. Mol. Biol.* **369**, 631-639 (2007).
8. Trepel, M., Arap, W. & Pasqualini, R. In vivo phage display and vascular heterogeneity: implications for targeted medicine. *Curr. Opin. Chem. Biol.* **6**, 399-404 (2002).
9. Poul, M.-A., Becerril, B., Nielsen, U.B., Morisson, P. & Marks, J.D. Selection of tumor-specific internalizing human antibodies from phage libraries. *J. Mol. Biol.* **301**, 1149-1161 (2000).

Appendix 1

Supplementary Data for DARPins Selected from the Phage DARPin Library

Contents

1. Introduction

Appendix one contains supplementary data of **Chapter 3** of my thesis. One of the main goals of my thesis was to validate the constructed phage DARPin library by selecting binders against a broad range of target proteins. In **Chapter 3**, a detailed characterization is described only for a small subset of the DARPins selected. To facilitate the use of the selected binders in future projects and collaborations, each subchapter of this **Appendix 1** summarizes data of the DARPins selected against one specific target protein. The characterizations include for all selected binders: sequence alignment, SEC analysis and specificity and affinity determination by ELISA (some data is redundant to **Chapter 3**). All experiments were performed in analogy to the protocols given in the **Material and Methods** section of **Chapter 3**. The last subchapter comprises a small statistical analysis of the sequences of naive library members and selected binders and an evaluation of the SEC measurements recorded for all selected DARPins. **Table 1** summarizes selections on the different target proteins and the resulting binders.

Table 1: Summary of the phage display selections of DARPins against different target proteins

Target (sel. Rounds)	Selection		Selected DARPins		
	No. positive clones[a]	No. different sequences[b]	**No ELISA signal** (false positive)	**Low ELISA signal** (low affinity binders)[c]	**High ELISA signal** (high affinity binders)[d]
huIgG1_Fc (R3)	82/94	11/21 (8/21)	I_10, I_14, I_15	I_06, I_03	**I_01, I_02, I_07, I_11, I_13, I_19**
TNFα (R2/3)[e]	102/188	29/52 (29/52)	-	T_03, T_04, T_06, T_10, T_11, T_19, T_33, T_35, T_41, T_44, T_51	**T_01, T_02, T_07, T_08, T_09, T_ 16, T_25, T_27, T_37, T_40**, T_12, T_13, T_15, T_30, T_45, T_47, T_49, T_52
ErbB1 (R2/3)[e]	97/369	5/64 (1/64)	E_17, E_31, E_36	E_64	**E_01**
ErbB1 (R1, ep.)[g]	81/105	4/20 (4/20)	-	E_72	**E_67, E_68, E_69**
ErbB2-509 (R3)	83/94	13/29 (13/29)	-	9_12, 9_33	**9_16, 9_26, 9_29**, 9_01, 9_02, 9_03 9_04, 9_10, 9_18, 9_20, 9_30
ErbB2-631 (R1, ep.)[g]	24/94	9/16 (8/16)[h]	H_11	H_13	**H_14**, H_01, H_03
ErbB4 (R3)	55/143	7/48 (5/48)	B4_11, B4_14	-	**B4_01, B4_02, B4_07, B4_33, B4_45**
ErbB4 (R1, ep.)[g]	84/94	12/20 (6/20)	B4_55, B4_56, B4_63, B4_64, B4_65, B4_68	B4_49, B4_53, B4_57, B4_60	**B4_50, B4_58**

[a]Ratio of the number of positive clones to the total number of clones screened in ELISA experiments. [b]Number of clones with different sequences, identified in the total number of clones sequenced. In parentheses number of different clones confirmed by competition ELISA experiments using purified DARPins to bind the target protein. [c]Binders giving low ELISA signal (signal/background < 3) indicating either low affinity of low concentrations of active binder (atypical SEC, no monodisperse population as judged by SEC). [d] In bold letters binders described in **Chapter 3** of my thesis. [e]Sum of the analysis of the 2nd and 3rd round of selection. [f]Sum of the analysis of the 2nd and 3rd round of different selection approaches. [g]One round of selection with epitope-masking (ep.) as described in **Chapter 3** of my thesis. [h]Four of the clones sequenced were already found in the selection on ErbB2-509 and are not listed.

2. DARPins binding the Fc domain of human IgG1

The "fragment crystallizable" region (Fc region) of antibodies is responsible for interaction with cell surface receptors (Fc receptors) and proteins of the complement system and thereby mediates effector functions such as activation of the complement system or cytotoxic cells[1]. The Fc domain of IgGs is a glycosylated disulfide-linked homodimer, composed of the second and third constant domain of the antibody's heavy chain. The aim of this project was to select binders with a broad range of affinities against the Fc domain of human IgG1 (huIgG1_Fc, P100 – K330). High affinity clones, when coupled to a label, could be used as in vitro detection reagents, alternative to commercially available secondary antibodies (e.g. Western blotting and ELISA). Additionally, for *in vivo* applications, binders with different affinities could be tested to construct fusion proteins (e.g. DARPin heterodimers) with a "tailored" serum half-life by hijacking of antibodies present in the blood stream.

Selection and screening of binders against huIgG1_Fc is described in detail in **Chapter 3** of my thesis. Based on ELISA and SDS-PAGE analysis, 21 clones were submitted for sequencing, resulting in eleven different sequences (**Fig. 1**). After expression and purification by immobilized metal ion chromatography (IMAC) purification in the 96-well format, all binders were analyzed by size exclusion chromatography (SEC) and compared to the well characterized, non-binding DARPin E3_5 (ref. 2) (**Fig. 2**). To investigate the specificity of the selected DARPins, ELISA experiments were performed. All of the binders were tested for interacting with full length human IgG1 (huIgG1), neutravidin, mouse IgG1 (muIgG1) and mouse IgG2b (muIgG2b). In the competition ELISA setup, DARPins were preincubated with free huIgG1 (**Fig. 3a, b**). As a result, highly specific DARPins to human IgG1 were obtained with affinities ranging from 2 to 140 nM. Due to the low binding signal, clones I_10, I_14 and I_15 were considered as false positives (no affinity for the target protein or affinity below the detection limit of the experiments). Clones I_03 and I_06 gave low binding signal, probably due to the low

concentration of active binder present (see SEC **Fig. 2**), which can probably be attributed to framework mutations (**Fig. 1**)

Four of the clones were further analyzed at multiple concentrations by surface plasmon resonance (SPR) (**Table 3** and **Supplementary Figure 2** of **Chapter 3**) and the data obtained were evaluated with a global kinetic fit. Additionally, the binding kinetics of these clones were determined by resonant acoustic profiling (RAP) performed by John Watkins and coworkers (Akubio Ltd., Cambridge, United Kingdom). Comparison of the SPR and RAP results is shown in **Table 2**. Unfortunately, DARPin concentrations for RAP measurements were only estimated by a single measurement using a NanoDrop ND-1000 spectrophotometer (NanoDrop Technologies, USA), affecting the accuracy of the association constants and thereof calculated affinity constants. DARPin concentrations for SPR measurements were determined directly before kinetic analysis using an Agilent 8453 UV-Visible Spectrophotometer (Agilent Technologies, Germany), giving highly reproducible values. Nevertheless, range and order of the affinities and binding kinetics measured with SPR and RAP are in good agreement.

Table 2: Comparison of the affinities and binding kinetics of huIgG1_Fc binding DARPins determined by SPR and RAP

Clone (NxC) [a]	Measurement [b]	K_D [nM]	k_{on} [10^4 $M^{-1}s^{-1}$]	k_{off} [$10^{-3}s^{-1}$]
I_02 (N2C)	SPR	41	28	12
	RAP	57	36	20
I_07 (N2C)	SPR	25	7.0	1.7
	RAP	14	18	2.5
I_11 (N3C)	SPR	140	49	67
	RAP	130	50	66
I_19 (N3C)	SPR	2.1	34	0.7
	RAP	3.2	47	1.5

[a] Name of the respective clone and in parentheses number internal of repeat modules (x) stacked between N-Cap (N) and C-Cap (C). [b] Association (k_{on}) and dissociation (k_{off}) constants were measured by using surface plasmon resonance (SPR) or resonant acoustic profiling (RAP) and respective dissociation constants K_D calculated as (k_{off}/k_{on}). Kinetic data and evaluation with a global kinetic fit of the SPR measurements is given in **Chapter 3: Supplementary Figure 2**. Data of the RAP measurements were produced John Watkins and coworkers (Akubio Ltd., Cambridge, United Kingdom).

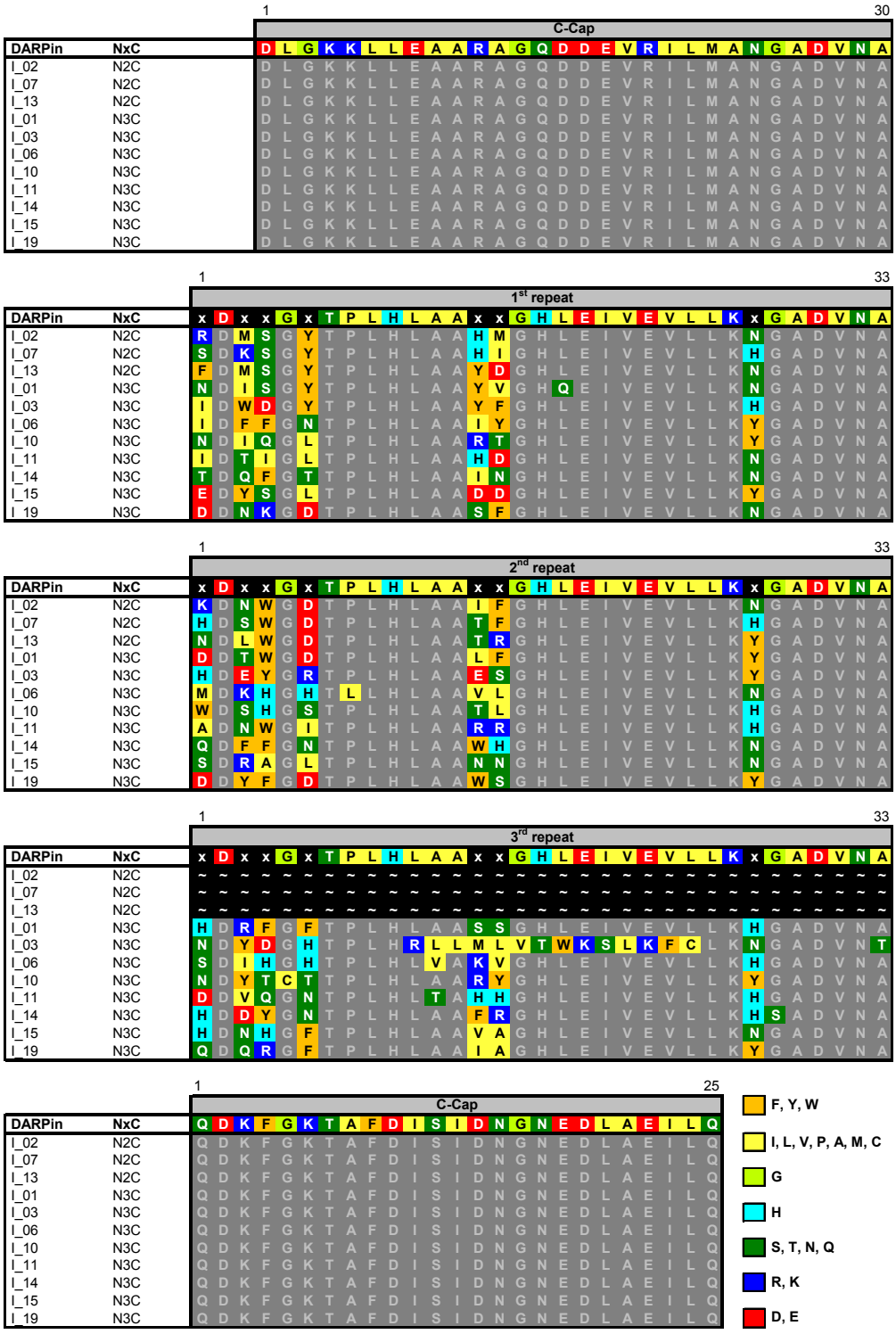

Figure 1: Sequences of selected huIgG1_Fc binding DARPins. The original consensus sequence is shown on top with randomized positions indicated by x. In the lines below, only residues that differ from the consensus sequence are printed in color, residues identical to the consensus sequence are printed in gray and deletions and missing amino acids are printed in black. Note that the N-terminal MRGSHHHHHHGS and the C-terminal KLN, which are not part of the DARPin sequence, are not shown. Amino acids are colored by type as indicated at the end of the alignment.

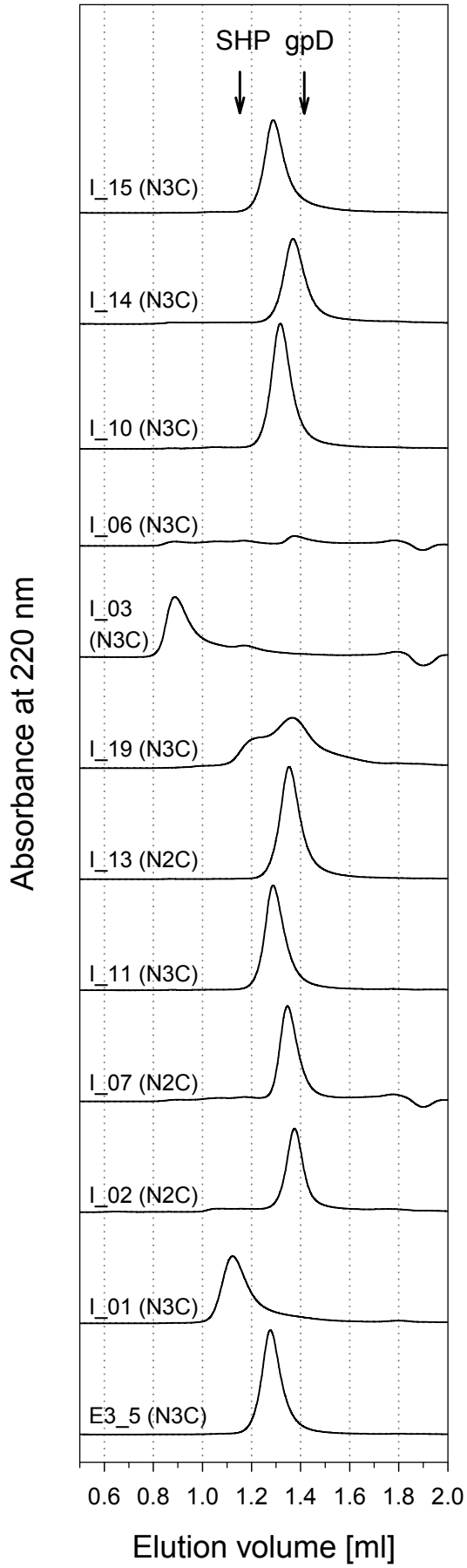

Figure 2: Size exclusion chromatography (SEC) of selected huIgG1_Fc-binding DARPins. The chromatograms of the eleven huIgG1_Fc binders and the unselected DARPin E3_5 are shown. For each DARPin the number of repeats stacked between N-Cap (N) and C-Cap (C) is given in parentheses. The molecular mass standards, phage protein D (gpD) with an apparent mass of 17.6 kDa and phage protein SHP, a trimer with an apparent mass of 50.2 kDa, are indicated with arrows.

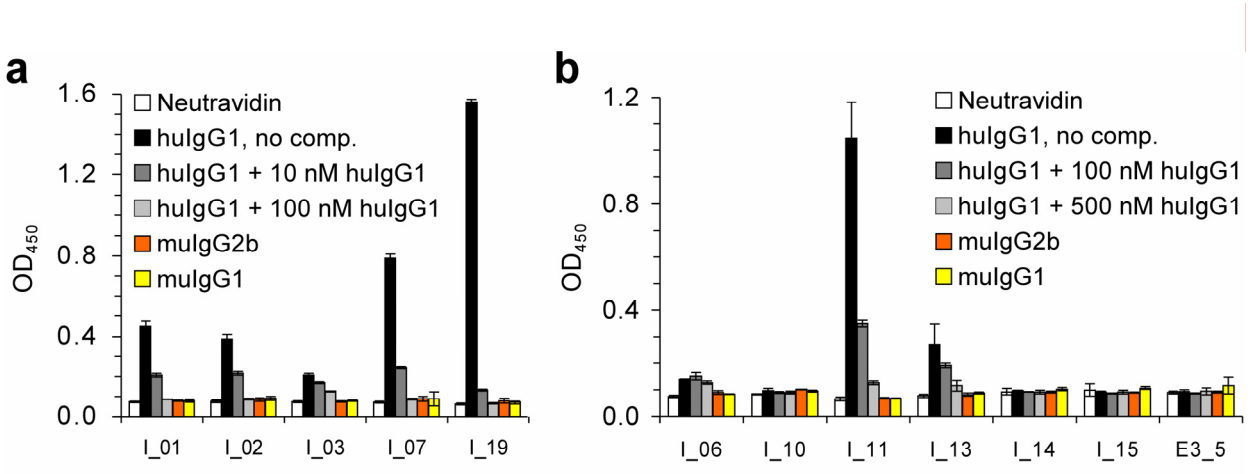

Figure 3: Specificity and affinity estimation of selected huIgG1_Fc binders. (a) ELISA with high affinity huIgG1_Fc binders. To analyze specificity, 1 nM solutions of the binders I_01, I_02, I_03, I_07 and I_19 were tested for binding on neutravidin, huIgG1, mouse IgG1 (muIgG1) and mouse IgG2b (muIgG2b) and, in parallel, competition experiments were performed by preincubation of 1 nM solutions of the DARPins with 10 nM or 100 nM free huIgG1 (10 nM or 100 nM) before binding on immobilized huIgG1. (b) ELISA with low affinity huIgG1_Fc binders and control DARPin E3_5. To analyze specificity, 5 nM solutions of the binders I_06, I_10, I_11, I_13, I_14, I_15 and control DARPin E3_5 were tested for binding on neutravidin, huIgG1, muIgG1 and muIgG2b and, in parallel, competition experiments were performed by preincubation of 5 nM solutions of the DARPins with 100 nM or 500 nM of free huIgG1 (100 nM or 500 nM) before binding on immobilized huIgG1. All full length IgGs were directly immobilized on solid supports. The first word in the legend denotes the protein immobilized, *no comp.* denotes the absence of a competitor and + *huIgG1* denotes the presence of competitor in 10 nM, 100 nM or 500 nM concentrations.

3. DARPins binding tumor necrosis factor alpha (TNFα)

Tumor necrosis factor alpha (TNFα) is a pro-inflammatory cytokine that is responsible for a broad range of signal events leading to apoptosis, cellular proliferation and differentiation[3]. TNFα is produced as a type II membrane protein which spontaneously assembles into homotrimers. Upon proteolytic cleavage, the soluble trimeric form of TNFα is released from the membrane. Both soluble and membrane bound form can interact with the two main receptors TNF-R1 and TNF-R2. Overexpression of TNFα has been identified as one of the key players in many human diseases such as rheumatoid arthritis. The aim of this project was to validate the phage DARPin library and to select binders to TNFα and test whether binders can be obtained that can block TNFα action in a similar fashion as the clinically used soluble recombinant receptor of TNFα Etanercept (Enbrel^{TM}) or the two antibodies Infliximab (Remicade^{TM}) and Adalimumab (Humira^{TM}).

Selection and screening of binders against the soluble form of TNFα is described in detail in **Chapter 3** of my thesis. Based on ELISA and SDS-PAGE analysis, 52 clones were submitted for sequencing, resulting in 29 different sequences (**Fig. 4**). Interestingly, all selected binders are N3C DARPins with a quite high prevalence of hydrophobic amino acids at the randomized positions of the first and second internal repeat, as well as many cysteines and deletions, without showing a selected consensus. After expression and purification by immobilized metal ion chromatography (IMAC) purification in the 96-well format, all binders were analyzed by size exclusion chromatography (SEC) and compared to the well characterized, non-binding DARPin E3_5 (ref. 2) (**Fig. 5**). To investigate the specificity of the selected DARPins, ELISA experiments were performed (**Fig. 6**). All of the binders do show specific binding to TNFα, do not interact with neutravidin and binding can be almost completely inhibited by preincubation of the immobilized TNFα with soluble Enbrel (for further experiments see below). In the competition ELISA setup, the binding of all clones to immobilized TNFα could also be well

inhibited by preincubation with free TNFα. From the competition ELISA signals obtained with 10 nM of free TNFα, the affinity of most of the binders was estimated to be in the low nM range.

To determine the affinity, a subset of the selected DARPins (T_02, T_07, T_08, T_25, T_37 and T_40) was further analyzed by competition ELISA measurements using dilution series of free TNFα for competition (**Fig. 7a**). Inhibition of ELISA signals to less than 50% was observed for all clones tested using 3 nM competitor, suggesting single digit nanomolar affinity. To determine the binding kinetics, the selected DARPins were further analyzed by surface plasmon resonance (SPR, Biacore) measurements. Interestingly, none of the selected DARPins did show binding to TNFα which had been immobilized via the biotin label (present at an N-terminal Avi-tag on TNFα) to a flow cell of a streptavidin coated chip (SA, Biacore), while Enbrel gave a high and specific binding signal, confirming the immobilization of the target protein. Unfortunately, the exact reason for this behavior could not be determined. However, the observation that the refractive index signal of the TNFα-coated flow cell decreased over time might indicate that the integrity of the TNFα homotrimer is not maintained under these experimental conditions. Thus, a possible explanation could be that the DARPins only bind to the intact trimer, while Enbrel also recognizes other forms of TNFα.

The SPR measurements were then also performed in the inverted setup. The DARPins T_02 and T_25 were directly coupled to a dextran-chip (CM5, Biacore) and soluble TNFα was injected at different concentrations over the flow cells (**Fig. 7b, c**). The kinetic data of the interactions were evaluated with a global fit using Scrubber 2 (BioLogic Software Ltd), resulting in a dissociation constant of 12 nM for T_02 and 7 nM for T_25, which is in reasonable agreement with the affinities estimated by the competition ELISA experiments (**Fig. 7a**).

Interestingly, in an ELISA setup the binding of all selected DARPins can be almost completely inhibited by preincubation of the immobilized TNFα with soluble Etanercept (Enbrel^{TM}, recombinant human soluble tumor necrosis factor alpha receptor fused to Fc domain of human IgG1) (Amgen, USA) (**Fig. 6 a, b**). However, in the same ELISA setup, when the

immobilized TNFα was preincubated with different DARPins (T_02, T_07, T_08, T_25, T_37, T_40), the binding of Enbrel could not be inhibited, even not at very low concentrations of Enbrel (**Fig. 8a**). This seemingly "unidirectional" competition of the two classes of binding molecules can probably be explained by their different affinities for the target protein. The affinities of the tested DARPins are in the low nanomolar range (see above). Literature values for the affinity of Enbrel range from 65 pM (ref. 4) to 1.15 nM (ref. 5). The former value seems to be much more realistic, since in the SPR experiments carried out here the evaluation of injections of Enbrel by a global fit resulted in an affinity of about 130 pM (data not shown). Due to this 100-fold difference in affinity of the two classes of binding molecules it might be possible that the dimeric Enbrel is able to displace the bound DARPins in the setup of the ELISA experiment.

The competition of the DARPin T_25 with Enbrel for binding to TNFα was further analyzed in kinetic SPR measurements. Enbrel was directly coupled to a dextran-chip (CM5, Biacore) and soluble TNFα alone or TNFα preincubated with an excess of the DARPin (200 nM) was injected at different concentrations over the flow cells (**Fig. 8b**). For all concentrations addition of the DARPin strongly reduced the binding signal obtained compared to TNFα alone, and at 1 nM TNFα concentration the DARPin (at 200 nM) could almost completely inhibit the binding of TNFα to the immobilized Enbrel. Therefore, the DARPins and Enbrel are competing for binding to the target protein, however in strong favor for the dimeric Enbrel.

In all experiments described above (phage selection, ELISA and SPR measurements), the binding and washing steps were carried out using standard buffers containing 0.1% (v/v) Tween-20 (buffers used are indicated in all figures). During further analysis, very much to my surprise, I discovered that all the selected DARPins show specific TNFα binding that is dependent on the presence of the detergent Tween-20 in the binding buffer. For example, in ELISA experiments, excellent and specific binding to the immobilized target protein was observed in buffer PBST (PBS containing 0.1% (v/v) Tween-20), but not in PBS alone (**Fig. 9**). Identical Tween-20

dependent binding in ELISA experiments was observed using TBS or HBS as buffers (data not shown) and also in SPR measurements, binding of TNFα to the immobilized DARPins could only be detected in HBST (HBS containing 0.1% (v/v) Tween-20) but not in HBS alone. In stark contrast, Enbrel did show identical TNFα binding signals independent of the buffer composition used (**Fig. 9)**. To further analyze if this effect of detergent-dependent binding can also be observed in solution, complex formation of the two DARPins T_07 and T_37 with the target protein was investigated by SEC using PBS and PBST as running buffers (**Fig. 10**). DARPins and TNFα alone and both co-injected were analyzed. The apparent molecular weight of TNFα was 45 kDa in PBS and 40 kDa in PBST, most probably representing the homo-trimeric form of the protein, which has a theoretical molecular weight of 52.2 kDa. As expected, only in the buffer containing Tween-20 a shift to higher molecular weight indicating complex formation was observed (**Fig. 10b, d**). In PBS, co-injection of the binders and TNFα resulted in an elution chromatogram identical to the sum of the chromatograms of the single components (**Fig. 10a, c**). One possible speculation to explain these findings is that Tween-20, present during all selections, induces conformational changes in TNFα needed for the accessibility of the DARPin epitopes.

To further investigate the composition of the DARPin- TNFα complex, DARPin T_07 and TNFα alone and both co-injected were analyzed by SEC-MALS as described[6]. Measurements and data evaluation was performed by Thomas Huber and the results obtained are depicted in **Figure 11**. For the DARPin T_07 the weight-average molar mass over the peak obtained from SEC-MALS measurements (MW_{MALS}) was determined to be 18.8 kDa, in good agreement with the molecular weight calculated from the amino acid composition (MW_{calc} = 18 kDa). For TNFα the MW_{MALS} was determined to be 52.8 kDa, also in good agreement with the MW_{calc} = 52.2 kDa of the homo-trimeric form of the protein. Complex formation of TNFα coinjected with an equimolar amount of the DARPin T_07 is clearly indicated by a shift of 0.6 ml of the elution peak to a smaller elution volume (bigger molecular size) relative to the uncomplexed TNFα. However, the MW_{MALS} was determined to be 53.5 kDa which cannot be

explained by the complex formation of one or more DARPins with the intact homo-trimeric form of TNFα, which would result in a MW_{calc} of at least 70.2 kDa (homo-trimeric TNFα plus one DARPin). One reasonable model to explain the measured molecular mass would be the complex formation of the homo-dimeric form of TNFα with one DARPin (MW_{calc} = 52.8 kDa). In the case of TNFα coinjected with a threefold lower amount of the DARPin T_07 complex formation can be observed, but the elution peak seems to be a mixture of different molecular species as indicated by the shape of the elution peak and the molar mass distribution over the peak. We cannot exclude a more complicated model containing mixtures of species, as the MALS can only detect the weight-average molar mass. All in all, the complex formation of TNFα with the DARPin can not be explained by the stable interaction of one or three DARPins with the homo-trimeric form of TNFα and seems to follow a more complicated mechanism.

To summarize, the selected DARPins seem to bind to a non-native epitope on TNFα, also depending on the presence of Tween-20. It should be remembered that the TNFα used (with and without Avi-tag) was recombinantly produced in *E. coli* (see **Chapter 3**). To prevent the enrichment of such binders, Tween-20 could be omitted or replaced by other detergents in new selection approaches on TNFα. I did not further analyze these DARPins, since I do not expect them to bind their target protein *in vivo*.

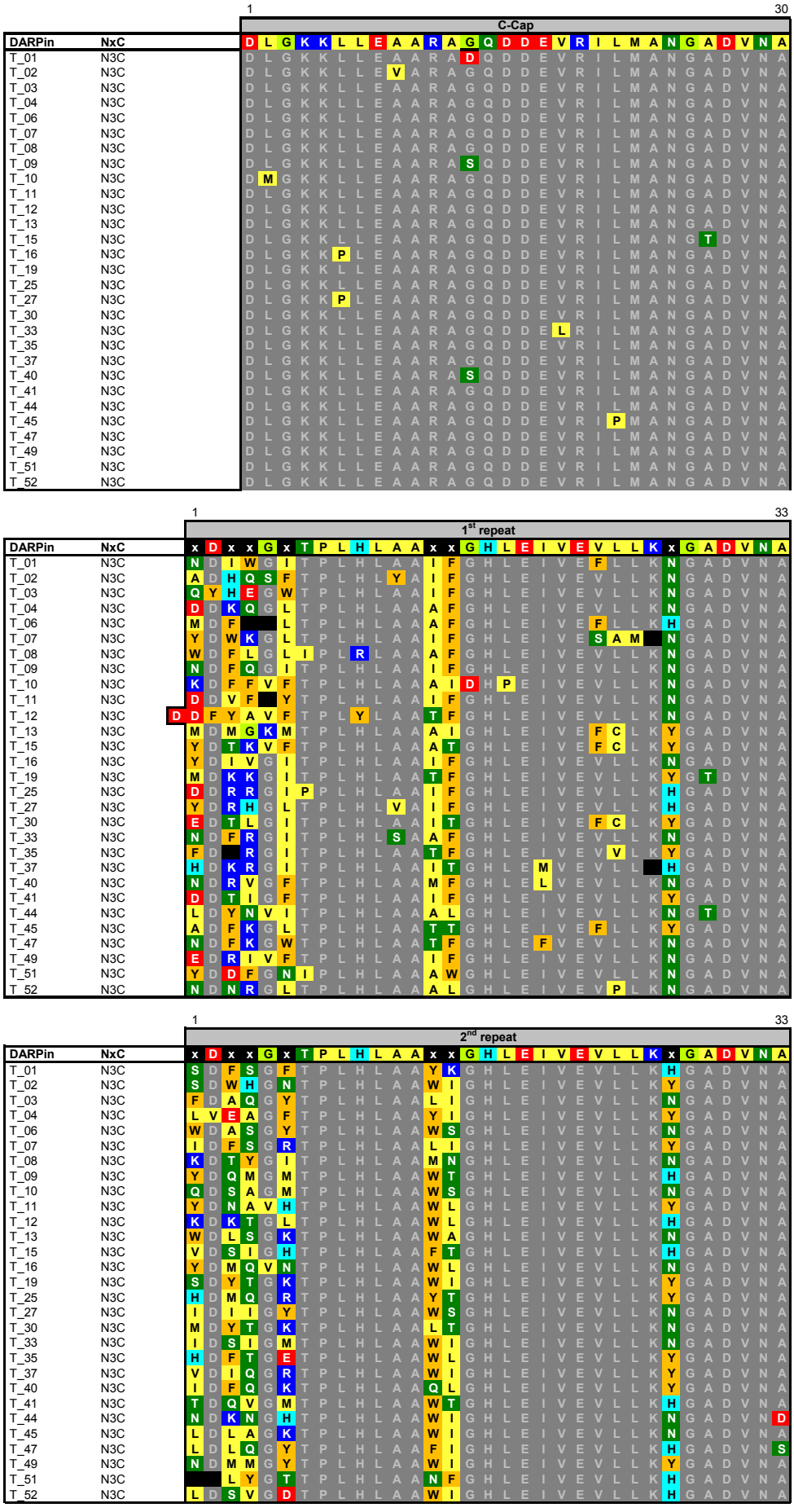

Figure 4: Continued next page.

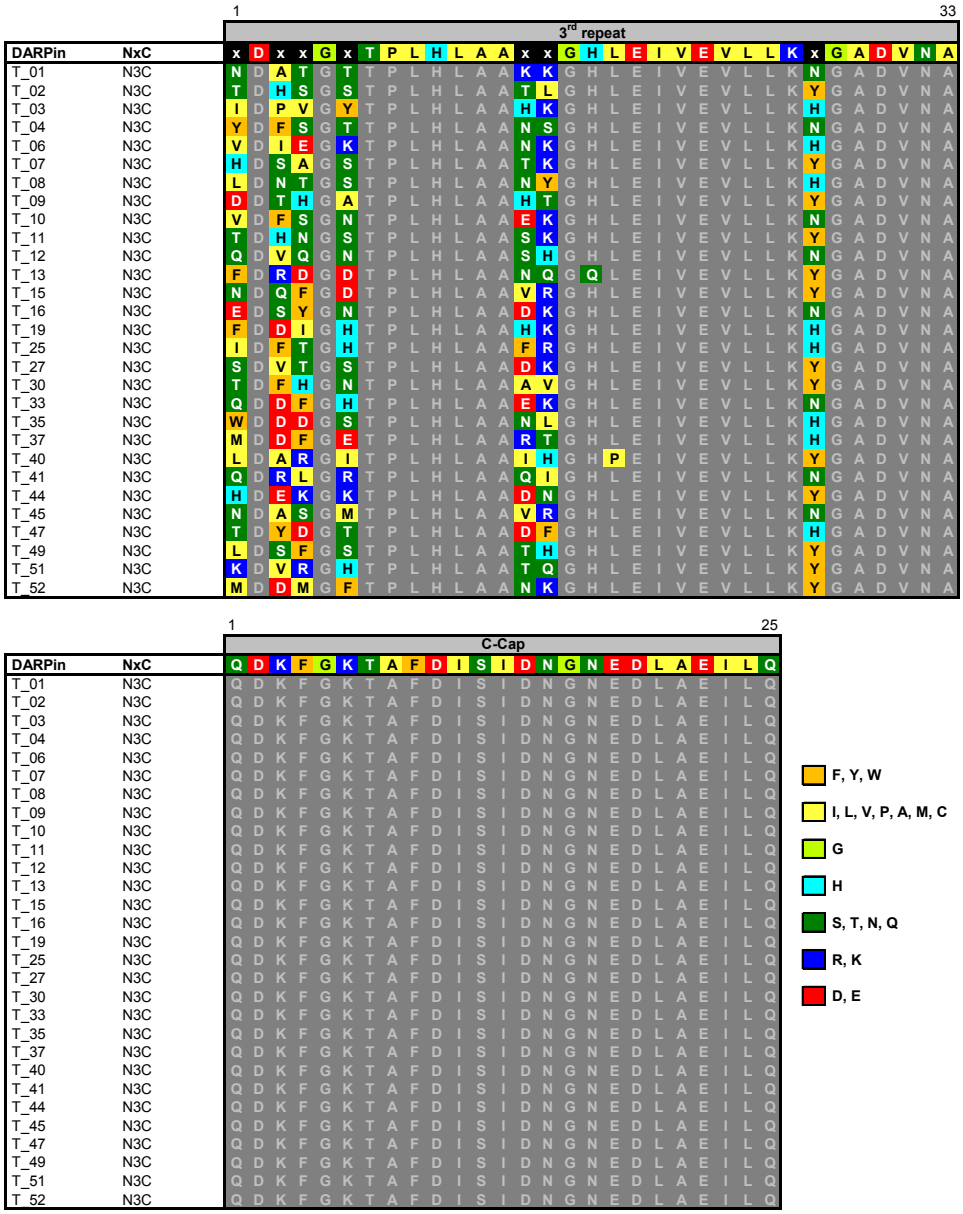

Figure 4: Sequences of selected TNFα binding DARPins. The original consensus sequence is shown on top with randomized positions indicated by x. In the lines below, only residues that differ from the consensus sequence are printed in color, residues identical to the consensus sequence are printed in gray and deletions and missing amino acids are printed in black. Note that the N-terminal MRGSHHHHHHGS and the C-terminal KLN, which are not part of the DARPin sequence, are not shown. Amino acids are colored by type as indicated at the end of the alignment.

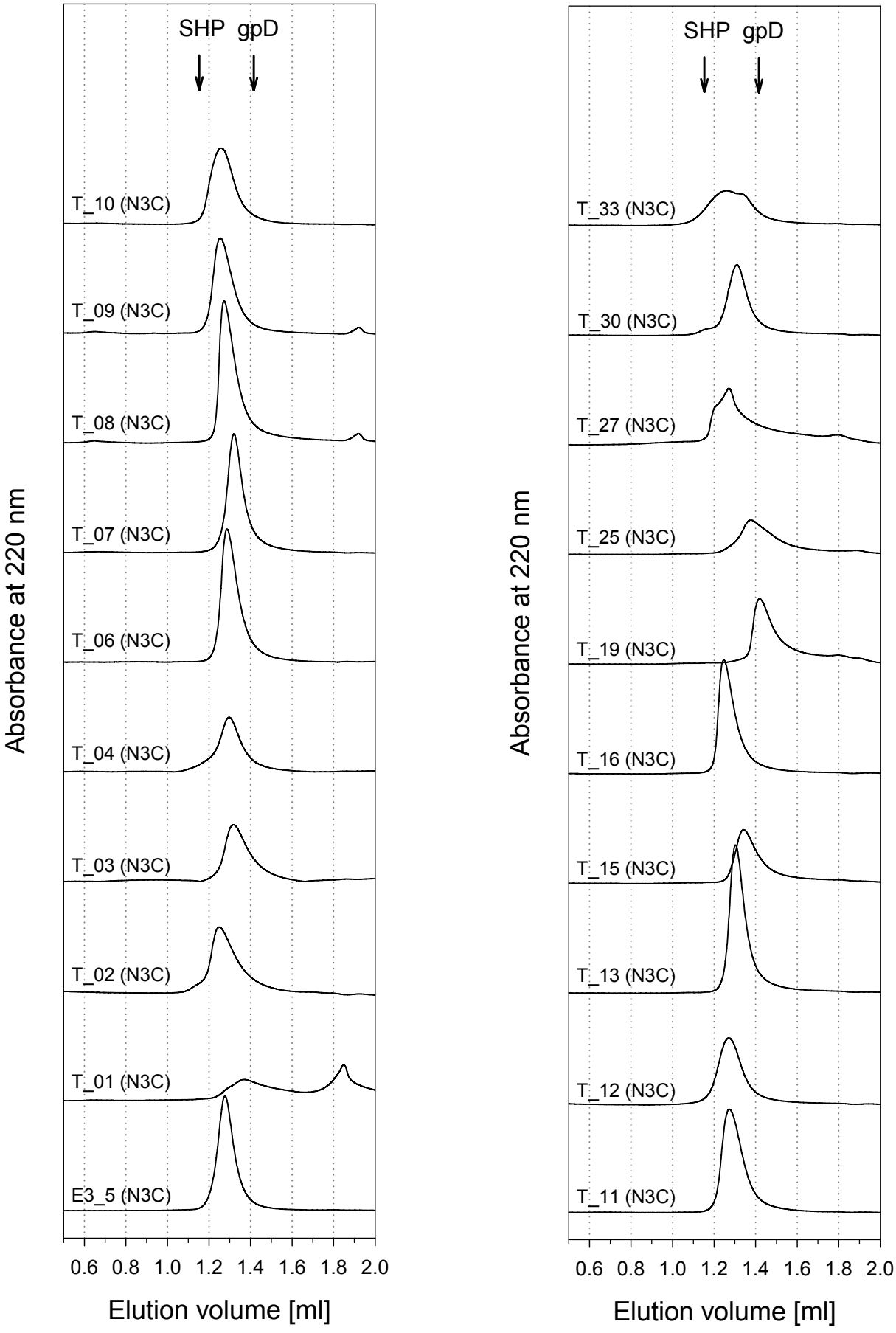

Figure 5: Continued next page.

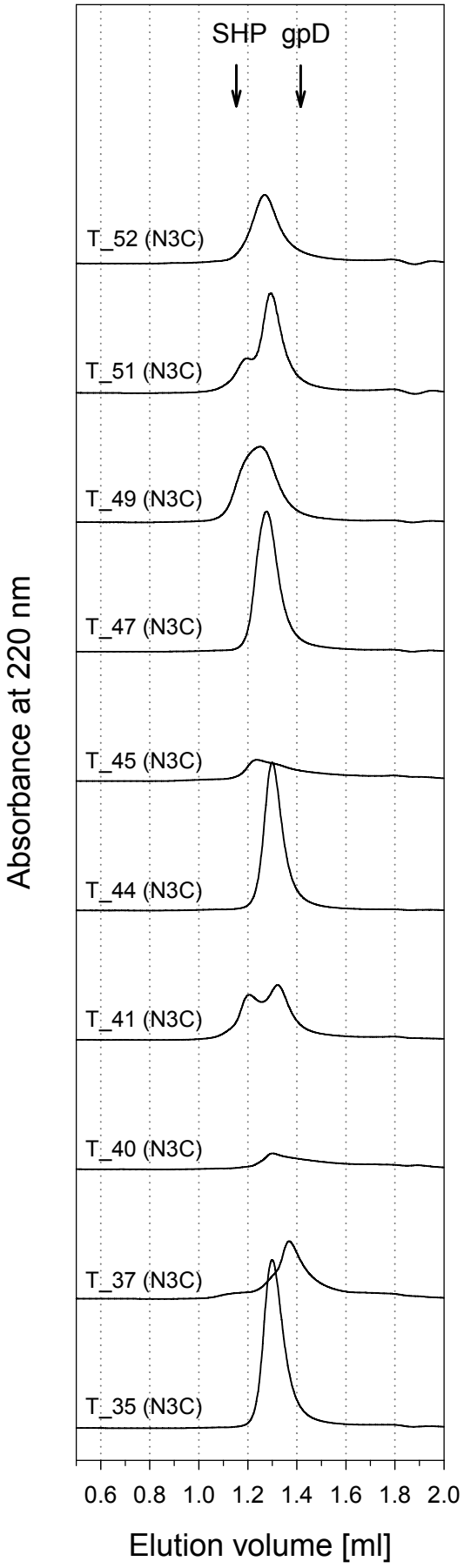

Figure 5: Size exclusion chromatography (SEC) of selected TNFα-binding DARPins. The chromatograms of the 34 TNFα binders and the unselected DARPin E3_5 are shown using PBS as running buffer. For each DARPin the number of repeats stacked between N-Cap (N) and C-Cap (C) is given in parentheses. The molecular mass standards, phage protein D (gpD) with an apparent mass of 17.6 kDa and phage protein SHP, a trimer with an apparent mass of 50.2 kDa, are indicated with arrows.

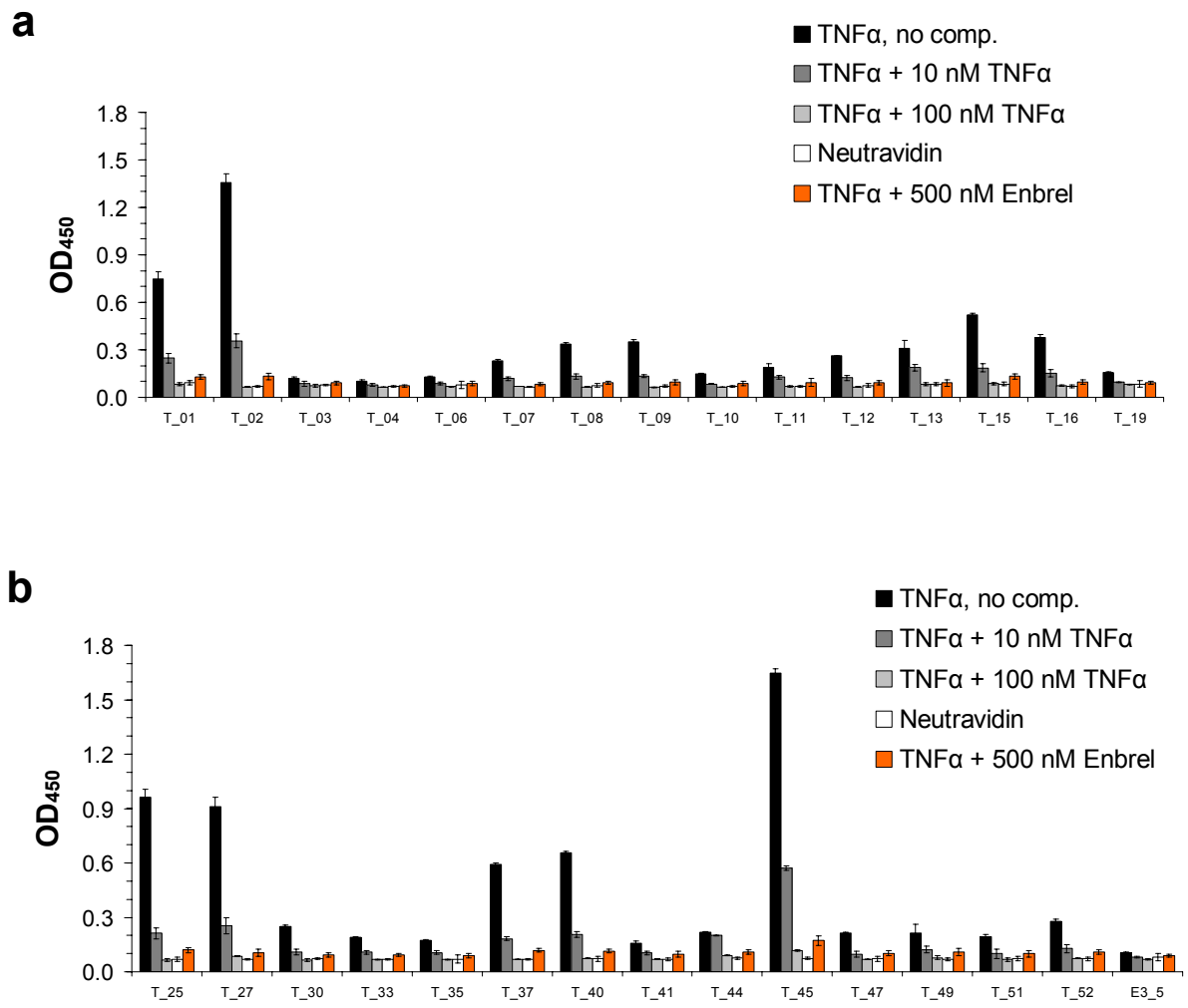

Figure 6: ELISA of selected TNFα binding DARPins. (a, b) To analyze specificity, 5 nM solutions of the selected DARPins were analyzed for binding on neutravidin, immobilized TNFα and immobilized TNFα preincubated with 500 nM Etanercept (Enbrel™) (recombinant human soluble tumor necrosis factor alpha receptor fused to Fc domain of human IgG1). In parallel, competition experiments were performed by preincubation of 5 nM solutions of the DARPins with free TNFα (10 nM or 100 nM) before binding on immobilized TNFα. DARPin E3_5 was used as negative control. For each sample applied, the signal of bound DARPins, detected with an anti RGS-His antibody is shown. The first word in the legend denotes the protein immobilized, *no comp.* denotes the absence of a competitor and + *TNFα* or + *Enbrel* denotes the presence of competitor (respective concentrations are given in nM). All binding and washing steps were carried out in PBST (PBS containing 0.1% (v/v) Tween-20) and concentrations for TNFα are given for the monomer.

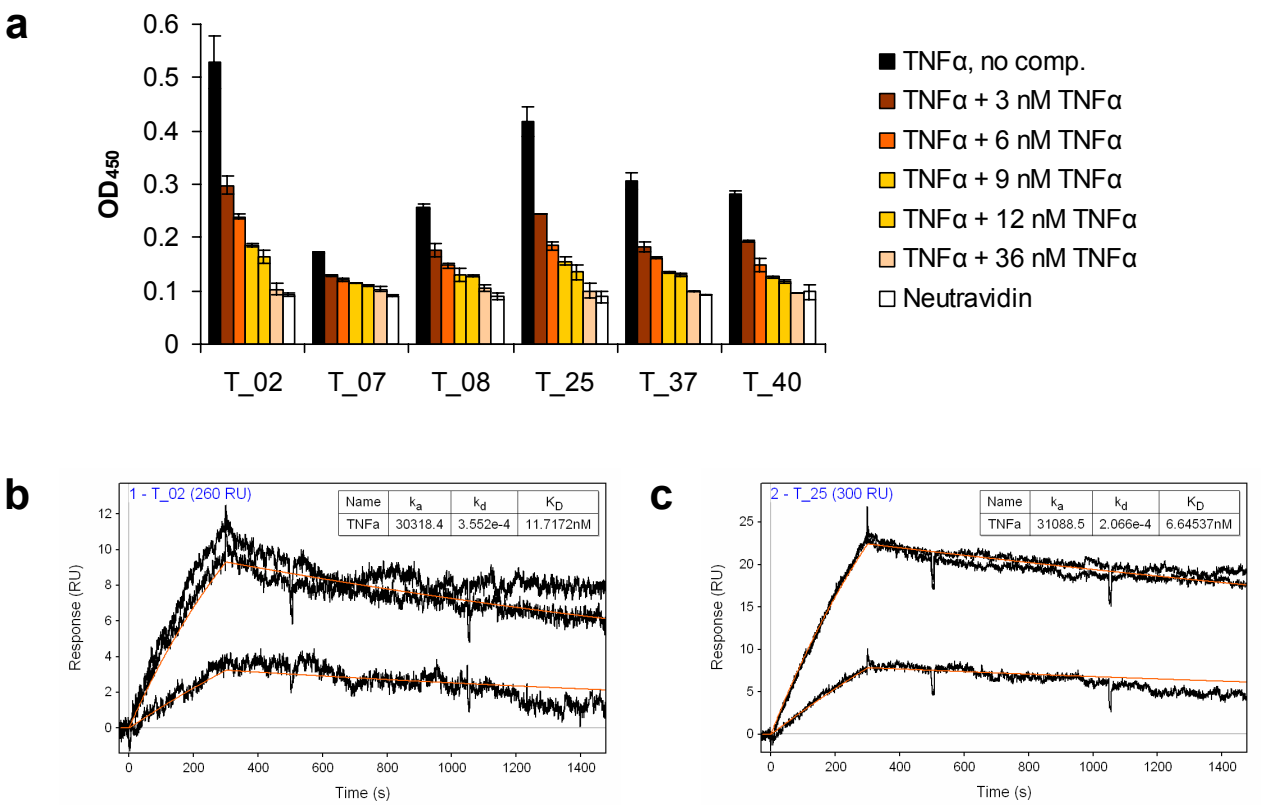

Figure 7: Affinity estimation for a subset of the selected TNFα binding DARPins: (a) To quantify the affinity by a competition ELISA experiment, 2 nM solutions of the DARPins (T_02, T_07, T_08, T_25 and T_40) were analyzed for binding on neutravidin and immobilized TNFα. In parallel, competition experiments were performed by preincubation of 2 nM solutions of the DARPins with free TNFα (3 nM, 6 nM, 9 nM 12 nM and 36 nM) before binding on immobilized TNFα. For each sample applied, the signal of bound DARPins, detected with an anti RGS-His antibody is shown. The first word in the legend denotes the protein immobilized, *no comp.* denotes the absence of a competitor and + *TNFα* denotes the presence of competitor (respective concentrations are given in nM). All binding and washing steps were carried out in PBST (PBS containing 0.1% (v/v) Tween-20) and concentrations for TNFα are given for the monomer. (b, c) Surface plasmon resonance (SPR) was measured using a BIAcore 3000 instrument (BIAcore, Uppsala Sweden). Measurements were performed in HBST buffer (20 mM HEPES, 150 mM NaCl, pH 7.4, 0.1% Tween-20) at a flow rate of 50 µl/min. The DARPins T_02 (b) and T_25 (c) were directly coupled to a dextran-chip (CM5, Biacore, 260 RU and 300 RU, respectively) and soluble TNFα (once 15 nM and twice 50 nM) injected for 4 minutes and the off-rate measured for 20 minutes with buffer flow. The signal of an uncoated reference cell was subtracted from the sensograms. The kinetic data of the measurements was evaluated with a global fit using Scrubber 2 (BioLogic Software Ltd). Curves with the corresponding fits are shown in the figure and the kinetic data are indicated in each graph.

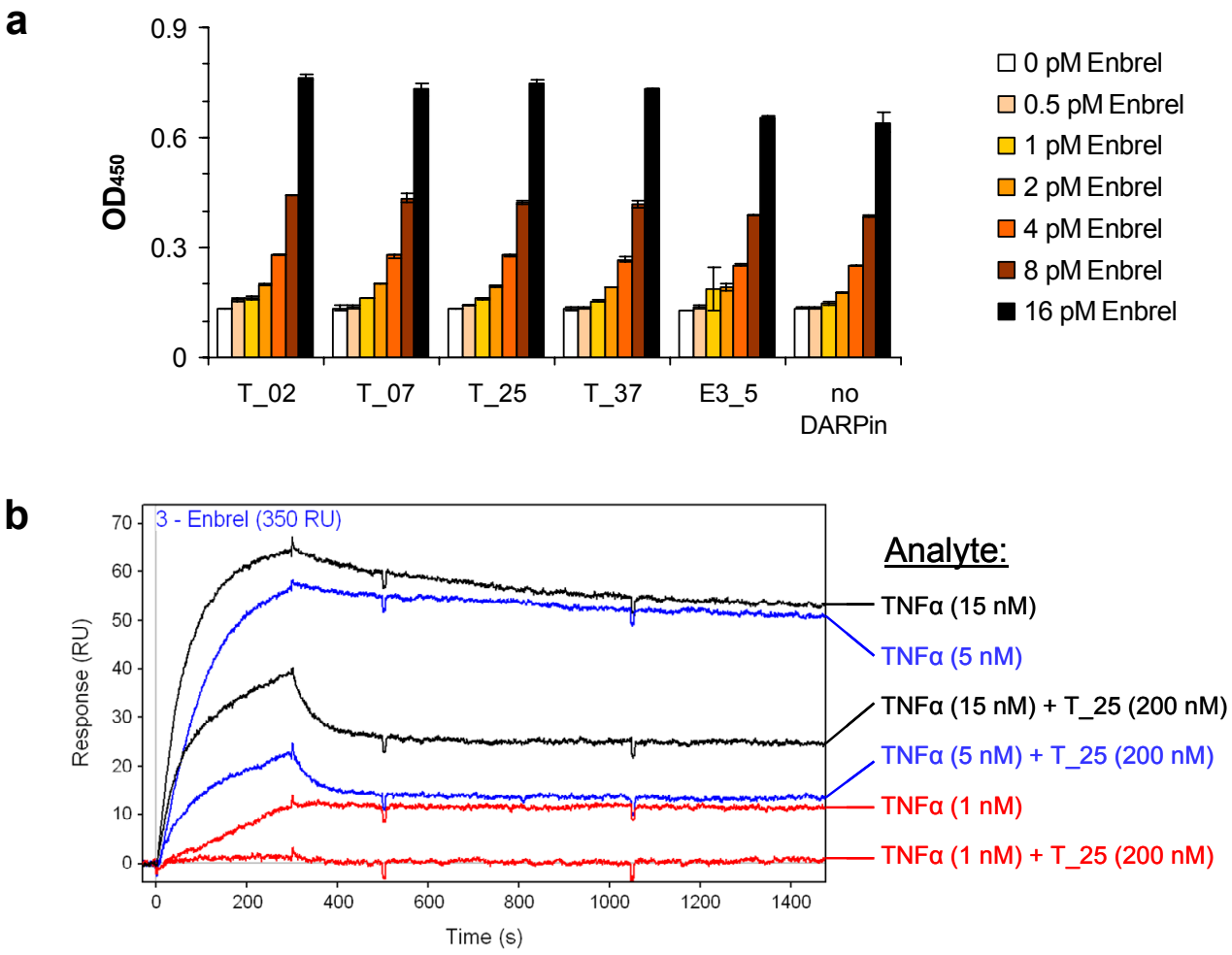

Figure 8: Competition of DARPins with recombinant TNF receptor fusion protein Enbrel for TNFα binding. (a) In the ELISA setup, solutions of Enbrel (0.5 pM to 16 pM) were analyzed for binding to immobilized TNFα (TNFα, no DARPin) and immobilized TNFα preincubated with and in the presence of 0.5 µM solutions of the DARPins T_02, T_07, T_25, T_37, E3_5 indicated on the x-axis. For each sample applied, the signal of bound Enbrel, detected with an anti-human antibody is shown. All binding and washing steps were carried out in PBST (PBS containing 0.1% (v/v) Tween-20). (b) Surface plasmon resonance (SPR) was measured using a BIAcore 3000 instrument (BIAcore, Uppsala Sweden). Measurements were performed in HBST buffer (20 mM HEPES, 150 mM NaCl, pH 7.4, 0.1% Tween-20) at a flow rate of 50 µl/min. Enbrel was directly coupled to a dextran-chip (CM5, Biacore, 350 RU) and soluble TNFα (1 nM, 5 nM and 15 nM) alone and preincubated with DARPin T_25 (200 nM) injected for 4 minutes and the dissociation recorded for 20 minutes with buffer flow. The signal of an uncoated reference cell was subtracted from the sensograms.

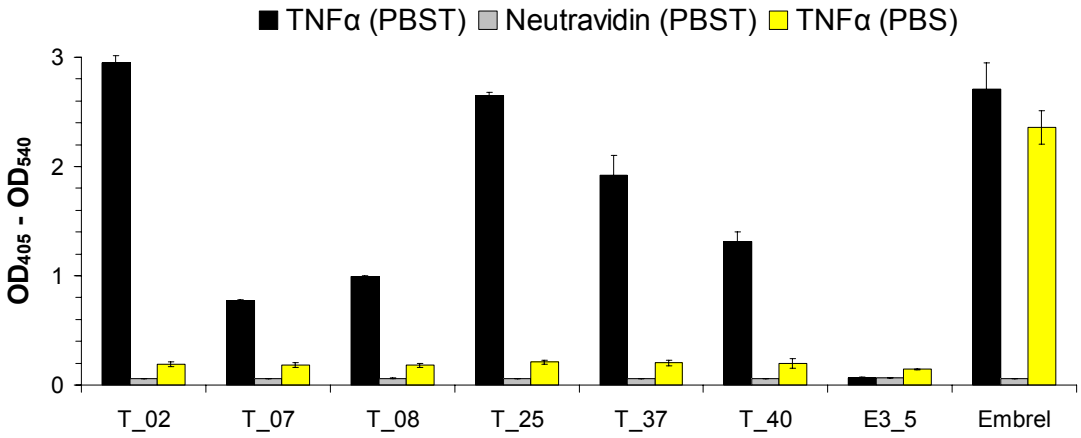

Figure 9: Buffer-dependent TNFα binding in ELISA. DARPins as described above and Enbrel were analyzed for binding to TNFα under different conditions. Ten nM solutions of the selected DARPins and Enbrel were tested for binding to neutravidin and TNFα immobilized via neutravidin (TNFα) in PBST (PBS containing 0.1% (v/v) Tween-20) or PBS alone. For each sample applied, the signal of bound DARPins, detected with an anti RGS-His antibody or the signal of bound Enbrel, detected with an anti-human antibody is shown. Identical results were obtained for buffers HBS and TBS (data not shown).

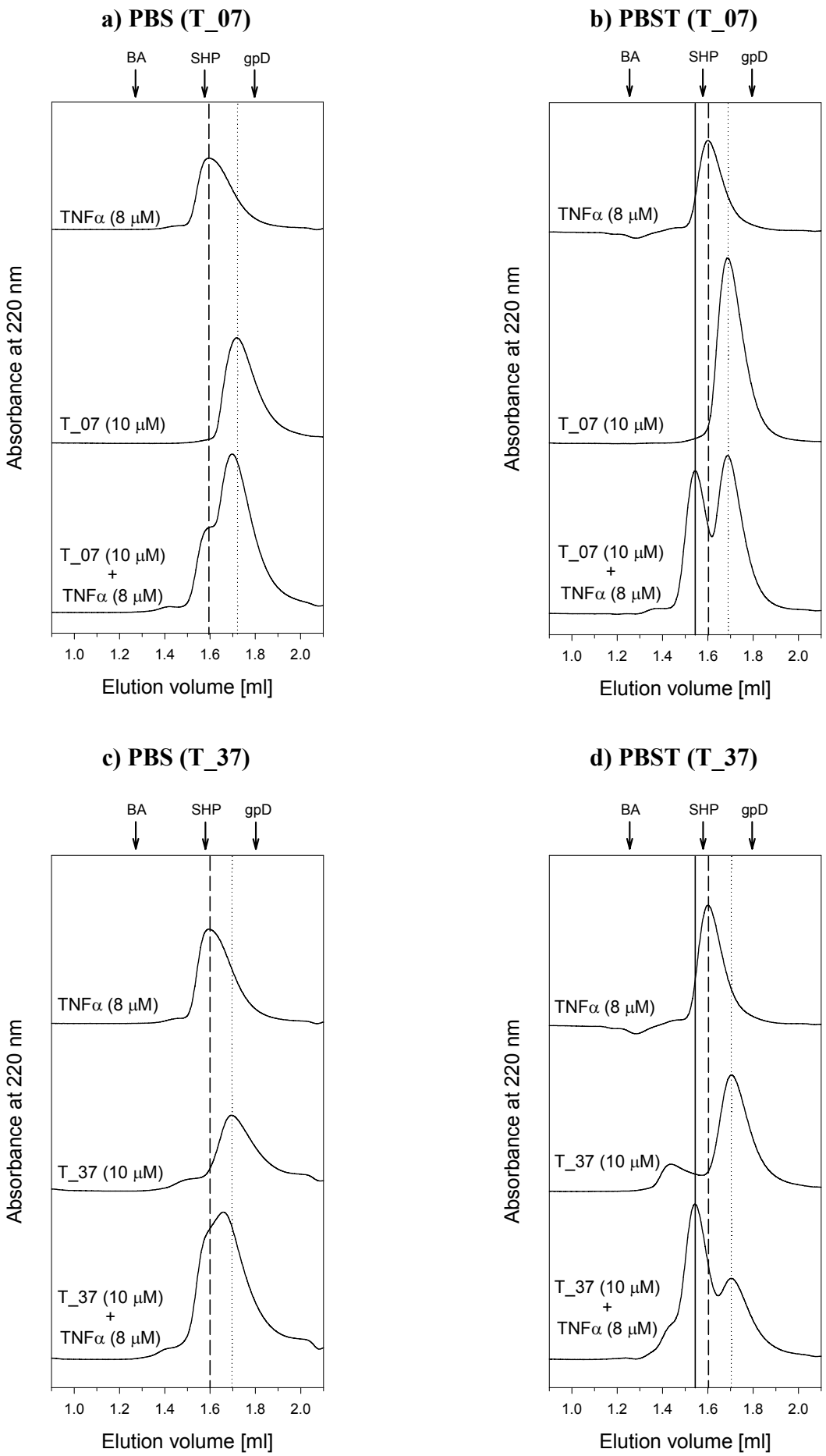
a) PBS (T_07)
b) PBST (T_07)
c) PBS (T_37)
d) PBST (T_37)
BA
SHP
gpD
TNFα (8 μM)
T_07 (10 μM)
T_37 (10 μM)
T_07 (10 μM) + TNFα (8 μM)
T_37 (10 μM) + TNFα (8 μM)
Absorbance at 220 nm
Elution volume [ml]
1.0
1.2
1.4
1.6
1.8
2.0

Figure 10

Figure 10: Tween-20 dependent binding of DARPins T_07 (**a, b**) and T_37 (**c, d**) to TNFα. The SEC elution chromatograms of TNFα (top), T_07 (middle) and both proteins coinjected (bottom) are shown using (**a, c**) PBS or (**b**, **d**) PBST (PBS containing 0.1% (v/v) Tween-20) as running buffer. TNFα was used at 8 µM and DARPins T_07 and T_37 at 10 µM concentrations. Elution volumes are indicated: T_07 and T_37 (dotted line), TNFα (dashed line) and TNFα-T_07 and TNFα-T_37 complexes (solid line). The molecular mass standards are described in **Figure 5** and indicated with arrows and concentrations for TNFα are given for the monomer.

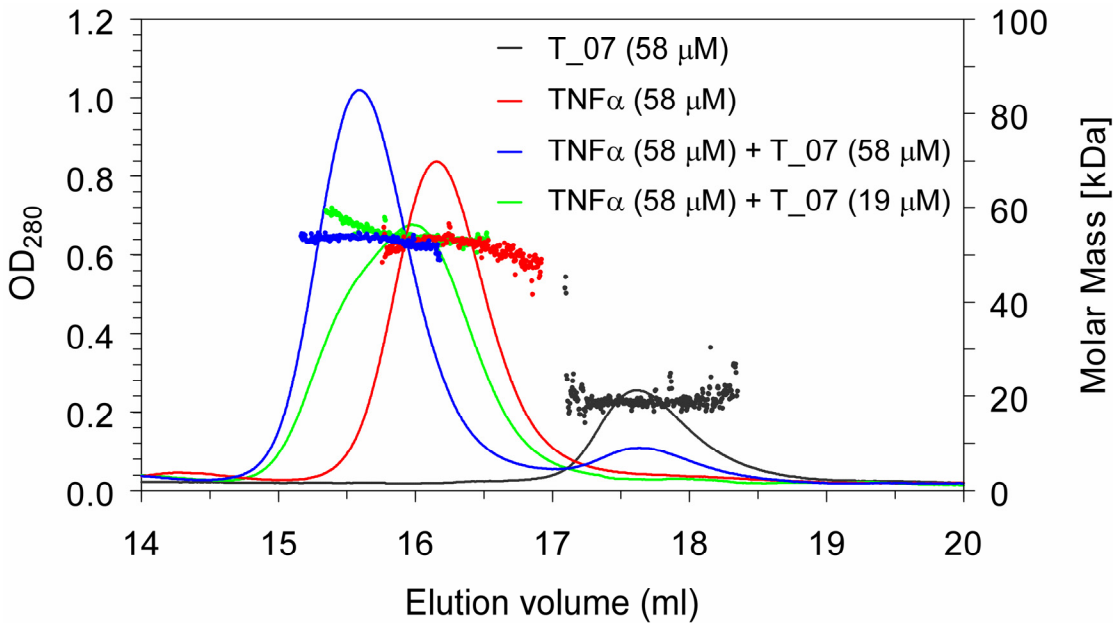

Figure 11: Characterization of the DARPin T_07 – TNFα complex formation by size-exclusion chromatography combined with multi-angle light scattering (SEC-MALS). The OD_{280} signals are depicted as solid lines (left y-axis) and the molar mass of the respective elution peak indicated with filled circles (right y-axis). TNFα alone (red line), T_02 alone (grey line), TNFα preincubated with an equimolar amount of DARPin (blue line) and TNFα preincubated with a threefold lower amount of DARPin (green line) were analyzed at the concentrations described in the figure. The weight-average molar mass over the respective elution peaks are: TNFα alone (52.8 kDa, red circles), T_02 alone (18.8 kDa, grey circles), TNFα preincubated with an equimolar amount of DARPin (53.5 kDa, blue circles) and TNFα preincubated with a threefold lower amount of DARPin (50 - 60 kDa, green circles). Protein samples were incubated in PBS containing 0.1% Tween-20 for at least 1 h at room temperature before injection and concentrations for TNFα are given for the monomer.

4. DARPins binding receptor tyrosine kinase ErbB1/EGFR

The ErbB receptor tyrosine kinase family comprises four members: ErbB1 (EGFR, Her1), ErbB2 (Her2), ErbB3 (Her3) and ErbB4 (Her4). They are all composed of an extracellular ligand binding region, a single membrane spanning region and a cytoplasmic tyrosine kinase domain. ErbB2 has no known ligand binding affinity and ErbB3 lacks tyrosine kinase activity[7]. The extracellular region of the ErbB receptors is composed of four domains (I-IV) which are quite heavily glycosylated (e.g. ErbB1 is glycosylated at eight positions[8]). Structural studies of these receptors have provided valuable insight into receptor activation by their ligands, leading to homo- and heterodimerization of the receptors[7]. In particular ErbB1 and ErbB2 have been implicated in the development of many human cancers and are therefore intensively pursued as therapeutic targets[9].

The target protein ErbB1 (ref. 10, 11) was kindly provided by Dr. Tim Adams (CSIRO, Melbourne, Australia) (L25 – S525 of human receptor tyrosine-protein kinase ErbB1 fused to huIgG1_Fc). This truncated version of the extracellular region of ErbB1 comprising domains I-III but not domain IV and is described in detail in ref. 12. The aim of this project was to select binders against ErbB1 which can inhibit activation of the receptor by its ligands in a similar fashion as the clinically used monoclonal antibodies (mAbs) Erbitux (Cetuximab)[13] or Panitumumab (ABX-EGF).

Primary selections, selection with epitope masking and screening of binders against ErbB1 are described in detail in **Chapter 3** of my thesis and resulted in nine different sequences (**Fig. 12**). Clones E_01, E_17, E_31 and E_36 are from primary selections and clones E_67, E_68, E_69, E_72 form the selection with epitope masking. After expression and purification by immobilized metal ion chromatography (IMAC) purification in the 96-well format, all binders were analyzed by size exclusion chromatography (SEC) and compared to the well characterized, non-binding DARPin E3_5 (ref. 2) (**Fig. 13**). To investigate the specificity of the selected DARPins, ELISA experiments were performed. Due to the low binding signal in all ELISA

experiments, clones E_17, E_31 and E_36 were considered as false positives (no affinity for the target protein or affinity below the detection limit of the experiments). As almost expected, none of the binders did show crossreactivity when analyzed in ELISA experiments for binding to other receptors of the ErbB-family (ErbB2 and ErbB4), which share about 50% sequence identity and have highly conserved structures (**Fig. 14a**). In the competition ELISA setup, either DARPins were preincubated with free ErbB1 or the immobilized receptor preincubated with its ligand epidermal growth factor (EGF) or the clinically used mAb Erbitux (**Fig. 15**). The clones E_01, E_64, E_67 and E_68 bind an epitope overlapping with Erbitux, whereas E_69 and E_72 recognize a non-overlapping epitope. Preincubation of the receptor with EGF did only partially reduce the binding signal of E_01, E_64, E_67 and E_68. This is a bit surprising, since Erbitux is known to compete with EGF for binding and, therefore, one would expect that these binders that share an overlapping epitope with Erbitux to compete with EGF for receptor binding. One possible explanation might be that ErbB1 partially loses its conformational flexibility upon immobilization and therefore can no longer adopt its extended conformation needed for high affinity ligand binding[11]. Therefore, the high affinity DARPins might displace the ligand from the receptor, resulting in the partial inhibition seen in **Figure 15**.

Furthermore, binding and epitope localization of the clones was analyzed by ELISA. All ErbB1 binders were tested for interaction with the respective immobilized target protein or the target protein bound to immobilized DARPin (E_01) which was used for “epitope-masking” during the selection (**Fig. 14b**). Of the clones selected by “epitope-masking” (E_67, E_68, E_69, E_72) only E_69 and E_72 recognize an epitope not competing with E_01, in good agreement with the results obtained for target binding in the presence of Erbitux (**Fig. 15**).

Four well behaved clones (E_01, E_67, E_68 and E_69) were further analyzed at multiple concentrations by surface plasmon resonance (SPR) (**Table 3** and **Supplementary Figure 2** of **Chapter 3**) and the data were evaluated with a global kinetic fit. Two of the binders showed affinities in the pM range and the other binders were in the low nM range.

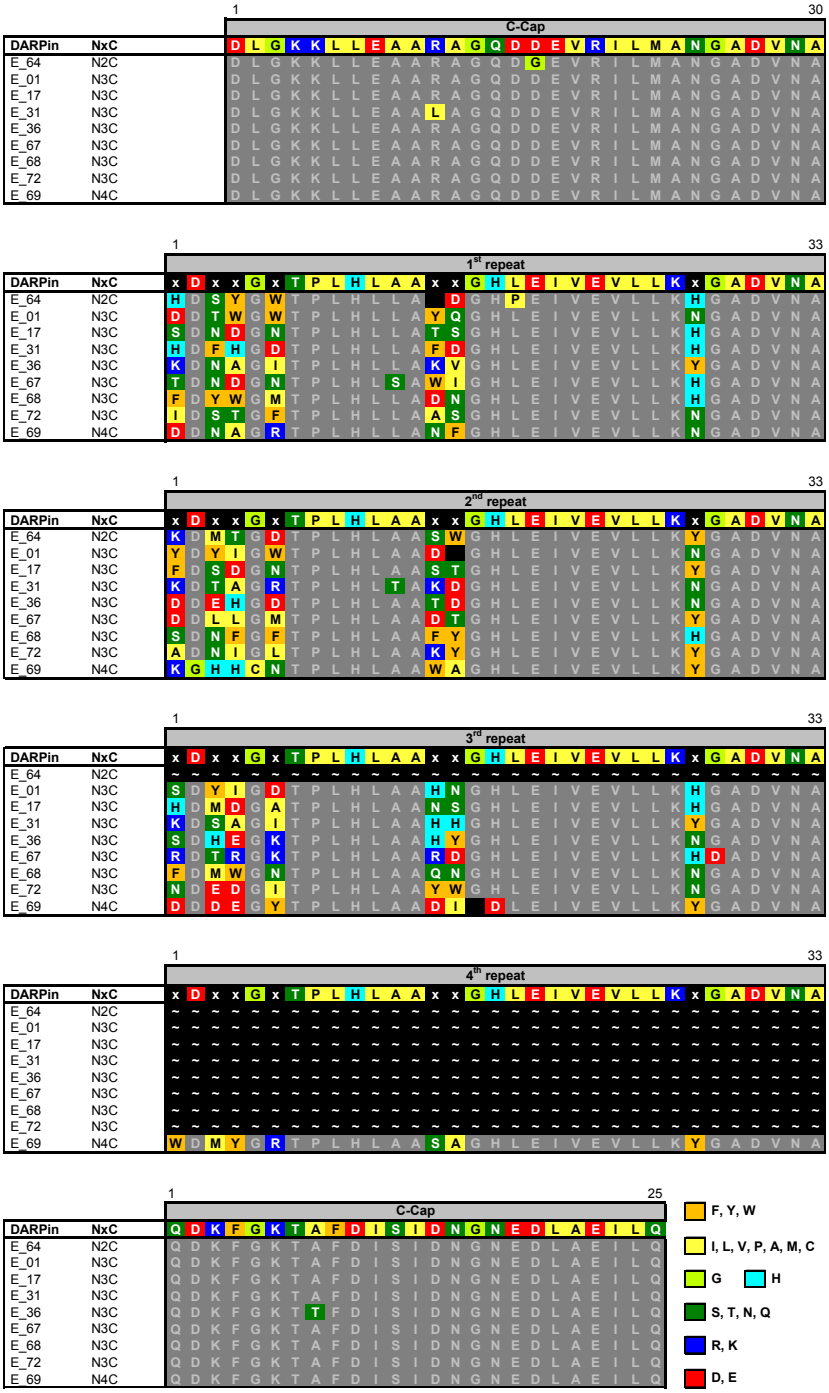

Figure 12: Sequences of selected ErbB1 binding DARPins. The original consensus sequence is shown on top with randomized positions indicated by x. In the lines below, only residues that differ from the consensus sequence are printed in color, residues identical to the consensus sequence are printed in gray and deletions and missing amino acids are printed in black. Note that the N-terminal MRGSHHHHHHGS and the C-terminal KLN, which are not part of the DARPin sequence, are not shown. Amino acids are colored by type as indicated at the end of the alignment.

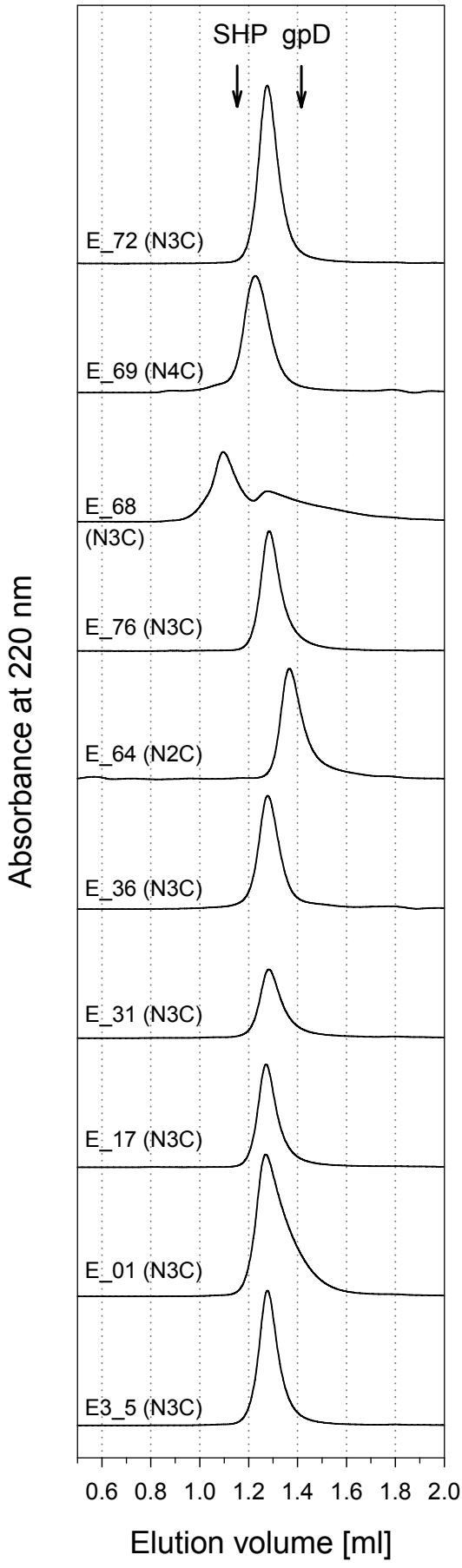

Figure 13: Size exclusion chromatography (SEC) of selected ErbB1-binding DARPins. The chromatograms of the nine ErbB1 binders and the unselected DARPin E3_5 are shown. For each DARPin the number of repeats stacked between N-Cap (N) and C-Cap (C) is given in parentheses. The molecular mass standards, phage protein D (gpD) with an apparent mass of 17.6 kDa and phage protein SHP, a trimer with an apparent mass of 50.2 kDa, are indicated with arrows.

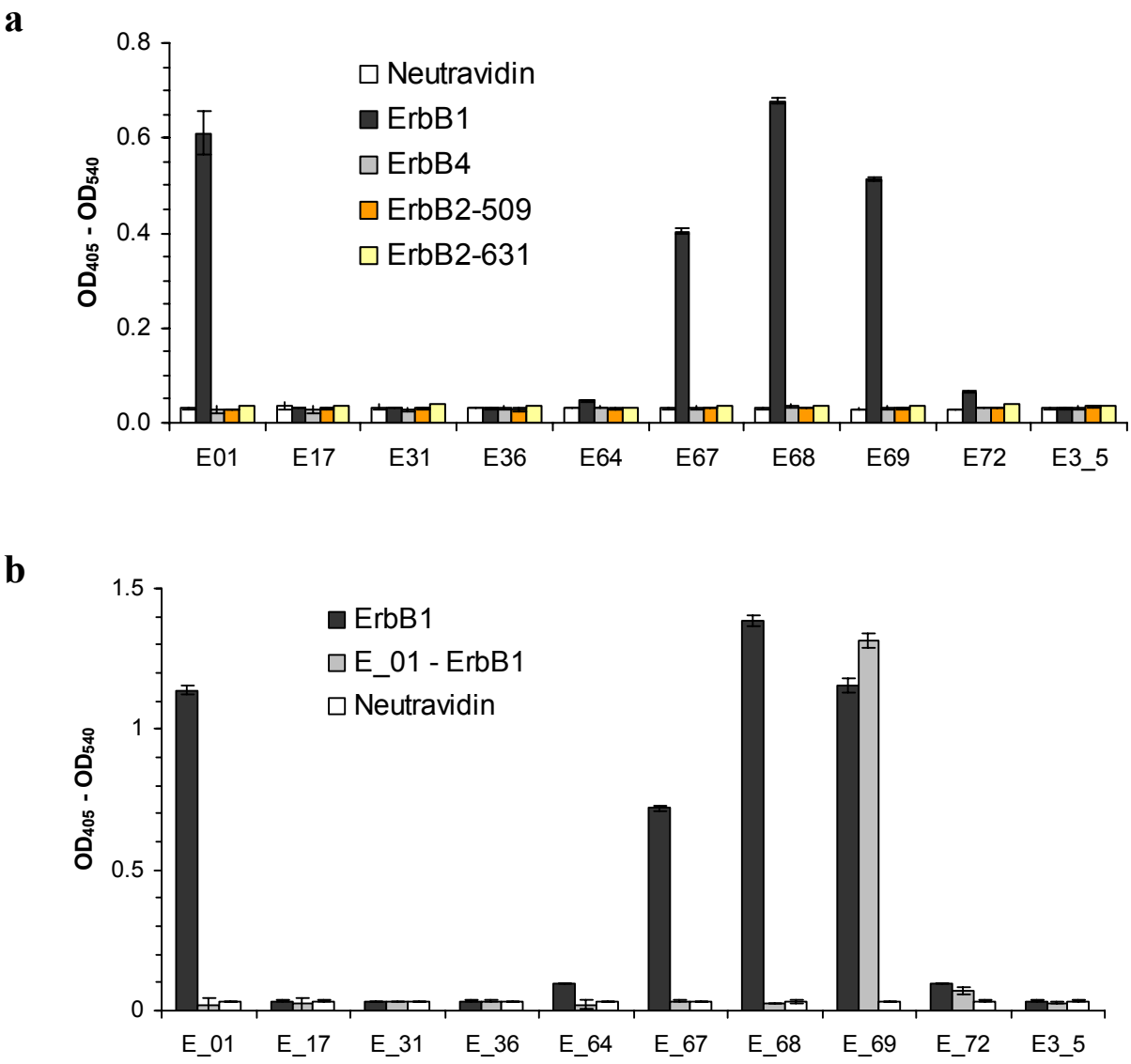

Figure 14: ELISA of selected ErbB1 binding DARPins. (**a**) Specificity was tested by applying 50 nM solutions of the selected ErbB1 binders on immobilized ErbB-receptors (ErbB1, ErbB2-631, ErbB2-509 and ErbB4). (**b**) To determine the epitope the binders were further tested for binding to immobilized target protein (ErbB1), target protein bound via immobilized DARPin used for epitope-masking during the selection round (E_01—ErbB1) and neutravidin. DARPin E3_5 was used as control in all experiments.

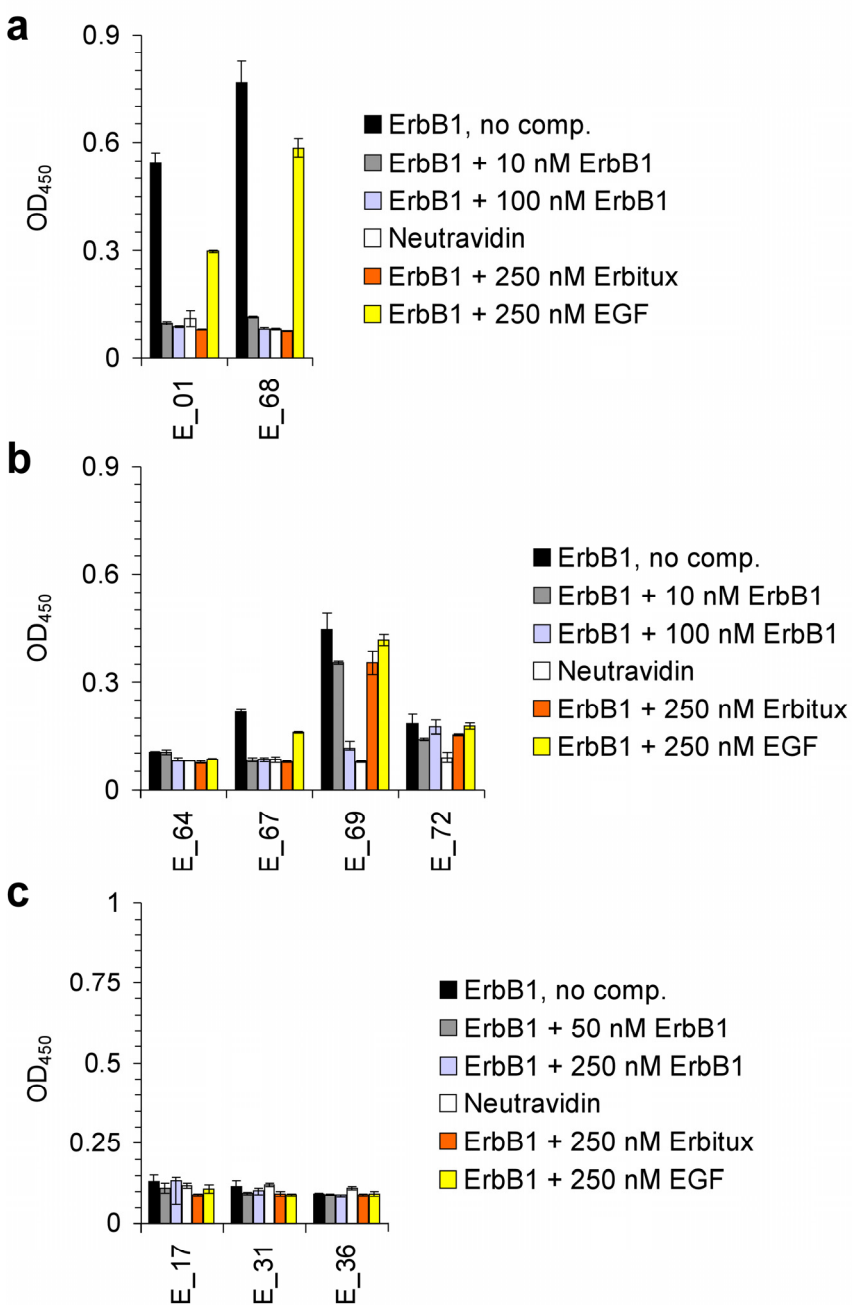

Figure 15: Specificity and affinity estimation of selected ErbB1 binders. (**a**) ELISA with high affinity ErbB1 binders. To analyze specificity, 1 nM solutions of the binders E_01 and E_68 were tested for binding on neutravidin and ErbB1 and, in parallel, competition experiments were performed by preincubation of 1 nM solutions of the DARPins with free ErbB1 (10 nM and 100 nM) before binding on immobilized ErbB1. (**b**) ELISA with medium affinity ErbB1 binders. To analyze specificity, 5 nM solutions of the binders E_64, E_67, E_69 and E_72 were tested as described above using 10 nM and 100 nM free ErbB1 for competition. (**c**) ELISA with low affinity ErbB1 binders. To analyze specificity, 25 nM solutions of the binders E_17, E_31and E_36 were tested as described above using 50 nM and 250 nM free ErbB1 for competition. The first word in the legend denotes the protein immobilized, *no comp.* denotes the absence of a competitor and + *ErbB1*, + *Erbitux* or + *EGF* denotes the presence of competitor (respective concentrations are given in nM).

5. DARPins binding receptor tyrosine kinase ErbB2/Her2

A general introduction to the ErbB receptor tyrosine kinase family is given in the ErbB1 subchapter four of Appendix one. Two different constructs of the target protein ErbB2 (ref. 7) were kindly provided by Dr. Tim Adams (CSIRO, Melbourne, Australia): ErbB2-631, the complete extracellular region of the human receptor (S22 – T652 of human receptor tyrosine-protein kinase ErbB2) containing domains I – IV and ErbB2-509, the truncated version (S22 – N530 of human receptor tyrosine-protein kinase ErbB2) comprising only domains I-III (see ref. 14 and ref. 15, respectively). The aim of this project was to select binders against ErbB2 which can either inhibit activity of the receptor in a similar fashion as the clinically used mAb Trastuzumab (Herceptin^{TM})[14] or that can block ErbB2 homo- or heterodimerization as described for the clinically used mAb Pertuzumab (Omnitarg^{TM} or 2C4)[16].

In previous selections using ribosome display high affinity DARPin binders have been generated against ErbB2 (ref. 17, 18). Surprisingly, these binders almost exclusively recognize domain IV of the receptor (data not shown), which seems to provide a dominant epitopes during the selection processes. To obtain binders that recognize domain I – III of the receptor I followed two selections strategies which are described in detail in **Chapter 3** of my thesis. Screening of the ErbB2 binding DARPins was done together with Christian Jost (C.J.) and is described in his Diploma thesis. Selection on ErbB2-509, lacking domain IV, resulted in 13 different sequences (**Fig. 16**, names starting with 9_). Selection on ErbB2-631 in the presence of a two-fold excess of the high affinity DARPin H10-2-G3 (ref. 18) (masking one of the dominant epitopes on domain IV) resulted in nine different sequences of which four were already found in the selection on ErbB2-509 (**Fig. 16**, names starting with H_). After expression and purification by immobilized metal ion chromatography (IMAC) purification in the 96-well format, all binders were analyzed by size exclusion chromatography (SEC) and compared to the well characterized, non-binding DARPin E3_5 (ref. 2) and ErbB2 binding DARPin H10-2-G3 (**Fig. 17**). To investigate the specificity of the selected DARPins, ELISA experiments were performed. As almost expected,

none of the binders showed crossreactivity when analyzed in ELISA experiments for binding to other receptors of the ErbB-family (ErbB1 and ErbB4), which share about 50% sequence identity and have highly conserved structures (**Fig. 18**). Comparing the binding of the clones to ErbB2-631 and ErbB2-509 revealed that only one of the selected DARPins (H_14) recognizes domain IV of the receptor, showing the success of the selection strategy used. Detailed analysis of DARPin H_14 was done by C.J. and is described in his Diploma thesis; H_14 has an affinity of about 0.2 nM (SPR measurement), competes in an ELISA experiment with H10-2-G3 for binding and can completely block interaction of Herceptin with the receptor (shown in an SPR experiment). In cell based assays, this clone was the only one showing significant anti-proliferative activity.

Furthermore, a subset of the ErbB2-509 binding DARPins was analyzed in the competition ELISA setup. Binding to the immobilized target protein was tested with and without preincubation with free ErbB2-509 (**Fig. 19**). Three well behaved ErbB2-509 binding DARPins (9_16, 9_26 and 9_29) and were further analyzed at multiple concentrations by surface plasmon resonance (SPR) (**Table 3** and **Supplementary Figure 2** of **Chapter 3**) and the data evaluated with a global kinetic fit. All of the measured binders showed affinities in the low nM range. None of the ErbB2-509 binders shows complete competition with Pertuzumab for binding to the receptor and also none of them shows anti-proliferative activity in cell based assays (experiments done by C.J., which are described in his Diploma thesis).

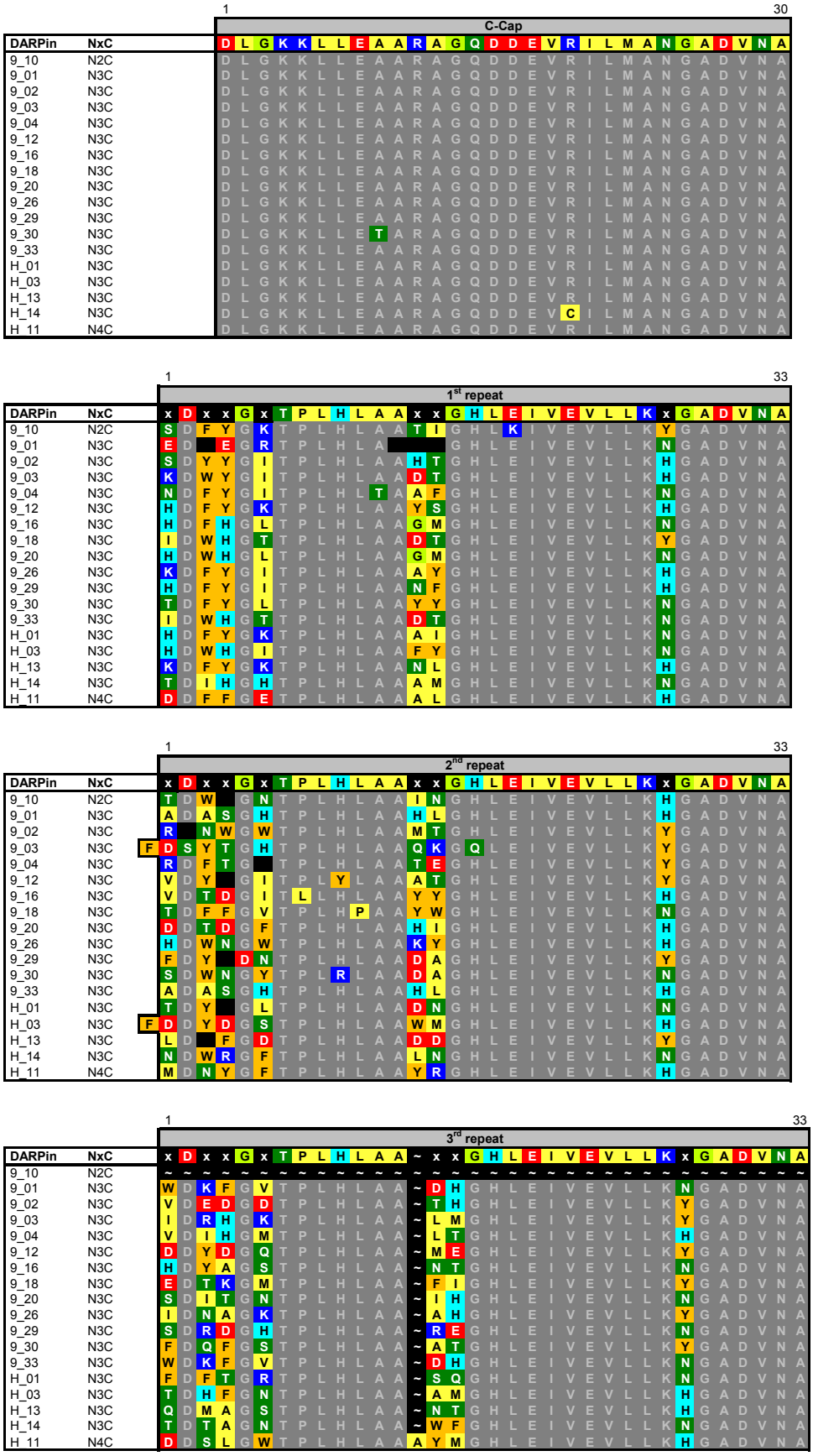

Figure 16: Continued next page.

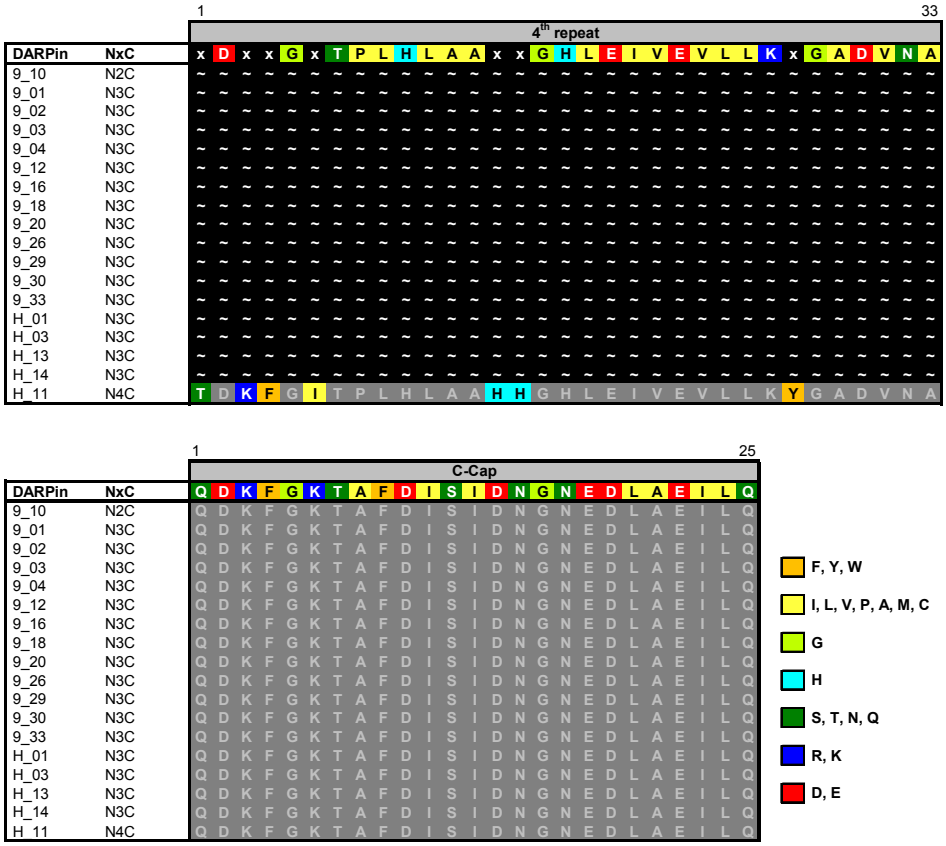

Figure 16: Sequences of selected ErbB2 binding DARPins. The original consensus sequence is shown on top with randomized positions indicated by x. In the lines below, only residues that differ from the consensus sequence are printed in color, residues identical to the consensus sequence are printed in gray and deletions and missing amino acids are printed in black. Note that the N-terminal MRGSHHHHHHGS and the C-terminal KLN, which are not part of the DARPin sequence, are not shown. Amino acids are colored by type as indicated at the end of the alignment.

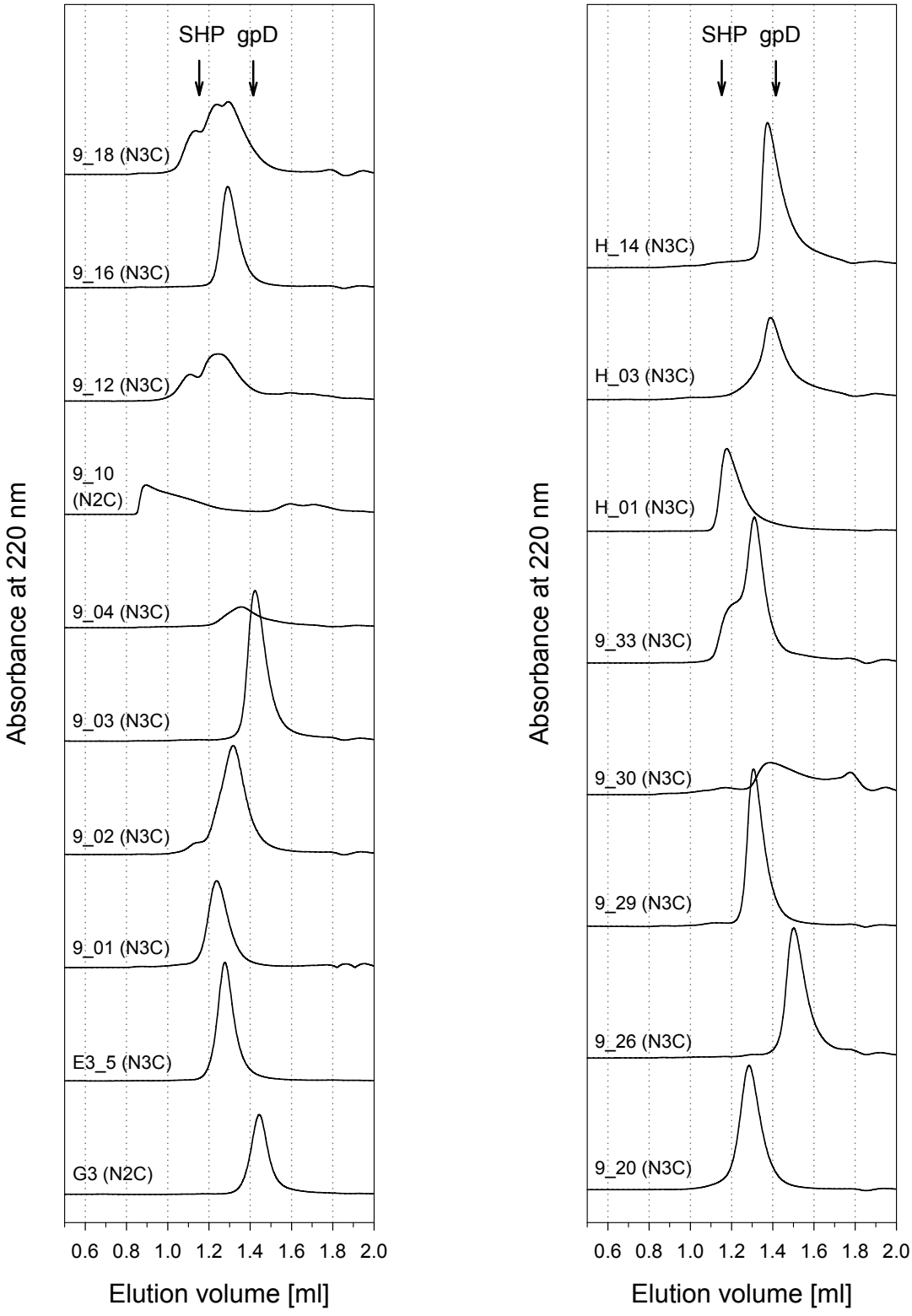

Figure 17: Size exclusion chromatography (SEC) of selected ErbB2 binding DARPins. The chromatograms of the 16 ErbB2 binders, the previously selected ErbB2 binding DARPin H10-2-G3 and unselected DARPin E3_5 are shown. For each DARPin the number of repeats stacked between N-Cap (N) and C-Cap (C) is given in parentheses. The molecular mass standards, phage protein D (gpD) with an apparent mass of 17.6 kDa and phage protein SHP, a trimer with an apparent mass of 50.2 kDa, are indicated with arrows.

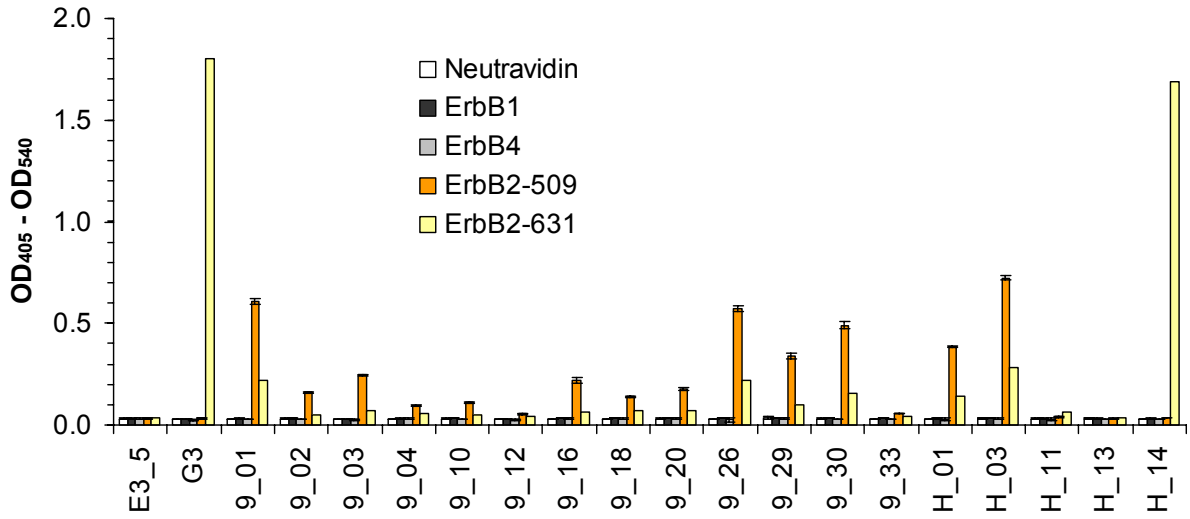

Figure 18: ELISA of selected ErbB2 binding DARPins. Specificity was tested by applying 50 nM solutions of the selected ErbB2 binders on immobilized ErbB-receptors (ErbB1, ErbB2-631, ErbB2-509 and ErbB4). DARPin E3_5 was used as control.

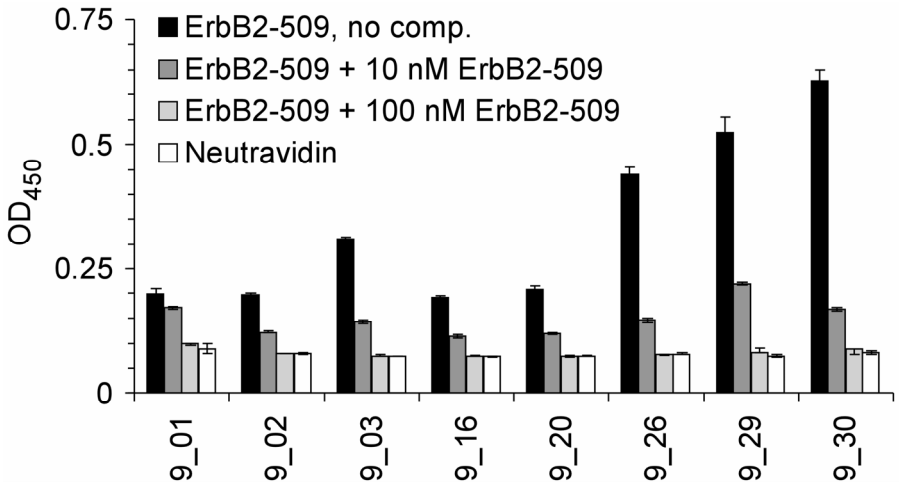

Figure 19: Specificity and affinity estimation of subset of selected ErbB2_509 binders. To analyze specificity, 5 nM solutions of the binders were tested for binding on neutravidin and ErbB2_509 (509) and, in parallel, competition experiments were performed by preincubation of 5 nM solutions of the DARPins with 10 nM or 100 nM of free ErbB2_509 (10 nM and 100 nM) before binding on immobilized ErbB2_509. The first word in the legend denotes the protein immobilized, *no comp.* denotes the absence of a competitor and + *ErbB2-509* denotes the presence of competitor in 10 nM or 100 nM concentrations.

6. DARPins binding receptor tyrosine kinase ErbB4

A general introduction to the ErbB receptor tyrosine kinase family is given in the ErbB1 subchapter four of Appendix one. The target protein ErbB4 (ref. 19) was kindly provided by Dr. Tim Adams (CSIRO, Melbourne, Australia) (Q26 – R525 of human receptor tyrosine-protein kinase ErbB4 fused to huIgG1_Fc). This truncated version of the extracellular region of ErbB4 comprises domains I-III but not domain IV. The aim of this project was to validate the phage DARPin library by selecting binders against ErbB4. Such binders could inhibit activation of the receptor by its ligands or prevent homo- and heterodimerization of the receptor. Since ErbB4 has no clinical relevance as yet, binders were not further investigated in any collaboration.

Primary selections, selections by epitope masking and screening of binders against ErbB4 are described in detail in **Chapter 3** of my thesis and resulted in 19 different sequences (**Fig. 20**). Clones B4_01 to B4_45 are from primary selections and clones B4_49 to B4_68 form the selection with epitope masking. After expression and purification by immobilized metal ion chromatography (IMAC) purification in the 96-well format, all binders were analyzed by size exclusion chromatography (SEC) and compared to the well characterized, non-binding DARPin E3_5 (ref. 2) (**Fig. 21**). To investigate the specificity of the selected DARPins, ELISA experiments were performed. As almost expected, none of the binders did show crossreactivity when analyzed in ELISA experiments for binding to other receptors of the ErbB-family (ErbB1 and ErbB2), which share about 50% sequence identity and have highly conserved structures (**Fig. 22a**). Further the ErbB4 binding DARPins were analyzed in the competition ELISA setup. Binding to the immobilized target protein was tested with and without preincubation with free ErbB4 (**Fig. 23**). Due to the low binding signal in this ELISA experiment, clones B4_11, B4_14, B4_55, B4_56, B4_63, B4_64, B4_65 and B4_68 were considered as false positives (no affinity for the target protein or affinity below the detection limit of the experiments).

Furthermore, binding and epitope localization was tested by ELISA. All ErbB4 binders were tested for interaction with the respective immobilized target protein or the target protein bound to immobilized DARPin (B4_02) which was used for “epitope-masking” during the selection (**Fig. 22b**). One of the clones (B4_01) selected in the primary selections and four of the clones selected by “epitope-masking” (B4_, B4_50, B4_57, B4_58 and B4_60) recognized another epitope than B4_02.

Four well behaved clones (B4_01, B4_02, B4_50 and B4_58) were further analyzed at multiple concentrations by surface plasmon resonance (SPR) (**Table 3** and **Supplementary Figure 2** of **Chapter 3**) and the data evaluated with a global kinetic fit. Three of the measured binders showed affinities in the pM range and the other binder is in the low nM range.

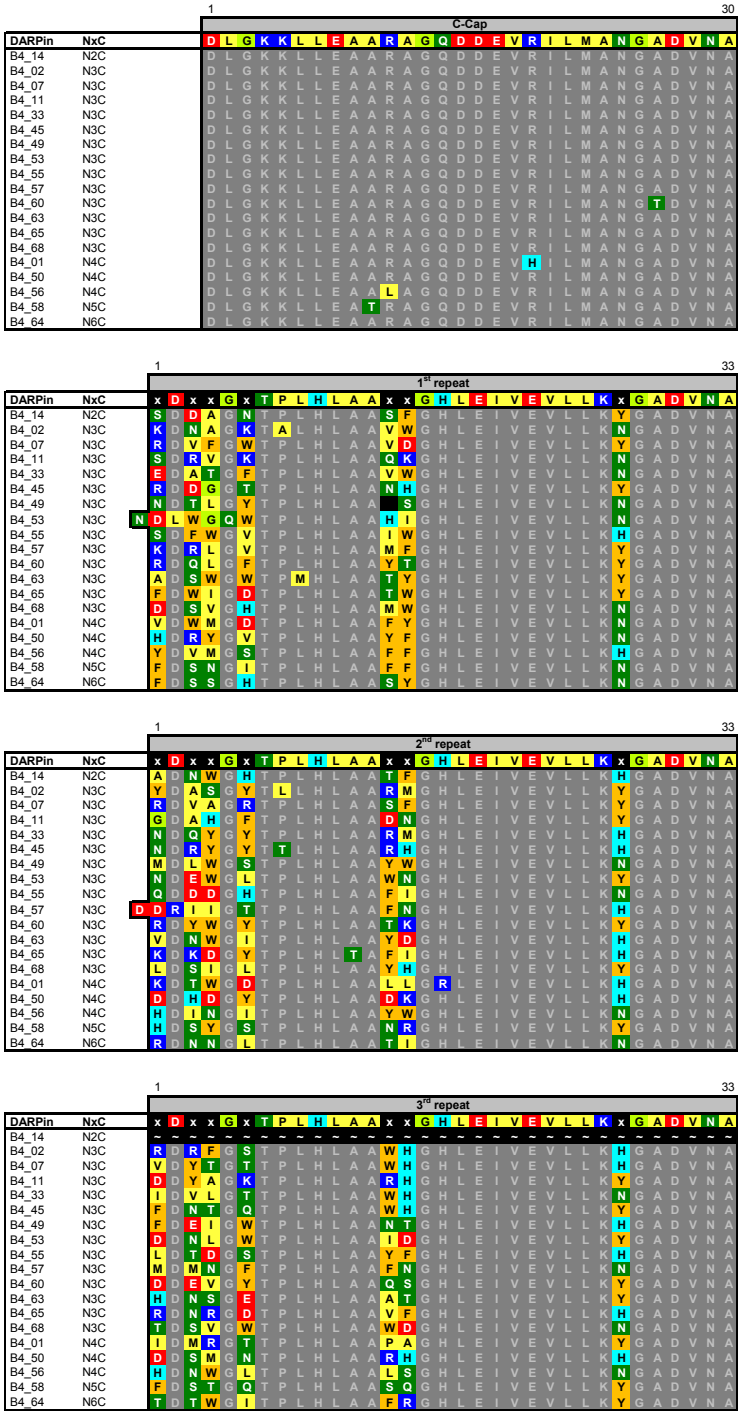

Figure 20: Continued next page.

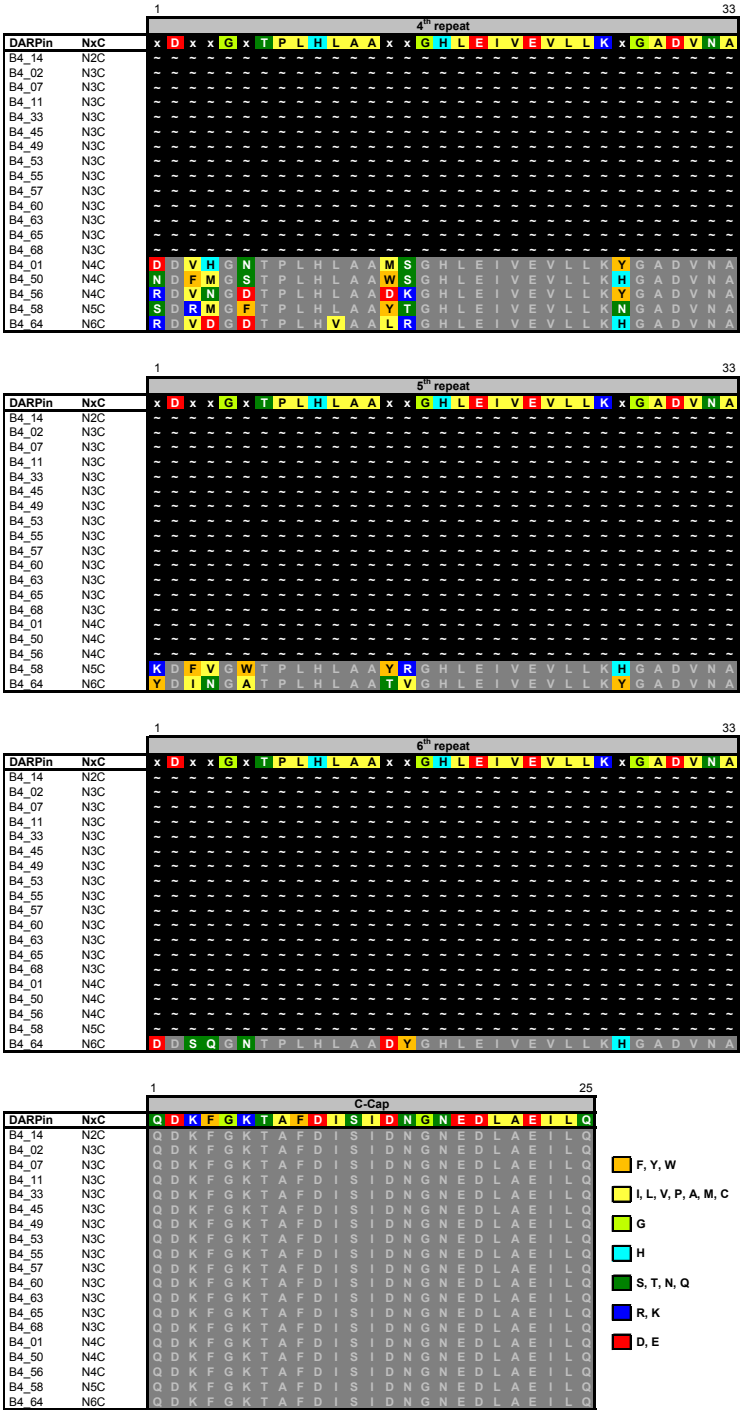

Figure 20: Sequences of selected ErbB4 binding DARPins. The original consensus sequence is shown on top with randomized positions indicated by x. In the lines below, only residues that differ from the consensus sequence are printed in color, residues identical to the consensus sequence are printed in gray and deletions and missing amino acids are printed in black. Note that the N-terminal MRGSHHHHHHGS and the C-terminal KLN, which are not part of the DARPin sequence, are not shown. Amino acids are colored by type as indicated at the end of the alignment.

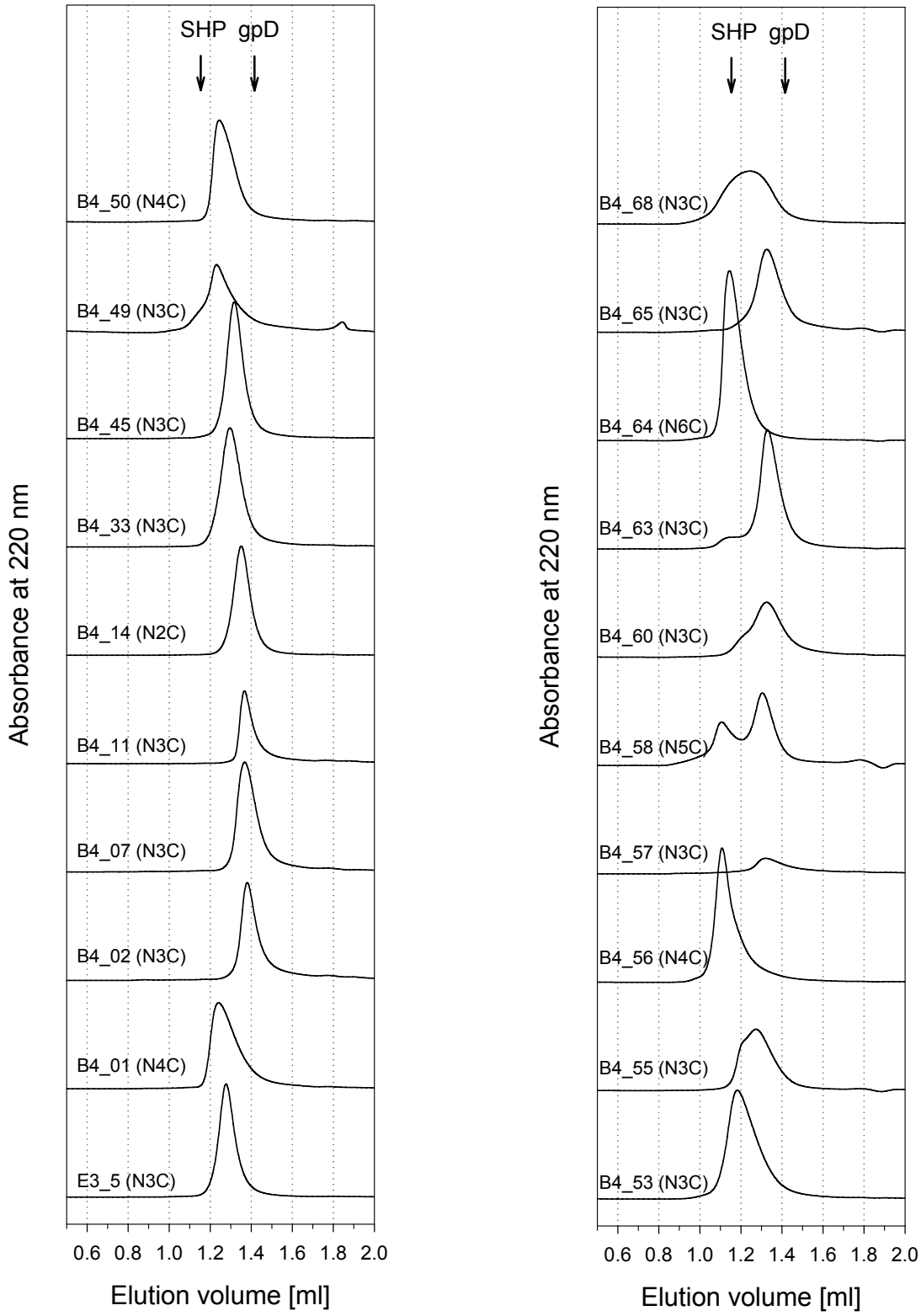

Figure 21: Size exclusion chromatography (SEC) of selected ErbB4 binding DARPins. The chromatograms of the 19 ErbB4 binders and the unselected DARPin E3_5 are shown. For each DARPin the number of repeats stacked between N-Cap (N) and C-Cap (C) is given in parentheses. The molecular mass standards, phage protein D (gpD) with an apparent mass of 17.6 kDa and phage protein SHP, a trimer with an apparent mass of 50.2 kDa, are indicated with arrows.

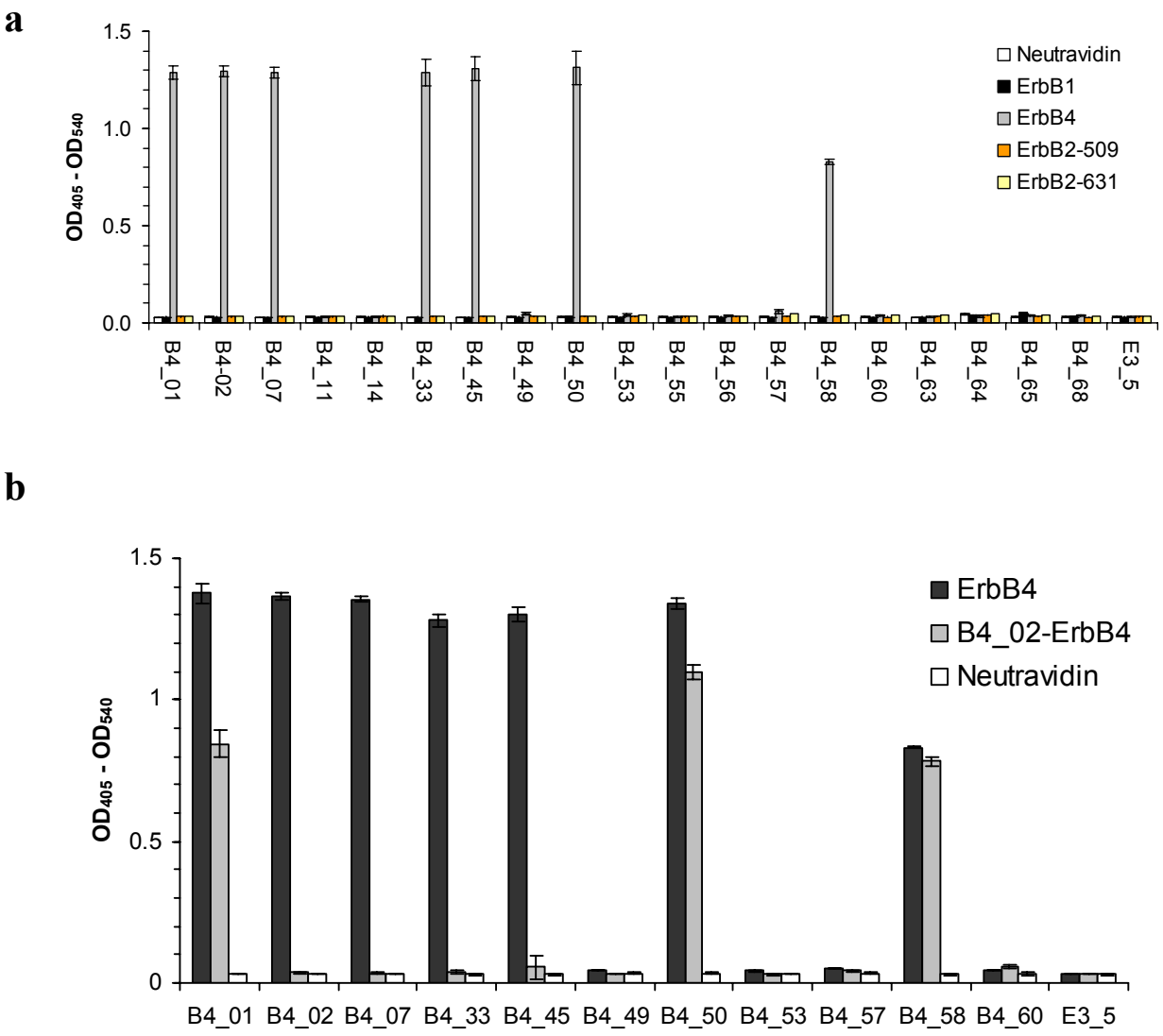

Figure 22: ELISA of selected ErbB4 binding DARPins. (**a**) Specificity was tested by applying 50 nM solutions of the selected ErbB4 binders on immobilized ErbB-receptors (ErbB1, ErbB2-631, ErbB2-509 and ErbB4). (**b**) To determine the epitope the binders giving a signal in (**a**) were further tested for binding to immobilized target protein (ErbB4), target protein bound to immobilized DARPin used for epitope-masking during the selection round (B4_02—ErbB4) and neutravidin. DARPin E3_5 was used as control in all experiments.

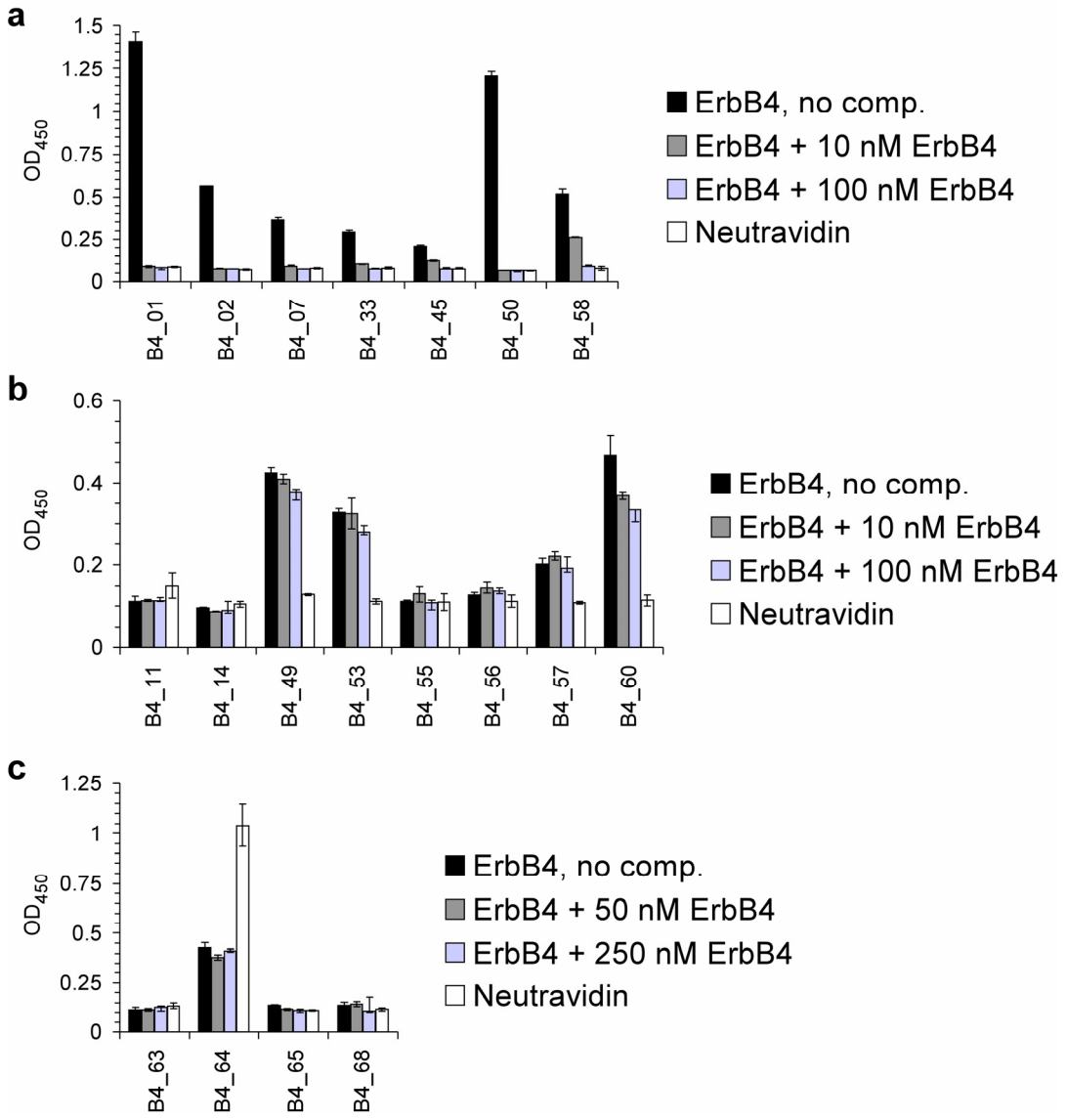

Figure 23: Specificity and affinity estimation of selected ErbB4 binders. (**a**) ELISA with high affinity ErbB4 binders. To analyze specificity, 1 nM solutions of the binders B4_01, B4_02, B4_07, B4_33, B4_45, B4_50 and B4_58 were tested for binding on neutravidin and ErbB4 and, in parallel, competition experiments were performed by preincubation of 1 nM solutions of the DARPins with free ErbB4 (10 nM and 100 nM) before binding on immobilized ErbB4. (**b**) ELISA with medium affinity ErbB4 binders. To analyze specificity, 5 nM solutions of the binders B4_11, B4_14, B4_49, B4_53, B4_55, B4_56, B4_57 and B4_60 were tested as described above using 10 nM and 100 nM of free ErbB4 for competition. (**c**) ELISA with low affinity ErbB4 binders. To analyze specificity, 25 nM solutions of the binders B4_63, B4_64, B4_65 and B4_68 were tested as described above using 50 nM and 250 nM of free ErbB4 for competition. The first word in the legend denotes the protein immobilized, *no comp.* denotes the absence of a competitor and + *ErbB4* denotes the presence of competitor in 10 nM, 50 nM, 100 nM or 250 nM concentrations.

7. Amino acid sequence and SEC analysis of selected and unselected DARPins

7.1 Amino acid sequence analysis

In this subchapter, an analysis of the amino acid sequences of selected and unselected DARPins of the phage DARPin library is described. DNA sequencing of 55 randomly picked clones of the naive library showed that about half of the clones (29) had either a frameshift in the DARPin sequence or contained no insert at all (non functional part of the library). Of the 26 clones with correct DARPin sequences 18 (69%) encode for N3C, 7 (27%) for N2C and 1 (4%) for N1C DARPin library members, all encoding different amino acids at randomized positions (**Fig. 24a**). The presence of library members containing less than three internal repeats (N1C and N2C) can be attributed to the stepwise library building or the repetitive nature of the DARPins, leading to an *in vitro* recombination during PCR amplification. DNA sequencing of selected clones resulted in 84 different sequences of which 72 (86%) encode for N3C, 6 (7%) for N2C, 4 (5%) for N4C, 1 (1%) for N5C and 1 (1%) for N6C DARPin library members, all encoding different amino acids at randomized positions (**Fig. 24b**). Only one of the clones giving specific binding signals encoded a non-functional member of the naive library (I_03, part of the third internal repeat is not consensus, **Fig. 1**). Comparing the size distribution of DARPins before and after selections reveals a clear shift to members with an increased number of internal repeat modules.

The reduced proportion of N1C and N2C DARPins after selections might be of experimental origin. Prior to the screening of single clones, the pools of selected DARPins had to be subcloned from the phagemid into the expression vector. During this process, which involves gel-purification of the inserts, minor populations of binders with a smaller size might have been reduced. DARPins containing more than three internal repeat modules are probably already present in the initial library but to a very low extent, since no repeat duplication indicating *in*

vivo recombination during amplification in *E. coli* was observed. Such clones are selected most probably due to their favorable binding properties in preference. A larger contiguous patch of randomized residues in the DARPins with more than three randomized repeats may allow binding to additional epitopes, where contacting by residues in the capping repeats might not have been favorable or where a larger binding surface is needed. An accumulation of these longer constructs during after selections with epitope masking supports this theory.

Furthermore, all sequences were analyzed for framework mutations, including point mutations of conserved framework residues and insertions or deletion at any sequence position. From this preliminary analysis of the first five selections described in my thesis, the number of clones containing one ore more framework mutations almost double from 41% for naive library members to 78% for selected DARPins (**Fig. 24**). Even more interesting is the distribution of the framework mutations over the sequence of the DARPin molecules (**Fig. 25**). To allow an overall analysis of DARPins varying in size form N2C to N6C, internal repeat modules were classified into three groups: first repeat (adjacent to N-Cap), middle repeat (no interface with N-Cap or C-Cap) and last repeat (adjacent to C-Cap). Members of the naive library show a more or less random distribution of such framework mutations over the whole sequence (**Fig. 25a**). In stark contrast, selected binders show a strong gradual decrease in framework mutations from the N- to the C-Cap (**Fig. 25b**). There are two potential explanations why binders with higher numbers of framework mutations and biased distribution of framework mutations were selected in preference. The first possible explanation is based on the selection system. Clones containing an increased number of framework mutations, especially in the more stable N-terminal part, might have lower stability and are therefore displayed at higher level on filamentous phage particles and are subsequently selected in preference. The high display level of one of the most stable DARPins E3_5 (ref. 2) by using SRP phage display[20] speaks against this hypothesis. However, I observed a slightly higher display level for selected DARPins having one or more framework mutations, compared to the display level of DARPins from the naive library having no

framework mutations (**Fig. 26**), supporting this hypothesis. The second possible explanation is based on the shape of the binding surface of the DARPins. Here, framework mutations would introduce flexibility into the rigid DARPin scaffold and thereby allow an adaptation of the binding surface, needed for the interaction with certain epitopes[18]. The biased distribution of framework mutations could be explained by the lower intrinsic stability of the C-Cap, already providing the flexibility needed for binding but at the same time also reducing the tolerance of destabilizing framework mutations in itself and in its close proximity.

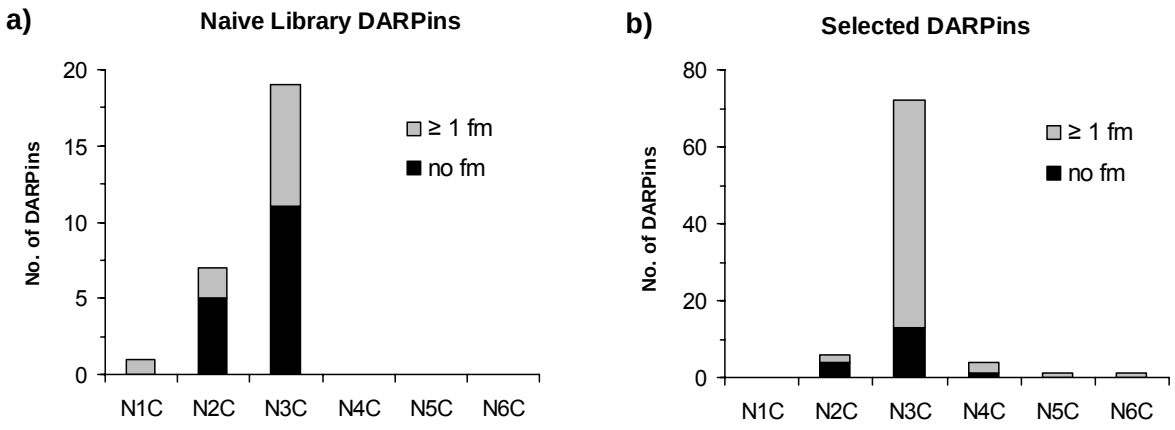

Figure 24: Size distribution and fraction of clones containing framework mutations: (a) naive library DARPins (unselected) and (b) selected DARPins. Depicted are the number of clones (y-axis) as a function of the DARPin size (x-axis; number of repeats stacked between N-Cap (N) and C-Cap (C)). The fraction of clones without framework mutation (no fm) are indicated in black and the fraction of clones having one or more framework mutations (≥ 1 fm) are indicated in gray. Point mutations of conserved framework residues and insertions or deletions at any sequence position were counted as framework mutations.

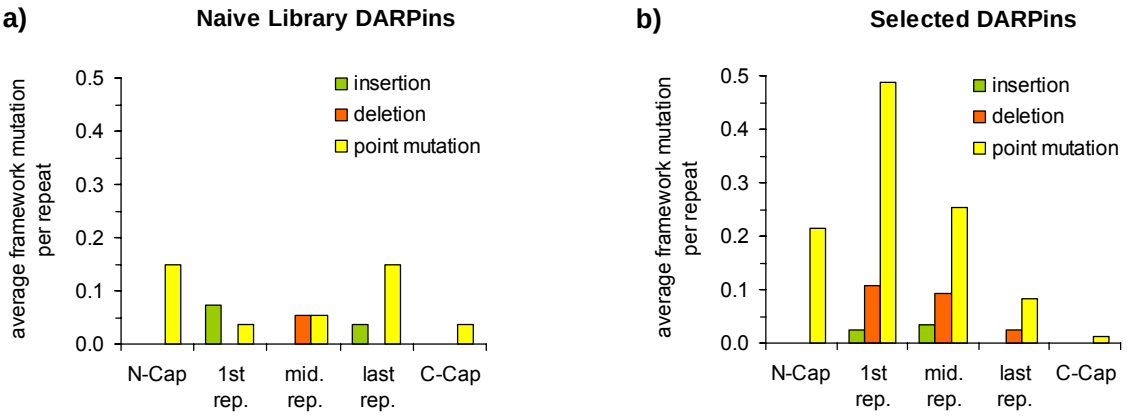

Figure 25: Distribution of the framework mutations over the DARPin sequences: (a) naive library DARPins and (b) selected DARPins. Depicted is the average of framework mutations (point mutations of conserved framework residues and insertions or deletions at any sequence position) found per repeat (y-axis). Different repeats are grouped into N-terminal capping repeat (N-Cap), fist repeat (1st. rep., adjacent to N-Cap), middle repeat (mid. rep., no interface with N-Cap or C-Cap), last repeat (last rep., adjacent to C-Cap) and C-terminal capping repeat (C-Cap).

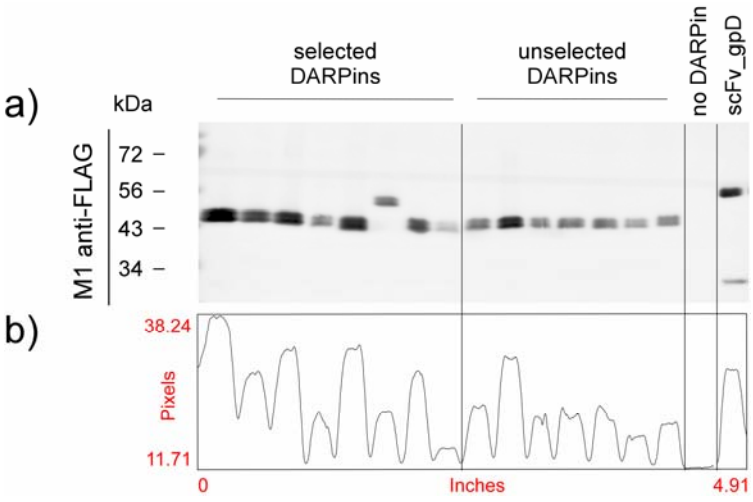

Figure 26: Display analysis of selected and unselected library members. (a) Phage particles produced in parallel by the use of the phagemid pPDV1 (encoding selected DARPins with framework mutations, unselected DARPins without framework mutations, no DARPin) or the phagemid pDST24 (encoding the PhoAss and the scFv_gpD[20]) purified by PEG/NaCl precipitation and normalized by UV absorbance to the same number of phage particles were separated by SDS-PAGE, blotted onto PVDF membranes and detected with an antibody specific for the FLAG-tag (M1 anti-FLAG) located at the N-terminus of the POI. The molecular weights of marker proteins are indicated in kDa at the left side of the blot. (b) Signal intensities were analyzed using Scion Image software (Scion Corporation, Release Alpha 4.0.3.2.). It should be noted that phage particles were not purified by CsCl gradient centrifugation and the error in the measured phage concentrations will be at least ±20%.

7.2 SEC analysis

SEC analysis was performed with all 84 DARPin binders obtained from the selections on the different target proteins (elution chromatograms are shown in each respective subchapter). Clones were divided into three groups based on their elution chromatogram (characteristic examples of each group are shown in **Figure 27**); 60 (71%) eluted in a single peak (potentially monomeric), 14 (17%) in multiple peaks (probably mixtures of monomeric and multimeric species) and 10 (12%) in ”atypical“ elution chromatograms (no defined peaks or peak in the void volume) (**Fig. 28a**).

Clones eluting in a single peak were further grouped, based on the shape of the elution peak (**Fig. 28b**). The shape of the elution peak of DARPin E3_5 was taken as reference for a symmetric peak and peak asymmetry judged by eye. Of the 60 clones giving a single peak, 35 (58%) eluted as a symmetric peak, 5 (8%) with a shoulder in front of these peaks and 20 (33%) with tailing (**Fig. 28b**). A shoulder in front of the elution peak probably indicates a small percentage of multimeric species and a tailing of the peak (front of peak steeper than rear) probably indicates interaction of the protein with the column material.

Furthermore, single peaks were grouped according to their apparent molecular weight (MW_{app}) derived from the elution volume of the peak maximum. DARPin E3_5 eluted at a factor 1.48 higher than the calculated molecular weight (MW_{calc}) as derived from the molecular weight standard on the column, slightly above the factor published[2]. Based on results from SEC multi-angle light scattering (SEC-MALS) measurements (see below), this factor ±25% was used to define a range in which the eluted DARPins are expected to be monomeric ($1.11 \times MW_{calc} \leq MW_{app} \leq 1.85 \times MW_{calc}$). Of the 60 clones giving a single peak, 46 (77%) eluted at the expected MW_{app}, 10 (17%) at too low MW_{app} (indicating column interaction) and 4 (7%) at too high MW_{app} (indicating oligomerization or an elongated shape, probably due to partial unfolding) (**Fig. 28c**).

DARPins eluting as a single peak but at too high or too low MW_{app} were further analyzed by SEC-MALS as described[6]. Measurements and data evaluation was performed by Thomas Huber and data from SEC and SEC-MALS are summarized in **Table 3**. The two binders (9_03 and 9_26) eluting at too low MW_{app} ($MW_{app}/MW_{calc} \leq 1.11$) as well as the two binders (T_09 and T_16) eluting at with a MW_{app} slightly above the expected value ($MW_{app}/MW_{calc} \sim 1.7$) clearly showed a monomeric mass calculated from SEC-MALS measurements (MW_{MALS}). In contrast, the four binders (B4_53, B4_56 I_01 and H_01) eluting at too high MW_{app} ($MW_{app}/MW_{calc} \geq 2.2$) showed a MW_{MALS} clearly indicating a dimeric mass or a high fraction of dimeric species, validating the chosen cutoff of ±25% with respect to E3_5.

Of the totally 84 clones analyzed by SEC, only 29 (35%) elute as a single symmetric peak with the elution volume expected for the monomer, including single peaks with a slight shoulder or tailing increases this number to 46 (55%). To estimate the percentage of all binders being monomeric, DARPins with a too low MW_{app} can also be counted, as shown by SEC-MALS, resulting in a final value of 56 (67%) of monomeric binders.

Table 3: Molecular weight calculations of DARPins with atypical elution volumes in SEC

DARPin	MW_{calc} (kDa)[a]	MW_{app} (kDa)[b]	MW_{MALS} (kDa)[c]
B4_53	18.6	42 (2.3)	30 (1.6)
B4_56	21.8	56 (2.6)	43 (2.0)
I_01	18.3	54 (3.0)	40 (2.2)
H_01	18.1	42 (2.3)	33 (1.8)
T_16	18.3	31 (1.7)	20 (1.1)
T_09	18.3	31 (1.7)	20 (1.1)
9_26	18.4	10 (0.6)	19 (1.0)
9_03	18.5	15 (0.8)	19 (1.0)

[a] Molecular weight calculated from the sequence. [b] Apparent molecular weight determined by gel-filtration, in parentheses MW_{app}/MW_{calc}. [c] Observed molecular weight determined by SEC-multi-angle light scattering (MALS) (measurements performed by T. Huber), in parentheses MW_{MALS}/MW_{calc}.

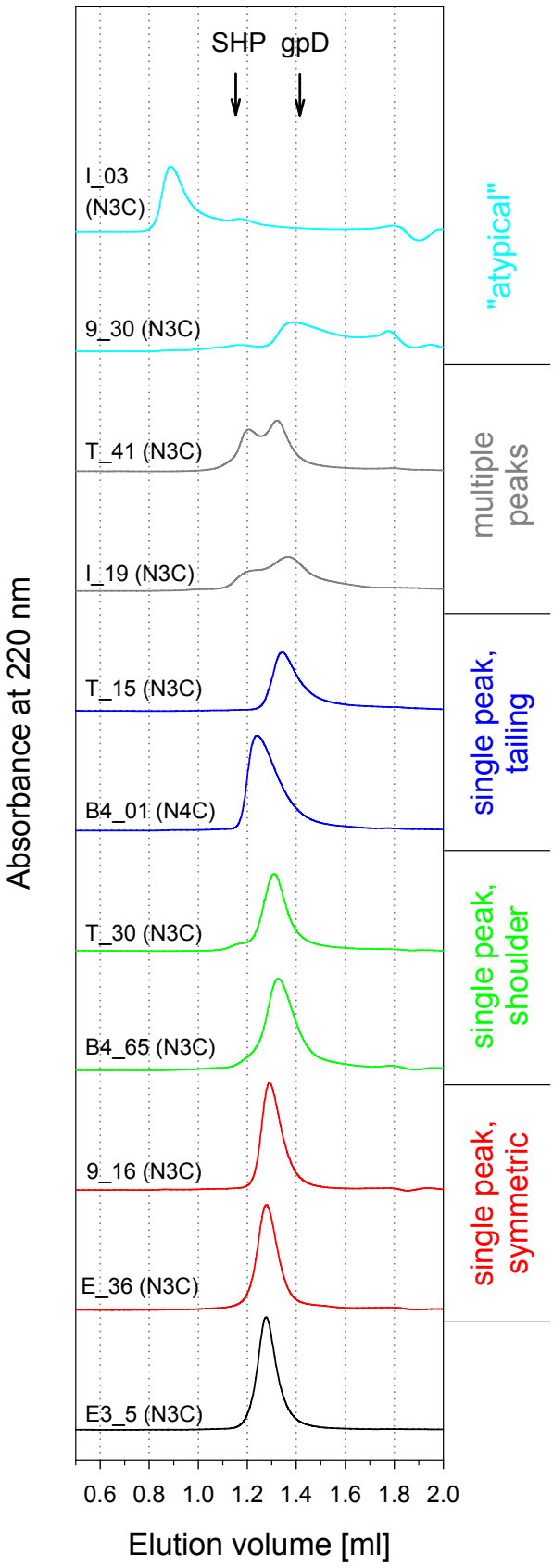

Figure 27: Grouping of DARPins based on SEC analysis. DARPins were divided into five groups based on their elution chromatogram: single symmetric peak, single peak with a shoulder, single peak with tailing, multiple peaks and "atypical" elution chromatogram. The elution chromatograms of two representative examples of each group and of the unselected DARPin E3_5 are shown. For each DARPin the number of repeats stacked between N-Cap (N) and C-Cap (C) is given in parentheses. The molecular mass standards, phage protein D (gpD) with an apparent mass of 17.6 kDa and phage protein SHP, a trimer with an apparent mass of 50.2 kDa, are indicated with arrows.

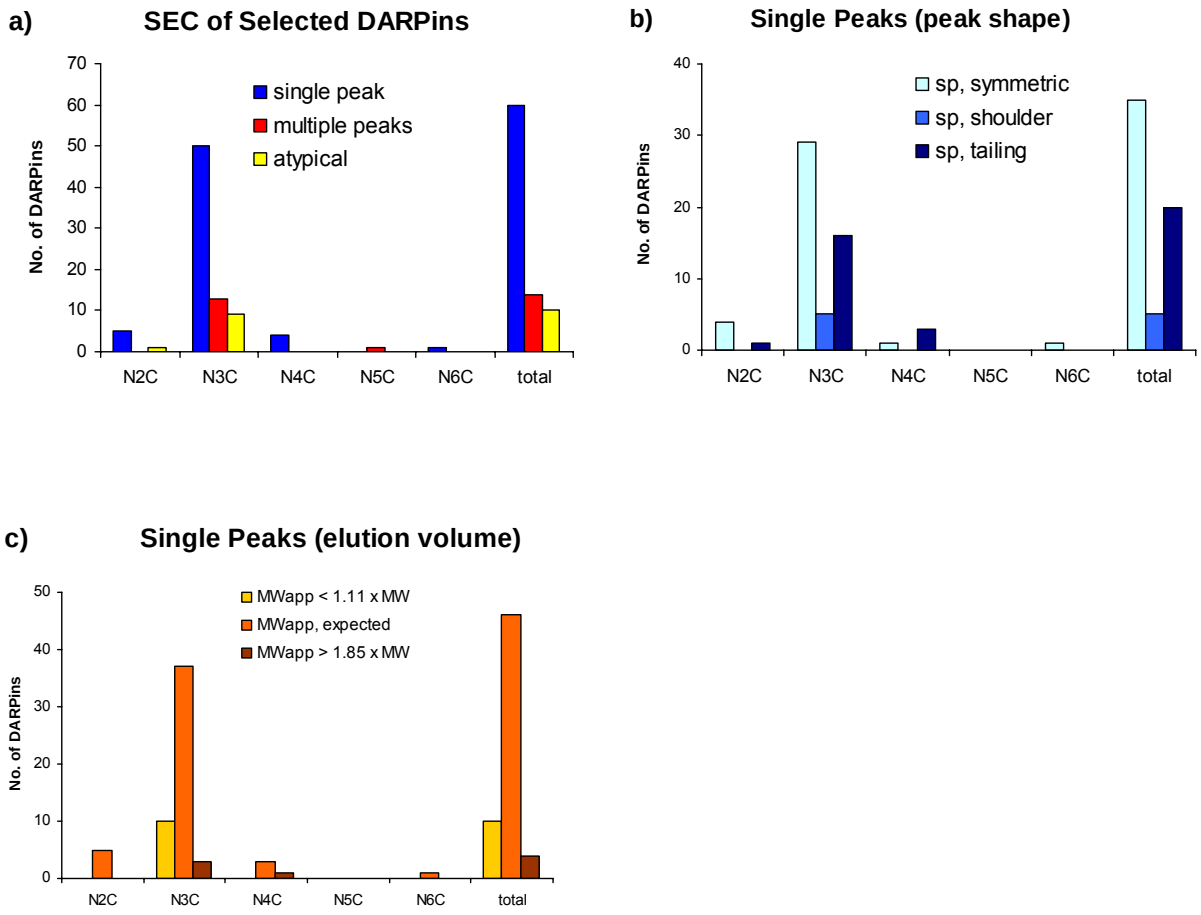

Figure 28: Summary of collected SEC data. (a) The number of clones eluting in a single peak, in multiple peaks or not as defined peaks or as peak in the void volume (atypical) are plotted for the DARPins of different length and the sum of all DARPins. (b) The clones eluting as a single peak (sp) were grouped according to the shape of their elution peak. The number of clones giving a sp that is symmetric, sp with a shoulder or sp with tailing are plotted as described above. (c) The clones eluting as a single peak were additionally grouped according to their elution volume. The number of clones eluting at too low ($MW_{app} \leq 1.11 \times MW_{calc}$), expected ($1.11 \times MW_{calc} \leq MW_{app} \leq 1.85 \times MW_{calc}$) or too high apparent molecular weight ($MW_{app} \geq 1.85 \times MW_{calc}$) are plotted as described above.

7.3 Comparing SEC and sequences

The aim of comparing the recorded SEC elution profiles with the sequences of the respective DARPins was to find out if there is a correlation between the behavior in SEC and the occurrence of framework mutations in general or certain patterns of framework mutations. Binders were grouped based on their behavior in SEC and framework mutations analyzed. One possible grouping is depicted in **Figure 29.** The only clear observation is the low occurrence of framework mutations in the C-Cap of binders eluting as a single symmetric peak or single peak with a shoulder. No correlation of a non-monomeric elution profile in SEC with an increased number of framework mutations or pattern of framework mutations was observed. Even more interesting, about half of the clones giving an ”atypical“ elution chromatogram in SEC had no framework mutations at all, indicating a high influence of the randomized positions on the SEC behavior of the DARPins.

Furthermore, all sequences were analyzed for the occurrence of charged or hydrophobic amino acid. Also in this case no correlation of a non-monomeric elution profile in SEC with over all increased or decreased charge or hydrophobicity was observed.

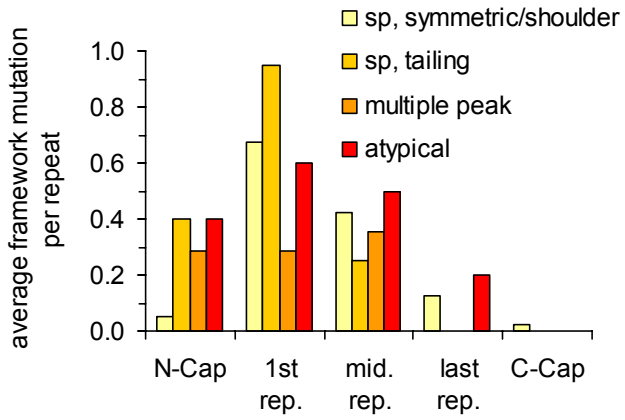

Figure 29: Distribution of the framework mutations over the DARPin sequences for groups of DARPins having different SEC behavior. Depicted is the average of framework mutations (point mutations of conserved framework residues and insertions or deletion at any sequence position) found per repeat (y-axis) plotted for the DARPins having different SEC behavior. Labeling of the SEC behavior is done as described in **Figure 28** and grouping of the different repeats as in **Figure 25.**

7.4 Surface analysis of selected DARPins

Since no clear correlation between amino acid sequence of the selected DARPins and behavior in SEC was found, the binders were further analyzed for the occurrence of hydrophobic patches or charge clusters on their surface which might lead to multimerisation or aggregation. All DARPins with a non-monomeric elution profile in SEC and a subset of the binders showing monomeric behavior were submitted for modeling of their three-dimensional structure (SWISS-MODEL[21]) using the "automated mode" which selects the template structure based on sequence similarity. Models of each DARPin were subsequently analyzed for surface charge distribution and surface hydrophobicity using MOLMOL[22] (**Fig. 30**).

Analysis of the hydrophobicity of the surface of the DARPins revealed that most DARPins selected by phage display show an increased occurrence of hydrophobic residues in the concave binding surface of the DARPins compared to the DARPins used as templates. Especially large hydrophobic patches were observed for the clones T_01, T_40, B4_57 and I_06 showing an atypical SEC behavior, clones T_49, T_41 and T_27 giving multiple peaks in SEC and the reference clone H10_2_G3. The hydrophobicity of the back side is unaltered in all clones analyzed.

Analysis of the charge distribution only shows a clustering of positive charges for the reference clone E3_19 and the two clones T_01 and T_25 showing atypical SEC behavior.

Over all the surface analysis showed that there is an increased occurrence of hydrophobic and positive charge patches for some clones with atypical SEC behavior and clones giving multiple peaks in SEC. This might be the reason for their non-ideal behavior. However, for most other clones no correlation was observed indicating that mutations disturbing hydrophobic core packing, salt bridges and H-bonds will probably affect the structural integrity of the DARPin and thereby influence their behavior in SEC.

Figure 30: Charge distribution and hydrophobicity of the surface of selected DARPins. The charge distribution (even pages: red indicates negative potential; blue, positive potential) and hydrophobicity (odd pages: hydrophobic side-chains colored in green) of the different DARPins are depicted. The front view of the concave binding surface of the DARPins is shown on the left side and the back view on the opposite side is shown on the right side. DARPins E3_5 (PDB entry: 1MJ0), H10_2_G3 (PDB entry: 2JABA), 3a (PDB entry: 2BKKB), E3_19 (PDB entry: 2BKGA), off7 (PDB entry: 1SVXA), and 1108_19 (PDB entry: 2J8SD) with known structures are shown as references (highlighted in purple). For orientation, corresponding ribbon representations of DARPin E3_5 are shown on top of the respective surface representation. Depicted below is the surface of models of the selected DARPins generated by using SWISS-MODEL[21]. For each selected DARPin the structure of the DARPin with highest sequence identity was used as a template (respective PDB entry given in brackets). DARPins with atypical SEC behavior (T_01, T_25, 9_30, 9_04, T_40, B4_57, I_06, T_45 and 9_10, highlighted in yellow), DARPins that elute in SEC with multiple peaks (T_49, T_33, T_41, T_27, I_19, B4_68, E_68, B4_60, B4_58, 9_18, 9_33, 9_12 and T_51, highlighted in light blue), DARPins having framework mutations (+fm) and eluting as a single peak at the expected molecular weight (T_08, I_14, I_11, I_10, E_67, B4_45 and I_15, highlighted in dark gray) and DARPins having no framework mutations (no fm) and eluting as a single peak at the expected molecular weight (E_72, E_36, E_17, 9_20 and B4_33, highlighted in light gray) are depicted. The figures and the charge calculations were made using MOLMOL[22].

		Charge Distribution of DARPin Surface	
SEC	Name (temp.)	Front (view into binding site)	Back (view on backbone)
single peak	E3_5 (1MJ0)		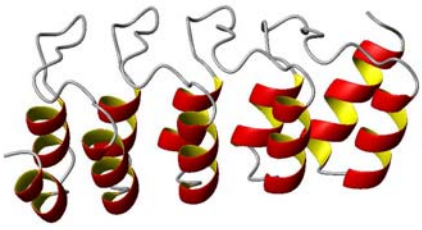
single peak	E3_5 (1MJ0)	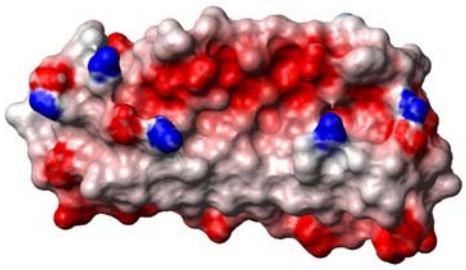	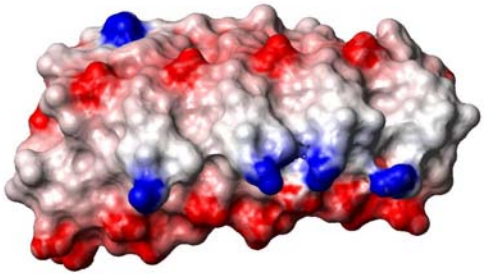
single peak	H10_2_G3 (2JABA)	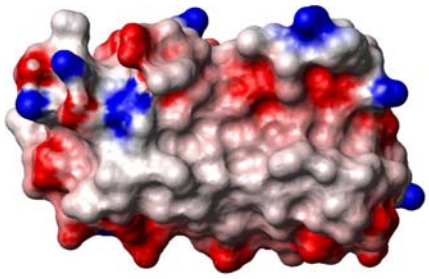	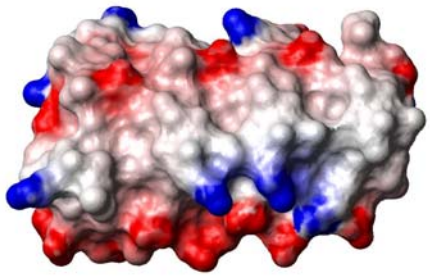
multiple peaks	3a (2BKKB)	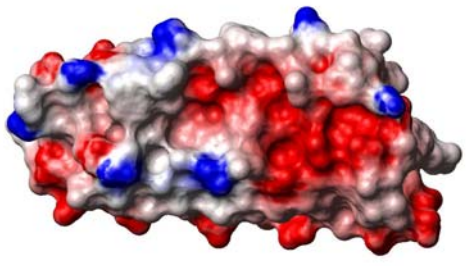	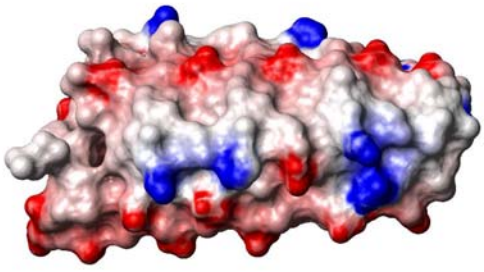
single peak	E3_19 (2BKGA)	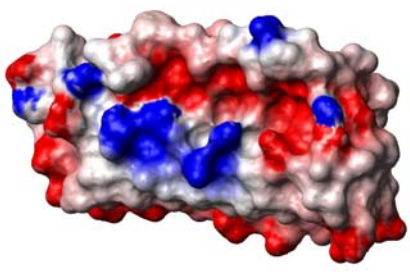	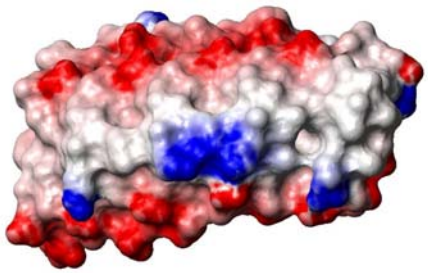

Figure 30: Continued next page

SEC	Name (temp.)	Hydrophobicity of DARPin Surface: Front (view into binding site)	Hydrophobicity of DARPin Surface: Back (view on backbone)
single peak	E3_5 (1MJ0)		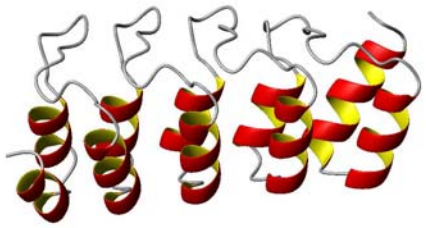
single peak	E3_5 (1mj0a)	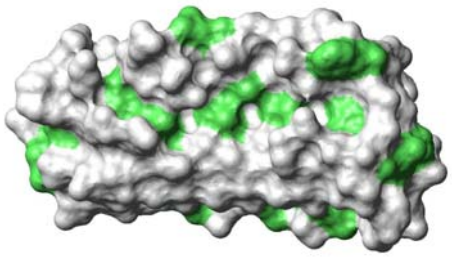	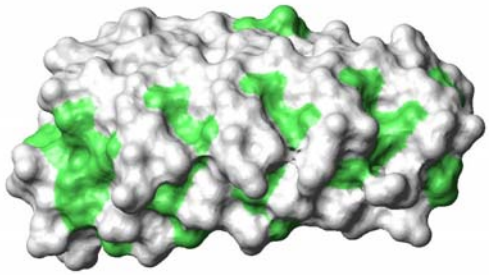
single peak	H10_2_G3 (2JABA)	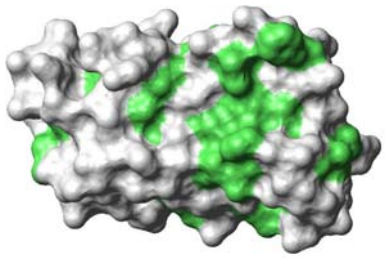	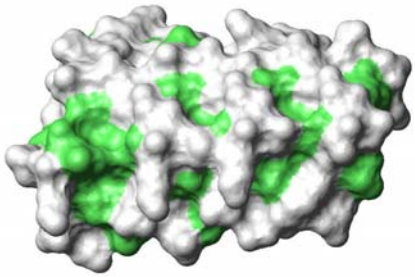
multiple peaks	3a (2BKKB)	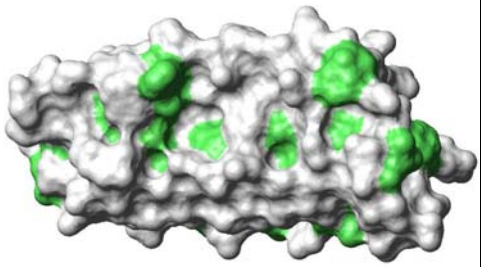	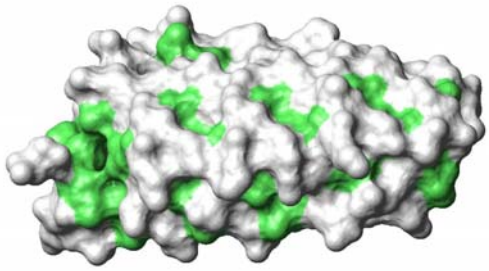
single peak	E3_19 (2BKGA)	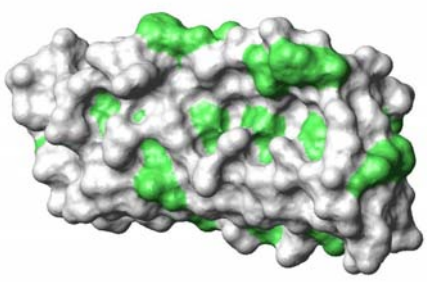	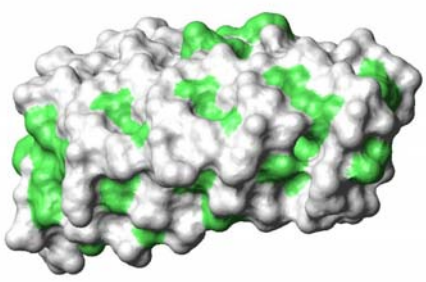

Figure 30: Continued next page

		Charge Distribution of DARPin Surface	
SEC	Name (temp.)	Front (view into binding site)	Back (view on backbone)
-	off7 (1SVXA)	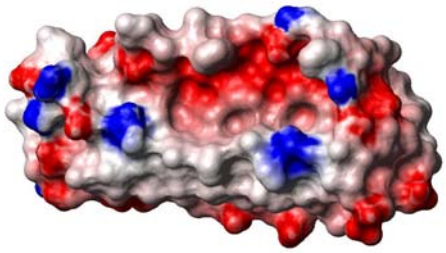	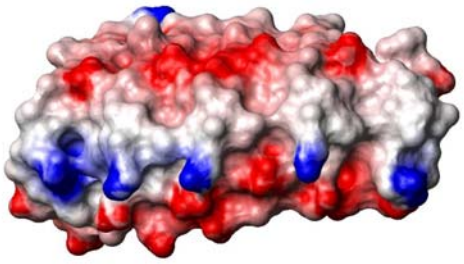
-	1108_19 (2J8SD)	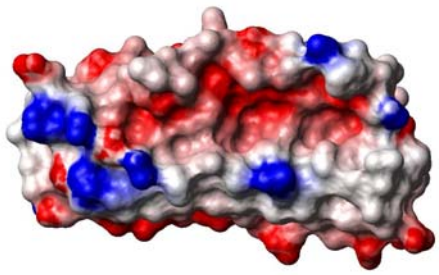	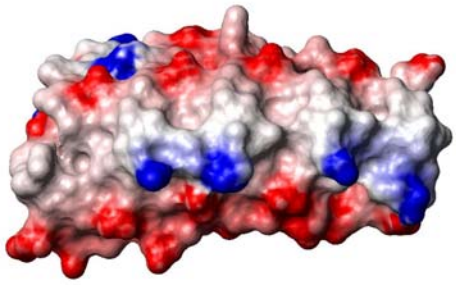
atypical	T_01 (2BKKB)	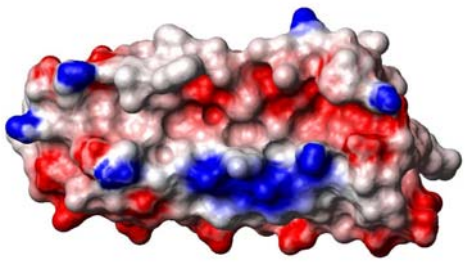	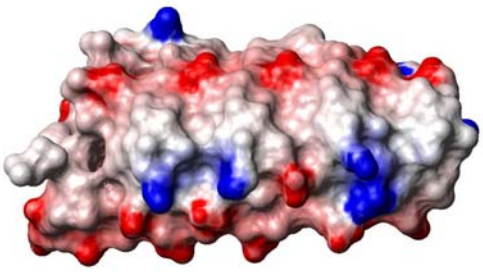
atypical	T_25 (2BKKB)	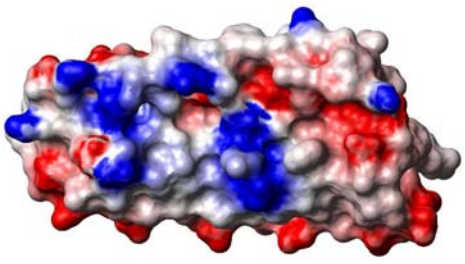	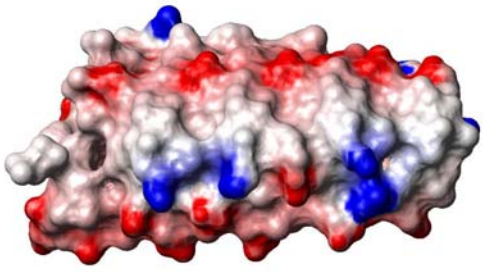
atypical	9_30 (2BKGA)	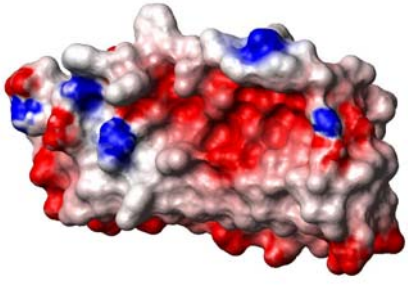	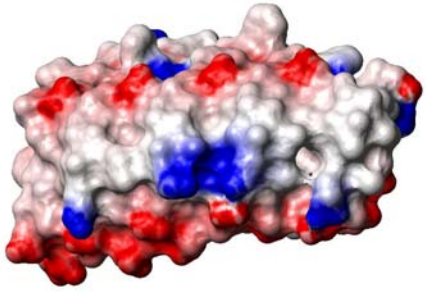

Figure 30: Continued next page

SEC	Name (temp.)	Hydrophobicity of DARPin Surface: Front (view into binding site)	Hydrophobicity of DARPin Surface: Back (view on backbone)
-	off7 (1SVXA)	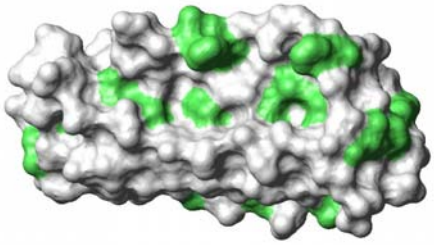	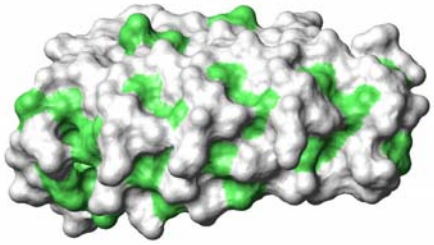
-	1108_19 (2J8SD)	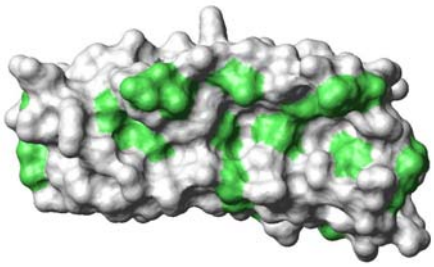	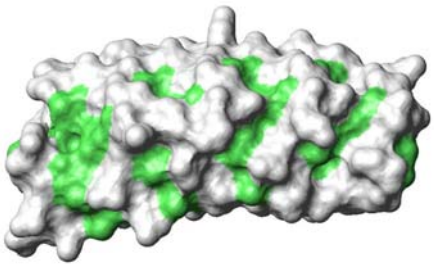
atypical	T_01 (2BKKB)	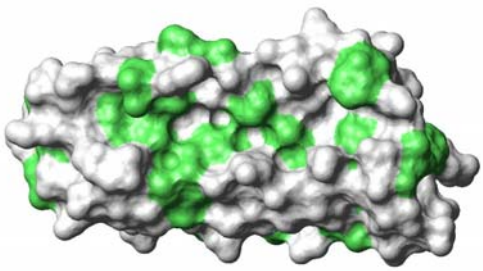	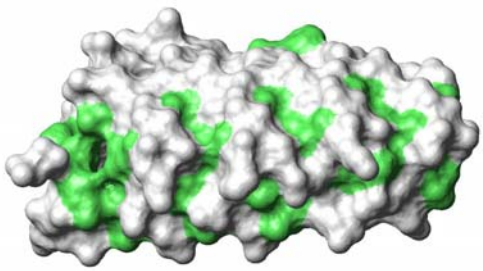
atypical	T_25 (2BKKB)	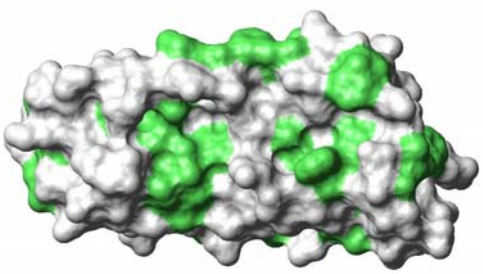	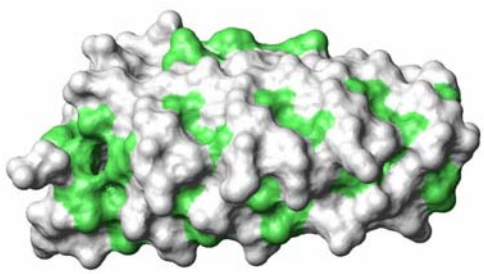
atypical	9_30 (2BKGA)	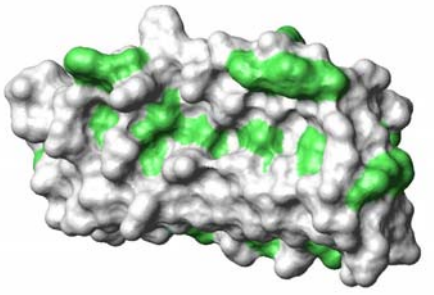	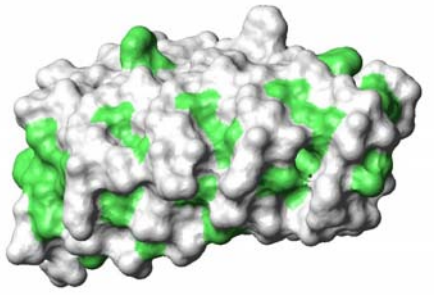

Figure 30: Continued next page

SEC	Name (temp.)	Charge Distribution of DARPin Surface: Front (view into binding site)	Charge Distribution of DARPin Surface: Back (view on backbone)
atypical	9_04 (2BKKB)	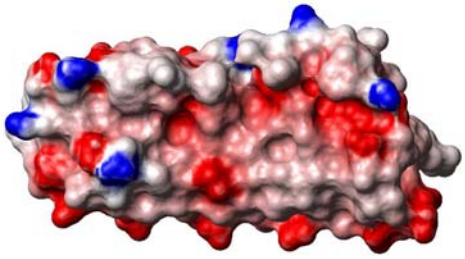	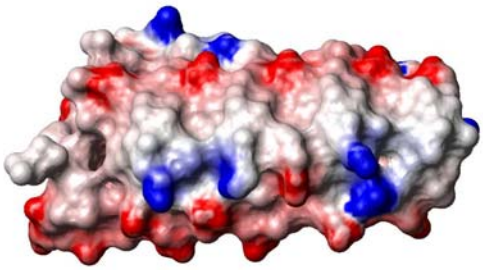
atypical	T_40 (2BKGA)	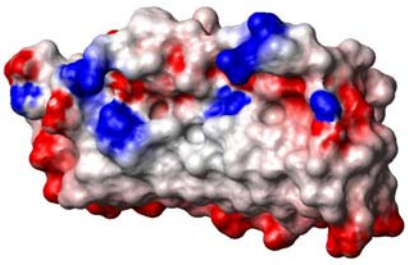	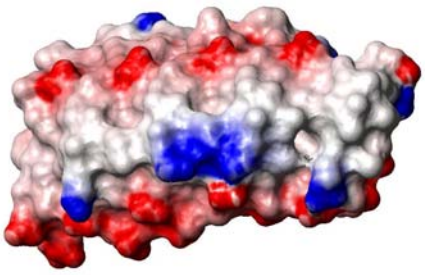
atypical	B4_57 (2BKKB)	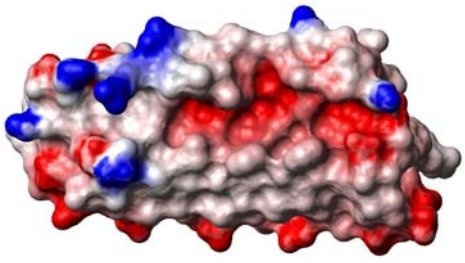	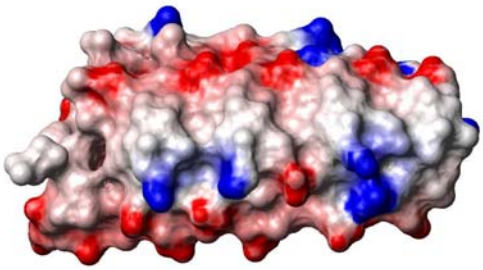
atypical	I_06 (2BKKB)	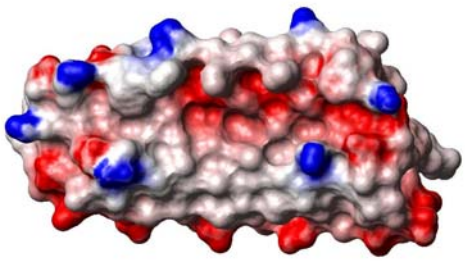	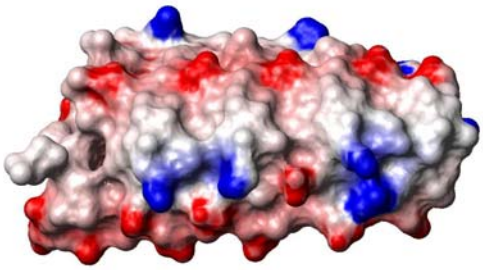
atypical	T_45 (1SVXA)	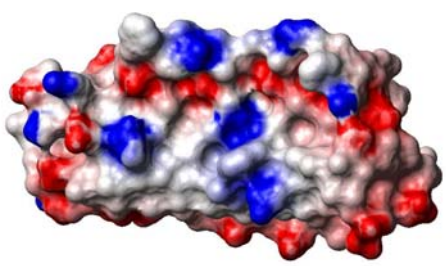	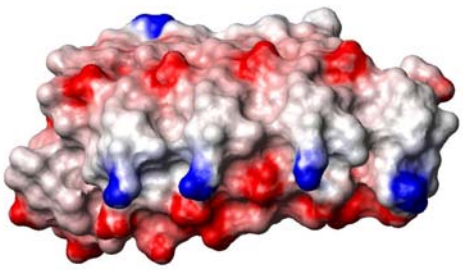

Figure 30: Continued next page

SEC	Name (temp.)	Hydrophobicity of DARPin Surface: Front (view into binding site)	Hydrophobicity of DARPin Surface: Back (view on backbone)
atypical	9_04 (2BKKB)	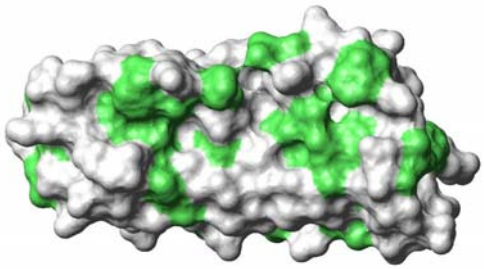	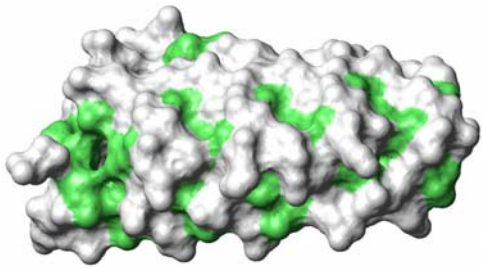
atypical	T_40 (2BKGA)	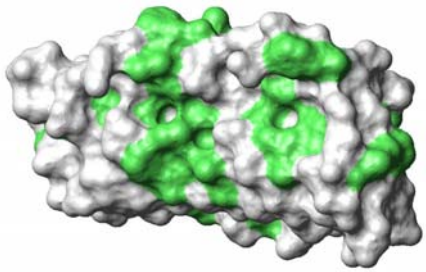	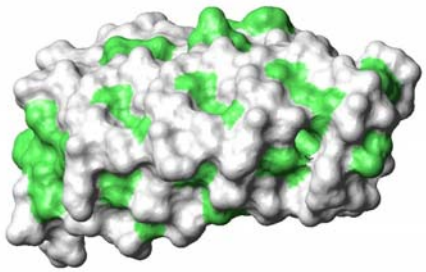
atypical	B4_57 (2BKKB)	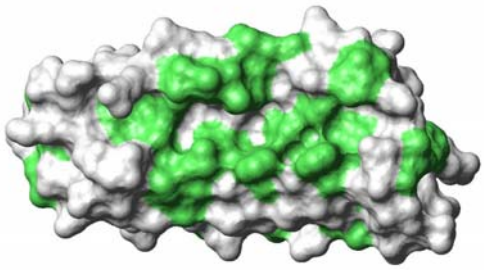	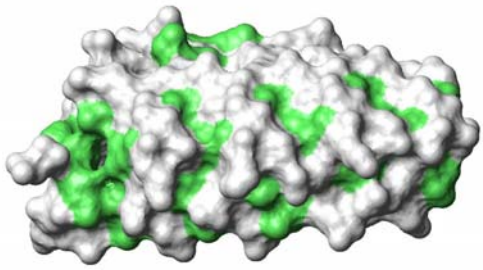
atypical	I_06 (2BKKB)	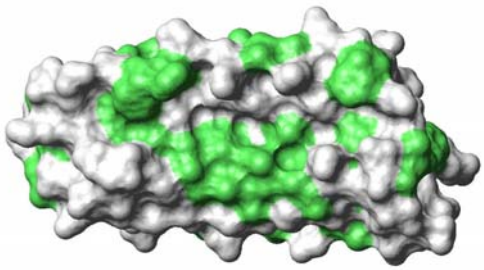	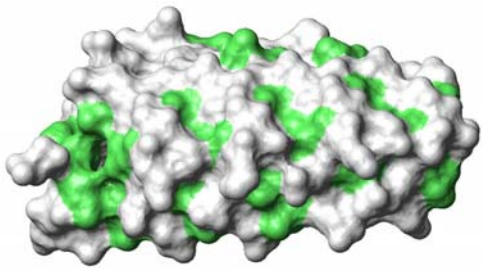
atypical	T_45 (1SVXA)	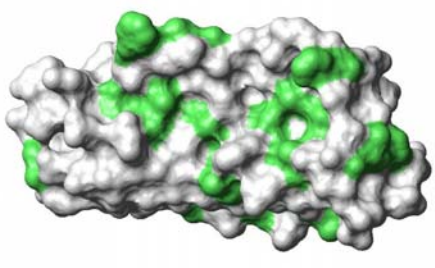	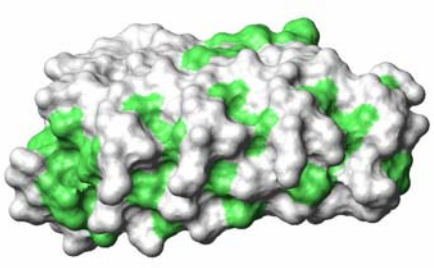

Figure 30: Continued next page

		Charge Distribution of DARPin Surface	
SEC	Name (temp.)	Front (view into binding site)	Back (view on backbone)
atypical	9_10 (2BKKB)	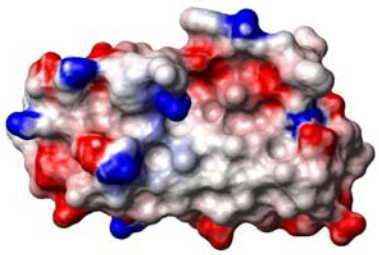	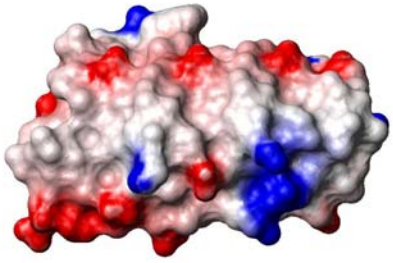
multiple peaks	T_49 (2BKGA)	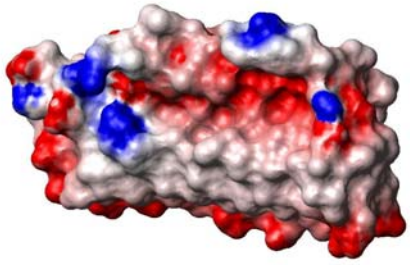	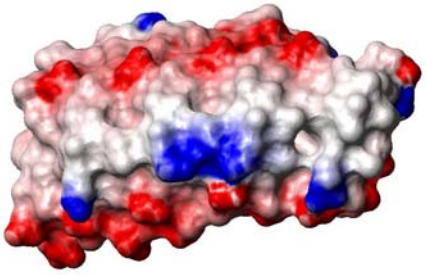
multiple peaks	T_33 (2J8SD)	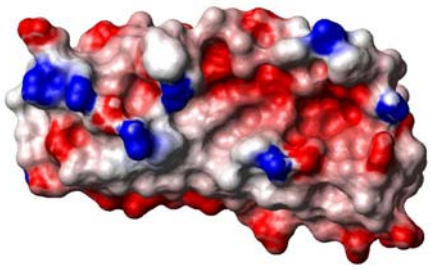	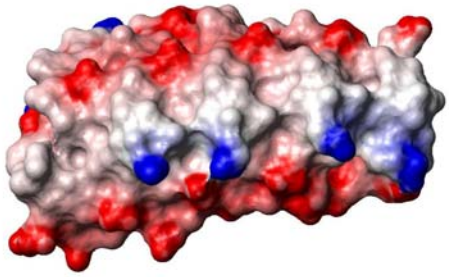
multiple peaks	T_41 (2BKKB)	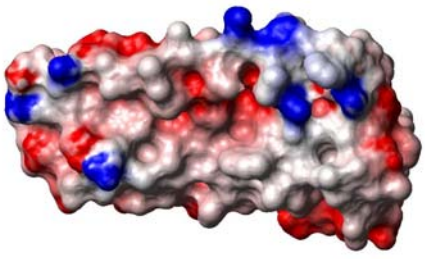	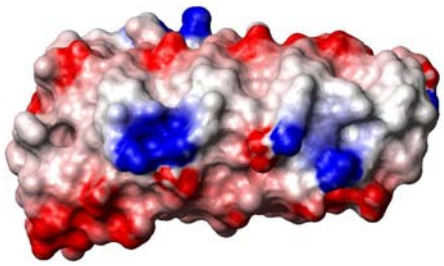
multiple peaks	T_27 (1SVXA)	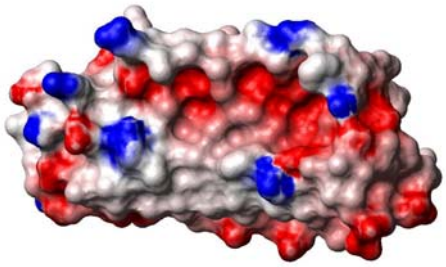	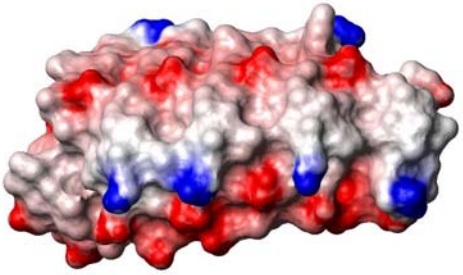

Figure 30: Continued next page

SEC	Name (temp.)	Hydrophobicity of DARPin Surface: Front (view into binding site)	Hydrophobicity of DARPin Surface: Back (view on backbone)
atypical	9_10 (2BKKB)	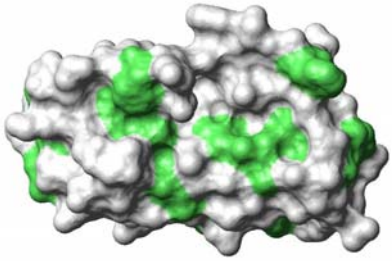	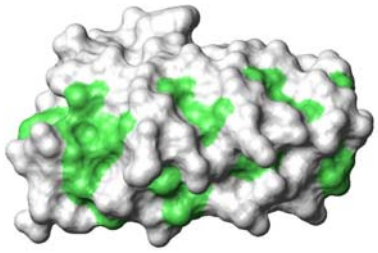
multiple peaks	T_49 (2BKGA)	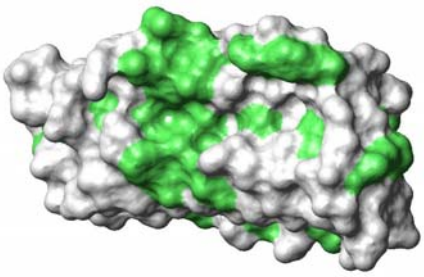	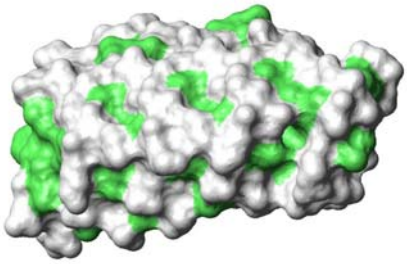
multiple peaks	T_33 (2J8SD)	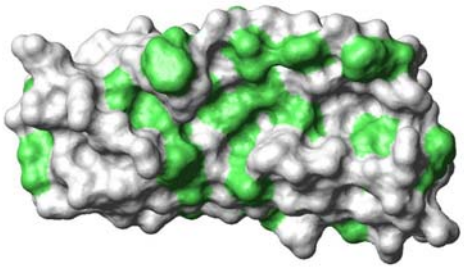	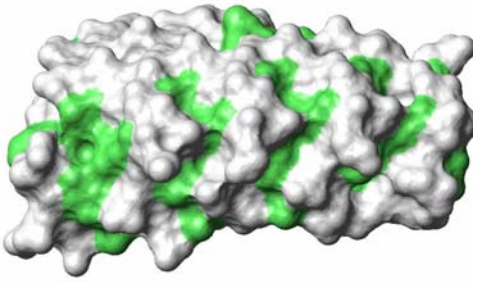
multiple peaks	T_41 (2BKKB)	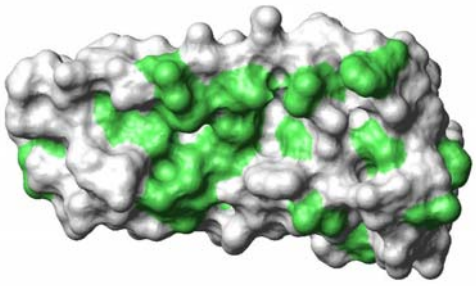	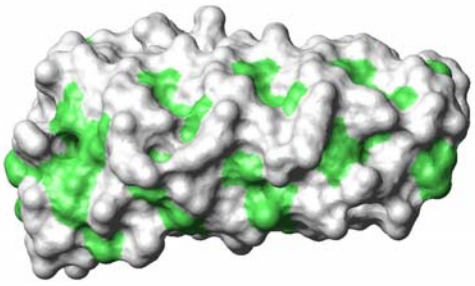
multiple peaks	T_27 (1SVXA)	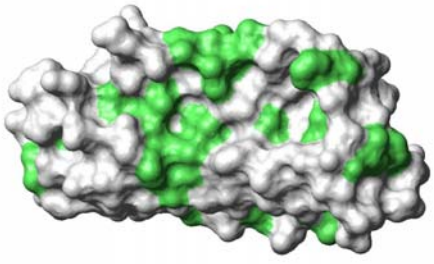	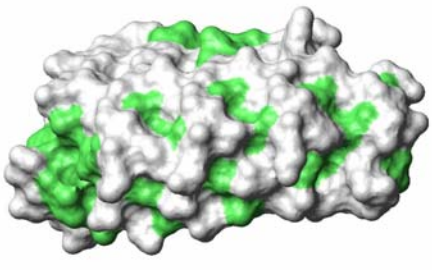

Figure 30: Continued next page

		Charge Distribution of DARPin Surface	
SEC	Name (temp.)	Front (view into binding site)	Back (view on backbone)
multiple peaks	I_19 (2BKGA)	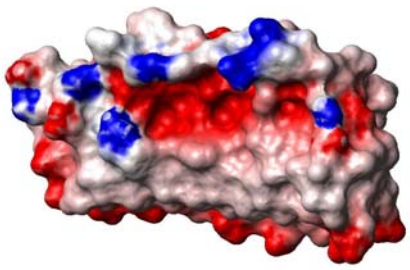	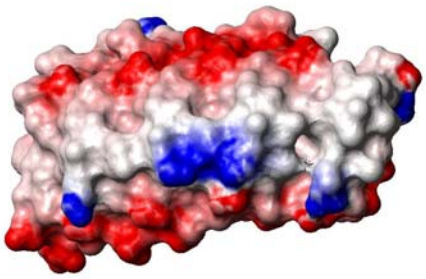
multiple peaks	B4_68 (2BKGA)	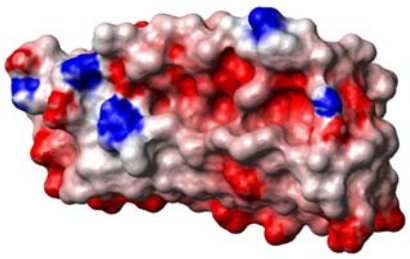	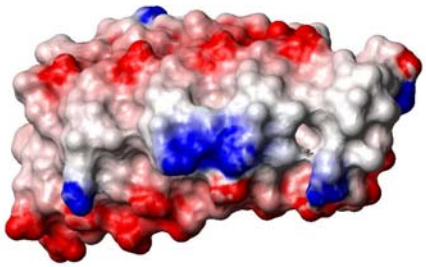
multiple peaks	E_68 (2BKKB)	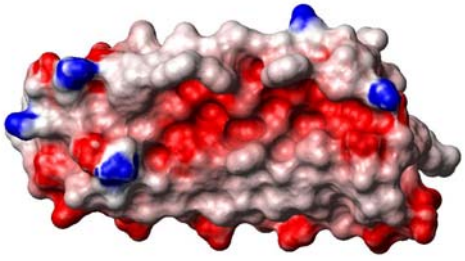	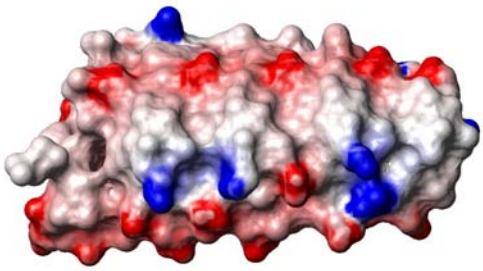
multiple peaks	B4_60 (2BKKB)	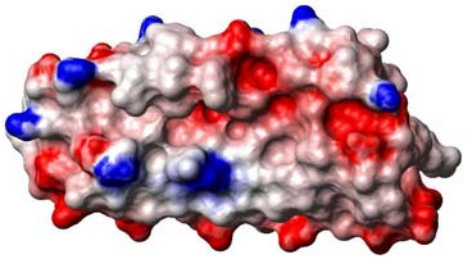	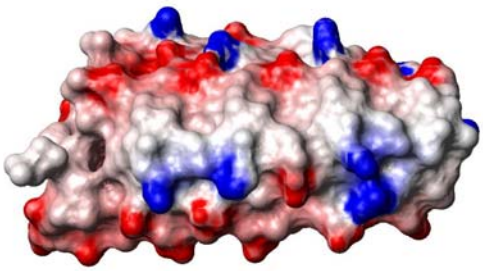
multiple peaks	B4_58 (2BKGA)	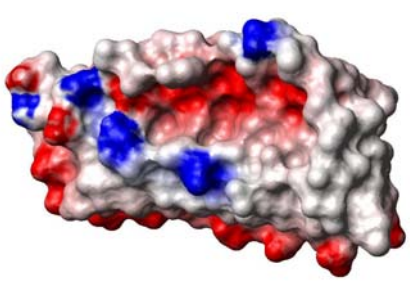	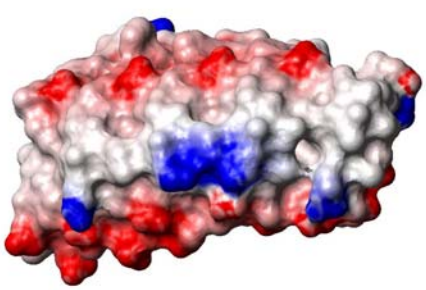

Figure 30: Continued next page

SEC	Name (temp.)	Hydrophobicity of DARPin Surface: Front (view into binding site)	Hydrophobicity of DARPin Surface: Back (view on backbone)
multiple peaks	I_19 (2BKGA)	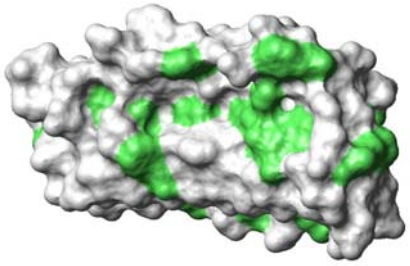	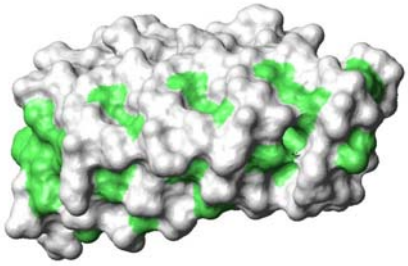
multiple peaks	B4_68 (2BKGA)	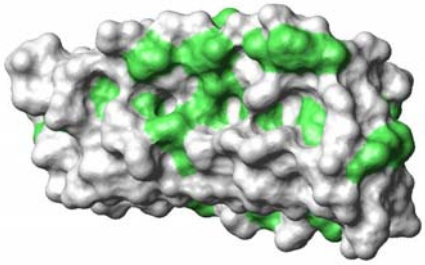	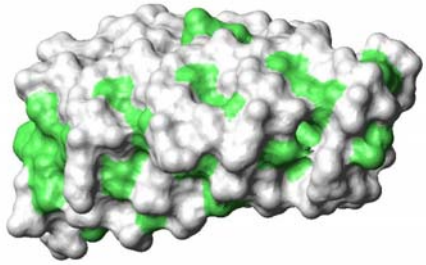
multiple peaks	E_68 (2BKKB)	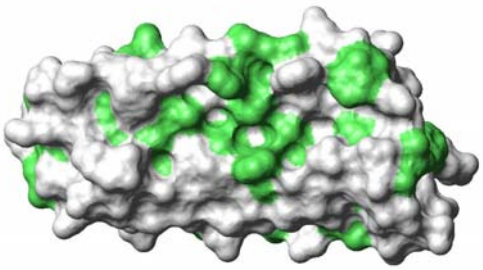	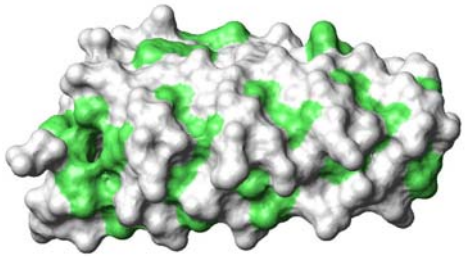
multiple peaks	B4_60 (2BKKB)	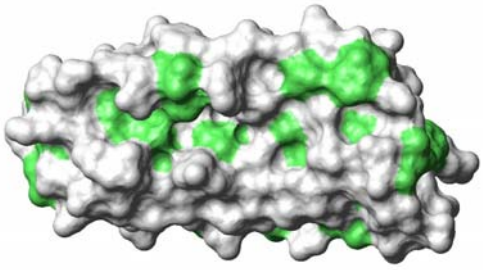	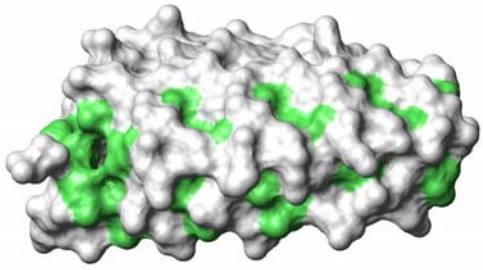
multiple peaks	B4_58 (2BKGA)	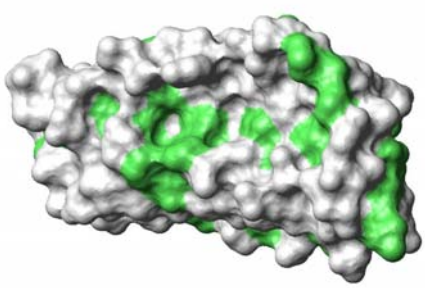	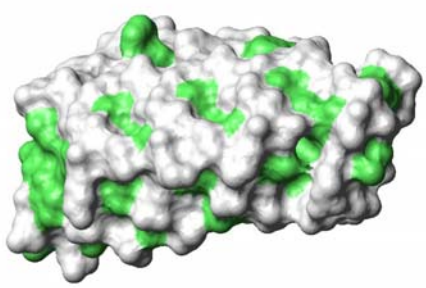

Figure 30: Continued next page

SEC	Name (temp.)	Charge Distribution of DARPin Surface: Front (view into binding site)	Back (view on backbone)
multiple peaks	9_18 (1SVXA)	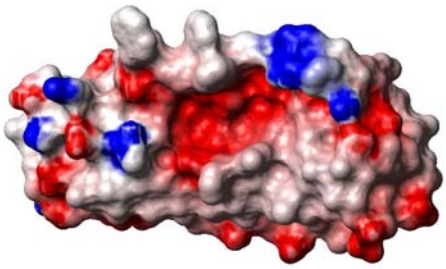	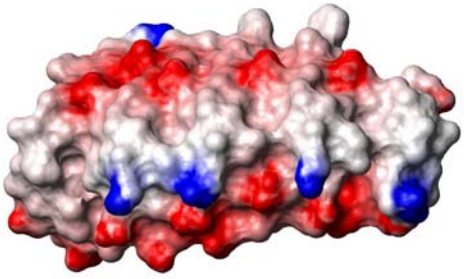
multiple peaks	9_33 (2BKKB)	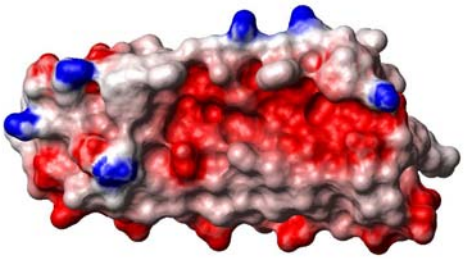	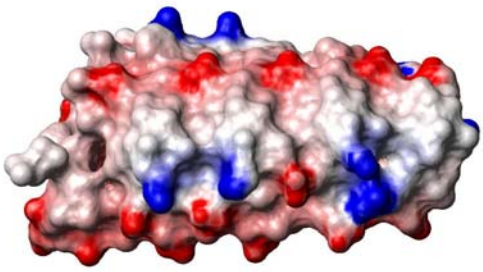
multiple peaks	9_12 (2BKGA)	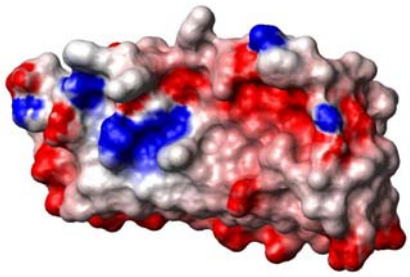	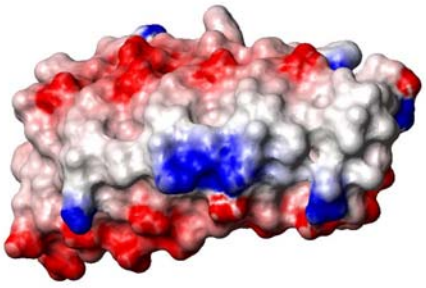
multiple peaks	T_51 (2J8SD)	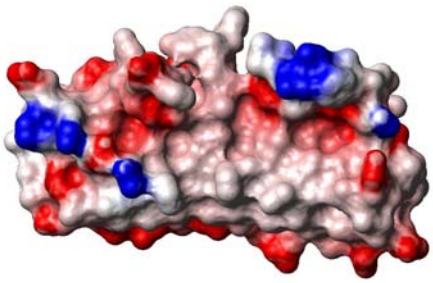	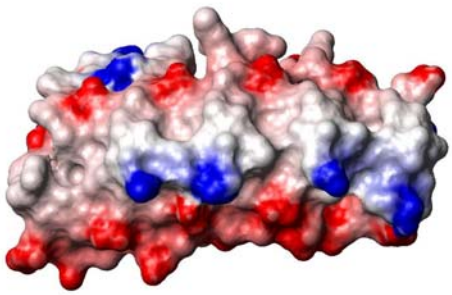
single peak (+ fm)	T_08 (1SVXA)	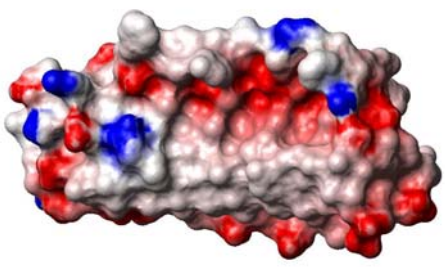	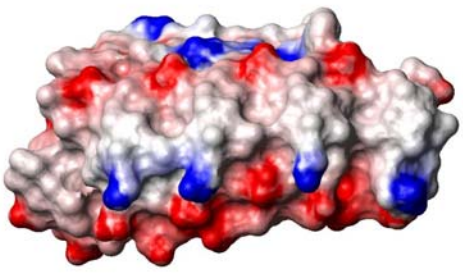

Figure 30: Continued next page

SEC	Name (temp.)	Hydrophobicity of DARPin Surface: Front (view into binding site)	Hydrophobicity of DARPin Surface: Back (view on backbone)
multiple peaks	9_18 (1SVXA)	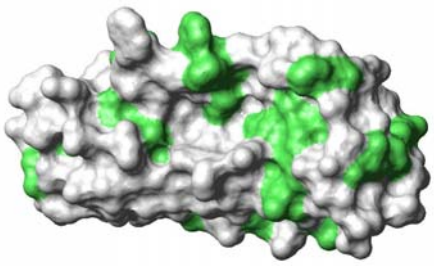	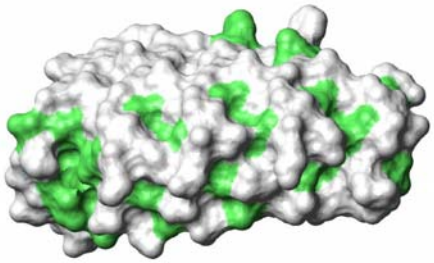
multiple peaks	9_33 (2BKKB)	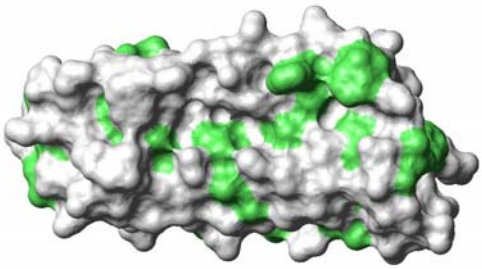	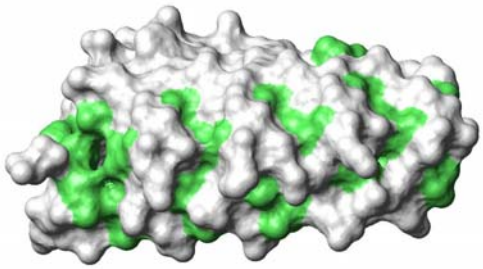
multiple peaks	9_12 (2BKGA)	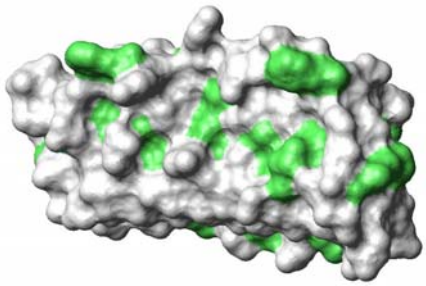	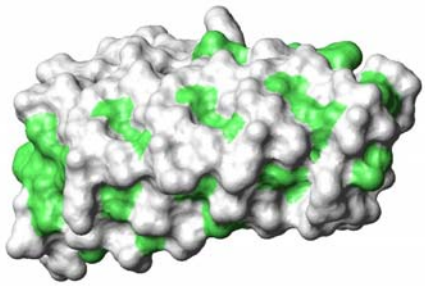
multiple peaks	T_51 (2J8SD)	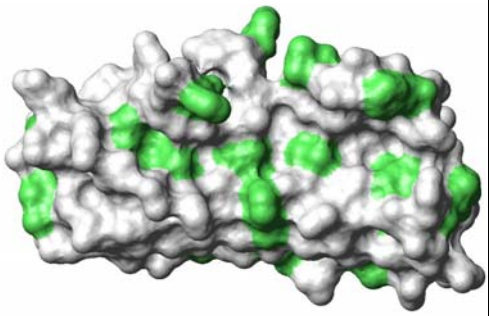	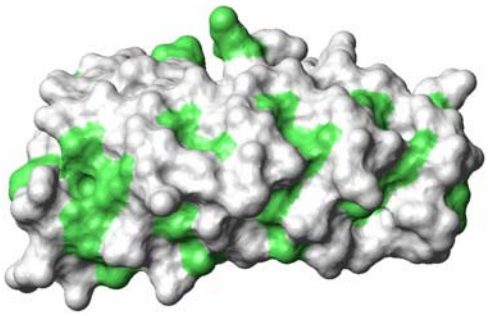
single peak (+ fm)	T_08 (1SVXA)	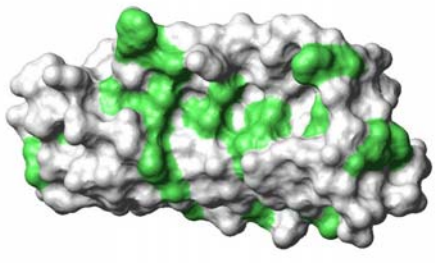	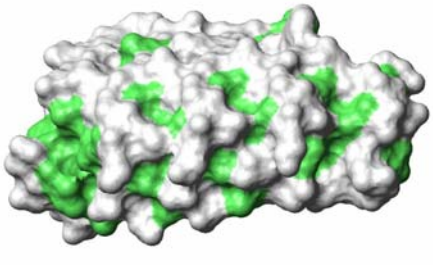

Figure 30: Continued next page

		Charge Distribution of DARPin Surface	
SEC	Name (temp.)	Front (view into binding site)	Back (view on backbone)
single peak (+ fm)	I_14 (1SVXA)	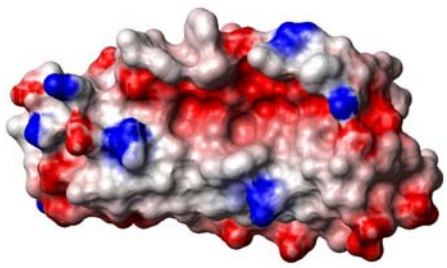	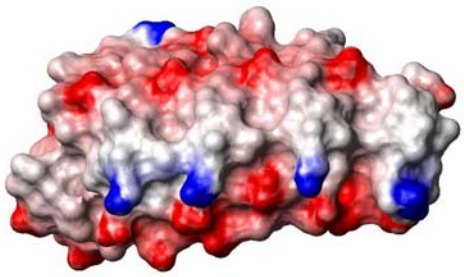
single peak (+ fm)	I_11 (2BKKB)	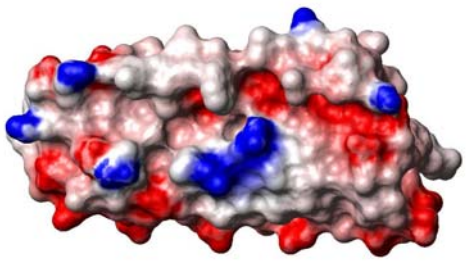	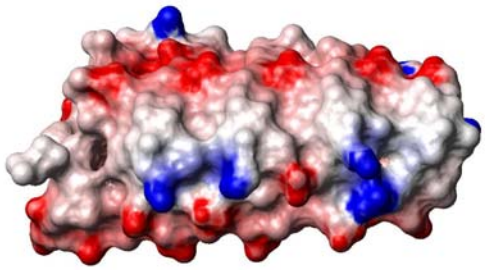
single peak (+ fm)	I_10 (2BKKB)	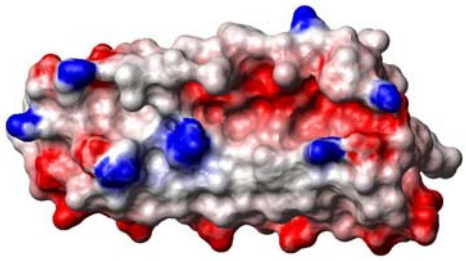	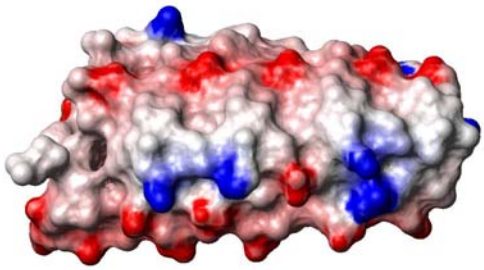
single peak (+ fm)	E_67 (1SVXA)	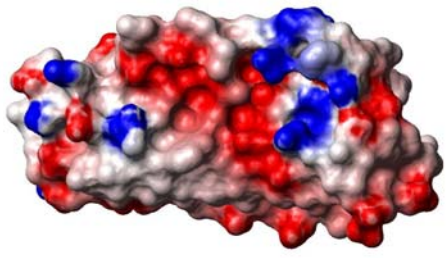	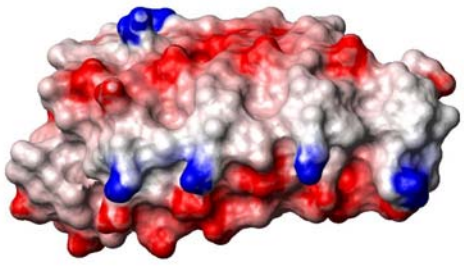
single peak (+ fm)	I_15 (2BKKB)	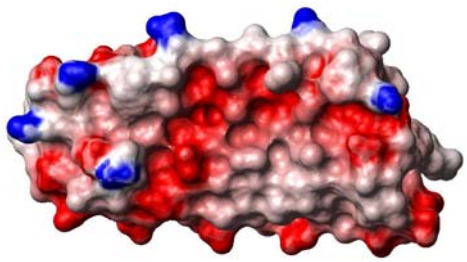	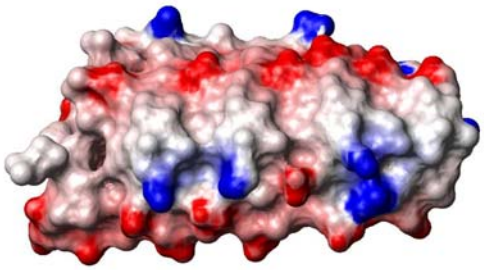

Figure 30: Continued next page

SEC	Name (temp.)	Hydrophobicity of DARPin Surface: Front (view into binding site)	Hydrophobicity of DARPin Surface: Back (view on backbone)
single peak (+ fm)	I_14 (1SVXA)	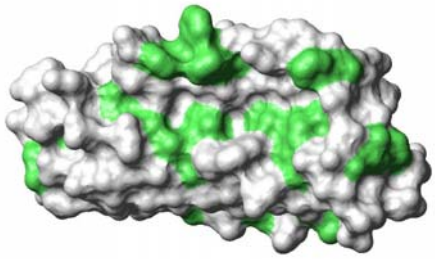	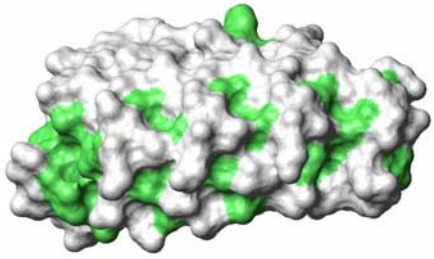
single peak (+ fm)	I_11 (2BKKB)	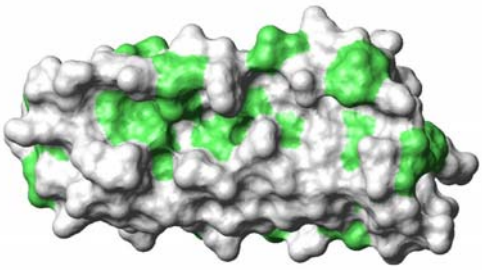	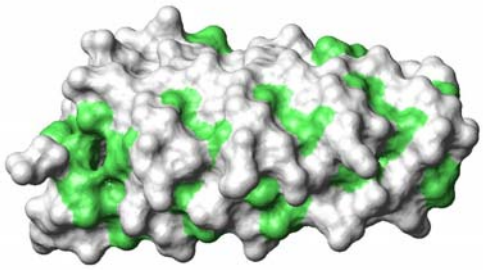
single peak (+ fm)	I_10 (2BKKB)	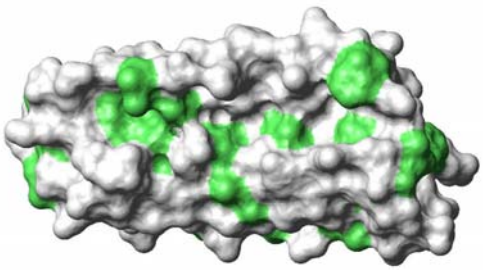	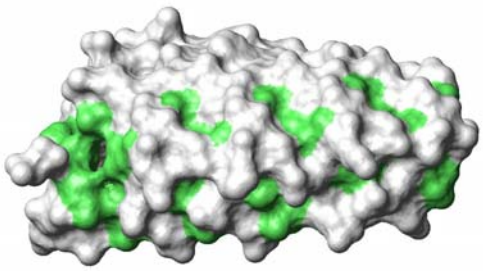
single peak (+ fm)	E_67 (1SVXA)	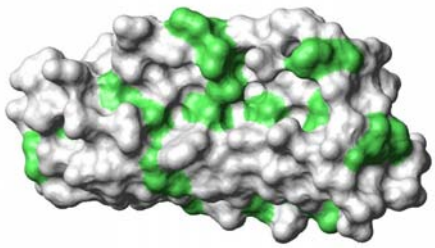	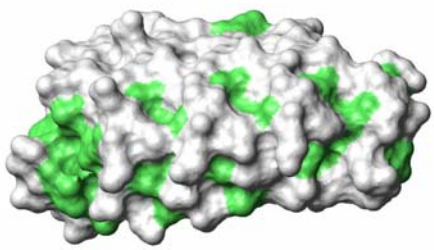
single peak (+ fm)	I_15 (2BKKB)	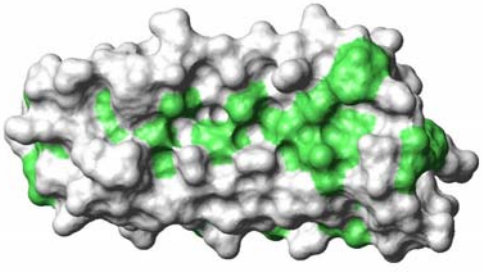	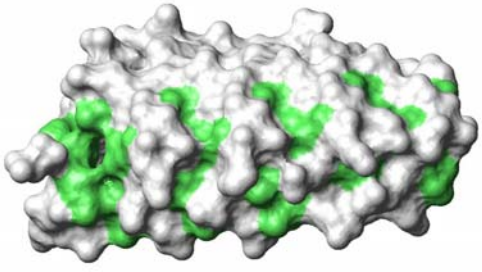

Figure 30: Continued next page

		Charge Distribution of DARPin Surface	
SEC	Name (temp.)	Front (view into binding site)	Back (view on backbone)
single peak (no fm)	E_72 (1SVXA)	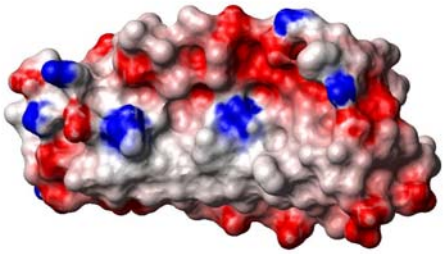	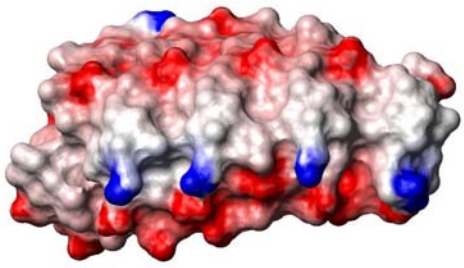
single peak (no fm)	E_36 (1SVXA)	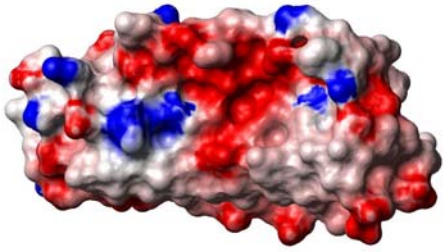	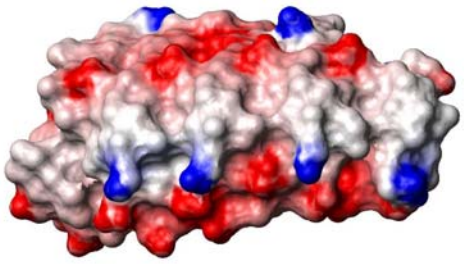
single peak (no fm)	E_17 (1SVXA)	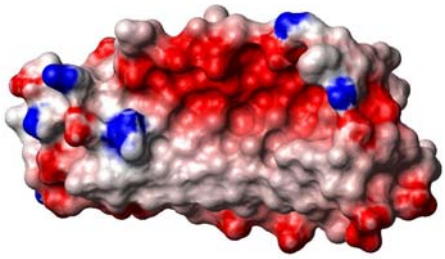	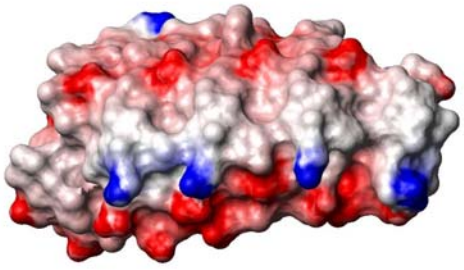
single peak (no fm)	9_20 (2BKKB)	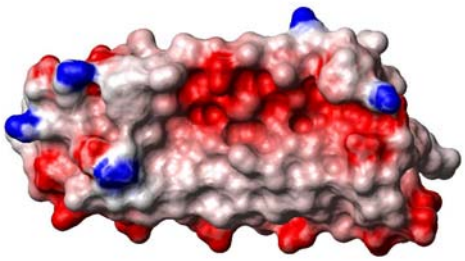	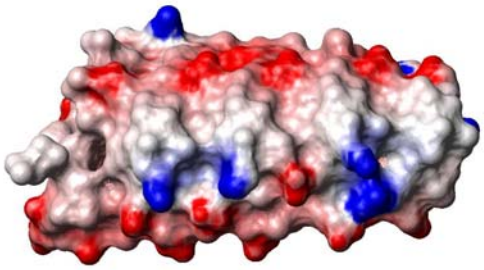
single peak (no fm)	B4_33 (1SVXA)	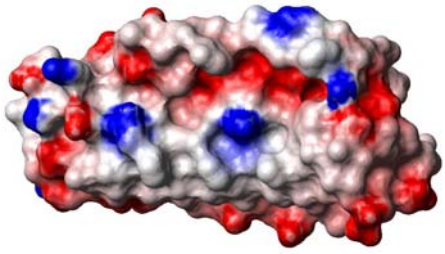	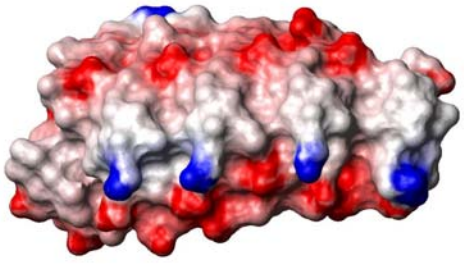

Figure 30: Continued next page

SEC	Name (temp.)	Hydrophobicity of DARPin Surface: Front (view into binding site)	Hydrophobicity of DARPin Surface: Back (view on backbone)
single peak (no fm)	E_72 (1SVXA)	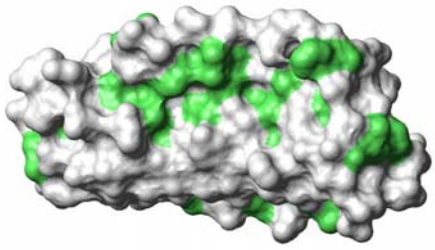	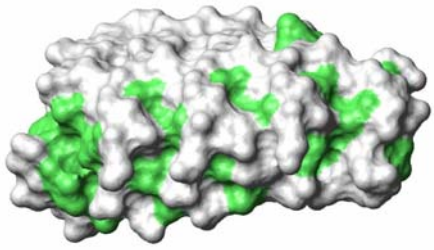
single peak (no fm)	E_36 (1SVXA)	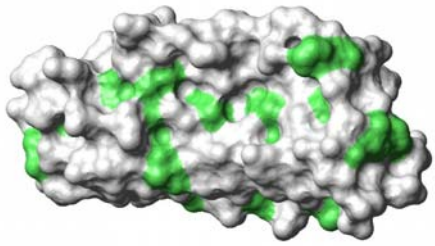	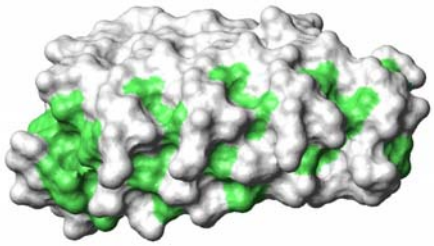
single peak (no fm)	E_17 (1SVXA)	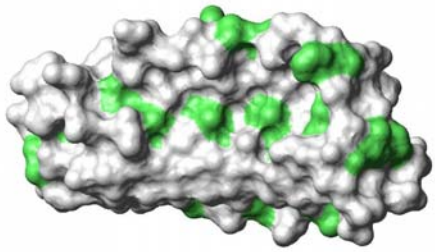	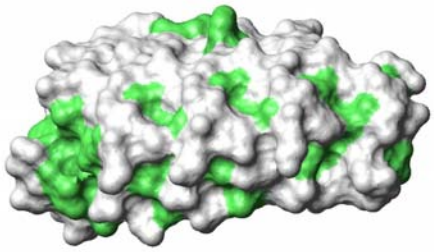
single peak (no fm)	9_20 (2BKKB)	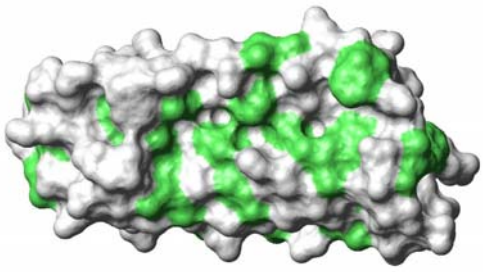	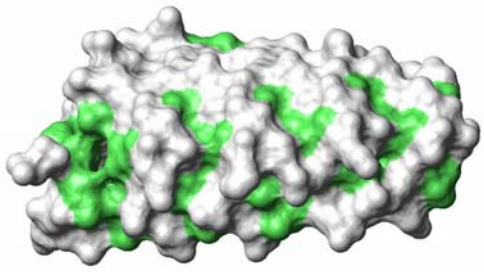
single peak (no fm)	B4_33 (1SVXA)	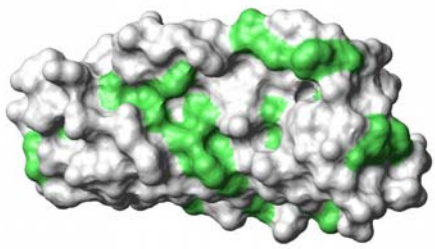	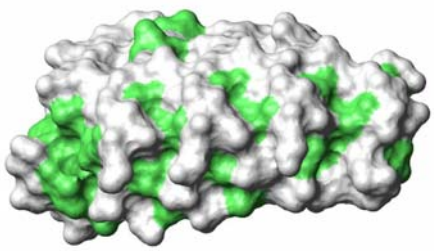

Figure 30: Continued next page

8. References

1. Späth, J.P. Structure and Function of Immunoglobulins. *Sepsis* **3**, 197-218 (1999).
2. Binz, H.K., Stumpp, M.T., Forrer, P., Amstutz, P. & Plückthun, A. Designing repeat proteins: Well-expressed, soluble and stable proteins from combinatorial libraries of consensus ankyrin repeat proteins. *J. Mol. Biol.* **332**, 489-503 (2003).
3. Haitham, T.I. & James, H.N. TNF and the TNF receptor superfamily: Structure-function relationship(s). *Microsc Res Tech.* **50**, 184-195 (2000).
4. Scallon, B., Cai, A., Solowski, N., Rosenberg, A., Song, X.Y., Shealy, D. & Wagner, C. Binding and functional comparisons of two types of tumor necrosis factor antagonists. *J. Pharmacol. Exp. Ther.* **301**, 418-426 (2002).
5. Mohammad Tabrizi, L.K.R. in Pharmacokinetics and Pharmacodynamics of Biotech Drugs. (ed. P.D.B. Meibohm) 295-3272006).
6. Huber, T., Steiner, D., Röthlisberger, D. & Plückthun, A. In vitro selection and characterization of DARPins and Fab fragments for the co-crystallization of membrane proteins: The Na^+-citrate symporter CitS as an example. *J. Struct. Biol.* **159**, 206-221 (2007).
7. Burgess, A.W., Cho, H.S., Eigenbrot, C., Ferguson, K.M., Garrett, T.P., Leahy, D.J., Lemmon, M.A., Sliwkowski, M.X., Ward, C.W. & Yokoyama, S. An open-and-shut case? Recent insights into the activation of EGF/ErbB receptors. *Mol. Cell* **12**, 541-552 (2003).
8. Zhen, Y., Caprioli, R.M. & Staros, J.V. Characterization of glycosylation sites of the epidermal growth factor receptor. *Biochemistry* **42**, 5478-5492 (2003).
9. Hynes, N.E. & Lane, H.A. ERBB receptors and cancer: the complexity of targeted inhibitors. *Nat Rev Cancer* **5**, 341-354 (2005).
10. Jorissen, R.N., Walker, F., Pouliot, N., Garrett, T.P.J., Ward, C.W. & Burgess, A.W. Epidermal growth factor receptor: mechanisms of activation and signalling. *Exp. Cell Res.* **284**, 31-53 (2003).
11. Dawson, J.P., Berger, M.B., Lin, C.-C., Schlessinger, J., Lemmon, M.A. & Ferguson, K.M. Epidermal Growth Factor Receptor Dimerization and Activation Require Ligand-Induced Conformational Changes in the Dimer Interface. *Mol. Cell. Biol.* **25**, 7734-7742 (2005).
12. Garrett, T.P., McKern, N.M., Lou, M., Elleman, T.C., Adams, T.E., Lovrecz, G.O., Zhu, H.J., Walker, F., Frenkel, M.J., Hoyne, P.A., Jorissen, R.N., Nice, E.C., Burgess, A.W. & Ward, C.W. Crystal structure of a truncated epidermal growth factor receptor extracellular domain bound to transforming growth factor alpha. *Cell* **110**, 763-773 (2002).
13. Li, S., Schmitz, K.R., Jeffrey, P.D., Wiltzius, J.J.W., Kussie, P. & Ferguson, K.M. Structural basis for inhibition of the epidermal growth factor receptor by cetuximab. *Cancer Cell* **7**, 301-311 (2005).
14. Cho, H.S., Mason, K., Ramyar, K.X., Stanley, A.M., Gabelli, S.B., Denney, D.W., Jr. & Leahy, D.J. Structure of the extracellular region of HER2 alone and in complex with the Herceptin Fab. *Nature* **421**, 756-760. (2003).
15. Garrett, T.P., McKern, N.M., Lou, M., Elleman, T.C., Adams, T.E., Lovrecz, G.O., Kofler, M., Jorissen, R.N., Nice, E.C., Burgess, A.W. & Ward, C.W. The crystal structure of a truncated ErbB2 ectodomain reveals an active conformation, poised to interact with other ErbB receptors. *Mol. Cell* **11**, 495-505 (2003).
16. Franklin, M.C., Carey, K.D., Vajdos, F.F., Leahy, D.J., de Vos, A.M. & Sliwkowski, M.X. Insights into ErbB signaling from the structure of the ErbB2-pertuzumab complex. *Cancer Cell* **5**, 317-328 (2004).

17. Zahnd, C., Pecorari, F., Straumann, N., Wyler, E. & Plückthun, A. Selection and Characterization of Her2 Binding-Designed Ankyrin Repeat Proteins. *J. Biol. Chem.* **281**, 35167-35175 (2006).
18. Zahnd, C., Wyler, E., Schwenk, J.M., Steiner, D., Lawrence, M.C., McKern, N.M., Pecorari, F., Ward, C.W., Joos, T.O. & Plückthun, A. A Designed Ankyrin Repeat Protein Evolved to Picomolar Affinity to Her2. *J. Mol. Biol.* **369**, 1015-1028 (2007).
19. Bouyain, S., Longo, P.A., Li, S., Ferguson, K.M. & Leahy, D.J. The extracellular region of ErbB4 adopts a tethered conformation in the absence of ligand. *PNAS* **102**, 15024-15029 (2005).
20. Steiner, D., Forrer, P., Stumpp, M.T. & Plückthun, A. Signal sequences directing cotranslational translocation expand the range of proteins amenable to phage display. *Nat. Biotechnol.* **24**, 823-831 (2006).
21. Schwede, T., Kopp, J., Guex, N. & Peitsch, M.C. SWISS-MODEL: an automated protein homology-modeling server. *Nucl. Acids Res.* **31**, 3381-3385 (2003).
22. Koradi, R., Billeter, M. & Wüthrich, K. MOLMOL: A program for display and analysis of macromolecular structures. *J. Mol. Graph.* **14**, 51-55 (1996).

Appendix 2

Phage Display Manual: Protocols for Filamentous Phage Display of DARPins

Version: 13/09/2007

Daniel Steiner, danstein@bioc.unizh.ch, +41 (0)44 635 55 76

Patrik Forrer, patrik.forrer@molecularpartners.com, +41 (0)44 755 77 04

Contents:

Glossary of terms

- CAT: chloramphenicol acetyl transferase
- cfu: colony forming units
- cam: chloramphenicol
- DARPin: designed ankyrin repeat protein
- *E. coli: Escherichia coli*
- kan: kanamycin
- p3: minor phage coat protein 3
- PBS: phosphate buffered saline
- PD: phage display
- pfu: plaque forming units
- ps: packaging signal
- SRP: signal recognition particle
- ssDNA: single stranded DNA
- TBS: Tris buffered saline
- tet: tetracycline

Introduction

Phage display readings and protocols

This manual describes the use of a designed ankyrin repeat protein (DARPin) phage display library (for details see Appendix data sheet: PD library #1) to select target-specific DARPins by filamentous phage display (**Fig. 1**). Before starting a phage display project we strongly recommend to understand the basic principles behind phage display. Compact and easy understandable general information on phage biology and phage display can be found in recent book chapters [1,2] or more detailed information in reviews [3,4] (a complete listing of all references can be found at the end of this manual)

- Ref. 1: Russel, M., Lowman, H. B. & Clackson, T. (2004). Introduction to phage biology and phage display. In *Phage Display: A Practical Approach* (Lowman, H. B. & Clackson, T., eds.), pp. 1-26. Oxford University Press, New York, USA.
- Ref. 2: Dennis, M. S. & Lowman, H. B. (2004). Phage selection strategies for improved affinity and specificity of proteins and peptides. In *Phage Display: A Practical Approach* (Lowman, H. B. & Clackson, T., eds.), pp. 61-83. Oxford University Press, New York, USA.
- Ref. 3: Smith, G. P. & Petrenko, V. A. (1997). Phage Display. *Chem Rev* 97, 391-410.
- Ref. 4: Bradbury, A. R. & Marks, J. D. (2004). Antibodies from phage antibody libraries. *J Immunol Methods* 290, 29-49.

Many protocols on phage display have been published. A list of some public available phage display manuals is given below:

- Protocols from G. Smith lab:
  → http://www.biosci.missouri.edu:16080/smithGp/PhageDisplayWebsite/PhageDisplayWebsiteIndex.html
- Protocols from A. Bradbury and G. Smith lab:
  → http://www.bio.com/protocolstools/
- Protocols from D. Neri lab: [5]
  → Ref 5: Viti, F., Nilsson, F., Demartis, S., Huber, A. & Neri, D. (2000). Design and use of phage display libraries for the selection of antibodies and enzymes. *Methods Enzymol* 326, 480-505.

→ http://www.pharma.ethz.ch/institute_groups/biomacromolecules/protocols/eth

- Protocols from S. Sidhu lab: [6]

  → Ref 6: Sidhu, S. S., Lowman, H. B., Cunningham, B. C. & Wells, J. A. (2000). Phage display for selection of novel binding peptides. *Methods Enzymol* 328, 333-63.

DARPins

DARPins constitute a novel substance class of binding molecules based on repeat proteins[7]. Repeat proteins are, next to antibodies, the most abundant class of binding molecules found in nature. They are found in all phyla, they occur intra- and extracellularly and they are involved in diverse biological processes, such as cell cycle control, transcription regulation, innate and adaptive immunity, vesicular trafficking, cell differentiation, apoptosis, cellular scaffolding or bacterial invasion. Interestingly, jawless fish have variable lymphocyte receptors, which consist of repeat protein modules instead of the immunoglobulin-type antigen receptors of jawed vertebrates[8].

High-affinity target-specific DARPins with great potential in biotechnological, diagnostic or therapeutic applications can easily be generated[9]. Selected DARPins possess the high specificities and high affinities of antibodies. Unlike antibodies, DARPins do not contain disulfide bonds enabling intracellular applications[10]. DARPins are built of consecutive homologous repeats, which assemble to form elongated domains with a continuous hydrophobic core. Combinatorial libraries of DARPins were constructed and members of these libraries are generally very well expressed, monomeric in solution, highly soluble, and possess high thermodynamic stabilities[11].

DARPin phage display

The very high stability and folding properties of DARPins made it necessary to develop a novel phage display vector for their efficient display on phage particles[12]. Translocation of proteins into the periplasm of *Escherichia coli* (*E. coli*) is an intermediate step in filamentous phage assembly and using the conventional posttranslational Sec-dependent translocation pathway was found to be the bottleneck in the display of DARPins. Using the cotranslational signal recognition particle (SRP) translocation pathway resulted in up to 700-fold improved display levels of DARPins when compared to using the Sec pathway. This novel method is termed “SRP phage display”.

- The phagemid vector pMPAG3 is used for the efficient display of DARPins on filamentous phage particles (for details see Appendix data sheet: pMPAG3).

→ Phagemid vector for monovalent filamentous phage display using the minor phage coat protein p3 as fusion partner (p3-DARPin fusion protein) for display.

→ Vector providing SRP phage display functionality for the efficient display of DARPins.

→ Vector carrying a f1 origin of replication to permit production of virions using an appropriate helper phage, such as VCSM13.

→ Vector carrying a plasmid origin (ColE1) and providing resistance to chloramphenicol (cam) to allow propagation in *E. coli.*

- The provided DARPin phage display library (for details see Appendix data sheet: PD library #1) is based on pMPAG3 and contains:

→ 2.6 x 10^{10} independent chloramphenicol resistant clones of which 42% are correct DARPins, resulting in the functional library size of 1.1 x 10^{10}.

→ 25% of the clones are N3C DARPin library members.

→ 17% of the clones are N2C DARPin library members

→ 58% of the clones (non functional part of the library) had either frame shifts in the DARPin sequence or no insert at all.

Advantages of DARPin phage display

- The high functional diversity of the PD library #1 provides the essential basics that high affinity DARPins can be selected; it is expected that low nM or even pM binders will be obtained on a regular basis.
- Selected DARPins maintain their excellent target-specificity and stability independent of being tethered to a phage particle or not.

→ Selected DARPins possess a very wide potential application range, ranging form *in vitro* applications such as immunohistochemistry, over intracellular applications for target validation to *in vivo* therapeutic applications.

- Most of the selected DARPins will have the excellent biophysical properties inherent in this novel substance class.
- It is anticipated that this DARPin phage display library will be an excellent tool for the selection of DARPins for target protein binding directly on cells, on tissue or even *in vivo* (in mice).
- So far successful selections against a panel of nine target proteins ranging form the detergent-solubilized Na^+-citrate symporter CitS of *Klebsiella pneumoniae* (T. Huber et al. *J. Struct. Biol.* **159**, 206-221(2007)) to the Fc domain of human IgG1 (D. Steiner et al. manuscript in preparation).

Work flow of a selection project and selection cycle

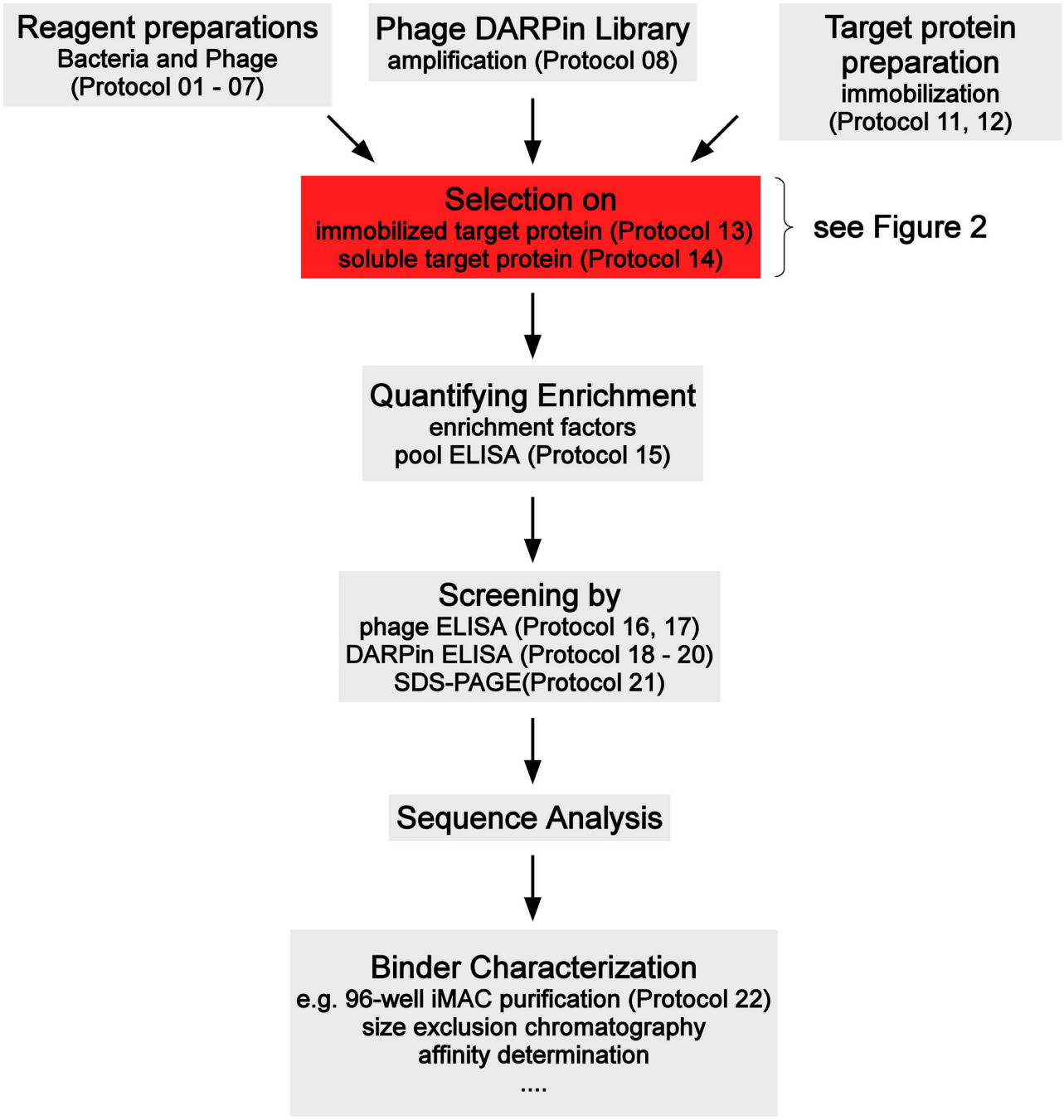

Figure 1: Work flow of a selection project

Schematic representation of the workflow of a selection project. Respective protocols found in this manual are given in parentheses.

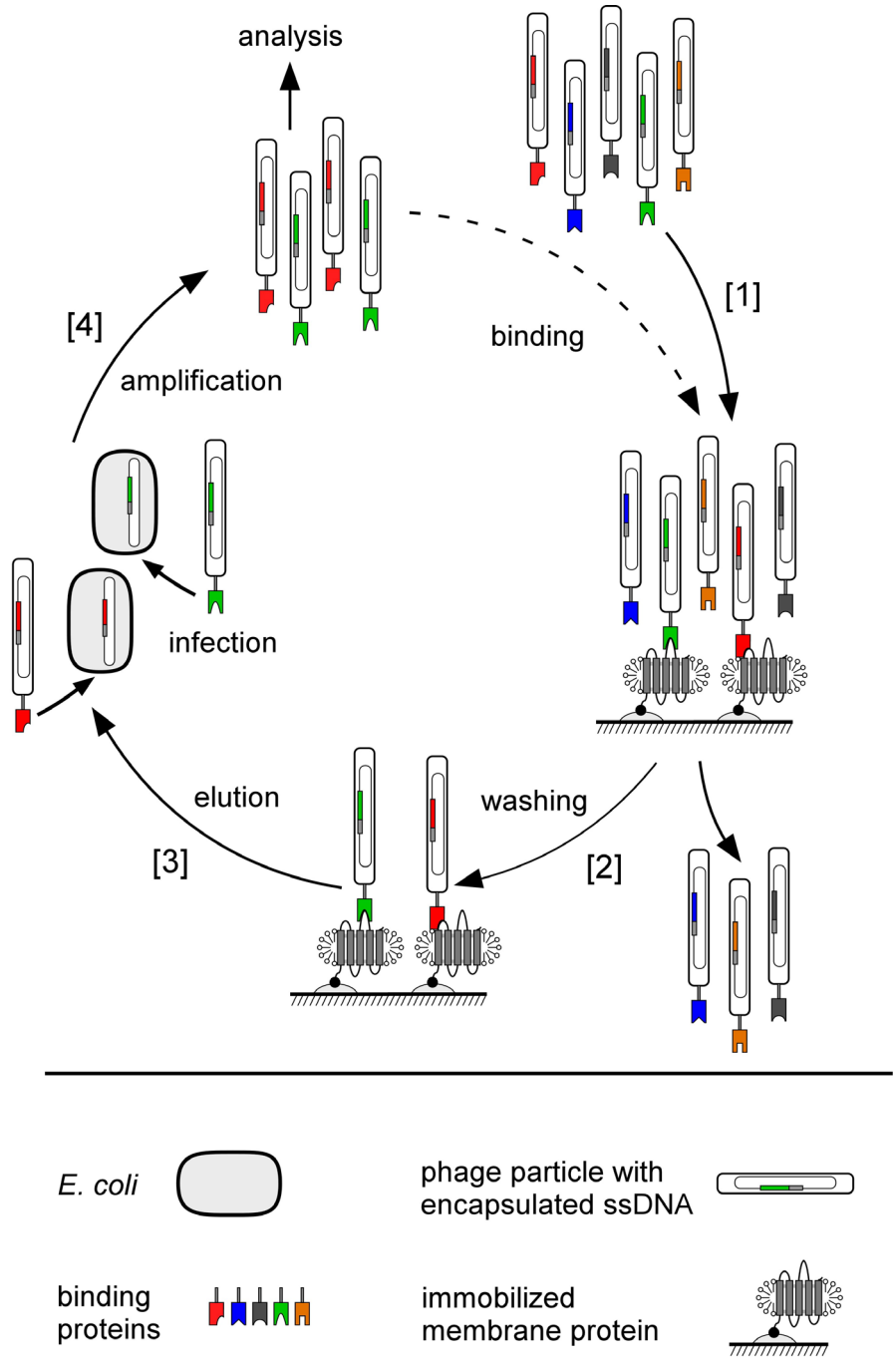

Figure 2: Work flow of a selection cycle

Schematic representation of a phage display selection cycle. A phage library displaying the proteins of interest on their surface while having the respective gene encapsulated inside the phage particle (coupling of the genotype and phenotype) is used for the binding selection on the immobilized target protein [1]. After formation of the complexes between the binding protein and the target protein (solubilised membrane protein depicted), unbound phage particles are washed off [2]. The bound phages are eluted from the immobilized target by a pH shift [3] and used for the infection of *E. coli.* Phage particles are amplified [4] and can then be analyzed or used as input for the next selection round.

General Reagents and Equipment

- For a detailed description of all equipments, reagents and solutions needed see **Materials** (p. 278 ff.)
- PD library #1 (for details see Appendix data sheet: PD library #1)
  → DARPin phage display library based on pMPAG3.
  → A procedure for repropagation of the PD library #1 is provided (**Protocol 08**).
- pMPAG3 (for details see Appendix data sheet: pMPAG3)
  → Phagemid, which was used to construct the PD library #1; may be used as a negative control phagemid.
- pMPAG6 and pDST67 (for details see Appendix data sheet: pMPAG6, pDST67)
  → Plasmids for the cytoplasmic expression of DARPins in *E. coli* (e.g. XL1-Blue).
  → pMPAG6 contains $lacI^q$, pDST67 not. Thus, pDST67 has to be used in a $lacI^q$ host background (e.g. XL1-Blue).
  → Single DARPin sequences or pools of DARPin sequences may be transferred from pMPAG3 into pMPAG6 or pDST67 using the corresponding *BamH*I and *HindIII* restriction sites (**Protocol 18**).
- Bacterial strain: *E. coli* XL1-Blue[13] (Stratagene, no 200268)
  → F' [$lacI^q$ *lacZ*Δ*M15 proAB*$^+$ Tn*10*(Tet^r)] *endA1 supE44 gyr*A96 *hsdR17 lac recA1 relA1 thi*
- VCSM13 helper phage (Stratagene, no 200251)
  → Helper phage derived from M13 K07, carries kanamycin (kan) resistance. A protocol for VCSM13 stock preparation and storage is provided (**Protocol 03**)
- Control DARPin (I_19) and control target protein (human IgG1 whole molecule)
  → DARPin I_19 binding to Fc part of human IgG1 with high affinity (K_D = 2 nM)
  → Using the phagemid pMPAG3 (I_19), phage particles displaying I_19 can be prepared which can be used as positive control in selection and phage ELISA experiments
  → Using the espression vector pDST67 (I_19) soluble I_19 can be expressed which can be used as positive control in ELISA experiments.
  → Full length human IgG1 is used as controll target protein (for immobilization and capturing see **Protocol 11**, **Protocol 12**)
- Solution for phage decontamination: Helipur (B.Braun Melsungen AG, no. 6505520)

General phage working rules

- Phage contaminations in flasks, bottles etc. may accumulate as one performs selections from phage display libraries. Precautions need to be taken throughout the protocol to **avoid any carry over of phage**. Autoclaving alone is not sufficient enough to remove all phage contamination. Ensure that all non-disposable plasticware and glassware (e.g. centrifuge bottles, shaker flasks) is completely phage free by soaking it for 3 hr in 2% (v/v) helipure solution (B.Braun Melsungen AG, no. 6505520), followed by manual washing, washing in dishwasher and then autoclaving.
- If available do all phage work in an extra “phage-room” or “phage-hood”.
- Wherever possible use disposable pipettes and **disposable plasticware**. The use of polypropylene tubes is recommended as phage may adsorb non-specifically to other types of plastic. Do all work with phage samples using a clearly labeled set of “**phage-pipettes**” and a clearly labeled “**phage waste**”.
- Use **filter tips** and “phage-pipettes” whenever working with solutions containing phage or phagemid particles.
- Be especially careful when working with highly concentrated phage particle solutions like described in **Protocol 04**.
- Wear **gloves** whenever working with phage samples, change before touching phage free equipment to keep contaminations as low as possible.
- Do not grow phage free cultures and phage cultures in the same incubator.
- **Always check log-phase *E. coli* XL1-Blue cultures for phagemid or helper phage contaminations** by antibiotic resistance (cam, kan). XL1-Bue is only tet^R. Contaminations are difficult to see because filamentous bacteriophages do not lyse the host cells but just lead to slower growth.
- Solutions containing phage must be collected. For decontamination add 2% (v/v) helipur, incubate for 24 h, autoclave and transfer to liquid waste.
- Aspirate phage containing supernatants (e.g. during selection) into filter flask containing helipure solution (Connect plastic tubing and Pasteur pipette to a filter flask).
- Remove phage solution from antigen coated wells either by aspirating or by rapidly inverting the plate over a plastic tray (decontaminate liquid as described above) followed by blotting dry on stacked paper towels (discard to phage-waste).
- Clean lab bench and hood frequently with 2% (v/v) **helipure** solution followed by water and 70% EtOH.

- Before starting a new selection clean phage free pipettes and “phage pipettes” by soaking 3 hr in 2% (v/v) helipure solution followed by extensive washing in water and 70% EtOH.
-

Bacteria, Filamentous Bacteriophage and Phagemid

Filamentous Bacteriophage:

- Most commonly, filamentous phages such as f1, M13 and fd that infect *E. coli* are used for phage display (termed Ff phages). In contrast to most other bacteriophages, filamentous phages do not lyse the host cells upon release of their progeny. The newly produced filamentous phage particles are assembled in the periplasmic membrane and continuously extruded from the cells into the culture medium, resulting in a reduced growth rate of infected cells.
- The phage coat encapsulates single stranded DNA (ssDNA) encoding 11 proteins needed for replication and assembly in the *E. coli* host cell (three for ssDNA generation, three for phage assembly and five for phage coat formation). Additionally, the replication origins for + and – strand synthesis and the packaging signal (ps) for ssDNA incorporation into the phage particles are encoded on the phage genome.

E. coli host cells

- Efficient filamentous bacteriophage infection depends on the presence of the F-pilus on the *E. coli* surface (only in F', male strains). Genetic information for F-pilus formation is contained on an F' plasmid. F-pilus expression is reduced when growing *E. coli* past log-phase and also when growing cells at temperatures below 34°C (ref. 1). Thus growth at 37°C to OD_{600} = 0.4 - 0.6 is recommended (**Protocol 01**).

Phagemid

- DARPins are displayed on phage particles by using a "**phagemid**" vector (for details see Appendix data sheet: pMPAG3). Such phagemid vectors are plasmids carrying an Ff origin and can thus be packaged into filamentous phage particles. pMAPG3 contains a gene coding for the DARPin fused to the gene of the phage coat protein 3 (p3) which is under the control of a weak promoter, a gene coding for an antibiotic resistance (cam), a plasmid origin of replication, a Ff origin of replication to allow production of single-stranded vector and a ps for encapsulation of the ssDNA into phage particles. All the information for phage replication and production is missing on phagemids.

Phage Particles

- Dependent on the DNA encapsulated one can differentiate between two types of phage particles: **helper phage particles** and **phagemid particles**.
- **Helper phage particles** (**VCSM13** is used in this manual) encapsulate helper phage ssDNA which contains all the genetic information of wild type filamentous phage M13 needed for phage replication and production. Additionally, VCSM13 carries a kanamycin resistance that allows antibiotic selection of helper phage infected cells, mutations in the ps that reduce packaging efficiency of its ssDNA and mutations that allow infection of bacteria already harboring a plasmid with Ff origin of replication (interference-resistance) [1]. (see **Protocol 02,Protocol 03**)
- **Phagemid particles** encapsulate phagemid ssDNA. To produce such phage particles *E. coli* cells harboring a phagemid need to be coinfected with **helper phage** (see above) which provides all information for phage replication and production in trans. The cells will then produce all phage proteins from the helper phage genome (large excess of wild-type-p3) as well as in a small amount phage p3 fusion protein encoded by the phagemid. Therefore, the majority of the phage particles extruded by the cell will display only wild-type-p3 (5 copies per phage particle) and less than 10% of the produced phage particles will contain one copy of the p3-DARPin fusion (phenotypic diversity, monovalent display). Because the helper phage ssDNA is poorly packaged, the majority of the phage particles will contain the phagemid ssDNA preserving the link between genotype and phenotype but all phagemid particle preparations will contain a low percentage of helper phage particles (genotypic diversity). The phagemid particles can infect *E. coli* were phagemid ssDNA is replicated as double stranded DNA without further phage replication. (see **Protocols 06, 07, 08, 09** and **10**)

Table 1: Comparison of helper phage and phagemid particles

	Phage particles	
	Helper phage particles	Phagemid particles
Encapsulated genome	helper phage ssDNA (VCSM13)	phagemid ssDNA (pMPAG3)
Packaging efficiency of encapsulated ssDNA	low	high
Infectious	yes	yes
Replicable as phage particles	yes	no (helper phage needed)
Antibiotic resistance of infected cells	kanamycin	chloramphenicol
Typical concentration in culture supernatant	~ 10^{11} pfu/ml	~ 10^{12} cfu/ml
Comments		preparations of phagemid particles do always contain helper phage particles

Protocol 01 Exponential bacterial cultures (log-phase cultures)

Comments

- This is a general protocol for the production of log-phase bacterial cultures.
- Phage infection depends on the presence of the F-pilus on the bacteria surface. F-pilus expression is reduced when growing *E. coli* past log-phase and also when growing cells at temperatures below 34°C (ref. 1). Thus growth at 37°C to OD_{600} = 0.4 - 0.6 is recommended.
- *E. coli* XL1-Blue is the preferred host for phage propagations giving high yields of page particles. Alternatively, *E. coli* TG 1 or other strains may be used (different protocols needed).
- *E. coli* XL1-Blue must be grown on agar plates and in media containing tetracycline (tet) to keep bacteria infective (tet resistance on F'-plasmid that contains genes encoding for F-pilus formation). Do always grow XL1-Blue from fresh colonies because subculturing can occasionally lead to emergence of tet resistant cells which are not infectable.
- Prepare your own glycerol stocks of *E. coli* XL1-Blue. Grow liquid culture (2YT/tet) of a single colony of *E. coli* XL1-Blue to late log phase (OD_{600} = 1 – 2), add 15% (v/v) of sterile glycerol, mix and freeze in liquid N_2. Prepare several glycerol stocks and store at -80°C and only use one at the time. Test the culture for phagemid and helper phage contaminations by plating on 2YT/tet/cam and 2YT/kan agar plates. Test as well for amp resistance and for plaque formation (**Protocol 02**). Additionally, test culture for proper infection with phagemid particles and helper phage particles (**Protocol 06**). This cumbersome procedure ensures that you are starting from a good stock of host cells necessary for the whole selection.
- It is strongly recommended to plate *E. coli* XL1-Blue from the glycerol stock in use each week on a fresh 2YT/tet agar plate.
- Test **every** *E. coli* XL1-Blue culture used during the selection for contamination by plating on a 2YT/tet/cam and a 2YT/kan agar plate.
- *E. coli* XL1-Blue at OD_{600} = 1 contains about 5 x 10^8 cfu/ml.

Equipment and Reagents (see p. 278 ff. for details)

- *E. coli* XL1-Blue
- 2YT/tet media
- 2YT/tet agar plates (round)
- 2YT/kan agar plates (round or square)
- 2YT/cam/tet agar plates (round or square)
- Culture flasks (100 ml or 300 ml)
- Culture tubes (14 ml)

Method

Day 1

1. Streak out *E. coli* XL1-Blue from your stock on a 2YT/tet agar plate and incubate overnight at 37°C. (Seal with parafilm and store plate at 4°C and use for max one week)

Day 2

2. Inoculate 5 ml of 2YT/tet media in a 14 ml culture tube with a single colony of *E. coli* XL1-Blue and grow overnight at 37°C with shaking at 220 rpm (pre-culture).

   Use medium without innoculation as negative control for medium contamination

Day 3 (log-phase culture)

3. Inoculate fresh 2YT/tet media with the pre-culture at a ratio of 1:25 to 1:200 (see below) and grow at 37°C with shaking to OD_{600} of 0.4-0.6 (log-phase culture)

   The efficiency of infection is greatly reduced above OD_{600} of 0.6. Adjust volume of log-phase culture depending on the amount needed for the experiment. Use shaker flasks without baffles. If you have problems estimating the time needed to be ready for infection, inoculate at different dilutions (see Table, e.g. 1:50, 1:100 and 1:200). This allows you to have log phase cultures for a time span of about 1.5 h (the doubling time of XL1-Blue is about 35 – 40 min).

Table 2: Inoculations for log-phase cultures

Inoculation ratio	Time to OD_{600} = 0.5
1:25	~ 1h 00 min
1:50	~ 1h 40 min
1:75	~ 2h 00 min
1:100	~ 2h 20 min
1:150	~ 2h 40 min
1:200	~ 3h 00 min

4. Use log-phase culture for the infections.
5. To check for contaminations plate 50 µl aliquots of the log-phase culture on 2YTcam/tet and 2YT/kan agar plates and incubate at 37°C overnight and 24 hours, respectively.

Day 4

6. Check 2YT/kan and 2YTcam/tet agar plates for colonies (contamination).

Titering, propagating and purifying helper phage particles

- There are two methods for determining the concentration of viable, infective helper phage particles: **titration by plaque forming units** and **titration by colony forming units**.
- **Titration by plaque forming units**: For helper phage particles, determining the concentration of viable particles involves counting phage plaques on a lawn of host bacteria (plaque forming units per ml, pfu/ml) (**Protocol 02**). Turbid plaques are visible due to the reduced growth of infected host cells. It is advisable to follow this procedure of plaque isolation whenever propagating helper phages to ensure that a pure culture of viable helper phage is obtained (**Protocol 03**).
- **Titration by colony forming units**: For helper phage particles containing an antibiotic resistance (e.g. kan for VCSM13) titration by colony forming units can be performed as described for phagemid particles (**Protocol 06**). However, this method gives only an estimate and is not recommended for accurate titration of helper phages. During recovery in solution helper phage particles that are released from host cells short time after infection will consequently re-infect other host cells. Therefore, concentration of viable particles will be strongly overestimated.
- A convenient alternative to determine the concentration phage particle preparations is the estimation by absorbance (**Protocol 05**). However, calculations based on absorbance normally overestimate the concentration of viable, infective particles by a factor 2-10.
- A typical yield of helper phage particles in the supernatant of XL1-Blue phage cultures grown in 2YT would be 10^{11}-10^{12} phage/ml.

Protocol 02 Helper Phage titration by plaque forming units (pfu)

Comments

- This is a general procedure for the titration of stocks of helper phage particles (e.g. VCSM13) to determine the concentration of infectious particles. A single plaque obtained should be used for amplification of the helper phage particles (**Protocol 03**).

Equipment and Reagents (see p. 278 ff. for details)

- Helper phage VCSM13
- *E. coli* XL1-Blue log-phase culture (**Protocol 01**)
- 2YT/cam/tet agar plates (round or square)
- 2YT/kan agar plates (round or square)
- 2YT/tet agar plate (round)
- 2YT top agar
- 50°C water bath

Method

Day 1,2

1. *E. coli* XL1-Blue plating and pre-culture (**Protocol 01**).

Day 3 (Titering of helper phage)

2. Prewarm 2YT/tet agar plates to 37°C.
3. Prepare 5 ml *E. coli* XL1-Blue log-phase culture (**Protocol 01**).
4. Perform serial dilutions of helper phage stock in 2YT media down to about 10^3-10^5 particles/ml.
5. Melt 2YT top agar by microwaving and cool to 50°C in a water bath.

   Complete melting of the top agar is essential.
6. Mix 0.01 ml of each phage dilution with 0.1 ml of log-phase XL1-Blue cells in a 14 ml tube.
7. To each tube, add 3 ml of 2YT top agar and mix carefully, but quickly.

   Avoid formation of bubbles, making plaques difficult to count
8. Immediately pour the top agar mixture evenly onto a 2YT/tet agar plate. To test for contamination do the same procedure using only log-phase XL1-Blue cells.

   If top agar is to cold, lumps will form, making plaques difficult to count.
9. Additionally, check for contamination of log-phase XL1-Blue cells by plating 50 µl on a

2YT/tet/cam and a 2YT/kan agar plate.

10. Allow the top agar to solidify at RT, and then incubate the plates at 37°C overnight.

Plaques should appear as turbid discs against a background lawn of cells.

11. Calculate the phage concentration in the original stock solution (pfu/ml) taking the serial dilutions into account.

Protocol 03 Helper Phage amplification from single plaque

Comments

- This is a procedure for propagation of helper phage particles (VCSM13) from a single plaque (**Protocol 02**).

Equipment and Reagents (see p. 278 ff. for details)

- 2YT/tet agar plate containing well separated single plaques (**Protocol 02**).
- *E. coli* XL1-Blue log-phase culture (**Protocol 01**)
- PBS-G (PBS containing 10 % v/v glycerol)
- 2YT/kan media
- 2YT/cam/tet agar plates (round or square)
- 2YT/kan agar plates (round or square)

Method

Day 1,2

1. *E. coli* XL1-Blue plating and pre-culture (**Protocol 01**).

Day 3 (Phage amplification from single plaques)

2. Prepare *E. coli* XL1-Blue log-phase culture (**Protocol 01**).
3. Pick a single isolated plaque using a sterile Pasteur pipette and add it to 1 ml of log phase XL1-Blue cells.
4. Check for contamination by plating 50 µl log-phase XL1-Blue cells on a 2YT/tet/cam and a 2YT/kan agar plate.
5. Incubate for 1 h at 37°C with shaking.
6. Dilute the cells into 25-1000 ml of 2YT/kan media.

   Volume dependent on amount of helper phage needed for the planed selection experiments (Can be stored for several months at -80°C). Use flasks without baffles.
7. Incubate the culture for 12-15 h at 37°C with shaking.
8. Precipitate and purify the helper phage as described in **Protocol 04.** Resuspend the phage in ~ 1:20 of culture volume PBS-G to a final concentration of about 10^{13} phage/ml (OD_{269} = 1.0 for a solution containing 5 x 10^{12} phage/ml).

9. For long term storage freeze small aliquots of helper phage in liquid N_2 and store at -80°C.

Helper phage stocks can be stored at 4°C for several weeks.

10. Determine the phage titer (**Protocol 02**) of a thawed helper phage sample (pfu/ml) and use this value for the selections. Test helper phage stock for phagemid contamination by plating infected cells on 2YT/tet/cam agar plate.

Protocol 04 Phage precipitation and purification

Comments

- This is a general procedure for the precipitation of helper phage and phagemid particles from cell culture supernatants.
- Typically, culture supernatants from XL1-Blue phage cultures grown in 2YT yield about 10^{11}-10^{12} phage/ml.
- This procedure is used to produce concentrated working stocks of helper phage particles (**Protocol 03**), stocks of phagemid particles (**Protocol 07**), phage library stocks (**Protocol 08**) and DARPin displaying phagemid particles during selection cycles (**Protocol 09** and **Protocol 10**) from the supernatant of respective cell cultures.
- To avoid contaminations with phage particles be especially careful when working with such highly concentrated phage particle solutions (see General Phage Working Rules p.201)

Equipment and Reagents (see p. 278 ff. for details)

- Cell culture containing helper phage or phagemid particles (**Protocol 03, 08, 11** and **12)**
- Polypropylene tubes (50 ml)
- Micro tubes (2 ml)
- PBS
- PBS-G
- PEG/NaCl (5x)

Method

Day 1

1. Centrifuge the culture containing phage particles for 10 min at 16'000g and 4°C.

   *If volume is not too large use 50 ml disposable tubes. You can also centrifuge for 15 min at 5'600 g and 4°C. This way you will have more cell debris in the supernatant which will be removed in **Step 4**.*

2. Transfer supernatant to a fresh tube and add 1/4 volume of ice cold PEG/NaCl (5x) solution (2 ml to every 8 ml culture supernatant) to precipitate phage. Incubate for 1 hour on ice.

   If the culture supernatant contains about $10^{11\text{-}12}$ phage/ml, precipitating phage will immediately be visible as turbid clouds after addition of the PEG/NaCl (5x) solution. For

phage samples with higher concentrations, 10 min incubation on ice can be sufficient to precipitate most of the phage particles. Longer incubation on ice (up to 12 h) will help to precipitate phage from less concentrated culture supernatants.

3. Centrifuge in a swing rotor for 15 min at 5'600g and 4°C. Decant the supernatant. Respin briefly and remove the remaining supernatant with a pipette.

It is important not to spin phage too fast, as they will be difficult to resuspend, and phage titer will decrease.

4. Resuspend phage pellet in 1/20 of the initial culture supernatant volume PBS-G using a pipette. Transfer into sterile 2 ml tubes. For complete resuspension incubate the phage solution on an orbital shaker at 800 rpm for 15 min at 4°C. Pellet insoluble matter (cell debris) by centrifugation for 10 min at 11'000g and 4°C.

Phage particles start to precipitate at concentrations higher than 10^{14} phage/ml

5. Transfer the supernatant to a clean tube and estimate the phage concentration by absorbance (**Protocol 05**)

6. Titrate helper phage or phagemid particles on XL1-Blue cells to determine the concentration of infectious phage particles (pfu or cfu) as described in **Protocol 02** and **Protocol 06**.

Ideally, the concentrated phage stock will have concentrations 10^{12-13} cfu/ml.

7. VCSM13 helper phage and phagemid particles may be kept at 4°C for days. Nevertheless, it is advisable to aliquot them and store them at -80°C after flash freezing in liquid nitrogen.

Protocol 05 Estimating of phage concentrations by absorbance

Comments

- Adapted form protocol by G. Smith, based on calculations done by Day et al. [14]
- This is a procedure for estimating the concentration of phage particles by absorbance. However, calculations based on absorbance normally overestimate the concentration of viable, infective particles by a factor 2-10.
- Unlike icosahedral phage like T4 and λ, which have roughly equal weight ratios of protein to DNA, filamentous phage have about 6 times more protein than DNA; the protein therefore contributes substantially to the absorption spectrum, accounting for the broad plateau at 260–280 nm, with a shallow maximum at 269 nm.

Equipment and Reagents (see p. 278 ff. for details)

- purified filamentous phage sample (**Protocol 04**)
- PBS-G

Method

Day 1

1. Measure UV absorption spectrum of purified filamentous phage sample (**Protocol 04**) dissolved in PBS-G, which also serves as the blanking solution in the reference cuvette.

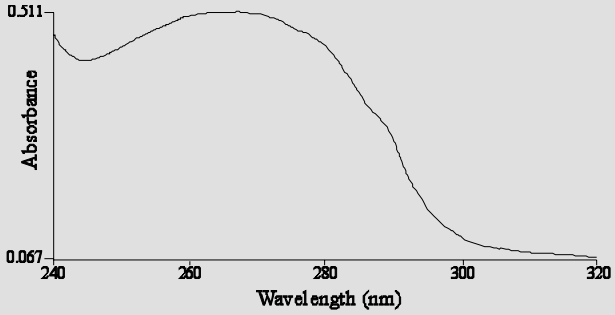

Figure 3: UV absorption spectrum of purified filamentous phage sample: Ideally, OD_{269} should be slightly higher than OD_{260}. To high OD_{260} indicate the presence of DNA debris in the sample. This calculation often overestimates the amount of infectious phage particles by a factor of 2-10.

2. Calculate the concentration of phage in virions/ml from the difference between A_{269} and

A_{320} as follows:

$$\text{virions/ml} = \frac{(A_{269} - A_{320}) \cdot 6 \times 10^{16}}{\text{number of bases/phage or phagemid particle}}$$

(VCSM13 = ~12’500 bases, pMPAG3_N3C = ~ 4’500 bases)

Titering and propagating phagemid particles

- It is important that whenever working with bacteria harboring the phagemid pMPAG3 the chloramphenicol concentration should not be above the recommended 10 μg/ml. Higher concentrations will strongly reduce transformation and infection efficiency, phagemid particle production and growth of host bacteria.
- After transformation or infection with phagemid pMPAG3 recovery in non-selective media for 1 h is essential before plating on or growing in selective media to allow accumulation of the resistance conferring protein (CAT).
- For more complete suppression of the lac-promoter of pMPAG3 under non-induced conditions, 1% glucose is added to all agar plates used.
- Determining the concentration of viable phagemid particles involves infection of bacteria and counting of resulting antibiotic-resistant colonies (colony forming units per ml, cfu/ml) (**Protocol 06**).
- Due to the lack of the genes (on phagemids) needed for replication as phage particles, titering for plaque forming units (**Protocol 02**) cannot be applied for phagemid particles.
- Each phagemid particle preparation will contain helper phage particles. In theory, the reduced efficiency of the helper phage packaging signal should significantly reduce the number of helper phage particles in any phagemid preparation. However, the number of helper phage can sometimes equal, or exceed, the number of phagemid particles, which can significantly compromise subsequent selections[15]. We never observed such excessive numbers of helper phage particles in our phagemid particle preparations. Nevertheless, we recommend when titering phagemid particle preparations for cfu on cam agar plates always to titer for helper phage particles on kan agar plates in parallel. The ratio of cfu (kan) to cfu (cam) should be below one (concentration of viable helper phage particles will be strongly overestimated (for explanation see p. 209)).
- A convenient alternative to determine the concentration of phage or phagemid particle preparations is an estimation of concentrations by absorbance (**Protocol 05**). However, calculations based on absorbance normally overestimate the concentration of viable, infective particles.
- Different protocols for the amplification phagemid particles will be given in this manual:
  - → **Protocol 07**: Amplification of monoclonal phagemid particles
  - → **Protocol 08**: Amplification of a library of phagemid particles

→ **Protocol 13, 14**: Two methods for the amplification of a polyclonal selection output of phage paritlces

→ **Protocol 16**: Amplification of monoclonal phagemid particles in a 96-well format for screening

- General information for the production of DARPin-displaying phagemid particles:
  → IPTG induces the expression of the p3-DARPin fusion protein and thus ensures their display (0.2 mM IPTG is sufficient for full induction).
  → Coinfection with helper phage VCSM13: There is no need to add kan to select for helper phage coinfected cells since helper phage particles are provided in excess over cells (>20 x multiplicity of infection). Addition of kan reduces cell growth and phage particle yield (In case of kan addition add final concentration of 12.5 µg/ml one hour after VCM13 addition. Not recommended.)
- A typical yield of phagemid particles in the supernatant of XL1-Blue phage cultures grown in 2YT would be 10^{11}-10^{12} phagemid particles/ml.

Protocol 06 Phagemid titration by colony forming units (cfu)

Comments

- This is a procedure to determine the phagemid or helper phage titers in terms of colony forming units (cfu) of a phage solution by counting the number of infectious phage particles either containing the phagemid or the helper phage genome, respectively.
- For helper phage (VCSM13), values obtained can vary strongly with the time of recovery in solution (helper phages will be propagated from infected cells short time after infection).

Equipment and Reagents (see p. 278 ff. for details)

- *E. coli* XL1-Blue log-phase culture (**Protocol 01**)
- Phagemid particle solution to be titrated
- 96-deep well plate
- 2YT/tet/cam agar plates (square)
- 2YT/kan agar plates (square)

Method

Day 1,2

1. *E. coli* XL1-Blue plating and pre-culture (**Protocol 01**).

Day 3

2. Prewarm 2YT/tet/cam and 2YT/kan agar plates to 37°C.

   Keep lid ajar to allow plates to dry.
3. Prepare *E. coli* XL1-Blue log-phase culture (**Protocol 01**).
4. Perform serial dilutions of phagemid particles in 2YT media down to about 10^3-10^5 phage/ml.

   *See below for 96-well plate titration and recommended dilutions for a phage sample prepared in **Protocol 04**.*
5. For each phage dilution, mix 0.1 ml of phage with 0.9 ml of log-phase XL1-Blue cells.
6. Incubate for 1 h at 37°C with shaking.

   Incubation for 1 h is essential before plating on selective media to allow accumulation of the resistance conferring proteins
7. Plate on 2YT/tet/cam (phagemid) or 2YT/kan (helper phage) agar plates.

By dispensing 10 µl of each sample onto the upper part of sloped (~ 45°) 2YT agar plates. The applied 10 µl drop should slowly run down the plate, but not reach its bottom. A maximum of 12 samples can be applied per square plate.

8. Check log-phase XL1-Blue cells for contamination by plating 10 µl on a 2YT/tet/cam and a 2YT/kan agar plate as described in **Step 7**.
9. Incubate plates overnight at 37°C.

   Incubation of up to 24 h is needed for the 2YT/kan (helper phage) agar plates. Sometimes, smaller and larger colonies can be observed on 2YT/kan agar plates (no reason for concern).
10. Count colonies at an appropriate dilution and calculate cfu/ml for each phage, phagemid solution.

    *Drops applied in **Step 7** should result in a lane of colonies that can be counted.*

11. If you have multiple samples to be titrated, serial dilutions may be performed in 96-deep well plates using a multichannel pipette. Clean pipette tips must be used for each dilution step.

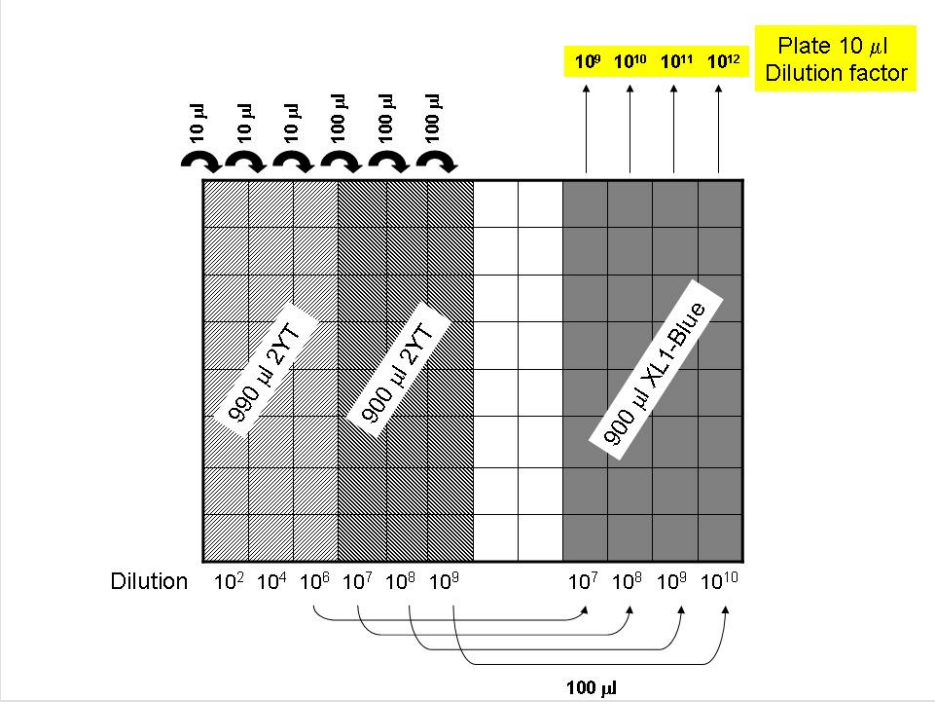

Figure 4: 96-well plate titration

96-well plate titration and recommended dilutions for a phage particle sample prepared in **Protocol 04**. (dilutions for initial phage particle concentrations ranging from 10^{10} to 10^{13} cfu/ml)

Protocol 07 Phagemid particle amplification from single colonies

Comments

- This protocol allows the medium scale production of individual phagemid clones in a 50 ml scale and should yield about 50 ml of supernatant containing 10^{11}-10^{12} cfu of phagemid particles per ml which can then be further purified as described in **Protocol 04**.

Equipment and Reagents (see p. 278 ff. for details)

- VCSM13 helper phage stock (**Protocol 03**)
- 2YT/cam/tet agar plates with plated cells harboring the phagemid to be analyzed (**Protocol 06**)
- 2YT/tet/cam media
- 2YT/tet/cam/Glu media
- IPTG
- Culture tubes (14 ml)
- Culture flasks, non-baffled (300 ml)

Method

Day 1

1. Inoculate 5 ml of 2YT/tet/cam/glu with a single colony of *E. coli* XL-1 Blue harboring the phagemid to be analyzed. Grow overnight at 30°C with shaking.

Day 2

2. Inoculate 5 ml of fresh 2YT/tet/cam with the overnight cultures at a ratio of 1:100 (OD_{600} = 0.04 - 0.06) and grow at 37°C to an OD_{600} of 0.5 with shaking (2-3 hours).
3. Dilute cells 1:10 in prewarmed 50 ml fresh 2YT/tet/cam containing IPTG at 0.22 mM and 10 minutes later add VCSM13 helper phage to a final concentration of 10^{10} pfu (plaque forming units) per ml and grow overnight at 37°C with shaking.

   Do not grow more than 16 h.

Day 3

4. Final cell density obtained should be between OD_{600} = 3-6. Precipitate and purify the phagemid particles displaying DARPins as described in **Protocol 04**. Resuspend in PBS-G (~ 1:20 of cell culture volume) or buffer needed for further experiments to a final concentration of about 10^{13} phage/ml.
5. Determine concentrations of viable phagemid particles by titration on *E. coli* XL1 Blue

(**Protocol 06**) or estimate concentrations of phage particles by UV absorption (**Protocol 05**).

6. The phagemid solution may be used directly or can be stored at 4°C for several days or at -80°C (flash freeze in liquid nitrogen) for several years.

Protocol 08 Phage library repropagation

Comments

- This protocol is optimized for the DARPin PD library #1 and allows their repropagation to produce fresh DARPin displaying phage particles that can be used immediately in selection experiments. Alternatively, the repropagated DARPin PD library may be stored at -80°C for later use.
- This protocol is sufficient for libraries with diversities less than 1×10^{11} to ensure that diversity of the library is not reduced during amplification.
- Phagemid particles displaying functional DARPins can be stored in an infectious state at -80°C for years. The functionality of the displayed DARPins is not expected to decrease under these storage conditions. Therefore, it is recommended to prepare large library stocks of displaying phage particles which can be tested for functionality and then be used for further selections.
- Fresh stocks of the library should always be prepared form the primary library by repropagation in *E. coli*.
- It is important that the number of repropagated unique phagemid particles is higher or at least equal to the size of the primary library.
- It is important to test the amplified library for functionality:
  → Quantify cfu and pfu of the new phage library stock
  → Analyze display levels of DARPins by Western-Blotting as described by Steiner et al. [12]
- When doing the first selection with the new phage library stock include control target protein for which fast and good enrichment of specific binders after two to three rounds is known (e.g. control target *human* IgG1_Fc). In parallel perform identical selection rounds using an old batch of the library as positive controll.

Equipment and Reagents (see p. 278 ff. for details)

- Primary DARPin PD library #1stock
- VCSM13 helper phage stock (**Protocol 03**)
- *E. coli* XL1-Blue log-phase culture (**Protocol 01**)
- PBS-G
- 2YT/tet media
- 2YT/tet/cam media
- IPTG
- 2YT/tet/cam agar plates
- 2YT/kan agar plates

Method

Day 1,2

1. Determine the infectivity titer of the phage library stock (**Protocol 06**).
2. *E. coli* XL1-Blue plating and pre-culture (**Protocol 01**).

Day 3

3. Prepare 400 ml of *E. coli* XL1-Blue log-phase culture (**Protocol 01**).

   Ideally, use a 2 l non-baffled flask with shaking at 200 rpm (shaking radius 50 cm).This corresponds to a total of about 1 x 10^{11} cells (E. coli XL1-Blue at OD_{600} = 1 contains about 5 x 10^{8} cfu/ml). Check for contamination of log-phase XL1-Blue cells by plating on a 2YT/tet/cam agar plate and a 2YT/kan agar plate.
4. Add 1 x 10^{11} infective phagemid particles (cfu) of the library stock and incubate at 37°C for 30 min without shaking.
5. Incubate the culture at 37°C for an additional 30 min with shaking. Remove a small aliquot to determine the efficiency of infection by titering 10 µl of 10^{-4} to 10^{-6} dilutions on selective media (2YT/cam/tet and 2YT/kan agar plates).
6. Transfer 100 ml culture to each of four 5 l flasks containing 1 l of 2YT/tet/cam media and incubate at 37°C to an OD_{600} = 0.5.

   Ideally, use a 5 l non-baffled flask with shaking at 200 rpm (shaking radius 50 cm).
7. Add IPTG to 0.2 mM and VCSM13 helper phage to 10^{10} phage/ml and grow overnight at 37°C with shaking.

   Do not grow for more than 16 hours.

Day 4

8. Final cell density obtained should be between OD_{600} = 3-6. Precipitate and purify the phage particles displaying DARPins as described in **Protocol 04**. Resuspend the phage in PBS-G (1:20 of culture volume) to a final concentration of about 10^{13} phage/ml.

   The protocol yields 200 ml of repropagated library phage stock.
9. The library phage stock may be used directly in phage selection experiments. For storage, aliquot, flash freeze in liquid nitrogen and store at -80°C.
10. Determine the phage titer (**Protocol 06**) of a thawed library phagemid sample (cfu/ml) and use this value for the selections.
11. After thawing, the DARPin-displaying phage particles should be used immediately in

phage selection experiments.

12. Perform test experiments with repropagated library as described in the introduction of this chapter.

Protocol 09 "In solution-amplification" of selection output

Comments

- After each round of selection the eluted pool of phage particles is amplified prior to the next round of selection by passage through *E. coli*.
- In order to maintain diversity use an excess of log-phase XL1-Blue over eluted phage particles to amplify each individual member of the eluted pool. This is most critical for the first selection round.
- "**In solution-amplification**": Amplification of the polyclonal phage particles eluted from a selection round can be done by directly growing the infected cells in selective liquid media, followed by infection with helper phage and subsequent phage production. This procedure allows performing a selection round each 24 hours. The potential risk when applying this method is, that, due to growth advantage or disadvantage, not every clone will be identically amplified and, therefore, the selection biased. Although we never observed any negative effects of direct "In solution-amplification" they can not be completely excluded. We recommend this method since we successfully selected binders against more than nine different target proteins by using direct "In solution-amplification".
- Alternatively, plate cells on large 2YT/tet/cam agar plate for "On plate-amplification" as described in **Protocol 10**.

Equipment and Reagents (see p. 278 ff. for details)

- Helper phage VCSM13 (stock from **Protocol 03**)
- *E. coli* XL1-Blue log-phase culture (**Protocol 01**)
- 2YT/tet/cam media
- 2YT/tet/cam agar plates (square)
- 2YT/kan agar plates (square)

Method

1. To each 100 µl neutralized eluate from the respective selection round (**Protocol 13** or **Protocol 14**), add 1 ml of the *E. coli* XL1-Blue log-phase culture.

   Dilute the eluate in at least 10-times larger volume of the log phase culture to guarantee proper infection.

2. Incubate the culture for 30 min at 37°C without shaking and 30 min at 37°C with shaking.

   If 50 ml polypropylene tubes are used, allow sufficient oxygen supply by not closing the

lid completely and fixing it with tape.

3. For monitoring enrichment and for controlling proper infection, the phagemid titers of the eluate should be determined by plating 10 µl of 10^{-1} to 10^{-4} dilutions (first selection round) and 10^{-2} to 10^{-5} dilutions (later selection rounds) of the culture on 2YT/tet/cam and 2YT/kan agar plates.

   For the first round 10^4 - 10^7 and for later rounds 10^5 – 10^9 eluted phagemid particles are expected. Check for contamination by plating 10 µl of log-phase XL1-Blue cells on a 2YT/tet/cam and a 2YT/kan agar plate.

4. Dilute infected cells 1:10 in prewarmed fresh 2YT/tet/cam (results in OD_{600} of about 0.1) and incubate in a non-baffled shaker flask at 37°C with shaking for 4-5 hours.

   The infected cells are grown in solution in the presence of chloramphenicol to select against uninfected and helper phage containing cells. During the recovery of 4-5 hours the cells infected with a phagemid will divide without producing phage particles. With the low amount of phages eluted in the first selection round (possibly also later rounds) it would take the culture very long to reach log-growth phase (OD_{600} = 0.5) where helper phage co-infection is done normally, nevertheless monitor OD_{600} of the culture.

5. Add IPTG to 0.2 mM and 10 minutes later VCSM13 helper phage to 10^{10} pfu/ml and grow overnight at 37°C with shaking.

   Do not grow for more than 16 hours.

Day 2

6. Final cell density obtained should be between OD_{600} = 3-6. Precipitate phage particles as described in **Protocol 04** and continue with selection (**Protocol 13** or **Protocol 14**).

Protocol 10 "On plate-amplification" of selection output

Comments

- After each round of selection the eluted pool of phage particles is amplified prior to the next round of selection by passage through *E. coli*.
- In order to maintain diversity use an excess of log-phase XL1-Blue over eluted phage particles to amplify each individual member of the eluted pool. This is most critical for the first selection round.
- "**On plate-amplification**": For the amplification of the polyclonal phage particles eluted from a selection round the infected cells can be plated and grown on selective agar plates. Provided that the cells are plated at low density this approach allows each cell to grow individually without growth competition. On the second day colonies are eluted from the agar plate and used as inoculum for a phage producing culture. The much lower number of cell cycles in liquid culture of the "On plate-amplification" protocol compared to "In solution-amplification" protocol should reduce the influence of growth advantage or disadvantage of certain clones.
- Alternatively, grow cells in solution "In solution-amplification" as described in **Protocol 09**.

Equipment and Reagents (see p. 278 ff. for details)

- Helper phage VCSM13 (stock from **Protocol 03**)
- *E. coli* XL1-Blue log-phase culture (**Protocol 01**)
- 2YT/tet/cam media
- 2YT/tet/cam agar plates (square)
- 2YT/kan agar plates (square)
- 2YT/tet/cam agar plate (large)
- 2YT/tet/cam/G media
- Cell scrapers

Method

Day 1

1. To each 100 µl neutralized eluate from the respective selection round (**Protocol 13** or **Protocol 14**), add 1 ml of the *E. coli* XL1-Blue log-phase culture.

   Dilute the eluate in at least 10-times larger volume of the log phase culture to guarantee proper infection.

2. Incubate the culture for 30 min at 37°C without shaking and 30 min at 37°C with shaking.

   If 50 ml polypropylene tubes are used, allow oxygen supply by not closing the lid completely and fixing it with tape.

3. For monitoring enrichment and for controlling proper infection, the phagemid titers of the eluate should be determined by plating 10 µl of 10^{-1} to 10^{-4} dilutions (first selection round) and 10^{-2} to 10^{-5} dilutions (later selection round) of the culture on 2YT/tet/cam and 2YT/kan agar plates.

   For the first round 10^4 - 10^7 and for later rounds 10^5 – 10^9 eluted phagemid particles are expected. Check for contamination by plating 10 µl of log-phase XL1-Blue cells on a 2YT/tet/cam and a 2YT/kan agar plate.

4. Spin down the culture of **Step 2** at 3'300 g for 10 min, resuspend the pellet of cells in 1 ml of 2YT and spread on a large 2YT/tet/cam agar plate. Incubate at 37°C overnight.

   Growth of the infected cells on agar plates in the presence of chloramphenicol allows each colony to grow individually without any growth competition with other clones However, colonies can be quite heterogeneous in size, resulting in different numbers of cells for individual clones.

Day 2

5. Add 10 ml of 2YT/tet/cam/G media to the plate resuspend the colonies with a cell scraper and incubate the eluted cells with shaking at 1'000 rpm for 15 min at 4°C to obtain a homogenous cell suspension. Measure OD_{600} of the cell suspension and inoculate 10 ml of 2YT/tet/cam with a calculated amount of cell suspension to yield an OD_{600} = 0.05 - 0.1. Grow cells at 37°C with shaking to an OD_{600} = 0.5 (takes ~ 2 hours). Expand 5 ml of the culture into 50 ml fresh prewarmed 2YT/tet/cam containing 0.22 mM IPTG and 10 minutes later add VCSM13 helper phage to a final concentration of 10^{10} pfu (plaque forming units) per ml and grow overnight at 37°C with shaking.

   Procedure described above is sufficient to amplify phages from about 2 x 10^7 individual colonies (>10-fold oversampling). If more than 2 x 10^7 individual colonies were plated the protocol should be upscaled (e.g. use 5-fold larger volumes for 10^8 individual colonies). Do not grow more than 16 h.

Day 3

6. Final cell density obtained should be between OD_{600} = 3-6. Precipitate phage particles as described in **Protocol 04** and continue with selection (**Protocol 13** or **Protocol 14**).

Target Presentation

- Throughout the whole selection procedure it is very important to fix parameters like buffer composition, temperature, target presentation,…in order to guarantee target presentation in its native state. Only then successful selections of binders against epitopes present on native target protein can be enriched. Phage particles and DARPins are stable in most buffers (also containing detergents) and over a wide range of temperatures.
- Targets for the phage display selections can be presented in many different ways. Mostly the purified target protein is immobilized but binding selections can also be performed on whole cells or even in vivo.
- The quality and purity of the target protein will strongly influence the selection.
- Many different methods for immobilization and capturing can be applied. The most important point is to keep the target protein in its native conformation during the whole selections process.
- The majority of phage display selections are done on target protein immobilized on a solid support or on target protein in solution which is subsequently captured.
- The lower the additional amount of components needed for immobilization the lower the chance to enrich binders directed against these components and not your target protein (e.g. immobilization via antibodies binding your target protein or an affinity tag)
- We strongly recommend the immobilization or capturing of biotinylated target protein via biotin binding proteins (NeutrAvidin, streptavidin). This method allows presentation of native target protein and almost irreversible immobilization or capturing.
- Biotinylated target protein can be used for selection on immobilized target protein (**Protocol 13**) or selection on soluble target protein (**Protocol 14**)
- Protocols for chemical biotinylation (**Protocol 11**) and immobilization of biotinylated proteins (**Protocol 12**) are described.
- Alternatively, proteins can be enzymatically biotinylated using an Avi-tag as described by Cull and Schatz[16] and Scholle [17] or other methods for site specific biotinylation[18].

Protocol 11 Chemical biotinylation of target proteins

Comments

- This protocol describes the chemical biotinylation of a target protein. This procedure is recommended to immobilize the target protein in a native conformation for most efficient binding and selection of DARPins.
- Biotin is linked to the exposed amino groups of the target protein by acylation with a biotinylating reagent. N -Hydroxysulfosuccinimide (Sulfo-NHS) efficiently reacts with primary amines and is coupled to the biotin moiety by a variable linker (e.g. NHS-LC-Biotin, Pierce).
- Once the biotins are attached, the modified proteins can be immobilized on solid supports (**Protocol 12**) or be captured from solution (**Protocol 14**).
- For storage of the biotinylation reagents and additional information see the manufacturer's instructions (Pierce).
- The amount of biotinylation is a very critical point for the selection. Optimal would be a single biotin attached to each protein. A too high degree of biotinylation leads to the blocking of epitopes or even the inactivation of the protein. On the other hand, incomplete biotinylation leads to an unconjugated fraction of the protein which is not accessible for capturing or immobilization. In "selection on immobilized target protein" (**Protocol 11**), unconjugated protein should not interfere as long as the streptavidin-, NeutrAvidin-coated tube or well is charged with an excess of biotinylated protein and carefully washed. In "selection on soluble target protein" (**Protocol 12**), reaction of target phage with unconjugated protein (making a complex that cannot be subsequently "captured" on streptavidin-coated beads) competes against reaction with conjugated protein (making a complex that can be captured); if target phage are limiting, this side-reaction can reduce the yield. This reduction in yield is most problematic in the first selection round but in most cases, however, not severe enough to interfere noticeably with affinity selection.
- The use of a 20-fold molar excess of biotinylating agent relative to an antibody molecule leads to the incorporation of approximately 6 biotin moieties per protein molecule. Such antibodies are effective in biopanning. Some proteins other than antibodies-particularly low-molecular-weight proteins may be inactivated by such high-level of biotinylation (blocking of epitopes by the biotin moiety). If you are uncertain, it may be advisable to biotinylate to a lesser extent. For example, we biotinylated *human* IgG1 Fc (amino acid P100 - K330) and Her2 (amino acid S1 - N509) by using a 4- respectively 6-fold molar

excess of biotinylating agent still getting good results for the selections.

- Test the biotinylated protein by ELISA or Western blotting. A good possibilty to quantify the percentage of protein having a biotin moiety attached is a pull down experiment using streptavidin-coated beads followed by western blotting. Detect protein in the supernatant, wash and elution fraction with streptavidin-AP conjugate and additionally, with an antibody directed against target protein or tag of the protein. For quantitation of biotinylation the EZ™ Biotin Quantitation Kit (HABA assay; Pierce) can be used, but concentrations of biotinylated target protein are mostly below the detection limit of the assay.
- Biotinylated control target protein (human IgG1 whole molecule)

Equipment and Reagents (see p. 278 ff. for details)

- EZ-Link Sulfo-NHS-LC-Biotin or EZ-Link Sulfo-NHS-ss-Biotin
- Dialyis tubing MWCO 3’500 kDa
- Nap 5 columns
- PBS (4°C)
- Streptavidin-AP conjugate
- antibody directed against target protein or tag of the protein

Method

All steps should be performed at 4°C using cold buffers. When working with low protein concentrations (< 0.5 mg/ml) use siliconized labware to store protein eluates to avoid losses due to hydrophobic interactions.

1. Prepare protein in PBS or other amine-free buffer at pH 7.2 – 8.0.

   The buffer should contain no primary or secondary amines or other groups that might react with the reagents, other than those on the protein itself. Proteins in Tris or other amine-containing buffers must be exchanged into a suitable buffer (use Nap 5 column as described in the supplier’s manual and elute protein with only 0.9 ml of PBS.)

2. Measure UV spectrum and calculate protein concentration.
3. Based on the target protein concentration and the sample volume calculate the amount of 2 mM solution of the biotinylating reagent which is needed to get a x-fold molar excess of biotinylating reagent relative to the protein.

   Only a fraction of the biotinylating reagent will react with your protein due to hydrolysis and, therefore, inactivation of the NHS group. The excess of biotinylating reagent nevertheless determines the degree to which your protein is biotinylated (see comments).

4. Remove the vial of biotin reagent from freezer and equilibrate it to room temperature before opening. Immediately before use, prepare a 2 mM solution of the biotin reagent: e.g. for EZ-Link Sulfo-NHS-LC-Biotin add 800 µl of PBS to 1 mg of reagent.

5. Quickly add the appropriate calculated volume (**Step 3**) of 2 mM biotin reagent solution to the protein solution and incubate reaction on ice for two hours.

6. Carefully remove excess of non-reacted and hydrolyzed biotin reagent that remains in the solution. First use a Nap 5 column as described in the suppliers manual and elute protein with 1 ml of PBS. Then dialyze eluate twice against 200-fold volume of PBS (MWCO of 3'500 kDa of the dialysis tubing is sufficient to remove biotin reagent.)

   Complete removal of free biotin is essential for successful selections

7. Measure UV spectrum and calculate protein concentration.

8. For storage at -80 °C add 10% (v/v) glycerol, sterile filter protein solution (0.22 µm), aliquot and freeze in liquid N_2.

9. The degree of biotinylation of the target protein should be controlled as described in the comments.

Protocol 12 Immobilization (Coating of plates and tubes)

Comments

- This protocol describes the native immobilization of a target protein in MaxiSorp 96-well plates or MaxiSorp Immunotubes by using a biotin moiety attached to the target. It is recommended to immobilize the target protein in its native conformation for most efficient binding and selection of DARPins.
- Different biotin-binding proteins can be used for the immobilization of biotinylated proteins: NeutrAvidin a deglycosylated form of avidin with low background binding or Streptavidin, a on the primary structure level unrelated protein, isolated from Streptomyces avidinii.
- Alternatively, a target protein may directly be coated to plastic surfaces. This leads to partial denaturation of the target. Nevertheless, there may be still enough native epitopes present allowing efficient DARPin binding. For this purpose you can use the protocol as described below and directly coat your target protein instead of NeutrAvidin.
- Cover the 96-well plates during all incubations steps with a lid or an appropriate plastic seal.
- For ELISA, appropriate positive and negative control should be included. (control target protein IgG1 can be directly immobilized or biotinylated as described in **Protocol 11** and then immobilized via biotin-binding proteins)
- Immobilize control target protein (human IgG1 whole molecule)

Equipment and Reagents (see p. 278 ff. for details)

- MaxiSorp Immunotubes
- Stoppers for Immunotubes
- MaxiSorp 96-well plate
- Tween20 (25%)
- PBS
- NeutrAvidin (300 x) or alternatively Strp (300 x)
- PBS-T
- PBS-TB
- Shaker for 96-well plates
- Equipment for end-over-end rotation

Method

Instructions for Immunotubes are given in brackets.

Day 1

1. Coat a MaxiSorp 96-well plate with 0.1 ml per well of 66 nM NeutrAvidin (4 μg/ml, 1:300 dilution of NeutrAvidin (300x) stock solution) in PBS overnight at 4°C. (for MaxiSorp Immunotubes, use 4 ml of 66 nM NeutrAvidin, incubate standing upright)

The amount of NeutrAvidin in solution is sufficient for maximum high density coating of MaxiSorp material. Alternatively, incubate for 1 h at RT. NeutrAvidin may be substituted by streptavidin (alternated use is recommended for the selection on plates, ***Protocol 13****)*

Day 2

2. Empty the plate and blot it dry on stacked paper towels. Add 300 μl/well of PBS-TB blocking buffer and incubate the plate at room temperature (RT) with orbital shaking (900 rpm) for 1h. (For MaxiSorp Immunotubes, use 4 ml PBS-TB, close tube with stopper and incubate with end-over-end mixing)
3. Wash the plate by emptying the plate as in **Step 2**, adding of 300 μl/well of PBS-T wash buffer and vortexing of the plate 5 seconds. Repeat wash cycle 3 times. (For MaxiSorp Immunotubes, rinse 4 times with PBS-T, wash stopper)
4. Empty the plate as in **Step 2**. Add 100 μl/well of 0.1 μM biotinylated target protein in PBS-TB (or respective buffer needed for target protein) and incubate the plate at RT/4°C (dependent on target protein) for 1 h. (For MaxiSorp Immunotubes, use 4 ml of 0.1 μM biotinylated target (minimum volume 0.4 ml of 1 μM biotinylated target), close tube with stopper, incubate with end-over-end mixing)

   This is an excess of biotinylated target protein, compared to the NeutrAvidin you immobilized, and the excess can be reduced. The more of target protein you get immobilized, the better for the selection process. For screening by ELISA you can easily reduce the amount of target protein immobilized to 100 μl/well of 15 nM biotinylated target protein. A pre-experiment with serial dilutions may be needed for the determination of minimal amounts of biotinylated target protein needed to detect binding signal over background. For ELISA prepare appropriate control wells by applying biotinylated control target protein (IgG1) or just PBS-TB to these wells.
5. Wash the plate or tube as in **Step 3**.
6. Proceed with selection on immobilized target protein (**Protocol 13)** or ELISA (**Protocol 17** and **Protocol 20**)

Affinity selection of DARPins

- This chapter describes the selection of DARPins from DARPin-displaying phage particles that recognize a specific target protein. The library of DARPin-displaying phage particles is exposed to immobilized target protein (**Protocol 13**) or soluble target protein (target protein in solution, **Protocol 14**) which is then subsequently captured. Both methods allow phage particles with affinity for the target protein to bind while the others not binding the target protein are washed away. The selected DARPin-displaying phage particles are amplified in host bacteria to create an enriched pool of phage particles with affinity for the target protein which can then be used as input for the next selection round.
- Throughout the whole selection procedure it is very important to fix parameters like buffer composition, temperature, target presentation,…in order to guarantee target presentation in its native state. Only then successful selections of binders against epitopes present on native target protein can be enriched. Phage particles and DARPins are stable in most buffers (also containing detergents) and over a wide range of temperatures.
- Optimal selection conditions can vary a lot with the target protein used and each of the two strategies described above has its advantages and disadvantages. Generally, selection on immobilized target protein gives higher recovery of phage particle in the first selection round and is cheaper, but the risk of selecting unspecific binders is much higher for this method. For selection on soluble target protein, we never observed an enrichment of background binders and, additionally, by lowering the concentration of target protein during selection high affinity binders can be favored. **The best combination in our hands is to perform the first selection round on immobilized target protein followed by the further selection rounds on soluble target protein.**
- Multiple rounds of selection are needed to enrich specifically binding phage above the background yield of non-binding phage. It is expected that after 2 to 4 selection rounds significant enrichment of specifically binding phage particles can be observed.
- Selection on target protein which is biotinylated on accessible amino groups (**Protocol 11**) is very convenient due to the native, rapid and irreversible immobilization and capturing using biotin binding proteins such as NeutrAvidin or streptavidin. The protocols described below are based on biotinylated target protein but can be adapted to other immobilization or capturing methods.
- Because of monovalent phage display, only a minor part of produced phage particles carry a displayed-DARPin and the corresponding phagemid. Thus, about 1000 times more chloramphenicol resistant cfu than the transformed library size should be applied to

represent all clones of interest in the first round. It is thus recommended to use about 2 ml of the Lot #1 (25.01.2006, 1.6 x 10^{13} cfu/ml) of the DARPin PD-library #1 as input phage for the first selection round to cover the full diversity (transformed library size 2.6 x 10^{10} cfu, functional library size 1.1 x 10^{10} cfu, for details see Appendix data sheet: PD library #1) of the library.

- The stringency of a selection round determines more or less the yield of eluted phage particles. Since in the first selection round every clone will only be represented a few times low stringency leading to high yield should be applied. Every clone that is lost in the first round can never be recovered. In the subsequent rounds every clone will be represented by hundreds to thousands of phage particles and, therefore, stringency can be increased.
- In selection rounds following the first round using about $10^{11\text{-}12}$ chloramphenicol resistant cfu of amplified phage are enough to oversample the selected diversity by far.
- Due to the differences in “selection volume” and “selection stringency”, independent protocols for round one and subsequent rounds will be described.
- It is very important to avoid carry over of input phage particles to late washing steps or to the eluted phage particles (each microliter of the input phage solution will contain 10^2 – 10^5 times more phage particles than the total amount of phage particles eluted after a selection round)
- There are two methods for amplification of the eluted pool of phagemid particles after a selection round: “**In solution-amplification**” (**Protocol 09**) and “**On plate-amplification**” (**Protocol 10**).
- For the quantification of enrichment see p. 252.
- For background enrichment and epitope focusing see “Troubleshooting” p.276.
- To perform a model selection spike phagemid particles displaying the DARPin (I_19) at a ratio of 1:100 into a sample of the phage library particles. Perform one round of selection on control target protein (human IgG1 whole molecule) which should enrich I_19 to almost 100 %.

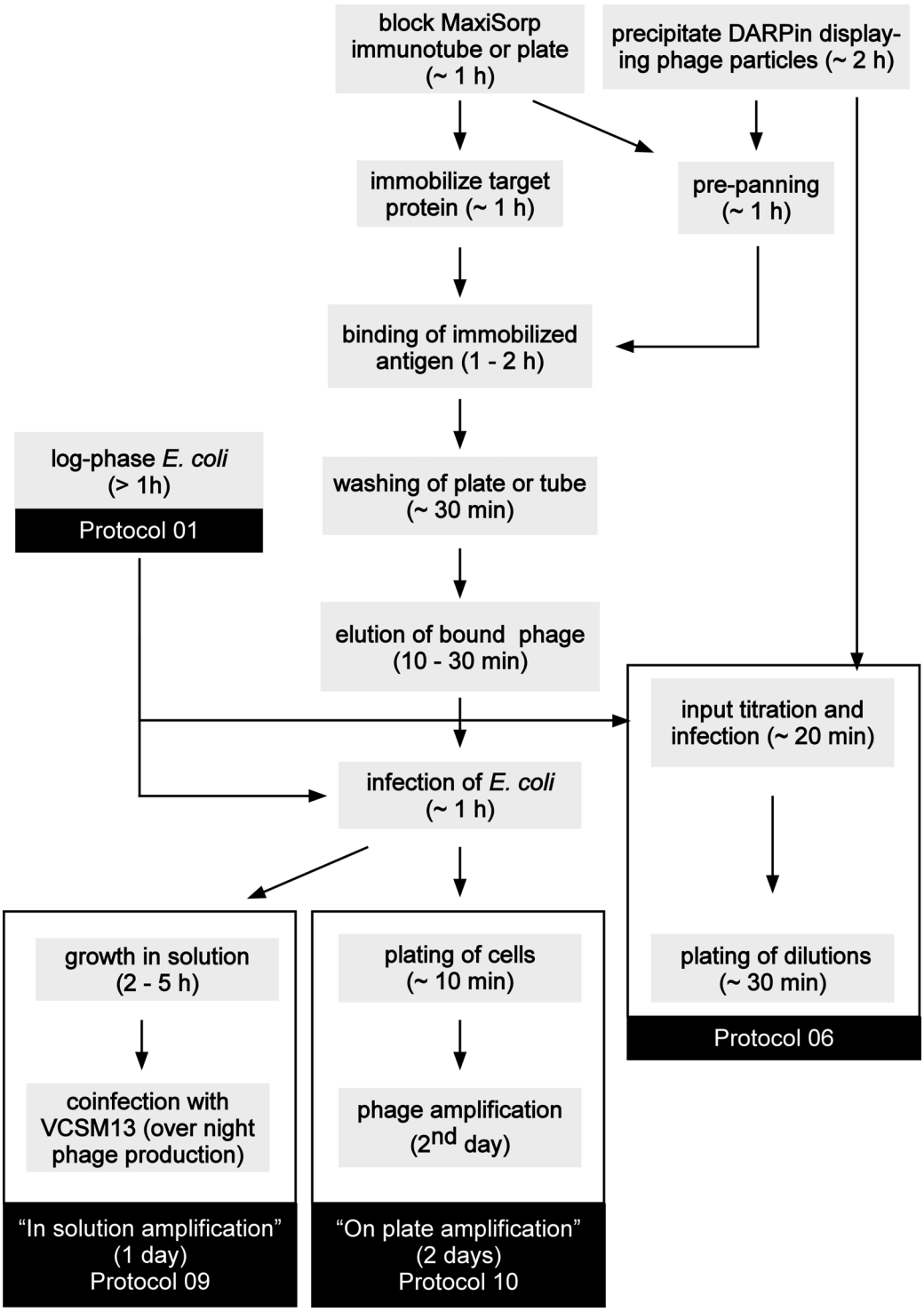

Figure 5: Work flow of Protocol 13

Schematic representation of the workflow for a selection round on immobilized target protein. Estimation of time needed for the respective steps is given in brackets. For the first selection round pre-panning is omitted.

Protocol 13 Selection on immobilized target protein

Comments

- This protocol describes the selection of DARPins from DARPin-displaying phage particles on target protein attached to a solid support: immunotube (MaxiSorp Immunotube) or plate (MaxiSorp 96-well plate).
- The protocol described is based on biotinylated target protein but can be adapted to other immobilization methods. The DARPin-displaying phage particles are exposed to the target protein which is immobilized via a biotin binding protein for the same amount of time. To reduce selection of NeutrAvidin binders it is recommended to alternate in the selection rounds between NeutrAvidin and streptavidin (different on sequence and structure level).
- Due to the large volume of the input phage library in the first round the selection is performed in a target protein coated immunotube whereas for the later rounds about 4 wells of a 96-well plate for each target protein are sufficient.
- See general phage working rules (p.201) for removal of phage solutions.

Equipment and Reagents (see p. 278 ff. for details)

- Helper phage VCSM13 (stock from **Protocol 03**)
- *E. coli* XL1-Blue log-phase culture (**Protocol 01**)
- Target protein coated immunotube for 1st round (NeutrAvidin) (**Protocol 12**)
- 4 target protein coated wells for >1st round (alternate Streptavidin, NeutrAvidin) (**Protocol 12**) and wells for background binding to determine enrichment factors.
- Blocked immunotube for >1st round (prepanning)
- glycine (200 mM, pH 2)
- Tris/base (2 M)
- PBS-T
- PBS-TB
- triethylamine (100 mM) (prepare on the day used)
- Tris/HCl (1 M, pH 7.4)
- Tween20 (25%)
- BSA (20%)
- 2YT/tet/cam agar plates (square)
- 2YT/kan agar plates (square)
- PBS-G
- PEG/NaCl (5x)
- Culture tubes (14 ml)
- Polypropylene tubes (50 ml)
- Equipment for end-over-end rotation
- For selection output amplification see: **Protocol 09, Protocol 10**

Method

Day 1,2

1. *E. coli* XL1-Blue plating and pre-culture (**Protocol 01**).
2. Coat immunotube (**Protocol 12**).
3. Book shakers, prepare Equipment and Reagents (see p. 278 ff. for details)

Day 3

4. Prewarm and dry 2YT/cam/tet and 2YT/kan agar plates at 37°C.

   Keep lid ajar to allow plates to dry.

5. Prepare *E. coli* XL1-Blue log-phase culture (**Protocol 01**).

   *For each selection you will need 13 ml of the E. coli XL1-Blue log-phase culture. Inoculate at the ratio calculate from the time needed for the selection experiment and time needed for the cells to grow into the log-phase (see **Protocol 01**).*

6. Prepare target protein coated immunotube (**Protocol 12**).
7. Wash the tube by emptying the tube, blotting it dry on stacked paper towels and rinsing with 4 -5 ml of PBS-T wash buffer. Repeat wash cycle 4 times. (wash stopper carefully)
8. Add 2-3 ml of DARPin-displaying phage solution to the tube, adjust with PBS-TB to 4 ml and add BSA and Tween 20 to a final concentration of 0.2% and 0.1%, respectively.

   *Input of DARPin PD library should be 1000-fold higher than actual library size to cover the full library diversity (see above). More DARPin-displaying phage particles or other buffer conditions than the storage buffer of the phage library (PBS-G) can be used by simply precipitating the phage particles as described in **Protocol 04** prior to the selection*

9. Cap the tube, close with parafilm, and incubate with end-over-end mixing on a rotary wheel at RT or 4°C for 2 h.

   Temperature of the binding reaction should be chosen depending on the target protein stability. If uncertain do at 4°C.

10. Remove the solution of phage and rinse the tube ten times as described in **Step 7**.

    Stringency of washing should be kept low in the first selection round to recover all binders (See above). If binding was done at 4°C use cold buffer for washing.

11. Add 500 µl of triethylamine (100 mM) (prepare on the day used) for elution.

12. Cap the tube (use a new cap), and incubate with end-over-end rotation for 5-8 min.

Longer incubation will reduce the infectivity of the phage particles

13. Transfer the solution to a 50 ml polypropylene tube containing 250 µl of Tris/HCl (1 M, pH 7.4) for neutralization. Mix to neutralize the triethylamine and keep on ice.

In round 1 an additional second elution is performed to recover all binding phage.

14. For second elution add 500 µl of glycine (200 mM, pH 2) to the tube.

15. Cap the tube, and incubate with end-over-end mixing on a rotary wheel for 10 min.

16. Transfer the solution to the same 50 ml polypropylene tube as the first elution and add 45 µl of Tris/base (2 M) for neutralization. Mix to neutralize and keep on ice.

Check pH (spot 1 µl of neutralized eluate on pH indicator paper), should be about 7. After neutralization the phage solution can be kept at 4°C for a few days before proceeding to the next step.

17. Amplify the eluted pool of phagemid particles and determine the phagemid titers of the eluates: see “In solution-amplification” (**Protocol 09**) or “On plate-amplification” (**Protocol 10**)

18. In the mean time titrate input phage solution as described in **Protocol 06**.

19. *For second selection round prepare: E. coli* XL1-Blue pre-culture (**Protocol 01**) coat wells of MaxiSorp plate (**Protocol 12**) for target protein and for background binding.

4 wells coated with target protein are sufficient for the second selection round.

Day 4

phage preparation (parallel to step 23 - 26)

20. Calculate the elution-titre of the selections by counting the colonies on the plates from the different dilutions (check control plate for *E. coli* XL1-Blue log-phase culture contaminations)

21. Precipitate and purify the amplified phage particles displaying DARPins as described in **Protocol 04**. Resuspend the phage in 1/20 of supernatant volume PBS-G (results in about 10^{12}-10^{13} phage/ml).

*Quantify the amount of phage particles obtained by absorbance as described in **Protocol 05**.*

22. The amplified phage pool may be used directly for the next round of selection. For storage, aliquot, flash freeze in liquid nitrogen and store at -80°C.

For further analysis keep about 50 µl of the phage pool at 4°C (e.g. pool ELISA analysis)

2nd selection cycle

23. Prewarm and dry 2YT/cam/tet and 2YT/kan agar plates at 37°C.

Keep lid ajar to allow plates to dry.

24. Prepare *E. coli* XL1-Blue log-phase culture (**Protocol 01**).

*For each selection you will need 5 ml of the E. coli XL1-Blue log-phase culture. Inoculate at the ratio calculate from the time needed for the selection experiment and time needed for the cells to grow into the log-phase (see **Protocol 01**).*

25. Prepare target protein coated wells (4 wells) (**Protocol 12**) and wells for background binding and blocked immunotubes for prepanning.

26. Wash the plate by empting the plate, blotting it dry on stacked paper towels, adding of 300 µl/well of PBS-T wash buffer and vortexing of the plate for 5 seconds. Repeat wash cycle 3 times.

27. Perform prepanning step by adding 500 µl of DARPin-displaying phage solution form **Step 21** to the blocked immunotube which contains 500 µl of PBS-TB and add BSA and Tween 20 to a final concentration of 0.2% and 0.1%, respectively. Cap the tube, close with parafilm, and incubate with end-over-end mixing on a rotary wheel at RT or 4°C for 1 h.

28. Add 100 µl DARPin-displaying phage solution from **Step 27** to each target protein coated well and to a well not containing target protein.

Always add an aliquot of input phages to a blocked well not containing the target protein to determine background binding.

29. Incubate with orbital shaking at 900 rpm for 1 - 2 hours at RT or 4°C.

Temperature of the binding reaction should be chosen depending on the target protein stability. If uncertain do at 4°C. Binding time can be reduced with selection cycles.

Remove the solution of phage and wash the plate by empting the plate (rapidly invert the plate over a plastic tray, see phage handling p.201 for details), blotting it dry on stacked paper towels, adding of 300 µl/well of PBS-T wash buffer and orbital shaking (900 rpm) for 1-2 min. Repeat wash cycle 12 times.

Stringency of washing can be increased by longer washing times or increased number of wash cycles (e.g. 12 cycles 1-2 min on shaker). If binding was done at 4°C use cold buffer for washing.

30. For elution add 100 µl of glycine (200 mM, pH 2) to each well.

31. Incubate with orbital shaking at 900 rpm for 10 - 15 min at RT to elute the phages.

32. Pool the 400 µl elution solution in a 14 ml polypropylene tube containing 36 µl of Tris/base (2 M). Mix to neutralize and keep on ice.

No additional second elution is needed. Check pH (spot 1 µl of neutralized eluate on pH indicator paper), should be about 7. After neutralization the phage solution can be kept at 4°C for a few days before proceeding to the next step.

33. Amplify the eluted pool of phagemid particles and determine the phagemid titers of the eluates: see “In solution-amplification” (**Protocol 09**) or “On plate-amplification” (**Protocol 10**)

34. In the mean time titrate input phage solution as described in **Protocol 06**.

35. *For third selection round prepare E. coli* XL1-Blue pre-culture (**Protocol 01**) coat MaxiSorp plate (**Protocol 12**) and wells not containing target protein to determine enrichment factors.

Day 5

36. Phage preparation and 3rd selection cycle as described for the second selection cycle on day 4.

Day 6

37. For monitoring the enrichment the amplified pools may be analyzed by phage ELISA as described in **Protocol 15** to determine the relative amounts of target binding phage particles present in the pools.

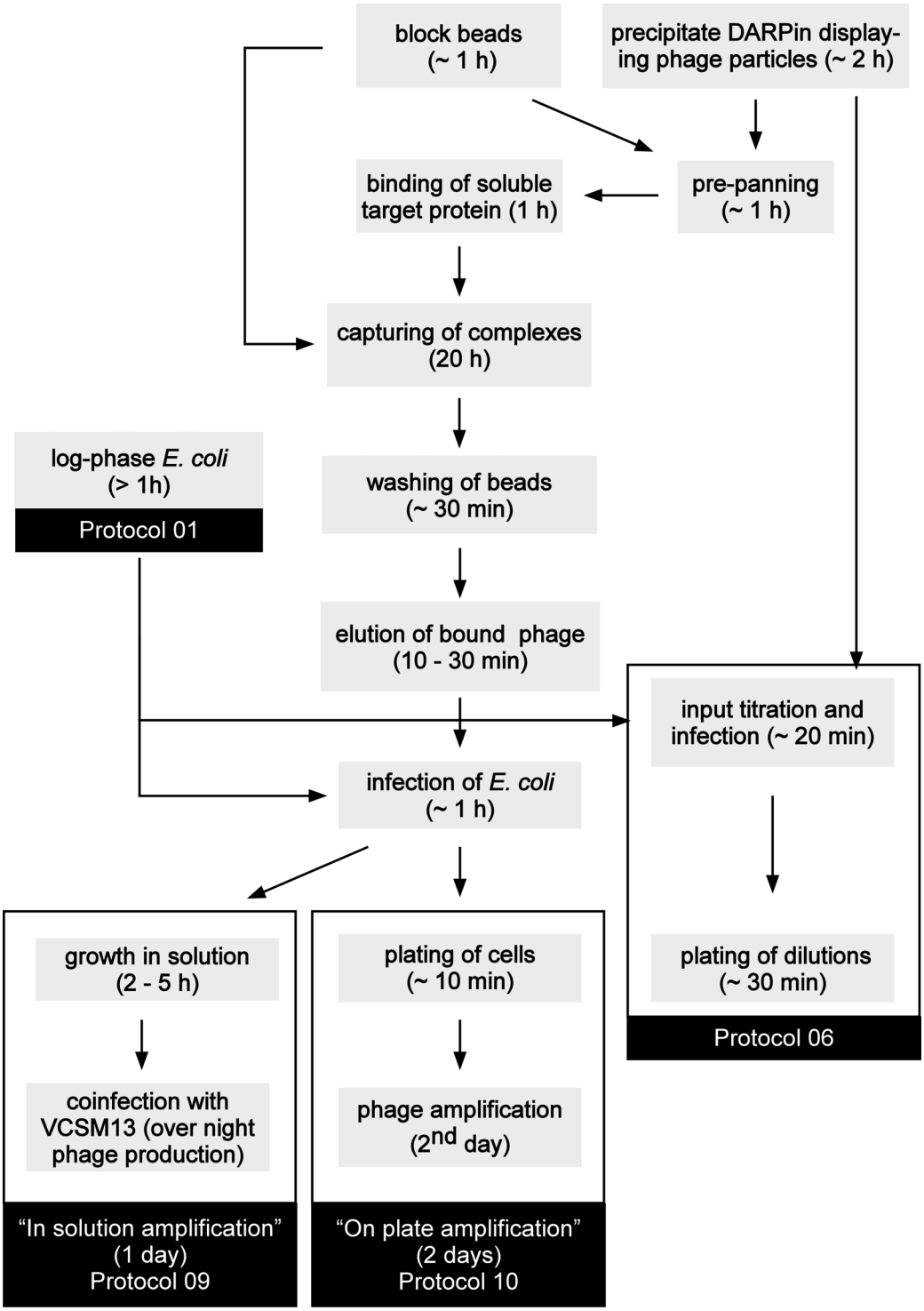

Figure 6: Work flow of Protocol 14

Schematic representation of the workflow for a selection round on soluble target protein. Estimation of time needed for the respective steps is given in brackets. For the first selection round pre-panning is omitted.

Protocol 14 Selection on soluble target protein

Comments

- This protocol describes the selection of DARPins from DARPin-displaying phage particles on soluble target protein. The library of phage particles is incubated with biotinylated target protein followed by a capturing of the phage-target protein complexes with streptavidin-coated magnetic beads.
- The protocol described is based on capturing of biotinylated target protein with streptavidin-coated magnetic beads but can be adapted to other capturing methods.
- Buffers used for the selection can be chosen depending on the target protein. Tween 20 can be replaced by other detergents and BSA by other proteins.
- To reduce enrichment of streptavidin binders a prepanning step on blocked streptavidin-coated magnetic beads should be performed from round two on. Alternatively, avidin coated beads could be used in an alternating mode.
- Target protein concentration can be reduced during the selection procedure to favor selection of high affinity clones. For successful selections on a new target protein we suggest to use a concentration of about 100 nM for the first three selection rounds. To increase the affinity of binders selection steps with reduced target protein concentrations can be repeated or added after specific enrichment is observed.
- Concentration of displayed DARPin and target protein concentration: For a concentration of 10^{12} cfu/ml of phagemid particles, containing 10% particles with monovalent display would give a DARPin concentration of 166 nM. This value will by far overestimate the concentration of target binding DARPins during a selection round. Therefore, it can be assumed that even at low nM concentration the amount of target protein should not be limiting. We never increased the selection pressure by reducing antigen and used a 100 nM trough out all the selection rounds.
- Agglutination of streptavidin-coated magnetic beads is one problem when performing selections on soluble biotinylated target protein. The reason is the attachment of multiple biotin moieties per protein molecule due to chemically biotinylation which leads to a cross-linking and, therefore, agglutination of the beads. Proper resuspension of the beads during the washing is essential to get rid of background phage particles without affinity for the target protein. In this respect enzymatic attachment of a single biotin moiety at defined position is the clear advantage of Avi-tagged targets.
- No experiments to determine background binding are performed (too high costs for

magnetic beads), therefore no monitoring of enrichment during the selection cycles is possible. The enrichment is quantified after three rounds by performing a polyclonal phage ELISA (**Protocol 15**)

- See general phage working rules (p.201) for removal of phage solutions.

Equipment and Reagents (see p. 278 ff. for details)

- Helper phage VCSM13 (stock from **Protocol 03**)
- *E. coli* XL1-Blue log-phase culture (**Protocol 01**)
- Biotinylated target protein (**Protocol 11**)
- Streptavidin-coated paramagnetic beads
- Magnetic tube holder for 2 ml micro tubes
- Micro tubes (2 ml)
- Culture tubes (14 ml)
- Polypropylene tubes (50 ml)
- Equipment for end-over-end rotation
- PBS-T
- PBS-TB
- Tween 20 (25%)
- BSA (20%)
- triethylamine (100 mM) (prepare on the day used)
- 1 M Tris/HCl
- 200 mM glycine. (pH 2)
- Tris/base (2 M)
- 2YT/tet/cam media
- 2YT/tet/cam agar plates
- 2YT/kan agar plates
- PBS-G
- PEG/NaCl (5x)
- For selection output amplification see: **Protocol 09, Protocol 10**

Method

Day 1,2

1. *E. coli* XL1-Blue plating and pre-culture (**Protocol 01**).
2. book shakers, prepare Equipment and Reagents (see p. 278 ff. for details)

Day 3

3. Prewarm and dry 2YT/cam/tet and 2YT/kan agar plates at 37°C.

   Keep lid ajar to allow plates to dry.
4. Prepare *E. coli* XL1-Blue log-phase culture (**Protocol 01**).

   For each selection you will need 5 ml of the E. coli XL1-Blue log-phase culture.

*Inoculate at the ratio calculate from the time needed for the selection experiment and time needed for the cells to grow into the log-phase (see **Protocol 01**).*

5. Add 1 ml of PBS-TB to five 2 ml micro tubes in order to block non-specific binding to the tube. Incubate with end-over-end rotation for 1 hour at RT.

Label the tubes with the name of the target protein and B (for binding), W1,2,3 (for wash 1,2 and 3) and E (for elution)

6. In a fresh 2 ml micro tube add 100 µl of streptavidin beads to 1 ml of PBS-TB order to block non-specific binding to the beads. Incubate with end-over-end rotation for 1 hour at RT.

To save time this step can also be performed overnight.

7. Discard the PBS-TB from the blocked binding tube (B).

8. Add 1.8 ml of DARPin-displaying phage solution, BSA and Tween 20 (final concentration of 0.2% and 0.1%, respectively) and biotinylated target protein to 100 nM final concentration. Adjust with PBS-TB to 2 ml.

*Input phage particles of DARPin PD library should be 1000-fold higher than the actual library size to cover the full library diversity (see above). More DARPin-displaying phage particles, other volumes or other buffer conditions than the storage buffer of the phage library (PBS-G) can be used by simply precipitating the phage particles as described in **Protocol 04** prior to the selection. Final concentration of the target protein in 2 ml binding solution should not be more than 100 nM to allow complete capturing with the streptavidin beads)*

9. Incubate with end-over-end rotation for 1 hour at RT or 4°C.

Temperature of the binding reaction should be chosen depending on the target protein stability. If uncertain do at 4°C.

10. Draw the pre-blocked streptavidin beads to one side of the tube with a magnetic tube holder and discard the supernatant. Add the solution from Step 9 containing phage and target protein to the pre-blocked beads, resuspend the beads.

11. Incubate the tube with end-over-end rotation for 20 min at room at RT or 4°C.

If beads start to form clots incubate with orbital shaking at 900 rpm (see Step 14).

12. Centrifuge at 100 g for 10 sec and place the tube in the magnetic tube holder for 1 min.

Buffers with high viscosity may increase the time needed to capture the beads in all steps.

13. Aspirate the supernatant from the tube.

14. Wash the beads by adding of 1 ml of PBS-T wash buffer, short resuspension by pipetting, centrifugation at 100 g for 10 sec, placing the tube it the magnetic tube holder for 1 min and aspirating the supernatant. Repeat wash cycle 9 times. After every second wash step resuspend the beads in 0.1 ml of PBS-T wash buffer and transfer to a fresh pre-blocked tube (W1,2,3 and E). By washing the old tube a second time with 0.9 ml of PBS-T and transferring it to the fresh tube loss of beads can be minimized.

Chemically biotinylated target protein with multiple biotin moieties per protein molecule attached can lead to cross-linking and, therefore, agglutination of the beads. Careful resuspension of the beads (e.g. orbital shaking at 900 rpm for 1 min) is needed to remove phages without affinity for the target protein.

Stringency of washing should be kept low in the first selection round to recover all binders (see above). If binding was done at 4°C use cold buffer for washing

15. Add 200 µl of triethylamine (100 mM) (prepare on the day used).

16. Incubate with end-over-end rotation for 5-8 min.

Longer incubation will reduce the infectivity of the phage particles

17. Centrifuge at 100 g for 10 sec and place the tube in the magnetic tube holder for 1 min.

18. Transfer the supernatant to a 14 ml polypropylene tube containing 100 µl of Tris/HCl (1 M, pH 7.4). Mix to neutralize the triethylamine and keep on ice.

In round 1 an additional second elution is performed to recover all binding phage.

19. For the second elution add 200 µl of glycine (200 mM, pH 2) to the tube containing the beads.

20. Incubate with end-over-end rotation for 10 min.

21. Centrifuge at 100 g for 10 sec and place the tube in the magnetic tube holder for 1 min.

22. Transfer the supernatant to the same 14 ml polypropylene tube as the first elution and add 18 µl of Tris/base (2 M). Mix to neutralize and keep on ice.

Check pH (spot 1 µl of neutralized eluate on pH indicator paper), should be about 7. After neutralization the phage solution can be kept at 4°C for a few days before proceeding to the next step.

23. Amplify the eluted pool of phagemid particles and determine the phagemid titers of the eluates: see “In solution-amplification” (**Protocol 09**) or “On plate-amplification” (**Protocol 10**)

24. In the mean time titrate input phage solution as described in **Protocol 06**.

25. For the second selection round prepare: *E. coli* XL1-Blue pre-culture (**Protocol 01**)

Day 4 (2nd selection cycle)

26. Prepare phages as described in **Protocol 13, Step 20** to **22**

27. Step 3 to **step 5** as described for the first round.

28. In two 2 ml micro tubes add 50 µl of streptavidin-coated paramagnetic beads (10 µg/ml) to 1 ml of PBS-TB. Incubate with end-over-end rotation for 1 hour at RT.

One tube is used for pre-panning to remove streptavidin-binding phage particles and the other one for capturing of the target protein.

29. With a magnetic tube holder draw the pre-blocked streptavidin beads to one side of the of the pre-panning tube and discard the supernatant. Resuspend the beads in 0.6 ml PBS-TB, add 200 µl of the amplified phage particles from round 1 and adjust with BSA and Tween 20 to a final concentration of 0.2% and 0.1%, respectively.

30. Incubate with end-over-end rotation for 1 hour at RT or 4°C.

31. With a magnetic tube holder draw the beads of the pre-panning tube to one side of the tube.

32. Discard the PBS-TB from the blocked binding tube and add the phage containing supernatant from **Step 31**. Add biotinylated target protein to 100 nM final concentration and adjust with PBS-TB to 1 ml.

Lower volumes can be used to save target protein.

33. Incubate with end-over-end rotation for 1 hour at RT or 4°C.

34. With a magnetic tube holder draw the pre-blocked streptavidin beads to one side of the capturing tube and discard the supernatant. Add the solution from **Step 32** containing phage and target protein to the pre-blocked beads, resuspend the beads.

35. Perform capturing and washing as described in **Step 11** to **step 14** of the first round.

Stringency of washing can be increased by longer washing times or increased number of wash cycles (e.g. 12 x 1 min). If binding was done at 4°C use cold buffer for washing.

36. For elution add 400 µl of glycine (200 mM, pH 2) to the tube.

37. Incubate with end-over-end rotation for 10 - 15 min.

38. Centrifuge at 100 g for 10 sec and place the tube in the magnetic tube holder for 1 min.

39. Transfer the supernatant to a 14 ml polypropylene tube containing 36 µl of Tris/base (2 M). Mix to neutralize and keep on ice.

No additional second elution is needed. Check pH (spot 1 µl of neutralized eluate on pH

indicator paper), should be about 7. After neutralization the phage solution can be kept at 4°C for a few days before proceeding to the next step..

40. Amplify the eluted pool of phagemid particles and determine the phagemid titers of the eluates: see “In solution-amplification” (**Protocol 09**) or “On plate-amplification” (**Protocol 10**)

41. For third selection round prepare: *E. coli* XL1-Blue pre-culture (**Protocol 01**)

Day 5 (3rd selection cycle)

42. Phage preparation and 3rd selection cycle as described for the second selection cycle on day 4.

Day 6

43. For monitoring the enrichment the amplified pools may be analyzed by phage ELISA as described in **Protocol 15** to determine the relative amounts of target binding phage particles present in the pools.

Quantifying enrichment

- There are two possibilities for monitoring the selection process:
- **a) Enrichment factors**: For each selection round equivalent amounts of the input phage particles have to be applied to the target protein coated wells and to wells not containing target protein (e.g. only NeutrAvidin for background binding). The enrichment factor is the ratio of input cfu to output cfu on target protein coated wells relative to the ratio of input cfu to output cfu on wells not containing target protein. Experimental determination of enrichment factors is only advisable from the 2^{nd} round on when doing selections on immobilized target protein. When doing selections in solution the costs for magnetic beads are too high to do this monitoring. Enrichment factors have the advantage that they can be done in parallel during the selection cycles. But when doing selections on multiple targets in parallel the amount of work will exceed the capacity of one person.
- **b) Pool ELISA (Protocol 15)**: A simple method for the quantification of enrichment after having performed the actual selection rounds. This method can be performed for many different selections in parallel and is advisable even if enrichment factors have been determined beforehand. The phage ELISA of the pools of amplified phage particles eluted from each round gives the information of how many phage particles are binding to the target versus the empty matrix (e.g. only NeutrAvidin). Monitoring enrichment by pool ELISA is very convenient and additional information about specificity can be obtained by immobilizing respective control proteins or doing competition experiments.
- For percentage of expected binders in a pool giving positive binding signal on target protein see **Figure 7:**.

Protocol 15 Polyclonal phage ELISA

Comments

- This protocol allows analyzing polyclonal DARPin-displaying phagemid particles for target protein binding by a simple ELISA procedure.
- This polyclonal phage ELISA procedure can be used to monitor phage enrichments and should be performed prior to screening of single clones for specific binding.
- For ELISA, appropriate positive and negative control should be included (coating of wells as described in **Protocol 12**; Use wells with immobilized target protein for specific binding and wells coated with NeutrAvidin (or streptavidin if used during the selection) for the control of background binding. In the example described below the target protein is immobilized via NeutrAvidin, therefore wells only coated with NeutrAvidin and blocked with BSA serve a control for background binding)
- See general phage working rules (p.201) for removal of phage solutions.
- If possible make triplicates for each measurement

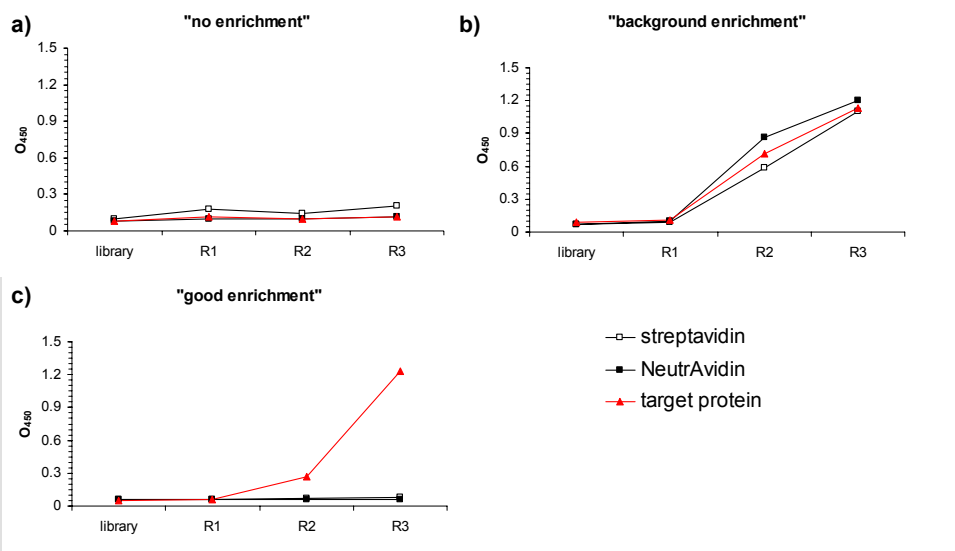

Figure 7: Example showing polyclonal phage ELISA

The binding to streptavidin (square, open), NeutrAvidin (square, closed) and antigen (triangle, closed) of the initial library and of pools of phage particles after selection rounds (R1 to R3) was analyzed by phage ELISA. (**a**) Selection without enrichment of phage particles having affinity for the target protein. (**b**) Selection with enrichment of background binding phage particles. (**c**) Selection with nice enrichment of phage particles having affinity for the target protein. Screening of single clones of R2 and R3 resulted in about 10% and 90% of target specific clones, respectively.

Equipment and Reagents (see p. 278 ff. for details)

- Target protein and NeutrAvidin or strepatavidin coated wells of a MaxiSorp 96-well plate (**Protocol 12**)
- PBS-T
- PBS-TB
- anti-M13 antibody HRP conjugate
- BM Blue POD substrate
- Shaker for 96-well plates
- Phage pools from different selection rounds to be analyzed. (**Protocol 13** or **Protocol 14**)

Method

Day 1

1. Coat wells of MaxiSorp 96-well plate (**Protocol 12**).

Day 2

2. Mix 1 µl of phage pools to be analyzed with 99 µl of PBS-TB in the target protein coated wells and in the NeutrAvidin coated wells (**Protocol 12**) and incubate at 4°C or RT for 1 h with orbital shaking (900 rpm).

   1 µl of concentrated phage pools should contain by far enough phage particles to obtain a binding signal in the phage ELISA. Applying higher amounts of the phage pools increases the risk of obtaining signals out of the linear range (can make differentiation between high, low binding signal and background binding impossible).

3. Wash the wells by empting the plate (rapidly invert the plate over a plastic tray, see phage handling for details), blotting it dry on stacked paper towels, adding of 300 µl/well of PBS-T wash buffer and orbital shaking (900 rpm) for 1-2 min. Repeat wash cycle 3 times.
4. Empty the plate as described in **Step 3**. Add 100 µl of 1:40'000 anti-M13 antibody HRP conjugate mAb in PBS-TB per well and incubate at 4°C or RT for 1 h.

   The optimal concentration of the anti-M13 antibody HRP conjugate depends strongly on the amounts of phage particles bound per well (in our hands 1:40'000 gives good signal in the linear range). Shorter incubation times can be compensated by higher antibody concentrations.

5. Wash wells as described in **Step 3**. (4 cycles)
6. Empty the plate as described in **Step 3**. Add 100 µl of soluble Blue POD substrate and quench after a few minutes with 50 µl of 1 M H_2S0_4.

   It is possible to measure the reaction before quenching at OD_{370} - OD_{492} but sensitivity

is lower. Usually, quenching should be performed after no more than 30 min (1 < OD_{370} - OD_{492}).

7. Measure OD_{450}.

Measure immediately after quenching. Substrate will precipitate over time making accurate measurements impossible.

8. Decide which pools to be screened on single clone level in the phage ELISA format (**Protocol 17**) or as soluble expressed DARPins (**Protocol 20**).

Screening

- Once target protein specific binding clones have been enriched individual clones can be screened for qualitative binding to the target protein by two different methods:
- **Screening by phage ELISA**: The fastest way to get single clone data is to screen on the phagemid particle level (**Protocol 16** and **Protocol 17**). This method has the clear disadvantage that each positive clone has to be individually subcloned into the expression vector pMPAG6 or pDST67 for soluble expression and also no secondary screening by SDS-PAGE can be performed (see below). However, for some applications it might be advisable to use this method due to the binding functionality of the detection antibody used (e.g. anti-M13 antibody HRP conjugate is functional in solutions containing 0.2% DDM in which many other antibodies fail).
- **Screening DARPins by ELISA:** The second possibility is to subclone the whole selected pool to be analyzed into the expression vector pMPAG6 or pDST67 (**Protocol 18**). The ELISA can then be performed directly by using crude *E. coli* lysate containing soluble expressed DARPin (**Protocol 19** and **Protocol 20**). The clear advantage of this method is the possibility to directly perform a secondary screening by **SDS-PAGE** before submitting clones for sequencing analysis.
- **Secondary screening by SDS-PAGE (Protocol 21)**: A frequently encountered problem in phage display is the reduction of diversity after two to three rounds of selection. In such a case many of the positive clones identified by ELISA will be identical on sequence level. To identify positive clones with different sequences by sequencing would be time consuming and expensive. One approach to circumvent this is the **secondary screening by SDS-PAGE**. Due to high expression level of DARPins, crude cell extracts can be directly analyzed. DARPins different on the sequence level do show different running behavior on SDS-PAGE (mainly due to their stability differences) and expression patterns. These two properties allow identifying clones different on sequence level. Differences in running behavior are for N2C not as clearly visible as for N3C (probably due to the generally lower stability of N2C compared to N3C).
- Use phage particle displaying DARPin (I_19) or purified DARPin (I_19) and control target protein (human IgG1 whole molecule) in the respective experiments.

Protocol 16 Production of phages in the 96-well format

Comments

- This protocol allows the production of individual phage clones in the 96-well format followed by analysis for target-specific binding by phage ELISA (**Protocol 17**) and subsequent sequencing and subcloning into pDST67 or pMPAG6 for soluble expression.

Equipment and Reagents (see p. 278 ff. for details)

- 2YT/cam/tet agar plates with colonies to be analyzed (**Day 1** this protocol and **Protocol 01**)
- 96-deep well plates for bacterial cell cultures
- IPTG
- VCSM13 helper phage stock (**Protocol 03**)
- 2YT/tet/cam media
- Incubator for 96-well bacterial cell cultures
- Gas permeable adhesive seals
- Autoclaved toothpicks
- Parafilm

Method

Day 1

1. Infect 0.9 ml of log-phase XL1-Blue cells with 100 µl of 10^8 and 10^9 dilutions of the phage pool to be screened (dilutions for phage samples containing about 10^{13} cfu/ml) and incubate for 30 min at 37°C without agitation and then for 30 min at 37° C with shaking.
2. Plate 100 µl of the infected cells on 2YT/cam/tet agar plates and grow overnight at 37°C.

   These final dilutions of 10^{10} and 10^{11} should give numbers of colonies per plate that allow easy picking of single ones.

Day 2

3. Aliquot 0.9 ml of 2YT/cam/tet into each well of a 96-deep well plate (phage plate).
4. Pick individual colonies into each well and seal the plate by applying a gas permeable adhesive seal.

   A simple method that avoids cross-contamination and double inoculation is to seal the plate with a piece of parafilm. Pick the colonies with sterile toothpicks and stab them

through the parafilm into the medium. The toothpicks can be removed after inoculation of all the wells.

5. Incubate the sealed plate in an orbital shaker (540 rpm) and grow at 37°C for 4 h
6. Aliquot 1.2 ml of 2YT/cam/tet into each well of a new 96-deep well plate (master plate) Transfer 0.05 ml from each well of the phage plate to the corresponding well of the master plate using a multichannel pipette. Incubate the sealed plate in an orbital shaker (540 rpm) and grow at 37°C overnight.
7. To each well of the phage plate add 0.2 ml of 2YT/cam/tet containing 1 mM IPTG and VCSM13 helper phage (5×10^{10} cfu/ml).
8. Incubate the sealed plate in an orbital shaker (540 rpm) and grow at 37°C overnight.

Day 3

9. Spin phage plate at 3'000g for 10 min. The supernatant is now used for the phage ELISA (**Protocol 17**)
10. Spin master plate at 3'000g for 10 min, empty the plate, blot it dry on stacked paper towels and store at -20°C for later preparation of plasmid DNA.

Protocol 17 Screening phages by ELISA

Comments

- This protocol allows the screening of individual phage DARPin clones for target-specific binding by phage ELISA
- Subcloning for large scale expression is needed and can be very cumbersome for large number of clones. If possible do screening of unfused DARPins by ELISA to avoid subcloning of single clones (**Protocol 18)**.
- Phages are expressed as described in **Protocol 16.**
- For ELISA, appropriate positive and negative controls should be included
- See general phage working rules (p.201) for removal of phage solutions.

Equipment and Reagents (see p. 278 ff. for details)

- Target protein and NeutrAvidin coated MaxiSorp 96-well plate (**Protocol 12**)
- PBS-T
- PBS-TB
- anti-M13 antibody HRP conjugate
- BM Blue POD substrate
- Shaker for 96-well plates
- 96-well plate containing phage supernatants (**Protocol 16, Step 9**)

Method

1. Mix 10 µl of supernatant from **Protocol 16, Step 9** with 90 µl of PBS-TB in the target protein coated plate and in the NeutrAvidin coated plate (**Protocol 12**) and incubate at RT for 1 h with orbital shaking (900 rpm).

   Use one ELISA plate prepared with immobilized target protein and one NeutrAvidin coated plate for the control of background binding. 10 µl of phage supernatant should contain by far enough phage particles to obtain a binding signal in the phage ELISA. Applying higher amounts of supernatant increases the risk of obtaining signals out of the linear range (difficult to differentiate between good and bad binders).

2. Wash the plate by empting the plate (rapidly invert the plate over a plastic tray, see phage handling for details), blotting it dry on stacked paper towels, adding of 300 µl/well of PBS-T wash buffer and orbital shaking (900 rpm) for 1-2 min. Repeat wash cycle 3 times.
3. Empty the plate as described in **Step 2**. Add 100 µl of 1:40'000 anti-M13 antibody HRP

conjugate in PBS-TB per well and incubate at RT for 1 h.

The optimal concentration of the anti-M13 antibody HRP conjugate depends strongly on the amounts of phage particles bound per well (in our hands 1:40'000 gives good signal in the linear range). Shorter incubation times can be compensated by higher mAb concentrations.

4. Wash plate as described in **Step 2**. (4 cycles)
5. Empty the plate as described in **Step 2**. Add 100 µl of soluble Blue POD substrate and quench after a few minutes with 50 µl of 1 M H_2S0_4.

   It is possible to measure the reaction before quenching at OD_{370} - OD_{492} but sensitivity is lower Usually, quenching should be performed after no more than 30 min (1 < OD_{370} - OD_{492}).
6. Measure OD_{450}.

   Measure immediately after quenching. Substrate will precipitate over time making accurate measurements impossible.
7. Prepare plasmid DNA from positive clones using a standard kit (e.g. from Qiagen). Directly add resuspension buffer to the respective well of the master plate (thaw plate which was stored at -20°C) and resuspend the cell pellets for about 10 min at RT with orbital shaking plate (900 rpm).
8. Submit for sequencing using the primer pUCM13r-57 or odst03 (for details see Appendix data sheet: pMPAG3).
9. Selected clones have to be subcloned from phagemid pMPAG3 into expression vectors pDST67 or pMPAG6 (for details see Appendix data sheets) by excising the DARPin sequence using the *BamH*I and *Hind*III restriction sites of pMPAG3 and subcloning of the gel-purified fragment into the corresponding *BamH*I and *Hind*III restriction sites of pDST67 or pMPAG6.

   pDST67 and pMPAG6 introduces an 6xHis-tag to the N-terminus of the DARPin allowing efficient Ni-NTA (Qiagen) purification of the DARPin after its high level cytoplasmic expression in E. coil XL1-Blue.

Protocol 18 Subcloning of phagemid pools into expression plasmid

Comments

- This protocol allows the subcloning of the DARPins of a polyclonal phagemid pool (pMPAG3) into the expression vector pDST67 or pMPAG6 (for details see Appendix data sheets)
- Both expression vectors introduce an 6xHis-tag to the N-terminus of the DARPin allowing detection of the protein in ELISA and efficient immobilized-metal affinity chromatography (IMAC) purification of the DARPin after its high level cytoplasmic expression in *E. coil* XL1-Blue.
- Analysis of the single DARPin clones in the expression vector by ELISA (**Protocol 20**) has the advantage that no individual subcloning of positive clones is needed and DARPins are tested independently of the phage particle and direct secondary screening by SDS-PAGE (**Protocol 21**) is possible.
- Restriction enzyme unit (U) definition: The amount of enzyme required to completely digest 1 µg of substrate DNA (mostly phage λ DNA, see supplier information) in a reaction volume of 50 µl in one hour using recommended buffer).

Equipment and Reagents (see p. 278 ff. for details)

- *BamHI* (20 U/µl)
- *HindIII* (20 U/µl)
- NEB2 buffer (10x)
- Chemically competent *E. coli* XL1 Blue
- 2YT/amp agar plates (round or square)
- CiAP (1u/µl)
- 1.2% agarose gel
- T4-Ligase
- T4-buffer (10x)
- SOC media
- Plasmid purification kit
- DNA purification kit

Method

Day 1

1. Infect 0.9 ml of log-phase XL1-Blue cells with 100 µl of 10^7 and 10^8 dilutions of the phagemid particle pool to be subcloned (dilutions for phage samples containing about 10^{13} cfu/ml) and incubate for 30 min at 37°C without agitation and then for 30 min at 37 C with shaking.

2. Plate 100 µl of the infected cells on 2YT/cam/tet agar plates and grow overnight at 37°C.

   These final dilutions of 10^9 and 10^{10} should give more than 1'000 colonies per plate that allow the subcloning the pool without loss of diversity.

Day 2

3. For subcloning use the plate with more than 1000 individual colonies.
4. Add 2 ml of 2YT/tet/cam/G media to the plate, resuspend the colonies with a cell scraper and incubate the eluted cells with shaking at 1000 rpm at 4°C for 15 min to obtain a homogenous solution.
5. Use 600 µl of the eluted cells to prepare phagemid DNA using a standard plasmid purification kit.

   This procedure should yield phagemid DNA at a concentration of 50 - 100 ng/µl

6. Digest phagemid DNA (~1 µg) with *BamHI* and *HindIII* (e.g. for three-fold over digest: 0.33 µl *BamHI* (20 U/µl), 0.28 µl *HindIII* (20 U/ µl), 0.5 µl BSA (100 x stock), 5 µl NEB2 buffer (10 x stock), 10 - 20 µl phagemid DNA (1 µg) and UHP to final volume of 50 µl, for 1 hour at 37°C)
7. Gel-purify the polyclonal DARPin fragments by using a standard DNA purification kit.

   Cut out complete gel piece from 300 to 600 base pairs to allow N1C to N4C to be recloned. Include bands up to 900 base pairs if visible.

8. Over-digest target vector pDST67 or pMPAG6 (~1 µg) with *BamHI* and *HindIII* and dephosphorylate (e.g. for fifteen-fold over digest:1.7 µl *BamHI* (20 U/µl), 1.4 µl *HindIII* (20 U/µl), 0.5 µl BSA (100 x stock), 5 µl NEB2 buffer (10 x stock), 10 – 20 µl pDST67 (1 µg), 1 µl CiAP and UHP to final volume of 50 µl, for 1 hour at 37°C)
9. Remove enzymes by using a standard DNA purification kit.
10. Ligate 5 µl of the DARPin fragments with 1 µl of the digested pDST67 or pMPAG6 from **Step 8** for 30 min at RT (0.5 µl T4-Ligase, 1 µl T4-buffer, 2.5 µl UHP).

    To quantify background transformation of uncut or relegated target vector make negative controls: digested pDST67 or pMPAG6 without and with ligase.

11. Transform 5 µl of the ligation mix into 50 µl of chemically competent *E. coli* XL1-Blue cells. (mix, keep 30 min on ice and heat shock for 30 sec at 42°C)
12. Add 200 µl of SOC and shake at 37°C for 1hour.
13. Plate 100 µl and 10 µl on 2YT/amp agar plates and incubate at 37°C overnight.

    This subcloning procedure should give numbers of colonies per plate that allow easy picking of more than 100 single clones. Check negative controls: background

transformation of uncut or relegated target vector should be <10% compared to ligations including insert.

14. Proceed with the screening of DARPin by ELISA (**Protocol 19** and **Protocol 20**).

Protocol 19 Expression of DARPins in the 96-well format

Comments

- This protocol describes the expression of individual DARPins clones in the 96-well format followed by analysis for target-specific binding by ELISA (**Protocol 20**).
- No further subcloning for large scale expression needed.

Equipment and Reagents (see p. 278 ff. for details)

- 96-deep well plate for bacterial cell cultures (round bottom)
- IPTG
- amp (1000x)
- 2YT media
- Glucose (20%)
- 2YT/Glu/amp media
- 2YT/amp media
- 2YT/amp/IPTG media
- B-PER II
- 96-well PCR plate
- Shaker for 96-well plates
- Incubator for 96-well bacterial cell cultures
- Gas permeable adhesive seals
- Autoclaved toothpicks

Method

Unless stated otherwise, all handling should be done with an 8 or 12-fold multichannel pipette to avoid cross-contamination between wells.

Day 1

1. Aliquot 1.2 ml of 2YT/Glu/amp into each well of a 96-deep well plate (master plate).

   Using 2YT instead of LB gives you higher cells densities of the overnight culture and subsequently higher plasmid DNA yields.

2. Pick individual colonies into each well and seal the plate by applying an air permeable membrane.

   A simple method that avoids cross-contamination and double inoculation is to seal the plate with a piece of parafilm during inoculation. Pick the colonies with sterile toothpicks and stab them through the parafilm into the medium. The toothpicks can be removed after inoculation of all the wells. As a negative control do at least leave one well without inoculation.

3. Incubate the sealed plate in an orbital shaker (540 rpm) and grow at 37°C overnight.

   Shaking below 500 rpm may result in reduced cell density of the overnight culture and shaking above 550 rpm increases the risk of cross-contamination between wells.

4. Start preparing target protein coated MaxiSorp 96-well plate and plate to test background binding (e.g. only NeutrAvidin coated plate) as described in **Protocol 12.**

Day 2

5. Parallel to the expression continue blocking and coating of MaxiSorp 96-well plates as described in **Protocol 12.**
6. Aliquot 0.9 ml of 2YT/amp media into each well of a 96-deep well plate (expression plate).
7. Transfer 0.1 ml from each well of the master plate to the corresponding well of the expression plate.

   If the overnight culture did grow properly this will approximately result in an OD_{600} = 0.4.

8. Incubate the sealed plate in an orbital shaker (540 rpm) and grow at 37°C for 45 min.

   *45 min are sufficient for the cells to get into the log growth phase and obtain high expression yields of DARPins. This time can be extended up to 2 hours which leads to even slightly higher amounts of expression (not necessary for crude extract ELISA but advisable for expression and further 96-well IMAC purification (**Protocol 22**)).*

9. In the mean time centrifuge master plate at 3'000g for 10 min, empty the plate, blot dry on stacked paper towels and store at -20°C for later preparation of plasmid DNA.
10. To each well of the expression plate add 110 µl of 2YT/amp/IPTG media and incubate the sealed plate in an orbital shaker (540 rpm) and grow at 37°C for 3-4 h.
11. Transfer 0.1 ml from each well of the expression plate to the corresponding well of a 96-well PCR plate, spin the plate at 3'000g for 6 min, empty the plate, blot it dry on stacked paper towels.

    *This cell pellets can be used for the secondary screening by SDS-PAGE (**Protocol 21**).*

12. Spin expression plate at 3'000g for 6 min, empty the plate, blot it dry on stacked paper towels.

    Longer centrifugation makes the resuspension of the cell pellet cumbersome.

13. To each well add 50 µl B-PER II and resuspend the cell pellet completely for 15 min at RT (e.g. on an orbital shaker at 500 rpm).
14. To each well add 950 µl of PBS-TB and spin the plate at 3'000g for 10 min to remove cell debris.

15. Proceed with the screening of DARPins as described in **Protocol 20.**

16. For further experiments store the plate at -20 °C.

Protocol 20 Screening DARPins by ELISA

Comments

- This protocol allows the screening of individual DARPins for target-specific binding by ELISA.
- No further subcloning for large scale expression or IMAC purification is needed.
- DARPins are expressed as described in **Protocol 19.**
- For ELISA, appropriate positive and negative control should be included

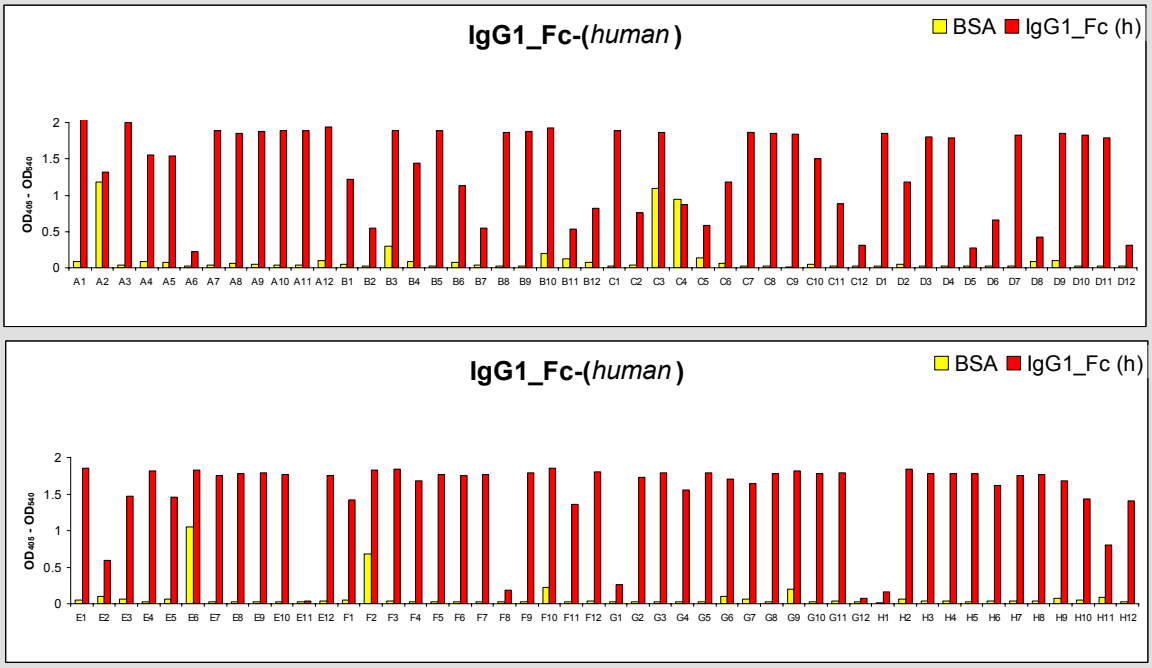

Figure 8: Example showing screening of DARPins by ELISA

Screening of IgG1_Fc binding DARPins by ELISA using crude cell extracts.

Equipment and Reagents (see p. 278 ff. for details)

- Target protein coated plate and control plate for background binding (**Protocol 12)**
- anti-RGS(His)$_4$ antibody
- anti-mouse antibody AP conjugate
- pNPP substrate
- PBS-T
- PBS-TB
- Shaker for 96-well plates
- 96-well plate containing crude extracts (**Protocol 19, Step 14**)

Method

Unless stated otherwise, all handling should be done with an 8 or 12-fold multichannel pipette to avoid cross-contamination between wells.

1. Add 90 µl of PBS-TB to each well of the target protein coated plate and control plate for background binding (**Protocol 12**).
2. Transfer 10 µl of the supernatant from **Protocol 19, Step 14** to both plates and incubate for 1 h at RT with orbital shaking (900 rpm).

   10 µl of the supernatant contain by far enough DARPins for the ELISA. Supernatants can be diluted up to 200-fold for further ELISA experiments (competition).
3. Wash the plate by empting the plate, blotting it dry on stacked paper towels, adding of 300 µl/well of PBS-T wash buffer and vortexing of the plate for 5 seconds. Repeat wash cycle 3 times.

   For washing you can use a squirt bottle filled with PBS-T.
4. Empty the plate and blot dry on stacked paper towels. Add 100 µl of 1:5'000 anti-RGS(His)$_4$ antibody in PBS-TB per well and incubate at RT for 1 h.
5. Wash plate as described in **Step 2**. (3 wash cycles)
6. Empty the plate and blot dry on stacked paper towels. Add 100 µl of 1:10'000 anti-mouse antibody AP conjugate in PBS-TB per well and incubate at RT for 1 h.
7. Wash plate as described in **Step 2**. (4 wash cycles)
8. Empty the plate as described in **Step 2**. Add 100 µl of pNPP substrate solution for the detection of bound protein.

   Develop the ELISA for up to 12 hours at RT. The reaction can be stopped by the addition of 3 M NaOH (100 µl) but background signal will be slightly increased.
9. Measure $OD_{405} - OD_{540}$.

   *Perform secondary screening by SDS-PGAE (**Protocol 21**).*
10. Prepare plasmid DNA from positive clones using a standard plasmid purification kit. Directly add resuspension buffer to the respective well of the master plate (thaw plate which was stored at -20°C) and resuspend the cell pellets for about 10 min at RT with orbital shaking plate (900 rpm).
11. Submit for sequencing using the primer Qe_30_for or Qe_30_rev for pDST67 (for details see Appendix data sheet: pDST67) or Qe_30_for or T7_term for pMPAG6 (for details see Appendix data sheet: pMPAG6).

Protocol 21 Secondary screening by SDS-PAGE

Comments

- This protocol describes the secondary screening of clones giving positive signal in ELISA experiments by SDS-PAGE.
- Due to high expression level of DARPins, crude cell extracts can be directly analyzed. DARPins different on the sequence level do show different running behavior on SDS-PAGE (mainly due to their stability differences) and expression patterns. These two properties allow identifying clones different on sequence level.

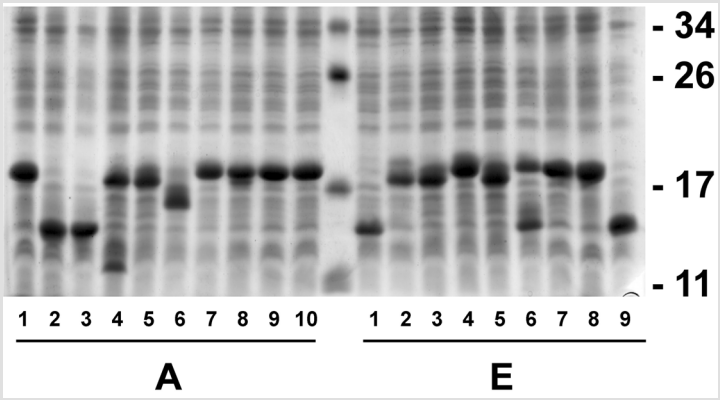

Figure 9: Example showing secondary screening of DARPins by SDS-PAGE

Analysis of whole cell extracts of a subset of IgG1_Fc binders (Binders from ELISA depicted in Figure 8:) by SDS-PAGE. On each lane cell extract from ~25 ul of the expression culture was loaded. Based on running behavior and expression pattern groups of presumably identical members DARPins can be formed (e.g. A1, A7, A8, A9, A10, E4, E7 and E8 what aligns quite well with ELISA signals seen in Figure 8:)

It should be noted that some DARPins having more than two internal repeats run at lower apparent molecular mass or show additional bands with faster running behavior. The same behavior was also observed for the respective purified proteins, even though they were subsequently shown by sequencing and MS to be precise in sequence and not degraded. As shown previously[11, 12] this is due to an incomplete denaturation of these stable molecules by SDS. N2C DARPins do not have this extreme SDS resistance and do run where expected

Equipment and Reagents (see p. 278 ff. for details)

- 96-well PCR plate containing cell pellets to be analyzed (**Protocol 19, Step 11**)
- SDS-PAGE (15%)
- SDS loading buffer

Method

1. Add 20 µl of SDS-PAGE loading buffer to each well of the PCR-plate (expression samples prepared in **Protocol 19, Step 11**) and resuspend the cell pellets by shaking at 1'000 rpm for 20 min and heat the samples to 95°C for 5 min using a 96-well PCR-machine. Load 5 µl of the samples to each lane of an 15% SDS-PAGE.
2. Run SDS-PAGE.
3. Stain with Coomassie Brilliant Blue solution and destain with 10% (v/v) acetic acid.
4. Together with ELISA data try to identify as many different positive clones as possible.

   *Differences in running behavior are for N2C not as clearly visible as for N3C (probably due to the generally lower stability of N2C compared to N3C, see **Figure 9:**)*
5. Prepare plasmid DNA from positive clones using a standard plasmid purification kit. Directly add resuspension buffer to the respective well of the master plate (thaw plate which was stored at -20°C) and resuspend the cell pellets for about 10 min at RT with orbital shaking plate (900 rpm).
6. Submit for sequencing using the primer Qe_30_for or Qe_30_rev for pDST67 (for details see Appendix data sheet: pDST67) or Qe_30_for or T7_term for pMPAG6 (for details see Appendix data sheet: pMPAG6).

96-well DARPin purification

Protocol 22 96-well IMAC purification of DARPins

Comments

- This protocol allows the IMAC purification of 96 individual DARPins in parallel.
- Using purified DARPins is recommended for the detailed characterization (competition, SEC,…) of clones identified as positive in the screening procedure. Clones should be sequenced in advance.
- About 0.25 to 1 mg of purified DARPins is obtained.
- All steps starting from 96-well transformation to 96-well purification will be described.
- DARPins are expressed with a modified version of **Protocol 19** optimized for maximal DARPin expression yields in small scale 96-well cultures.
- An alternative 96-well purification protocol using Ni-NTA material from QIAgen can be found on the supplier's homepage (http://www1.qiagen.com/literature/protocols/pdf/QE04.pdf).
- **It is absolutely essential to regenerate the plate after each use.**
- **Be careful not to lose IMAC resin during plate handling, the material is not fixed in the plate.**

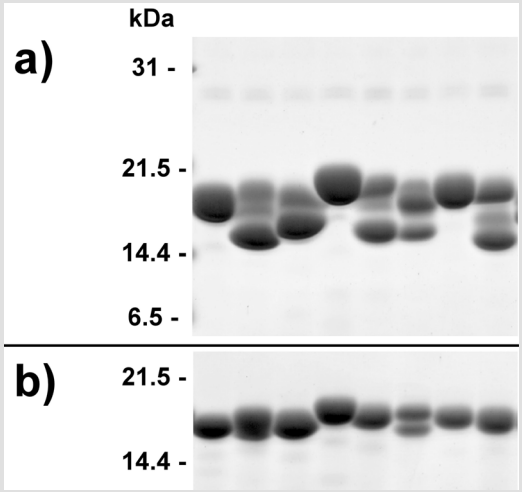

Figure 10: Example showing SDS-PAGE of 96-well IMAC purified DARPins

SDS-PAGE analysis of 96-well IMAC purified DARPins (all N3Cs) (**a,b**). 4 µl of pooled

eluates was loaded per lane and SDS-PAGE performed at room temperature (**a**), showing incomplete denaturation (refolding) of the highly stable DARPins and thereofe appearance of multiple bands. If SDS-PAGE of the same samples is run at 60°C (**b**) most of the multiple bands disapear.

Equipment and Reagents (see p. 278 ff. for details)

- Chemically competent *E. coli* XL1 Blue cells
- 96-well PCR plate
- SOC media
- 2YT/amp agar plate (square)
- 96-deep well plate for bacterial cell cultures (round bottom)
- 2YT media
- $NiCl_2$ (200 mM)
- 2YT/Glu/amp media
- 2YT/amp media
- 2YT/amp/IPTG media
- IMAC adjusting buffer
- IMAC wash buffer
- IMAC elution buffer
- Vacuum manifold
- IMAC 96-well plate
- GdnHCl (6 M), HCl (0.2 M)
- NaOH (0.5 M)

Method

Unless stated otherwise, all handling should be done with an 8 or 12-fold multichannel pipette to avoid cross-contamination between wells. Filter tips are not needed if you pipet carefully.

Day 1 (transformation)

1. Prewarm a metal 96-well PCR block to 42°C.
2. Put 96-well PCR plate on ice and aliquot 5 µl of chemically competent *E. coli* XL1 Blue cells into each well.
3. Add to each well 0.1 µl of respective plasmid DNA and incubate for 30 min on ice.

   Time can be reduced but transformation yield will be lower.
4. Heat shock for 30 sec at 42°C and add 50 µl of SOC media.

   LB or 2YT-media can be used instead but transformation yield will be lower.

5. Incubate at 37°C for 1 hour.

   Time can be reduced but transformation yield will be lower.

6. Plate drops of 3 µl on a 2YT/amp agar plate by using a multichannel pipette

   Take care to avoid cross contamination.

Day 2 (preculture)

7. Aliquot 1.2 ml of 2YT/Glu/amp into each well of a 96-deep well plate (master plate).

   Using 2YT instead of LB gives you higher cells densities of the overnight culture and subsequently higher plasmid DNA yields.

8. Pick multiple colonies from each transformation into wells of a 96-deep well plate and seal the plate with an air permeable membrane

   A simple method that avoids cross-contamination and double inoculation is to seal the plate with a piece of parafilm during inoculation. Pick the colonies with sterile toothpicks and stab them through the parafilm into the medium. The toothpicks can be removed after inoculation of all the wells. As a negative control do at least leave one well without inoculation.

9. Incubate the sealed plate in an orbital shaker (540 rpm) and grow at 37°C overnight.

   Shaking below 500 rpm may result in reduced cell density of the overnight culture and shaking above 550 rpm increase the risk of cross-contamination between wells.

Day 3 (expression)

10. Aliquot pre-warmed (37°C) 0.99 ml of 2YT/amp into each well of eight 96-deep well plates (expression plates).

    Use round–bottom 96-deep well plates. By using eight expression plates in parallel a final culture volume of about 10 ml for each clone will be obtained giving enough starting material for the IMAC purification.

11. Transfer 0.11 ml from each well of the master plate to the corresponding well of the eight expression plates.

    If the overnight culture did grow properly this will approximately result in an OD_{600} = 0.4-0.6. If you need to prepare plasmid DNA from positive clones, add fresh 2YT/Glu/amp media to the master plate (max final volume 1.3 ml), grow for 10 hours at 37°C and prepare plasmid DNA using a standard kit.

12. Incubate the sealed plates in an orbital shaker (540 rpm) at 37°C for 2 hours.

Higher cell density at the time point of induction yields higher amounts of DARPin per ml of culture.

13. Add 133 µl of 2YT/amp/IPTG to each well of the expression plate and incubate the sealed plate in an orbital shaker (540 rpm) at 37°C for 4-5 h.

The culture will have a final OD_{600} = 3-4.

14. Transfer 0.1 ml from each well of one of the expression plates to the corresponding well of a 96-well PCR plate, spin the plate at 3'000g for 6 min, empty the plate, blot it dry on stacked paper towels.

*This cell pellets can be used for SDS-PAGE expression analysis of the single clones as described (**Protocol 21**).*

15. Spin expression plate at 3'000g for 6 min, empty the plate, blot it dry on stacked paper towels.

Longer centrifugation makes the resuspension of the cell pellet cumbersome.

16. Freeze cell pellets at -80°C for at least 1 hour.

*Freezing the cells increases the yield of lysis in **Step 17**. Do not freese in liquid nitrogen which can lead to cracking of the plate.*

Day 4 (purification)

17. Add 50 µl B-PER II to each well. Resuspend the cell pellet and lyse the cells by shaking on an orbital shaker at 800 rpm for 30 min at RT.

Good lysis is essential to obtain high amounts of purified protein.

18. Pool the lysates of all expression plates into one expression plate, add 400 µl of the IMAC adjusting buffer and mix by orbital shaking.

19. Centrifuge the plate at 3'000 g for 30 min.

20. During the mean time prepare IMAC 96-well plate by re-hydrating the nickel-charged chelating agarose with 0.5 ml 30% EtOH for 10 min, wash twice with 0.5 ml UHP and equilibrate by washing twice with 0.5 ml IMAC wash buffer. Omit EtOH wash if regenerated material is used.

21. Transfer 0.6 ml of the combined and centrifuged lysate into the wells of the IMAC 96-well plate and let the liquid pass through the filter plate by gravity flow. Re-centrifuge plate with lysate at 3'000 g for 15 min before transferring the rest of the supernatant to the IMAC 96-well plate. Wait until samples have completely passed through the IMAC resin.

Take care not to load cell debris into the Ni-NTA plate as this will clog the plate. Some wells may flow slower than others, if necessary slight vacuum might be applied to

speed up loading of the samples. Be aware that slow passage through the resin is essential for efficient binding of the His-tagged DARPins to the Ni-NTA matrix.

22. Perform wash steps with IMAC wash buffer on a vacuum manifold. Pipette 0.6 ml of IMAC wash buffer into each well, draw buffer completely through the filter by applying slight vacuum. Wash filter plate thoroughly from lower side by using a squirt bottle filled with UHP.

23. Perform another three wash cycles as described in **Step 22**.

24. Place the IMAC-plate on an empty collection plate and centrifuge at 100 x g for 2 min to remove residual wash buffer.

25. Place IMAC-plate on an empty collection plate add 200 µl IMAC elution buffer into each well, incubate for 1 min at RT and elute the protein by centrifugation at 50 x g for 2 min.

26. Perform second and third elution step as described in **Step 25**.

27. Pool eluted fractions, measure UV spectra and run SDS-PAGE.

Extinction coefficients of DARPins can vary strongly, dependent on the amount of aromatic residues. If sequence data of the DARPins is not yet available use other methods to quantify protein concentration (e.g. BCA, Breadford)

Day 4 (plate regeneration)

28. Perform all regeneration steps on a vacuum manifold. Pipette 0.6 ml of respective solution into each well, draw solution completely through the filter by applying slight vacuum.

2 x UHP, 2 x GdnHCl (6 M), HCl (0.2 M), 2 x UHP, 2 x NaOH (0.5 M), 2 x UHP, 2 x TBS_{500} (for more stringent purification Ni can be stripped from resin by using 100 mM EDTA)

29. Add 0.2 ml of $NiCl_2$ (200 mM) and let run through by gravity flow. Wash plate with 3 x UHP and 1 x 30% v/v EtOH

30. For storage pipette 0.6 ml of 30% v/v EtOH, seal plate with adhesive seal, put on empty collection plate and seal with parafilm

Troubleshooting

- **Background binding**: During selections on immobilized target protein an increase of clones showing unspecific background binding has been observed. The reason for this effect can probably be attributed to the “bad state” of the immobilized antigen. There are several possibilities to get rid of such background binders.
  - → Increasing the prepanning step (e.g. 2 hours in blocked MaxiSorp Immunotube), did lower but not completely avoid background binding in our hands.
  - → Change blocking buffer. BSA seems to have some properties that increase the interaction with sticky background binders. In a test-experiment none of these background binders did show signal on casein-blocked wells (most other blocking proteins tested behaved as BSA). Casein does contain low amounts of biotin that will block NeutrAvidin or streptavidin binding sites. Do dialyze casein stock extensively against PBS or add an excess of free biotin binding proteins during blocking of the plate and target immobilization. This approach has not been tested in selection conditions but is very promising.
  - → The simplest and most effective way is to do one or multiple rounds of selection in solution. In our hands this completely eliminated all background binders.
- **Low diversity of selection output**: Early epitope focusing, meaning that only one very dominant binder under all the positive clones is found has been reported for phage display and also observed for the DARPin phage library.
  - → We solved this problem by purifying the dominant DARPin and adding it to target protein during the selection. The DARPin will bind the target protein and thereby block its epitope. Therefore, the selection will be forced to find binders against different epitopes. In our hands the addition of different concentrations of purified DARPins to the target protein (e.g. for a 100 nM target protein concentration we added 200 nM and 4 µM DARPin) resulted in a panel of new DARPins binding the target protein.
- **No enrichment:** There are many possibilities why selections on a certain target protein might fail. One reason might be the instability of the target protein under the chosen selection conditions.
  - → e.g. in our hands reducing the temperature during the selection to 4°C made it possible to find binders against Her2 (1-509) which did fail under all selection approaches performed at RT.

References

1. Russel, M., Lowman, H.B. & Clackson, T. in Phage Display: A Practical Approach. (eds. H.B. Lowman & T. Clackson) 1-26 (Oxford University Press, New York, USA; 2004).
2. Dennis, M.S. & Lowman, H.B. in Phage Display: A Practical Approach. (eds. H.B. Lowman & T. Clackson) 61-83 (Oxford University Press, New York, USA; 2004).
3. Smith, G.P. & Petrenko, V.A. Phage Display. *Chem. Rev.* **97**, 391-410 (1997).
4. Bradbury, A.R. & Marks, J.D. Antibodies from phage antibody libraries. *J. Immunol. Methods* **290**, 29-49 (2004).
5. Viti, F., Nilsson, F., Demartis, S., Huber, A. & Neri, D. Design and use of phage display libraries for the selection of antibodies and enzymes. *Methods Enzymol.* **326**, 480-505 (2000).
6. Sidhu, S.S., Lowman, H.B., Cunningham, B.C. & Wells, J.A. Phage display for selection of novel binding peptides. *Methods Enzymol.* **328**, 333-363 (2000).
7. Forrer, P., Stumpp, M.T., Binz, H.K. & Plückthun, A. A novel strategy to design binding molecules harnessing the modular nature of repeat proteins. *FEBS Lett.* **539**, 2-6 (2003).
8. Alder, M.N. et al. Diversity and function of adaptive immune receptors in a jawless vertebrate. *Science* **310**, 1970-1973 (2005).
9. Binz, H.K. et al. High-affinity binders selected from designed ankyrin repeat protein libraries. *Nat. Biotechnol.* **22**, 575-582 (2004).
10. Amstutz, P. et al. Intracellular kinase inhibitors selected from combinatorial libraries of designed ankyrin repeat proteins. *J. Biol. Chem.* **280**, 24715-24722 (2005).
11. Binz, H.K., Stumpp, M.T., Forrer, P., Amstutz, P. & Plückthun, A. Designing repeat proteins: Well-expressed, soluble and stable proteins from combinatorial libraries of consensus ankyrin repeat proteins. *J. Mol. Biol.* **332**, 489-503 (2003).
12. Steiner, D., Forrer, P., Stumpp, M.T. & Plückthun, A. Signal sequences directing cotranslational translocation expand the range of proteins amenable to phage display. *Nat. Biotechnol.* **24**, 823-831 (2006).
13. Bullock, W.O., Fernandex, J.M. & Short, J.M. XI1-Blue: A High Efficiency Plasmid Transforming recA Escherichia coli Strain With Beta-Galactosidase Selection. *BioTechniques* **5**, 376-379 (1987).
14. Day, L.A. Conformations of single-stranded DNA and coat protein in fd bacteriophage as revealed by ultraviolet absorption spectroscopy. *J. Mol. Biol.* **39**, 265-277 (1969).
15. Chasteen, L., Ayriss, J., Pavlik, P. & Bradbury, A.R. Eliminating helper phage from phage display. *Nucleic Acids Res* **34**, e145 (2006).
16. Cull, M.G. & Schatz, P.J. Biotinylation of proteins in vivo and in vitro using small peptide tags. *Methods Enzymol.* **326**, 430-440 (2000).
17. Scholle, M.D., Collart, F.R. & Kay, B.K. In vivo biotinylated proteins as targets for phage-display selection experiments. *Protein Expr. Purif.* **37**, 243-252 (2004).
18. Chattopadhaya, S., Tan, L.P. & Yao, S.Q. Strategies for site-specific protein biotinylation using in vitro, in vivo and cell-free systems: toward functional protein arrays. **1**, 2386-2398 (2006).
19. Inoue, H., Nojima, H. & Okayama, H. High efficiency transformation of Escherichia coli with plasmids. *Gene* **96**, 23-28 (1990).

Materials

Equipment

- **Culture flasks**: non-baffled (100 ml, 300 ml, 2 l, 5 l), sterile, phage free flask (re-autoclave if you want to be sure)
- **Equipment for end-over-end rotation**: for Nunc Immunotubes and 2 ml micro tubes (e.g. Stuart scientific roller mixer SRT1, Aldrich no. Z316474 or MACSmix tube rotator, Miltenyi Biotech, no. 130-090-753)
- **Incubator for 96-well bacterial cell** cultures: e.g. Edmund Bühler, no 6161 000 and 6167 000
- **Magnetic tube holder for 2 ml micro tubes**: e.g. Dynal, MPC-S, no. 120.20
- **Shaker for 96-well plates**: e.g. Mikrotiterplattenschüttler TiMix 5, Edmund Bühler, no 6166 000
- **Vacuum manifold**: e.g. Millipore, no. MAVM 096 0R
- **Water bath (heatable)**: e.g. Heating Circulator with Open Bath Julabo, ED-5, no 9115405

Consumables

- **96-deep well plate for bacterial cell cultures (round bottom)**: e.g. AbGene, no. AB-0932
- **96-well PCR plate**: e.g. Costar, no. 6511
- **Cell scrapers**: e.g. BD Falcon, no 353085
- **Culture tubes (14 ml)**: Sterile 14 ml culture tubes (e.g. Falcon, no. 352059)
- **Dialyis tubing MWCO 3'500 kDa**: e.g. Spectra/Por, no 132720
- **DNA purification kit**: e.g. Macherey-Nagel, NucleoSpin Extract II, no 740609.50
- **Gas permeable adhesive seals**: e.g. ABgene, no AB-0718
- **IMAC 96-well plate**: e.g. SwellGel Nickel Chelated Discs, 96-well filter plate, Pierce, no 75824
- **MaxiSorp 96-well plate**: e.g. Nunc MaxiSorp 96-well plate (Nunc, no. 442404)

- **MaxiSorp Immunotubes**: e.g. Nunc MaxiSorp Immunotubes (Nunc, no. 444202)
- **Micro tubes (2 ml)**: Sterile 2 ml polypropylene micro tubes (e.g. Sarstedt, no. 72.695)
- **Nap 5 columns**: e.g. GE healthcare, no. 17-0853-01
- **Parafilm**: e.g. Pechiney Plastic Packaging (10cm x 38m), no:PM996
- **Petri plates large**: e.g. Nunc Tc Dish 245x245x25, no 166508
- **Petri plates round**: e.g. Sarstedt, 92 x 16 mm, no. 83.1473
- **Petri plates square**: e.g. Nunc Tc Dish 245x245x25, no 166508
- **Plasmid purification kit**: e.g. Macherey-Nagel, NucleoSpin Plasmid, no 740588.50
- **Polypropylene tubes (50 ml)**: Sterile 50 ml polypropylene tubes (e.g. Sarstedt, no. 62.547.24)
- **Stoppers for Immunotubes** : Nunc stoppers (Nunc, no. 348801)
- **Toothpicks autoclaved**

Reagents from third parties

- **anti-M13 antibody HRP conjugate**: mouse anti-M13 antibody horseradish peroxidase conjugate (Amersham Pharmacia Biotech, UK, No. 27-9421-01)
- **anti-mouse antibody AP conjugate**: : goat anti–mouse IgG alkaline phosphatase conjugate (Sigma, No. A3562)
- **anti-RGS(His)$_4$ antibody**: mouse anti RGS(His)$_4$ IgG1 (Qiagen, no. 34650)
- ***BamHI* (20 U/µl):** e.g. NEB, 20 U/µl, no R0136S
- **BM Blue POD substrate**: Roche Diagnostics, no. 11484281001
- **B-PER II**: Bacterial Protein Extraction Reagent (Pierce, no.78260)
- **CiAP (1u/µl)**: Calf Intestine Alkaline Phosphatase (e.g. Fermentas, 1U/µl, no #EF0341)
- ***E. coli* XL1-Blue**: Bacterial strain: *E. coli* XL1-Blue[13] (Stratagene, no 200268): F' [lacI^q lacZΔM15 proAB$^+$ Tn10(Tet^r)] endA1 supE44 gyrA96 hsdR17 lac recA1 relA1 thi
- **EZ-Link Sulfo-NHS-LC-Biotin**: Pierce, no. 21335
- **EZ-Link Sulfo-NHS-ss-Biotin**: Pierce, no. 21331

- ***HindIII* (20 U/µl)**: e.g. NEB, 20 U/µl, no R0104S
- **NEB2 buffer (10x)**: e.g. NEB, no B7002S
- **NeutrAvidin**: Pierce, no. 31000
- **Primary DARPin PD library #1stock**:
- **Streptavidin (Strp)**: Sigma, no. S-0677
- **Streptavidin-coated paramagnetic beads**: Dynabeads MyOne Streptavidin T1, Dynal, no. 656-02 or Dynabeads M-280 Streptavidin, no. 112-06D (10 µg/ml)
- **Streptavidin-AP conjugate**: e.g. Roche Diagnostics, no 1089161
- **T4-buffer (10x)**: Supplied with enzyme
- **T4-Ligase**: e.g. Fermentas, 5u/µl, #EL0014
- **VCSM13 Helper phage**: Stratagene, no 200251 (alternatively, M13K07 helper phage (New England Biolabs) may be used)

Reagents and Solutions

- **1.2% TAE/agarose gel**: TAE buffer, 1.2% (w/v) agarose, heat to dissolve, cool to 50°C, add 1:5'000 ethidium bromide and pour gel
- **2YT agar**: 2YT media, 1.5% agar (15 g/l) and 1% glucose (10 g/l); autoclave, cool
- **2YT media**: 1% bacto-yeast extract (10 g/l), 1.6% bacto-tryptone (16 g/l), 0.5% NaCl (5 g/l); adjust pH to 7.0 with NaOH; autoclave and cool (To avoid contaminations we recommend to heat up media to >80°C in the microwave after each use)
- **2YT top agar**: 2YT media containing 0.75% agar (7.5 g/l); autoclave, cool to 50°C
- **2YT/amp agar plates (round or square)**: melt 2YT agar, cool to 55°C, add 50 µg/ml amp, pour into petri plates (round: ~ 20 ml/plate), (square: ~ 60 ml/plate)
- **2YT/amp media**: 2YT media, 50 µg/ml amp
- **2YT/amp/IPTG media**: 2YT media, 50 µg/ml amp, 5 mM IPTG
- **2YT/cam/tet agar plates (round, square or large)**: melt 2YT agar, cool to 55°C, add 15 µg/ml tet and 10 µg/ml cam, pour into petri plates (round: ~ 20 ml/plate), (square: ~ 60 ml/plate), (large :~ 100 ml/plate)

- **2YT/Glu/amp media**: 2YT media, 1% glucose, 50 μg/ml amp
- **2YT/Glu/amp media**: 2YT media, 1% glucose, 50 μg/ml amp
- **2YT/kan agar plates (round or square)**: melt 2YT agar, cool to 55°C, add 10 μg/ml kan, pour into petri plates (round: ~ 20 ml/plate), (square: ~ 60 ml/plate)
- **2YT/kan media**: 2YT media, 10 μg/ml kan
- **2YT/tet agar plates (round)**: melt 2YT agar, cool to 55°C, add 15 μg/ml tet, pour into round petri plates (~ 20 ml/plate)
- **2YT/tet media**: 2YT media, 15 μg/ml tet
- **2YT/tet/cam media**: 2YT media, 15 μg/ml tet, 10 cam
- **2YT/tet/cam/G media**: 2YT media containing 20% v/v glycerol, autoclave and cool, add tetracycline to 15 μg/ml and chloramphenicol to 10 μg/ml
- **2YT/tet/cam/Glu media**: 2YT/tet/cam media containing 1% w/v glucose
- **amp (1000x)**: Ampicilin (amp, 1000 x stock) (50 mg/ml ampicilin dissolve in UHP, filter through 0.22 μm filter, store at -20°C)
- **BSA (20%)**: 20% BSA (20% w/v BSA in UHP, filter through 0.22 μm filter, store at -20°C)
- **Chemically competent *E. coli* XL1 Blue**: Protocol by P.Forrer based on method published by Inoue et al [19])
- **cam (1000x)**: 1000 x chloramphenicol (cam) stock (10 mg/ml chloramphenicol dissolve in EtOH, filter through 0.22 μm filter, store at -20°C)
- ***E. coli* XL1-Blue glycerol stock**: *E. coli* XL1-Blue[13] (Stratagene, no 200268): F' [*lacI*^{q} *lacZ*Δ*M15 proAB*$^+$ Tn*10*(Tet^r)] *endA1 supE44 gyr*A96 *hsdR17 lac recA1 relA1 thi* (see **Protocol 1** for glycerol stock preparation)
- **Glucose (20%)**: 20% glucose (20% w/v glucose (200 g/l) in UHP, autoclave and cool)
- **glycine (200 mM, pH 2)**: 200 mM glycine (1.50 g/100 ml) adjust to pH 2, autoclave or filter through 0.22 μm filter, store at RT
- **GdnHCl (6 M), HCl (0.2 M)**: 6 M GdnHCl (57.3 g/100 ml), 0.2 M HCl (0.63 ml/100ml) dissolve in UHP, store at RT
- **IMAC adjusting buffer**: TBS_{500} containing 20% v/v glycerol and 40 mM imidazol
- **IMAC elution buffer**: TBS_{500} containing 10% v/v glycerol and 250 mM imidazol

- **IMAC wash buffer**: TBS_{500} containing 10% v/v glycerol and 20 mM imidazol
- **IPTG**: isopropyl-β-D-thiogalactoside (IPTG) stock (1 M IPTG (238 mg/ml) dissolve in UHP, filter through 0.22 µm filter, store at -20°C)
- **kan (1000x)** : 1000 x kanamycin (kan) stock (10 mg/ml kanamycin dissolve in UHP, filter through 0.22 µm filter, store at -20°C)
- **NaOH (0.5 M)**: 0.5 M NaOH (2g/100 ml) dissolve in UHP, store at RT
- **Neutravidin (300x)**: 300 x NeutrAvidin (Neu) stock (Pierce, no. 31000) (1.2 mg/ml NeutrAvidin dissolve in UHP, filter through 0.22 µm filter, store at -80°C) (final working concentration ~ 66 nM of tetrameric Neu)
- **$NiCl_2$ (200 mM)**: 200 mM $NiCl_2.6H_2O$ (4.75 g/100 ml) dissolve in UHP, store at RT
- **PBS**: 10 x PBS stock (1.37 M NaCl (80.1 g/l), 30 mM KCl (2.24 g/l), 80 mM $Na_2HPO_4.2H_2O$ (14.24 g/l), 15 mM KH_2PO_4 (2.04 g/l), do not adjust pH, autoclave) for 1xPBS dilute 10 x PBS stock into UHP, should be about pH 7.4, check first time stock is used
- **PBS-G**: PBS containing 10% v/v of glycerol, filter through 0.22 µm filter, store at 4°C
- **PBS-T**: PBS containing 0.1% (v/v) Tween20 (4 ml/l of 25% Tween20)
- **PBS-TB**: PBS-T containing 0.2% (w/v) BSA
- **PEG/NaCl (5x)** : 5 x PEG/NaCl (solve 20% w/v Polyethylene glycol (PEG) 6000 (20g/100ml) in warm 2.5 M NaCl (146.1 g/l), store at 4°C for max 1 week (hydrolysis of PEG)
- **pNPP buffer**: 50 mM $NaHCO_3$ (4.2 g/l), 50 mM $MgCl_2.6H_2O$ (10.2 g/l) dissolve in UHP, store at RT
- **pNPP stock (1M)**: 1 M stock solution of di-sodium 4-nitrophenyl phosphate (pNPP) (371 mg/ml), dissolve in UHP, store at -20°C
- **pNPP substrate**: Add 3 mM pNPP from stock (1M) to the pNPP buffer, final pNPP substrate is stable at 4°C for 1-2 weeks (discard when turning yellowish)
- **SOC media**: 0.5% bacto-yeast extract (5 g/l), 2% bacto-tryptone (20 g/l), 1mM NaCl (0.58 g/l) 2.5 mM KCl (0.19 g/l); pH should be about 7.2 otherwise adjust with NaOH; autoclave and cool, before use add sterile 10 mM $MgCl_2$,10 mM $MgSO_4$ and 20 mM glucose (To avoid contaminations we recommend to heat up media to >80°C in the microwave after each use)

- **Strp (300x)**: 300 x Streptavidin (Strp) stock (Sigma, no. S-0677) (1.2 mg/ml streptavidin dissolve in UHP, filter through 0.22 µm filter, store at -80°C) (final working concentration ~ 66 nM of tetrameric Strp)
- **TAE:** 50x TAE stock (2 M Tris (242g/l), 50 mM EDTA (100 ml/l of 0.5 M EDTA, pH 8) and adjust with glacial acetic acid (~ 57 ml) to pH 8, autoclave, cool
- **TBS_{500}**: 50 mM Tris.HCl (6.06 g/l), 500 mM NaCl (29.2 g/l), adjust with HCl to pH 8
- **Tet (1000x)**: 1000 x tetracycline (tet) stock (15 mg/ml tetracycline dissolve in 50% (v/v) EtOH containing 3 drops of 6 M HCl/10 ml, filter through 0.22 µm filter, store at -20°C)
- **triethylamine (100 mM)**: 100 mM triethylamine (140 µl triethylamine in 10 ml UHP), prepare on the day used
- **Tris/base (2 M)**: 2 M Tris (14.22 g/100 ml), autoclave or filter through 0.22 µm filter, store at RT
- **Tris/HCl (1 M, pH 7.4)**: 1 M Tris/HCl (12.11 g/100 ml) adjust to pH 7.4, autoclave or filter through 0.22 µm filter, store at RT
- **Tween20 (25%)**:25% Tween20 (25% (v/v) Tween20 stock solution in UHP, sterile filter 0.22 µm, store at 4°C)

Appendix

Data sheet: pDST67

- The plasmid vector pDST67 allows the expression of protein of interests (POI), such as designed ankyrin repeat proteins (DARPins), in the cytoplasm of *Escherichia coli.* The vector uses a strong regulated T5 phage promoter for the inducible high level expression of the POI. The open reading frame encodes a MRGS-His_6-tag for simple purification of the POI by immobilized metal affinity chromatography (IMAC). pDST67 relies on a *lacI* repressor gene presented in trans on a separate plasmid (pREP4, Qiagen) or by the strain (e.g. XL1-Blue has *lacI*^{q} on F' plasmid) for efficient repression of the promoter.

Handling

- Storage: -20°C in TE (10 mM TrisHCl, 1 mM EDTA, pH 8.5)
- Amplification: pDST67 can be amplified in *E. coli* (e.g. XL1-Blue) using a Luria Broth medium supplemented with 50 μg/ml of ampicillin and 1% glucose.

Vector Map

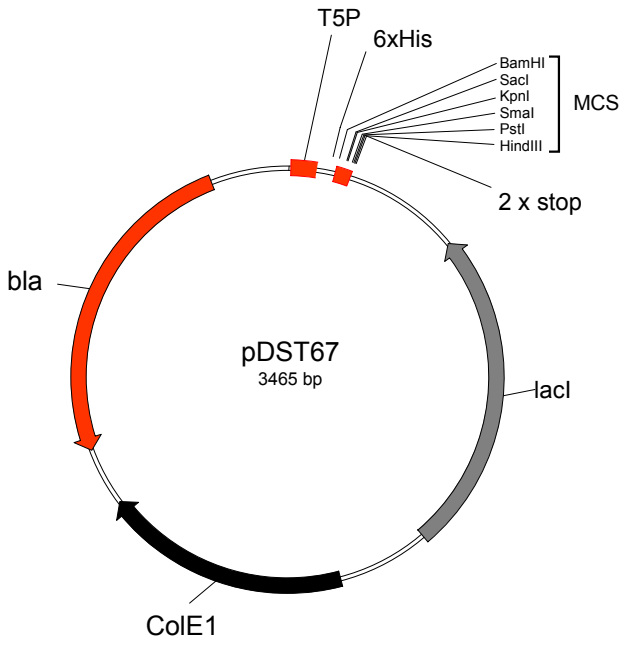

Cloning site region

```
 M  R  G  S  H  H  H  H  H  H  G  S  A  C  E  L  G  T  P  G  R  P  A  A  K  L  N  *  *
ATGAGAGGATCGCATCACCATCACCATCACGGATCCGCATGCGAGCTCGGTACCCCGGGTCGACCTGCAGCCAAGCTTAATTAATGA

                          BamHI       SacI  KpnI SmaI       PstI    HindIII
                          146         162   168  170        184     188
```

Features

- pDST67 is derived from pQE30 (Qiagen). From the MCS the *Stu*I restriction site was removed and in the resulting plasmid the single stop codon (TAA, position 196-196) replaced by two stop codon (ochre & opal; TAATGA, position 196-201), leaving the rest of the plasmid unchanged.
- Plasmid vector for high level cytoplasmic protein expression in *E. coli*.
- pDST67 contains no $lacI^q$ therefore has to be used in a $lacI^q$ host background (e.g. XL1-Blue).
- Excellent expression yields can be obtained in XL1-Blue cells.
- Sequences to be expressed are inserted in the MCS. The MCS is compatible to vectors of the pMPAG vector series, including the phagemid vector pMPAG3.
- For example, DARPins selected using pMPAG3 can be shuffled into pDST67 by simple transfer of the DARPin encoding *Bam*HI/*Hin*dIII vector fragment.
- The expression of the POI is under the control of a phage T5 promoter/*lac* operator element and the *lacI*^{q} gene has to be provided in trans.
  - → The phage T5 promoter is recognized by the endogenous *E. coli* RNA polymerase.
  - → Two lac operator sequences increase lac repressor binding and ensure efficient repression of the powerful T5 promoter.
  - → High-level expression is induced by addition of 0.5 mM of Isopropyl-beta-D-thiogalactopyranoside (IPTG) to the expression culture (typically at OD600 = 0.8).
  - → The addition of 1% glucose to the growth media helps to further repress the promoter in its uninduced state by catabolite repression, but has no negative effects on expression levels achievable upon induction.
- Synthetic ribosomal binding site for efficient translation initiation.
- 6xHis-tag coding sequence 5' to the multiple cloning site (MCS).
- The expressed His-tagged POI can be purified by IMAC.
- Two consecutive stop codons (ochre & opal; TAATGA) after the MCS ensure efficient translation termination in one reading frame.
- Strong transcriptional terminators prevent read-through transcription and ensure stability of the expression construct.
- Vector has a plasmid origin (ColE1) and an ampicillin resistance marker (Amp^R) to allow propagation as a plasmid in *E. coli.* The Amp^R is provided by β-lactamase (*bla*), which is constitutively expressed from the vector.

- The oligonucleotide Qe_30_for (5'-CTTTCGTCTTCACCTCGAG-3'; position 3453 to 6; reading forward) or Qe_30_rev (5'- CCAAGCTAGCTTGGATTCTC -3'; position 300 to 319 of the complement strand; reading reverse) may be used to sequence inserts present in the MCS(both oligonucleotides are available at www.microsynth.ch for sequencing).

Data sheet: pMPAG3 (pPDV1)

- The phagemid vector pMPAG3 allows the display of a protein of interest (POI) on filamentous phage. The vector uses the cotranslational signal recognition particle (SRP) pathway for the translocation of the POI across the cytoplasmic membrane into the periplasm of *Escherichia coli*. This feature (SRP phage display) allows the efficient display of stable and fast folding proteins, such as designed ankyrin repeat proteins (DARPins), on phage particles.

Handling

- Storage: at -20°C in TE (10 mM TrisHCl, 1 mM EDTA, pH 8.5)
- Amplification: pMPAG3 can be amplified in *E. coli* (e.g. XL1-blue) using a Luria Broth medium supplemented with 15 μg/ml of chloramphenicol

Vector Map

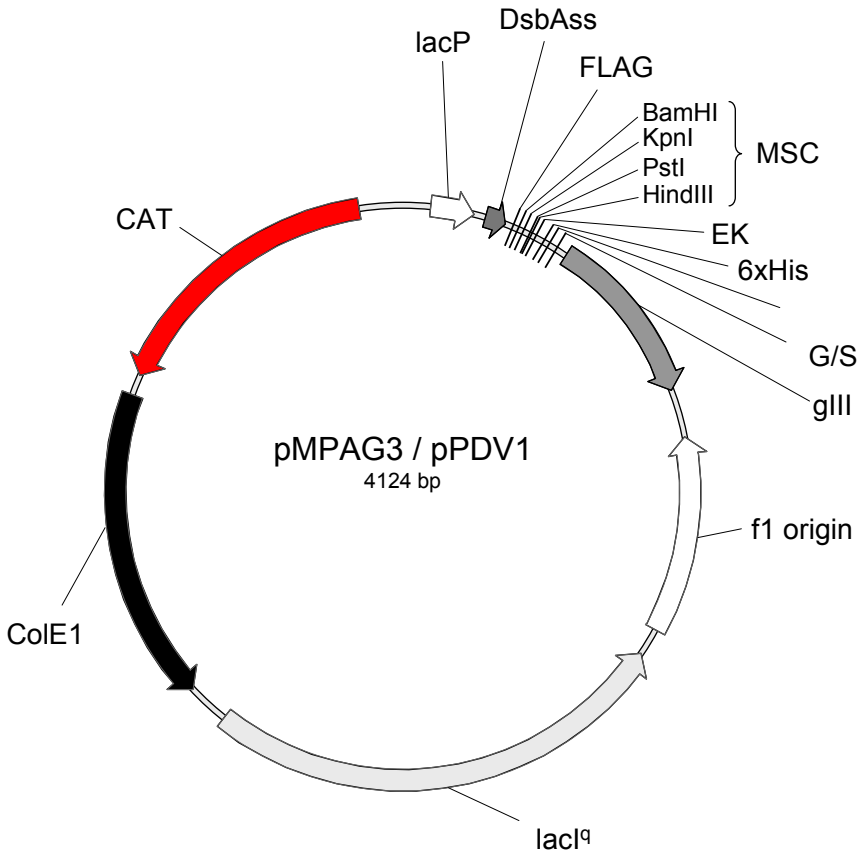

Cloning site region

```
   M   (DsbAss-Flag) G  S  G  G  T  *  *  *  P  A  A  K  L   (EK-6xHis) T  S  *  (gpIII)
CATATG---------------GGATCCGGTGGTACCTAATGATAACCTGCAGCCAAGCTT------------ACTAGTTAGGGT----
NdeI                BamHI    KpnI           PstI    HindIII           SpeI
193                 264      277            293     297               348
```

Features

- Phagemid vector for monovalent filamentous phage display.
- The signal sequence of *E. coli* DsbA (DsbAss) ensures efficient SRP phage display.
- Sequences for display are inserted in the multiple cloning site (MCS) between the DsbAss and a super short variant of filamentous phage gene III (gIII, encoding aa 250-406).
- The fusion protein (gpIII fusion) is under the control of a lac promoter/operator element and the $lacI^q$ gene provides high levels of the lac repressor in cis.
- An amber stop codon (TAG) is interposed between the displayed sequence and the gene III
  - → Allows expression of the POI independent of the gene III product (gpIII) in a non-supE host (e.g. JM83).
  - → Requires a supE suppressor host (e.g. XL1-blue) to produce displaying phage particles.
  - → Reduces the level of the gpIII fusion produced as a function of the *supE* suppressor host chosen to reduce potential toxic effect of the gpIII overexpression.
- The fusion protein contains a Flag-tag, a protease cleavage site (enterokinase site, EK) and a 6xHis-tag.
- Vector carries a f1 origin of replication to permit production of virions using an appropriate helper phage, such as VCSM13.
- Vector has a plasmid origin (ColE1) and an antibiotic resistance marker (the gene for chloramphenicol acetyl transferase (CAT) providing resistance to chloramphenicol (cam)) to allow propagation as a plasmid in *E. coli*.
- Two different oligonucleotides can be used for sequencing inserts present in the MCS: The oligonucleotide odst03 (5'-CATAATCAAAATCACCGGAACCAG-3'), corresponds to position 390 to 367 of the complement strand of pMPAG3 reading upstream the p3 fusion gene. Alternatively, the oligonucleotides pUCM13r-57 (5'-TGCTTCCGGCTCGTATGTTG-3'), corresponds to position 116 to 135 of the direct strand of pMPAG3 reading downstream the p3 fusion gene (oligonucleotides pUCM13r-57 is available at www.microsynth.ch for sequencing)

Data sheet: pMPAG6

- The plasmid vector pMPAG6 allows the expression of protein of interests (POI), such as designed ankyrin repeat proteins (DARPins), in the cytoplasm of *Escherichia coli.* The vector uses a strong regulated T5 phage promoter for the inducible high level expression of the POI. The open reading frame encodes a MRGS-His_6-tag for simple purification of the POI by immobilized metal affinity chromatography (IMAC). In addition, the vector has a $lacI^q$ gene providing lac repressor for efficient repression of the promoter.

Handling

- Storage: -20°C in TE (10 mM TrisHCl, 1 mM EDTA, pH 8.5)
- Amplification: pMPAG6 can be amplified in *E. coli* (e.g. XL1-Blue) using a Luria Broth medium supplemented with 50 μg/ml of ampicillin and 1% glucose.

Vector Map

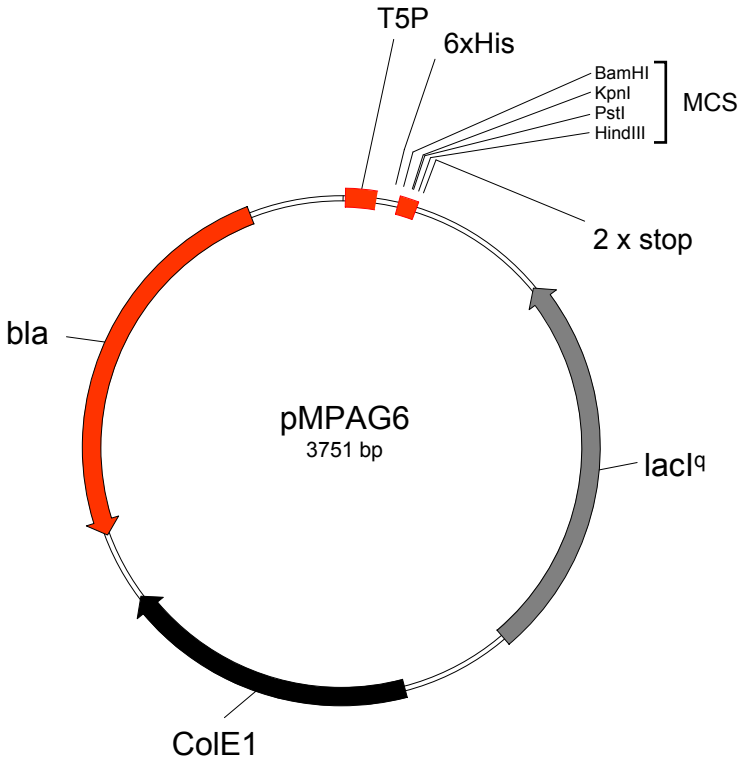

Cloning site region

```
   M  R  G  S  H  H  H  H  H  H  G  S  G  G  T  *  *  *  P  A  A  K  L  N  *  *  *
CATATGAGAGGATCGCATCACCATCACCATCACGGATCCGGTGGTACCTAATGATAACCTGCAGCCAAGCTTAATTAATGATAG
NdeI                            BamHI    KpnI           PstI    HindIII
113                             145      158            174     178
```

Features

- Plasmid vector for high level cytoplasmic protein expression in *E. coli*.
- No special expression host needed. Excellent expression yields can be obtained in XL1-Blue cells.
- Sequences to be expressed are inserted in the MCS. The MCS is compatible to vectors of the pMPAG vector series, including the phagemid vector pMPAG3.
- For example, DARPins selected using pMPAG3 can be shuffled into pMPAG6 by simple transfer of the DARPin encoding *Bam*HI/*Hin*dIII vector fragment.
- The expression of the POI is under the control of a phage T5 promoter/*lac* operator element and the *lacI*^{q} gene provides high levels of the lac repressor *in cis.*
  - → The phage T5 promoter is recognized by the endogenous *E. coli* RNA polymerase.
  - → Two lac operator sequences increase lac repressor binding and ensure efficient repression of the powerful T5 promoter.
  - → High-level expression is induced by addition of 0.5 mM of Isopropyl-beta-D-thiogalactopyranoside (IPTG) to the expression culture (typically at OD600 = 0.8).
  - → The addition of 1% glucose to the growth media helps to further repress the promoter in its uninduced state by catabolite repression, but has no negative effects on expression levels achievable upon induction.
- Synthetic ribosomal binding site for efficient translation initiation.
- 6xHis-tag coding sequence 5' to the multiple cloning site (MCS).
- The expressed His-tagged POI can be purified by IMAC.
- Two consecutive stop codons (ochre & opal; TAATGA) after the MCS ensure efficient translation termination in one reading frame.
- Strong transcriptional terminators prevent read-through transcription and ensure stability of the expression construct.
- Vector has a plasmid origin (ColE1) and an ampicillin resistance marker (Amp^R) to allow propagation as a plasmid in *E. coli.* The Amp^R is provided by β-lactamase (*bla*), which is constitutively expressed from the vector.
- The oligonucleotides Qe_30_for (5'-CTTTCGTCTTCACCTCGAG-3'; position 3739 to 6; reading forward) or T7_term (5'-TGCTAGTTATTGCTCAGCGG-3'; position 277 to 258 of the complement strand; reading reverse) may be used to sequence inserts present in the MCS (both oligonucleotides are available at www.microsynth.ch for sequencing).

Data sheet: PD Library #1

The phage display library PD library #1 allows the selection of target-specific designed ankyrin repeat proteins (DARPins) by monovalent filamentous phage display.

Lot #1 (25.01.2006)

- The library is provided as a frozen stock of DARPin-displaying phage particles in PBS (pH 7.4) supplemented with 10% glycerol.
- **Phage concentration**: 1.6 x 10^{13} chloramphenicol resistant colony forming units (cfu) per ml
- **Diversity**:
  - → 2.6 x 10^{10} independent chloramphenicol resistant clones of which 42% are correct DARPins, resulting in the functional library size of 1.1 x 10^{10}.
  - → 25% of the clones are N3C DARPin library members.
  - → 17% of the clones are N2C DARPin library members
  - → 58% of the clones (non functional part of the library) had either frame shifts in the DARPin sequence or no insert at all.
- The N2C library members comprise two randomized internal repeat modules between the N- and the C-terminal capping repeat, while the N3C library members have three randomized repeats

Handling

- Background information and protocols for the use of the PD library #1 are provided in the Phage Display Manual.
- Storage: Store at -80°C until use.
  - → Samples may be further aliquoted by thawing, splitting and flash freezing in liquid nitrogen. Repeated cycles of freezing and thawing should be avoided.
  - → Long term storage at 4°C may result in loss of displayed DARPins.
- Because displayed DARPins remain functional upon freezing, defrosted phage samples can directly be used for the first selection round without the need of reamplifying them.
- Repropagation: Repropagation of the library is possible. See **Protocol 8** of the Phage Display Manual.

Key features

- Allows the selection of highly stable target-specific DARPins against native proteins.

- The excellent biophysical properties of DARPins ensure that they normally will keep their target-specificity and well-behavior independent of being tethered to a phage particle.
- Based on the phagemid pMPAG3 (for details see Appendix data sheet: pMPAG3)
  → Monovalent phage display allowing the selection of high (even sub-nanomolar) affinity DARPins.
  → SRP phage display ensures the efficient display of the highly stable and fast folding DARPins.

Appendix 3

A Designed Ankyrin Repeat Protein Evolved to Picomolar Affinity to Her2

Zahnd, C., Emanuel, W., Schwenk, J. M., Steiner, D., Lawrence, M. C., McKern, N. M., Pecorari, F., Ward, C. W., Joos, T. O. & Plückthun, A. (2007)

J. Mol. Biol. 369, 1015-1028 (2007).

(**My contribution**: Cristallisation collaboration with C. Ward and coworkers (CSIRO, Melbourne, Australia))

Contents

doi:10.1016/j.jmb.2007.03.028 *J. Mol. Biol.* (2007) **369**, 1015–1028

JMB

Available online at www.sciencedirect.com

ScienceDirect

ELSEVIER

A Designed Ankyrin Repeat Protein Evolved to Picomolar Affinity to Her2

Christian Zahnd[1]†, Emanuel Wyler[1]†, Jochen M. Schwenk[2] Daniel Steiner[1], Michael C. Lawrence[3], Neil M. McKern[3] Frédéric Pecorari[1], Colin W. Ward[3], Thomas O. Joos[2] and Andreas Plückthun[1]*

[1]*Biochemisches Institut der Universität Zürich Winterthurerstr. 190 CH-8057 Zürich, Switzerland*

[2]*NMI Naturwissenschaftliches und Medizinisches Institut an der Universität Tübingen Markwiesenstr. 55, D-72770 Reutlingen, Germany*

[3]*CSIRO, Molecular and Health Technologies 343 Royal Parade, Parkville Victoria 3052, Australia*

**Corresponding author*

Designed ankyrin repeat proteins (DARPins) are a novel class of binding molecules, which can be selected to recognize specifically a wide variety of target proteins. DARPins were previously selected against human epidermal growth factor receptor 2 (Her2) with low nanomolar affinities. We describe here their affinity maturation by error-prone PCR and ribosome display yielding clones with zero to seven (average 2.5) amino acid substitutions in framework positions. The DARPin with highest affinity (90 pM) carried four mutations at framework positions, leading to a 3000-fold affinity increase compared to the consensus framework variant, mainly coming from a 500-fold increase of the on-rate. This DARPin was found to be highly sensitive in detecting Her2 in human carcinoma extracts. We have determined the crystal structure of this DARPin at 1.7 Å, and found that a His to Tyr mutation at the framework position 52 alters the inter-repeat H-bonding pattern and causes a significant conformational change in the relative disposition of the repeat subdomains. These changes are thought to be the reason for the enhanced on-rate of the mutated DARPin. The DARPin not bearing the residue 52 mutation has an unusually slow on-rate, suggesting that binding occurred *via* conformational selection of a relatively rare state, which was stabilized by this His52Tyr mutation, increasing the on-rate again to typical values. An analysis of the structural location of the framework mutations suggests that randomization of some framework residues either by error-prone PCR or by design in a future library could increase affinities and the target binding spectrum.

Keywords: ErbB2/Her2; designed ankyrin repeat protein (DARP)in; *in vitro* selection; ribosome display

Introduction

Antibodies with high affinity to disease-relevant antigens, such as tumor markers or chemokines, have been widely investigated for their use in therapy and diagnostics. Antibody engineering techniques have facilitated the generation of high affinity protein binders for targeted therapy.[1,2] The introduction of antibody-fragments and novel selection methods such as phage display or ribosome display has allowed the fast isolation of specific binding proteins from vast synthetic libraries *in vitro*.[3,4] Selections from such libraries have been shown to routinely yield specific binders, with the

† C.Z. and E.W. contributed equally to this work.

Present addresses: C. Zahnd, Molecular Partners AG, Grabenstrasse 11a, CH-8952 Schlieren, Switzerland; E. Wyler, Institute of Biochemistry, ETH Zürich, CH-8093 Zürich, Switzerland; F. Pecorari, Unité de Biochimie Structurale – CNRS URA 2185, Institut Pasteur, 25 rue du Dr Roux, 75724 Paris Cedex 15, France.

Abbreviations used: ECD, extracellular domain; IHC, immunohistochemistry; RIA, radioimmuno assay; RMS, root mean square; SPR, surface plasmon resonance.

E-mail address of the corresponding author: plueckthun@bioc.unizh.ch

0022-2836/$ - see front matter

highest affinity binders typically being in the low nanomolar affinity-range.

For therapeutic and diagnostic applications, particularly against cell-surface targets, the retention time on the target is usually a crucial factor limiting the efficacy of the antibody reagent.[5] Affinity maturation of binders is therefore considered to be an important means to improve the properties of previously selected binders, and the selection for slower dissociation-rates with competitive off-rate selections has proved to be a powerful method for improving affinity.[6,7] This strategy is based on the observation that, usually, the on-rates for forming protein–protein interactions fall into a narrow window[8] and affinity is thus normally correlated with off-rate. Such evolved high-affinity antibodies have been used with great success in many applications.[2]

An alternative, novel approach to developing high-affinity binding reagents takes advantage of another natural class of binding proteins, termed ankyrin repeat proteins.[8] Ankyrin repeat proteins are built from a single structural motif, which is assembled into a protein domain. Due to the relatively high sequence homology within these ankyrin repeats, a consensus sequence module could be deduced from the natural ankyrin repeat proteins, identifying putative structure-determining framework residues (i.e. residues which on the basis of sequence conservation appear to be important for maintaining the repeat structure) and interaction-mediating binding residues.[9,10] A synthetic consensus repeat module of the ankyrin repeat protein family could be assembled into complex libraries of designed ankyrin repeat proteins (DARPins), from which binding proteins could be isolated that showed exceptional expression yields, stabilities[9,11] and affinities in the low nanomolar range.[11] Due to the modularity of the design, DARPins with more binding modules and consequently larger binding interfaces are feasible and a stepwise enlargement of the binding interface could even be considered as a way of affinity maturation. The exceptional stability and folding efficiency of DARPins might also allow novel therapeutic approaches such as potent DARPin-toxin fusions or bivalent DARPin constructs.

Epidermal growth factor receptor 2 (Her2) is a cell surface receptor, which has been shown to be over-expressed in several cancer tissues, including breast and colon carcinoma, and its over-expression has been linked to poorer prognosis of the patients. Only 20–30% of all breast cancer patients, however, show over-expression of Her2, making the determination of the state of the Her2 expression of a cancer patient an important diagnostic step in assessing the suitability of anti-Her2 therapy for the patient. Currently, one antibody against Her2 has been approved for the treatment of breast cancer and several other tumor types are in clinical trials.

In a previous study, DARPins binding to the extracellular domain of Her2 (Her2 ECD) with high specificity and low nanomolar affinities had been selected[12] from large synthetic libraries *in vitro* using ribosome display.[3] After six rounds of selection, several binders with nanomolar affinities were obtained and characterized. They were shown to bind the cognate antigen both as a purified protein and on different Her2-overexpressing cell lines and *in situ* in tissue sections of Her2-positive mammary carcinomas. For both therapeutic and diagnostic applications, the affinity of the Her-2 binding molecule is expected to be crucial. Therefore, Her2 is an ideal model system to explore the potential for affinity maturation of DARPins.

Here, we aimed to explore the affinity limits obtainable for DARPins by subsequent randomization of the selected pools in combination with *in vitro* selection under very stringent conditions, and particularly to investigate the structural consequences of affinity maturation in this scaffold.

For the present study we used rather small DARPin molecules containing only two randomized repeat modules (termed N2C). These N2C DARPins display an interaction surface that is smaller than the average interaction surface of an antibody. The small size of the DARPin, which should allow good tumor penetration, in combination with its high stability and expression yield, would provide the basis for the development of an *in vitro* and possibly also *in vivo* diagnostic test for the expression state of Her2 in cancer tissues. We have characterized the binding properties of the affinity-matured DARPins, including their ability to detect Her2 in solubilized tumor tissue. In addition, we have determined the crystal structure of the N2C DARPin with the highest affinity, which has allowed us to demonstrate that the selected mutations cause a change in the positioning of the side-chain of the residue at position 52 and, as a consequence of this mutation, cause a significant conformational change in the relative disposition of the repeat domains in this structure compared with their counterparts in the previously determined structures. These structural changes are thought to be the cause of the enhanced on-rate of the mutated DARPin.

Results

DARPins had been selected from large synthetic libraries *in vitro* using ribosome display[3] and binders specific for Her2 with nanomolar affinities were obtained.[12] We wished to affinity-mature these binders for their potential application as diagnostics and therapeutics and characterize the biophysical and structural consequences of affinity maturation in this protein architecture.

Selection procedure

Analysis of the previously selected pools revealed that most binders belonged to only a few sequence families. To increase the diversity in these pools and to extend the randomization to framework po-

sitions, which were fixed in the original library design,[9] error-prone PCR was performed in the presence of dNTP analogs as described earlier.[6,13] Several new pools were generated using all previously isolated pools as a starting point. The average mutation rate in the different reactions (with different mutation rates) was determined by sequencing to be 1.3–5.9 mutations per gene. For the following selection, the libraries with different mutation rates were combined.

The pools obtained were converted into the ribosome display format and subjected to three rounds of off-rate selection.[6] The selection pressure is mainly defined by the incubation time of the pools in the presence of a large molar excess of competitor antigen. It was increased from round to round, from 10 h initially to 100 h in the second round. In the third selection round, a first aliquot was isolated after five days and a second after 25 days. It has been shown that after very stringent off-rate selections, the fraction of remaining binders is very low compared to non-binding background clones.[7] This fraction can be increased by applying an additional selection round at low stringency, thereby enriching the diluted binders. Thus an additional panning round with no additional selection pressure was applied. The percentage increase in the binder clones after this non-selective selection round could be monitored by radioimmuno assay of the pools, resulting in a fivefold increase of the binding signal (data not shown). In addition, after cloning of the pools in an expression vector in *E. coli*, crude extract ELISA of single clones also indicated that there was an increase in specific binding clones. After the last off-rate selection round, five out of 92 analyzed clones (5%) showed specific binding. After the additional non-selective panning round, this ratio increased to 68 out of 92 (74%).

Sequences of binders

Those binders giving a specific binding signal in a crude extract ELISA were sequenced. Four major sequence families were found in the selected pool. According to the amino acid sequence in the first four randomized positions, the sequence families were termed the LWRF, the LWRL, the KEYL and the KWIF family. Representative sequences of binders are shown in Figure 1, kinetic parameters from BIAcore measurements are shown in Table 1 and Figure 2. Interestingly, an N1C DARPin showing target binding was also isolated, which might have been generated by recombination from an N2C DARPin gene.

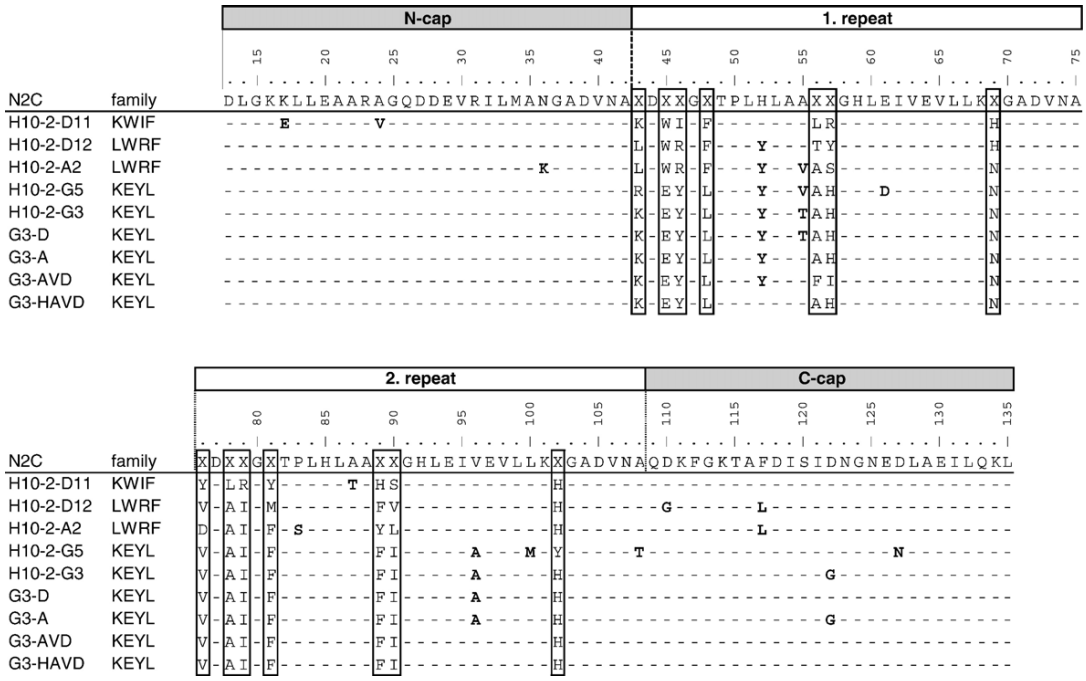

Figure 1. Sequences of selected DARPins and framework mutants of H10-2-G3. The sequences of different DARPins are shown. Randomized positions in the N2C family sequence (first line) are indicated by X. In the lower lines, only residues that differ from the consensus sequence of an N2C DARPin are printed. Residues that had been randomized in the original design are boxed. Mutations that showed up at framework positions (outside the boxes) are printed in bold. Four major sequence families were found after affinity maturation, termed KEYL, KWIF, LWRL and LWRF, according to the first randomized positions in the first module. The respective sequence family is also indicated. The clone with the highest affinity found was H10-2-G3. It contained four framework mutations (at residues 52, 55, 96 and 122) in addition to those residues that had been randomized by design. To investigate the effect of the different framework mutations, several mutants of this clone were constructed, turning the sequence back to the consensus sequence. These clones are listed in the lower part.

Table 1. Kinetic parameters of the binding of different DARPins

Clone name	Sequence family	K_D/nM	$k_{on}/10^4$ $M^{-1}s^{-1}$	$k_{off}/10^{-3}s^{-1}$
H10-2-G3	KEYL	0.091±0.001	112.3±0.19	0.102±0.001
G3-D	KEYL	1.48±0.008	76.8±0.36	1.14±0.002
G3-A	KEYL	1.21±0.006	61.8±0.26	0.745±0.002
G3-AVD	KEYL	10.2±0.055	43.5±0.22	4.42±0.008
G3-HAVD	KEYL	269±1.19	0.275±0.001	0.739±0.003
H10-2-G5	KEYL	0.670±0.005	26.6±0.036	0.178±0.001
H10-2-D11	KWIF	35.8±0.149	15.4±0.057	5.52±0.011
H10-2-D12	LWRF	93.9±1.12	30.5±0.31	28.6±0.17
H10-2-A2	LWRF	3.46±0.017	11.9±0.019	0.411±0.002

The statistical errors in the parameters given are those obtained from the best fit error.

As described below, the binder with the highest affinity, H10-2-G3 (KEYL family) has a picomolar affinity to the target. The K_D is about one order of magnitude better compared to the second best binder analyzed from the KEYL family. Interestingly, despite its high affinity, clone H10-2-G3 was only found once out of 68 sequenced clones. Only six out of the 68 analyzed clones belonged to the KEYL family. This indicates that high affinity is either not the only important factor for survival in the applied selection system or that the enrichment for high affinities has not yet reached its limit.

Compared to the sequences found in the selected pools prior to error-prone PCR, many mutations were found at so-called framework positions[9] as a consequence of the applied randomization. The average number of amino acid substitutions at framework positions was about 2.5 per sequence, ranging from several clones having no framework mutation, up to seven amino acid substitutions at framework positions per gene. It is likely that variable positions had also been randomized during error-prone PCR. This would not be detectable in the final sequence, although the actual number of mutations in the selected clones was increased.

The same sequence families that were present before off-rate selection could also be found after off-rate selection. However, the relative abundance of the different sequence families had changed. Whereas about 50% of the binders found before off-rate selection belonged to the KWIF-family, only 14% of the binders found after error-prone PCR and off-rate selections were of the KWIF-type. The LWRL-family, which finally contributed 28% of all binders, had not been found before off-rate selection.

Compared to previously described selection experiments against other targets, such as maltose binding protein and MAP kinases,[11] it was striking that most of the randomized variable positions in the selected Her2 ECD binders were hydrophobic. Up to 11 out of 14 variable residues were either aromatic or aliphatic amino acids. Ten of these built up an extended hydrophobic patch on the binding interface of the ankyrin repeat protein in the most extreme case. Since the interaction interface of the chosen DARPin library (consisting of only two ankyrin repeats) was limited in size, this might have been the only molecular solution to generate binders with affinities high enough to survive the selection pressure. However, despite the relatively large contiguous hydrophobic surface of the selected binders, no non-specific binding was observed (see below).

Affinities of Her2 binders

Based on the binding signals obtained in crude extract ELISA and the competition behavior with free Her2 ECD, several clones were chosen for expression, purification, affinity determination and further analysis. For each sequence family, several DARPins were expressed in the *Escherichia coli* strain XL1-blue. Despite the framework mutations, expression yields were similarly high as found previously[9,11] and also similar among the various clones, corroborating the robustness of the framework to also carry high mutational loads outside the randomized positions. The clones were purified to 95% purity *via* IMAC, and affinities were determined using kinetic and equilibrium surface plasmon resonance (SPR) measurements.

To get an initial affinity ranking, all expressed and purified clones were injected at a single concentration and the most promising binders were chosen for detailed measurements. Affinities were determined by kinetic SPR measurements with protein samples having any minor potential non-monomeric fractions removed by preparative gel filtration. The dissociation constants K_D of the measured affinities were found to be between 91 pM and 94 nM (Table 1). The binder with the highest affinity, termed H10-2-G3, was measured several times independently with different protein preparations and both kinetic and equilibrium measurements.[14–16] The kinetic measurements revealed an association rate constant of 1.1×10^6 $M^{-1}s^{-1}$ and a dissociation rate constant of 1.0×10^{-4} s^{-1}, giving rise to an equilibrium dissociation constant of 90 pM. Equilibrium measurements of the dissociation constant resulted in a K_D of 91 pM (Figure 2).

Clone H10-2-G5 (K_D of 670 pM) differed mainly at framework positions from H10-2-G3 (six differences), but had very similar amino acids at the variable positions (only two residues differ at positions 43 and 102; Figure 1). Although they belong to the same sequence family, their affinities differ by one order of magnitude. Most other binders showed affinities in the low nanomolar range (Table 1).

In the non-affinity-matured pools (starting material for this study), the clone with the highest affinity, termed H6-2-A7, had an affinity of 7.3 nM,[12] which is 80-fold lower than the affinity shown by H10-2-G3. Interestingly, clone H6-2-A7 had the same amino acid sequence in the first variable module as H10-2-G3, but a completely different sequence in the second variable module.

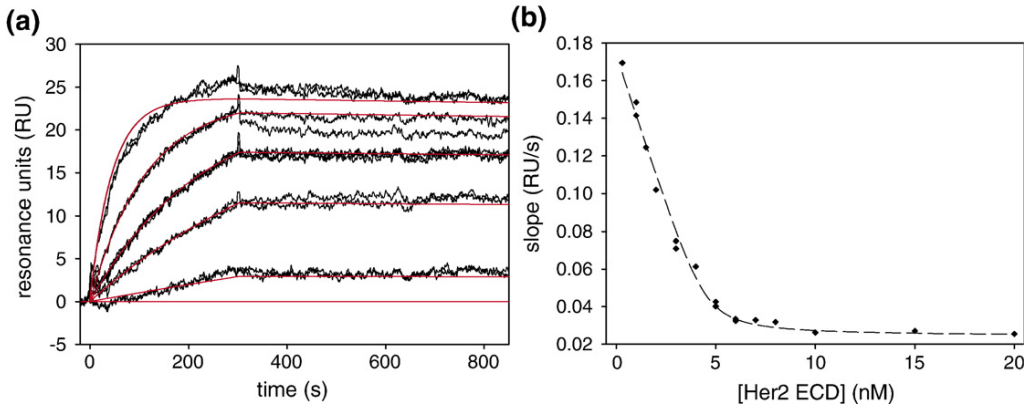

Figure 2. Affinity determination of clone H10-2-G3 using SPR. (a) The kinetics of binding of clone H10-2-G3 to Her2 ECD was monitored using Biacore. Her2 ECD was immobilized on a flow cell at low concentrations. Binding of the DARPin to the immobilized target protein was compared to binding to an empty flow cell at increasing concentrations of the DARPin (1 nM, 5 nM, 10 nM, 20 nM, 30 nM). The data were evaluated using global fitting with the software CLAMP.[26] The predicted curves are drawn in red. (b) The affinity was also determined at equilibrium using competition Biacore. The affinity values obtained by both methods were consistent.

Influences of framework mutations on affinity

The use of error-prone PCR allowed the introduction of framework mutations. However, in earlier selection rounds, several framework mutations already had become enriched. This intrinsic randomization of pools that are selected by ribosome display has been described before.[16] At position 52, the framework mutation histidine to tyrosine (H52Y) was found in 86% of all binders. Even before error-prone PCR, this mutation was found in some members of the KEYL-sequence family, suggesting that this mutation evolved independently several times.[12] Since this mutation has not been found in any of the other selection experiments performed with DARPins, we concluded that this mutation would be important for binding to the target Her2.

To test the influence of the observed framework mutations on the affinity of H10-2-G3, several mutants were constructed restoring the original framework residues (Figure 1). The four framework mutations found in H10-2-G3 were: H52Y and A55T, both residing in the first variable repeat module, V96A in the second variable repeat module and D122G in the C-terminal capping repeat. We generated four clones, the first termed G3-D, lacking the D122G mutation, the second termed G3-A, lacking the A55T mutation, the third G3-AVD without the mutations A55T, V96A and D122G and finally clone G3-HAVD, which corresponds to

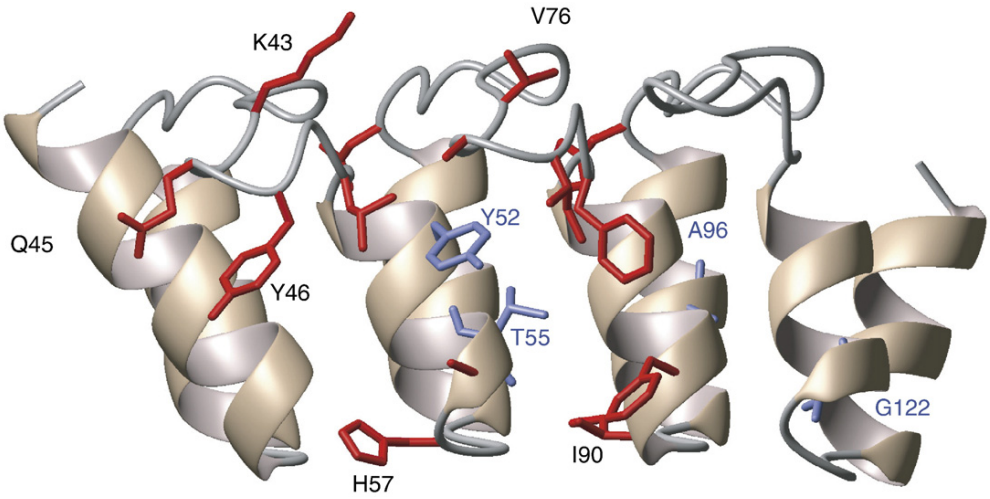

Figure 3. Crystal structure of H10-2-G3. The overall structure is shown in ribbon representation in front view, looking towards the putative binding surface. The side-chains of residues that had been randomized in the synthetic library are drawn in red. Side-chains of framework residues that had been mutated in the course of affinity maturation are drawn in blue. Note that only some of the side-chains that have been drawn are labeled.

H10-2-G3 with the original DARPin framework. All clones were expressed and purified and affinities were determined using kinetic SPR (Supplementary Data Figure).

All back-mutated clones had lower binding affinities than clone H10-2-G3 (Table 1). The reversion of the single mutations A55T and D122G had similar effects on the equilibrium dissociation constant, decreasing the affinity by about 15-fold each. The reversion of the triple mutation in G3-AVD reduced the affinity by over 100-fold, while the reversion of the additional mutation H52Y lead to a further 26-fold decreased affinity (compare G3-AVD with G3-HAVD) and an about 3000-fold decreased affinity compared to H10-2-G3. Interestingly, reversion of the mutation H52Y influenced mostly the on-rate, and since the off-rate changes much less, the affinity is lowered by about two orders of magnitude in the mutant.

The major contribution to the improved affinity obtained by the evolutionary approach was thus due to an increase in the association rate constant of the binding. This was not expected, since the association rate constant is usually governed by translational diffusion and orientation-dependent collisions, at least in solutions of moderate or high ionic strength. Therefore, it tends to be rather similar in most protein–protein interactions. For interacting proteins with molecular masses similar to the present example, association constants of 10^5–10^6 s^{-1} M^{-1} would be expected, if the process was diffusion-controlled.[8] The association rate constant of H10-2-G3 was determined to be 1.1×10^6 s^{-1} M^{-1}, which is in the expected range. For most of the non-affinity matured binders, the association rate constant was two to tenfold lower. However, in the quadruple "back"-mutant of the KEYL family, G3-HAVD, k_{on} was dramatically reduced (400-fold, compared to H10-2-G3 and 160-fold compared to G3-AVD, which differs only by carrying His52 instead of Tyr52). This strongly indicates that there is a rate-limiting step in the formation of the DARPin Her2-ECD complex other than simple diffusion. This could either be due to slowly forming structural rearrangements that have to occur prior to binding or be due to rapidly equilibrating conformations, of which an only sparsely populated one is able to bind. In the other protein families (KWIF and LWRF), the H52Y mutation does not correlate with k_{on}, suggesting that this effect is connected to the epitope recognized by the members of the KEYL-family (see below).

It should also be noted that most of the framework mutations are not at the putative binding site of the DARPin. While D122G could be involved in binding, and maybe also H52Y, mutations A55T and V96A are most likely not part of the binding interface, based on their location (see Figure 3). The differences between H10-2-G3 and H10-2-G5 (Figure 1) involve amino acid residues that are part of the hydrophobic core or reside on the back of the DARPin, except for K43R. Possible explanations for these observations are detailed in Discussion.

Crystal structure of H10-2-G3

To further analyze the influence of framework mutations on the binding kinetics, the crystal structure of the clone H10-2-G3 was determined to a final resolution of 1.7 Å, an *R*-value of 17.8% and an R_{free} of 21.2% (Table 2). The structure solution with three molecules of H10-2-G3 found in the crystallographic asymmetric unit was achieved *via* molecular replacement. The overall backbone of H10-2-G3 (Figure 3) was similar to the previously determined structures of DARPins,[11,12,19] with an overall root mean square (RMS) displacement of the backbone atoms of 1.13 Å compared to the N2C model.

However, there are two striking differences compared to representative N3C structures. The first is a rotameric[17] change at position 52 in conformation of the side-chain from *m*80° if it is occupied by histidine to *t*80° if it is occupied by Tyr in H10-2-G3. This mutation causes a change in the inter-repeat disposition (see below). H10-2-G3 has four mutations in the designed framework, H52Y, A55T, V96A and D122G. After testing the influence of all four mutations on the binding affinity (see above), mutation H52Y was shown to have the most substantial influence on the on-rate and its structural consequences were therefore analyzed in detail. This mutation, as well as D122G, is located on the side of the DARPin potentially facing the target, while the other two mutations are buried inside the molecule.

Analysis of the crystal structures of unselected N3C DARPins[18] reveals that the histidine at position 52 participates in an extended hydrogen bond network: His52 $N^{\delta1}$ to Thr49 $O^{\gamma1}$ and His52 $N^{\varepsilon2}$ to the carbonyl oxygen of residue 81 (Figure 4(a)). These inter-repeat unit hydrogen bonds likely contribute to the known extraordinary stability of DARPins (see below). However, the H52Y mutation and the concomitant rotameric change at that position causes a loss of both these hydrogen bonds, replacing them with a single hydrogen bond between Tyr52 O^{η} and Asp77 $O^{\delta2}$ (Figure 4(b)). No disruption is caused to the hydrogen-bonding pattern within the α-helical backbone at that mutation site. Rotameric rearrangement of the side-chain

Table 2. X-ray data collection and processing statistics

	Data set 1	Data set 2
Detector 2θ (°)	0	15
Resolution range (Å)	∞–2.00 (2.03–2.00)	∞–1.70 (1.73–1.70)
No. of frames	200	310
Oscillation range (°)	1	1
No. of measurements	144,477	225,321
No. of reflections	35,218	58,105
Redundancy	4.1 (3.7)	3.8 (2.4)
Completeness (%)	97.7 (94.6)	98.6 (93.3)
R_{merge}[a]	0.11 (>1.0)	0.12 (0.88)
$\langle I\rangle/\langle\sigma\rangle$	15.5 (1.6)	13.2 (1.3)

Numbers in parentheses refer to the statistics for the outer resolution shell.

[a] $R_{merge} = \sum_h\sum_i | \langle I_h\rangle - I_{h,i} | / \sum_h | \langle I_h\rangle |$.

at Leu86 is also evident, presumably to relieve steric clash with the Tyr52 side-chain. The second, more dramatic difference is that the positioning of the phenol ring of Tyr52 in the groove formed by the first helices of the two randomized repeats necessitates an opening-up of the N2C structure with respect to its unmutated counterparts (Figure 4(c)), effected by an $\omega = 13(\pm 1)°$ rotation of the second randomized and C-cap repeat (grouped as a single domain) with respect to the N-cap and first randomized repeat (grouped as a single domain). The hinge point of this rotation lies in the vicinity of residue 76. Whilst the size of ω and the direction of the rotation axis are closely similar for all pairwise N2C-to-N3C comparisons conducted here, the spatial location of the rotation axis itself is somewhat ill-defined, a mathematical consequence of ω being small. The relative rotation of the N and C-terminal halves of the N2C structure results in the loss of the hydrogen bond between the backbone carbonyl at position 46 and the backbone amide at position 78, the respective O and N atoms of these residues now being about 6 Å apart (Figure 4(a) and (b)).

Since all clones of the KEYL family having this H52Y mutation had an association rate constant that was increased by up to two orders of magnitude to reach values expected for protein–protein interactions (see above), the importance of this residue on the overall structure of the DARPin may not surprise. It is in principle possible that Tyr52 directly interacts with Her2 ECD, but we have no evidence for or against this. It is likely that the "opened-up" structure is the one that interacts optimally with the target. The original framework could adopt, as a sparsely populated state, an overall conformation that is similar to the conformation found with Tyr52. Such a break-up of the repeats could even allow His52 to adopt a similar rotameric conformation as seen here for Tyr52 (i.e. directed away from the N2C structure and towards the target), but this does not imply productive interaction of His52 with the target. A similar interaction of Tyr and His with the target would be difficult to conceive because of the different side-chain characteristics. If binding occurs by conformational selection, i.e. if only a minor fraction of the binding molecules is in the reactive "open" conformation, the bimolecular binding reaction would appear to be slow. Note that this effect would not affect the off-rate. The mutation H52Y most likely stabilizes the outward rotated conformation and thereby increases the active concentration of the binder, giving rise to a "normal" on-rate. In addition, the other mutations might optimize existing interactions or introduce new ones. The change in the overall conformation might assist adaptation to the antigen.

Note that the change in on-rate, interpreted as a conformational selection that gets stabilized by mutation, is a phenomenon only found in the KEYL family. In the other families, completely normal rates of association are found, despite the fact that they all contain His52. We interpret this as indicating a necessity for an open conformation only for binding to the epitope of the KEYL family, but clearly not a general phenomenon of DARPins. Consistent with this view, all association rates measured with binders to other targets fell in the usual windows, and all crystal structures determined so far[11,12,19] indicated a consensus spacing of repeats.

Conformational variability or even partial unfolding can be an important parameter controlling interactions of some natural ankyrin repeat proteins,[21–24] whereas other natural ankyrin repeat proteins[19] have been shown to be very stable and display two-state folding. The consensus-designed DARPins have previously been shown to be particularly stable.[9] We were thus interested in determining whether the His52Tyr mutation had an effect on the thermal stability of H10-2-G3 and therefore measured it and compared it to that of the "restored" consensus framework variant, G3-HAVD. We found that G3-HAVD is significantly more stable than H10-2-G3: the mutations in the framework acquired in affinity maturation did indeed lead to a decrease of the midpoint of denaturation from 89.4(±0.6) °C to 69.1(±0.02) °C (Figure 5). For both proteins, H10-2-G3 and G3-HAVD, the measurement was performed with material that had been purified by gel filtration to remove any potential non-monomeric species. Furthermore, the protein had been analyzed by multi-angle light scattering (MALS) to verify its monomeric state. These MALS results exclude that the observed stability change was due to the presence of dimers of G3-HAVD. Neither of the two proteins showed significant dimeric fractions even at very high concentrations of more than 100 μM (data not shown).

Therefore, the conformational change caused by the introduction of these evolved framework mutations destabilizes the molecule, but not to the point of imparting any handling disadvantage on this evolved protein, as even the affinity-matured H10-2-G3 still has a stability in the upper range of typical globular proteins, and no difference in handling was noticed in purification or any treatment compared to other DARPins. In particular, the high soluble expression yield is fully maintained for the evolved DARPin. The consensus protein G3-HAVD, a typical member of the original library from which the directed evolution had presumably started, has such a high stability that the conformational changes and some ensuing loss of stability are easily tolerated. This high stability of the consensus-designed libraries is one of the key features ensuring that affinity maturation still leads to molecules with very favorable properties without further stability engineering.

A more complete analysis of the influence of the mutations could be obtained by the analysis of the binding interface in a co-crystal of Her2 and H10-2-G3. Presumably not only the randomized positions (those designed to be variable in the original library) participate in binding of the DARPin to its target, but also at least some of the selected framework positions, as shown, for example, by the considerably lower K_D of the G3-D mutant compared to H10-

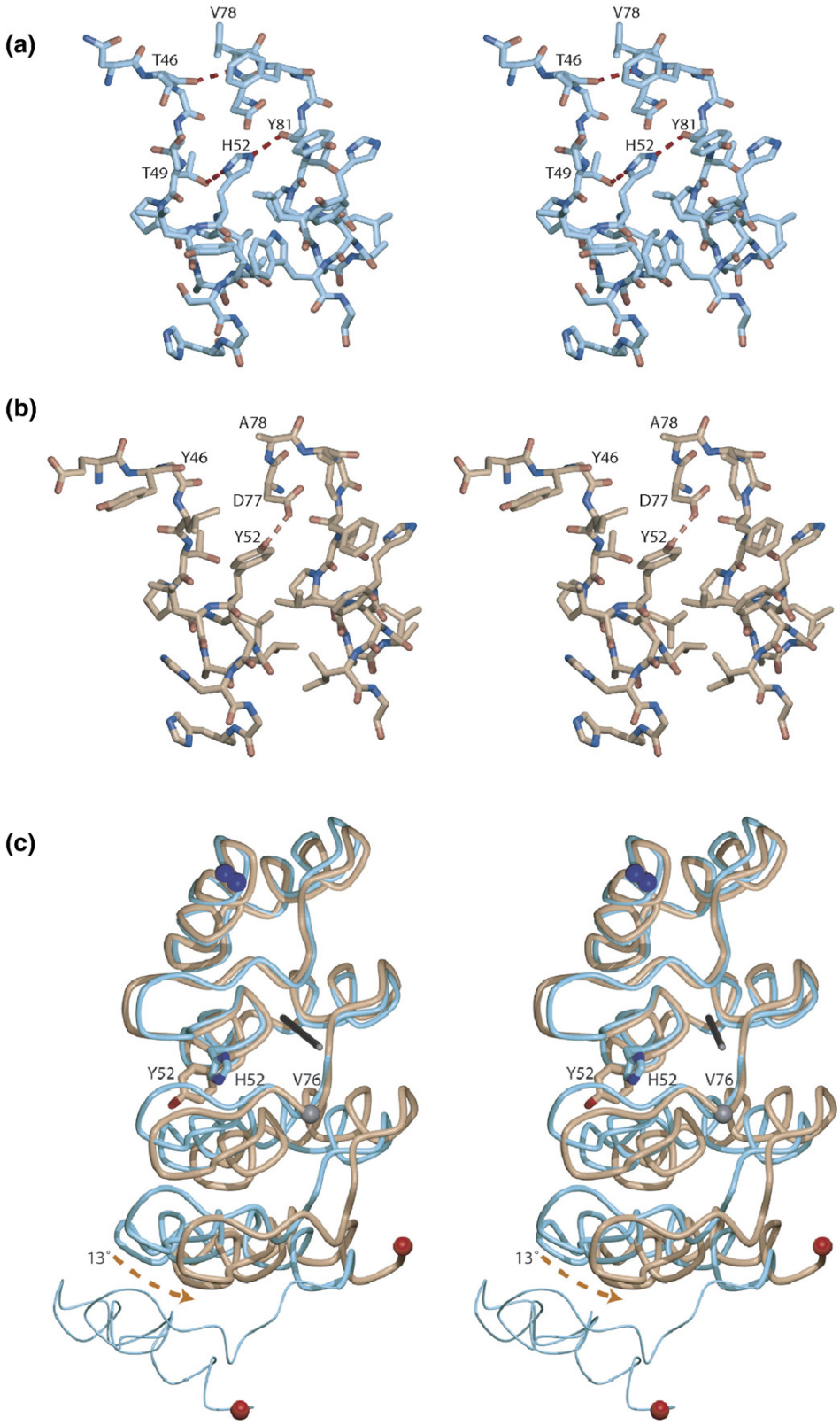

Figure 4 (*legend on next page*)

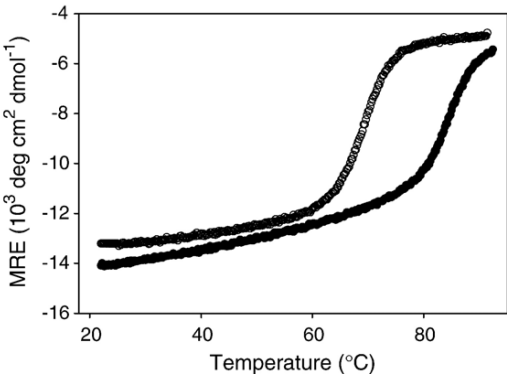

Figure 5. Thermal denaturation of H10-2-G3 (open circles) and G3-HAVD (filled circles), a variant of H10-2-G3 that carries no mutations at framework positions. Both proteins were heated from room temperature to 95 °C and the circular dichroism was measured at 222 nm. The midpoints of denaturation were estimated from extrapolation of the curves to be at 69 °C and 89 °C, respectively.

2-G3. The residue where G3-D differs, Gly122, is in the C-cap, and it could make a direct contact or the original interaction with Asp122 could have been unfavorable, even by indirect electrostatic effects. In a biochemical analysis and in the absence of a structure of a complex, however, it is difficult to distinguish between mutations that help the adaptation of the DARPin structure to the antigen epitope and mutations of amino acids that actually bind to the target.

Epitope characterization and specificity of affinity matured binders

DARPins selected before affinity maturation were shown to bind to different epitopes and some competed for the same epitope with trastuzumab (Herceptin™), an antibody used in therapy. We therefore tested if the binding of the affinity-matured DARPins could still be inhibited with antibodies. We assayed the selected clones with trastuzumab, which has been shown to bind to the membrane-adjacent cysteine-rich domain IV[20] and pertuzumab, another antibody under development for its use in therapy, which binds to domain II.[21] In competition ELISA, all binders of the KWIF-sequence family competed with trastuzumab for the epitope as shown previously for the non-affinity matured DARPins.[12] None of the selected and analyzed binders competed with pertuzumab for Her2 ECD (data not shown).

The highest affinity DARPins were investigated for their cross-reactivity with unrelated proteins, including epidermal growth factor receptor 1 (EGFR). As shown in the previous work for non-matured binders,[12] none of the affinity-matured binders showed non-specific binding (data not shown).

Sensitivity analysis of the selected DARPins

To evaluate the use of the selected and affinity-matured DARPins for the quantification of Her2 in sandwich immunoassays, we tested five binders (three representative ones are listed in Figure 6(a)) in a multiplexed format. For this purpose, the DARPins were expressed with N-terminally fused phage lambda protein D (pD) containing an avi-tag, to allow site-specific biotinylation with the *E. coli* biotin ligase BirA. Each of the biotinylated DARPins was immobilized on a different population of spectrally distinguishable avidin-coated Luminex microspheres. These beads were incubated with various concentrations of the recombinant ECD of Her2. After the binding step, detection was performed by either adding a second DARPin bearing a myc-tag or commercially available anti-Her2 antibodies to set up a sandwich assay. This method allowed a fast screening for the best combination of the five DARPins and three different commercially available murine monoclonal antibodies against Her2. Although several of the DARPin-DARPin combinations could be used in the sandwich format (data not shown), the best sandwich combination turned out to be when using a DARPin for capturing and the antibody sp185 for detection. This is most likely due to the fact that the investigated high-affinity DARPins do not make suitable sandwich pairs because they bind to the same or to nearby epitopes.

Large differences were seen when using the different DARPins as capture reagents in this assay

Figure 4. A stereo diagram showing detail of the accommodation of the imidazole ring of His52 in a representative N3C structure (PDB entry 1SVX) is shown in (a). Oxygen atoms are shown in red, nitrogen atoms in blue and carbon atoms in cyan. The hydrogen bonds between the imidazole ring of His52 and the respective atoms Thr49 $O^{\gamma 1}$ and Tyr81 O are indicated by broken red lines, as is the inter-repeat hydrogen bond between Thr46 O and Val78 N. (b) Stereo diagram showing detail of the accommodation of the phenol ring of Tyr52 in the N2C structure presented here. Oxygen atoms are shown in red, nitrogen atoms in blue and carbon atoms in copper. The single hydrogen bond between the side-chain hydroxyl of Tyr52 and the side-chain carboxylate of Asp77 is indicated by a broken red line. The increased separation (ca 6 Å) of the respective backbone atoms at positions 46 and 78 compared to the N3C structure shown in (a) is apparent. (c) Stereo diagram showing an overlay of the backbone traces of H10-2-G3 (copper) with an N3C structure (PDB entry 1SVX, cyan) generated by superimposing the C^{α} atoms of residues 12 to 74 of the two structures. The rotameric change at position 52 is indicated. The 13° relative rotation of the two C-terminal ankyrin repeats of H10-2-G3 with respect to their N3C counterparts is apparent, with the grey line showing the approximate location of the rotation axis and the sphere at residue 76 indicating the approximate point in the backbone trace at which the overlaid structures begin to diverge. The Figures were generated using Molmol[35] and POVScript+.[39]

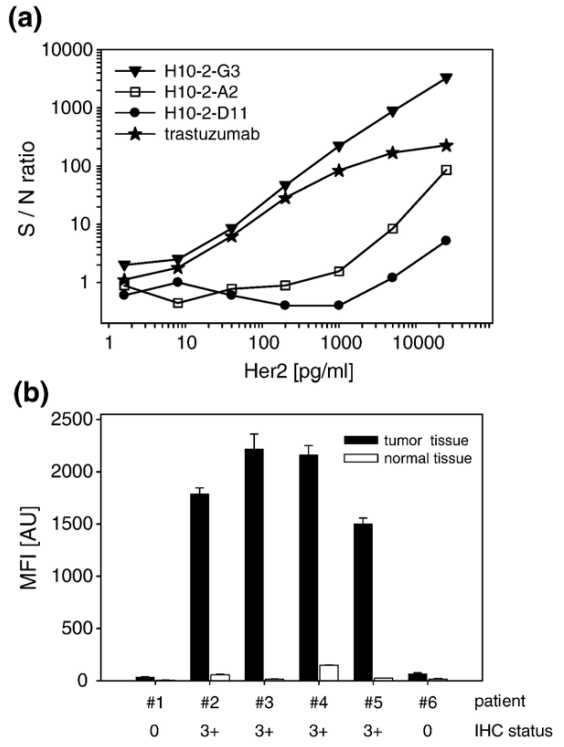

Figure 6. DARPins in immunoassays for Her2 detection. (a) The capture activities of three representative DARPins were compared in a sandwich immunoassay. These DARPins were biotinylated and site-specifically immobilized on Luminex microspheres. In a six-plex assay format including bead-coupled trastuzumab, capture activities were analyzed in a titration series of Her2 ECD. The monoclonal anti-Her2 antibody sp185 was applied for detection of bound Her2. The sensitivity of the DARPins appeared to correlate with the affinity. The ratio of signal over background (S/N: signal to noise ratio) was chosen to display qualitative differences of capture activities. (b) Clone H10-2-G3 was used as a capture reagent to detect Her2 from solubilized breast tissue of patient samples in a sandwich assay, with monoclonal antibody sp185 as detection agent. The measurements were performed in triplicates. Tumor and normal breast tissue from six patients were used for the assay that had been classified for Her2 expression using IHC in a routine clinical laboratory. The Her2 status of patient tumors 2, 3, 4 and 5 were rated 3+ on a scale from 0 to 3+. Tumor samples 1 and 6 were judged as 0. Using bead-based assays, Her2 positive tumor tissues were measured with median fluorescence intensities (MFIs) > 1000 AU, whereas Her2 negative tumor tissue resulted in MFIs < 100 AU. Moreover, a basal Her2 expression was detected from normal tissue with MFIs < 150 AU.

(Figure 6(a)). The overall performance seemed to correlate with the affinities of the clones. H10-2-G3 proved to be the most sensitive DARPin and was capable of detecting Her2 ECD down to a concentration of 20 pg/ml (0.2 pM), which is comparable to commercial ELISA kits. The dynamic range of the assay covered more than three orders of magnitude. The capturing potential of the DARPin H10-2-G3 was further compared to the mAb trastuzumab, which was immobilized on a microsphere by NHS-ester chemistry. The sensitivity of this setup was comparable to the capturing potential of the DARPin H10-2-G3. However, trastuzumab showed some deviations from linearity at high Her2 concentrations, possibly because of its dimeric nature and the higher molecular weight. In addition, trastuzumab showed a more than fivefold higher background signal with the applied detection system than H10-2-G3.

The combination of H10-2-G3 as a capture molecule and the monoclonal mouse antibody sp185 as the detector was used in a sandwich assay to quantify Her2 expression in tumor lysates. Samples from mammary carcinomas and normal breast tissue that had been analyzed by immuno-histochemistry (IHC) in a routine clinical laboratory were used, performing the assay with only 1 μg of total protein per sample. Data from the bead-based assays explicitly show a distinction between Her2-expressing tumors and normal tissue. A clear correlation of the Her2 expression from the sandwich assay with the clinical data from IHC could be observed (Figure 6(b)).

Discussion

Using ribosome display with a combination of error-prone PCR and stringent off-rate selection, we generated the highest affinity DARPin described up to now, with a monovalent affinity of 90 pM. This affinity surpasses the high-affinity natural ankyrin repeat proteins, such as the mouse GA binding protein (GABP) β1 binding GABPα, which was described to bind with an affinity of 0.78 nM,[22] and IκBα, whose affinity lies in the low nanomolar range.[23] When comparing the affinity to the size of the interaction surface, the difference becomes even more obvious: while the selected DARPins accomplish the binding with only two repeat modules, most natural ankyrin repeat proteins involve several repeat modules in binding.[24] A high percentage of hydrophobic interactions were found in the putative selected interaction interface. These contacts can contribute much to the free energy of the interaction within a small interaction surface. Nevertheless, specificity is maintained.

The use of error-prone PCR for the affinity maturation of DARPins proved to be a powerful approach. The random mutation of framework residues produced a kink in the rigid backbone of the DARPin and thereby added some variability to the scaffold by increasing the diversity of molecular shapes. Many mutations that contribute to high affinity, when comparing H10-G3 to the wild-type framework or to H10-G5 are most likely not part of the binding interface. We think that these mutations lead to subtle changes in the overall conformation. These changes are fundamental for a tight adaptation of the structure to the target and therefore for highest affinities. Introducing random mutations in the whole gene, followed by stringent selection, might be a general

means to adapt the binding site to the target surface. In a very stable framework such as that of a DARPin, such adaptations by directed evolution are possible, since the favorable biophysical properties can still be maintained. In addition, structural and kinetic analysis of the binding revealed some insight into the dynamics of framework residues.

We propose that a sparsely population of a kinked conformation was stabilized by a framework mutation at position 52 in the evolved DARPins. This would also explain the unusually slow association rate constants of the non-affinity matured clone G3-HAVD, which did not contain a tyrosine residue at position 52. Since the association rate of the DARPin with its antigen is a bimolecular event that is directly proportional to changes in concentration, the presence of two conformations of one binding partner would directly lead to a decrease of the association rate constant. Mutation of histidine 52 to tyrosine, however, forces residue 52 to rotate into the putative binding pocket due to the larger size of the side-chain ring and the additional hydroxyl group, thereby inducing the putative active conformation, resulting in a dramatic increase of the association rate constant to the level typical for protein–protein interactions.[8] This particular conformation appears to be crucial when binding the epitope of the KEYL family, but not for the epitopes recognized by the other families, as the other k_{on} values are normal, with and without the Tyr52 mutation.

An unexpected finding of our affinity maturation was that, even though we used off-rate selection, proteins with improved on-rates were obtained. We believe, however, that a plausible, albeit purely speculative rationalization can be proposed. It is useful to consider the single point mutants of G3 (G3-D, G3-A, G3-AVD, G3-HAVD, Table 1), even though these clones have not actually been observed as intermediates in the selection, but have only been constructed afterwards to investigate the selection procedure. The "wild-type" H3-HAVD (with unmutated framework) has a K_D of only 288 nM and it would be easily out-competed at equilibrium by G3-AVD (K_D 10 nM), carrying the His52Tyr mutation, especially since it also equilibrates much faster. This mutant, the putative precursor of G3-2-H10, has a relatively fast off-rate of 4.1×10^{-3} s^{-1} and from this point on, the off-rate decreased (40-fold), whereas the on-rate increased only slightly (2.5-fold), as expected for a classical off-rate selection.

The affinity maturation did not influence the specificity of H10-2-G3. For this mutant as well as all other tested, still no cross-reactivity was observed, and competition with trastuzumab was seen for several clones. Also, fusion to phage λ pD and modification with biotin did not influence the beneficial behavior of H10-2-G3. In a sandwich-ELISA approach, similar sensitivities for Her2 were observed as with a commercial antibody such as trastuzumab. Compared to the antibody-based assay, H10-2-G3 showed a lower background.

The accumulated mutations destabilized the DARPin compared to the clones not carrying framework mutations. The still high stability and the unchanged expression properties of the evolved DARPins show that the DARPin scaffold is well suited to tolerate multiple mutations at framework positions in addition to the randomized residues. These favorable biophysical properties in combination with the exceptional affinity, selectivity and sensitivity data make DARPins such as clone H10-2-G3 ideal candidates for miniaturized and even multiplexed assay systems, useful tools for diagnostic tests on microarray platforms or candidates for further drug development.

Materials and Methods

Error-prone PCR

Error-prone PCR in the presence of dNTP analogues[25] was performed to generate second generation libraries of pools that were previously selected.[12] Therefore, the pools isolated after round six in this previous study were used as template for error-prone PCR. Several reactions were performed with different concentrations of the dNTP analogues dPTP (6-(deoxy-β-D-erythro-pentofuranosyl)-3,4-dihydro-8H-pyrimido- [4,5-c][1,2]oxazine-7-one-5′-triphosphate) and 8-oxo-dGTP (8-oxo-2′-deoxyguanosine-5′-triphosphate) ranging from 2.5 μM to 20 μM each. The amplification was performed in a 50 μl reaction in the presence of 0.25 μM primers, one unit of Vent polymerase exo minus (NEB), 5% DMSO, 1.5 mM $MgCl_2$ and 200 μM dNTPs. A total of 23 cycles of PCR were performed, and the mutational load was determined by sequencing to be 1.3–5.9 mutations per DARPin. The distribution of transitions and transversions was similar to published values.[13]

Ribosome display selection rounds

For selection experiments, biotinylated Her2 ECD was immobilized *via* neutravidin as described.[12] For ELISA and RIA experiments, 250–500 ng of Her2 ECD were directly coated to 96-well MaxiSorp polystyrene plates (Nunc) by overnight incubation at 4 °C in phosphate-buffered saline (PBS).

Ribosome display off-rate selections were performed as described.[12,15] Biotinylated Her2 ECD was added to the stopped translation reaction at a concentration of 0.7 nM and equilibrated by shaking overnight at 4 °C. Non-biotinylated Her2 ECD was added in 500-fold excess (350 nM). This mixture was kept under slow shaking at 4 °C for times ranging from 10 h up to 27 days.

Ternary complexes that were still bound to the biotinylated Her2 ECD were isolated using streptavidin-coated magnetic beads (Roche). For recovery, 60 μl (0.6 mg) beads were washed three times in WBT (50 mM Tris acetic acid (pH 7.5), 150 mM NaCl, 50 mM $Mg(CH_3COO^-)_2$, 0.05% Tween 20) and then blocked for 1 h in WBT plus 0.5% (w/v) BSA at room temperature. After adding the beads, the ribosomal complexes were allowed to bind by shaking for 30 min at 4 °C. The beads were then washed three times for 3 min and three times 15 min with WBT before elution.

Crude extract ELISA, protein expression and surface plasmon resonance spectroscopy

For affinity analysis of single clones, the selected pools were cloned into plasmid pQE30 (Qiagen) *via* BamHI and HindIII. Because of the very strong expression of the DARPins, the single stop codon on pQE30 is partially read over leading to a C-terminal extension bearing a cysteine, which made an additional purification step for crystallization necessary. This step could be circumvented in the future by using a vector with two stop codons in tandem ($pQE30_{SS}$) (D.S. *et al.*, unpublished). Crude extract ELISAs were performed as described earlier[11] from lysates of 1 ml expression cultures. For SPR analysis, the DARPins were expressed in *E. coli* strain XL1-blue in 500 ml scale and purified over immobilized metal-ion affinity chromatography (IMAC) on a Superflow NTA matrix (Qiagen) as described.[11]

All SPR measurements were performed using a Biacore 3000 (Biacore). A CM5 chip was prepared according to the manufacturer's protocol. For the immobilization of neutravidin, a solution of 50 μg/ml neutravidin in 10 mM sodium acetate, 125 mM NaCl (pH 4.5) was used. Biotinylated Her2 ECD was then immobilized on the neutravidin-modified flow cells. For kinetic measurements, a chip was coated with 220 RU of biotinylated Her2 and for inhibition measurements with 2500 RU.

Kinetic measurements were performed by the serial injection of a DARPin in concentrations ranging from 1 nM to 250 nM at a buffer-flow of 30 μl/min in HBST (20 mM Hepes (pH 7.4), 150 mM NaCl, 0.05% Tween 20). Inhibition measurements were done as described[3] at a constant concentration of DARPin of 5 nM and different concentrations of soluble Her2 ECD as a competitor in concentrations ranging from 50 pM to 20 nM. The slope of the binding to a high-density chip was monitored in the linear range as a function of the concentration of competitor at a flow of 25 μl/min. Data evaluation was performed using BIAEVAL (Biacore), CLAMP[26] and SigmaPlot (Systat Software) as described.[16]

Construction of point mutants

To study the influence of the four framework mutations of H10-2-G3, several clones were constructed where one or more of these mutations were changed back to the consensus sequence. The following variants were constructed: G3-D (without mutation D122G), G3-A (without A55T), G3-AVD (without A55T, V96A, D122G) and G3-HAVD (without A55T, V96A, D122G, V96A, which corresponds to H10-2-G3 having no framework mutations).

The mutations were introduced by a PCR-based approach. Two fragments were amplified overlapping in the region of the desired mutation. In a second PCR reaction with outer primers only, the fragments were joined to yield the mutated sequence. Clone G3-D was constructed with a single PCR reaction using a long reverse primer, as the mutation was near to the C terminus. DNA of all clones was isolated from agarose gels and cloned *via* BamHI and HindIII into pQE-30 (Qiagen). Plasmids were prepared, sequenced and the mass of the expressed and purified clones was verified with mass spectrometry (MALDI-TOF).

Protein crystallization and X-ray data collection

Prior to crystallization, protease inhibitors and oligomeric protein species were removed from the protein solution by size-exclusion chromatography on a Superdex 200 10/30 column. Eluted protein was concentrated to 6 mg/ml using a Millipore Centricon 3 kDa centrifugal concentrator in 20 mM sodium phosphate (pH 7.4), 75 mM NaCl.

An initial screen of 808 commercial and in-house conditions was performed using a Cartesian Honeybee robot (Genomic Solutions, Michigan) to set up 96-well round-bottomed plates (Greiner, Germany) with 100 μl screening solution per well, 100 nl protein plus 100 nl well solution in the drops. The screen gave several leads, which were scaled up using protein at 10 mg/ml and optimized manually in hanging drops (24 well Linbro plates, 1 ml of solution per well, 1 μl protein plus 1 μl of well solution in drops, at room temperature). Crystals grew within three weeks from a solution containing 0.1 M Tris-HCl (pH 8.5), 2.3 M $(NH_4)_2SO_4$, 10% (v/v) glycerol. The crystal used for data collection exhibited a trapezoidal plate-like morphology, ca 0.25 mm × 0.08 mm × 0.15 mm.

A single crystal of the H10-2-G3 DARPin molecule was transferred to a cryo-protectant solution containing 2.3 M $(NH_4)_2SO_4$, 20% glycerol, 0.1 M Tris-HCl (pH 8.5) and mounted at −160 °C in a rayon loop[27] on a RU-3R X-ray generator (RigakuMSC, Texas) equipped with monocapillary focusing optics (AXCO, Australia). The crystal diffracted to at least 1.7 Å resolution. Two X-ray diffraction data sets were collected using the oscillation method; the first data set was collected with the camera set at $2\theta = 0°$ and the second at $2\theta = 15°$. Both data sets were processed using the software HKL.[28] The space-group of the crystal was *C*2 with unit cell dimensions $a = 152.40$ Å, $b = 51.97$ Å, $c = 70.07$ Å, $\beta = 105.21°$. X-ray data collection and processing statistics are presented in Table 2. We note that the R_{merge} statistics is high in the outer resolution shells of both data sets, however, the $<I>/<s>$, completeness and data redundancy statistics in this shell were judged satisfactory and these data were thus retained.

Structure determination and analysis

A molecular model encompassing 123 residues of the protein of an N2C DARPin, constructed from the two previously solved structures of N3C DARPins, E3_5 and E3_19 (with no framework mutations) was used for the molecular replacement search, employing the first diffraction data set and the program MOLREP[29] within the CCP4 suite.[30] Three copies of the search molecule (subsequently labelled A, B and C) were located within the asymmetric unit. The structure factor phases obtained by molecular replacement were then further improved using the program RESOLVE[31] and an atomic model built using the automated model-building procedure within that program. The atomic model was further improved by iterative cycles of crystallographic refinement against the second diffraction data set using REFMAC5[32] within the CCP4 suite and manual model building using O.[33] The final atomic model encompassed residues A12 to A135, B12 to B135 and C12 to C136 and included 488 ordered solvent molecules. Crystallographic refinement included a bulk solvent model, refinement of restrained individual atomic temperature factors and the refinement of individual TLS parameters[34] for the three monomers. Crystallographic refinement statistics are presented in Table 3. The structure was analyzed using the programs MolMol[35] and Swiss PDB viewer.

Structural comparison with N3C ankyrins

Each of the three copies of H10-2-G3 in the crystallographic asymmetric unit was overlaid using the pro-

Table 3. Crystallographic refinement statistics

Resolution range (Å)	15.0–1.7
No. of reflections in working set	53,757 (3768)
No. of reflections in free set	2929 (188)
R_{cryst} [a]	0.178 (0.287)
R_{free}	0.212 (0.395)
RMSD bond lengths (Å)	0.014
RMSD bond angles (°)	1.3
No. of protein atoms	2792
No. of solvent molecules	488
$<B>$ protein atoms (Å^2)	34.5
$<B>$ solvent molecules (Å^2)	38.9
Ramachadran plot details[36] (no. of residues)	
Most favored regions	299
Additional allowed region	26
Generously allowed region	0
Disallowed region	0

[a] $R_{cryst} = \sum_h | F_h^{obs} - k F_h^{calc} | / \sum_h | F_h^{obs} |$.

gram LSQMAN[36] onto the three N-terminal ankyrin repeats of three representative N3C structures extracted from the Protein Data Bank (entries 2BBK, 1MJ0 and 1SVX). Analysis of the resultant geometric transformations was conducted manually, whilst analysis of relative changes in the hydrogen bonding patterns was conducted using HBPLUS.[37]

Thermal denaturation

Thermal denaturation experiments were performed and evaluated as described.[11] Briefly, 15 μM purified protein in PBS were brought from 20 °C to 92 °C with a heating rate of 0.5 deg./min and the CD signal at 222 nm was recorded. Data were recorded with a Jasco J-715 instrument.

Sensitivity analysis of selected DARPins in Luminex assays

Biotinylated DARPins H10-2-A2, H10-2-D11, H10-2-G3, H10-2-G11 and DARPin H6-3-B3, which is an N3C DARPin that has been described earlier[12] were expressed with the N-terminal fusion protein avi-pD by cloning into vector pAT224 (GenBank accession number AY327139) and purified as described above. By co-expression with BirA, the biotin ligase of *E. coli*, the DARPins could be biotinylated site-specifically *in vivo* as described earlier.[11]

Each sample was immobilized on Luminex beads of distinguishable color-code according to the manufacturer's protocol (Luminex-Corp., Austin, Tx, USA). Biotinylated DARPins were immobilized on avidin-coated beads (LumAvidin Microspheres). Trastuzumab was coupled to carboxylated beads (COOH Microspheres). A recombinant Her2 ECD (BenderMed Systems, Vienna, Austria) served as antigen in sandwich-ELISA set-up. Breast cancer tumor tissue and corresponding normal tissue were kindly provided by Helmut Deissler (University of Ulm, Medical School, Germany). All tissue samples were solubilized as described.[38] The total amount of protein was determined by the Bradford assay.

Immobilized DARPins were studied in multiplexed sandwich immunoassays to compare capture activities for quantitative Her2 analysis. All assays were performed in Blocking Reagent for ELISA (Roche) with 0.005% Tween at pH 7.4 under permanent shaking in microtiter plates. Six differently color-coded Luminex beads, each loaded with a different DARPin or trastuzumab, were mixed. Titration series of recombinant Her2 protein or tissue samples were incubated with the bead mixture in a volume of 50 μl overnight at 4 °C. After filtering the assay mixture in a 96-well filter plate (Pall, East Hills, NY, USA) the beads were resuspended in 30 μl of assay buffer containing 1 μg/ml of anti-Her2 antibody sp185 (BenderMed Systems) and incubated for 60 min. Bound antibody was detected using R-phycoerythrin (R-PE) labeled, Fc fragment-specific goat anti-mouse antibody (Dianova, Hamburg, Germany) at a concentration of 2.5 μg/ml over 45 min incubation. The beads were analyzed in a Luminex 100 IS System. Results are presented as median fluorescence intensity (MFI) of 100 events counted per bead population.

Protein Data Bank accession code

Atomic coordinates for the high affinity DARPin have been deposited in the PDB under accession code 2jab.

Acknowledgements

We thank Helmut Deissler from the University of Ulm, Germany, for kindly providing breast cancer tissues. We further thank Thomas Huber for his help and valuable discussions in data evaluation. This work was supported by a grant from the Swiss National Center of Competence in Research in Structural Biology.

Supplementary Data

Supplementary data associated with this article can be found, in the online version, at doi:10.1016/j.jmb.2007.03.028

References

1. Allen, T. M. (2002). Ligand-targeted therapeutics in anticancer therapy. *Nature Rev. Cancer*, **2**, 750–763.
2. Moroney, S. & Plückthun, A. (2005). Modern antibody technology: the impact on drug development. In *Modern Biopharmaceuticals* (Knäblein, J. & Müller, R. H., eds), pp. 1147–1185, WILEY-VCH Verlag GmbH & Co. KGaA, Weinheim.
3. Hanes, J. & Plückthun, A. (1997). In vitro selection and evolution of functional proteins by using ribosome display. *Proc. Natl Acad. Sci. USA*, **94**, 4937–4942.
4. Smith, G. P. (1985). Filamentous fusion phage: novel expression vectors that display cloned antigens on the virion surface. *Science*, **228**, 1315–1317.
5. Chen, Y., Wiesmann, C., Fuh, G., Li, B., Christinger, H. W., McKay, P. *et al.* (1999). Selection and analysis of an optimized anti-VEGF antibody: crystal structure of an affinity-matured Fab in complex with antigen. *J. Mol. Biol.* **293**, 865–881.
6. Jermutus, L., Honegger, A., Schwesinger, F., Hanes, J. & Plückthun, A. (2001). Tailoring in vitro evolution for protein affinity or stability. *Proc. Natl Acad. Sci. USA*, **98**, 75–80.
7. Zahnd, C., Spinelli, S., Luginbühl, B., Amstutz, P.,

Cambillau, C. & Plückthun, A. (2004). Directed in vitro evolution and crystallographic analysis of a peptide-binding single chain antibody fragment (scFv) with low picomolar affinity. *J. Biol. Chem.* **279**, 18870–18877.
8. Northrup, S. H. & Erickson, H. P. (1992). Kinetics of protein-protein association explained by Brownian dynamics computer simulation. *Proc. Natl Acad. Sci. USA*, **89**, 3338–3342.
9. Binz, H. K., Stumpp, M. T., Forrer, P., Amstutz, P. & Plückthun, A. (2003). Designing repeat proteins: well-expressed, soluble and stable proteins from combinatorial libraries of consensus ankyrin repeat proteins. *J. Mol. Biol.* **332**, 489–503.
10. Forrer, P., Binz, H. K., Stumpp, M. T. & Plückthun, A. (2004). Consensus design of repeat proteins. *ChemBioChem.* **5**, 183–189.
11. Binz, H. K., Amstutz, P., Kohl, A., Stumpp, M. T., Briand, C., Forrer, P. *et al.* (2004). High-affinity binders selected from designed ankyrin repeat protein libraries. *Nature Biotechnol.* **22**, 575–582.
12. Zahnd, C., Pecorari, F., Straumann, N., Wyler, E. & Plückthun, A. (2006). Selection and characterization of Her2-binding designed ankyrin repeat proteins. *J. Biol. Chem.* **281**, 35167–35175.
13. Zaccolo, M. & Gherardi, E. (1999). The effect of high-frequency random mutagenesis on in vitro protein evolution: a study on TEM-1 beta-lactamase. *J. Mol. Biol.* **285**, 775–783.
14. Karlsson, R. (1994). Real-time competitive kinetic analysis of interactions between low- molecular-weight ligands in solution and surface-immobilized receptors. *Anal. Biochem.* **221**, 142–151.
15. Nieba, L., Krebber, A. & Plückthun, A. (1996). Competition BIAcore for measuring true affinities: large differences from values determined from binding kinetics. *Anal. Biochem.* **234**, 155–165.
16. Hanes, J., Jermutus, L., Weber-Bornhauser, S., Bosshard, H. R. & Plückthun, A. (1998). Ribosome display efficiently selects and evolves high-affinity antibodies in vitro from immune libraries. *Proc. Natl Acad. Sci. USA*, **95**, 14130–14150.
17. Lovell, S. C., Word, J. M., Richardson, J. S. & Richardson, D. C. (2000). The penultimate rotamer library. *Proteins: Struct. Funct. Genet.* **40**, 389–408.
18. Kohl, A., Binz, H. K., Forrer, P., Stumpp, M. T., Plückthun, A. & Grütter, M. G. (2003). Designed to be stable: crystal structure of a consensus ankyrin repeat protein. *Proc. Natl Acad. Sci. USA*, **100**, 1700–1705.
19. Mosavi, L. K., Williams, S. & Peng Zy, Z. Y. (2002). Equilibrium folding and stability of myotrophin: a model ankyrin repeat protein. *J. Mol. Biol.* **320**, 165–170.
20. Cho, H. S., Mason, K., Ramyar, K. X., Stanley, A. M., Gabelli, S. B., Denney, D. W., Jr & Leahy, D. J. (2003). Structure of the extracellular region of HER2 alone and in complex with the Herceptin Fab. *Nature*, **421**, 756–760.
21. Franklin, M. C., Carey, K. D., Vajdos, F. F., Leahy, D. J., de Vos, A. M. & Sliwkowski, M. X. (2004). Insights into ErbB signaling from the structure of the ErbB2-pertuzumab complex. *Cancer Cell*, **5**, 317–328.
22. Suzuki, F., Goto, M., Sawa, C., Ito, S., Watanabe, H., Sawada, J. & Handa, H. (1998). Functional interactions of transcription factor human GA-binding protein subunits. *J. Biol. Chem.* **273**, 29302–29308.
23. Malek, S., Huxford, T. & Ghosh, G. (1998). IκBα functions through direct contacts with the nuclear localization signals and the DNA binding sequences of NF-κB. *J. Biol. Chem.* **273**, 25427–25435.
24. Mosavi, L. K., Cammett, T. J., Desrosiers, D. C. & Peng, Z. Y. (2004). The ankyrin repeat as molecular architecture for protein recognition. *Protein Sci.* **13**, 1435–1448.
25. Zaccolo, M., Williams, D. M., Brown, D. M. & Gherardi, E. (1996). An approach to random mutagenesis of DNA using mixtures of triphosphate derivatives of nucleoside analogues. *J. Mol. Biol.* **255**, 589–603.
26. Myszka, D. G. & Morton, T. A. (1998). CLAMP: a biosensor kinetic data analysis program. *Trends Biochem. Sci.* **23**, 149–150.
27. Teng, T. Y. (1990). Mounting of crystal for macromolecular crystallography in a free standing thin film. *J. Appl. Crystallog.* **23**, 387–391.
28. Otwinowski, Z. & Minor, W. (1997). Processing of X-ray diffraction data collected in oscillation mode. *Methods Enzymol.* **276**, 307–326.
29. Vagin, A. & Teplyakov, A. (1997). MOLREP: an automated program for molecular replacement. *J. Appl. Crystallog.* **30**, 1022–1025.
30. CCP4. (1994). The CCP4 Suite: programs for protein crystallography. *Acta Crystallog. sect. D*, **50**, 760–763.
31. Terwilliger, T. (2004). SOLVE and RESOLVE: automated structure solution, density modification and model building. *J. Synchrotron Radiat.* **11**, 49–52.
32. Murshudov, G. N., Alexei, A. V. & Dodson, E. J. (1997). Refinement of macromolecular structures by the maximum-likelihood method. *Acta Crystallog. sect. D*, **53**, 240–255.
33. Jones, T. A., Zou, J. Y., Cowan, S. W. & Kjeldgaard (1991). Improved methods for building protein models in electron density maps and the location of errors in these models. *Acta Crystallog. sect. A*, **47**, 110–119.
34. Winn, M. D., Isupov, M. N. & Murshudov, G. N. (2001). Use of TLS parameters to model anisotropic displacements in macromolecular refinement. *Acta Crystallog. sect. D*, **57**, 122–133.
35. Koradi, R., Billeter, M. & Wüthrich, K. (1996). MOLMOL: a program for display and analysis of macromolecular structures. *J. Mol. Graph.* **14**, 51–5, 29–32.
36. Kleywegt, G. J. & Jones, T. A. (1994). A super position. *CCP4/ESF-EACBM News. Protein Crystallog.* **31**, 9–14.
37. McDonald, I. K. & Thornton, J. M. (1994). Satisfying hydrogen bonding potential in proteins. *J. Mol. Biol.* **238**, 777–793.
38. Schneiderhan-Marra, N., Kirn, A., Döttinger, A., Templin, M. F., Sauer, G., Deissler, H. & Joos, T. O. (2005). Protein microarrays - a promising diagnostic tool for cancer. *Cancer Genomics Proteomics*, **2**, 37–42.
39. Fenn, T. D., Ringe, D. & Petsko, G. A. (2003). POVScript+: a program for model and data visualization using persistence of vision ray-tracing. *J. Appl. Crystallog.* **36**, 944–947.

Edited by I. Wilson

(Received 13 July 2006; received in revised form 10 March 2007; accepted 13 March 2007)
Available online 20 March 2007

A designed ankyrin repeat protein evolved to picomolar affinity to Her2

Christian Zahnd, Emanuel Wyler, Jochen M. Schwenk, Daniel Steiner, Michael C. Lawrence, Neil M. McKern, Frédéric Pecorari, Colin W. Ward, Thomas O. Joos and Andreas Plückthun

Supplementary Figure 1. The affinities of different DARPins were determined by surface Plasmon resonance (SPR) using a Biacore 3000 instrument. Her2 ECD was immobilized on a flow cell at low concentrations. Binding of the DARPin to the immobilized target protein was compared to binding to an empty flow cell at different concentrations of the DARPin. Data were processed by the software Scrubber and evaluated by global fitting using the software CLAMP[32]. Each DARPin was injected several times at different concentrations. Note that H3-HAVD was injected at significantly higher concentrations than the other DARPins. DARPins G3-D and G3-A were injected at 20 nM, 50 nM, 100 nM and 150 nM, G3-AVD was injected at 50 nM, 100 nM, 200 nM and 300 nM, G3-HAVD was injected at 500 nM, 1000 nM, 2000 nM, 4000 nM, 6000 nM and 8000 nM, H10-2-G5 was injected at 1 nM, 5 nM, 10 nM, 20 nM, 30 nM, 50 nM, 75 nM, 100 nM and 150 nM, H10-2-D11 was injected at 10 nM, 20 nM, 30 nM, 50 nM, 75 nM, 100 nM and 150 nM, H10-2-D12 was injected at 0 nM, 100 nM, 200 nM, 300 nM and 400 nM and H10-2-A2 was injected at 0 nM, 1 nM, 5 nM, 10 nM, 20 nM, 30 nM, 50 nM, 100 nM and 150 nM.

Supplementary Figure 1

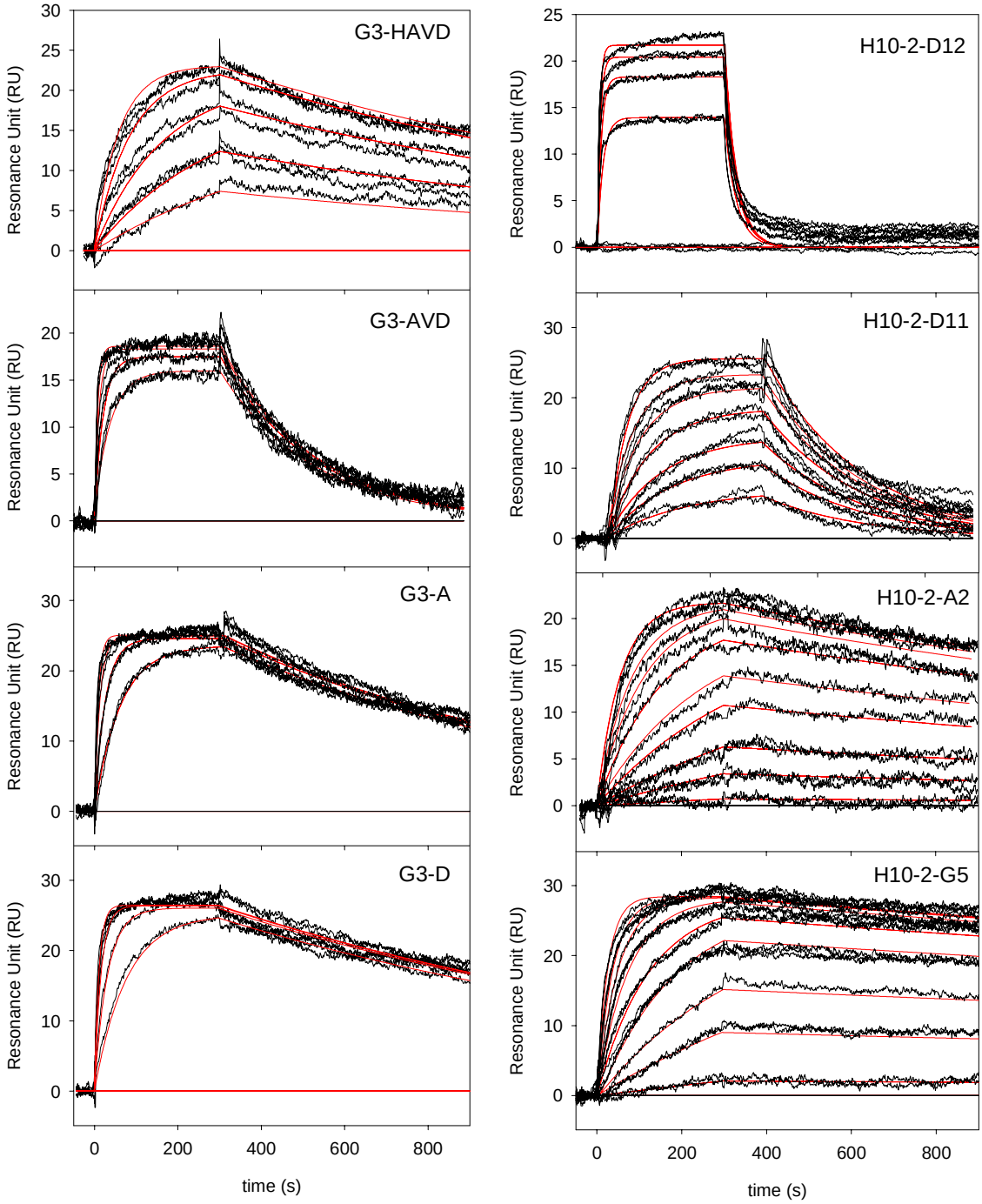

Appendix 4

Contents

1. Abbreviations

AP	alkaline phosphatase
APH	aminoglycoside phosphotransferase IIIa
BAD	biotin acceptor domain
BCIP	substrates 5-bromo-4-chloro-3-indolyl phosphate
BSA	bovine serum albumin
cat	chloramphenicol acetyl transferase
CDR	complementary determining region
cfu	Colony forming units
CitS	Citrate carrier CitS
cml or cam	chloramphenicol
ColE1 *ori*	plasmid origin of replication ColE1
CTp3	C-terminal domain (amino acids 250-406) of protein 3 of filamentous phage M13
DARPin	designed ankyrin repeat protein
DDM	n-dodecyl-α-D-maltopyranoside
DsbAss	the signal sequence of the *E. coli* DsbA
E. coli	*Escherichia coli*
ECL	electrochemiluminescence
EK	enterokinase site
ELISA	enzyme-linked immunosorbent assay
ErbB1	human receptor tyrosine-protein kinase ErbB1
ErbB2	human receptor tyrosine-protein kinase ErbB2
ErbB4	human receptor tyrosine-protein kinase ErbB4
f1 *ori*	f1 origin of replication
Fc	fragment crystallizable
FLAG	DNA sequences encoding a FLAG-tag
gpD	phage λ coat protein D
gpD	phage protein D
HBS	Hepes buffered saline
HuCAL	human combinatorial antibody library
huIgG1_Fc	Fc domain of human IgG1
Ig	immunoglobulin
IMAC	immobilized metal ion chromatography
IPTG	isopropyl-β-D-thiogalactoside
JNK2	c-jun N-terminal kinase 2α2
kan	kanamycin
K_D	equilibrium dissociation constant
k_{off}	dissociation rate constants
k_{on}	association rate constants
*lac*P	*lac* promoter/operator element
lacZ p/o	promoter/operator element of the *lacZ* gene of *E. coli*
LB	Luria-Bertani
λPP	bacteriophage λ protein-phosphatase

MALS	multi-angle static light scattering
MBP	maltose binding protein
MCS	multiple cloning site
muIgG	mouse IgG
myc	DNA sequences encoding a myc-tag
NBT	nitroblue tetrazolium
NCCR	Swiss National Center of Competence in Research
p3	minor phage coat protein 3
PBS	phosphate buffered saline
PD	phage display
PEG	polyethyleneglycol
PelBss	signal sequence of the *Erwinia carotovora* PelB
pfu	plaque forming units
PhoAss	signal sequence of the *E. coli* PhoA
pNPP	di-sodium 4-nitrophenyl phosphate
POD	peroxidase
POI	protein of interest
ps	packaging signal
PVDF	polyvinylidene fluoride
RD	Ribosome display
scFv	single-chain Fv antibody
SDS-PAGE	sodium dodecyl sulfate polyacrylamide gel electrophoresis
SEC	size exclusion chromatography
SHP	phage protein SHP
SPR	Surface plasmon resonance
SRP	signal recognition particle
ss	signal sequence
ssDNA	single stranded DNA
Strp	streptavidin
Taq	Taq DNA polymerase
TBS	Tris buffered saline
tet	tetracycline
TMS	transmembrane segment
TNFα	human tumor necrosis factor precursor
TrxA	thioredoxin
2HCT	2-hydroxy-carboxylate transporters
4NPP	4-nitrophenyl phosphate

2. List of prepared plasmids

Name	Source	Ori(s)	Res.	Use/ORF
pAT223	PAT	ColE1	amp	Avi-tag:pDΔN2:His_6-tag (GenBank accession number AY327138)
pDST022	DST (#2)	ColE1, f1	cam	Phagemid pMorph7 containing: PhoAss_ DARPin 3a
pDST023	DST (#2)	ColE1, f1	cam	Phagemid pMorph7 containing: DsbAss_ DARPin 3a
pDST024	DST (#2)	ColE1, f1	cam	Phagemid pMorph7 containing: PhoAss_ scFv_gpD
pDST030	DST (#2)	ColE1, f1	cam	Phagemid pMorph7 containing: PhoAss_ DARPin E3_5
pDST031	DST (#2)	ColE1, f1	cam	Phagemid pMorph7 containing: DsbAss_ scFv_gpD
pDST032	DST (#2)	ColE1, f1	cam	Phagemid pMorph7 containing: DsbAss_ DARPin E3_5
pDST034	DST (#2)	ColE1, f1	cam	Phagemid pMorph7 containing: PhoAss_ DARPin JNK2_2_3
pDST037	DST (#2)	ColE1, f1	cam	Phagemid pMorph7 containing: DsbAss_ DARPin JNK2_2_3
pDST039	DST (#2)	ColE1, f1	cam	Phagemid pMorph7 containing: PhoAss_ GCN4
pDST040	DST (#2)	ColE1, f1	cam	Phagemid pMorph7 containing: DsbAss_ GCN4
pDST041	DST (#2)	ColE1, f1	cam	Phagemid pMorph7 containing: PhoAss_ pDΔN2
pDST042	DST (#2)	ColE1, f1	cam	Phagemid pMorph7 containing: DsbAss_ pDΔN2
pDST045	DST (#2)	ColE1, f1	cam	Phagemid pMorph7 containing: PhoAss_ JNK2α2
pDST046	DST (#2)	ColE1, f1	cam	Phagemid pMorph7 containing: DsbAss_ JNK2α2
pDST047	DST (#2)	ColE1, f1	cam	Phagemid pMorph7 containing: PhoAss_ TrxAwt
pDST048	DST (#2)	ColE1, f1	cam	Phagemid pMorph7 containing: DsbAss_ TrxAwt
pDST051	DST (#2)	ColE1, f1	cam	Phagemid pMorph7 containing: PhoAss_ Taq polymerase
pDST052	DST (#2)	ColE1, f1	cam	Phagemid pMorph7 containing: DsbAss_ Taq polymerase
pDST053	DST (#2)	ColE1, f1	cam	Phagemid pMorph7 containing: PhoAss_λ-phosphatase
pDST054	DST (#2)	ColE1, f1	cam	Phagemid pMorph7 containing: DsbAss_λ-phosphatase
pDST055	DST (#2)	ColE1, f1	cam	Phagemid pMorph7 containing: PhoAss_ APH
pDST056	DST (#2)	ColE1, f1	cam	Phagemid pMorph7 containing: DsbAss_ APH
pDST065	DST (#2)	ColE1, f1	cam	Phagemid pMorph7 containing: PhoAss_ DARPin E3_19
pDST066	DST (#2)	ColE1, f1	cam	Phagemid pMorph7 containing: DsbAss_ DARPin E3_19
pDST067	DST (#3)	ColE1	amp	Modified pQE30, double stop codon (TAA TGA) after the *Hind*III restriction site: expression of the selected DARPins containing an N-terminal MRGS$(H)_6$ tag
pDST067_ (T_xx)	DST (#3, Ap. #1)	ColE1	amp	pDST67 containing a DARPin selected against TNF alpha : MRGS$(H)_6$ _DARPin (T_01, T_02, T_03, T_04, T_06, T_07, T_08, T_09, T_10, T_11, T_12, T_13, T_15, T_16, T_19, T_25, T_27, T_30, T_33, T_35, T_37, T_40, T_41, T_44, T_45, T_47, T_49, T_51, T_52)
pDST067_ (E_xx)	DST (#3, Ap. #1)	ColE1	amp	pDST67 containing a DARPin selected against ErbB1: MRGS$(H)_6$ _DARPin (E_01, E_17, E_31, E_36, E_64, E_67, E_68, E_72)
pDST067_ (9_xx)	DST (#3, Ap. #1)	ColE1	amp	pDST67 containing a DARPin selected against ErbB2-509: MRGS$(H)_6$ _DARPin (9_01, 9_02, 9_03, 9_04, 9_10, 9_12, 9_16, 9_18, 9_20, 9_26, 9_29, 9_30, 9_33)
pDST067_ (H_xx)	DST (#3, Ap. #1)	ColE1	amp	pDST67 containing a DARPin selected against ErbB2-631: MRGS$(H)_6$ _DARPin (H_01, H_03, H_14)
pDST067_ (B4_xx)	DST (#3, Ap. #1)	ColE1	amp	pDST67 containing a DARPin selected against ErbB4: MRGS$(H)_6$ _DARPin (B4_01, B4_02, B4_07, B4_11, B4_14, B4_33, B4_45, B4_49, B4_50, B4_53, B4_55, B4_56, B4_57, B4_58, B4_60, B4_63, B4_64, B4_65, B4_68)
pDST067_ (I_xx)	DST (#3, Ap. #1)	ColE1	amp	pDST67 containing a DARPin selected against Fc domain of human IgG1: MRGS$(H)_6$ _DARPin (I_01, I_02, I_03, I_06, I_07, I_10, I_11, I_13, I_14, I_19)
pDST072	DST (#3)	ColE1	amp	pDST67 containing the selected DARPin G3 (H2R10G3): MRGS$(H)_6$ _G3
pDST080	DST (#2)	ColE1, f1	cam	Phagemid pMorph7 containing: PelBss_DARPin 3a
pDST081	DST (#2)	ColE1, f1	cam	Phagemid pMorph7 containing: PelBss_DARPin JNK2_2_3
pDST084	DST (#2)	ColE1, f1	cam	Phagemid pMorph7 containing: TolBss_DARPin 3a
pDST085	DST (#2)	ColE1, f1	cam	Phagemid pMorph7 containing: TolBss_DARPin JNK2_2_3
pDST086	DST (#2)	ColE1, f1	cam	Phagemid pMorph7 containing: SfmCss_DARPin 3a
pDST087	DST (#2)	ColE1, f1	cam	Phagemid pMorph7 containing: SfmCss_DARPin JNK2_2_3
pDST088	DST (#2)	ColE1, f1	cam	Phagemid pMorph7 containing: TorTss_DARPin 3a
pDST089	DST (#2)	ColE1, f1	cam	Phagemid pMorph7 containing: TorTss_DARPin JNK2_2_3
pDST103	DST (#2)	ColE1, f1	cam	Phagemid pMorph7 containing: OmpAss_DARPin E3_5
pDST104	DST (#2)	ColE1, f1	cam	Phagemid pMorph7 containing: OmpAss_TrxAwt

Name	Source	Ori(s)	Res.	Use/ORF
pDST105	DST (#2)	ColE1, f1	cam	Phagemid pMorph7 containing: PelBss_DARPin E3_5
pDST106	DST (#2)	ColE1, f1	cam	Phagemid pMorph7 containing: TolBss_DARPin E3_5
pDST107	DST (#2)	ColE1, f1	cam	Phagemid pMorph7 containing: TorTss_DARPin E3_5
pDST108	DST (#2)	ColE1, f1	cam	Phagemid pMorph7 containing: SfmCss_DARPin E3_5
pDST109	DST (#2)	ColE1, f1	cam	Phagemid pMorph7 containing: MalEss_DARPin E3_5
pDST110	DST (#2)	ColE1, f1	cam	Phagemid pMorph7 containing: LamBss_DARPin E3_5
pDST111	DST (#2)	ColE1, f1	cam	Phagemid pMorph7 containing: MglBss_DARPin E3_5
pDST112	DST (#2)	ColE1, f1	cam	Phagemid pMorph7 containing: PelBss_TrxAwt
pDST113	DST (#2)	ColE1, f1	cam	Phagemid pMorph7 containing: TolBss_TrxAwt
pDST114	DST (#2)	ColE1, f1	cam	Phagemid pMorph7 containing: TorTss_TrxAwt
pDST115	DST (#2)	ColE1, f1	cam	Phagemid pMorph7 containing: SfmCss_TrxAwt
pDST116	DST (#2)	ColE1, f1	cam	Phagemid pMorph7 containing: MalEss_TrxAwt
pDST117	DST (#2)	ColE1, f1	cam	Phagemid pMorph7 containing: LamBss _TrxAwt
pDST118	DST (#2)	ColE1, f1	cam	Phagemid pMorph7 containing: MglBss _TrxAwt
pDST126	DST (#3)	ColE1	amp	pAT223 containing DARPin E_01
pDST127	DST (#3)	ColE1	amp	pAT223 containing DARPin B4_02
pPDV1 / pMPAG3	DST (#3)	ColE1, f1	cam	Phagemid for SRP phage display used for library construction

Abbreviations used: DST, Daniel Steiner; PAT, Patrik Forrer; #, Chapter in this thesis; Ap. #, Appendix; Res., antibiotics resistance; cam, chloramphenicol; amp, ampicilin

3. List of oligonucleotides

Name	Source	Sequence	Comment
oDST01	DST (#2)	5'- TTCCTCCATGGGTATGAGAGGATCGCATCACC ATCACCATCACGGATCCGACCTGGG-3'	Fwd. primer: amplification of DARPins (*Nco*I, *BamH*I)
oDST02	DST (#2)	5'- TCGAATTCGGCTGCAGATTGCAGGATTTCAGC CAGGTCCTCG-3'	Rev. primer: amplification of DARPins (*Pst*I, *EcoR*I)
oDST04	DST (#2)	5'-AGAGCATGCGTAGGAGAAAATAAAATGAAA AAGATTTGGCTGGCGCTGGCTGG-3'	Inner fwd. primer DsbAss
oDST05	DST (#2)	5'-TCTTTGTAGTCCGCCGATGCGCTAAACGCTAA AACTAAACCAGCCAGCGCCAGCC-3'	Inner rev. primer DsbAss
oDST06	DST (#2)	5'-GCTCTAGAGCATGCGTAGGAG-3'	Outer fwd. primer for all ss amplification (*Xba*I)
oDST07	DST (#2)	5'-GCCAATTGCACTTCATCTTTGTAGTCCGCCG-3'	Outer rev. primer for DsbAss amplification, special for scFv 31 containing pDST (*Mfe*I)
oDST08	DST (#2)	5'-GCGGATCCATCTTTGTAGTCCGCCG-3'	Outer rev. primer for DsbAss amplification (*BamH*I)
oDST09	DST (#2)	5'-CGGGATCCCGTATGAAACAGCTGGAAGACAA AGTTGAATTGCTTCCGAAAAATTATCAC-3'	Fwd. primer: amplification of GCN4 (*BamH*I)
oDST10	DST (#2)	5'-CGGAATTCGGCTGCAGAGCGTTCGCCAACTAA TTTCTTTAATC-3'	Rev. primer: amplification of GCN4 (*Pst*I, *EcoR*I)
oDST11	DST (#2)	5'-CGAGATCTGGCACCGCAACCGCG-3'	Fwd. primer: amplification of pDΔN2 (*Bgl*II)
oDST12	DST (#2)	5'-CGGAATTCGGCTGCAGAGCCAACGATGCTGA TTGCCG-3'	Rev.: amplification of pDΔN2 (*Pst*I, *EcoR*I)
oDST13	DST (#2)	5'-CGGAATTCGGCTGCAGATCGACAGCCTTCAA GG-3'	Rev. primer: amplification of JNK2 (*Pst*I, *EcoR*I)
oDST14	DST (#2)	5'-CGGGATCCTCCGACTCTAAATGTGAC-3'	Fwd. primer: amplification of JNK2 (*BamH*I)
oDST15	DST (#2)	5'-CGGGATCCGGCAGCGATAAAATTATTCACC-3'	Fwd. primer: amplification of TrxA (*BamH*I)
oDST16	DST (#2)	5'-CGGAATTCGGCTGCAGAGGCCAGGTTAGCGT CG-3'	Rev. primer: amplification of TrxA (*Pst*I, *EcoR*I)
oDST19	DST (#2)	5'-GAAGATCTGGCAGCCCCAAGGCCCTG-3'	Fwd. primer: amplification of Taq (*Bgl*II)
oDST20	DST (#2)	5'-CGGAATTCGGCTGCAGACTCCTTGGCGGAGA GC-3'	Rev. primer: amplification of Taq (*Pst*I, *EcoR*I)
oDST21	DST (#2)	5'-GAGGATCCATGCGCTATTACGAAAAAATTGA TGG-3'	Fwd. primer: amplification of λ-phosphatase (*BamH*I)
oDST22	DST (#2)	5'-CGGAATTCGGCTGCAGAACCTGCGCCTTCTCC CTG-3'	Rev. primer: amplification of λ-phosphatase (*Pst*I, *EcoR*I)
oDST23	DST (#2)	5'-CGGGATCCGCTAAAATGAGAATATCACC-3'	Fwd. primer: amplification of APH (*BamH*I)
oDST24	DST (#2)	5'-CGGAATTCGGCTGCAGAAAACAATTCATCCA GTAAAA-3'	Rev.: amplification of APH (*Pst*I, *EcoR*I)
oDST29	DST (#3)	5'- GGCCAAGCTTAATTAATGACTGAGCTTGGACT CCTG-3'	Fwd. primer: Introducing TAA TAG into pQE30 (*Hind*III)
oDST30	DST (#3)	5'- AAAGCCAAGCTAGCTTGGATTCTC-3'	Rev. primer: Introducing TAA TAG into pQE30 (*Nhe*I)
oDST47	DST (#2)	5'-GCGGATCCATCTTTGTAGTC-3'	Outer rev. primer for all ss amplification (*BamH*I)

Name	Source	Sequence	Comment
oDST48	DST (#2)	5'-AGAGCATGCGTAGGAGAAAATAAAATGAAATACCTATTGCCTACGGCAGCCGCTGG-3'	Inner fwd. primer PelBss
oDST52	DST (#2)	5'-AGAGCATGCGTAGGAGAAAATAAAATGAAGCAGGCATTACGAGTAGCATTTGGTTTCCTC-3'	Inner fwd. primer TolBss
oDST53	DST (#2)	5'-GGATCCATCTTTGTAGTCAGCATGCAGAACTGATGCCCACAGTATGAGGAAACCAAATGCTACTCG-3'	Inner rev. primer TolBss
oDST54	DST (#2)	5'-AGAGCATGCGTAGGAGAAAATAAAATGATGACTAAAATAAAGTTACTCATGCTCATTATATTTTACCTG-3'	Inner fwd. primer SfmCss
oDST55	DST (#2)	5'-GGATCCATCTTTGTAGTCAGCATGGGCGCTGGCCGAAATGATCAGGTAAAATATAATGAGCATGAG-3'	Inner rev. primer SfmCss
oDST56	DST (#2)	5'-AGAGCATGCGTAGGAGAAAATAAAATGCGCGTACTGCTATTTTTACTGCTTTCCCTTTTCATGCTG-3'	Inner fwd. primer TorTss
oDST57	DST (#2)	5'-GGATCCATCTTTGTAGTCCGAAAATGCCGGCAGCATGAAAAGGGAAAGCAG-3'	Inner rev. primer TorTss
oDST60	DST (#2)	5'-AGAGCATGCGTAGGAGAAAATAAAATGAATAAGAAGGTGTTAACCCTGTCTGCTGTGATGGCCAGC-3'	Inner fwd. primer MglBss
oDST61	DST (#2)	5'-GGATCCATCTTTGTAGTCAGCGTGTGCAGCGGCACCGAATAACATGCTGGCCATCACAGCAGAC-3'	Inner rev. primer MglBss
oDST62	DST (#2)	5'-AGAGCATGCGTAGGAGAAAATAAAATGATGATTACTCTGCGCAAACTTCCTCTGGCGGTTGCCGTCG-3'	Inner fwd. primer LamBss
oDST63	DST (#2)	5'-GGATCCATCTTTGTAGTCAGCCATTGCCTGAGCAGACATTACGCCCGCTGCGACGGCAACCGCCAGAG-3'	Inner rev. primer LamBss
oDST64	DST (#2)	5'-AGAGCATGCGTAGGAGAAAATAAAATGAAAATAAAAACAGGTGCACGCATCCTCGCATTATCCGCATTAACGACG-3'	Inner fwd. primer MalEss
oDST65	DST (#2)	5'-GGATCCATCTTTGTAGTCGGCGAGAGCCGAGGCGGAAAACATCATCGTCGTTAATGCGGATAATGC-3'	Inner rev. primer MalEss
oDST66	DST (#2)	5'-AGAGCATGCGTAGGAGAAAATAAAATGAAAAAGACAGCTATCGCGATTGCAGTGGCACTGGC-3'	Inner fwd. primer OmpAss
oDST67	DST (#2)	5'-GGATCCATCTTTGTAGTCGGCCTGCGCTACGGTAGCGAAACCAGCCAGTGCCACTGCAATCG-3'	Inner rev. primer OmpAss
EWT3	HKB	5'-TTCCGCGGATCCGACCTGGG-3'	Fwd. primer: amplification of DARPin library (*Bam*HI)
WTC4	HKB	5'-TTTGGGAAGCTTTTGCAGGATTTCAGC-3'	Rev. primer: amplification of DARPin library (*Hind*III)

Abbreviations used: DST, Daniel Steiner; HKB, Hans Kaspar Binz; #, Chapter in this thesis; fwd., forward; rev., reverse, Restriction enzymes are given in brackets and underlined in the sequence.

4. Curriculum vitae

Personal data:

Name:	Steiner
First Name:	Daniel
Date of Birth:	11th of September 1976
Place of birth:	Zürich
Nationality:	Swiss/German

Education:

2003-2007	Dissertation in the group of Prof. Andreas Plückthun, Department of Biochemistry, University of Zürich, Switzerland. Title: „Filamentous Phage Display of Designed Ankyrin Repeat Proteins: from Conception to Applications“
2003	Advanced Studies in Nutrition and Health at the Swiss Federal Institute of Technology in Zürich (ETH Zürich)
2002	Diploma in Biochemistry and organic chemistry at the ETH Zürich
2001	Diploma Thesis in the Biochemistry Institute at the ETH Zürich, Advisor: Prof. Joseph Brunner, Title: „Synthesis and Biochemical Evaluation of Bifunctional Photoaffinity Amino Acid“
1999-2000	ERASMUS exchange at the Imperial College London, England
1997-2002	Studies in Biochemistry and Organic Chemistry at the ETH Zürich
1992-1997	„Matura Typus B“, Kantonsschule Wattwil, Switzerland

5. Oral presentations and invited talks

December 2005 **IBC's Antibody Engineering Conference,** San Diego, California, USA. *Novel Aspects of Phage Display*

September 2006 **GlycoVaxyn AG**, Wädenswil, Switzerland. *SRP Phage Display: Expanding the Scope of Phage Display by using Cotranslational Translocation*

May 2007 **CHI's Phage Display of Antibodies and Peptides Conference**, Boston, Massachusetts, USA. *Efficient Selection of Subnanomolar DARPins by SRP Phage Display*